INFLUENCE OF ENVIRONMENTAL VARIABILITY ON CLIMATE CHANGE IMPACTS IN MARINE ECOSYSTEMS

EDITED BY: Christian Pansch, Michael Raatz, Steeve Comeau, Tin Yan Hui, Christopher Edward Cornwall and Jon Havenhand

PUBLISHED IN: Frontiers in Marine Science

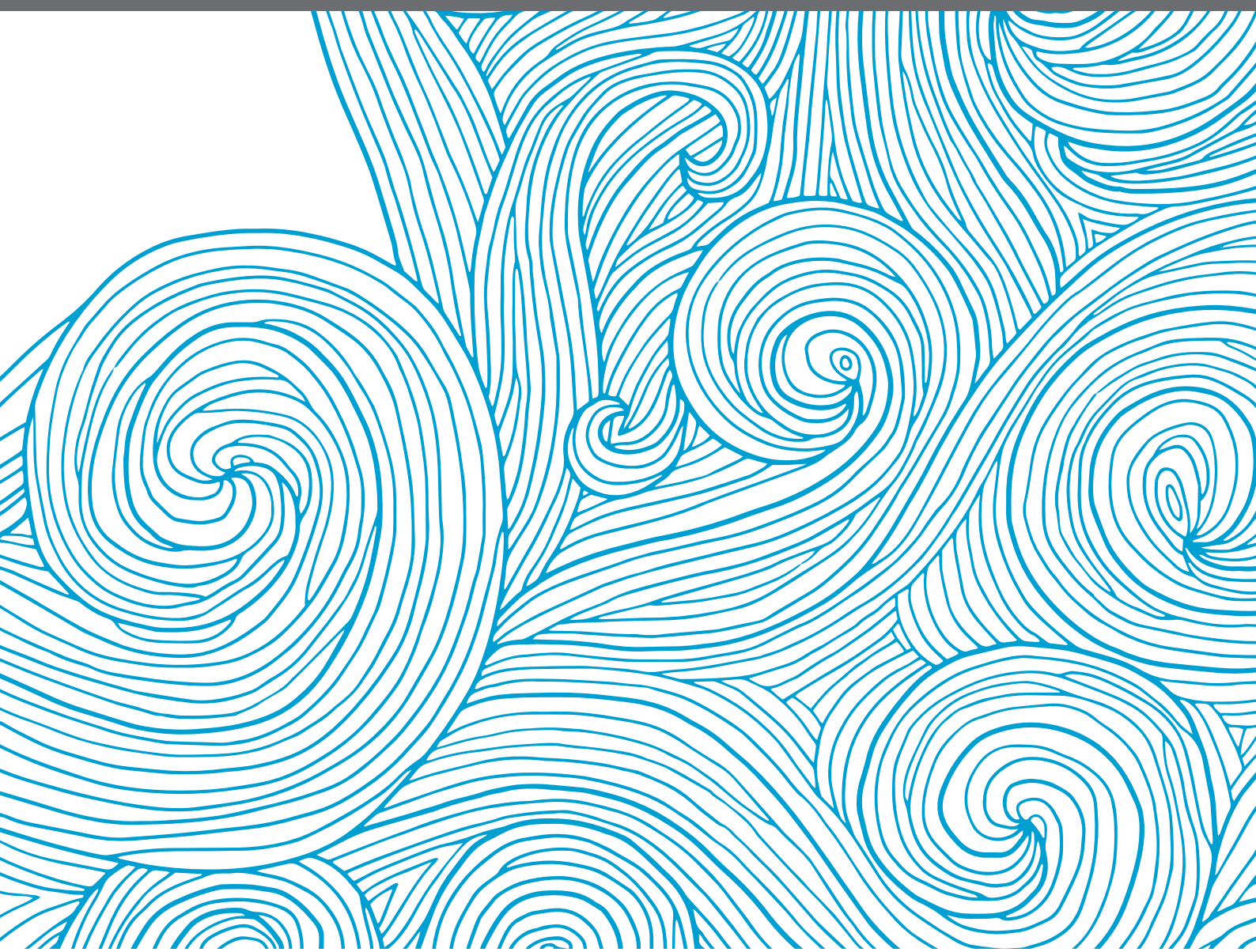

frontiers Research Topics

frontiers

ISSN 1664-8714
ISBN 978-2-83250-074-3
DOI 10.3389/978-2-83250-074-3

About Frontiers

Frontiers is more than just an open-access publisher of scholarly articles: it is a pioneering approach to the world of academia, radically improving the way scholarly research is managed. The grand vision of Frontiers is a world where all people have an equal opportunity to seek, share and generate knowledge. Frontiers provides immediate and permanent online open access to all its publications, but this alone is not enough to realize our grand goals.

Frontiers Journal Series

The Frontiers Journal Series is a multi-tier and interdisciplinary set of open-access, online journals, promising a paradigm shift from the current review, selection and dissemination processes in academic publishing. All Frontiers journals are driven by researchers for researchers; therefore, they constitute a service to the scholarly community. At the same time, the Frontiers Journal Series operates on a revolutionary invention, the tiered publishing system, initially addressing specific communities of scholars, and gradually climbing up to broader public understanding, thus serving the interests of the lay society, too.

Dedication to Quality

Each Frontiers article is a landmark of the highest quality, thanks to genuinely collaborative interactions between authors and review editors, who include some of the world's best academicians. Research must be certified by peers before entering a stream of knowledge that may eventually reach the public - and shape society; therefore, Frontiers only applies the most rigorous and unbiased reviews.
Frontiers revolutionizes research publishing by freely delivering the most outstanding research, evaluated with no bias from both the academic and social point of view. By applying the most advanced information technologies, Frontiers is catapulting scholarly publishing into a new generation.

What are Frontiers Research Topics?

Frontiers Research Topics are very popular trademarks of the Frontiers Journals Series: they are collections of at least ten articles, all centered on a particular subject. With their unique mix of varied contributions from Original Research to Review Articles, Frontiers Research Topics unify the most influential researchers, the latest key findings and historical advances in a hot research area! Find out more on how to host your own Frontiers Research Topic or contribute to one as an author by contacting the Frontiers Editorial Office: frontiersin.org/about/contact

INFLUENCE OF ENVIRONMENTAL VARIABILITY ON CLIMATE CHANGE IMPACTS IN MARINE ECOSYSTEMS

Topic Editors:
Christian Pansch, Åbo Akademi University, Finland
Michael Raatz, Max Planck Institute for Evolutionary Biology, Germany
Steeve Comeau, UMR7093 Laboratoire d'océanographie de Villefranche (LOV), France
Tin Yan Hui, The University of Hong Kong, SAR China
Christopher Edward Cornwall, Victoria University of Wellington, New Zealand
Jon Havenhand, University of Gothenburg, Sweden

Citation: Pansch, C., Raatz, M., Comeau, S., Hui, T. Y., Cornwall, C. E., Havenhand, J., eds. (2022). Influence of Environmental Variability on Climate Change Impacts in Marine Ecosystems. Lausanne: Frontiers Media SA.
doi: 10.3389/978-2-83250-074-3

Table of Contents

frontiers | Frontiers in Marine Science

TYPE Editorial
PUBLISHED 11 August 2022
DOI 10.3389/fmars.2022.994756

OPEN ACCESS

EDITED AND REVIEWED BY
Rui Rosa,
University of Lisbon, Portugal

*CORRESPONDENCE
Christian Pansch
ch.pansch@gmail.com

SPECIALTY SECTION
This article was submitted to Global Change and the Future Ocean, a section of the journal Frontiers in Marine Science

RECEIVED 15 July 2022
ACCEPTED 27 July 2022
PUBLISHED 11 August 2022

CITATION
Pansch C, Raatz M, Comeau S, Hui TTY, Havenhand JN, Vajedsamiei J and Cornwall CE (2022) Editorial: Influence of environmental variability on climate change impacts in marine ecosystems. *Front. Mar. Sci.* 9:994756. doi: 10.3389/fmars.2022.994756

Editorial: Influence of environmental variability on climate change impacts in marine ecosystems

Christian Pansch[1]*, Michael Raatz[2], Steeve Comeau[3], Tommy T. Y. Hui[4], Jonathan N. Havenhand[5], Jahangir Vajedsamiei[6] and Christopher E. Cornwall[7,8]

[1]Department of Environmental and Marine Biology, Åbo Akademi University, Turku, Finland, [2]Department for Evolutionary Theory, Max Planck Institute for Evolutionary Biology, Plön, Germany, [3]Sorbonne Université-CNRS, Laboratoire d'Océanographie de Villefranche, Villefranche, France, [4]The Swire Institute of Marine Science and School of Biological Sciences, The University of Hong Kong, Hong Kong, Hong Kong SAR, China, [5]Department of Marine Sciences - Tjärnö, University of Gothenburg, Strömstad, Sweden, [6]Department of Marine Ecology, GEOMAR Helmholtz Centre for Ocean Research, Kiel, Germany, [7]School of Biological Sciences, Victoria University of Wellington, Kelburn, Wellington, New Zealand, [8]Coastal People; Southern Skies, Centre of Research Excellence, Victoria University of Wellington, Kelburn, Wellington, New Zealand

KEYWORDS

multiple drivers, environmental variability, Climate change, marine heatwaves, stress memory, Ecological memory, Thermal performance curves, acclimation

Editorial on the Research Topic
Influence of environmental variability on climate change impacts in marine ecosystems

Phenotypic responses and selection in populations that lead to ecosystem shifts are often driven by environmental variability and extremes (Grant et al., 2017; Al-Janabi et al., 2019). Marine environments, particularly coastal and shallow-water habitats,

experience strong fluctuations of abiotic drivers at multiple temporal scales (Boyd et al., 2016; Pansch and Hiebenthal, 2019). This environmental variability can arise from biological activity, irradiance variation, tides, weather-driven changes in water level, waves, and up/downwelling events, but also from seasonal, annual, and semi-decadal cycles such as El Niño and La Niña (Boyd et al., 2016; Choi et al., 2019). Diurnal and seasonal temperature fluctuations (driven by irradiation cycles) form basic cycles on top of which stochastic processes operate (Lima and Wethey, 2012; Wang and Dillon, 2014). These include marine heatwaves (MHWs; Oliver et al., 2018), which can have strong and lasting negative impacts on the physiology of marine species and the composition of entire ecosystems (Pansch et al., 2018; Smale et al., 2019). Likewise, the seawater carbonate system (and oxygen tension) varies in response to the same drivers (Hofmann et al., 2011), although this can be more strongly influenced by the metabolism of organisms in areas with high biomass and high seawater residence times (Rivest et al., 2017; Noisette et al., 2022).

There has been increasing research interest in how organisms respond to environmental variability and how this will interact with future effects of anthropogenic climate change. In habitats where organisms are near, or at, their physiological limits, environmental variability will exacerbate future effects of climate change (Cornwall et al., 2018; Morón Lugo et al., 2020). Alternatively, some fluctuations and cycles can mimic the mean conditions expected due to ongoing ocean warming or acidification, which can precondition resident taxa to greater tolerance (Pansch et al., 2014; Vargas et al., 2017). In all cases, environmental variability can lead to periods where environmental conditions are favorable (Cornwall et al., 2014; Wahl et al., 2018; Vajedsamiei et al., 2021), and variability has therefore been proposed to also provide temporal refugia in a future ocean.

This special issue hosts a range of research that explores concepts relating to environmental variability and climate change. From microbes to corals, and microns to ocean basins, these studies explore the effects of variability in light, temperature, and seawater carbonate chemistry.

Including environmental variability in our projections is essential if we are to accurately assess the impacts of climate change. McClanahan et al. demonstrate that projections of the impacts of MHWs and thermal stress are much more accurate if models include components of variability such as bimodality and standard deviation in temperature, rather than more simplistic assumptions of cumulative thermal stress such as the degree heating day/week models (Maynard et al., 2008; Cornwall et al., 2021). MHWs are complex and comprise different components, such as intensity, duration, and frequency, that will all change in the future (Frölicher et al., 2018). Wolf et al. demonstrate that longer continual MHWs have stronger negative effects on sea star physiology than equivalent MHWs that are broken up into several shorter periods of heat stress (and therefore allow for recovery from stress). Vajedsamiei et al. demonstrate that MHWs may select for mussel recruits with higher heat tolerance and such tolerance may be mediated by lower metabolic demand, but also that mussels' capacity for beneficial heat acclimation is limited. Samuels et al. indicate that MHW intensity controls responses of diatoms, but that past thermal history and genotypic differences modulate responses further. Collectively, these works exemplify the complexity of MHWs, and show that projections based on traditional research models of slow onset of thermal stress (simulating ocean warming/acidification), or which ignored sequential phases of impact and recovery, should be considered with caution.

Historical variability in temperature can affect species' responses to MHWs or ongoing ocean warming, such that populations exposed to greater extremes in temperatures often have higher thermal tolerances than populations of the same species not exposed to such extremes (Schoepf et al., 2015; Marshall et al., 2018; Moyen et al., 2020). Kunze et al. demonstrate that responses of phytoplankton to temperature fluctuations vary depending on the frequency of the fluctuations, with faster fluctuations having more positive outcomes. Hennigs et al. indicate that the responses of mysids to temperature fluctuations are dependent on their sex, with females being metabolically more active than males, and female ingestion rates being negatively impacted by temperature fluctuations. Jimenez et al. find sex-related responses to temperature fluctuations in intertidal crabs, where thermal extremes but not latitudinal gradients explain the responses. These three studies collectively reinforce earlier findings that the impacts of thermal variability in experimental work and the impacts of past exposure to temperature variability are complex and context-dependent and that these cannot easily be generalized. This complexity must be well understood and acknowledged if we are to accurately project the impacts of climate change (McClanahan et al.). In this issue, Sylvester et al. support this premise, showing that it is difficult to tease apart the response of krill population growth to ocean warming from responses to the large natural temperature variability in the Southern Ocean. Further complications arise when accounting for the impacts of environmental variability on microbial adaptive plasticity and evolution. The review by Arromrak et al. indicates the importance of these aspects, but also points out the apparent knowledge gaps around the interplay of climate change, environmental variability, and adaptation, as a vast majority of past research has focused on single drivers applying constant environmental regimes.

Variability in drivers besides temperature, such as light, water motion, and seawater carbonate chemistry, are also important for the physiology of marine species. For example, the quality and quantity of fluctuating light can radically alter the physiology of photosynthetic species. Neun et al. demonstrate that responses to light variability of phytoplankton are species-specific. Light also modifies indirectly the seawater chemistry experienced by many marine organisms in nearshore ecosystems. In an extreme example, Houlihan et al. show that increasing light (and therefore photosynthesis) and decreasing water velocity increase pH and the thickness of the diffusion boundary layer (Hurd et al., 2011; Cornwall et al., 2015; Noisette et al., 2022) of crustose coralline algae, which represents µm to mm habitats in which sea urchin larvae settle. However, during the night, respiration processes impose contrasting pH shifts leading to strong diurnal pH variability.

This special issue highlights the complex and context-dependent nature of environmental variability. It shows that responses to variability cannot be generalized from concepts such as Jensen's inequality and from experimental studies applying constant environmental regimes. In addition, previous experience (carry-over effects, stress memory and cross-stress tolerance, ecological memory, or trans-generational plasticity; Jackson et al., 2021) can all change organisms' responses to (multiple) fluctuating drivers. Nonetheless, environmental variability is fundamentally important and must be considered in future research that investigates the impacts of climate change on marine taxa.

We propose (Figure 1) future research combining experimental and conceptual/theoretical studies that investigate the effects of multiple (including biotic) fluctuating environmental drivers across relevant spatial and temporal scales on marine organisms and ecosystems. Ideally, drivers would be applied along a species' performance gradient, i.e., from optimal to stressful conditions. Experiments testing whether performance curves are adaptive in the short- (via phenotypic plasticity) or the long-run (by evolution) will be a highly valuable contribution to the existing literature. Thus, the complexity of this rapidly growing research field may be overcome only by integrating disciplines (from physiology and evolutionary biology to behavioral biology and ecology) and by combining studies from the Petri dish to large-scale mesocosm infrastructure and field observations across environmental gradients.

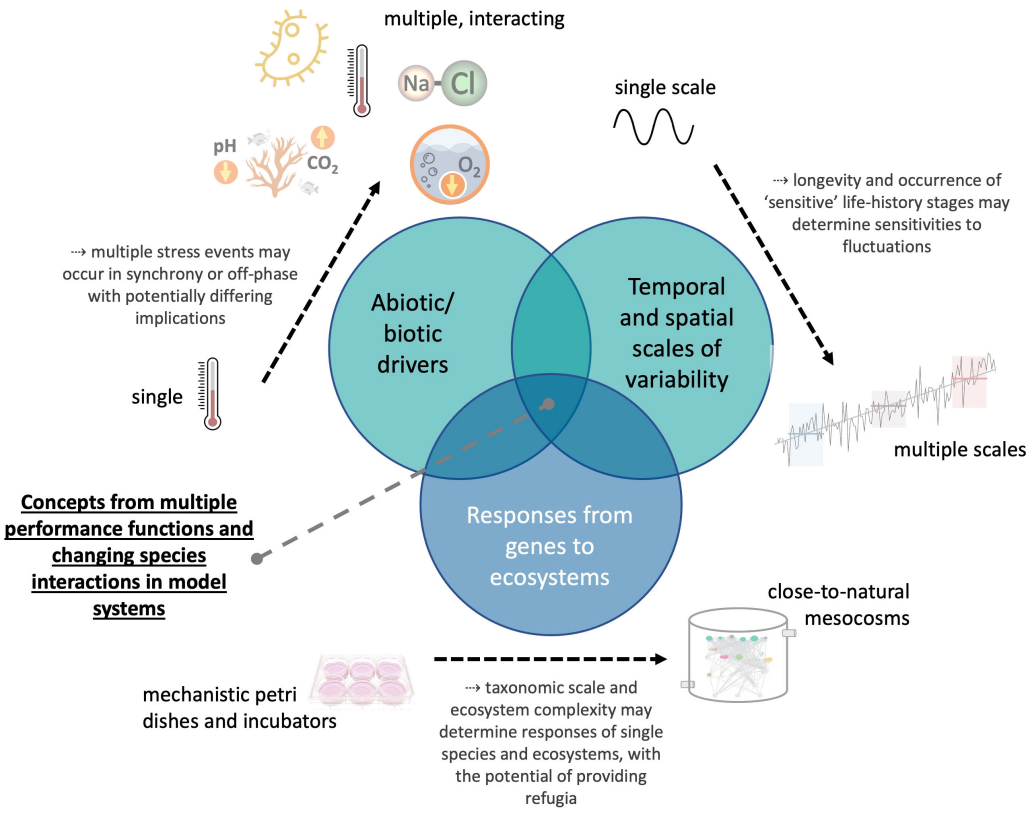

FIGURE 1
Aspects to be considered in theoretical to experimental research that aims to delineate the consequences of environmental variability and climate change for marine life.

Author contributions

CP initiated this topic. CP and CC framed the text and CP drafted the figure. All authors contributed substantially to the editorial process of this topic and the article and approved the submitted version.

Funding

CEC was funded by a Rutherford Discovery Fellowship from the Royal Society of New Zealand Te Apārangi.

Conflict of interest

The authors declare that the research was conducted in the absence of any commercial or financial relationships that could be construed as a potential conflict of interest.

Publisher's note

All claims expressed in this article are solely those of the authors and do not necessarily represent those of their affiliated organizations, or those of the publisher, the editors and the reviewers. Any product that may be evaluated in this article, or claim that may be made by its manufacturer, is not guaranteed or endorsed by the publisher.

References

Al-Janabi, B., Wahl, M., Karsten, U., Graiff, A., and Kruse, I. (2019). Sensitivities to global change drivers may correlate positively or negatively in a foundational marine macroalga. *Sci. Rep.* 9, 14653. doi: 10.1038/s41598-019-51099-8

Boyd, P. W., Cornwall, C. E., Davison, A., Doney, S. C., Fourquez, M., Hurd, C. L., et al. (2016). Biological responses to environmental heterogeneity under future ocean conditions. *Global Change Biol.* 22, 2633–2650. doi: 10.1111/gcb.13287

Choi, F., Gouhier, T., Lima, F., Rilov, G., Seabra, R., and Helmuth, B. (2019). Mapping physiology: biophysical mechanisms define scales of climate change impacts. *Conserv. Physiol.* 7, coz028. doi: 10.1093/conphys/coz028

Cornwall, C. E., Boyd, P. W., McGraw, C. M., Hepburn, C. D., Pilditch, C. A., Morris, J. N., et al. (2014). Diffusion boundary layers ameliorate the negative effects of ocean acidification on the temperate coralline macroalga *Arthrocardia corymbosa*. *PloS One* 9, e97235. doi: 10.1371/journal.pone.0097235

Cornwall, C. E., Comeau, S., DeCarlo, T. M., Moore, B., D'Alexis, Q., and McCulloch, M. T. (2018). Resistance of corals and coralline algae to ocean acidification: physiological control of calcification under natural pH variability. *Proc. R. Soc. B: Biol. Sci.* 285, 20181168. doi: 10.1098/rspb.2018.1168

Cornwall, C. E., Comeau, S., Kornder, N. A., Perry, C. T., van Hooidonk, R., DeCarlo, T. M., et al. (2021). Global declines in coral reef calcium carbonate production under ocean acidification and warming. *Proc. Natl. Acad. Sci.* 118, e2015265118. doi: 10.1073/pnas.2015265118

Cornwall, C. E., Pilditch, C. A., Hepburn, C. D., and Hurd, C. L. (2015). Canopy macroalgae influence understorey corallines' metabolic control of near-surface pH and oxygen concentration. *Mar. Ecol. Prog. Ser.* 525, 81–95. doi: 10.3354/meps11190

Frölicher, T. L., Fischer, E. M., and Gruber, N. (2018). Marine heatwaves under global warming. *Nature* 560, 360–364. doi: 10.1038/s41586-018-0383-9

Grant, P. R., Grant, B. R., Huey, R. B., Johnson, M. T. J., Knoll, A. H., and Schmitt, J. (2017). Evolution caused by extreme events. *Philos. Trans. R. Soc. B: Biol. Sci.* 372, 20160146. doi: 10.1098/rstb.2016.0146

Hofmann, G. E., Smith, J. E., Johnson, K. S., Send, U., Levin, L. A., Micheli, F., et al. (2011). High-frequency dynamics of ocean pH: A multi-ecosystem comparison. *PloS One* 6, e28983. doi: 10.1371/journal.pone.0028983

Hurd, C. L., Cornwall, C. E., Currie, K. I., Hepburn, C. D., McGraw, C. M., Hunter, K. A., et al. (2011). Metabolically-induced pH fluctuations by some coastal calcifiers exceed projected 22nd century ocean acidification: a mechanism for differential susceptibility? *Global Change Biol.* 17, 3254–3262. doi: 10.1111/j.1365-2486.2011.02473.x

Jackson, M. C., Pawar, S., and Woodward, G. (2021). The temporal dynamics of multiple stressor effects: From individuals to ecosystems. *Trends Ecol. Evol.* 36, 402–410. doi: 10.1016/j.tree.2021.01.005

Lima, F. P., and Wethey, D. S. (2012). Three decades of high-resolution coastal sea surface temperatures reveal more than warming. *Nat. Commun.* 3, 704. doi: 10.1038/ncomms1713

Marshall, D. J., Brahim, A., Mustapha, N., Dong, Y., and Sinclair, B. J. (2018). Substantial heat tolerance acclimation capacity in tropical thermophilic snails, but to what benefit? *J. Exp. Biol.* 221, jeb187476. doi: 10.1242/jeb.187476

Maynard, J. A., Turner, P. J., Anthony, K. R. N., Baird, A. H., Berkelmans, R., Eakin, C. M., et al. (2008). ReefTemp: An interactive monitoring system for coral bleaching using high-resolution SST and improved stress predictors. *Geophysical Res. Lett.* 35, L05603. doi: 10.1029/2007GL032175

Morón Lugo, S. C., Baumeister, M., Nour, O. M., Wolf, F., Stumpp, M., and Pansch, C. (2020). Warming and temperature variability determine the performance of two invertebrate predators. *Sci. Rep.* 10, 6780. doi: 10.1038/s41598-020-63679-0

Moyen, N. E., Crane, R. L., Somero, G. N., and Denny, M. W. (2020). A single heat-stress bout induces rapid and prolonged heat acclimation in the California mussel, Mytilus californianus. *Proc. R. Soc. B: Biol. Sci.* 287, 20202561. doi: 10.1098/rspb.2020.2561

Noisette, F., Pansch, C., Wall, M., Wahl, M., and Hurd, C. L. (2022). Role of hydrodynamics in shaping chemical habitats and modulating the responses of coastal benthic systems to ocean global change. *Global Change Biol.* 28, 3812–3829. doi: 10.1111/gcb.16165

Oliver, E. C. J., Donat, M. G., Burrows, M. T., Moore, P. J., Smale, D. A., Alexander, L. V., et al. (2018). Longer and more frequent marine heatwaves over the past century. *Nat. Commun.* 9, 1324. doi: 10.1038/s41467-018-03732-9

Pansch, C., and Hiebenthal, C. (2019). A new mesocosm system to study the effects of environmental variability on marine species and communities. *Limnol Oceanography-Methods* 17, 145–162. doi: 10.1002/lom3.10306

Pansch, C., Schaub, I., Havenhand, J., and Wahl, M. (2014). Habitat traits and food availability determine the response of marine invertebrates to ocean acidification. *Global Change Biol.* 20, 765–777. doi: 10.1111/gcb.12478

Pansch, C., Scotti, M., Barboza, F. R., Al-Janabi, B., Brakel, J., Briski, E., et al. (2018). Heat waves and their significance for a temperate benthic community: A near-natural experimental approach. *Global Change Biol.* 24, 4357–4367. doi: 10.1111/gcb.14282

Rivest, E. B., Comeau, S., and Cornwall, C. E. (2017). The role of natural variability in shaping the response of coral reef organisms to climate change. *Curr. Climate Change Rep.* 3, 271–281. doi: 10.1007/s40641-017-0082-x

Schoepf, V., Stat, M., Falter, J. L., and McCulloch, M. T. (2015). Limits to the thermal tolerance of corals adapted to a highly fluctuating, naturally extreme temperature environment. *Sci. Rep.* 5, 17639–17639. doi: 10.1038/srep17639

Smale, D. A., Wernberg, T., Oliver, E. C. J., Thomsen, M., Harvey, B. P., Straub, S. C., et al. (2019). Marine heatwaves threaten global biodiversity and the provision of ecosystem services. *Nat. Climate Change* 9, 306–312. doi: 10.1038/s41558-019-0412-1

Vajedsamiei, J., Melzner, F., Raatz, M., Morón Lugo, S. C., and Pansch, C. (2021). Cyclic thermal fluctuations can be burden or relief for an ectotherm depending on fluctuations' average and amplitude. *Funct. Ecol.* 35, 2483–2496. doi: 10.1111/1365-2435.13889

Vargas, C. A., Lagos, N. A., Lardies, M. A., Duarte, C., Manríquez, P. H., Aguilera, V. M., et al. (2017). Species-specific responses to ocean acidification should account for local adaptation and adaptive plasticity. *Nat. Ecol. Evol.* 1, 0084. doi: 10.1038/s41559-017-0084

Wahl, M., Covacha, S. S., Saderne, V., Hiebenthal, C., Muller, J. D., Pansch, C., et al. (2018). Macroalgae may mitigate ocean acidification effects on mussel calcification by increasing pH and its fluctuations. *Limnol Oceanography* 63, 3–21. doi: 10.1002/lno.10608

Wang, G., and Dillon, M. E. (2014). Recent geographic convergence in diurnal and annual temperature cycling flattens global thermal profiles. *Nat. Climate Change* 4, 988–992. doi: 10.1038/nclimate2378

frontiers in Marine Science

ORIGINAL RESEARCH
published: 13 November 2020
doi: 10.3389/fmars.2020.577562

Diffusive Boundary Layers and Ocean Acidification: Implications for Sea Urchin Settlement and Growth

Erin P. Houlihan[1], Nadjejda Espinel-Velasco[1,2], Christopher E. Cornwall[3], Conrad A. Pilditch[4] and Miles D. Lamare[1]*

[1] Department of Marine Science, University of Otago, Dunedin, New Zealand, [2] Fram Centre, Norwegian Polar Institute, Tromsø, Norway, [3] School of Biological Sciences, Victoria University of Wellington, Wellington, New Zealand, [4] School of Science, Waikato University, Hamilton, New Zealand

Chemical changes in the diffusive boundary layer (DBL) generated by photosynthesising macroalgae are expected to play an important role in modulating the effects of ocean acidification (OA), but little is known about the effects on early life stages of marine invertebrates in modified DBLs. Larvae that settle to macroalgal surfaces and remain within the DBL will experience pH conditions markedly different from the bulk seawater. We investigated the interactive effects of seawater pH and DBL thickness on settlement and early post-settlement growth of the sea urchin *Pseudechinus huttoni*, testing whether coralline-algal DBLs act as an environmental buffer to OA. DBL thickness and pH levels (estimated from well-established relationships with oxygen concentration) above the crustose coralline algal surfaces varied with light availability (with photosynthesis increasing pH to as high as pH 9.0 and respiration reducing pH to as low as pH 7.4 under light and dark conditions, respectively), independent of bulk seawater pH (7.5, 7.7, and 8.1). Settlement success of *P. huttoni* increased over time for all treatments, irrespective of estimated pH in the DBL. Juvenile test growth was similar in all DBL manipulations, showing resilience to variable and low seawater pH. Spine development, however, displayed greater variance with spine growth being negatively affected by reduced seawater pH in the DBL only in the dark treatments. Scanning electron microscopy revealed no observable differences in structural integrity or morphology of the sea urchin spines among pH treatments. Our results suggest that early juvenile stages of *P. huttoni* are well adapted to variable pH regimes in the DBL of macroalgae across a range of bulk seawater pH treatments.

Keywords: *Pseudechinus huttoni*, macroalgae, seawater pH, settlement substrates, early post-settlement, juveniles

OPEN ACCESS

Edited by:
Iris Eline Hendriks, University of the Balearic Islands, Spain

Reviewed by:
Benjamin Mos, Southern Cross University, Australia
Narimane Dorey, UMR 8539 Laboratoire de météorologie dynamique (LMD), France

****Correspondence:***
Erin P. Houlihan
erinphoulihan@gmail.com

Specialty section:
This article was submitted to Global Change and the Future Ocean, a section of the journal Frontiers in Marine Science

Received: *29 June 2020*
Accepted: *22 October 2020*
Published: *13 November 2020*

Citation:
Houlihan EP, Espinel-Velasco N, Cornwall CE, Pilditch CA and Lamare MD (2020) Diffusive Boundary Layers and Ocean Acidification: Implications for Sea Urchin Settlement and Growth. Front. Mar. Sci. 7:577562. doi: 10.3389/fmars.2020.577562

INTRODUCTION

Ocean acidification (OA) occurs when seawater pH decreases due to the uptake of elevated atmospheric CO_2 by the surface ocean water (Caldeira and Wickett, 2003). Reduced mainstream (or bulk) seawater pH due to OA poses a major threat to marine ecosystems including calcifying organisms (Dupont et al., 2010; Hendriks et al., 2010; Byrne, 2011; Dupont and Thorndyke, 2013; Kroeker et al., 2013). To date, most research on the effects of OA on marine invertebrates has

utilized constant pH conditions representative of bulk seawater pH levels (Wahl et al., 2015; Boyd et al., 2016). However, newly-settled and metamorphosing organisms are likely to experience pH conditions different from the bulk seawater when settled on marine algae and biofilms, which may account for some of the variability found in settlement and post-settlement development of invertebrate responses to OA (Dupont et al., 2010; Albright et al., 2012; Wangensteen et al., 2013; Wolfe et al., 2013a; García et al., 2015). For example, Mos et al. (2019) observed greater survival and growth in newly settled *Tripneustes gratilla* raised on concrete substrates, attributed to the chemical buffering of reduced seawater pH in the boundary layers.

The diffusive boundary layer (DBL) is a micro-layer of seawater (μm to cm scale) around marine organisms where, due to biological activity, the chemical and physical environment is different from the surrounding bulk seawater (Denny and Wethey, 2000; Cornwall et al., 2013b). The potential thickness of the DBL near the surface of macroalgae and marine biofilms is inversely correlated to water velocity, with thicker DBLs resulting in greater gradients between the near-surface and bulk seawater in concentrations of metabolically used or excreted dissolved substances (Cornwall et al., 2015). Within DBLs around macroalgae, variations in light availability drive pH variability (Hurd et al., 2011), with pH generally increasing during the day due to photosynthetic uptake of dissolved inorganic carbon and decreasing at night due to respiration of CO_2 (De Beer and Larkum, 2001; Cornwall et al., 2013b). The pH experienced by organisms within the DBL above photosynthesizing surfaces, therefore, likely differs greatly from surrounding seawater pH.

Thick DBLs that form at the surface of macroalgae may ameliorate some of the negative effects of OA due to the formation of a microenvironment where pH is increased during the day, resulting in exposure to higher mean pH over diel cycles (Hurd et al., 2011; Cornwall et al., 2013b, 2014). However, the potential impacts of seaweed DBLs are yet to be considered on early life stages of invertebrates under future OA conditions (Koehl and Hadfield, 2010; Espinel-Velasco et al., 2018), and a better understanding of how pH fluctuations within the DBL will amplify or alleviate the impacts of reduced bulk seawater pH on surrounding marine organisms is needed (Shaw et al., 2012; Cornwall et al., 2014; Wahl et al., 2015).

Sea urchins (Echinodermata: Echinoidea) are thought to be vulnerable to OA and their early life-history stages and adults have been widely used to investigate the effects of reduced seawater pH (Dupont and Thorndyke, 2013). Within indirect lifecycles, settlement, and early post-settlement stages are particularly vulnerable to OA and other environmental stressors, and therefore are a potential population bottleneck (Gosselin and Qian, 1997; Wolfe et al., 2013a). The effects of OA on the development of echinoderms in the settlement and early post-settlement period can be variable (Dupont et al., 2010; Byrne, 2011; Kroeker et al., 2013; Przeslawski et al., 2015; Byrne et al., 2017; Espinel-Velasco et al., 2018). Previous studies have found negative effects on settlement success in sea urchins due to reduced seawater pH, including delayed metamorphosis (Dupont et al., 2013; García et al., 2015), while other studies have found no effects (Byrne et al., 2010a; Wangensteen et al., 2013). Early post-settlement growth in response to reduced pH is similarly varied, with some juvenile sea urchin survival or test diameter growth being relatively robust to OA (Wolfe et al., 2013a), and even increasing (García et al., 2015). Spine development is similarly robust with reductions usually occurring under only the lowest pH levels (7.4) tested (Wolfe et al., 2013a). Byrne et al. (2010a) and Wangensteen et al. (2013) observed a reduction in size and a smaller proportion of juveniles with normal morphology in reduced bulk seawater pH.

Here, we investigated the ecological implications of pH modifications in the DBL, created by crustose coralline algae (CCA) under OA conditions, on the settlement and early post-settlement juvenile stage of sea urchin *Pseudechinus huttoni* Benham 1908 (Echinoidea, Temnopleuridae). *P. huttoni* is a species endemic to New Zealand found in slow-flow environments along the continental shelf (<60 m) and southern fjords (McClary and Sewell, 2003; Kirby et al., 2006). CCA are well-known settlement inducers of marine invertebrate larvae and also a food source for many (McCoy and Kamenos, 2015) including mollusks (Roberts, 2001; Roberts et al., 2010), corals (Foster and Gilmour, 2016), and echinoderms (Uthicke et al., 2013). Coralline algae were selected for this study, being the most abundant encrusting taxa on New Zealand's shallow rocky reefs (Shears and Babock, 2007) and have been shown to be a key larval settlement substrate for sea urchins (Lamare and Barker, 2001). The pH and thickness of the DBLs were experimentally manipulated via light intensity in contemporary (pH_T 8.1) or near-future bulk seawater pH levels (pH_T 7.5 and 7.7) predicted for the end of century and beyond (IPCC 2019). We determined settlement and metamorphosis success of *P. huttoni* as well as early post-settlement growth (test diameter and spine length 4 day post-settlement) across these treatment combinations. Urchin skeletal elements and spines were also examined using scanning electron microscopy (SEM) to visualize effects on calcification and growth.

MATERIALS AND METHODS

CCA Collection and Storage

Small CCA encrusted cobbles (0.5–2 cm diameter) were collected from the shallow subtidal (<2 m depth) adjacent to the Portobello Marine Laboratory (PML), Otago Harbor, New Zealand (45°52.51'S, 170°30.9'E) during July and August 2018. These cobbles consisted of a natural assemblage of CCA, likely containing multiple species, reflecting *in situ* conditions. While different cobbles were used during experiments, all cobbles were collected in the same location, were the same approximate size and had estimated coverage of about 80% CCA (**Supplementary Figure 1**). Prior to use in experiments, cobbles were visually examined for extraneous organisms, which were removed using a scalpel without damaging the CCA. Cobbles were kept at PML in 50 L flow-through tanks supplied with filtered seawater (10 μm). Tanks were covered with black mesh to limit excessive light. Typically during winter and spring, seawater from the Otago Harbor has a salinity of 33 and temperature 7–11°C (Nelson, 2016).

DBL Measurements

Oxygen profiles were measured above CCA substrates submerged in 3 L plastic experimental aquaria under six experimental treatment conditions: two irradiance levels (dark and light) and three bulk seawater pH levels (pH_T 7.5, 7.7, and 8.1). Dark treatments received <1 μmol photons m^{-2} s^{-1} irradiance, while light treatments received a photosynthetically active radiation (PAR; 400 to 700 nm) of 10 μmol photons m^{-2} s^{-1}. PAR was provided by overhead standard fluorescent tubes in an under-verandah housing, suspended approximately 1 m above the experimental aquaria. The tubes were cool white 845, producing approximately 80% of the natural spectrum at a color temperature of 4500K. Incident irradiance was measured using a flat terrestrial LI-250A quantum sensor (LI-COR, Lincoln, United Kingdom). These measurements were completed under static (no) flow conditions. Within macroalgal turf communities, flows can be extremely slow (<1 cm s^{-1}; Pöhn et al., 2001; Cornwall et al., 2015). Measurements of the DBL were also completed above CCA covered acrylic disks in an annular flume to characterize and compare the DBL under quantifiable flow speeds (Methods, **Supplementary Material**).

Oxygen Profiles

Oxygen concentration profiles were measured using a microsensor from the Unisense MicroRespiration System (Unisense, Aarhus, Denmark) connected to a Unisense Microsensor Multimeter and controlled by a Unisense automatic micromanipulator. SensorTrace Profiling software was used to log the microsensor profiles. Prior to use, the oxygen microsensor was first pre-polarized with -0.80 V for a minimum 10 min period and then calibrated in a fully aerated (100% value) and anoxic (0% value) solution in the SensorTrace Logger software as per the Unisense Oxygen Sensor User Manual.

The sensor was manually lowered with the micromanipulator until it was touching the surface of the substrate, this was considered to be 0 μm above the substrate surface. In this position, a 40 min equilibration period was allowed for the DBL to re-establish before vertical profiles began. The micromanipulator was used to automatically raise the sensor and record 60 s of oxygen concentration (μmol O_2 l^{-1}) measurements at each height. The wait time between each measurement was 0.1 s and the measurement period was 0.9 s. Of the 60 measurements at each height, the first and last 5 measurements were discarded in case movement of the sensor affected readings, and the remaining 50 measurements were averaged. Measurements were taken every 100 μm from 0 to 4 mm above the substrate and then every 1 mm from 4–10 mm. A minimum of four replicate oxygen profiles was measured above CCA substrates for each experimental treatment.

DBL Calculations

Diffusive boundary layer thickness was defined as the distance above the surface of the CCA substrate at which the changes in concentrations of O_2 (raw value) were <5% per 0.1 mm for four subsequent measurements. This 5% cutoff (Layton et al., 2019) balances the robustness of previous methods that used 10% (Hurd et al., 2011; Cornwall et al., 2013b; Lichtenberg et al., 2017) and the sensitivity of changes <1% (Cornwall et al., 2015; Noisette and Hurd, 2018). In order to account for small variation among replicates in bulk seawater oxygen concentration, oxygen profiles were standardized by dividing the concentration at any given height by the bulk seawater concentration (the oxygen concentration 10 mm above the CCA substrate).

H^+ (pH) and O_2 concentrations have a strong relationship within the DBL above CCA substrates (R^2 = 0.82; Cornwall et al., 2014) due to the uptake and release of CO_2 and O_2 during photosynthesis and respiration (Cornwall, 2013; Chan et al., 2016; Noisette and Hurd, 2018). The magnitude and direction of pH changes within the DBL have been found to be almost identical to changes in O_2 concentrations (Cornwall et al., 2014). Thus, O_2 is commonly used as a robust proxy for H^+ and pH (Cornwall et al., 2014; Layton et al., 2019). Standardized O_2 concentrations were converted into H^+ concentrations using separate relationships previously determined for CCA (Cornwall, 2013). These relationships were derived from measurements conducted in the DBL of coralline algae collected from the same region as those in this study (Cornwall et al., 2013b) and take into account potential modification of pH due to calcification and dissolution:

In the dark (R^2 = 0.85):

$$[H^+] = 0.0621[O_2]^{-1.942[O_2]}$$

and light (R^2 = 0.73):

$$[H^+] = 0.000004e^{-0.005[O_2]}$$

H^+ concentrations were converted into pH_T values using the equation pH_T = -log [H^+]. Seawater pH values were standardized for each profile by dividing the concentration at any given height by the bulk seawater pH concentration to get pH deviation in the DBL from the bulk (mainstream) pH. Estimated pH values were calculated by adding the pH deviation to the mean bulk seawater pH value for the respective treatment.

In order to estimate the pH conditions that metamorphosing and newly settled *P. huttoni* experienced during experiments (pH_{EXP}), pH was averaged from 0 to 0.5 mm above the CCA surface. A height of 0 to 0.5 mm was chosen since the test diameter of newly settled *P. huttoni* ranged between 400 to 500 μm.

Sea Urchin Collection, Spawning and Rearing

Adult *P. huttoni* were collected from Doubtful Sound, Fiordland in June 2018 by SCUBA divers and transported to PML where they were kept in a flow through system prior to experiments. Four days after collection, adults were induced to spawn by an intra-coelomic injection of 0.5 M KCL per animal. The gametes obtained were visually inspected for viability under the microscope (swimming sperm and healthy eggs), and deemed suitable for fertilization. Sperm stock solution was added to the egg solution until reaching a final fertilization success of more than 95% (indicated by the appearance of the fertilization membrane). The resulting larvae were reared until competency (i.e., ready to settle) at 10–13°C and under ambient pH_T = 8.1

in 20 glass jars (2.5 L) at densities ranging from 3 to 20 larvae per mL. Larvae were daily fed a combination of *Rhodomonas sp.* and *Dunaliella primolecta* at a total concentration of ∼8,000 cells ml^{-1}. To keep larvae and food suspended, cultures were stirred continuously with large plastic paddles, at a rate of 10 cycles per minute. Water was changed every third day and jars were cleaned periodically. Most larvae showed signs of competency (e.g., well-developed rudiments) from 60 to 75 day post-fertilisation (dpf).

Settlement Experiment

Competent larvae were used to examine settlement and metamorphosis of *P. huttoni* in response to pH and light intensity (therefore DBL characteristics). CCA covered cobbles (0.5 to 2 cm diameter) were placed in custom-made inverted settlement chambers, as per methodology specifically developed for such experiments (Espinel-Velasco et al., 2020). The chambers were closed by a 100 μm mesh cap on the top end to allow water circulation while keeping the larvae inside. The chambers were then placed in 3 L airtight aquaria containing water at the desired target pH (bulk pH) in both light and dark conditions. Three pH treatments were used for this experiment (pH_T 7.5, 7.7, and 8.1). Each treatment (3 L aquaria) contained four inverted chambers and was replicated 3 times. Competent larvae of all the glass cultures were pooled and homogenized before using for the settlement assay. Approximately 30 competent larvae (61 dpf) were added into each chamber and left to settle. After 6, 18, 30, and 51 h, the chambers were checked for settlement under a dissecting microscope. Larvae were counted and placed into two categories: (1) settled and metamorphosed: indicated by the presence of juveniles at the bottom of the chambers, and (2) not-settled: remaining larvae, still in the larval form, swimming in the water column or crawling on the bottom.

Post-settlement Growth Experiment

Post-settlement growth of *P. huttoni* was determined in response to pH and light intensity (therefore DBL characteristics). For this, approximately 4,700 competent larvae (69 dpf) were placed into a 3 L, airtight aquaria with ∼200 CCA covered cobbles, with a diameter between 0.5 and 2 cm. The larvae were left for 24 h to settle on the cobbles, based on results from the settlement experiment. After 24 h, cobbles were visually examined under the dissecting microscope. Cobbles with at least one juvenile attached to them were used for experiments. A total of six cobbles were placed into each experimental tank and left there for a total of 4 days (5 days after introduction to the cue), given that sea urchin juveniles undergo a perimetamorphic period that generally lasts at least 4 day, where they are unable to feed because they have yet to develop a digestive system and other internal structures (Gosselin and Jangoux, 1998; Rahman et al., 2012). Newly settled *P. huttoni* juveniles were grown under six experimental treatment conditions, comprised of three bulk seawater pH levels (pH_T 7.5, 7.7, and 8.1) and two irradiance levels (light and dark), with each treatment replicated three times.

After 4 days in the treatment conditions, cobbles were examined under a dissecting microscope and juveniles were removed from the substrate by a strong water blast with a Pasteur pipette. After removal, juveniles were transferred into eppendorf tubes and fixed with 0.5 mL of paraformaldehyde solution (4% PFA in FSW, buffered). Juveniles were stored in a fridge and photographed with a camera (Olympus XC50) under a compound microscope (Olympus BX51) within the three following days, since preliminary tests had showed no signs of post-fixation change. Images were discarded if juveniles were (1) not lying flat on their aboral or oral surface, (2) covered by algae, another urchin or other unknown material, or (3) if the sea urchin showed signs of disintegration (i.e., did not successfully metamorphose and survive). Each juvenile was photographed multiple times in different focal planes. Average spine length and test diameter were measured for each juvenile with ImageJ (NIH, Cary, NC, United States; **Figure 1**). Two test diameters were measured, approximately perpendicular to each other at the longest diameter of the test, and subsequently averaged. The three longest spines were measured from the outer edge of the test to the tip of the spine and subsequently averaged. The number of juveniles measured per replicate (3 replicates per treatment), ranged from 3 to 11, with an average of 7 juveniles measured per replicate.

Juveniles from the post-settlement growth experiment were prepared for analysis with SEM in order to determine calcification patterns of skeletal elements. Juveniles were placed in a 1% NaClO treatment for 30 min in order to remove organic material. The juveniles were consequently rinsed three times with distilled water and placed in a drying oven at 45°C for 48 h (Wolfe et al., 2013a). The juvenile skeletons lost their structure after the treatment, leaving disarticulated pieces of the spine and skeleton. These pieces were mounted on stubs with conductive double-sided tape and coated with gold using a Quorum gold coater. Observations and photographs were taken using a Hitachi TM3000 tabletop SEM.

Water Chemistry

Target experimental seawater pH was obtained in a 90 L tank for each treatment that was constantly maintained at each target pH level by controlled bubbling of 100% CO_2 gas into the system as required via TUNZE pH/CO_2 controllers (TUNZE AQUARIENTECHNIK GMBH, Penzberg, Germany; Comeau et al., 2018). Seawater pH and temperature were recorded at the beginning and end of every profile during measurements of the DBL in the 3 L aquaria (**Table 2**). Temperature was measured using a mercury thermometer, while pH was measured spectrophotometrically using Cresol purple dye (Dickson et al., 2007). Seawater pH is reported on the total scale in this manuscript, unless specifically mentioned otherwise. Target bulk pH levels were maintained in the settlement experiment by adding new water from the 90 L header tanks at the target pH every 6, 18, 30, and 51 h (**Supplementary Table 1**) and every 24 h in the post-settlement growth experiment (**Supplementary Table 2**). One liter seawater samples for A_T and DIC were fixed with saturated HgCl. Seawater samples for A_T and DIC for each treatment were taken at the beginning of the settlement experiment.

Dissolved inorganic carbon and total alkalinity were later determined by a Single Operator Multi-parameter Metabolic Analyzer (SOMMA) and closed-cell potentiometric titration,

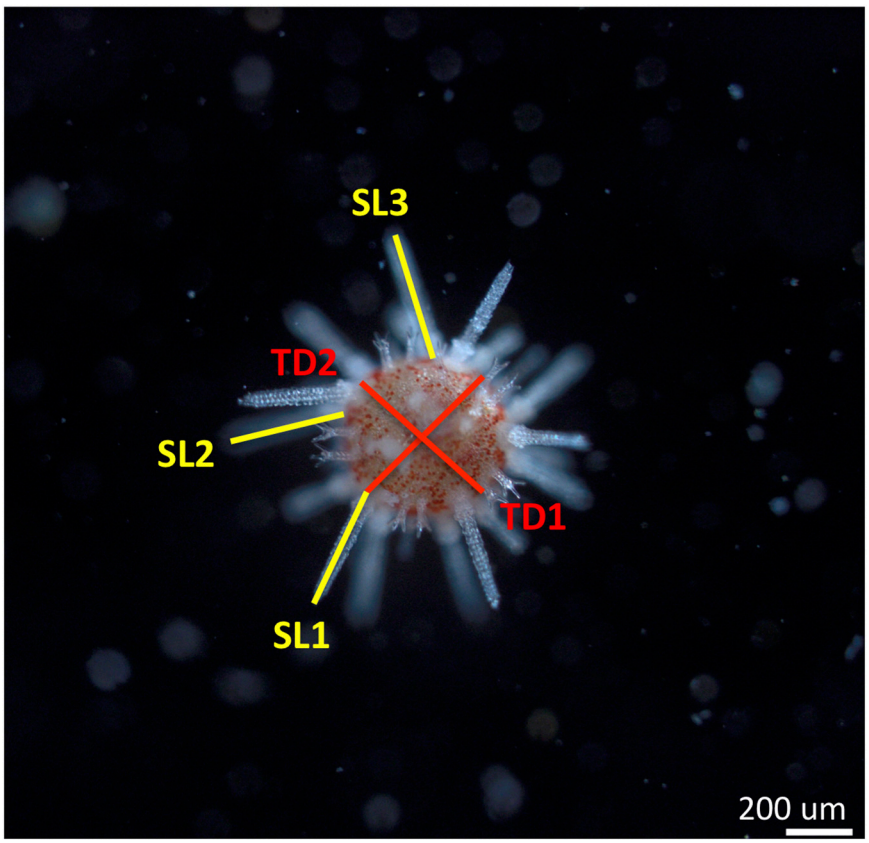

FIGURE 1 | Image taken with a compound microscope of a juvenile sea urchin *Pseudechinus huttoni* 4 days post-settlement. Morphometric measurements are spine length (average of three longest spines or SL) and test diameter (average of two longest diameters or TD). Scale bar 200 μm.

TABLE 1 | Average seawater carbonate chemistry parameters in bulk seawater samples.

	pH_T	A_T (μmol kg^{-1})	DIC (μmol kg^{-1})	Temperature (°C)	Salinity	CO_3^{2-} (μmol kg^{-1})	Ω_{Ar}	Ω_{ca}	pCO_2 (μatm)
pH 8.1	8.09	2290	2090	10.5	34.2	147	2.23	3.51	350
pH 7.7	7.68	2290	2240	10.5	34.2	63.1	0.96	1.51	999
pH 7.5	7.48	2280	2290	10.5	34.2	40.7	0.62	0.97	1620

One water sample was taken per treatment at the beginning of the settlement experiment.

TABLE 2 | Bulk pH values (pH_T) of treatment conditions during oxygen profiling in the 3 L aquaria.

Light Bulk pH 8.1	Dark Bulk pH 8.1	Light Bulk pH 7.7	Dark Bulk pH 7.7	Light Bulk pH 7.4	Dark Bulk pH 7.4
8.10 ± 0.01	8.08 ± 0.01	7.63 ± 0.00	7.72 ± 0.01	7.48 ± 0.01	7.48 ± 0.01

Values represent mean ± 1 SE and n = 8.

respectively (Dickson et al., 2007). CRM batch number 168 was used for this analysis in September and October 2018. During which, the precision of the DIC analyses was 0.72 μmol kg^{-1}. The analyzed DIC values were corrected by a factor CRMcertified/CRManalyzed, determined daily. The analysis accuracy is 0.7 μmol kg^{-1}. Other carbonate system parameters, including the partial pressure of CO_2 (pCO_2) and the saturation states for calcite ($\Omega_{calcite}$) and aragonite ($\Omega_{aragonite}$), were calculated using $SWCO_2$ (Mosley et al., 2010). Seawater properties were determined using CO_2 equilibrium constants from Mehrbach et al. (1973) refitted by Dickson and Millero (1987).

Statistical Analysis

Statistical analyses were performed using RStudio, v1.1.453 (RStudio Team, 2016) unless otherwise mentioned. Data was checked for homogeneity of variance using Levene's tests and checked for normality using QQplots and Shapiro–Wilk Tests.

DBL Measurements

We tested for significant differences in DBL thickness and O_2 concentration at the surface of CCA among treatments using non-parametric Kruskal–Wallis tests (**Table 3**), since assumptions of normality and heteroscedasticity were not met. Kruskal–Wallis tests were supported by results of a Welch's analysis of variance (ANOVA) with unequal variances. *Post hoc* Dunn tests (**Supplementary Table 3**) were used to show pairwise differences in all of the independent treatment conditions in DBL thickness and O_2 concentration at the surface of CCA.

Settlement Data

The settlement data was analyzed by means of fitting a general linear mixed regression model (linear model with binomial distribution: function glmer, family: binomial, R v.2.13) to describe the effect of the pH treatment (bulk seawater pH) and irradiance (light vs. dark) on the percentage settlement of the larvae over time. This model, using a binomial distribution and settlement chambers as random factor, allowed us to include the information of the repeated measures of settlement in the chambers over time. Model selection included all variables initially (bulk seawater pH, irradiance, and time) and was based on selecting the best model based on the Akaike information criterion (AIC) value. Significance and model fit (AIC, residual plots) can be found in **Supplementary Material** (**Supplementary Table 4**).

Post-settlement Data

The post-settlement data was analyzed using a linear mixed model (function: lmer, R v.3.5.2) to describe the effect of the bulk seawater pH treatment (treated as a continuous variable) and irradiance (light vs. dark) on spine length and test diameter of 4-day-old juvenile sea urchins. Replicate containers were used as a random factor in the model (3 replicate containers per treatment). Significance and model (AIC, residual plots) can be found in **Supplementary Material** (**Supplementary Table 5**).

RESULTS

Water Chemistry

Seawater carbonate chemistry was taken at the beginning of the settlement experiment from the 90 L header tanks (**Table 1**, and for additional experiments reported in **Supplementary Table 6**). During the course of the settlement and post-settlement experiments, pH stayed relatively stable (±0.1 units) between water changes (**Supplementary Tables 1, 2**). While completing DBL measurements in the 3 L aquaria, bulk seawater pH also remained similar between oxygen profiles, with clear differences among the three bulk pH treatments and no effect of light on bulk pH (**Table 2**).

DBL Measurements

DBL Measurements in Static Conditions

The chemical environment immediately above the coralline algal surface differed from that of the bulk seawater. At all levels of bulk seawater pH, pH increased in the light treatment above CCA and decreased in the dark treatment (**Figure 2** and **Supplementary Figure 2**), with irradiance having a significant effect on substrate surface oxygen concentration (Chi Square = 17.28, $p < 0.001$, df = 1, and **Table 3**). In the light, estimated pH deviated by up to ∼0.8 units from bulk pH (**Figure 2**), with the pH at the surface of the CCA in bulk seawater pH 7.5 being estimated as above that of today's average seawater pH levels of 8.1 (**Figure 2**). In the dark, oxygen concentration at the surface of CCA had much smaller deviations, with pH varying less than 0.1 units below median values in all bulk seawater conditions (**Figure 2**). In the dark, pH values at the surface of CCA were similar to those of the bulk seawater pH and bulk seawater pH had no significant effect on oxygen concentration at the surface of CCA (Chi Square = 0.215, p-value > 0.1, df = 2, and **Table 3**).

The release of CO_2 due to the respiration of CCA, was evidently too low to generate a measurable DBL in the dark treatments. DBLs were significantly different (thicker) in the

TABLE 3 | Non-parametric Kruskal–Wallis examining the effects of treatments, bulk pH, flow, and irradiance on DBL thickness and O_2 Concentration at surface of CCA in 3 L aquaria and the annular flume.

	Experiment	Factor	Df	Chi-squared	*p*-value
DBL thickness	3 L Aquaria	Bulk pH	2	0.009998	0.995
		Irradiance	1	19.74	**<0.001**
		Treatment	5	19.76	**0.001**
DBL thickness	Annular Flume	Bulk pH	1	0.5375	0.464
		Irradiance	1	10.62	**0.001**
		Flow	1	7.670	**0.006**
		Treatment	7	26.04	**<0.001**
O_2concentration at surface of CCA	3 L Aquaria	Bulk pH	2	0.215	0.898
		Irradiance	1	17.28	**<0.001**
		Treatment	5	18.35	**0.003**
O_2concentration at surface of CCA	Annular Flume	Bulk pH	1	0.2784	0.598
		Irradiance	1	21.14	**<0.001**
		Flow	1	0.2401	0.624
		Treatment	7	26.32	**<0.001**

p values less than 0.05 are in bold.

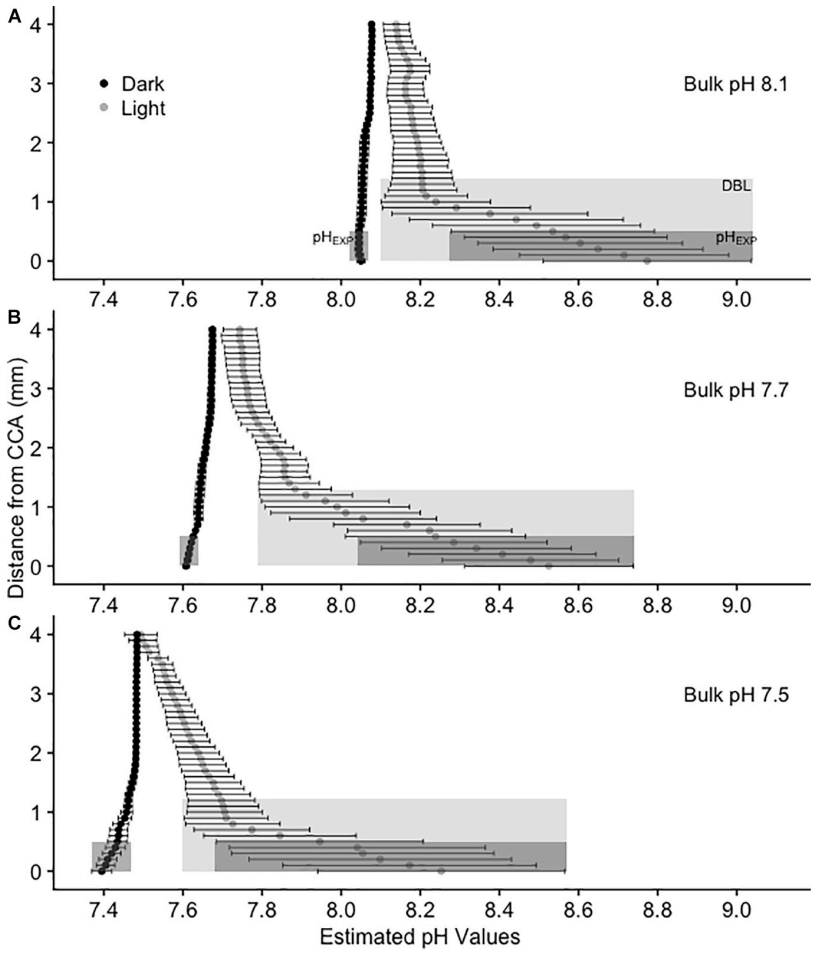

FIGURE 2 | Calculated average $pH_{(T)}$ values above CCA in 3 L experimental aquaria at three bulk pH levels: **(A)** 8.1, **(B)** 7.7, and **(C)** 7.5. Values are mean pH ± SE, n = 4. pH values were estimated using oxygen as a proxy. Black circles represent dark treatments and gray circles represent light treatments. The light gray shaded rectangle represents the diffusion boundary layer and the dark gray shaded rectangle represents the pH from 0 to 0.5 mm above the CCA surface (pH_{EXP}), or the average pH that metamorphosing and newly settled *P. huttoni* on CCA substrates experience.

light than in the dark (Chi Square = 19.74, $p < 0.001$, df = 1, and **Table 3**). In the light, mean (±SE) DBL thickness was 1.4 mm ± 0.53 at bulk pH 8.1, 1.3 mm ± 0.40 at bulk pH 7.7 and 1.2 mm ± 0.4 at bulk pH 7.5 but these differences were not significant (Chi Square = 0.01, $p > 0.1$, df = 2, and **Table 3**).

In the dark treatments, *P. huttoni* likely experienced pH levels similar to the bulk seawater (pH_{EXP} was reduced by less than 0.1 units below mainstream values), whereas in the light, *P. huttoni* experienced pH levels substantially higher (pH_{EXP} increased by 0.5 to 0.7 units above mainstream values). Values are reported in **Supplementary Table 7**. Due to the DBL, the pH_{EXP} that *P. huttoni* experienced in light treatments with bulk seawater pH 7.5, was estimated to be 8.05, comparable to contemporary seawater pH levels of 8.1.

DBL Measurements in Flow

Oxygen profiles were also completed above CCA covered acrylic disks in an annular flume to characterize oxygen and pH conditions above CCA under quantifiable flow speeds (Methods, **Supplementary Material**). This allowed us to compare the DBL under more ecologically relevant flow speeds to the static flow conditions used in this experiment that enabled us to settle and grow *P. huttoni* juveniles. The DBL profiles and DBL thicknesses in static flow in the 3 L experimental aquaria displayed similar trends to those at slow flow speeds of 1 cm s^{-1} in the annular flume (**Supplementary Figures 3, 4**). In the light, pH varied up to ∼0.8 units above the bulk seawater pH in static (no) flow, and up to ∼0.6 units above the bulk seawater pH in slow (1 cm s^{-1}) flow. In the dark, pH varied by <0.1 units under both static and slow flow. As under static flow, irradiance had a significant effect on substrate surface oxygen concentration in slow flow ($p < 0.001$, df = 1, and **Table 3**), while bulk seawater pH did not ($p > 0.1$, df = 1, and **Table 3**). In the light under slow flow, mean (±SE) DBL thickness was 0.78 mm ± 0.28 in the pH 8.1 treatment and 0.50 mm ± 0.14 in the pH 7.4 treatment. In the dark under slow flow, mean (±SE) DBL thickness was 0.1 mm ± 0.04 in the pH 8.1 treatment and 0.08 mm ± 0.03 in the pH 7.4 treatment. The static flow

conditions used in these sea urchin experiments are similar to slow flow speeds (1 to 2 cm s^{-1}, **Supplementary Figure 5**) found *in situ* in the fiord environment where the *P. huttoni* used in this study were collected.

Increased speeds of flow altered the shape of oxygen (and accordingly the pH) profiles and DBL thickness. Oxygen profiles at fast flow speeds of 5.5 cm s^{-1} displayed a thinner DBL and a smaller range of O_2 and pH values (**Supplementary Figures 3, 4**). At 5.5 cm s^{-1}, mean pH values varied by only up to ∼0.2 units in the light. Additionally, flow had a significant effect on DBL thickness ($p = 0.006$, df = 1, and **Table 3**). In the light, mean (±SE) DBL thickness under slow flow was 0.78 mm ± 0.28 in the pH 8.1 treatment and 0.50 mm ± 0.14 in the pH 7.4 treatment compared to 0.05 mm ± 0.05 and 0.10 ± 0.00 in fast flow, respectively.

Settlement

After 6 h, 14% to 33% of larvae had settled on the CCA. Cumulatively, percentage settlement on CCA increased with time for all treatments, reaching a final settlement of 58% to 77% after 51 h (**Figure 3** and **Supplementary Table 7**). Bulk seawater pH showed no significant effect on its own, but light conditions and their interaction with the bulk seawater pH of the water were significant factors influencing settlement success in *P. huttoni* over the course of the experiment (**Supplementary Table 4**). After the initial 6 h, percentage settlement was significantly lower in bulk pH 8.1:dark conditions (pH_{EXP} 8.01) compared to the other treatments (14%). After 18 h, percentage settlement in bulk pH 7.7:light conditions (pH_{EXP} 8.38) did not increase as greatly compared to the other treatments (37%). However, toward the end of the experiment (after 30 and 51 h), only the settlement in bulk pH 8.1:light conditions (pH_{EXP} 8.64) was significantly greater than in the remaining treatments (68% and 77%, respectively). The pH that the sea urchins likely experienced while settling on CCA substrate (pH_{EXP}) showed no consistent or strong effect on settlement success.

Post-settlement Growth

Test diameter was similar across all treatments, with no significant effect of bulk seawater pH or irradiance (**Figure 4**, $p = 0.290$ and $p = 0.755$, **Supplementary Table 5**). Spine length displayed greater variance across all treatments, but also showed no significant effect of bulk seawater pH on its own ($p = 0.090$, **Supplementary Table 5**). However, the results of the linear mixed modeling indicated that irradiance and the interaction of pH and irradiance had a significant effect on spine length of 4-day-old juveniles ($p = 0.039$ and $p = 0.035$, respectively, **Supplementary Table 5**). In the dark, mean spine length increased with increasing bulk seawater pH, while in the light, mean spine length decreased with increasing bulk seawater pH. The shortest mean spine length was found in the treatment with the highest pH_{EXP}, bulk pH 8.1:light. The pH that juvenile sea urchins likely experienced while settling on CCA substrate (pH_{EXP}) showed no consistent or strong effect on test diameter or spine length.

Additionally, SEM revealed no observable differences in structural integrity or morphology of the sea urchin spines in any of the treatments (and thus at any levels of pH_{EXP}; **Figure 5**, **Supplementary Figure 6**). This suggests, visually, that calcification was not impaired, nor was there any indication of degradation of calcified surfaces. Juvenile skeletal element morphology appeared similar in all treatments, showing no loss of structural integrity, while bearing smooth surfaces and no evidence of pitting or erosion on the primary and secondary spines. Evidence of fine calcification (i.e., secondary spination) was present along the edges of the juvenile spine. Additionally, stereom lattice structure was well developed in the spines and test.

DISCUSSION

Marine invertebrates that settle and live on algal surfaces experience pH levels that differ from the bulk seawater pH due to biologically driven changes within the DBL associated with irradiance and water flow. Our observations align with previous investigations showing that macroalgae modify the chemical environment immediately above their surface in the DBL (De Beer and Larkum, 2001; Hurd et al., 2011; Cornwall et al., 2013b; Hurd, 2015; Noisette and Hurd, 2018; Wahl et al., 2018; Comeau et al., 2019; Layton et al., 2019). In this respect, we focused on how the DBL could influence settlement success and early post-settlement growth in the sea urchin *P. huttoni* under contemporary and future OA conditions. It was hypothesized that reduced bulk seawater pH would negatively affect settlement success and post-settlement growth of sea urchins, but that thick macroalgal DBLs in the daytime (light), where pH is raised, would protect against these effects. If this occurred, we would observe higher settlement success under thick DBLs in the light, compared to the dark in our OA treatments. However, the observed settlement success and growth of newly settled sea urchins was relatively similar across all treatments, suggesting that *P. huttoni* juveniles are able to grow in a range of pH levels, even when pH is reduced in the DBL.

Settlement rates showed high variability among treatments, but settlement success was not significantly reduced at low pH levels in the DBL. Juveniles in our study were examined only 4 day post-settlement, so it is possible that the growth period was too short to reveal potential greater differences in skeletal morphology. Preliminary experiments yielded similar results of no differences among treatments, and our observations are also consistent with previous studies on sea urchins, where no direct effects of OA on larval settlement have been reported (Dupont et al., 2013; Wangensteen et al., 2013; Espinel-Velasco et al., 2020). The few significant differences on settlement in this study were primarily observed in the bulk pH 8.1 treatments, suggesting that high pH can reduce settlement success, as seen in Mos et al. (2020). While not tested, other environmental factors, that covaried with pH in our experiment, such as light, may also have significant effects on sea urchin settlement success (Rodriguez et al., 1993; Scheibling and Robinson, 2008). Additionally, *in situ* juveniles may also be able to undergo post-settlement transport or movement to improve the environmental conditions under which they first settled (Pilditch et al., 2015).

Early post-settlement growth also showed high variability among treatments, however, *P. huttoni* juveniles successfully grew in a range of pH levels within the DBL (pH 7.4 to 9.0).

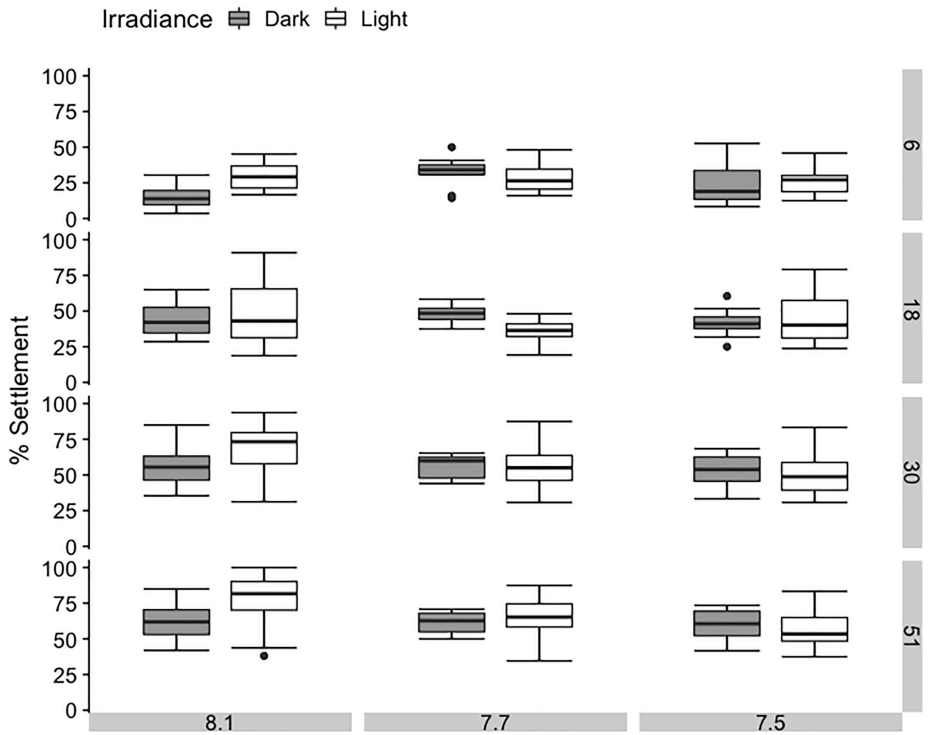

FIGURE 3 | Average percentage settlement of sea urchins *Pseudechinus huttoni* during a 51-h period under three bulk seawater pH and two irradiance treatments. Each treatment (3 L aquaria) contained four inverted chambers and was replicated three times. Error bars are ±1 SE of the mean.

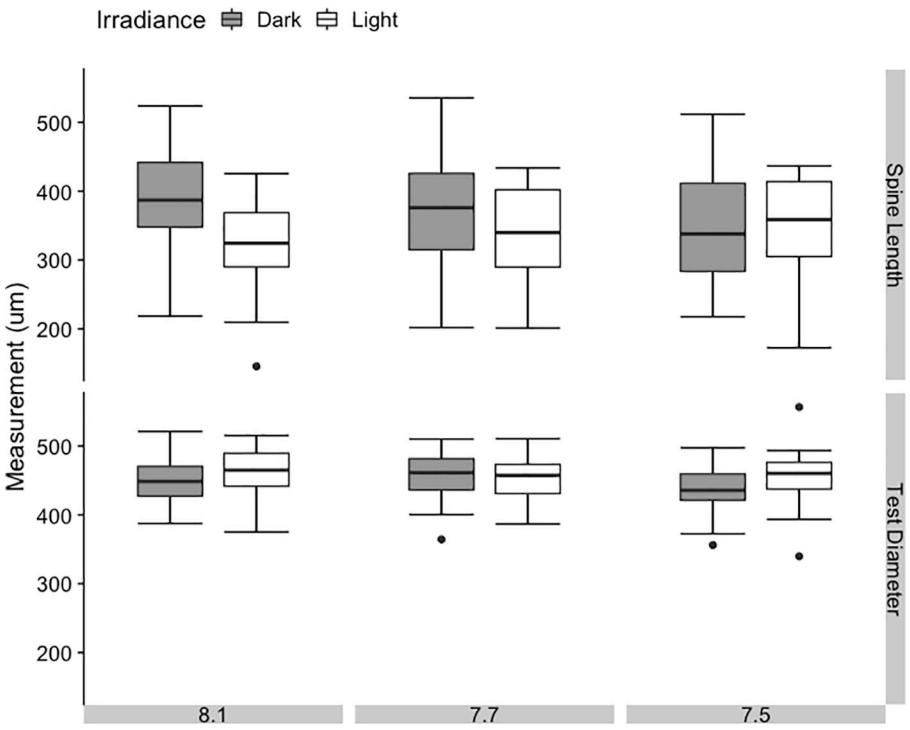

FIGURE 4 | Average spine length and test diameter in juvenile sea urchins *Pseudechinus huttoni* at 4 days post-settlement under three bulk seawater pH and two irradiance treatments. Each treatment (3 L aquaria) was replicated three times. Error bars are ±1 SE of the mean.

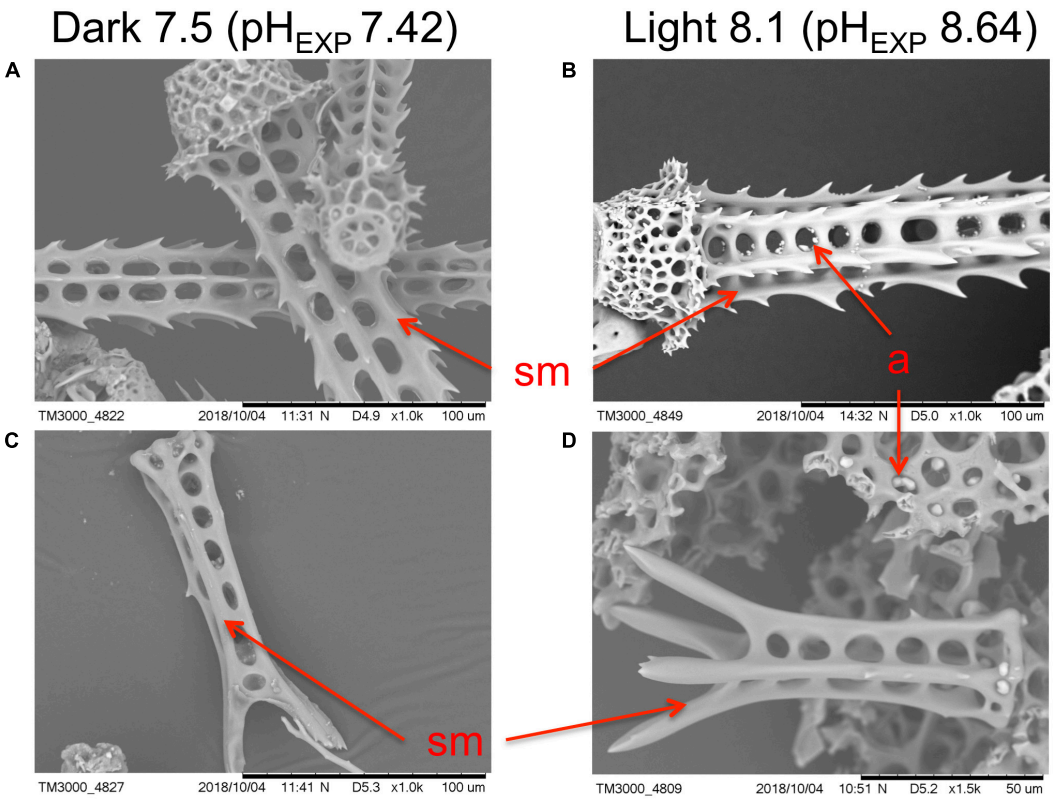

FIGURE 5 | Examples of scanning electron micrographs of *Pseudechinus huttoni* juveniles reared in the dark at bulk seawater pH 7.5 (pH$_{EXP}$ 7.42) and in the light at bulk seawater pH 8.1 (pH$_{EXP}$ 8.64), for 4 days post-settlement. Scale bars are **(A–C)** 100 μm and **(D)** 50 μm, as indicated on SEM micrographs. Micrographs depict **(A,B)** base and attachment site of adult spines, and **(C,D)** juvenile spines. *sm* smooth surface. *a* artifact (a product of sample preparation for the SEM).

Thus, low pH levels in the DBL do not appear to impair growth. Our observations are consistent with those of previous studies on sea urchins, which have found that test diameter is robust to low pH, although spine length can be altered under extremely low pH values (7.4; Wolfe et al., 2013a). Our SEM observations revealed no apparent differences in structural details of the juvenile *P. huttoni* skeletons in any of the treatments. SEM micrographs have highlighted some of the greatest differences in calcification and supported other growth measurements in other sea urchin species, such as quantitative reductions in weight (Albright et al., 2012). Thus, our visual observations qualitatively suggest that growth was not substantially reduced at lower pH levels in the DBL.

This is one of the first studies to measure sea urchin settlement and early post-settlement development under DBLs of measured thicknesses. Previous work on the sea urchin *Centrostephanus rodgersii* accounting for the DBL, found that both low pH and high pH conditions have effects on settlement and post-settlement growth (Mos et al., 2020). Additionally, chemical buffering of reduced seawater pH has been found in the boundary layers above concrete surfaces (Mos et al., 2019). Our study examines a similar effect above macroalgal surfaces. Our results suggest that juvenile sea urchins may, to a certain extent, already be adapted to lower pH, with effects of low pH potentially only seen at extreme levels in the bulk seawater (pH$_T$ 7.4 and below; Byrne et al., 2009, 2017; Dupont et al., 2010; Byrne, 2011; Wolfe et al., 2013a; Espinel-Velasco et al., 2018). This has previously been seen in other marine taxa; for example, some oyster species have the potential to acclimatize to OA over multiple generations, where carryover effects mediate impacts of reduced seawater pH on later generations (Parker et al., 2011, 2015). Similarly, newly-settled sea urchins may be more tolerant to pH variability over temporal scales of hours/days because previous generations have already experienced significant natural pH variability, as has been suggested for other taxa in such environments (Melzner et al., 2009; Hurd et al., 2011; Wahl et al., 2015, 2018; Boyd et al., 2016; Noisette and Hurd, 2018). Indeed, organisms experiencing greater environmental variability are thought to possess higher phenotypic plasticity, and generally have greater resistance to mean changes in the environment due to global change (Boyd et al., 2016). Fluctuations in seawater carbonate chemistry *in situ* may mean that many taxa are already acclimatized or adapted to calcify in these extreme pH levels (Wolfe et al., 2013a; Eriander et al., 2015). Presently, there are no published *in situ* measurements of pH within the DBL of nearshore marine organisms, and the role of the DBL pH variability has largely gone underappreciated.

In addition to environmental history, fluctuations in pH during exposure to stressors will also likely modify responses to OA conditions (Rivest et al., 2017). Fluctuating environments may ameliorate negative effects of OA because either mean pH is higher (i.e., reductions at night being less than the increases during the day) or the fluctuations may yield periods of favorable pH conditions for organisms where they are able, for example, to calcify (Melzner et al., 2009; Cornwall et al., 2014; Wahl et al., 2015, 2018; Noisette and Hurd, 2018). Previous research has found that fluctuating pH treatments can elicit different effects on organisms than stable acidified conditions. For example, diurnal pH fluctuations increased the variance in growth of the barnacle *Balanus improvisus*, but not its mean growth (Eriander et al., 2015). The timing of exposure to different pH levels impacted larval development of the mussel *Mytilus galloprovincialis*, while larval shell growth was correlated with mean exposure regardless of variability (Kapsenberg et al., 2018). This may be another explanation for the lack of detectable results on effects of pH in the DBL on settlement and post-settlement growth in this study; our irradiance treatments were constant rather than on a diel cycle. Further research is needed to understand how natural small-scale temporal pH fluctuations will interact with bulk seawater pH decreases due to OA.

While juvenile sea urchins appeared robust to reduced pH in this study, it is also possible that a physiological limit may be surpassed when natural fluctuations are superimposed onto mean predictions of global change (Boyd et al., 2016), particularly in kelp beds with large diurnal pH changes (Cornwall et al., 2013a). Calcifying organisms living in these fluctuating environments already likely experience a degree of stress, and the combined effects of environmental fluctuations and global change related stressors (e.g., reduced seawater pH due to OA) may expose organisms to conditions beyond their thresholds of tolerance (Hofmann et al., 2011; Boyd et al., 2016). Effects of reduced pH may only become discernible at very extreme pH values below those used in this experiment (bulk seawater pH 7.5). Indeed, negative effects on skeleton growth (test diameter, spine number, and stereom pore size) and spine growth of juvenile *H. erythrogramma* were largely restricted to the lowest pH treatments used (pH 7.4 and below; Wolfe et al., 2013a,b).

The effects of OA on sea urchins are almost certainly life history specific, with effects on juveniles being variable and in some cases undetectable (Byrne et al., 2009, 2010b, 2017; Dupont et al., 2010; Byrne, 2011; Dupont and Thorndyke, 2013; Wolfe et al., 2013a; Chan et al., 2015; Espinel-Velasco et al., 2018). The negative effects of reduced seawater pH previously seen in larval *P. huttoni* (Clark et al., 2009) are not reflected in the responses of juveniles in this study. However, the larval urchins used in this study were reared in present-day conditions. Carry-over effects from the larval stage, such as energy reserves, may have allowed juveniles to grow successfully in varying pH conditions. There is a possibility for negative carryover effects from the juvenile stage to later life stages or future generations that this study did not explore (Karelitz et al., 2019). Thus, the larval rather than the juvenile stage may be a potential life-history bottleneck under OA conditions, as previously suggested (Byrne et al., 2013; Lamare et al., 2016). Life in the DBL may have pre-adapted juvenile *P. huttoni* to living and calcifying in a range of pH levels, thus conferring potential resilience to OA conditions at this life-history stage.

DATA AVAILABILITY STATEMENT

The raw data supporting the conclusions of this article will be made available by the authors, without undue reservation.

AUTHOR CONTRIBUTIONS

EH and ML conceived and designed the research, with input from NE-V for the settlement assay and CC for the boundary layer measurements. EH and NE-V carried out the experimentation. CP provided experimental resources for the boundary layer measurements in the annular flume. EH and NE-V analyzed the data. EH drafted the manuscript, with editorial input from all co-authors. All authors contributed to the article and approved the submitted version.

FUNDING

EH received funding from a Fulbright US Graduate Award. ML contributions were supported by CARIM (Coastal Acidification: Rate, Impacts and Management), funded by the New Zealand Ministry of Business, Innovation and Employment. CC was supported by a Rutherford Discovery Fellowship by the Royal Society of New Zealand Te Apârangi (RDF-VUW1701).

ACKNOWLEDGMENTS

Thanks to Dr. Kim Currie and Judith Murdoch at the National Institute of Water and Atmospheric Research (NIWA), New Zealand, for the dissolved inorganic carbon and total alkalinity measurements. Thank you to Anna Kluibenschedl at the University of Otago, New Zealand for the use of the CCA disks.

SUPPLEMENTARY MATERIAL

The Supplementary Material for this article can be found online at: https://www.frontiersin.org/articles/10.3389/fmars.2020.577562/full#supplementary-material

REFERENCES

Albright, R., Bland, C., Gillette, P., Serafy, J. E., Langdon, C., and Capo, T. R. (2012). Juvenile growth of the tropical sea urchin *Lytechinus variegatus* exposed to near-future ocean acidification scenarios. *J. Exp. Mar. Biol. Ecol.* 426–427, 12–17. doi: 10.1016/j.jembe.2012.05.017

Boyd, P. W., Cornwall, C. E., Davison, A., Doney, S. C., Fourquez, M., Hurd, C. L., et al. (2016). Biological responses to environmental heterogeneity under future ocean conditions. *Glob. Change Biol.* 22, 2633–2650. doi: 10.1111/gcb.13287

Byrne, M. (2011). "Impact of ocean warming and ocean acidification on marine invertebrate life history stages: vulnerabilities and potential for persistence in a changing ocean," in *Oceanography and Marine Biology: An Annual Review*, eds R. N. Gibson, R. Atkinson, J. Gordon, I. Smith, and D. Hughes (Boca Raton, FL: CRC Press), 1–42. doi: 10.1155/2011/473615

Byrne, M., Ho, M., Selvakumaraswamy, P., Nguyen, H. D., Dworjanyn, S. A., and Davis, A. R. (2009). Temperature, but not pH, compromises sea urchin fertilization and early development under near-future climate change scenarios. *Proc. R. Soc. B Biol. Sci.* 276, 1883–1888. doi: 10.1098/rspb.2008.1935

Byrne, M., Ho, M., Wong, E., Soars, N. A., Selvakumaraswamy, P., Shepard-Brennand, H., et al. (2010a). Unshelled abalone and corrupted urchins: development of marine calcifiers in a changing ocean. *Proc. R. Soc. B Biol. Sci.* 278, 2376–2383. doi: 10.1098/rspb.2010.2404

Byrne, M., Soars, N., Selvakumaraswamy, P., Dworjanyn, S. A., and Davis, A. R. (2010b). Sea urchin fertilization in a warm, acidified and high pCO2 ocean across a range of sperm densities. *Mar. Environ. Res.* 69, 234–239. doi: 10.1016/j.marenvres.2009.10.014

Byrne, M., Ho, M. A., Koleits, L., Price, C., King, C. K., Virtue, P., et al. (2013). Vulnerability of the calcifying larval stage of the Antarctic sea urchin *Sterechinus neumayeri* to near-future ocean acidification and warming. *Glob. Change Biol.* 19, 2264–2275. doi: 10.1111/gcb.12190

Byrne, M., Ross, P. M., Dworjanyn, S. A., and Parker, L. (2017). "Larval ecology in the face of changing climate–impacts of ocean warming and ocean acidification," in *Evolutionary Ecology of Marine Invertebrate Larvae*, eds T. Carrier, A. Reitzel, and A. Heyland (Oxford: Oxford University Press), 251–272.

Caldeira, K., and Wickett, M. E. (2003). Anthropogenic carbon and ocean pH. *Nature* 425:365. doi: 10.1038/425365a

Chan, K. Y. K., García, E., and Dupont, S. (2015). Acidification reduced growth rate but not swimming speed of larval sea urchins. *Sci. Rep.* 5:9764. doi: 10.1038/srep09764

Chan, N. C. S., Wangpraseurt, D., Kühl, M., and Connolly, S. R. (2016). Flow and coral morphology control coral surface pH: implications for the effects of ocean acidification. *Front. Mar. Sci.* 3:10. doi: 10.3389/fmars.2016.00010

Clark, D., Lamare, M., and Barker, M. (2009). Response of sea urchin pluteus larvae (Echinodermata: Echinoidea) to reduced seawater pH: a comparison among a tropical, temperate, and a polar species. *Mar. Biol.* 156, 1125–1137. doi: 10.1007/s00227-009-1155-8

Comeau, S., Cornwall, C., Pupier, C., DeCarlo, T., Alessi, C., Trehern, R., et al. (2019). Flow-driven micro-scale pH variability affects the physiology of corals and coralline algae under ocean acidification. *Sci. Rep.* 9:12829.

Comeau, S., Cornwall, C. E., DeCarlo, T. M., Krieger, E., and McCulloch, M. T. (2018). Similar controls on calcification under ocean acidification across unrelated coral reef taxa. *Glob. Change Biol.* 24, 4857–4868. doi: 10.1111/gcb.14379

Cornwall, C. E. (2013). *Macroalgae as Ecosystem Engineers and the Implications for Ocean Acidification*. Ph.D. thesis, University of Otago, Dunedin.

Cornwall, C. E., Boyd, P. W., McGraw, C. M., Hepburn, C. D., Pilditch, C. A., Morris, J. N., et al. (2014). Diffusion boundary layers ameliorate the negative effects of ocean acidification on the temperate coralline macroalga *Arthrocardia corymbosa*. *PLoS One* 9:e97235. doi: 10.1371/journal.pone.0097235

Cornwall, C. E., Hepburn, C. D., McGraw, C. M., Currie, K. I., Pilditch, C. A., Hunter, K. A., et al. (2013a). Diurnal fluctuations in seawater pH influence the response of a calcifying macroalga to ocean acidification. *Proc. R. Soc. B Biol. Sci.* 280:20132201. doi: 10.1098/rspb.2013.2201

Cornwall, C. E., Hepburn, C. D., Pilditch, C. A., and Hurd, C. L. (2013b). Concentration boundary layers around complex assemblages of macroalgae: implications for the effects of ocean acidification on understory coralline algae. *Limnol. Oceanogr.* 58, 121–130. doi: 10.4319/lo.2013.58.1.0121

Cornwall, C. E., Pilditch, C. A., Hepburn, C. D., and Hurd, C. L. (2015). Canopy macroalgae influence understorey corallines' metabolic control of near-surface pH and oxygen concentration. *Mar. Ecol. Prog. Ser.* 525, 81–95. doi: 10.3354/meps11190

De Beer, D., and Larkum, A. (2001). Photosynthesis and calcification in the calcifying algae *Halimeda discoidea* studied with microsensors. *Plant Cell Environ.* 24, 1209–1217. doi: 10.1046/j.1365-3040.2001.00772.x

Denny, M. W., and Wethey, D. S. (2000). "Physical processes that generate patterns in marine communities," in *Marine Community Ecology*, eds M. Bertness, M. Hay, and S. Gaines (Sunderland, MA: Sinauer Associates), 3–37.

Dickson, A., and Millero, F. (1987). A comparison of the equilibrium constants for the dissociation of carbonic acid in seawater media. *Deep Sea Res. A Oceanogr. Res. Pap.* 34, 1733–1743. doi: 10.1016/0198-0149(87)90021-5

Dickson, A. G., Sabine, C. L., and Christian, J. R. (2007). *Guide to Best Practices for Ocean CO2 Measurements*. Sidney: North Pacific Marine Science Organization.

Dupont, S., Dorey, N., Stumpp, M., Melzner, F., and Thorndyke, M. (2013). Long-term and trans-life-cycle effects of exposure to ocean acidification in the green sea urchin *Strongylocentrotus droebachiensis*. *Mar. Biol.* 160, 1835–1843. doi: 10.1007/s00227-012-1921-x

Dupont, S., Ortega-Martínez, O., and Thorndyke, M. (2010). Impact of near-future ocean acidification on echinoderms. *Ecotoxicology* 19, 449–462. doi: 10.1007/s10646-010-0463-6

Dupont, S., and Thorndyke, M. (2013). "Direct impacts of near-future ocean acidification on sea urchins," in *Climate Change Perspective from the Atlantic: Past, Present and Future*, eds J. M. Fernández-Palacios, L. de Nascimento, J. C. Hernández, S. Clemente, A. González, and J. P. Díaz-González (La Laguna: Universidad de La Laguna), 461–485.

Eriander, L., Wrange, A.-L., and Havenhand, J. (2015). Simulated diurnal pH fluctuations radically increase variance in—but not the mean of—growth in the barnacle *Balanus improvisus*. *ICES J. Mar. Sci.* 73, 596–603. doi: 10.1093/icesjms/fsv214

Espinel-Velasco, N., Agüera, A., and Lamare, M. (2020). Sea urchin larvae show resilience to ocean acidification at the time of settlement and metamorphosis. *Mar. Environ. Res.* 159:104977. doi: 10.1016/j.marenvres.2020.104977

Espinel-Velasco, N., Hoffmann, L., Agüera, A., Byrne, M., Dupont, S., Uthicke, S., et al. (2018). Effects of ocean acidification on the settlement and metamorphosis of marine invertebrate and fish larvae: a review. *Mar. Ecol. Prog. Ser.* 606, 237–257. doi: 10.3354/meps12754

Foster, T., and Gilmour, J. (2016). Seeing red: coral larvae are attracted to healthy-looking reefs. *Mar. Ecol. Prog. Ser.* 559, 65–71. doi: 10.3354/meps11902

García, E., Hernández, J. C., Clemente, S., Cohen-Rengifo, M., Hernández, C. A., and Dupont, S. (2015). Robustness of *Paracentrotus lividus* larval and post-larval development to pH levels projected for the turn of the century. *Mar. Biol.* 162, 2047–2055. doi: 10.1007/s00227-015-2731-8

Gosselin, P., and Jangoux, M. (1998). From competent larva to exotrophic juvenile: a morphofunctional study of the perimetamorphic period of *Paracentrotus lividus* (Echinodermata, Echinoida). *Zoomorphology* 118, 31–43. doi: 10.1007/s004350050054

Gosselin, L. A., and Qian, P. Y. (1997). Juvenile mortality in benthic marine invertebrates. *Mar. Ecol. Prog. Ser.* 146, 265–282. doi: 10.3354/meps146265

Hendriks, I. E., Duarte, C. M., and Álvarez, M. (2010). Vulnerability of marine biodiversity to ocean acidification: a meta-analysis. *Estuar. Coast. Shelf Sci.* 86, 157–164. doi: 10.1016/j.ecss.2009.11.022

Hofmann, G. E., Smith, J. E., Johnson, K. S., Send, U., Levin, L. A., Micheli, F., et al. (2011). High-frequency dynamics of ocean pH: a multi-ecosystem comparison. *PLoS One* 6:e28983. doi: 10.1371/journal.pone.0028983

Hurd, C. L. (2015). Slow-flow habitats as refugia for coastal calcifiers from ocean acidification. *J. Phycol.* 51, 599–605. doi: 10.1111/jpy.12307

Hurd, C. L., Cornwall, C. E., Currie, K., Hepburn, C. D., McGraw, C. M., Hunter, K. A., et al. (2011). Metabolically induced pH fluctuations by some coastal calcifiers exceed projected 22nd century ocean acidification: a mechanism for differential susceptibility? *Glob. Change Biol.* 17, 3254–3262. doi: 10.1111/j.1365-2486.2011.02473.x

Kapsenberg, L., Miglioli, A., Bitter, M. C., Tambutté, E., Dumollard, R., and Gattuso, J.-P. (2018). Ocean pH fluctuations affect mussel larvae at key developmental transitions. *Proc. R. Soc. B Biol. Sci.* 285:20182381. doi: 10.1098/rspb.2018.2381

Karelitz, S., Lamare, M. D., Mos, B., De Bari, H., Dworjanyn, S. A., and Byrne, M. (2019). Impact of growing up in a warmer, lower pH future on offspring performance: transgenerational plasticity in a pan-tropical sea urchin. *Coral Reefs* 38, 1085–1095. doi: 10.1007/s00338-019-01855-z

Kirby, S., Lamare, M. D., and Barker, M. F. (2006). Growth and morphometrics in the New Zealand sea urchin *Pseudechinus huttoni* (Echinoidea: Temnopleuridae). *N. Z. J. Mar. Freshwater Res.* 40, 413–428. doi: 10.1080/00288330.2006.9517432

Koehl, M. A. R., and Hadfield, M. G. (2010). Hydrodynamics of larval settlement from a larva's point of view. *Integr. Comp. Biol.* 50, 539–551. doi: 10.1093/icb/icq101

Kroeker, K. J., Kordas, R. L., Crim, R., Hendriks, I. E., Ramajo, L., Singh, G. S., et al. (2013). Impacts of ocean acidification on marine organisms: quantifying sensitivities and interaction with warming. *Glob. Change Biol.* 19, 1884–1896. doi: 10.1111/gcb.12179

Lamare, M., and Barker, M. (2001). Settlement and recruitment of the New Zealand sea urchin *Evechinus chloroticus*. *Mar. Ecol. Prog. Ser.* 218, 153–166. doi: 10.3354/meps218153

Lamare, M. D., Liddy, M., and Uthicke, S. (2016). *In situ* developmental responses of tropical sea urchin larvae to ocean acidification conditions at naturally elevated *pCO2* vent sites. *Proc. R. Soc. B Biol. Sci.* 283:20161506. doi: 10.1098/rspb.2016.1506

Layton, C., Cameron, M. J., Shelamoff, V., Fernández, P. A., Britton, D., Hurd, C. L., et al. (2019). Chemical microenvironments within macroalgal assemblages: implications for the inhibition of kelp recruitment by turf algae. *Limnol. Oceanogr.* 64, 1600–1613. doi: 10.1002/lno.11138

Lichtenberg, M., Nørregaard, R. D., and Kühl, M. (2017). Diffusion or advection? Mass transfer and complex boundary layer landscapes of the brown alga *Fucus vesiculosus*. *J. R. Soc. Interface* 14:20161015. doi: 10.1098/rsif.2016.1015

McClary, D. J., and Sewell, M. A. (2003). Hybridization in the sea: gametic and developmental constraints on fertilization in sympatric species of *Pseudechinus* (Echinodermata: Echinoidea). *J. Exp. Mar. Biol. Ecol.* 284, 51–70. doi: 10.1016/s0022-0981(02)00487-2

McCoy, S. J., and Kamenos, N. A. (2015). Coralline algae (*Rhodophyta*) in a changing world: integrating ecological, physiological, and geochemical responses to global change. *J. Phycol.* 51, 6–24. doi: 10.1111/jpy.12262

Mehrbach, C., Culberson, C. H., Hawley, J. E., and Pytkowicz, R. M. (1973). *Constants of Carbonic Acid in Seawater at Atmospheric Pressure*. Corvallis, OR: Oregon State University.

Melzner, F., Gutowska, M., Langenbuch, M., Dupont, S., Lucassen, M., Thorndyke, M., et al. (2009). Physiological basis for high CO2 tolerance in marine ectothermic animals: pre-adaptation through lifestyle and ontogeny? *Biogeosciences* 6, 2313–2331. doi: 10.5194/bg-6-2313-2009

Mos, B., Byrne, M., and Dworjanyn, S. A. (2020). Effects of low and high pH on settlement and post-settlement growth of a sea urchin in culture. *Aquaculture* 528:735618. doi: 10.1016/j.aquaculture.2020.735618

Mos, B., Dworjanyn, S. A., Mamo, L. T., and Kelaher, B. P. (2019). Building global change resilience: concrete has the potential to ameliorate the negative effects of climate-driven ocean change on a newly-settled calcifying invertebrate. *Sci. Total Environ.* 646, 1349–1358. doi: 10.1016/j.scitotenv.2018.07.379

Mosley, L., Peake, B., and Hunter, K. (2010). Modelling of pH and inorganic carbon speciation in estuaries using the composition of the river and seawater end members. *Environ. Model. Softw.* 25, 1658–1663. doi: 10.1016/j.envsoft.2010.06.014

Nelson, K. S. (2016). *Biofilm Response to Ocean Acidification and the Effects on Serpulid Polychaete Settlement*. Masters of Science thesis, University of Otago, Dunedin.

Noisette, F., and Hurd, C. (2018). Abiotic and biotic interactions in the diffusive boundary layer of kelp blades create a potential refuge from ocean acidification. *Funct. Ecol.* 32, 1329–1342. doi: 10.1111/1365-2435.13067

Parker, L. M., O'Connor, W. A., Raftos, D. A., Pörtner, H.-O., and Ross, P. M. (2015). Persistence of positive carryover effects in the oyster, *Saccostrea glomerata*, following transgenerational exposure to ocean acidification. *PLoS One* 10:e0132276. doi: 10.1371/journal.pone.0132276

Parker, L. M., Ross, P. M., and O'Connor, W. A. (2011). Populations of the Sydney rock oyster, *Saccostrea glomerata*, vary in response to ocean acidification. *Mar. Biol.* 158, 689–697. doi: 10.1007/s00227-010-1592-4

Pilditch, C. A., Valanko, S., Norkko, J., and Norkko, A. (2015). Post-settlement dispersal: the neglected link in maintenance of soft-sediment biodiversity. *Biol. Lett.* 11:20140795. doi: 10.1098/rsbl.2014.0795

Pöhn, M., Vopel, K., Grünberger, E., and Ott, J. (2001). Microclimate of the brown alga *Feldmannia caespitula* interstitium under zero-flow conditions. *Mar. Ecol. Prog. Ser.* 210, 285–290. doi: 10.3354/meps210285

Przeslawski, R., Byrne, M., and Mellin, C. (2015). A review and meta-analysis of the effects of multiple abiotic stressors on marine embryos and larvae. *Glob. Change Biol.* 21, 2122–2140. doi: 10.1111/gcb.12833

Rahman, M. A., Yusoff, F. M., Arshad, A., Shamsudin, M. N., and Amin, S. (2012). Embryonic, larval, and early juvenile development of the tropical sea urchin, *Salmacis sphaeroides* (Echinodermata: Echinoidea). *Sci. World J.* 2012:938482.

Rivest, E. B., Comeau, S., and Cornwall, C. E. (2017). The role of natural variability in shaping the response of coral reef organisms to climate change. *Curr. Clim. Change Rep.* 3, 271–281. doi: 10.1007/s40641-017-0082-x

Roberts, R. (2001). A review of settlement cues for larval abalone (*Haliotis* spp.). *J. Shellfish Res.* 20, 571–586.

Roberts, R. D., Barker, M. F., and Mladenov, P. (2010). Is settlement of *Haliotis iris* larvae on coralline algae triggered by the alga or its surface biofilm? *J. Shellfish Res.* 29, 671–678. doi: 10.2983/035.029.0317

Rodriguez, S. R., Ojeda, F. P., and Inestrosa, N. C. (1993). Settlement of benthic marine invertebrates. *Mar. Ecol. Prog. Ser.* 97, 193–207. doi: 10.3354/meps097193

RStudio Team (2016). *RStudio: Integrated Development Environment for R*. Boston, MA.

Scheibling, R. E., and Robinson, M. C. (2008). Settlement behaviour and early post-settlement predation of the sea urchin *Strongylocentrotus droebachiensis*. *J. Exp. Mar. Biol. Ecol.* 365, 59–66. doi: 10.1016/j.jembe.2008.07.041

Shaw, E. C., McNeil, B. I., and Tilbrook, B. (2012). Impacts of ocean acidification in naturally variable coral reef flat ecosystems. *J. Geophys. Res. Oceans* 117:C03038.

Shears, N. T., and Babock, R. C. (2007). Quantitative description of mainland New Zealand's shallow subtidal reef communities. *Sci. Conserv.* 280, 5–14.

Uthicke, S., Pecorino, D., Albright, R., Negri, A. P., Cantin, N., Liddy, M., et al. (2013). Impacts of ocean acidification on early life-history stages and settlement of the coral-eating sea star *Acanthaster planci*. *PLoS One* 8:e82938. doi: 10.1371/journal.pone.0082938

Wahl, M., Covachã, S. S., Saderne, V., Hiebenthal, C., Müller, J. D., Pansch, C., et al. (2018). Macroalgae may mitigate ocean acidification effects on mussel calcification by increasing pH and its fluctuations. *Limnol. Oceanogr.* 63, 3–21. doi: 10.1002/lno.10608

Wahl, M., Saderne, V., and Sawall, Y. (2015). How good are we at assessing the impact of ocean acidification in coastal systems? Limitations, omissions and strengths of commonly used experimental approaches with special emphasis on the neglected role of fluctuations. *Mar. Freshw. Res.* 67, 25–36. doi: 10.1071/MF14154

Wangensteen, O. S., Dupont, S., Casties, I., Turon, X., and Palacín, C. (2013). Some like it hot: temperature and pH modulate larval development and settlement of the sea urchin *Arbacia lixula*. *J. Exp. Mar. Biol. Ecol.* 449, 304–311. doi: 10.1016/j.jembe.2013.10.007

Wolfe, K., Dworjanyn, S. A., and Byrne, M. (2013a). Effects of ocean warming and acidification on survival, growth and skeletal development in the early benthic juvenile sea urchin (*Heliocidaris erythrogramma*). *Glob. Change Biol.* 19, 2698–2707. doi: 10.1111/gcb.12249

Wolfe, K., Dworjanyn, S. A., and Byrne, M. (2013b). Thermal and pH/pCO2 fluctuations in the intertidal habitat of *Heliocidaris erythrogramma*: effects on post-metamorphic juveniles. *Cah. Biol. Mar.* 54, 657–666.

Conflict of Interest: The authors declare that the research was conducted in the absence of any commercial or financial relationships that could be construed as a potential conflict of interest.

frontiers in Marine Science

ORIGINAL RESEARCH
published: 27 January 2021
doi: 10.3389/fmars.2021.600343

Surviving Heatwaves: Thermal Experience Predicts Life and Death in a Southern Ocean Diatom

Toby Samuels[1†], Tatiana A. Rynearson[2†] and Sinéad Collins[1†]*

[1] Institute of Evolutionary Biology, School of Biological Sciences, The University of Edinburgh, Edinburgh, United Kingdom,
[2] Graduate School of Oceanography, University of Rhode Island, Kingston, RI, United States

OPEN ACCESS

Edited by:
Michael Raatz,
Max Planck Institute for Evolutionary Biology, Germany

Reviewed by:
Miriam Gerhard,
Institute for Chemistry and Biology of the Marine Environment, Germany
Peng Jin,
Guangzhou University, China
Anke Kremp,
Leibniz Institute for Baltic Sea Research (LG), Germany

***Correspondence:**
Sinéad Collins
s.collins@ed.ac.uk

†ORCID:
Toby Samuels
orcid.org/0000-0001-9850-1230
Tatiana A. Rynearson
orcid.org/0000-0003-2951-0066
Sinéad Collins
orcid.org/0000-0003-3856-4285

Specialty section:
This article was submitted to Global Change and the Future Ocean, a section of the journal Frontiers in Marine Science

Received: 29 August 2020
Accepted: 05 January 2021
Published: 27 January 2021

Citation:
Samuels T, Rynearson TA and Collins S (2021) Surviving Heatwaves: Thermal Experience Predicts Life and Death in a Southern Ocean Diatom. Front. Mar. Sci. 8:600343. doi: 10.3389/fmars.2021.600343

Extreme environmental fluctuations such as marine heatwaves (MHWs) can have devastating effects on ecosystem health and functioning through rapid population declines and destabilization of trophic interactions. However, recent studies have highlighted that population tolerance to MHWs is variable, with some populations even benefitting from MHWs. A number of factors can explain variation in responses between populations including their genetic variation, previous thermal experience and the cumulative heatwave intensity (°C d) of the heatwave itself. We disentangle the contributions of these factors on population mortality and post-heatwave growth rates by experimentally simulating heatwaves (7.5 or 9.2°C, for up to 9 days) for three genotypes of the Southern Ocean diatom *Actinocyclus actinochilus*. The effects of simulated heatwaves on mortality and population growth rates varied with genotype, thermal experience and the cumulative intensity of the heatwave itself. Firstly, hotter and longer heatwaves increased mortality and decreased post-heatwave growth rates relative to milder, shorter heatwaves. Secondly, growth above the thermal optimum before heatwaves exacerbated heatwave-associated negative effects, leading to increased mortality during heatwaves and slower growth after heatwaves. Thirdly, hotter and longer heatwaves resulted in more pronounced changes to thermal optima (T_{opt}) immediately following heatwaves. Finally, there is substantial intraspecific variation in post-heatwave growth rates. Our findings shed light on the potential of Southern Ocean diatoms to tolerate MHWs, which will increase both in frequency and in intensity under future climate change.

Keywords: marine diatoms (Bacillariophyceae), thermal acclimation, marine heatwaves, growth rates, mortality, Southern Ocean, *Actinocyclus*

INTRODUCTION

Extreme temperature fluctuations in terrestrial and marine systems have occurred with increasing frequency and duration over the past century, and will increase further with continued anthropogenic climate change (Frölicher et al., 2018; Lyon et al., 2019; Oliver et al., 2019; Rohini et al., 2019). Marine heatwaves (MHWs) are one such example of temperature fluctuations, and are defined as "discrete prolonged anomalous warm water events" (Hobday et al., 2016) that can result in rapid population declines and reduced ecosystem functioning (Frölicher and Laufkötter, 2018; Oliver et al., 2019; Smale et al., 2019). Recent work has uncovered a broad range of organismal

response to MHWs, from negative to positive (Stuhr et al., 2017; Pansch et al., 2018; Bartosiewicz et al., 2019; Saha et al., 2019; Britton et al., 2020). Furthermore, varied responses among species to MHWs can lead to significant food web alterations in marine habitats (Ryan et al., 2017; Jones et al., 2018; Peña et al., 2019; von Biela et al., 2019; Piatt et al., 2020), illustrating that the responses of individual species will influence the resilience of entire marine ecosystems under global change.

The ecological impact of marine heatwaves in the Southern Ocean has not previously received as much attention as MHWs in Arctic, temperate or tropical locations. However, between 2002 and 2018 nineteen heatwave events were detected across the Southern Ocean (Montie et al., 2020) and MHWs are predicted to increase in frequency in the Southern Ocean in coming decades (Frölicher et al., 2018). Indeed, heatwaves recorded across Antarctica in the summer of 2019–2020 are likely to have significant implications, both negative and positive, for the Antarctic ecosystem. For example, enhanced ice melt due to heatwaves can provide relief from drought stress for terrestrial plant species, but temperature extremes can simultaneously also enhance thermal stress (Robinson et al., 2020). These recent events highlight the urgent need to understand how Southern Ocean organisms respond to MHWs. Diatoms dominate phytoplankton blooms in the Southern Ocean, are important primary producers that support the Southern Ocean ecosystem and are major exporters of silica and carbon from surface waters to marine sediments (Deppeler and Davidson, 2017). Constant elevated temperature can affect both population dynamics and the nutritional value of Southern Ocean diatoms (Boyd et al., 2016), indicating that diatom responses to future warming could have significant implications for trophic interactions and biogeochemical cycling. These findings are echoed by a large body of literature that concludes that environmental change is affecting marine phytoplankton, and will continue to do so in the future (Collins et al., 2020). Despite this, only a handful of studies have directly investigated the effect of MHWs on diatoms under controlled laboratory conditions (Bedolfe, 2015; Remy et al., 2017; Feijão et al., 2018). Microcosm experiments with marine phytoplankton communities exposed to simulated heatwaves and increased turbidity demonstrated that milder heatwaves (+4°C from control) enhanced diatom growth rates, resulting in their dominance of the community, while in contrast, diatoms were completely absent in communities exposed to more intense heatwaves (+6°C) (Remy et al., 2017). Feijão et al. (2018) identified a number of physiological changes in the diatom *Phaeodactylum tricornutum* when exposed to heatwaves, including reduced photosynthetic efficiency and biomass production. These studies provide insight into how diatoms can respond to rapid temperature increases, but do not explore how diatoms behave under more complex, thermally variable environments.

From a physiological perspective, two key mechanisms affect the responses of organisms to thermal extremes, (a) the cellular stress response (Schroda et al., 2015) and (b) acclimation, which can result in "heat hardening" (Bowler, 2005). The cellular stress response, defined as the upregulation of stress response genes including those that express heat shock proteins, enhances tolerance to stressful conditions (Schroda et al., 2015). Acclimation, or gradual phenotypic plasticity (Kremer et al., 2018), describes the effect of altered gene expression and epigenetic modifications to adjust a phenotype (e.g., growth rate) in response to an environmental change (Angilletta, 2009; Kronholm and Ketola, 2018). In phytoplankton, acclimation can alter organismal fitness in the new environment over several asexual generations, and is reversible if the environmental cue stops (Brand et al., 1981; Anning et al., 2001; Kremer et al., 2018). Across a wide variety of marine taxa, numerous studies have demonstrated that previous acclimation to elevated temperatures can enhance tolerance (heat hardening) when exposed to thermal extremes (Magozzi and Calosi, 2015; Scharf et al., 2015; Stuhr et al., 2017; Pansch et al., 2018; Hughes et al., 2019; Sasaki and Dam, 2019).

Across both terrestrial and marine taxa, physiological responses to elevated temperature depend on the intensity and duration of thermal conditions within the context of the organism's thermal niche. For example, environmental warming that occurs below the thermal optimum, the temperature at which growth rate is fastest, can be beneficial by enhancing metabolic activity (Angilletta, 2009). However, environmental warming that occurs near or above the thermal optimum induces a number of physiological stress responses (Viant et al., 2003; Madeira et al., 2013; Leung et al., 2017; Low et al., 2018) that depend upon the duration of the thermal stress, ranging from acute (hours to days) to chronic (days to weeks) (Huey and Bennett, 1990). Energy and resource investment into the expression of acclimation and stress response genes, such as those that produce heat shock proteins, incur fitness costs (Krebs and Feder, 1997; Viant et al., 2003; Geider et al., 2009; Kingsolver and Woods, 2016) and if these are high they can limit responses to future environmental change (Sokolova et al., 2012). In the context of marine heatwaves, the impact of elevated temperatures will be dependent upon the thermal niche of the organisms present, which is subject to both interspecific and intraspecific variation (Boyd et al., 2013). Furthermore, the state of cellular condition (i.e., how stressed the cells are) before heatwaves has the potential to affect population resistance to heatwaves when they do occur (Short et al., 2015; Ainsworth et al., 2016; Stuhr et al., 2017; Siegle et al., 2018; Saha et al., 2019).

Several studies in marine organisms show that responses to MHWs depend upon multiple factors, including temperatures experienced prior to the thermal extreme (Siegle et al., 2018) and temperature variability (Stuhr et al., 2017; Saha et al., 2019; Lugo et al., 2020), and that responses vary between species (Magozzi and Calosi, 2015; Saha et al., 2019; Lugo et al., 2020). Given these factors, it is not surprising that studies have a range of findings. Stuhr et al. (2017) demonstrate that episodic heatwaves enabled maintenance of growth and activity in corals where chronic exposure reduced them. In contrast, Lugo et al. (2020) found that low-temperature periods in a fluctuating thermal regime did not provide relief after elevated temperature exposure in sea stars. Although these studies suggest that thermal experience interacts with taxonomic variation to constrain responses to marine heatwaves, this has not been explicitly addressed in marine phytoplankton, including diatoms.

To understand how intraspecific variation and thermal experience interact to determine mortality and population growth, we investigated the growth response of an Antarctic diatom species to heatwaves. Three genotypes of *Actinocyclus actinochilus* were used to assess the potential for intraspecific variation in heatwave responses. These genotypes were used in a complex experimental design in which we examined mortality (%) and maximum growth rates (asexual divisions per day) in response to differing thermal regimes, which had three phases: (1) growth below (2.5°C) or above (5.8°C) the thermal optimum before heatwaves, (2) exposure to heatwaves (7.5 or 9.2°C) for up to 9 days and (3) growth after heatwaves at seven temperatures spanning the organisms thermal niche to produce thermal performance curves (TPCs).

We examined whether experiencing high temperatures immediately before heatwaves dampens the negative consequences (decreased mortality and/or increased post-heatwave growth rates) of heatwave exposure by "heat hardening," or if previous growth at a higher temperature exacerbates these negative effects which is consistent with deteriorating cellular condition rather than heat hardening. In addition, we show how heatwave mortality and acute post-heatwave growth depend on cumulative heatwave intensity. Finally, we explored the evidence for intraspecific variation in these heatwave responses.

MATERIALS AND METHODS

Genotype Isolation and Culture Maintenance

Seawater samples were collected from surface waters (20 m depth) of the Ross Sea, Antarctica in January 2017. Individual cells and chains of the centric diatom *A. actinochilus* were isolated using a stereomicroscope (Olympus, Center Valley, United States) and a pipette, washed in sterile seawater and then incubated at 2°C in 1:10 F/2 medium under continuous light at 80–100 μmol photons m^{-2} s^{-1} in 24 and 48-well microtiter plates. Successfully cultivated isolates were then grown at 3°C under constant light intensity (∼50 μmol photons m^{-2} s^{-1}, measured using a 2-pi sensor) and an aliquot transferred to F/2 medium (Guillard, 1975) every 3–4 weeks. The three isolates used in this study (A4, B7, D8) were collected from two sites (1) 74.64° S, 157° W (A4), (2) 73.91° S, 151.1° W (B7, D8). These isolates were identified to species using the 18S rDNA sequence. We describe isolate cultures as unique genotypes as they were founded from single cells isolated from natural seawater, where genetic diversity within diatom populations is high (Godhe and Rynearson, 2017). Furthermore, each isolate had distinct and repeatable growth responses to the temperature range investigated, as determined from preliminary experiments. For these reasons, we describe these isolates as unique genotypes throughout this study.

To determine the 18S rDNA sequences for each genotype, genomic DNA was extracted from filtered biomass using the DNeasy 96 Plant Kit (Qiagen, Hilden, Germany) following the manufacturer's protocol, with additional lysis of biomass at 65°C for 10–20 min. The 18S was amplified using a 15 μL reaction mixture containing 1–2 ng DNA, 1X colorless GoTaq master mix (Promega, Madison, United States), and 0.5 mol L^{-1} each of the universal 18SA and 18SB primers (Medlin et al., 1988) in a thermal cycler (Eppendorf AG 22331 Mastercycler, Hamburg, Germany) at 94°C for 2 min, 40 cycles of 94°C for 30 s, 60°C for 60 s, and 72°C for 2 min followed by 10 min at 72°C. PCR amplicons were purified by ethanol precipitation (Zeugin and Hartley, 1985) and quantified by a Nanodrop 1000 (Thermo Scientific, Waltham, United States). Amplicons were sequenced unidirectionally using the 18SB primer either on a 3500XL Genetic Analyzer (Applied Biosystems, Foster City, CA, United States) at the University of Rhode Island Genomics and Sequencing Center, or on an ABI 3730XL (Applied Biosystems, Foster City, CA, United States) at Yale University's Keck DNA Sequencing Facility. Sequences were analyzed using Genomics Workbench software, V9.0.1 (Qiagen, Hilden, Germany) and BLAST (Altschul et al., 1990).

Experimental Design

The effect of thermal experience on mortality and post-heatwave growth rates of *A. actinochilus* was assessed in an experiment with three phases (**Figure 1**). In phase one (acclimation) a single stationary-phase culture of each genotype, cultivated at 2.5°C, was used to inoculate six 25 mL cultures, three of which were kept at 2.5°C (below their thermal optima, or T_{opt}) and three of which were transferred to 5.8°C (above T_{opt}). Thermal optima was estimated from preliminary growth experiments to range between 3 and 4.5°C across the three genotypes. Phase one was comprised of 18 experimental populations (3 genotypes × 2 temperatures × 3 biological replicates). All cultures were inoculated at low density (200–700 cells/mL) and incubated for 19 days. This period provided sufficient time for experimental populations to reach carrying capacity (1.25×10^4 – 1.25×10^5 cells/mL), having grown for 5.8–7.5 generations (∼0.3–0.4 generations per day).

In phase two (heatwaves), 1 mL volumes from the 25 mL, phase one cultures were aliquoted into individual wells of 48-well microtitre plates and incubated on a thermal gradient block at one of two heatwave temperatures (7.5 or 9.2°C). Each 1 mL population in this second phase was used as a sacrificial sample, so that a well was used for determination of mortality at a single time point and/or for propagation into the third phase. Phase two lasted between zero (non-exposed, no heatwave) and 9 days, with sacrificial samples collected for live-dead staining at 0, 1, 3, 6, and 9 days to determine mortality. Determining mortality for populations at day zero (non-exposed to heatwaves) provided a baseline for further comparison, and also allowed us to investigate the effect of growth above T_{opt} in the first phase of the experiment on mortality. In total, 162 experiment populations were in the heatwave phase and underwent live-dead staining, 18 non-exposed populations and 144 heatwave exposed populations (4 heatwave durations × 2 heatwave temperatures × 18 acclimation phase experimental populations). In phase three (acute TPCs), experimental populations not exposed to heatwaves (d0) and populations exposed to 3 and 9 days heatwaves were transferred

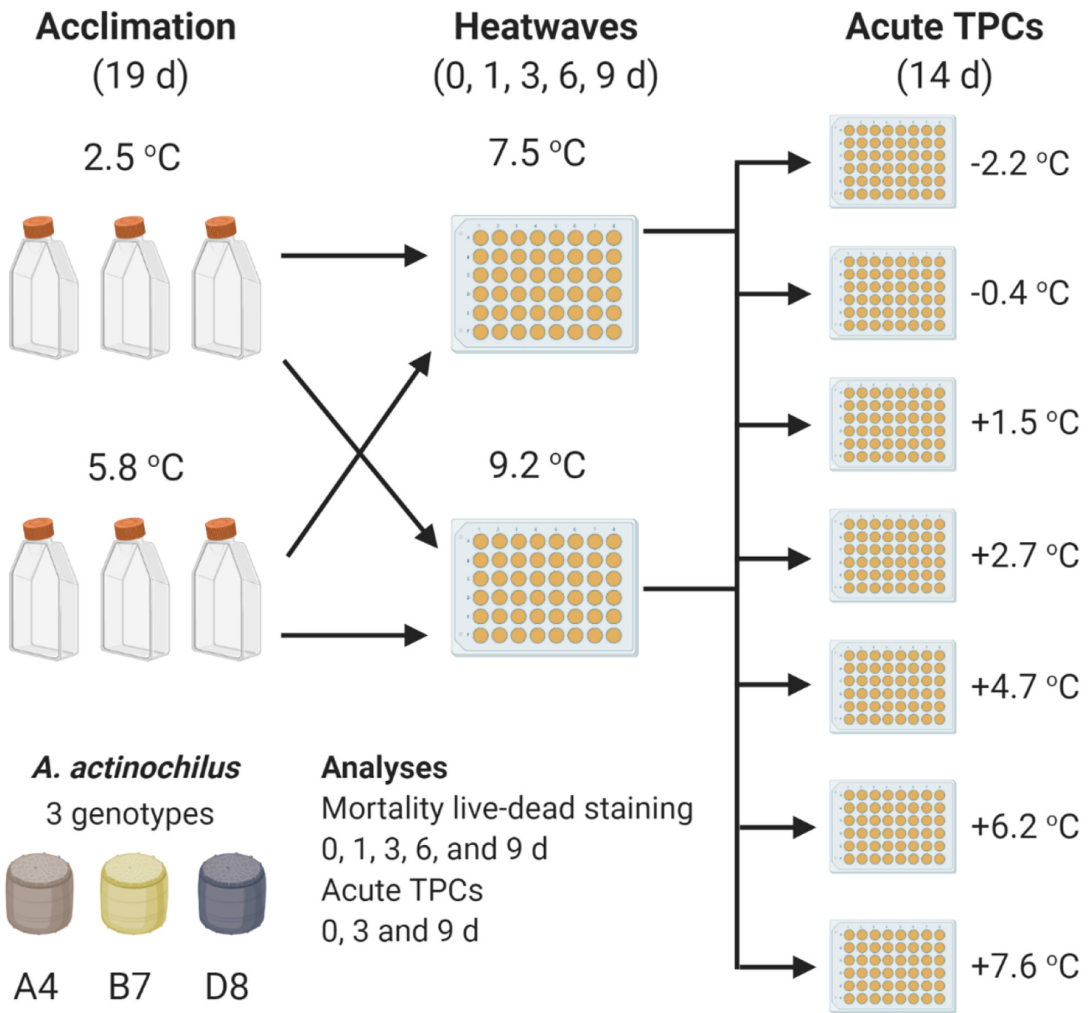

FIGURE 1 | Overview of experimental design for the heatwave treatment. All temperatures shown are absolute temperatures for incubation. A near-identical design was used for the control treatment, in which cultures grown at 2.5 and 5.8°C in the first (acclimation) phase are maintained near these temperatures (2.7 and 6.2°C) in the second (heatwave) phase (**Supplementary Figure 1**).

into nutrient-replete media in 48-well microtitre plates and allowed to recover and grow at a range of temperatures (−2.2, −0.4, +1.5, +2.7, +4.7, +6.2, and +7.6°C) for 14 days on a thermal gradient block to produce acute thermal performance curves. This totals to 630 experimental populations in this final phase of the experiment, 126 non-exposed populations (18 populations × 7 temperatures) and 504 heatwave exposed populations (72 populations × 7 temperatures).

Heatwave temperatures (7.5 and 9.2°C) were chosen to simulate thermally stressful environments for *A. actinochilus,* in which temperatures are either near to or beyond thermal maxima the for *A. actinochilus* and other Southern Ocean diatom species (Boyd, 2019). These temperatures, although not currently experienced in the Ross Sea where the genotypes used in this study were isolated, can occur in other parts of the Southern Ocean during heatwave events (Montie et al., 2020), and as such could be experienced by this species more broadly.

In phase three, experimental populations from phase two were diluted (1:20) into fresh media and allowed to grow until reaching stationary phase. Growth rates measured in this study are acute (Schulte et al., 2011). This enabled us to explore the role of recent thermal experience to extreme environmental fluctuations, when temperature changes over days rather than weeks; our setup reflects immediate recovery from a heatwave rather than the acclimated growth usually used in laboratory experiments aimed at identifying the thermal niche of organisms (Boyd et al., 2013).

An inherent limitation of this experiment comes from known interactions between thermal stress and nutrient limitation (Rhee and Gotham, 1981; Thomas et al., 2017). When stationary phase experimental populations were transferred from the first to the second phase of the experiment they were not diluted into fresh media; they were exposed to elevated temperature under nutrient limitation. This was necessary for accurate measurements of

mortality during heatwaves. Growth needed to be arrested, or mortality would be confounded by the growth of new cells.

We have accounted for this in two ways. First, for each heatwave duration (0–9 days), each experimental population, regardless of thermal history (2.5 or 5.8°C), was exposed to nutrient limitation for the same length of time. Thus, differences in mortality and post-heatwave growth rates between treatment groups after a specific heatwave duration are directly comparable. Second, we performed control treatments to maintain nearly constant temperatures between the first and second phases (2.5–2.7°C or 5.8–6.2°C), so that experimental populations were exposed to nutrient limitation only, without heatwaves (**Supplementary Figure 1**). Due to space limitations, it was not possible to perform the heatwave treatments and control treatments simultaneously. Because of this, we treated these two data sets separately in our statistical analyses and compared the results of those analyses to test for nutrient limitation effects. The mortality analysis in this treatment was potentially confounded by the growth of new cells, so changes in density (both live and dead cells) over time were calculated.

Incubation Conditions

Experimental populations were grown in a cooled incubator (Panasonic MIR-154) set to 3 or 6°C for the first phase of both experiments. Temperature within flasks was measured in triplicate on four occasions, with the temperatures in the 3 and 6°C incubators averaging 2.50 ± 0.24°C and 5.77 ± 0.13°C, respectively. Incubation during the heatwave and post-heatwave growth phases were performed on two thermal gradient blocks (TGBs). Both TGBs were identical in materials and set-up, and were made of thick aluminum sheets (41 cm × 92 cm), with two channels drilled through the width of the block at either length end, enabling water or anti-freeze to be pumped through, producing a thermal gradient along the length of the block. Each TGB was covered with sheets of insulation foam, with slots for microtitre plates to be in direct contact with the block surface. Slots were arranged in two rows of seven columns, allowing two microtitre plates per temperature. To enhance thermal conductivity between the block and the plates, custom cut aluminum sheets were inserted into the base of microtitre plates. Temperature values for each column were determined by taking measurements in 1 mL volumes of seawater within 48-well microtitre plates, with six wells recorded per measurement with a minimum of three measurements taken. Simulated heatwave temperatures (mean average ± standard deviation) were 7.45 ± 0.34 and 9.24 ± 0.51. Temperatures included in analyses for the TPCs were −2.24 ± 0.66, −0.36 ± 0.40, +1.53 ± 0.43, 2.73 ± 0.46, 4.68 ± 0.28, 6.19 ± 0.4, 7.6 ± 0.42. Simulated heatwave temperatures for the control treatment were 2.73 and 6.19°C. Samples in incubators and TGBs were lit from above using cool white aquarium LED lights at 45–55 μmol m^{-2} s^{-1}, measured using a 2-pi sensor.

Mortality Analysis

On each of the heatwave analysis days (0, 1, 3, 6, and 9), samples of either 1 mL (from flask cultures, for control treatments at day zero) or 0.5 mL (from microtiter plates after heatwave exposure, diluted to a volume of 1 mL) were obtained from experimental populations, aliquoted into micro-centrifuge tubes and stained with Evans Blue dye at a final concentration of 0.02%. Stained samples were incubated at 2.5°C for a minimum of 1 h. Samples were kept on ice until imaging (performed within 8 h of staining). The order of sample imaging was randomized. This method was adapted from Garrison and Tang (2014). Samples were loaded onto 1 mL Sedgewick rafter chambers and images acquired at 100× magnification using a mounted EOS 800D Canon digital SLR camera. Images were taken to obtain counts per sample of >600 cells total, or until images of 300 squares (300 μL) were acquired. Live cells ranged in color from dark to golden brown. Dead cells ranged in color from light to dark blue.

Determination of Acute Post-heatwave Growth Rates – Thermal Performance Curves (TPCs)

Acute growth rates of experimental populations were determined at seven temperatures ranging between −2.2 and +7.6°C on a TGB. These temperatures broadly covered the thermal tolerance range of *A. actinochilus*. On d0 (before heatwave), and on d3 and d9 of heatwave exposure, a single replicate from each experimental population was sub-cultured from the acclimation (2.5 or 5.8°C) or heatwave temperatures (7.5 or 9.2°C) directly to temperatures ranging from −2.2 to 7.6°C. Chlorophyll-a fluorescence was measured daily (Tecan Spark plate reader). Experimental populations were mixed by pipette every second day to disperse cellular aggregates (Siegel et al., 2020). Although fluorescence intensity per cell can vary with thermal stress in phytoplankton (Voznesenskiy et al., 2016), we measured relative changes of *in vivo* fluorescence in the same culture maintained under constant thermal conditions over time. Therefore, measurements within individual time series are comparable, allowing us to calculate maximum growth rates from the data. All growth curves were measured in 48 well plates.

Data and Statistical Analysis

All data analyses were performed in the R statistical environment (R Core Team, 2019) and plots were produced in the package *ggplot2* (Wickham, 2016). Maximum growth rates were calculated from chlorophyll-a fluorescence data using the equation below, where x_1 and x_2 are the estimated chlorophyll fluorescence values at the beginning (t_1) and end (t_2) of the fitted regression through the exponential phase of growth curves.

$$\mu = \frac{ln(x2) - ln(x1)}{t2 - t1} \quad (1)$$

The maximum slope gradient was estimated from the growth curves using a sliding window approach across the 14 days growth period, with the window providing the highest estimated value of growth rate accepted. The window length in all growth rate analyses was seven points, taken across consecutive days with the exception of anomalous data points removed from some growth series.

All estimated growth rates were assessed using R^2 confidence values. Fit confidence of growth rates varied with temperature

and growth rate (**Supplementary Figure 2**), and varied most at the lowest temperature (−2.24°C) and at lower growth rate values ($\mu < 0.2\ d^{-1}$). Estimation of growth rates at extreme low temperatures and/or slower growth is more difficult due to small values of, and changes in, experimental population size. For this reason, we chose not to exclude growth rates based upon an R^2 value cut-off. Visual assessment of all growth rate fits was used to confirm low, positive growth rates. Of the 598 positive growth rates, 589 had R^2 values above 0.4, and 518 had R^2 values above 0.75. The majority of growth rate estimates with R^2 values below 0.75 were from the lowest (−2.24°C, 34/80) and second lowest (−0.4°C, 31/80), while eight out of nine growth rate estimates with R^2 values below 0.4 were at −2.24°C (**Supplementary Figure 2**).

Relative growth differences (g) of experimental populations exposed to heatwaves after three or nine days (d_x) of heatwave exposure, relative to the growth of non-exposed experimental populations (d_0), was calculated using the following equation:

$$g = \frac{dx - d0}{d0} \quad (2)$$

Since T_{opt} has been shown to shift in response to recent thermal experience (Staehr and Birkeland, 2006; Padfield et al., 2016; Bernhardt et al., 2018; Kremer et al., 2018), T_{opt} values were obtained from curves fitted using a modified Norberg function (Thomas et al., 2012) within the growthTools package (Kremer, 2020), using the function *get.nbcurve.tpc()*. Thermal optima values for were obtained from each individual set of fit parameters. Curves were fit from growth data across the thermal gradient for each biological replicate. There were thus triplicate curves per treatment, and ninety curves in total. Fits were assessed visually, with poor fits removed from the analysis. Eight fits were removed after visual inspection, with remaining fits having R^2 values > 0.4 (78 fits had R^2 values > 0.8). All data for genotype D8 acclimated to 5.8°C and then exposed to 9.2°C heatwaves for 9 days were removed, due to erratic growth. Furthermore, due to enhanced growth at the lower thermal extremes in populations of genotype A4 acclimated at 2.5°C and then exposed to 7.5°C heatwaves for 3 days, the relationship between growth and temperature was no longer quadratic, and as such all data for this treatment was also removed from the analysis. Thermal plasticity of the TPCs was calculated as the slope of the TPC below T_{opt}, while the thermal plasticity of the thermal optimum (T_{opt}) was calculated from shifts in T_{opt} values between experimental conditions.

Mortality data after the acclimation phase was analyzed using a general linear model. Data after the heatwave treatment was analyzed using generalized linear models with binomial distributions in the *glm* function. Maximum growth rates from the acute TPCs were analyzed using general linear mixed models within the *lmer* function [package *lme4* (Bates et al., 2014)] and T_{opt} data was analyzed within a general linear model using the *lm* function. Due to collinearity between heatwave intensity (°C) and heatwave duration (d), we were unable to interpret results for these two variables independently. Because of this collinearity, we combined these two variables into a single variable, "cumulative heatwave intensity" (°C d), which was then used as the sole variable for heatwave treatment. For analysis of the mortality data, genotype, acclimation temperature, cumulative heatwave intensity and percentage of live cells at day zero were used as predictor variables, with proportional relative live cells ($d_0 = 1$) as the response variable. Percentage of live cells at day zero was included within our statistical analyses due to differences in mortality during the acclimation phase. For the analysis of maximum growth rate data, genotype, growth temperature (both as a linear and a quadratic function), acclimation temperature and cumulative heatwave intensity were used as predictor variables, with growth rate as the response variable. TPC phase plate ID was included as random effect within this model, as ninety experimental populations were split across two plates per temperature. In the analysis of T_{opt}, acclimation temperature, cumulative heatwave intensity and genotype were used as predictor variables, with T_{opt} values as the response variable. Note that cumulative heatwave intensity (°C d) was modeled as a numeric variable in the analysis of mortality, but as a factor variable in the analysis of growth rates and T_{opt}, due to the non-linear trends observed in the growth rate data with respect to this term. *Post hoc* testing was performed using the emmeans package *emmeans()* function with Tukey tests to assess the significance of pairwise treatment comparison.

For statistical analyses of mortality and thermal optimum data, all possible models were explored and selection based upon comparisons of differences in the corrected Akaike Information Criterion (ΔAICc) (Zuur et al., 2009). To analyze differences in maximum growth rate, a full model with all possible interactions was built and then run through the *dredge()* function in the package MuMIn, which produces all possible models and ranks them by AIC values (Barton and Barton, 2015). In analyses the top ranked model, either with AIC or AICc, was used. Model assumptions were checked for all selected models and were found not to have been violated.

RESULTS

Effects of Growth Temperature and Heatwaves on Population Mortality

Analysis of mortality at the conclusion of the acclimation phase revealed that acclimation temperature ($F = 45.03$, df = 1, $p < 0.001$), genotype ($F = 4.47$, df = 2, $p = 0.035$) and the interaction between them ($F = 4.55$, df = 2, $p = 0.034$) had significant effects on the percentage of live cells in experimental populations on day 19. The average percentage of live cells on day 19 for each genotype was 95–98% for experimental populations acclimated at 2.5°C, and 86–93% for experimental populations acclimated at 5.8°C. Day 19 populations from the acclimation phase of the experiment were used to seed phase two of the experiment (heatwaves).

Analysis of mortality during the phase two heatwave treatments (**Figure 2** and **Supplementary Figure 3**) showed that the effects of cumulative heatwave intensity (°C d) (GiLM, $\chi^2 = 12.3685$, df = 1, $p = 0.0004$) and acclimation temperature (GiLM, $\chi^2 = 3.4029$, df = 1, $p = 0.0651$) explain survivorship in these treatments, although acclimation temperature was only

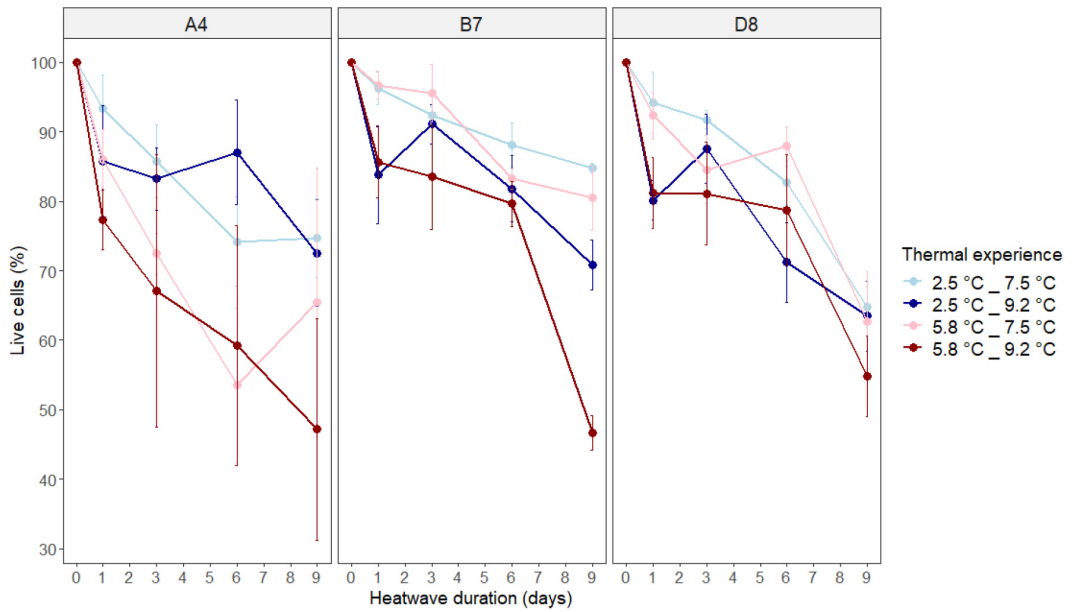

FIGURE 2 | Mortality of experimental populations during simulated heatwaves, shown as the percentage of live cells in experimental populations relative to the percentage of live cells on day 0. Thermal experience is defined by the combination of acclimation temperature (2.5 or 5.8°C) and heatwave temperature (7.5 or 9.2°C). Panels show the results for each genotype (A4, B7, and D8) of *A. actinochilus*. Data points represent average values for three independent replicates ± one standard deviation.

marginally significant (alpha = 0.05; **Supplementary Table 1**). By the end of heatwave exposure, average values of live cells remaining in populations were between 47 and 85% of values at the start of phase two. For two of three genotypes, A4 and B7, experimental populations grown at 2.5°C in the first phase of the experiment survived better when exposed to heatwaves than experimental populations grown at 5.8°C in the first phase. However, in genotype D8, mortality increased consistently regardless of acclimation temperature (**Figure 2** and **Supplementary Figure 3**).

We saw patterns consistent with warmer heatwaves (9.2°C, darker lines) increasing mortality more than cooler heatwaves (7.5°C, lighter lines) for genotypes B7 and D8 (**Figure 2**), although this could not be statistically tested due to collinearity between heatwave intensity and duration. Cumulative heatwave intensity (°C d) increased mortality in all three genotypes, with experimental populations acclimated to 2.5°C experiencing lower mortality during heatwaves than those acclimated to 5.8°C (**Figure 2** and **Supplementary Figure 3**). There was no statistical evidence for genotype influencing mortality (GiLM, $\chi^2 = 1.8158$, df = 2, $p = 0.4034$) (**Supplementary Table 1**). Adding interactions between response variables reduced model AICc values, and none of these terms were significant.

In the control treatment, experimental populations were maintained in a stable thermal environment for up to 9 days to determine if time spent in stationary phase alone impacted mortality. We collected data for five of the six control treatment groups (genotypes A4, B7, and D8, in two thermal regimes) due to culturing failure in experimental populations of genotype D8 acclimated at 5.8°C. In a statistical analysis of the control treatment, the effect of cumulative heatwave intensity (°C d^{-1}) was not significant (GiLM, $\chi^2 = 0.3944$, df = 1, $p = 0.53$) (**Supplementary Table 2**). In general, populations in the control treatment maintained high percentages of live cells relative to day zero of phase two (**Supplementary Figure 5**). After 9 days, percentages of live cells relative to day zero ranged between 88 and 99% in four of the five control treatment groups. In contrast, experimental populations exposed to 9 days of heatwave treatment had only 47–85% of live cells remaining relative to day zero (**Supplementary Figure 5**). It should be noted that in the fifth control treatment group, genotype D8 acclimated at 5.8°C and then exposed to 6.2°C for 9 days, mortality increased substantially (70% live cells after 9 days). While cumulative heatwave intensity (°C d) had a significant effect in the second phase of the heatwave treatment (GiLM, $\chi^2 = 12.3685$, df = 1, $p = 0.0004$) (**Supplementary Table 1**), the incubation of cultures at the control temperatures (2.7 and 6.2°C) in the second phase of the control treatment did not significantly influence mortality (**Supplementary Figure 5**). It should be noted that the effect acclimation temperature in the control treatment was significant (GiLM, $\chi^2 = 6.4280$, df = 1, $p = 0.0112$) (**Supplementary Table 2**) but was not significant at the 0.05 significance level in the heatwave treatment (GiLM, $\chi^2 = 3.4029$, df = 1, $p = 0.0651$) (**Supplementary Table 1**).

Overall cell densities (cells/mL, total live and dead cells) in experimental populations for both the heatwave and control treatments remained relatively constant over time (**Supplementary Figures 4**, **6**). Minor fluctuations in density occurred, but these were not the large increases that would be associated with sustained growth. This indicates that the observed

decline in live cells within experimental populations was not confounded by growth in our experiments.

Effects of Heatwaves on Thermal Performance Curves

In phase three, we characterized the plastic responses of experimental populations to changes in temperature using thermal performance curves spanning temperatures from −2.2 to +7.6°C. First we examined thermal performance of control populations that were held at constant temperatures. There was intraspecific variation in plasticity, defined as change in growth rate with increasing temperature below T_{opt}, and in the effect of previous growth temperature (acclimation) on growth rates (**Figure 3**, left-hand panels). For example, genotype A4 showed limited plasticity from the lowest temperature assayed (−2.2°C, $\mu = 0.37 \pm 0.02$) to the temperature at which the highest growth rate was recorded (+4.7°C, $\mu = 0.49 \pm 0.02$), when previously grown at 3°C (top-left panel, blue line). In contrast, genotype B7 was more plastic, with growth rate increasing by more than three-fold from −2.2°C (0.11 ± 0.01) to 2.7°C (0.35 ± 0.02) (middle-left panel, blue line). For genotypes A4 and B7, the effect of previous growth temperature had minimal influence on plasticity (blue and red lines substantially overlap in top-left and middle left panels). However, previous growth at 5.8°C for genotype D8 resulted in significantly decreased growth rates across the central and upper temperature range, compared to experimental populations grown previously at 2.5°C (bottom-left panel).

To assess how heatwaves affected subsequent plastic responses to temperature change, we constructed thermal performance curves for experimental populations after exposure to 3 and 9 day heatwaves (**Figure 3**). Heatwave exposure affected subsequent thermal performance curves, and cases of both increases and decreases in growth rates relative to experimental populations not exposed to heatwaves were observed (**Figure 4**). We explored the factors affecting changes in growth rates using a general linear mixed model (GLMM, **Supplementary Table 3**). Since not all temperature response curves had the same shape, we described the relationship between temperature and growth rate using a linear function (GLMM, $F = 71.7293$, df = 1, $p < 0.001$) and a quadratic function (GLMM, $F = 76.0014$, df = 1, $p < 0.0001$). Together, these terms captured the shape of the temperature response curves and explained 21% of the total variation explained by the model, as calculated by the sum of squares value for this term divided by the total sum of squares across the model and presented as a percentage. Genotype (GLMM, $F = 239.8280$, df = 2, $p < 0.0001$) and acclimation temperature (GLMM, $F = 133.9460$, df = 1, $p < 0.0001$) together explained the majority (53%) of the variance in growth rate (**Figure 3** and **Supplementary Table 3**). Here, experimental populations that were acclimated at a lower temperature generally grew faster at a given temperature than those acclimated at a higher temperature, particularly after the first 3 days of heatwave exposure (**Figure 3, central** and **right** hand panels).

Cumulative heatwave intensity (°C d) had a large and significant effect on experimental population growth rates (GLMM, $F = 67.8707$, df = 4, $p < 0.0001$). *Post hoc* testing (**Supplementary Tables 4A–C**) revealed that the effect of cumulative heatwave intensity was not linear. In general, growth was unaffected or enhanced by mild heatwaves, but reduced by intense heatwaves, relative to non-exposed populations. The extent of this alteration was modulated by genotype and acclimation temperature. For example, the most extreme growth rate increases occurred in B7 acclimated to 2.5°C, where all but the most intense heatwaves (79.83°C d, 9.2°C for 9 days) significantly increased growth rates relative to pre-heatwave values (**Figure 4** and **Supplementary Table 4B**). However, the most intense heatwaves (79.83°C d, 9.2°C for 9 days) significantly decreased growth rate, relative to both pre-heatwave values and to experimental populations exposed to milder heatwaves, in almost all pairwise comparisons across genotypes (**Supplementary Tables 4A–C**). After intense heatwaves, growth at lower temperatures was either significantly reduced or completely arrested in all three genotypes. Furthermore, genotype D8 exposed to 9.2°C heatwaves decreased across the entire range of temperatures measured.

A number of interactions between all individual variables within the main growth rate statistical model were also identified (**Supplementary Table 3**), but these had much smaller effect sizes than the individual variables, so only three interactions will be examined in detail here. First, the interaction with the largest effect size was genotype with growth temperature (GLMM, $F = 56.2742$, df = 2, $p < 0.0001$), which can be explained by the differences in plasticity between genotypes described above.

Second, growth temperature also interacted with cumulative heatwave intensity (GLMM, $F = 17.7256$, df = 4, $p < 0.0001$). Growth at both temperature range extremes was most affected by cumulative heatwave intensity, with less intense heatwaves elevating growth rates while more intense heatwaves reduced them. Very high cumulative heatwave intensities (9-day heatwaves of 9.2°C) resulted in the largest reductions in growth rate, particularly at low temperatures (**Figure 4**, right-hand panels). For genotypes B7 and D8, growth at both −2.2 and −0.4°C was completely inhibited after a thermal experience where experimental populations had been grown at 5.8°C, and then exposed to a 9.2°C heatwave for 9 days. Finally, acclimation temperature also interacted with genotype (GLMM, $F = 12.8787$, df = 2, $p < 0.0001$).

Due to the lower confidence of growth rate fits at the extreme low temperature (−2.24°C), the statistical analysis of growth rates was repeated but without data from this temperature (**Supplementary Table 5**). Despite some minor changes in relative effect sizes and the significance of low-effect interactions, the relative size and significance of major terms and interactions remained consistent. As such, we decided to continue to use the full dataset in further analyses of the experiment.

Differences in thermal optima (T_{opt}) between experimental populations depended on cumulative heatwave intensity (GLM, df = 4, $F = 12.08$, $p < 0.0001$) and genotype (GLM, df = 2, $F = 8.08$, $p < 0.0001$). There were also significant interactions between genotype and acclimation temperature (GLM, df = 2, $F = 5.99$, $p = 0.0041$), as well as genotype and cumulative heatwave intensity (GLM, df = 2, $F = 2.19$, $p = 0.040$) (**Figure 5** and **Supplementary Table 6**).

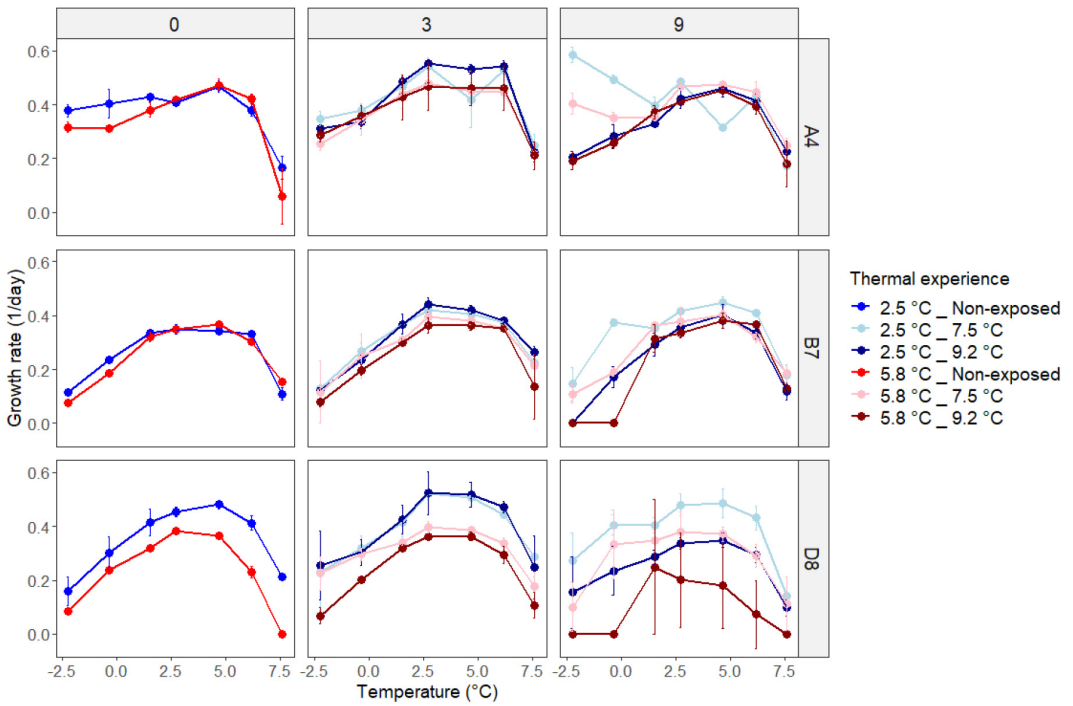

FIGURE 3 | Maximum growth rates of non-exposed (d0) and heatwave-exposed (d3 and d9) experimental populations at seven temperatures for each genotype. Thermal experience combines acclimation temperature (2.5 or 5.8°C) and heatwave temperature (7.5 or 9.2°C). Data shown are average values across three replicates ± one standard deviation.

In general, hotter heatwaves resulted in a higher T_{opt}. Over time, the difference in T_{opt} between hotter and cooler heatwaves either held steady or grew, but did not get smaller. The magnitude of the effects of acclimation temperature and cumulative heatwave intensity on T_{opt} were genotype specific. For example, before heatwave exposure, experimental populations of A4 acclimated at 5.8°C had a T_{opt} higher than those acclimated at 2.5°C. In comparison, genotype B7 had the same T_{opt} regardless of acclimation temperature (**Figure 5**). Heatwaves raised T_{opt} values in genotype A4, regardless of acclimation temperature, but the cumulative heatwave intensity required to do this depended on acclimation temperature: both 7.5 and 9.2°C heatwaves caused an upward shift in T_{opt} for experimental populations acclimated to 2.5°C (**Figure 5**, top left), but only 9.2°C for 9 days (79.83°C d) was able to further increase T_{opt} values for those acclimated at 5.8°C (**Figure 5**, top right). In contrast, heatwaves caused no significant shifts in T_{opt} in genotype D8, regardless of heatwave intensity or duration (**Figure 5**, bottom panels).

Post hoc testing of the effect of cumulative heatwave intensity, with all other variables kept equal, showed that heatwaves of 9.2°C significantly increased T_{opt} relative to pre-heatwave experimental populations by 0.4°C for 3 days (26.61°C d, $p < 0.0001$) and 0.5°C for 9 days (79.83°C d, $p < 0.0001$). In contrast, heatwaves of 7.5°C did not significantly alter T_{opt} from pre-heatwave values, for either 3 days (21.87°C d, $p = 0.2024$) or 9 days (65.61°C d, $p = 0.9812$) heatwaves.

DISCUSSION

Previous studies have found both negative and positive effects of heatwaves on marine organisms (Stuhr et al., 2017; Pansch et al., 2018; Siegle et al., 2018; Bartosiewicz et al., 2019; Roberts et al., 2019; Lugo et al., 2020). Here, we systematically disentangled how thermal experience and genotype affect the mortality and growth responses of the Southern Ocean diatom *A. actinochilus* to simulated heatwaves, and show how both negative and positive heatwave effects can occur in the same study system. A wide range of growth and mortality effects occur during and after exposure to heatwaves, and this range of effects can be attributed to differences in temperature regimes. As expected, more intense heatwaves result in increased mortality and affect post-heatwave growth rates more than more moderate heatwaves, and the extent of this depends on previous growth temperature. We also found that genotypes vary in their responses to heatwaves. Our data show that the effects of marine heatwaves on primary producers depend on both environmental and genetic context. While there are general patterns in responses to heatwaves, a range of responses should be expected between populations with different thermal histories, and to a lesser extent, within genetically variable populations with the same history.

More intense heatwaves consistently resulted in increased mortality across all three genotypes (**Figure 2** and **Supplementary Table 1**). This supports previous work showing that cumulative thermal stress is a strong predictor of population

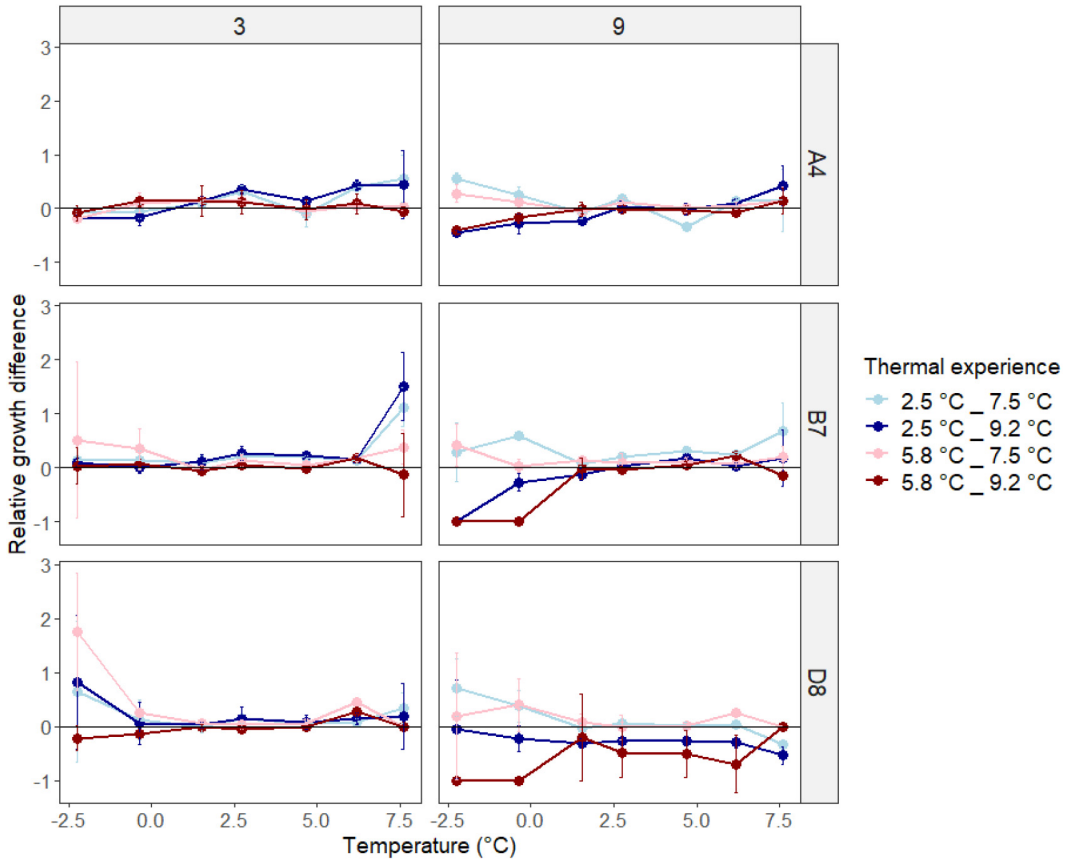

FIGURE 4 | Relative growth difference of experimental populations grown at seven temperatures after exposure to 3 or 9 days heatwaves compared to non-exposed experimental populations, for each genotype. Data represent average values across three replicates ± one standard deviation.

decline in marine populations and ecosystems (Eakin et al., 2010; Marbà and Duarte, 2010; Stuhr et al., 2017; Pansch et al., 2018; Siegle et al., 2018). Accumulated stress beyond a critical threshold results in mortality due to the degradation of cellular components and disruption of physiological functioning (Lesser, 2006; Magozzi and Calosi, 2015; Schroda et al., 2015; Feijão et al., 2018). Although exposure to non-lethal temperatures can also increase tolerance to further stress in some marine organisms (Clapp et al., 1997; Magozzi and Calosi, 2015; Sasaki and Dam, 2019), we do not find evidence for this in our experiment. Instead, we found that experimental populations grown at 5.8°C (above T_{opt}) prior to heatwave exposure had higher levels of mortality than those grown at 2.5°C (below T_{opt}), in both the heatwave and control treatments. This effect (F-value) was 3.40 (p = 0.0651) and 6.43 (p = 0.0112) in our heatwave and control treatments, respectively. It is unclear why the effect of acclimation temperature had a lower p-value in the control treatment. One potential explanation is that the negative effect of increasing cumulative heatwave intensity on the percentage of live cells partially masked previous acclimation effects, particularly in genotypes A4 and B7 (**Figure 2** and **Supplementary Figure 3**).

Growing in warmer temperatures before heatwaves exacerbated the negative consequences of heatwaves in this experiment. A number of studies have come to similar conclusions; that previous growth at elevated, sub-lethal temperatures weakened the capacity to respond to further stress, rather than providing a "heat-hardening" effect (Marbà and Duarte, 2010; Pansch et al., 2018; Siegle et al., 2018). For example, Siegle et al. (2018) found that copepods isolated from splash pools with differing thermal histories responded differently to simulated heatwaves. Individuals that had experienced sub-lethal but warmer temperatures were less likely to survive simulated heatwaves, with this effect exacerbated by increasing heatwave intensity (Siegle et al., 2018). We suggest that in our study, the effect of previous heat exposure is related to whether experimental populations were acclimated above T_{opt}, and nearer to the upper limit of temperatures normally experienced in the Southern Ocean during diatom blooms (5.8°C), or below T_{opt}, and within the normal temperature range for diatoms growing in the Southern Ocean (2.5°C) (Boyd, 2019). Above T_{opt}, one could reasonably suppose that cells would be stressed, and could accumulate damage, even if they are able to grow in the short term, which is consistent with, for example, reactive oxygen associated with rapid growth due to CO_2 enrichment (Lindberg and Collins, 2020). In contrast, cells growing below T_{opt} can be expected to be operating normally, if slowly, and even

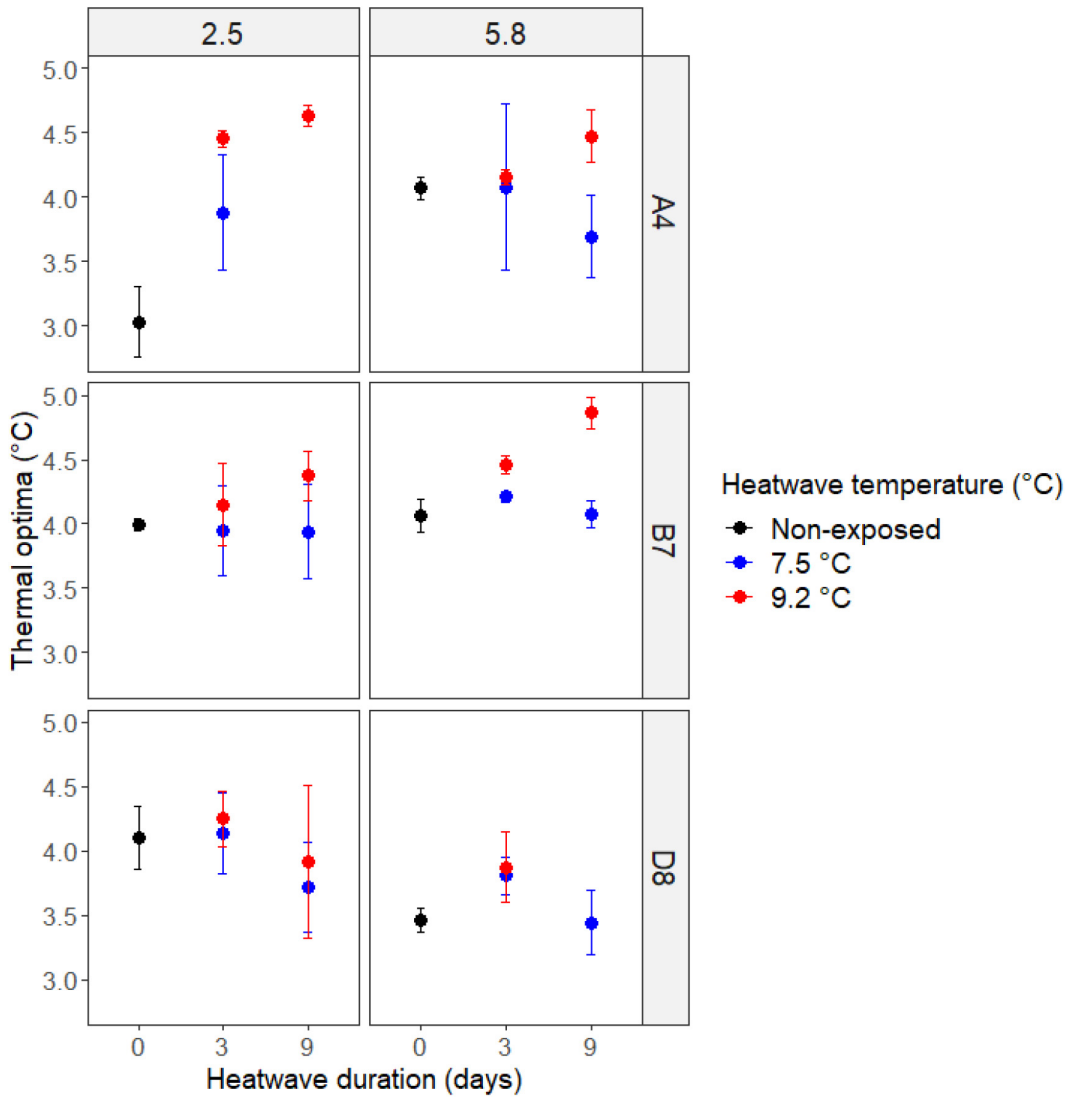

FIGURE 5 | Growth rate thermal optima (°C) of non-exposed (black) and heatwave exposed (red/blue) experimental populations. Thermal performance curves were produced for non-exposed populations (d0) and populations exposed to 3 and 9 days of heatwave exposure, for different acclimation temperatures (columns) and genotypes (rows). Error bars represent ± one standard deviation across three biological replicates.

if they are not under ideal conditions, it is unlikely that they are experiencing severe thermal stress.

We investigated the effect of thermal experience on growth immediately following heatwaves by comparing thermal performance curves before and after heatwave exposure. Previous studies on Southern Ocean diatoms (Boyd et al., 2013, 2016; Xu et al., 2014; Coello-Camba and Agustí, 2017; Andrew et al., 2019; Boyd, 2019) produced acclimated TPCs, where growth rate at a given temperature is recorded after several generations of acclimation to a stable thermal environment (Brand et al., 1981). In contrast, we have used acute thermal responses. Our rationale for measuring acute responses is that population dynamics, and the ecological consequences of them, immediately following heatwaves will be driven by acute responses to the post-heatwave temperatures, as ecological and evolutionary processes will not pause while populations acclimate for days or weeks. We found that plastic responses to warming depended on genotype and thermal experience. Exposure to heatwaves affected growth in all three genotypes (**Supplementary Table 3**), but the extent of this impact differed between them (**Figure 3**). Broadly, genotype A4 appeared to have the largest tolerance (low mortality and high growth rates) to simulated heatwaves, while genotype D8 displayed the lowest tolerance. However, the effect of genotype was not statistical significant for mortality (p = 0.4034). This suggests that genotype effects are mainly important in post-heatwave performance rather than heatwave survival itself, at least in this study. Interestingly, 3 days of heatwave exposure did not have negative consequences for growth in any genotype (**Figure 4** and **Supplementary Tables 4A–C**). This high tolerance to

short but very warm heatwaves was surprising, as a previous study found that exposure to simulated heatwaves (+6°C above control temperature) for 3 days reduced growth rates in the model diatom *P. tricornutum* (Feijão et al., 2018). In contrast, we identified that 3-day heatwaves sometimes had positive effects on growth rate at either thermal extreme in all three genotypes tested (**Figures 2**, **3**). An increase in growth rate at upper thermal extremes after heatwave exposure could indicate acclimation (Magozzi and Calosi, 2015; Scharf et al., 2016; Stuhr et al., 2017) where growth at elevated temperatures causes rapid physiological alterations that limit the negative impact of stress at temperatures above T_{opt} (Low et al., 2018). However, we also observed high variation among genotype replicates at the upper temperature range, indicating that acclimation at very high temperatures was variable (**Figure 4**). Cells at very high temperatures may be more stressed, and cell function may deteriorate idiosyncratically (Sørensen et al., 2013; Magozzi and Calosi, 2015; Feijão et al., 2018).

The most intense heatwaves (79.83°C d, 9.2°C for 9 days) resulted in the largest reductions in growth rate in this study, in some cases completely arresting growth at thermal extremes (**Figures 3**, **4**). This is consistent with our mortality measurements, and other studies where growth rate and survival decline as populations reach a critical level of accumulated thermal stress (Marbà and Duarte, 2010; Pansch et al., 2018; Siegle et al., 2018). The largest increases in mortality occurred between 6 and 9 days of heatwave exposure (**Figure 2**), indicating that differences in population growth rates for different heatwave durations is likely driven by increased cellular stress here (**Figure 3**). Strikingly, even after 9 days of heatwave exposure, a subset of experimental populations displayed remarkable tolerance to elevated temperature, measured as growth rate (**Figures 3**, **4**). In genotypes A4 and B7, growth at 7.6°C was enhanced after heatwave exposure, further supporting the hypothesis that acclimation can partially mitigate the negative effects of growth under elevated temperatures, at least in some cases (Magozzi and Calosi, 2015; Scharf et al., 2016; Stuhr et al., 2017). Interestingly, some experimental populations exposed to 9 days heatwaves also displayed enhanced growth rates at low temperatures (**Figure 4**). As with experimental populations exposed to shorter heatwaves, there was high variation within genotypes in lower temperature growth rates, which suggests that the effects of stress may be idiosyncratic in extreme cases, where the breakdown versus improvement of cellular function may have a high stochastic component.

These results are in line with previous studies that have used genomic and transcriptomic approaches to characterize the thermal adaptations of Southern Ocean diatoms, demonstrating that cells may employ common stress mechanisms at both thermal extremes (Mock et al., 2017; Pargana et al., 2020). Growth of *Fragilariopsis cylindrus* under both thermal extremes (−2, +11°C) revealed similarities in altered gene expression relative to ambient conditions, indicating that generic stress responses were potentially employed in both thermal environments (Mock et al., 2017), and in *Leptocylindrus aporus*, expression of heat shock proteins (HSPs) was upregulated in both high and low temperature incubations (Pargana et al., 2020). The production of HSPs is known to increase during growth above T_{opt} (Rousch et al., 2004; Leung et al., 2017), and has been shown to be maximized as temperatures approach thermal maxima (T_{max}) (Low et al., 2018). However, HSPs are also produced during cold shock responses, which is consistent with the observation that heat shocks can enhance tolerance to subsequent cold shocks (Burton et al., 1988; Goto and Kimura, 1998; Scharf et al., 2015, 2016). Further work using molecular approaches would be required to confirm if these same mechanisms are in play in *A. actinochilus*.

Analysis of a key thermal trait, T_{opt}, revealed that the plastic response to warming in *A. actinochilus* can change, and lead to enhanced growth in a warming environment, but that this does not occur in all genotypes (**Figure 5**). Increases in T_{opt} of up to 1.5°C occurred in genotypes A4 and B7 grown at warmer acclimation temperatures and exposed to hotter heatwaves. We also found evidence of a limit to shifts in T_{opt}, after which additional exposure to elevated temperatures did not increase T_{opt} further. Recent work has shown that previous environmental history can influence thermal performance, with higher acclimation temperatures resulting in upward T_{opt} shifts for a number of phenotypic traits (Seebacher et al., 2015; Padfield et al., 2016; Luhring and DeLong, 2017; Strock and Menden-Deuer, 2020). Our study, alongside others, confirms that thermal performance curves, which are often used to understand the thermal niche a taxon can occupy is plastic and can respond to rapid environmental change.

Taken together, our data show that whether heatwaves have a positive or a negative effect on growth depends on thermal experience. Though both genotype and cumulative heatwave intensity can affect growth, experimental populations acclimated to 2.5°C prior to heatwave exposure generally performed better than those acclimated to 5.8°C (**Figure 3**), indicating that growth temperatures above T_{opt} prior to heatwaves generally had a negative impact on growth after heatwaves. However, thermal extremes experienced during the heatwaves themselves can enhance growth rates at thermal extremes (**Figure 4**) and result in upward shifts of thermal optima (**Figure 5**).

It is interesting to consider whether the acute phenotypic changes that we observed immediately after heatwave exposure (**Figures 3–5**) would persist or if genotypes would revert back to pre-heatwave states. Although numerous studies have investigated the long-term effects of warming on phytoplankton populations via adaptation (Listmann et al., 2016; Padfield et al., 2016; Baker et al., 2018; Jin and Agustí, 2018; O'Donnell et al., 2018; Schaum et al., 2018), few have investigated intermediate time scales between rapid acclimation processes and long-term evolution. Further research is needed to resolve the effects of prolonged acclimation periods before adaptive processes start to occur. In addition, the state of other environmental parameters such as nutrient availability have been shown to alter the effect of heatwaves on population dynamics in natural ecosystems (Hayashida et al., 2020), and this is worth exploring under controlled laboratory conditions.

The thermal niches of studied Southern Ocean diatoms largely fall within the thermal annual range of the Southern Ocean (−1.5 and 8°C) (Boyd, 2019), with thermal optima ranging

between 0 and 7°C for the majority of species (Coello-Camba and Agustí, 2017). Growth of *A. actinochilus* in this study is consistent with this range, with thermal optimum values (3–5°C) depending on previous thermal experience (**Figure 5**). The ability of populations to shift their T_{opt} toward warmer temperatures after experiencing thermal extremes may enable them to better tolerate further environmental change (Seebacher et al., 2015). However, the shifts in thermal responses identified in this study may be influenced by trade-offs under less permissive growth conditions, in particular under nutrient limitation. Boyd et al. (2016) investigated trait responses in the Southern Ocean diatom *Pseudonitzschia multiseries* to a number of predicted future climate scenarios. Temperature, along with iron availability, were found to be predominant drivers of phenotypic plasticity, with populations having faster growth rates and carrying capacity in warmed environments, but at the cost of reduced cellular quality. This is expected to have ecological consequences, as cells grown in warmer environments also had lower nutritional value. Their findings show that responses of SO diatoms to changing thermal environments can have important implications for trophic energy transfer and biogeochemical cycling. The enhanced growth (**Figure 3**) and T_{opt} shifts (**Figure 5**) observed in this study may well have correlated effects on ecologically important traits such as nutritional value, and future work using additional trait assays, such as determination of cellular stress and elemental analysis, could reveal them.

In marine ecosystems, historical warming and heatwave events have resulted in a number of long-term changes to population responses to further warming, often driven by changes in the genetic structure of populations (Hughes et al., 2019; Coleman et al., 2020; Voolstra et al., 2020). Our study underscores the importance of intraspecific variation in heatwave responses, as genotype explained 35% of the total variation in growth rate after heatwaves (**Figure 3** and **Supplementary Table 3**), and affected thermal optimum shifts after heatwaves (**Figure 5** and **Supplementary Table 6**). Our findings add to a growing body of literature showing that intraspecific variation in responses to environmental change is common in phytoplankton, and that multiple genotypes should be considered in studies that aim to understand species-level or general responses (Schaum et al., 2013; Zhang et al., 2014; Pancic et al., 2015; Godhe and Rynearson, 2017; Wolf et al., 2018). Focus on a single genotype in this study would have produced misleading conclusions about the response of *A. actinochilus* to marine heatwaves, with either over estimation (e.g., A4) or under estimation (e.g., D8) of thermal tolerance. Our findings show that marine heatwaves can influence population dynamics and, through differential effects on lineage mortality during and growth rates after heatwaves, have the potential to result in rapid evolution in genetically-diverse diatom populations.

DATA AVAILABILITY STATEMENT

The raw data supporting the conclusions of this article will be made available by the authors, without undue reservation, to any qualified researcher.

AUTHOR CONTRIBUTIONS

TR and SC obtained research funding. TS, SC, and TR conceptualized the study and designed the experiments. TS performed the experiments and the data analysis and wrote the first draft of the manuscript. SC and TR contributed to final manuscript preparation. All authors approved the manuscript before submission.

FUNDING

This work was supported by an NSF GEO-NERC grant to TR (NSF - grant code 1543245) and SC (NERC - grant code NE/P006981/1).

ACKNOWLEDGMENTS

We would like to thank Stephanie Anderson for assisting with the design of the multi-well growth plate, S. Anderson and Kerry Whittaker for cell isolations during the 2016–2017 research cruise, Celia Gelfman for culture maintenance at URI, Katy McDonald, Jana Hinners and Ignacio Melero Jiménez for assistance in data collection, Ian Bishop for providing R code for growth rate calculations and, Albert Phillimore and Nick Colegrave for advice on statistical approaches. Part of this research was conducted using the University of Rhode Island's Marine Science Research Facility, supported by NSF EPSCoR awards 1004057 and 1655221. This manuscript has been released as a pre-print on BioRxiv (doi: https://doi.org/10.1101/2020.08.25.264028) Samuels et al. (2020).

SUPPLEMENTARY MATERIAL

The Supplementary Material for this article can be found online at: https://www.frontiersin.org/articles/10.3389/fmars.2021.600343/full#supplementary-material

REFERENCES

Ainsworth, T. D., Heron, S. F., Ortiz, J. C., Mumby, P. J., Grech, A., Ogawa, D., et al. (2016). Climate change disables coral bleaching protection on the Great Barrier Reef. *Science* 352, 338–342. doi: 10.1126/science.aac7125

Altschul, S. F., Gish, W., Miller, W., Myers, E. W., and Lipman, D. J. (1990). Basic local alignment search tool. *J. Mol. Biol.* 215, 403–410.

Andrew, S. M., Morell, H. T., Strzepek, R. F., Boyd, P. W., and Ellwood, M. J. (2019). Iron availability influences the tolerance of Southern Ocean phytoplankton to warming and elevated irradiance. *Front. Mar. Sci.* 6:681. doi: 10.3389/fmars.2019.00681

Angilletta, M. (2009). *Thermal acclimation. Thermal Adaptation: A Theoretical and Empirical Synthesis*. Oxford: Oxford University Press, 126–156.

Anning, T., Harris, G., and Geider, R. J. (2001). Thermal acclimation in the marine diatom Chaetoceros calcitrans (*Bacillariophyceae*). *Eur. J. Phycol.* 36, 233–241. doi: 10.1080/09670260110001735388

Baker, K. G., Radford, D. T., Evenhuis, C., Kuzhiumparam, U., Ralph, P. J., and Doblin, M. A. (2018). Thermal niche evolution of functional traits in a tropical marine phototroph. *J. Phycol.* 54, 799–810. doi: 10.1111/jpy.12759

Barton, K., and Barton, M. K. (2015). *Package 'MuMIn'. Version 1, 18*.

Bartosiewicz, M., Przytulska, A., Deshpande, B. N., Antoniades, D., Cortes, A., MacIntyre, S., et al. (2019). Effects of climate change and episodic heat events on cyanobacteria in a eutrophic polymictic lake. *Sci. Total Environ.* 693:133414. doi: 10.1016/j.scitotenv.2019.07.220

Bates, D., Mächler, M., Bolker, B., and Walker, S. (2014). Fitting linear mixed-effects models using lme4. *arXiv* [Preprint]. Avaliable at: https://arxiv.org/abs/1406.5823 (accessed April 1, 2020).

Bedolfe, S. (2015). *Heatwaves Decrease Production in Benthic Diatom Communities*. Faculty of Science and Engineering. Groningen

Bernhardt, J. R., Sunday, J. M., Thompson, P. L., and O'connor, M. I. (2018). Nonlinear averaging of thermal experience predicts population growth rates in a thermally variable environment. *Proc. R. Soc. B Biol. Sci.* 285:20181076. doi: 10.1098/rspb.2018.1076

Bowler, K. (2005). Acclimation, heat shock and hardening. *J. Therm. Biol.* 30, 125–130. doi: 10.1016/j.jtherbio.2004.09.001

Boyd, P., Dillingham, P., Mcgraw, C., Armstrong, E. A., Cornwall, C. E., Feng, Y.-Y., et al. (2016). Physiological responses of a Southern Ocean diatom to complex future ocean conditions. *Nat. Clim. te Change* 6, 207–213. doi: 10.1038/nclimate2811

Boyd, P. W. (2019). Physiology and iron modulate diverse responses of diatoms to a warming Southern Ocean. *Nat. Clim. Change* 9, 148–152. doi: 10.1038/s41558-018-0389-1

Boyd, P. W., Rynearson, T. A., Armstrong, E. A., Fu, F., Hayashi, K., Hu, Z., et al. (2013). Marine phytoplankton temperature versus growth responses from polar to tropical waters–outcome of a scientific community-wide study. *PLoS One* 8:e63091. doi: 10.1371/journal.pone.0063091

Brand, L. E., Guillard, R. R., and Murphy, L. S. (1981). A method for the rapid and precise determination of acclimated phytoplankton reproduction rates. *J. Plankton Res.* 3, 193–201. doi: 10.1093/plankt/3.2.193

Britton, D., Schmid, M., Noisette, F., Havenhand, J. N., Paine, E., McGraw, C. M., et al. (2020). Adjustments in fatty acid composition is a mechanism that can explain resilience to marine heatwaves and future ocean conditions in the habitat-forming seaweed Phyllospora comosa (Labillardière) C. Agardh. *Glob. Change Biol.* 26, 1–13.

Burton, V., Mitchell, H. K., Young, P., and Petersen, N. S. (1988). Heat shock protection against cold stress of *Drosophila melanogaster*. *Mol. Cell. Biol.* 8, 3550–3552. doi: 10.1128/mcb.8.8.3550

Clapp, D. F., Bhagwat, Y., and Wahl, D. H. (1997). The effect of thermal stress on walleye fry and fingerling mortality. *N. Am. J. Fish. Manag.* 17, 429–437. doi: 10.1577/1548-8675(1997)017<0429:teotso>2.3.co;2

Coello-Camba, A., and Agustí, S. (2017). Thermal thresholds of phytoplankton growth in polar waters and their consequences for a warming polar ocean. *Front. Mar. Sci.* 4:168. doi: 10.3389/fmars.2017.00168

Coleman, M. A., Minne, A. J., Vranken, S., and Wernberg, T. (2020). Genetic tropicalisation following a marine heatwave. *Sci. Rep.* 10, 1–11.

Collins, S., Boyd, P. W., and Doblin, M. A. (2020). Evolution, microbes, and changing ocean conditions. *Annu. Rev. Mar. Sci.* 12, 181–208. doi: 10.1146/annurev-marine-010318-095311

Deppeler, S. L., and Davidson, A. T. (2017). Southern Ocean phytoplankton in a changing climate. *Front. Mar. Sci.* 4:40. doi: 10.3389/fmars.2017.00040

Eakin, C. M., Morgan, J. A., Heron, S. F., Smith, T. B., Liu, G., Alvarez-Filip, L., et al. (2010). Caribbean corals in crisis: record thermal stress, bleaching, and mortality in 2005. *PLoS One* 5:e13969. doi: 10.1371/journal.pone.0013969

Feijão, E., Gameiro, C., Franzitta, M., Duarte, B., Caçador, I., Cabrita, M. T., et al. (2018). Heat wave impacts on the model diatom *Phaeodactylum tricornutum*: searching for photochemical and fatty acid biomarkers of thermal stress. *Ecol. Ind.* 95, 1026–1037. doi: 10.1016/j.ecolind.2017.07.058

Frölicher, T. L., Fischer, E. M., and Gruber, N. (2018). Marine heatwaves under global warming. *Nature* 560, 360–364. doi: 10.1038/s41586-018-0383-9

Frölicher, T. L., and Laufkötter, C. (2018). Emerging risks from marine heat waves. *Nat. Commun.* 9:650.

Garrison, H. S., and Tang, K. W. (2014). Effects of episodic turbulence on diatom mortality and physiology, with a protocol for the use of Evans Blue stain for live-dead determinations. Hydrobiologia, 738, 155–170.

Geider, R. J., Moore, C. M., and Ross, O. N. (2009). The role of cost–benefit analysis in models of phytoplankton growth and acclimation. *Plant Ecol. Divers.* 2, 165–178. doi: 10.1080/17550870903300949

Godhe, A., and Rynearson, T. (2017). The role of intraspecific variation in the ecological and evolutionary success of diatoms in changing environments. *Philos. Trans. R. Soc. B Biol. Sci.* 372:20160399. doi: 10.1098/rstb.2016.0399

Goto, S. G., and Kimura, M. T. (1998). Heat-and cold-shock responses and temperature adaptations in subtropical and temperate species of *Drosophila*. *J. Insect Physiol.* 44, 1233–1239. doi: 10.1016/s0022-1910(98)00101-2

Guillard, R. R. (1975). Culture of phytoplankton for feeding marine invertebrates. in *Culture of marine invertebrate animals* 29–60. Springer, Boston, MA.

Hayashida, H., Matear, R. J., and Strutton, P. G. (2020). Background nutrient concentration determines phytoplankton bloom response to marine heatwaves. *Glob. Change Biol.* 26, 4800–4811. doi: 10.1111/gcb.15255

Hobday, A. J., Alexander, L. V., Perkins, S. E., Smale, D., Straub, S., Oliver, E. C. J., et al. (2016). A hierarchical approach to defining marine heatwaves. *Prog. Oceanogr.* 141, 227–238. doi: 10.1016/j.pocean.2015.12.014

Huey, R. B., and Bennett, A. F. (1990). Physiological adjustments to fluctuating thermal environments: an ecological and evolutionary perspective. *Stress Proteins Biol. Med.* 1, 37–59.

Hughes, T. P., Kerry, J. T., Connolly, S. R., Baird, A. H., Eakin, C. M., Eakin, S. E., et al. (2019). Ecological memory modifies the cumulative impact of recurrent climate extremes. *Nat. Clim. Change* 9, 40–43. doi: 10.1038/s41558-018-0351-2

Jin, P., and Agustí, S. (2018). Fast adaptation of tropical diatoms to increased warming with trade-offs. *Sci. Rep.* 8, 1–10.

Jones, T., Parrish, J. K., Peterson, W. T., Bjorkstedt, E. P., Bond, N. A., Ballance, L. T., et al. (2018). Massive mortality of a planktivorous seabird in response to a marine heatwave. *Geophys. Res. Lett.* 45, 3193–3202. doi: 10.1002/2017gl076164

Kingsolver, J. G., and Woods, H. A. (2016). Beyond thermal performance curves: modeling time-dependent effects of thermal stress on ectotherm growth rates. *Am. Nat.* 187, 283–294. doi: 10.1086/684786

Krebs, R. A., and Feder, M. E. (1997). Deleterious consequences of Hsp70 overexpression in Drosphilla melanogaster larvae. *Cell Stress Chaperones* 2, 60–71. doi: 10.1379/1466-1268(1997)002<0060:dcohoi>2.3.co;2

Kremer, C. T. (2020). *growthTools: Tools for Analyzing Time Series of Microbial Abundances to Estimate Growth Rates. R Package Version 0.1.2*.

Kremer, C. T., Fey, S. B., Arellano, A. A., and Vasseur, D. A. (2018). Gradual plasticity alters population dynamics in variable environments: thermal acclimation in the green alga *Chlamydomonas reinhartdii*. *Proc. R. Soc. B Biol. Sci.* 285:20171942. doi: 10.1098/rspb.2017.1942

Kronholm, I., and Ketola, T. (2018). Effects of acclimation time and epigenetic mechanisms on growth of Neurospora in fluctuating environments. *Heredity* 121, 327–341. doi: 10.1038/s41437-018-0138-2

Lesser, M. P. (2006). Oxidative stress in marine environments: biochemistry and physiological ecology. *Annu. Rev. Physiol.* 68, 253–278. doi: 10.1146/annurev.physiol.68.040104.110001

Leung, P. T., Yi, A. X., Ip, J. C., Mak, S. S., and Leung, K. M. (2017). Photosynthetic and transcriptional responses of the marine diatom *Thalassiosira pseudonana* to the combined effect of temperature stress and copper exposure. *Mar.Pollut. Bull.* 124, 938–945. doi: 10.1016/j.marpolbul.2017.03.038

Lindberg, R. T., and Collins, S. (2020). Quality–quantity trade-offs drive functional trait evolution in a model microalgal 'climate change winner'. *Ecol. Lett.* 23, 780–790. doi: 10.1111/ele.13478

Listmann, L., Leroch, M., Schlüter, L., Thomas, M. K., and Reusch, T. B. (2016). Swift thermal reaction norm evolution in a key marine phytoplankton species. *Evol. Appl.* 9, 1156–1164. doi: 10.1111/eva.12362

Low, J. S., Chew, L. L., Ng, C. C., Goh, H. C., Lehette, P., and Chong, V. C. (2018). Heat shock response and metabolic stress in the tropical estuarine copepod Pseudodiaptomus annandalei converge at its upper thermal optimum. *J. Therm. Biol.* 74, 14–22. doi: 10.1016/j.jtherbio.2018.02.012

Lugo, S. C. M., Baumeister, M., Nour, O. M., Wolf, F., Stumpp, M., and Pansch, C. (2020). Warming and temperature variability determine the performance of two invertebrate predators. *Sci. Rep.* 10, 1–14. doi: 10.1002/9781444300932.ch1

Luhring, T. M., and DeLong, J. P. (2017). Scaling from metabolism to population growth rate to understand how acclimation temperature alters thermal performance. *Integr. Comp. Biol.* 57, 103–111. doi: 10.1093/icb/icx041

Lyon, B., Barnston, A. G., Coffel, E., and Horton, R. M. (2019). Projected increase in the spatial extent of contiguous US summer heat waves and associated attributes. *Environ. Res. Lett.* 14:114029. doi: 10.1088/1748-9326/ab4b41

Madeira, D., Narciso, L., Cabral, H., Vinagre, C., and Diniz, M. (2013). Influence of temperature in thermal and oxidative stress responses in estuarine fish. *Comp. Biochem. Physiol. Part A Mol. Integr. Physiol.* 166, 237–243. doi: 10.1016/j.cbpa.2013.06.008

Magozzi, S., and Calosi, P. (2015). Integrating metabolic performance, thermal tolerance, and plasticity enables for more accurate predictions on species vulnerability to acute and chronic effects of global warming. *Glob. Change Biol.* 21, 181–194. doi: 10.1111/gcb.12695

Marbà, N., and Duarte, C. M. (2010). Mediterranean warming triggers seagrass (Posidonia oceanica) shoot mortality. *Glob. Change Biol.* 16, 2366–2375. doi: 10.1111/j.1365-2486.2009.02130.x

Medlin, L., Elwood, H. J., Stickel, S., and Sogin, M. L. (1988). The characterization of enzymatically amplified eukaryotic 16S-like rRNA-coding regions. *Gene* 71, 491–499. doi: 10.1016/0378-1119(88)90066-2

Mock, T., Otillar, R. P., Strauss, J., McMullan, M., Paajanen, P., Schmutz, J., et al. (2017). Evolutionary genomics of the cold-adapted diatom *Fragilariopsis cylindrus*. *Nature* 541, 536–540.

Montie, S., Thomsen, M. S., Rack, W., and Broady, P. A. (2020). Extreme summer marine heatwaves increase chlorophyll a in the Southern Ocean. *Antarct. Sci.* 32, 1–2.

O'Donnell, D. R., Hamman, C. R., Johnson, E. C., Kremer, C. T., Klausmeier, C. A., and Litchman, E. (2018). Rapid thermal adaptation in a marine diatom reveals constraints and trade-offs. *Glob. Change Biol.* 24, 4554–4565. doi: 10.1111/gcb.14360

Oliver, E. C., Burrows, M. T., Donat, M. G., Sen Gupta, A., Alexander, L. V., Perkins-Kirkpatrick, S. E., et al. (2019). Projected marine heatwaves in the 21st century and the potential for ecological impact. *Front. Mar. Sci.* 6:734. doi: 10.3389/fmars.2019.00734

Padfield, D., Yvon-Durocher, G., Buckling, A., Jennings, S., and Yvon-Durocher, G. (2016). Rapid evolution of metabolic traits explains thermal adaptation in phytoplankton. *Ecol. Lett.* 19, 133–142. doi: 10.1111/ele.12545

Pancic, M., Hansen, P. J., Tammilehto, A., and Lundholm, N. (2015). Resilience to temperature and pH changes in a future climate change scenario in six strains of the polar diatom *Fragilariopsis cylindrus*. *Biogeosciences* 12, 4235–4244. doi: 10.5194/bg-12-4235-2015

Pansch, C., Scotti, M., Barboza, F. R., Al-Janabi, B., Brakel, J., Briski, E., et al. (2018). Heat waves and their significance for a temperate benthic community: a near-natural experimental approach. *Glob. Change Biol.* 24, 4357–4367. doi: 10.1111/gcb.14282

Pargana, A., Musacchia, F., Sanges, R., Russo, M. T., Ferrante, M. I., Bowler, C., et al. (2020). Intraspecific diversity in the cold stress response of transposable elements in the diatom *Leptocylindrus aporus*. *Genes* 11:9. doi: 10.3390/genes11010009

Peña, M. A., Nemcek, N., and Robert, M. (2019). Phytoplankton responses to the 2014–2016 warming anomaly in the northeast subarctic Pacific Ocean. *Limnol. Oceanogr.* 64, 515–525. doi: 10.1002/lno.11056

Piatt, J. F., Parrish, J. K., Renner, H. M., Schoen, S. K., Jones, T. T., Arimitsu, M. L., et al. (2020). Extreme mortality and reproductive failure of common murres resulting from the northeast Pacific marine heatwave of 2014-2016. *PLoS One* 15:e0226087. doi: 10.1371/journal.pone.0226087

R Core Team (2019). *R: A Language and Environment for Statistical Computing*. Vienna: R Foundation for Statistical Computing.

Remy, M., Hillebrand, H., and Flöder, S. (2017). Stability of marine phytoplankton communities facing stress related to global change: Interactive effects of heat waves and turbidity. *J. Exp. Mar. Biol. Ecol.* 497, 219–229. doi: 10.1016/j.jembe.2017.10.002

Rhee, G. Y., and Gotham, I. J. (1981). The effect of environmental factors on phytoplankton growth: temperature and the interactions of temperature with nutrient limitation 1. *Limnol. Oceanogr.* 26, 635–648. doi: 10.4319/lo.1981.26.4.0635

Roberts, S. D., Van Ruth, P., Wilkinson, C., Bastianello, S. B., and Bansemer, M. S. (2019). Marine heatwave, harmful algae blooms and an extensive fish kill event during 2013 in South Australia. *Front. Mar. Sci.* 6:610. doi: 10.3389/fmars.2019.00610

Robinson, S. A., Klekociuk, A. R., King, D. H., Rojas, M. P., Zúñiga, G. E., and Bergstrom, D. M. (2020). The 2019/2020 summer of Antarctic heatwaves. *Glob. Change Biol.* 26, 1–3.

Rohini, P., Rajeevan, M., and Mukhopadhay, P. (2019). Future projections of heat waves over India from CMIP5 models. *Clim. Dyn.* 53, 975–988. doi: 10.1007/s00382-019-04700-9

Rousch, J. M., Bingham, S. E., and Sommerfeld, M. R. (2004). Protein expression during heat stress in thermo-intolerant and thermo-tolerant diatoms. *J. Exp. Mar. Biol. Ecol.* 306, 231–243. doi: 10.1016/j.jembe.2004.01.009

Ryan, J., Kudela, R., Birch, J., Blum, M., Bowers, H., Chavez, F. P., et al. (2017). Causality of an extreme harmful algal bloom in Monterey Bay, California, during the 2014–2016 northeast Pacific warm anomaly. *Geophys. Res. Lett.* 44, 5571–5579. doi: 10.1002/2017gl072637

Saha, M., Barboza, F. R., Somerfield, P. J., Al-Janabi, B., Beck, M., Brakel, J., et al. (2019). Response of foundation macrophytes to near-natural simulated marine heatwaves. *Glob. Change Biol.* 26, 417–430. doi: 10.1111/gcb.14801

Samuels, T., Rynearson, T. A., and Collins, S. (2020). Surviving heatwaves: thermal experience predicts life and death in a Southern Ocean diatom. *bioRxiv* [Preprint]. doi: 10.1101/2020.08.25.264028

Sasaki, M. C., and Dam, H. G. (2019). Integrating patterns of thermal tolerance and phenotypic plasticity with population genetics to improve understanding of vulnerability to warming in a widespread copepod. *Glob. Change Biol.* 25, 4147–4164. doi: 10.1111/gcb.14811

Scharf, I., Galkin, N., and Halle, S. (2015). Disentangling the consequences of growth temperature and adult acclimation temperature on starvation and thermal tolerance in the red flour beetle. *Evol. Biol.* 42, 54–62. doi: 10.1007/s11692-014-9298-z

Scharf, I., Wexler, Y., Macmillan, H. A., Presman, S., Simson, E., and Rosenstein, S. (2016). The negative effect of starvation and the positive effect of mild thermal stress on thermal tolerance of the red flour beetle. *Tribolium castaneum. Sci. Nat.* 103:20.

Schaum, C.-E., Buckling, A., Smirnoff, N., Studholme, D., and Yvon-Durocher, G. (2018). Environmental fluctuations accelerate molecular evolution of thermal tolerance in a marine diatom. *Nat. Commun.* 9, 1–14. doi: 10.1016/j.marmicro.2007.05.002

Schaum, E., Rost, B., Millar, A. J., and Collins, S. (2013). Variation in plastic responses of a globally distributed picoplankton species to ocean acidification. *Nat. Clim. Change* 3, 298–302. doi: 10.1038/nclimate1774

Schroda, M., Hemme, D., and Mühlhaus, T. (2015). The Chlamydomonas heat stress response. *Plant J.* 82, 466–480.

Schulte, P. M., Healy, T. M., and Fangue, N. A. (2011). Thermal performance curves, phenotypic plasticity, and the time scales of temperature exposure. *Integr. Comp. Biol.* 51, 691–702. doi: 10.1093/icb/icr097

Seebacher, F., Ducret, V., Little, A. G., and Adriaenssens, B. (2015). Generalist–specialist trade-off during thermal acclimation. *R. Soc. Open Sci.* 2:140251. doi: 10.1098/rsos.140251

Short, J., Foster, T., Falter, J., Kendrick, G. A., and Mcculloch, M. T. (2015). Crustose coralline algal growth, calcification and mortality following a marine heatwave in Western Australia. *Cont. Shelf Res.* 106, 38–44.

Siegel, P., Baker, K. G., Low-Décarie, E., and Geider, R. J. (2020).) High predictability of direct competition between marine diatoms under different temperatures and nutrient states. *Ecol. Evol.* 10, 7276–7290.

Siegle, M. R., Taylor, E. B., and O'connor, M. I. (2018). Prior heat accumulation reduces survival during subsequent experimental heat waves. *J. Exp. Mar. Biol. Ecol.* 501, 109–117.

Smale, D. A., Wernberg, T., Oliver, E. C., Thomsen, M., Harvey, B. P., Straub, S. C., et al. (2019). Marine heatwaves threaten global biodiversity and the provision of ecosystem services. *Nat. Clim. Change* 9, 306–312.

Sokolova, I. M., Frederich, M., Bagwe, R., Lannig, G., and Sukhotin, A. A. (2012). Energy homeostasis as an integrative tool for assessing limits of environmental stress tolerance in aquatic invertebrates. *Mar. Environ. Res.* 79, 1–15.

Sørensen, J. G., Loeschcke, V., and Kristensen, T. N. (2013). Cellular damage as induced by high temperature is dependent on rate of temperature change–investigating consequences of ramping rates on molecular and organismal phenotypes in *Drosophila melanogaster*. *J. Exp. Biol.* 216, 809–814.

Staehr, P. A., and Birkeland, M. J. (2006). Temperature acclimation of growth, photosynthesis and respiration in two mesophilic phytoplankton species. *Phycologia* 45, 648–656.

Strock, J. S., and Menden-Deuer, S. (2020). Temperature acclimation alters phytoplankton growth and production rates. *Limnol. Oceanogr.* 9999, 1–13.

Stuhr, M., Reymond, C. E., Rieder, V., Hallock, P., Rahnenführer, J., Westphal, H., et al. (2017). Reef calcifiers are adapted to episodic heat stress but vulnerable to sustained warming. *PLoS One* 12:e0179753. doi: 10.1371/journal.pone.0179753

Thomas, M. K., Aranguren-Gassis, M., Kremer, C. T., Gould, M. R., Anderson, K., Klausmeier, C. A., et al. (2017). Temperature–nutrient interactions exacerbate sensitivity to warming in phytoplankton. *Glob. Change Biol.* 23, 3269–3280.

Thomas, M. K., Kremer, C. T., Klausmeier, C. A., and Litchman, E. (2012). A global pattern of thermal adaptation in marine phytoplankton. *Science* 338, 1085–1088.

Viant, M., Werner, I., Rosenblum, E., Gantner, A., Tjeerdema, R., and Johnson, M. (2003). Correlation between heat-shock protein induction and reduced metabolic condition in juvenile steelhead trout (*Oncorhynchus mykiss*) chronically exposed to elevated temperature. *Fish Physiol. Biochem.* 29, 159–171.

von Biela, V. R., Arimitsu, M. L., Piatt, J. F., Heflin, B., Schoen, S. K., Trowbridge, J. L., et al. (2019). Extreme reduction in nutritional value of a key forage fish during the Pacific marine heatwave of 2014-2016. *Mar. Ecol. Prog. Ser.* 613, 171–182.

Voolstra, C. R., Buitrago-López, C., Perna, G., Cárdenas, A., Hume, B. C., Rädecker, N., et al. (2020). Standardized short-term acute heat stress assays resolve historical differences in coral thermotolerance across microhabitat reef sites. *Glob. Change Biol.* 26, 4328–4343.

Voznesenskiy, S., Popik, A. Y., Gamayunov, E., Markina, Z. V., and Orlova, T. Y. (2016). The dependence of phytoplankton fluorescence on the thermal stress factor. *Biophysics* 61, 73–77.

Wickham, H. (2016). *ggplot2: Elegant Graphics for Data Analysis*. Berlin: Springer.

Wolf, K. K., Hoppe, C. J., and Rost, B. (2018). Resilience by diversity: Large intraspecific differences in climate change responses of an Arctic diatom. *Limnol. Oceanogr.* 63, 397–411.

Xu, K., Fu, F. X., and Hutchins, D. A. (2014). Comparative responses of two dominant Antarctic phytoplankton taxa to interactions between ocean acidification, warming, irradiance, and iron availability. *Limnol. Oceanogr.* 59, 1919–1931.

Zeugin, J. A., and Hartley, J. L. (1985). Ethanol precipitation of DNA. *Focus* 7, 1–2.

Zhang, Y., Klapper, R., Lohbeck, K. T., Bach, L. T., Schulz, K. G., Reusch, T. B., et al. (2014). Between-and within-population variations in thermal reaction norms of the coccolithophore Emiliania huxleyi. *Limnol. Oceanogr.* 59, 1570–1580.

Zuur, A., Ieno, E. N., Walker, N., Saveliev, A. A., and Smith, G. M. (2009). *Mixed Effects Models and Extensions in Ecology With R*. Berlin: Springer Science & Business Media.

Conflict of Interest: The authors declare that the research was conducted in the absence of any commercial or financial relationships that could be construed as a potential conflict of interest.

frontiers in Marine Science

BRIEF RESEARCH REPORT
published: 23 March 2021
doi: 10.3389/fmars.2021.660427

The Higher the Needs, the Lower the Tolerance: Extreme Events May Select Ectotherm Recruits With Lower Metabolic Demand and Heat Sensitivity

Jahangir Vajedsamiei[1], Martin Wahl[1], Andrea Lee Schmidt[1], Maryam Yazdanpanahan[2] and Christian Pansch[3]*

[1] Department of Marine Ecology, GEOMAR Helmholtz Centre for Ocean Research Kiel, Kiel, Germany, [2] Faculty of Life Sciences and Biotechnology, Shahid Beheshti University, Tehran, Iran, [3] Department of Environmental and Marine Biology, Åbo Akademi University, Turku, Finland

OPEN ACCESS

Edited by:
Christopher Edward Cornwall, Victoria University of Wellington, New Zealand

Reviewed by:
Jonathon H. Stillman, San Francisco State University, United States
Jenny Marie Booth, King Abdullah University of Science and Technology, Saudi Arabia

***Correspondence:**
Jahangir Vajedsamiei
jahangir.vajedsamiei@gmail.com; jvajedsamiei@geomar.de

Specialty section:
This article was submitted to Global Change and the Future Ocean, a section of the journal Frontiers in Marine Science

Received: *29 January 2021*
Accepted: *02 March 2021*
Published: *23 March 2021*

Citation:
Vajedsamiei J, Wahl M, Schmidt AL, Yazdanpanahan M and Pansch C (2021) The Higher the Needs, the Lower the Tolerance: Extreme Events May Select Ectotherm Recruits With Lower Metabolic Demand and Heat Sensitivity. Front. Mar. Sci. 8:660427. doi: 10.3389/fmars.2021.660427

Ongoing climate warming demands a better understanding of whether or how the ectotherms that evolved in response to fluctuating stress regimes may acquire increased heat tolerance. Using blue mussels, *Mytilus* spp., a globally important and well-studied species, we provide empirical evidence supporting that (i) extremely warm (future) summer conditions may select rare recruits that are more capable of expressing metabolic (feeding and respiration) suppression and recovery in response to daily thermal fluctuations in mild to critical temperature range, (ii) this higher heat tolerance can be mediated by lower baseline metabolic demand, possibly decreasing the risks of heat-induced supply and demand mismatch and its associated stress during thermal fluctuations, and (iii) the capacity to acquire such heat tolerance through acclimation is minor. We discuss our results, methodological limitations and offer a perspective for future research. Further evaluation of mechanistic hypotheses such as the one tested here (based on the role of metabolic demand) is needed to generalize the significance of drivers of fast warm adaptation in ectothermic metazoan populations.

Keywords: acclimation, climate change, energy budget, heatwave, metabolic depression, variability

INTRODUCTION

Marine ectotherms that have evolved in response to fluctuating stress regimes in environments such as shallow habitats can express remarkable suppression and recovery of metabolic performance over successive phases of critical and benign temperatures (Marshall and McQuaid, 1991). Metabolic suppression is expressed as substantial declines in feeding activities followed by partial decreases in aerobic respiration or extensive transition from aerobic to anaerobic respiration (Sokolova and Pörtner, 2001). By suppressing the rate of energy-intensive processes (e.g., feeding and growth), these organisms reduce their demand for metabolic substrates and energy (Schulte et al., 2011). Otherwise, their demands rise sharply with increasing temperature and eventually exceed the capacity to supply the required substrates from internal reserves. The supply capacity is related

to the rates of resource uptake, internal reserve formation, and reserve mobilization (Kooijman, 2010) and is generally less temperature-dependent than the metabolic demand (Pörtner, 2012; Rall et al., 2012; Ritchie, 2018). The heat-induced mismatch between metabolic supply and demand can give rise to internal entropy, stress, and damage, exacerbating organismal performance over time (Pörtner, 2012; Ritchie, 2018). Therefore, metabolic suppression may allow organisms to minimize the negative impacts of critical temperatures during short-term (e.g., daily) thermal fluctuations (Vajedsamiei et al., unpublished).

Ongoing ocean warming increases the probability of exposure to high, beyond-optimal temperatures for marine organisms (Brewer et al., 2014). Due to this warming, periods of suppression may become longer while recovery phases may shorten, assuming no change in the temperature fluctuation amplitude and length. Enforcing metabolic suppression in response to more intense or extended periods of high critical temperatures may cause or exacerbate the supply and demand mismatch and its associated stress, limiting an organism's capacity to resume activity during the shortened recovery phases (Vajedsamiei et al., unpublished). Thus, it is crucial to know whether and how exposure to warming trends is associated with increased heat tolerance in the form of elevated thermal thresholds of metabolic suppression or increased capacity for recovery during thermal fluctuations.

Within- and between-generational acclimation to warmer ambient regimes may increase heat tolerance in ectotherm individuals, leading to warm adaptation in some populations (Davenport and Davenport, 2005; Wittmann et al., 2008). For example, acclimation to a stressful event (e.g., heatwave) may functionally prepare or disturb the organism for successive stress events (Walter et al., 2013; Giomi et al., 2016; Bernhardt et al., 2020). Nonetheless, beneficial acclimation capacity may be limited for species from highly fluctuating environments (Stillman, 2003; Somero, 2010; Seebacher et al., 2014) due to a tradeoff in favor of the capacity for metabolic suppression and recovery (McMahon et al., 1995). Additionally, increases in heat tolerance through beneficial genetic mutation alone might not be fast enough to adapt populations to ocean warming (Somero, 2010) as suggested by the observed warming-induced extinctions and changes of biogeographical distributions of species (Barry et al., 1995; Sagarin et al., 1999; Wethey and Woodin, 2008). Finally, emerging evidence suggests that directional selection in favor of heat-tolerant individuals may enforce a shift in a population's mean thermal performance (Logan et al., 2014, 2018; Ma et al., 2014; Gilbert and Miles, 2017). Many marine ectothermic species express their lowest heat-tolerance during the spawning, egg, and larval stages (Pörtner and Farrell, 2008; Nasrolahi et al., 2012). Therefore, in theory, directional selection may be imposed by extreme events on these sensitive life-history stages, a critical phenomenon to investigate since such extreme events are being enforced by climate change (Grant et al., 2017; Al-Janabi et al., 2019).

Whether through directional selection or acclimation, ectothermic individuals or populations may need to acquire lowered metabolic demand to decrease the risks of heat-induced supply and demand mismatch and its associated stress during critically warm phases of thermal fluctuations. This hypothesis also corroborates the *temperature compensation* (Hazel and Prosser, 1974) or *metabolic cold adaptation* (Clarke, 2003) hypotheses proposing that individuals adapted to warmer environments, compared to cold-adapted ones, usually have lower metabolic demand (represented by the respiration rate of non-stressed individuals) at similar benign temperatures. This allows individuals to optimize their metabolic performances according to their local thermal regimes (Le Lann et al., 2011).

Using blue mussels, *Mytilus* spp., an economically and ecologically important species, and a model system for studying metabolic suppression capability of ectotherms, this research evaluates (i) whether extremely warm summer conditions would select for individuals with higher heat tolerance in their daily metabolic suppression and recovery responses and (ii) whether such a potentially warm-adaptive shift in the metabolic responses is linked to lower metabolic demand of the individuals. In a quasi-natural flow-through benthocosm system, mussels from the western Baltic Sea (Kiel Fjord) introduced as juveniles (transplanted organisms) or as larvae (recruited organisms) were grown under the *current* (+0°C) vs. *future* (+4°C) thermal history levels, imposed onto summer 2018 natural temperature regimes. After incubation for 4 months, the performance traits feeding and aerobic respiration were recorded in response to a mild temperature (20.8°C) for 6 h (baseline performance) followed by two 24 h thermal fluctuation cycles with extreme amplitudes (20.8–30.5°C).

The hypotheses of this study were: (i) The warmer thermal history would result in individuals with higher heat tolerance as evidenced by warmer thresholds of metabolic suppression or higher recovery or both responses to daily thermal fluctuation cycles (**Figure 1A**), and (ii) such higher heat tolerance would be mediated by a lower baseline metabolic demand (**Figure 1B**).

MATERIALS AND METHODS

The study organism is the filter feeder *Mytilus edulis trossulus*, the species complex that forms extensive mussel beds in the Baltic Sea (Larsson et al., 2017; Stuckas et al., 2017) where the tidal range is minimal (<few cm). However, ambient temperature regimes fluctuate in time due to daily irradiance variation (by 1–6°C at depths ca. 1 m) or days- to weeks-long weather events (up to 8°C at depths ca. 2 m) (Franz et al., 2019; Pansch and Hiebenthal, 2019). By the end of the 21st century, the average sea surface water temperature is projected to increase by 1.5–4°C in the Baltic Sea (Meier et al., 2012; Gräwe et al., 2013).

Long-Term Incubations and Short-Term Assays

The long-term incubation was conducted as a part of a 4 month community-level study on the effects of warming and upwelling on a Baltic Sea benthic community, including *Fucus* sp., and *Agarophyton vermiculophylla* and the associated grazer species (*Idotea balthica*, *Gammarus* sp., *Littorina littorea* and *Rissoa membranacea*), as well as mussel predators *Asterias rubens* and *Carcinus maenas* (kept in isolated baskets) during summer 2018 (Wahl et al., unpublished; Pansch et al., unpublished). Natural

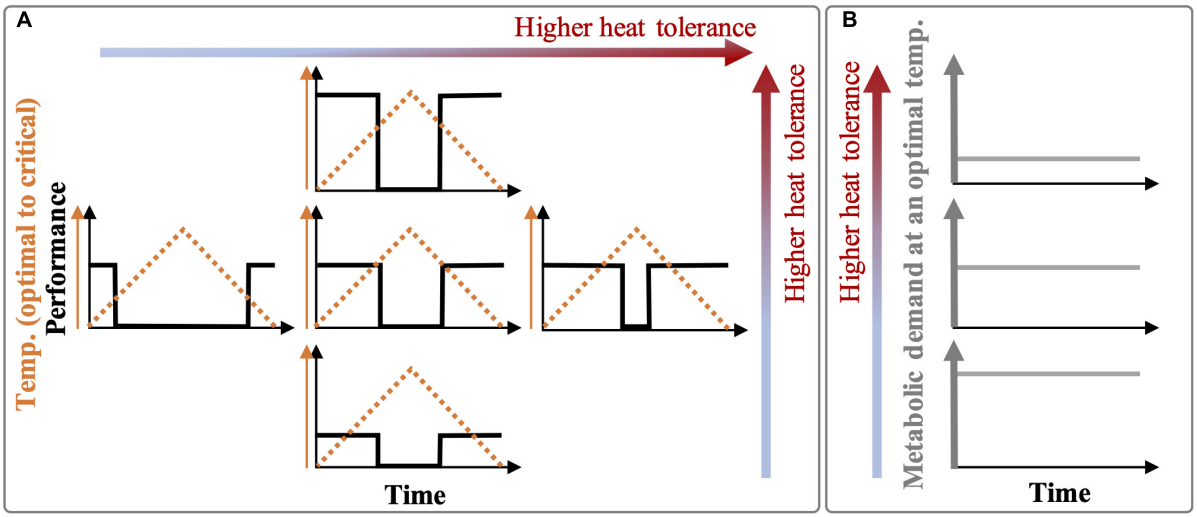

FIGURE 1 | Hypotheses sketch. **(A)** Organisms selected by or acclimated to extreme summer baselines (e.g., prolonged heatwaves) may express higher heat tolerance in the form of (i) higher thermal thresholds of feeding and respiration suppression and recovery (i.e., a broader temperature range for optimal performance; horizontal axis in **A**) or (ii) a generally higher metabolic performance (recovery) at benign phases of thermal fluctuations (vertical axis in **A**), or both. **(B)** Compared to non-selected or non-acclimated individuals, heat-tolerant individuals may have lower metabolic demands (baseline performances) but with a normally high demand/supply ratio (not presented here) under a mild ambient temperature. When an organism's initial thermal performance (middle plot) is maintained over several daily fluctuation cycles, it means that the heat tolerance has not changed over time (i.e., elastic metabolic suppression and recovery in response to thermal fluctuations). However, the initial thermal performance (middle plot) can change over time due to acclimation or stress (plastic responses to fluctuations), resulting in other forms of responses. Notes: To simplify, we assumed there are no gradual thermal changes in the performance due to thermodynamics (Q_{10} effects), and the slope of fast changes in the performance is infinity leading to immediate suppression and recovery.

recruitment of hard- and soft-bottom species was allowed on tank walls, introduced panels, and soft sediment. On May 23, 2018, juvenile mussels (7–13 mm) were collected in 0.5 m water depth from a jetty area (50 m^2) in Kiel Fjord, Germany (54.4330891° N, 10.1711679° E). Batches of 40 specimens were transplanted (transplanted mussels) inside two separate baskets (3 mm^2 pore size and ca. 500 cm^3 volume of each basket) within each 1500 L tank of the Kiel Outdoor Benthocosms (KOBs, located alongside a jetty in the Kiel Fjord; 54.330119° N, 10.149742° E). The KOB system automatically regulated heaters and coolers by commercial aquarium controllers, which allowed accurately simulation of real-time Kiel Fjord (pier) thermal conditions (even daily thermal fluctuations of 1–3°C) as well as warmed (baseline-shifted) regimes within the tanks, as generally described in the protocol by Wahl et al. (2015). Each tank received a flow-through of unfiltered Kiel Fjord seawater (ca. 8,500 L d^{-1}), which allowed near-natural abiotic (salinity, pH, oxygen, and nutrients) and biotic (bacterial load, phytoplankton, and zooplankton) conditions (Wahl et al., 2015).

In two short-term assays, we focused on measuring metabolic performance traits (filtration and respiration) for mussels from the two benthocosm tanks in which we simulated the current fjord temperature and a warmed future-expected thermal regime (hereafter, + 0°C and + 4°C *thermal history* levels). The thermal history regimes and variations of the dissolved oxygen concentration in these two benthocosm tanks during the long-term incubation are presented in **Figure 2A** and **Supplementary Figure 1**, respectively. There was only one benthocosm tank per treatment level (see "Shortcomings and Perspectives" in the section "Results and Discussion"). In the Kiel Fjord, summer 2018 was an extremely warm season, involving two subsequent marine heatwaves (durations of 20 and 26 days) with maximum temperatures reaching 24–25°C for a few days in the whole summer period (Wolf et al., 2020). The 24°C was previously established as the high temperature threshold for initiation of mussels' metabolic suppression in response to short-term (hours-long) warming (Vajedsamiei et al., 2021a; Vajedsamiei et al., unpublished). The +4°C thermal history level represented a future extreme summer regime, which will probably occur by the end of the 21st century (Meier et al., 2012; Gräwe et al., 2013). In this treatment level, the transplants had been exposed for ca. 1 month to temperatures above 24°C (**Figure 2A**). Therefore, the two thermal history levels represent current vs. future extreme summer-time thermal regimes.

We conducted lab assays for two periods. The first assay was performed in the period from August 29 to September 10, during which filtration and respiration of 18 transplanted mussels (from +0°C and +4°C thermal history levels) were recorded in six temporally replicated (independent) trials. In each trial, filtration and respiration of three different specimens, randomly selected from the samples incubated under +0°C and +4°C levels, were recorded in response to a constant mild temperature condition (20.8°C) followed by two 24 h thermal fluctuation cycles (**Figure 2B**) using a Fluorometer- and Oximeter-equipped Flow-through Setup (FOFS; Vajedsamiei et al., 2021a). In each trial, mussel-induced changes in the chlorophyll and dissolved oxygen concentrations were recorded as the difference between measurements taken from three flow-through paths containing

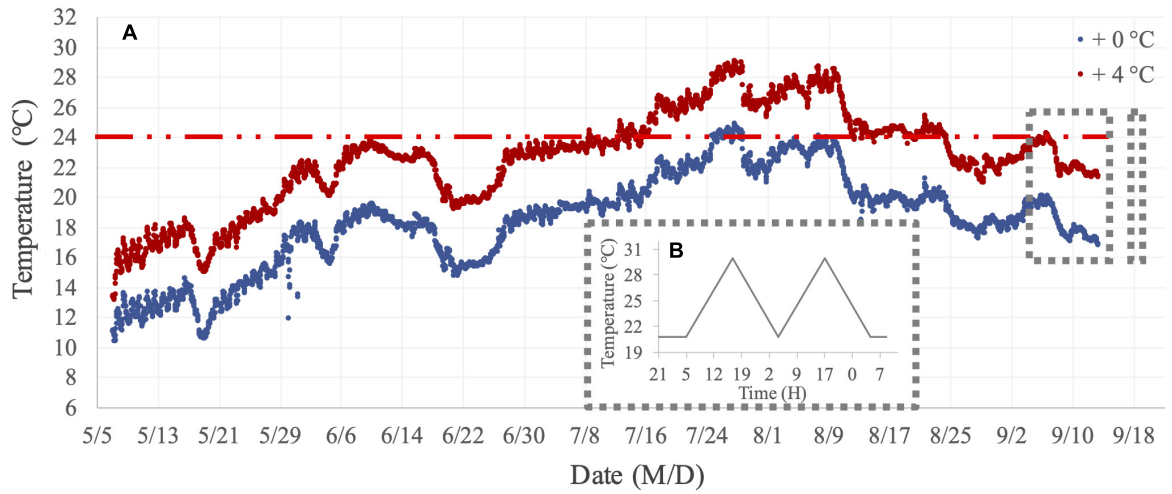

FIGURE 2 | Temperature regimes of the long-term incubation and short-term assays. **(A)** *Thermal history* treatment levels (+0°C and +4°C, above natural Kiel Fjord temperatures) imposed on mussels transplanted or recruited in summer 2018 in the two mesocosm tanks of the Kiel Outdoor Benthocosms (KOBs). **(B)** The assay treatment included the before-fluctuation phase (when mussels were exposed to constantly 20.8°C) and the fluctuation phase when the maximum temperature reached 30.5°C.

mussels and the measurements taken from one mussel-free flow-through path. Minimum and maximum temperatures in the cycles were 20.8 and 30.5°C, respectively, the former representing a current high (ca. the 90-percentile limit) daily thermal average in summer and the latter representing a future daily extreme (Gräwe et al., 2013; Pansch et al., 2018; Franz et al., 2019). During the performance trials, mussels were continuously fed with *Rhodomonas salina*, maintained at the concentration of their surrounding solution (**Supplementary Figure 2**) within the range (1,000–7,000 cells mL^{-1}) needed for mussel's optimal filtration activity (Riisgård et al., 2012).

For the second assay, we collected mussels recruited and grown on baskets located in the KOBs (recruited mussels) on September 12, 2018. Four hundred eighty specimens had recruited under the current thermal history level (+0°C), while 17 were found under the +4°C level. The recruited mussels were kept in filtered seawater at 20°C for five days before the assay. In total, we recorded filtration and respiration rates of six batches of 5 or 6 mussels with similar shell lengths (three batches from each thermal history level) in temporally replicated trials of the same treatment, as explained earlier. Batches were randomly assigned to the repeated trials.

The size traits and assignments of replicates (individuals or batches of mussels) to trials are presented in **Supplementary Table 1**. Mussel dry tissue weights were measured after each assay and later used as proxies for tissue volumes (Hamburger et al., 1983; Riisgård, 2001). The data of the assays are accessible in PANGAEA (Vajedsamiei et al., 2021b).

Initial Data Processing

Data collected in each short-term assay were processed separately. Initial data processing was conducted using Python (Python Software Foundation) based on the scripts and the protocol described in Vajedsamiei et al. (2021a). In short, the initial data processing had two main steps: (i) *Trial-by-trial processing* denoised the time series of dissolved oxygen and Chlorophyll (or cell) concentrations (measured in each trial) using the robust estimation technique, corrected for the effect of temperature, and converted to units of interest. The cell concentration measurement was time-lagged compared to the oxygen measurement, as the Chl sensor was positioned after the oximeter in each path of FOFS. The time lag was corrected using linear differential modeling. The revised time series of the measured variables were then applied to calculate the response variables (i.e., filtration, feeding, and respiration rates), all saved into the respective trial's output data frame. The variables' definitions, as used in the trial-by-trial processing Python script, are provided in **Supplementary Script 1**. (ii) *Integrative processing* scaled filtration and respiration rates for each replicate with respect to the average responses over the before-fluctuation phase and combined the revised output data frames of each assay.

Hypothesis Testing

Statistical hypothesis testing was done in R (R Core Team, 2019) using the packages *mgcv*, *visreg*, and *itsadug* (Breheny and Burchett, 2017; Wood, 2017; van Rij et al., 2020). The testing was done for transplanted and recruited mussels separately.

To test the first hypothesis, we used Generalized Additive Mixed-effect Models (GAMMs) to explain sources of variation in the scaled filtration (potential for feeding) and respiration rates observed during the whole assay. We tested for the significance of the fixed (intercept or average) effect of *thermal history*, the smoothed effect of *time*, and the interactive effect of *thermal history* and *time*. The number of the basis functions (knots) in the GAMMs was chosen to maximize the k-index considering the tradeoff between the models' non-linearity (degree of freedom) and the goodness of fit (Wood, 2017).

To test the second hypothesis, we used GAMMs to explain the sources of variation observed during the before fluctuation phase (at the constant temperature of 20.8°C). The potential for feeding (J h^{-1}), estimated based on the filtration rate at a constant medium food level (3,000 cell mL^{-1}), and the respiration rates (J h^{-1}) were used as the response variables. The number of knots in the GAMMs was restricted to 3, limiting the smooths' maximum allowed non-linearity. Considering all possible sources of variation in the potential for feeding, we tested for the fixed effect of *thermal history*, the smooth effect of *dry tissue weight* (as a measure of body volume), and the smooth effect of *time* and its interactions with *thermal history*. For modeling the respiration rate, besides these factors, we also tested for the smooth effect of *real-time feeding rate* since the feeding rate could have influenced the respiration rate (due to the cost of feeding activities; Secor, 2009). Therefore, in our hypothesis testing, we assumed that the smoothers explaining the responses as functions of *dry tissue weight* or *real-time feeding rate* would be relatively similar for mussels with different thermal histories.

Notably, in all GAMMs, *thermal history* was defined as an *ordered factor* to structure the model in the form of an ANOVA contrast, enabling direct comparison of the reference level smooth (+0°C) with the elevated one (+4°C) (van Rij et al., 2020). As measurements were longitudinal (with temporal dependency), *replicate* was defined as the random intercept factor, and the residual autocorrelation was considered by including a lag-one autoregressive term or *AR(1)* parameter in the GAMMs (Wood, 2017; van Rij et al., 2020). We also used Restricted Maximum Likelihood (REML) for the unbiased estimation of variance components (Wood et al., 2016). After the tests, we checked residuals' normality and independence through QQ and ACF plots, respectively. The general version of the R scripts can be found in **Supplementary Script 2**.

RESULTS AND DISCUSSION

The Future Summer Thermal Extreme Resulted in Rare Recruits of Higher Heat Tolerance

Over the daily cycles of our short-term assays, all transplanted and recruited mussels with different thermal histories (+0°C and +4°C) expressed some levels of metabolic suppression and recovery (**Figure 3**). Their metabolic performance traits, represented by scaled rates of potential for feeding (filtration) and aerobic respiration, were depressed in response to the temperature exceeding a specific threshold range (24–26°C) during the warming phases. The responses recovered to some extent at subsequent exposures to less extreme temperatures (recovery phases).

For recruited mussels, the variation of both metabolic traits was significantly explained by thermal history, as both the intercept (*future–current*) and the smooth term [*s(time):future*] were very significant ($p < 0.0001$; **Supplementary Table 2**). Indeed, compared to the recruits from the colder regime (+0°C), recruited mussels from the warmer regime (+4°C) were better able to restore their respiration and feeding rates during recovery phases to before-fluctuation levels (**Figures 3A,B,E,F**). The thermal thresholds of respiration suppression and recovery were relatively comparable between these two groups of recruited mussels (**Figure 3B**), and so was the threshold of feeding suppression (**Figure 3A**). However, the thermal threshold of feeding recoveries was lower for recruited mussels from +4°C compared to the recruits from +0°C (**Figure 3A**).

Recruitment under the +4°C regime was reduced by ca. 96.5% of what was found in the current regime (+0°C) (see section "Materials and Methods"). Jointly, these findings propose that high selective pressure imposed by the intensified (>24°C) thermal regime on mussels at very early life stages might have resulted in a selection for increased heat tolerance (the capability for metabolic recovery). Most marine ectotherms at the spawning, embryo, and larval stages have the narrowest thermal tolerance window and are most vulnerable to thermal extremes (Pörtner and Farrell, 2008; Nasrolahi et al., 2012).

Instead, for transplanted mussels, thermal history's effects were not significant, both in terms of the intercept (*future–current*) and the smooth [*s(time):future*] ($p > 0.26$; **Supplementary Table 2**). Mussels with different thermal histories, on average, showed very similar metabolic depression or recovery patterns (**Figures 3C,D,G,H**). Additionally, the feeding recovery of these mussels weakened over the short-term assay, probably in response to the critical temperatures. These patterns generally suggest that the studied species have a limited capacity to improve their metabolic performance under critical temperatures through physiological acclimation. Accordingly, at +4°C, growth rates of mussels' shell length, dry shell weight, and dry tissue weight over the summer were ca. 80, 60, and 40% of that found under +0°C (**Supplementary Table 3**). All these findings corroborate previous empirical evidence, suggesting that marine organisms from shallow habitats with pronounced thermal fluctuations generally have a limited capacity to acclimate to warm extreme conditions (Stillman, 2003; Somero, 2010; Seebacher et al., 2014).

Metabolic suppression and recovery, mediated by thermal fluctuations, may allow eurytherms such as mussels to improve their fitness, which may be instead detrimental under constant regimes (Vajedsamiei et al., unpublished). Such refuge effects are more relevant to organisms as ongoing ocean climate warming generally increases the probability of beyond-optimal temperature exposures. Our findings are partly in line with emerging evidence, proposing that extreme events may result in a directional selection of heat-tolerant individuals, which can potentially lead to increases in the populations' mean heat tolerance over generations (Logan et al., 2014, 2018; Ma et al., 2014; Gilbert and Miles, 2017). Yet, selection by one environmental factor may cause cross-tolerance or increased sensitivity to other environmental factors (Al-Janabi et al., 2019). Such selective forces may substantially decrease the recruitment success and population size in time, raising the risks of extinction due to reduced population size and genetic variation (Grant et al., 2017).

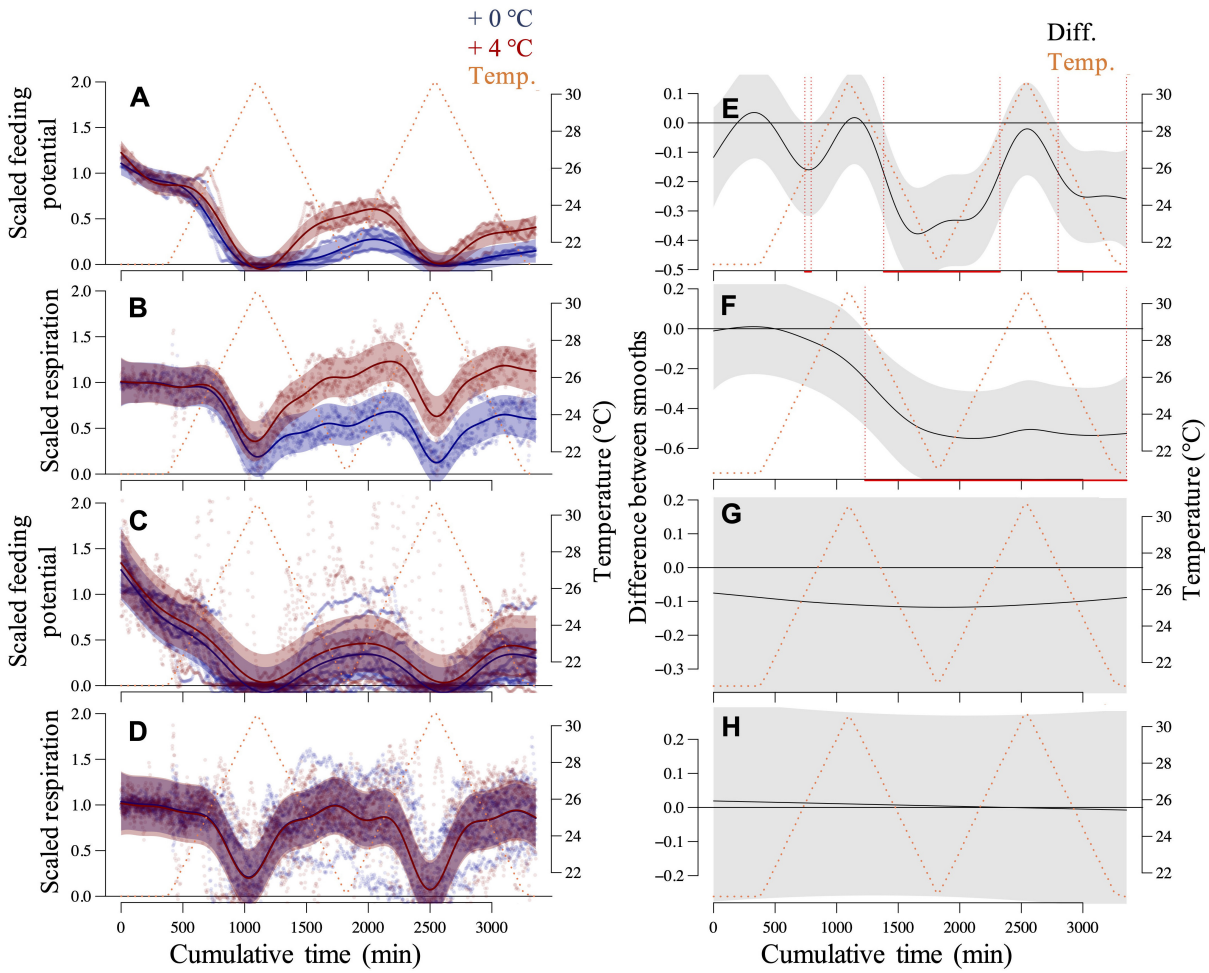

FIGURE 3 | Mussel responses in the short-term assays. Generalized Additive Mixed-effect Models (GAMMs) of the scaled potential for feeding and respiration rates of recruited **(A,B)** and transplanted **(C,D)** mussels over diurnal thermal fluctuation cycles. The specimens experienced a *thermal history* of +0°C and +4°C imposed onto summer 2018 ambient conditions. Responses of single transplanted mussels and the recruited mussels, in groups of 5–6 specimens as a replicate, were assessed using the Fluorometer- and Oximeter-equipped Flow-through Setup (FOFS; Vajedsamiei et al., 2021a). Each replicated time series was normalized concerning the average responses over the before-fluctuation phase. Respective *post hoc* curve comparison plots are presented on the right (**E**–**H**) in which the predictions of the treated-level smoother (+4°C) are subtracted from the reference level smoother (+0°C). Red lines denote the intervals of significant differences between smoothers.

Lower Metabolic Demand Might Have Led to Higher Heat Tolerance in Recruited Mussels

In the before-fluctuation phase, recruited mussels from +4°C showed, on average, significantly lower respiration and potential for feeding (**Figures 4A,B**) as the intercepts (*future–current*) of the models were very significant ($p < 0.0001$; **Supplementary Table 4**). Instead, transplanted mussels from +4°C expressed slightly lower potential for feeding and respiration rates than transplanted mussels from +0°C (**Figures 4C,D**; $p > 0.21$; **Supplementary Table 4**). The ratio of respired energy to energy uptake from feeding (fed energy) can be calculated using the parametric coefficients' "Estimate" values (intercept or averages) presented in **Supplementary Table 4**. The ratios were nearly identical, on average 0.17 vs. 0.19 (J h^{-1}), for the recruited mussels from the +0°C vs. +4°C, respectively. This pattern suggests that the lower metabolic demand (represented by the aerobic respiration) in recruits of the +4°C regime was coupled with the lower supply-to-reserve rate. The latter process is mainly represented by the potential for feeding but can include all processes involved in uptake and transport of metabolic substrates and energy into appropriate internal storage reservoirs (Kooijman, 2010). In contrast, the respired energy to fed energy ratios were on average 0.29 vs. 0.36 (J h^{-1}) for transplanted mussels from the +0°C vs. + 4°C, respectively, suggesting that the heat-treated transplants were more at the risk of heat-induced mismatch of metabolic supply and demand.

These findings suggest that recruits of marine ectotherms with lower metabolic demand (but enough supply rate) may have higher heat tolerance regarding their metabolic responses to transient critical exposures during short-term thermal

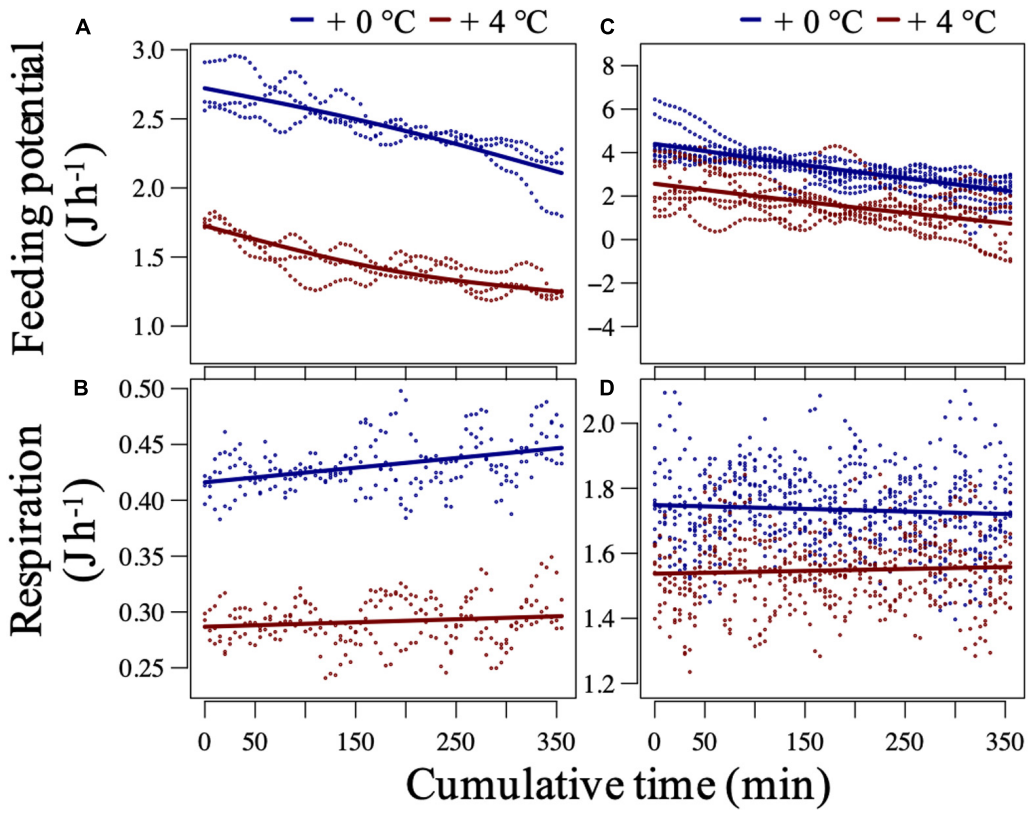

FIGURE 4 | Mussel baseline performance at constantly 20.8°C in the short-term assay. Potential-for-feeding and respiration rates of recruited **(A,B)** and transplanted **(C,D)** mussels at an ambient food concentration ca. Three thousand cells mL^{-1} during the before-fluctuation phase of the short-term assay. The plots are Generalized Additive Mixed-effect Model (GAMM) outputs after setting the median tissue dry weight (and a median feeding rate for predicting the respiration) and a specific replicate level. The dots represent partial residual for each model. For recruited mussels, the fixed effects of thermal history on both responses were significant ($p < 0.001$, adjusted-$R^2 > 0.95$), while for transplanted mussels, the effect was only significant for the potential for feeding ($p = 0.03$ and 0.39, and adjusted-$R^2 = 0.97$ and 0.94, for feeding and respiration, respectively). For tests on the significance of smooth and random effects (**Supplementary Table 2**).

fluctuations. The link between lower metabolic demand and higher heat tolerance can be explained through a heat-induced limitation in marine ectotherms' capacity to supply their demand for metabolic substrates and energy, as discussed in the following.

For individuals of a marine ectotherm population (at a specific life-stage and the whole organism level), thermal dependency (denoted by Q_{10}) is usually higher for the metabolic demand than for the feeding (Rall et al., 2012). Besides, oxygen supply capacity can also become limited at high temperatures (Pörtner, 2012; Verberk et al., 2016; Giomi et al., 2019). At the cellular level, Q_{10} may also be higher for metabolic product formation (or demand) as compared to substrate diffusion and transport processes (or supply) (Ritchie, 2018). For a growing juvenile mussel, for example, a temperature-induced rise in feeding rate (Q_{10} ca. 1.5; Kittner and Riisgård, 2005) may be enough to compensate for a relatively higher increase in energy demand (Q_{10} 2–3; Widdows, 1976; Vajedsamiei et al., unpublished) only if the food resource is sufficiently nutritious. However, after a specific temperature threshold or period of exposure is exceeded, the feeding activities may become too costly, as they usually consume a large portion (ca. 20%) of the whole metabolic expenditure (Widdows and Hawkins, 1989; Secor, 2009). When organisms restrict their supply-to-reserve rate due to the high costs, the supply-from-reserve will become time-limited, meaning that the organisms may become more and more in debt, specifically regarding metabolic substrates and energy. Therefore, in theory, and as our findings suggest, more heat-tolerant ectothermic individuals compared to less tolerant ones would tend to have lower metabolic demand to better control metabolic supply and demand mismatch. The associated debt and stress of such a mismatch would be directly linked to an organism's basic levels of metabolic demand.

Shortcomings and Perspectives

Our short-term assays were conducted as post-incubations to a community-level 4 month long incubation experiment, the results of which are mainly reported in two associated papers (Pansch et al., unpublished; Wahl et al. unpublished; but see also section "Materials and Methods"). The sample size and the level of between-replicate dependency were not ideal in our short-term assays. The number of recruited mussels in the end-of-century treatment level was only 17; therefore, just three replicated time series could be measured for three batches of 5–6 recruited mussels. Additionally, since replicate mussels shared

one benthocosm tank during the summer, we could not exclude (or account for) the confounding effects of between-replicate dependency in the modeling. Nonetheless, some factors could have lowered the dependency of replicate mussels, including the potential difference in their genetics, the large size of the tanks, and the high seawater exchange rate (see section "Materials and Methods"). Notably, the growth and recruitment data collected in the two treatment levels (+0°C and +4°C) fitted well into thermal performance curves which were created using the whole dataset from all six thermal history levels (+0°C to +5°C) of the 4 months long incubation (see **Supplementary Figure 3**), inferring that the mussels under the +4°C regime were mainly impacted by the temperature and no other confounding factors.

Nevertheless, more investigations are needed to support the two general propositions: (i) Extreme seasons (events) select for ectothermic early-stage individuals with more heat-tolerant metabolic performance and (ii) such heat tolerance is due to the lowered metabolic demand enabling these organisms to more efficiently control the mismatch between metabolic supply and demand at high temperatures. In a second step, we must understand if the directional selection of less metabolically demanding recruits can lead to rapid evolutionary warm adaptation of populations of ectothermic benthic metazoans, as recently shown for a microbial alga (Padfield et al., 2016). Such elevated heat resistance may not result in population persistence in response to future warming when it involves a substantial decrease in new cohorts' abundance and genetic diversity. Besides, it remains to be tested if community-level processes may provide refuge from stress effects, such as photosynthetically active organisms providing refuge from thermal stress due to oxygen supply (Giomi et al., 2019).

DATA AVAILABILITY STATEMENT

All data of the assays are archived and accessible in PANGAEA (https://doi.pangaea.de/10.1594/PANGAEA.928922).

AUTHOR CONTRIBUTIONS

JV, MW, and CP designed the study. JV developed the hypotheses and performed the modeling and analyses, and wrote the manuscript. JV, MY, and AS conducted the experiments. All co-authors discussed the results, reviewed and contributed to the final manuscript.

FUNDING

This work and JV were funded through the Deutsche Forschungsgemeinschaft (DFG) project: The neglected role of environmental fluctuations as a modulator of stress and driver of rapid evolution (Grant Number: PA 2643/2/348431475) and through GEOMAR. The project was also supported by EU project Aquacosm—731065 as well as the Cluster of Excellence "The Future Ocean" funded within the framework of the Excellence Initiative by the DFG on behalf of the German federal and state governments. CP was funded by the postdoc program of the Helmholtz- Gemeinschaft Deutscher Forschungszentren and by GEOMAR.

ACKNOWLEDGMENTS

We would like to acknowledge Claas Hiebenthal, KIMOCC, and Ulrike Panknin for providing the *Rhodomonas* culture and technical assistance. We would also like to thank Björn Bucholz for the maintenance of the KOB system and DO measurements during the long-term incubation.

SUPPLEMENTARY MATERIAL

The Supplementary Material for this article can be found online at: https://www.frontiersin.org/articles/10.3389/fmars.2021.660427/full#supplementary-material

REFERENCES

Al-Janabi, B., Wahl, M., Karsten, U., Graiff, A., and Kruse, I. (2019). Sensitivities to global change drivers may correlate positively or negatively in a foundational marine macroalga. *Sci. Rep.* 9:14653. doi: 10.1038/s41598-019-51099-8

Barry, J. P., Baxter, C. H., Sagarin, R. D., and Gilman, S. E. (1995). Climate-related, long-term faunal changes in a California rocky intertidal community. *Science* 267, 672–675. doi: 10.1126/science.267.5198.672

Bernhardt, J. R., O'Connor, M. I., Sunday, J. M., and Gonzalez, A. (2020). Life in fluctuating environments: Adaptation to changing environments. *Philos. Trans. R. Soc. B Biol. Sci.* 375:20190454. doi: 10.1098/rstb.2019.0454rstb20190454

Breheny, P., and Burchett, W. (2017). Visualization of Regression Models Using visreg. *The R Journal.* 9, 56–71.

Brewer, P. G., Fabry, V. J., Hilmi, K., Jung, S., Poloczanska, E., and Sundby, S. (2014). "Chapter 30. The Ocean," in *Climate Change 2014: Impacts, Adaptation, and Vulnerability. Working Group II Contribution to the Fifth Assessment Report of the IPCC: Australasia Intergovernmental Panel on Climate Change*, eds V. R. Barros, C. B. Field, D. J. Dokken, M. D. Mastrandrea, K. J. Mach, T. E. Bilir, et al. (Cambridge: Cambridge University Press), 1–138.

Clarke, A. (2003). Costs and consequences of evolutionary temperature adaptation. *Trends Ecol. Evol.* 18, 573–581. doi: 10.1016/j.tree.2003.08.007

Davenport, J., and Davenport, J. L. (2005). Effects of shore height, wave exposure and geographical distance on thermal niche width of intertidal fauna. *Mar. Ecol. Prog. Ser.* 292, 41–50. doi: 10.3354/meps292041

Franz, M., Lieberum, C., Bock, G., and Karez, R. (2019). Environmental parameters of shallow water habitats in the SW Baltic sea. *Earth Syst. Sci. Data* 11, 947–957. doi: 10.5194/essd-11-947-2019

Gilbert, A. L., and Miles, D. B. (2017). Natural selection on thermal preference, critical thermal maxima and locomotor performance. *Proc. R. Soc. B Biol. Sci.* 284:20170536. doi: 10.1098/rspb.2017.0536

Giomi, F., Barausse, A., Duarte, C. M., Booth, J., Agusti, S., Saderne, V., et al. (2019). Oxygen supersaturation protects coastal marine fauna from ocean warming. *Sci. Adv.* 5, 1–8. doi: 10.1126/sciadv.aax1814

Giomi, F., Mandaglio, C., Ganmanee, M., Han, G. D., Dong, Y. W., Williams, G. A., et al. (2016). The importance of thermal history: Costs and benefits of heat exposure in a tropical, rocky shore oyster. *J. Exp. Biol.* 219, 686–694. doi: 10.1242/jeb.128892

Grant, P. R., Rosemary Grant, B., Huey, R. B., Johnson, M. T. J., Knoll, A. H., and Schmitt, J. (2017). Evolution caused by extreme events. *Philos. Trans. R. Soc. B Biol. Sci.* 372, 5–8. doi: 10.1098/rstb.2016.0146

Gräwe, U., Friedland, R., and Burchard, H. (2013). The future of the western Baltic Sea: Two possible scenarios. *Ocean Dyn.* 63, 901–921. doi: 10.1007/s10236-013-0634-0

Hamburger, K., Møhlenberg, F., Randløv, A., and Riisgård, H. U. (1983). Size, oxygen consumption and growth in the mussel *Mytilus edulis*. *Mar. Biol.* 75, 303–306. doi: 10.1007/BF00406016

Hazel, J. R., and Prosser, C. L. (1974). Molecular mechanisms of temperature compensation in poikilotherms. *Physiol. Rev.* 54, 620–677. doi: 10.1152/physrev.1974.54.3.620

Kittner, C., and Riisgård, H. U. (2005). Effect of temperature on filtration rate in the mussel *Mytilus edulis*: no evidence for temperature compensation. *Mar. Ecol. Progr. Ser.* 305, 147–152.

Kooijman, S. A. L. M. (2010). *Dynamic Energy Budget Theory for Metabolic Organisation*. Cambridge, UK: Cambridge Univ. Press, doi: 10.1098/rstb.2010.0167

Le Lann, C., Wardziak, T., van Baaren, J., and van Alphen, J. J. M. (2011). Thermal plasticity of metabolic rates linked to life-history traits and foraging behaviour in a parasitic wasp. *Funct. Ecol.* 25, 641–651. doi: 10.1111/j.1365-2435.2010.01813.x

Larsson, J., Lind, E. E., Corell, H., Grahn, M., Smolarz, K., and Lönn, M. (2017). Regional genetic differentiation in the blue mussel from the Baltic Sea area. *Estuar. Coast. Shelf Sci.* 195, 98–109. doi: 10.1016/j.ecss.2016.06.016

Logan, C. A., Dunne, J. P., Eakin, C. M., and Donner, S. D. (2014). Incorporating adaptive responses into future projections of coral bleaching. *Glob. Chang. Biol.* 20, 125–139. doi: 10.1111/gcb.12390

Logan, M. L., Curlis, J. D., Gilbert, A. L., Miles, D. B., Chung, A. K., McGlothlin, J. W., et al. (2018). Thermal physiology and thermoregulatory behaviour exhibit low heritability despite genetic divergence between lizard populations. *Proc. R. Soc. B Biol. Sci.* 285:20180697. doi: 10.1098/rspb.2018.0697

Ma, F. Z., Lü, Z. C., Wang, R., and Wan, F. H. (2014). Heritability and evolutionary potential in thermal tolerance traits in the invasive Mediterranean cryptic species of *Bemisia tabaci* (Hemiptera: Aleyrodidae). *PLoS One* 9:1–7. doi: 10.1371/journal.pone.0103279

Marshall, D. J., and McQuaid, C. D. (1991). Metabolic rate depression in a marine pulmonate snail: pre-adaptation for a terrestrial existence? *Oecologia* 88, 274–276. doi: 10.1007/BF00320822

McMahon, R. F., Russell-Hunter, W. D., and Aldridge, D. W. (1995). Lack of metabolic temperature compensation in the intertidal gastropods. Littorina saxatilis (Olivi) and L. obtusata (L.). *Hydrobiologia* 309, 89–100. doi: 10.1007/BF00014475

Meier, H. E. M., Eilola, K., Gustafsson, B. G., Kuznetsov, I., Neumann, T., and Savchuk, O. P. (2012). *Uncertainty Assessment of Projected Ecological Quality Indicators in Future Climate. Rapport Oceanografi No. 112*. Norrköping: SMHI.

Nasrolahi, A., Pansch, C., Lenz, M., and Wahl, M. (2012). Being young in a changing world: how temperature and salinity changes interactively modify the performance of larval stages of the barnacle *Amphibalanus improvisus*. *Mar. Biol.* 159, 331–340. doi: 10.1007/s00227-011-1811-7

Padfield, D., Yvon-Durocher, G., Buckling, A., Jennings, S., and Yvon-Durocher, G. (2016). Rapid evolution of metabolic traits explains thermal adaptation in phytoplankton. *Ecol. Lett.* 19, 133–142. doi: 10.1111/ele.12545

Pansch, C., and Hiebenthal, C. (2019). A new mesocosm system to study the effects of environmental variability on marine species and communities. *Limnol. Oceanogr. Methods* 17, 145–162. doi: 10.1002/lom3.10306

Pansch, C., Scotti, M., Barboza, F. R., Al-Janabi, B., Brakel, J., Briski, E., et al. (2018). Heat waves and their significance for a temperate benthic community: a near-natural experimental approach. *Glob. Chang. Biol.* 24, 4357–4367. doi: 10.1111/gcb.14282

Pörtner, H. (2012). Integrating climate-related stressor effects on marine organisms: unifying principles linking molecule to ecosystem-level changes. *Mar. Ecol. Progr. Ser.* 470, 273–290. doi: 10.3354/meps10123

Pörtner, H. O., and Farrell, A. P. (2008). Physiology and climate change. *Science* 322, 690–692. doi: 10.1126/science.1163156

Rall, B. C., Brose, U., Hartvig, M., Kalinkat, G., Schwarzmüller, F., Vucic-Pestic, O., et al. (2012). Universal temperature and body-mass scaling of feeding rates. *Philos. Trans. R. Soc. B Biol. Sci.* 367, 2923–2934. doi: 10.1098/rstb.2012.0242

R Core Team (2019). *R: A Language and Environment for Statistical Computing*. Vienna: R Foundation for Statistical Computing.

Riisgård, H. U., Lundgreen, K., and Larsen, P. S. (2012). Field data and growth model for mussels *Mytilus edulis* in Danish waters. *Mar. Biol. Res.* 8, 683–700. doi: 10.1080/17451000.2012.678857

Riisgård, H. (2001). On measurement of filtration rate in bivalves-the stony road to reliable data: review and interpretation. *Mar. Ecol. Prog. Ser.* 211, 275–291. doi: 10.3354/meps211275

Ritchie, M. E. (2018). Reaction and diffusion thermodynamics explain optimal temperatures of biochemical reactions. *Sci. Rep.* 8, 1–10. doi: 10.1038/s41598-018-28833-9

Sagarin, R. D., Barry, J. P., Gilman, S. E., and Baxter, C. H. (1999). Climate-related change in an intertidal community over short and long time scales. *Ecol. Monogr.* 69, 465–490. doi: 10.2307/2657226

Schulte, P. M., Healy, T. M., and Fangue, N. A. (2011). Thermal performance curves, phenotypic plasticity, and the time scales of temperature exposure. *Integr. Comp. Biol.* 51, 691–702. doi: 10.1093/icb/icr097

Secor, S. M. (2009). Specific dynamic action: A review of the postprandial metabolic response. *J. Comp. Physiol. B Biochem. Syst. Environ. Physiol.* 179, 1–56. doi: 10.1007/s00360-008-0283-7

Seebacher, F., White, C. R., and Franklin, C. E. (2014). Physiological plasticity increases resilience of ectothermic animals to climate change. *Nat Clim Chang.* 5, 61–66. doi: 10.1038/NCLIMATE2457

Sokolova, I. M., and Pörtner, H. O. (2001). Physiological adaptations to high intertidal life involve improved water conservation abilities and metabolic rate depression in *Littorina saxatilis*. *Mar. Ecol. Prog. Ser.* 224, 171–186. doi: 10.3354/meps224171

Somero, G. N. (2010). The physiology of climate change: how potentials for acclimatization and genetic adaptation will determine "winners" and "losers.". *J. Exp. Biol.* 213, 912–920. doi: 10.1242/jeb.037473

Stuckas, H., Knöbel, L., Schade, H., Breusing, C., Hinrichsen, H. H., Bartel, M., et al. (2017). Combining hydrodynamic modelling with genetics: can passive larval drift shape the genetic structure of Baltic Mytilus populations? *Mol. Ecol.* 26, 2765–2782. doi: 10.1111/mec.14075

Stillman, J. H. (2003). Acclimation capacity underlies susceptibility to climate change. *Science* 301, 65. doi: 10.1126/science.1083073

Vajedsamiei, J., Melzner, F., Raatz, M., Kiko, R., Khosravi, M., and Pansch, C. (2021a). Simultaneous recording of filtration and respiration in marine organisms in response to short-term environmental variability. *Limnol. Oceanogr. Methods* 1–13. doi: 10.1002/lom3.10414

Vajedsamiei, J., Wahl, M., Schmidt, A. L., Yazdanpanahan, M., and Pansch, C. (2021b). FOFS measurements and metabolic performance records for transplants and recruits of *Mytilus* sp. incubated using KOBs in summer 2018. *PANGAEA*. doi: 10.1594/PANGAEA.928922

van Rij, J., Wieling, M., Baayen, R., and van Rijn, H. (2020). *Itsadug: Interpreting Time Series and Autocorrelated Data Using GAMMs. R package version 2.4.*

Verberk, W. C. E. P., Overgaard, J., Ern, R., Bayley, M., Wang, T., Boardman, L., et al. (2016). Does oxygen limit thermal tolerance in arthropods? *A critical Rev. curr. Evidence. Comp. Biochem. Physiol. -Part A Mol. Integr. Physiol.* 192, 64–78. doi: 10.1016/j.cbpa.2015.10.020

Wahl, M., Buchholz, B., Winde, V., Golomb, D., Guy-Haim, T., Müller, J., et al. (2015). A mesocosm concept for the simulation of near-natural shallow underwater climates: the kiel outdoor benthocosms (KOB). *Limnol. Oceanogr. Methods* 13, 651–663. doi: 10.1002/lom3.10055

Walter, J., Jentsch, A., Beierkuhnlein, C., and Kreyling, J. (2013). Ecological stress memory and cross stress tolerance in plants in the face of climate extremes. *Environ. Exp. Bot.* 94, 3–8. doi: 10.1016/j.envexpbot.2012.02.009

Wethey, D. S., and Woodin, S. A. (2008). Ecological hindcasting of biogeographic responses to climate change in the European intertidal zone. *Hydrobiologia* 606, 139–151. doi: 10.1007/s10750-008-9338-8

Widdows, J. (1976). Physiological adaptation of *Mytilus edulis* to cyclic temperatures. *J. Comp. Physiol. B* 105, 115–128. doi: 10.1007/BF00691115

Widdows, J., and Hawkins, A. J. S. (1989). Partitioning of Rate of Heat Dissipation by *Mytilus edulis* into Maintenance. Feeding, and Growth Components. *Physiol. Zool.* 62, 764–784. doi: 10.1086/physzool.62.3.30157926

Wittmann, A. C., Schröer, M., Bock, C., Steeger, H. U., Paul, R. J., and Pörtner, H. O. (2008). Indicators of oxygen- and capacity-limited thermal tolerance

in the lugworm *Arenicola marina*. *Clim. Res.* 37, 227–240. doi: 10.3354/cr00763

Wolf, F., Bumke, K., Wahl, S., Nevoigt, F., Hecht, U., Hiebenthal, C., et al. (2020). *High Resolution Water Temperature Data Between January 1997 and December 2018 at the GEOMAR pier Surface*. Bremen: PANGAEA, doi: 10.1594/PANGAEA.919186

Wood, S. N. (2017). *). Generalized Additive Models: An Introduction with R*, 2nd Edn. Boca Raton FL: CRC.

Wood, S. N., Pya, N., and Säfken, B. (2016). Smoothing parameter and model selection for general smooth models. *J. Am. Stat. Assoc.* 111, 1548–1563. doi: 10.1080/01621459.2016.1180986

Conflict of Interest: The authors declare that the research was conducted in the absence of any commercial or financial relationships that could be construed as a potential conflict of interest.

frontiers in Marine Science

ORIGINAL RESEARCH
published: 15 June 2021
doi: 10.3389/fmars.2021.669508

Detecting Climate Signals in Southern Ocean Krill Growth Habitat

Zephyr T. Sylvester[1], Matthew C. Long[2] and Cassandra M. Brooks[1]*

[1] Environmental Studies Program, University of Colorado Boulder, Boulder, CO, United States, [2] National Center for Atmospheric Research, Boulder, CO, United States

Climate change is rapidly altering the habitat of Antarctic krill (*Euphausia superba*), a key species of the Southern Ocean food web. Krill are a critical element of Southern Ocean ecosystems as well as biogeochemical cycles, while also supporting an international commercial fishery. In addition to trends forced by global-scale, human-driven warming, the Southern Ocean is highly dynamic, displaying large fluctuations in surface climate on interannual to decadal timescales. The dual roles of forced climate change and natural variability affecting Antarctic krill habitat, and therefore productivity, complicate interplay of observed trends and contribute to uncertainty in future projections. We use the Community Earth System Model Large Ensemble (CESM-LE) coupled with an empirically derived model of krill growth to detect and attribute trends associated with "forced," human-driven climate change, distinguishing these from variability arising naturally. The forced trend in krill growth is characterized by a poleward contraction of optimal conditions and an overall reduction in Southern Ocean krill habitat. However, the amplitude of natural climate variability is relatively large, such that the forced trend cannot be formally distinguished from natural variability at local scales over much of the Southern Ocean by 2100. Our results illustrate how natural variability is an important driver of regional krill growth trends and can mask the forced trend until late in the 21st century. Given the ecological and commercial global importance of krill, this research helps inform current and future Southern Ocean krill management in the context of climate variability and change.

Keywords: Southern Ocean, Antarctic krill, climate-change impacts, natural variability, time of emergence, Earth system modeling, marine biology, projection and prediction

OPEN ACCESS

Edited by:
Michael Raatz, Max Planck Institute for Evolutionary Biology, Germany

Reviewed by:
Bettina Meyer, Alfred Wegener Institute Helmholtz Centre for Polar and Marine Research (AWI), Germany
Alexei B. Ryabov, University of Oldenburg, Germany
Stuart Corney, University of Tasmania, Australia
Devi Veytia, Institute for Marine and Antarctic Studies, University of Tasmania, Australia, contributed to the review of Stuart Corney

****Correspondence:***
Zephyr T. Sylvester
zephyr.sylvester@colorado.edu

Specialty section:
This article was submitted to Global Change and the Future Ocean, a section of the journal Frontiers in Marine Science

Received: *19 February 2021*
Accepted: *19 May 2021*
Published: *15 June 2021*

Citation:
Sylvester ZT, Long MC and Brooks CM (2021) Detecting Climate Signals in Southern Ocean Krill Growth Habitat. Front. Mar. Sci. 8:669508. doi: 10.3389/fmars.2021.669508

INTRODUCTION

The Southern Ocean, which surrounds Antarctica, is a critical component of the Earth system and supports a marine ecosystem of immense economic and intrinsic value. It is also among the most sensitive areas to climate change (Hagen et al., 2007) and has already experienced physical changes in ocean temperature, sea-ice dynamics, stratification, and currents (Flores et al., 2012). The cumulative impact of these changes on the marine ecosystem and its primary keystone species, Antarctic krill (*Euphausia superba*), is predicted to increase considerably during the present century (Doney et al., 2012; McBride et al., 2014). However, in addition to trends forced by global-scale, human-driven warming, the Southern Ocean is also subject to highly-dynamic natural climate variability, which can exert important influence on the system on interannual to multi-decadal timescales (Mayewski et al., 2009). This research presents an analysis of the superposition of forced

climate change and natural variability on Antarctic krill habitat. In the context of climate change and the highly dynamic Southern Ocean, the framework we present provides insights that are important for decision makers to consider regarding climate change adaptation strategies.

Antarctic krill (hereafter krill) are at the center of the Southern Ocean food web as well as the target of the largest commercial fishery in the Southern Ocean (Nicol et al., 2012). Krill are a large bodied (up to ∼6 cm), fast swimming, aggregating, zooplankton known as a dominant species in the food web and in biogeochemical cycles (Tarling and Fielding, 2016; Trathan and Hill, 2016; Cavan et al., 2019). Krill are one of the most abundant wild animal species on Earth, with a biomass estimated between 300 and 500 million tons (Nicol and Mangel, 2018). The rate at which krill biomass is produced, or productivity, is central to the success of the ecosystem; thus, changes in krill distribution and abundance have ramifications across the ecosystem (Murphy et al., 2012; Constable et al., 2014; Larsen et al., 2014). A wide variety of Antarctic species feed on krill and they are the main energy pathway connecting primary producers to higher order predators (Quetin and Ross, 2003; Atkinson et al., 2009; Schmidt et al., 2011). Localized industrial fishing efforts, however, are growing rapidly (Nicol et al., 2012) and remove krill biomass in direct competition with krill-dependent species. These ecological and economic activities, however, are situated in the context of a highly dynamic climate system. Climate variability and change has the potential to drive important fluctuations in krill biomass, yielding widespread ecological impacts and causing variations in the definition of sustainable catch. Prediction of climate variability and change is therefore of high importance for effective long-term management of the ecosystem.

Concerns over the ecosystem impacts of growing commercial fishing interest for krill in the 1980s spurred the creation of the Convention on the Conservation of Marine Living Resources (CCAMLR) to govern the Southern Ocean (Nicol et al., 2012). Since the early 2000s human interest in krill has been rising and now represents the largest fishery, by biomass, in the Southern Ocean (Nicol and Foster, 2016). The krill fishery is managed under a mandated precautionary, ecosystem-based approach—including managing for environmental change, and based on the best available science (Constable, 2000). Currently, krill are managed with catch limits that are deemed to be precautionary, however, these limits are set using a stock assessment that does not account for environmental variability or climate change impacts (Constable and Kawaguchi, 2018; Watters et al., 2020). Fisheries compete with natural predators for krill biomass, making coordinated management critical for sustaining the Antarctic marine ecosystem (Meyer et al., 2020; Watters et al., 2020). Variation in climate, however, independently affects krill productivity, yielding bottom-up fluctuations in krill biomass (Atkinson et al., 2019). Effective management of the krill fishery, therefore, depends on sound understanding of climate-driven variations in krill populations. This research is thus motivated to inform this critical gap in management regarding the impacts of natural variability and climate change.

Climate affects krill through direct impacts (e.g., physiological thresholds, habitat use) and indirect impacts such as ecosystem interactions, including impacts on food supply and predation. The influence of natural climate variability is a large factor in understanding krill abundance, distribution, and productivity. However, accurate measurements of krill biomass are sparse, making it difficult to develop mechanistic connections between possible environmental drivers and krill production. In spite of uncertainty regarding specific mechanistic connections, there is broad consensus that krill populations are likely to be impacted by future changes in climate (Murphy et al., 2012; Constable et al., 2014; Rogers et al., 2020; Veytia et al., 2020). Attributing trends in krill production to anthropogenic climate change is challenged by the confounding influence of natural variability on top of limited observational data. The Southern Ocean's natural system is sufficiently dynamic such that important environmental fluctuations are likely even in the absence of human-driven warming.

It is critical to recognize that "climate" is not static, but rather manifests as a superposition of naturally-driven variability and human-driven trends (Hawkins and Sutton, 2009; Deser et al., 2012). Natural climate variability is an intrinsic feature of the earth system; it is attributable to nonlinear dynamical processes and interactions between climate system components that integrate information over different timescales (Hasselmann, 1976). Anthropogenic forcing from human-driven trends, like emissions of heat-trapping gases, externally forces the climate system. The characteristics of the superposition of internal variability on anthropogenic forcing in the Southern Ocean are illustrated by the Westerly Winds that drive the Antarctic Circumpolar Current (Allison et al., 2010) (Locations are referenced in **Figure 1**). The strength and position of the Westerlies naturally fluctuate in association with the Southern Annular Mode (Rogers and van Loon, 1982; Thompson and Wallace, 2000). Human-driven trends are superimposed on this variability: ozone depletion, followed by CO_2-driven warming has resulted in an intensification of the SAM index, a trend that is projected to continue over the next several decades (Fogt and Marshall, 2020; Goyal et al., 2021). Understanding the how, where, and by how much the fluctuations of natural variability may obscure observed trends (Ryabov et al., 2017) in anthropogenic climate change on different timescales is highly important for effective and long term resource management.

In the context of developing future projections, natural climate variability makes important contributions to uncertainty. Determining the uncertainty attributed to the two components of climate variability is a function of time horizons and scale (Commission on Geosciences, Environment, and Resources, Climate Research Committee, National Research Council, and Division on Earth and Life Studies, 1996). Internal variability is often the dominant source of uncertainty at regional scales or over less than two decades. Comparatively anthropogenic forcing is associated with longer-term trends at larger spatial scales (Hawkins and Sutton, 2009). When superimposed, fluctuations in natural variability have the potential to temporarily reverse or partially offset forced trends on interannual to decadal timescales. For example, in the western Atlantic Peninsula (WAP), the long term trend shows significant warming and sea ice loss overall (Henley et al., 2019) while short-term regional observations from

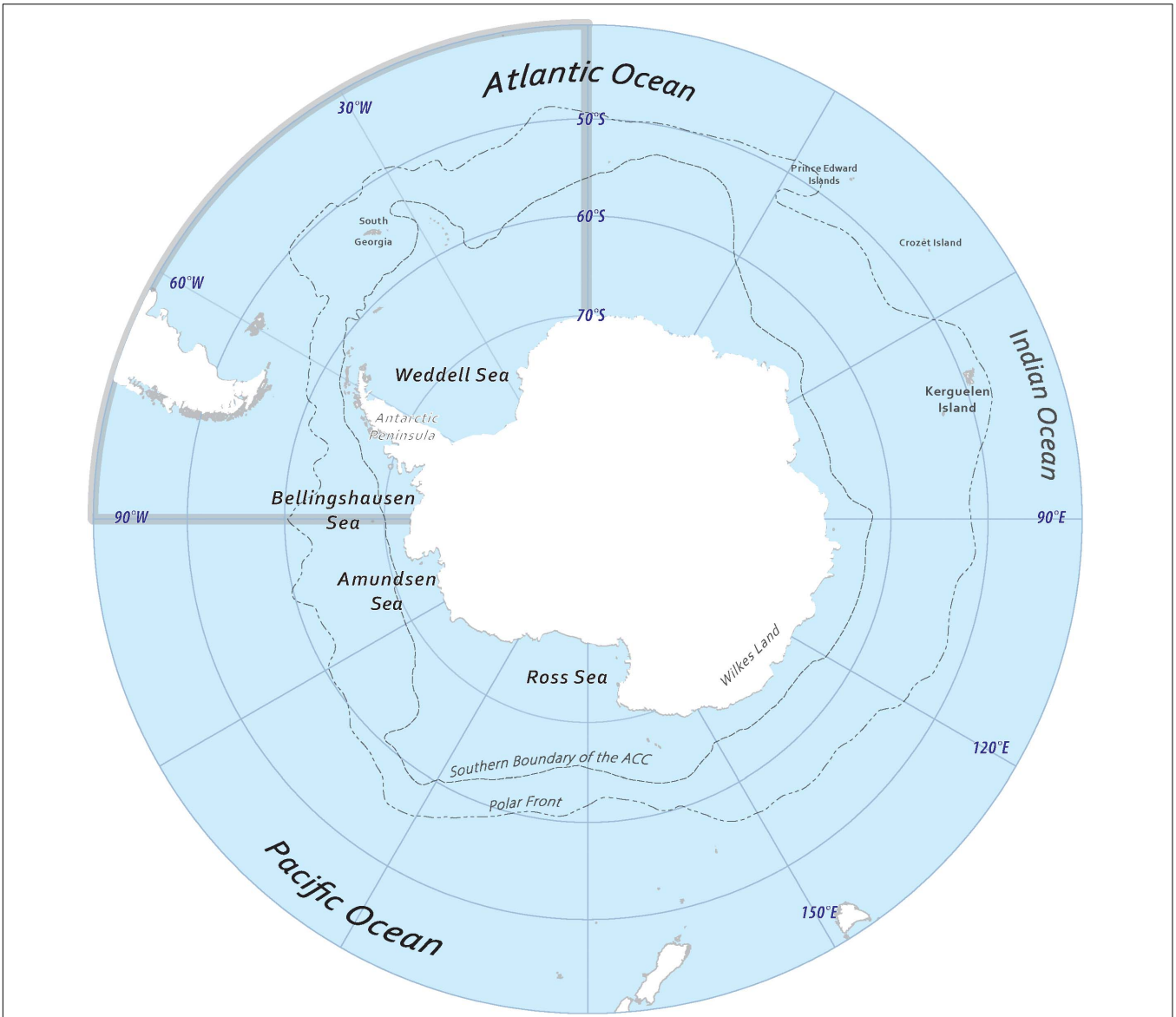

FIGURE 1 | This map illustrates the study area containing the locations and features referenced throughout paper. Notably, the Atlantic quadrant is highlighted in gray as the area between 0° and 90°W. All spatially averaged data is constrained by the 45°S latitude. Figure prepared by ZS, frontal data from Orsi et al. (1995).

the late 1990s and late 2000s showed a trend of increasing sea-ice extent (Stammerjohn et al., 2012). The long-term trend in the WAP was superimposed by significant natural variability in the regional climate resulting in short-term variation in sea ice dynamics (Hobbs et al., 2016; Turner et al., 2016; Stammerjohn and Maksym, 2017). Trends associated with the forced signal are unlikely to be reversed on short timescales or can only be reversed through intervention. Quantifying climate-change related impacts provides fundamental knowledge that can help inform management, including a framework for considering when and where to employ climate mitigation strategies.

Detection and attribution of forced trends must be approached against the backdrop of natural variability (Hawkins, 2011; Deser et al., 2012). Detecting trends and attributing them to forced climate change can be approached as a signal-to-noise problem: the forced trends represent a "signal" and the natural climate variability is "climate noise" (Feldstein, 2000). The forced signal will arise from the envelope of background climate noise if it is sufficiently large for an extended period of time (Hasselmann, 1993; Santer et al., 2011). A climate change signal is easier to detect in a system where the magnitude of the forced trends is large relative to the natural variability. The point in time when the anthropogenic climate change signal can be detected from the noise of internal climate variability is known as the "Time of Emergence" (ToE). Determining the ToE can help us determine if the state of the system is past the expected natural variability as well as what it could mean for the system to start to move outside of the noise of

natural variability (Deser et al., 2012; Hawkins and Sutton, 2012; Bonan and Doney, 2018).

Assessing when expected changes can be detected or if observed changes can be attributed to the forced trend is challenging to address definitively through observational records alone (Deser et al., 2012; Hawkins and Sutton, 2012; Bonan and Doney, 2018). When either observational records are scarce, like in the Southern Ocean, or we want to observe the future, modeling studies can provide insight. Earth system models (ESMs) are climate models that include a variety of ecological processes with the aim of simulating a fully-prognostic global carbon cycle (e.g., Hurrell et al., 2013). While ESMs may have significant biases relative to observations, they are formulated on the basis of physical principles, conserve mass and energy, and are internally consistent. Through the ability to run multiple realizations of the climate system as it transits through different forcing scenarios, ESMs can be used to examine detection and attribution of trends associated with forced climate change. ESMs include ocean biogeochemistry models as a component of the carbon cycle. As ESMs have evolved, there has been increasing recognition of their relevance to questions beyond carbon biogeochemistry, and in particular related to ocean ecosystems in the context of climate variability and change (Stock et al., 2011; Bopp et al., 2013; Tommasi et al., 2017).

Prior research has used outputs from ESMs to explore how changes in Southern Ocean climate will impact regional and circumpolar krill habitat. These studies have mainly used projected changes from multi-model ensembles from the Coupled Model Intercomparison Project Phase 5 (CMIP5) in combination with empirically-derived models (Atkinson et al., 2006; Hill et al., 2013; Piñones and Fedorov, 2016; Veytia et al., 2020). However, these multi-model ensemble studies have not considered the role of naturally occurring internal climate variability. The large-ensemble framework of a single ESM allows for quantification of the uncertainties from internal variability, identifying trends forced by human-driven climate change and identifying when those trends can be formally distinguished from natural variability. This study expands upon the previous work by considering the distinct roles of forced climate change and natural variability in driving fluctuations in krill habitat. Thus, we present an approach to differentiate the impacts of internal variability from forced trends on krill growth rates, also referred to as growth potential (GP).

MATERIALS AND METHODS

Earth System Model

We used output from the Community Earth System Model Large Ensemble (CESM-LE) (Kay et al., 2015). The model configuration included atmosphere, ocean, land, and sea ice component models based on a 1° horizontal integration (Hunke and Lipscomb, 2010; Danabasoglu et al., 2012; Holland et al., 2012; Lawrence et al., 2012). The CESM-LE began with multicentury, 1850-control simulation with constant preindustrial forcing; a single ensemble member was branched off this simulation and integrated from 1850 to 1920, at which point additional members were added. We used 28 members with ocean biogeochemistry output from the CESM-LE integrated over the period from 1920 to 2100, each using the same historical and future-scenario (RCP 8.5; Long et al., 2016) external forcing. Each ensemble member simulation has a unique climate trajectory because of small round-off level differences (10^{-14} K) in the air temperature field at initialization in 1920 (Kay et al., 2015). The climate system is sufficiently chaotic that these small deviations grow rapidly, leading to substantial spread across the ensemble that reflects the amplitude of internally-generated variability. When an ensemble is sufficiently large, the ensemble mean provides a robust estimate of the deterministic response of the climate system to external forcing, i.e., the forced trend. The ensemble spread, then, is indicative of the "noise," inclusive of changes in variance that may occur as a function of climate state (Deser et al., 2012; Long et al., 2016). The large ensemble framework therefore allows for assessment of internal climate variability relative to the magnitude of the forced anthropogenic change (Deser et al., 2012; Hawkins and Sutton, 2012; Lovenduski et al., 2016; Brady et al., 2017).

Most ESMs, including the CESM-LE, incorporate prognostic representations of zooplankton as a component of their ocean biogeochemistry simulation (Le Quéré et al., 2016). However, ESMs typically simplify diverse groups of planktonic organisms into plankton functional types (Quéré et al., 2005), which are delineated based on ecological or biogeochemical roles. ESMs do not typically simulate specific zooplankton species as state variables; moreover, krill are typically larger and have more complicated life-history than the included phytoplankton functional types. We use the ocean biogeochemistry model output from the CESM-LE to represent bottom-up drivers and apply the krill growth model from Atkinson et al. (2006) offline to quantify changes in krill growth potential over the duration of the simulation. Since the krill growth potential model is applied offline, this approach precludes representing feedbacks between krill potential and other aspects of the biogeochemical simulation.

Bias in mean state and variability of sea surface temperature (SST) and chlorophyll can dramatically affect the characteristics of the simulated krill growth potential due to the highly nonlinear krill growth potential equation, therefore it is important to understand the model's ability to reproduce observed SST and chlorophyll during austral summer. To address this, we compared an austral summer (December through February, referred to as DJF) climatology from the CESM-LE to climatologies constructed from observational datasets and regridded onto the nominally-1° CESM ocean component grid (**Figure 2**). Surface chlorophyll data from September 1997 to December 2010 was obtained from SeaWiFS OC4v6 (NASA Ocean Biology Processing Group, 2018) (**Figure 2a**). SST observations from 1981 to 2015 were obtained from the Hadley Centre Global Sea Ice and SST (HadISST) dataset (Hadley Centre for Climate Prediction and Research, 2000) (**Figure 2d**). The SeaWiFs data set was used in the derivation of the original krill growth model (Atkinson et al., 2006) (**Figure 2e**). The simulated SST values were positively biased beyond the Polar Front and slightly negatively biased along the western Antarctic Peninsula

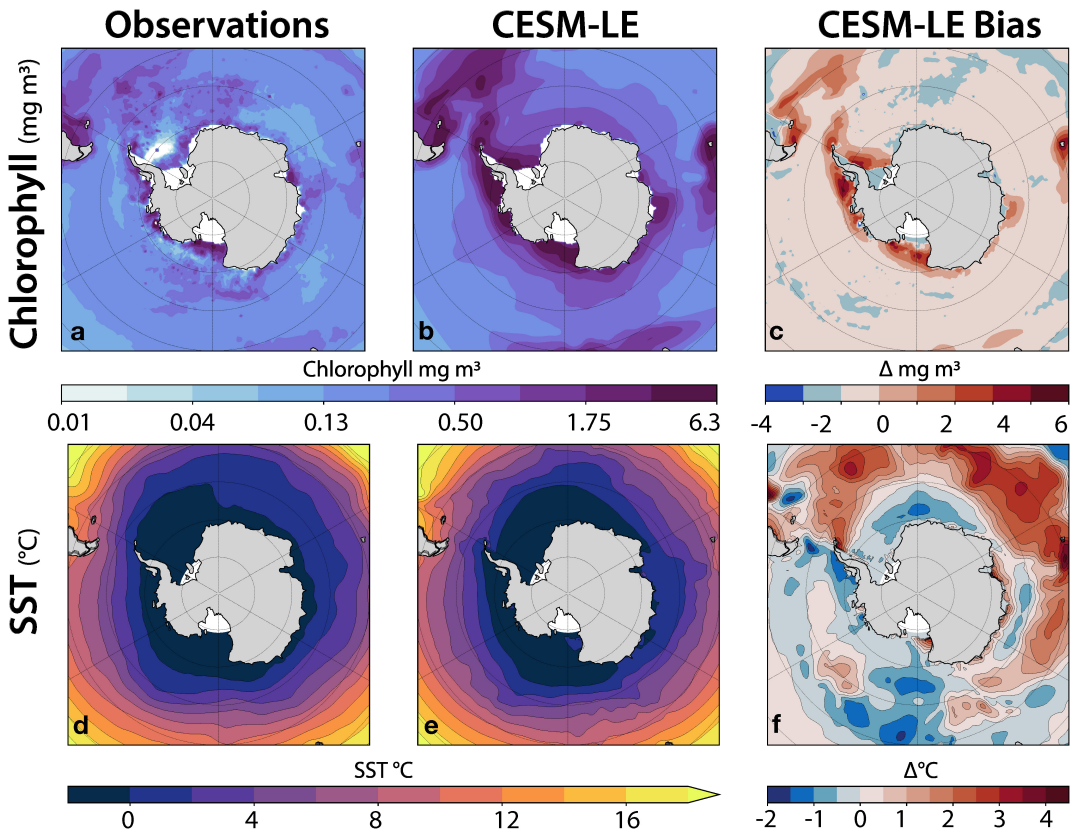

FIGURE 2 | CESM-LE model bias in chlorophyll (top row) and SST (bottom row) for DJF (austral summer). The left column shows observations, the middle column shows the corresponding simulated CESM-LE fields, and the right column shows the simulated bias as the difference between the simulated fields and the observations.

and into the Scotia Sea region (**Figure 2f**). Chlorophyll in the model was positively biased along the coastlines from the Scotia Sea region to the Bellingshausen Sea region, to the Ross Sea region (**Figure 2c**). It was further determined that the model biases were not outside the range of reasonable natural variability, but should be considered in evaluating results.

Krill Growth Potential

This study coupled an existing empirical krill growth model with the CESM-LE. The empirical model from Atkinson et al. (2006) was used to estimate the daily growth rate of krill (DGR mm day^{-1}) from sea surface temperature (T_{surf}, °C), food availability, indicated by surface chlorophyll a concentration (Chl, mg m^{-3}), and starting length of krill (L, mm):

$$DGR = -0.006 + 0.002L - 0.000061L^2 + [0.385Chl/(0.328 + Chl)] + 0.0078T_{surf} - 0.0101T_{surf}^2 \quad (1)$$

The model estimates a daily krill growth rate given temperature and the concentration of food in the summer season. The growth rate equation was derived using in-situ data from instantaneous growth rate experiments in the southwest Atlantic sector during the summer (January and February) of 2002 and 2003. It was further tested with SeaWiFS-derived chlorophyll to generate a predictive model of growth based on satellite-derivable environmental data (Atkinson et al., 2006). Previous studies have applied the growth model across the Southern Ocean at varying spatial and temporal scales to assess changes in habitat suitability (Hill et al., 2013; Murphy et al., 2017; Veytia et al., 2020). The growth rate provides a descriptive measurement of habitat suitability where a positive growth rate indicates habitat that can maintain and support adult krill productivity.

The variability of the environmental drivers (SST and chlorophyll) about a particular mean-state can dramatically affect the characteristics of the growth rate, due to the highly nonlinear nature of Eq. 1. While prior studies have used annual-mean climatologies to calculate GP rates results, we chose to calculate GP on monthly data (the highest frequency available from the model) to remain closer to the temporal resolution of the data used to develop the model. Seasonal estimates of krill GP at a starting length of an average adult krill (40 mm) were calculated from the growth period (December through February, referred to as DJF). The observed mean length of adult krill (40 mm) (Atkinson et al., 2009) was assumed as the starting length for an individual krill as previous analyses found that projected differences between future and historical epochs remained the

same irrespective of starting length (Veytia et al., 2020). Krill GP was calculated as a rate of mm day^{-1} where environmental conditions were within the temperature parameters that the growth model was derived from (−1 to 5°C).

The growth model predicts both positive and negative GP rates. Negative GP rates can occur when food concentrations are too low causing krill to undergo shrinkage (Hofmann and Lascara, 2000; Fach et al., 2002). Growth habitat was defined as habitat with a GP rate > 0 mm day^{-1} where higher GP rates indicated that habitat was more supportive of increasing krill growth and thus of higher quality. Habitat with a GP rate ≤ 0 mm day^{-1} was defined as "unsuitable habitat" where krill could survive but would not grow or where they would experience starvation and potentially undergo shrinkage.

Time of Emergence

We include a formal assessment of the time of emergence (ToE) of forced signals in the context of natural variability. ToE is the time when trends attributable to external forcing can be statistically distinguished from natural variability, which amounts to a signal to noise problem; detection is possible only when the magnitude of the forced response, the signal, exceeds the noise attributable to natural variability. Following Long et al. (2016), a time evolving spatial pattern of a variable in ensemble member i (ψ_i) is the sum of the internal variability and forced trend signal:

$$\psi_i = \psi_i' + \psi^s \quad (2)$$

The forced climate signal is represented by ψ^s while the component due to internal variability is represented as ψ_i'. In the CESM-LE, the number of ensemble members (m) is sufficiently large (Deser et al., 2012) that an average across the ensemble provides a reasonable estimate of the forced signal, ψ^S:

$$\psi^s = \frac{1}{n}\sum_{i=1}^{n}\psi_i \quad (3)$$

To assess the temporal evolution of trends and normalize the data, anomalies were calculated by removing the ensemble mean of a representative period of unperturbed climate: 1920–1950, from each ensemble member. We adapted a ToE method (Henson et al., 2017) that computes the start of a climate change signal (inflection point), the trend in the climate change signal (ω), and the year of emergence of the signal (ToE). For each grid cell, across all ensemble members, the ensemble mean (ψ^s) was cumulatively integrated over time using the composite trapezoidal rule in order to identify the year when the start of the climate change signal began, or the 'inflection point'. The 'inflection point' was defined as the year when the cumulative integral exceeded or dropped below zero (depending on the sign of the climate trend) for the remainder of the time series. With the inflection point identified, the trend of the climate change signal (ω) was calculated using a least squares polynomial fit function on the ensemble mean.

The timescale of the ToE was computed by multiplying the standard deviation of climate anomalies in the "unperturbed climate" (σ) by two and dividing it by the climate change trend (ω):

$$ToE = (2^*\sigma)/\omega \quad (4)$$

Using the ToE timescale, the year of detection was then calculated by adding the ToE to the starting year of the simulation, 1920 ($T_{detect} = T_0 + ToE$).

RESULTS

In our examination of simulated GP distributions prior to significant influence from the forced trend, spatial patterns in the distribution of krill GP rates were closely related to their thermotolerance range during the summer season. GP habitat was found within the Atlantic sector (30–70°W) along the latitudinal bands around the South Orkney Islands and along the eastern coastal regions near Wilkes Land (90–120°E) (**Figure 3a**). Temperature exerted a strong control on GP, with elevated GP values typically found within the optimal temperature range (−1 to 2°C) and located in coastal regions with high chlorophyll concentrations. The distribution of growth habitat was strongly constrained on its northern boundary by the edge of the 5°C isotherm that coincides with the Polar Front of the Antarctic Circumpolar Current (ACC) (**Figure 1**). Habitat within krill's thermotolerance with insufficient chlorophyll concentrations for growth (unsuitable habitat) were located in the Ross Gyre and Weddell Gyre and in the latitudinal range of the Polar Front (**Figure 3e**).

The CESM-LE simulated a poleward contraction in growth habitat and an overall decline in the spatial average of krill GP over the course of the 21st century. The circumpolar habitat area with positive growth potential rate decreased by ∼30% by 2100 (**Figure 3c**) from the mean state (**Figure 3a**). The spatially averaged mean growth potential rate within the habitat area with positive GP, also declined from the mean state by 29%. The contraction of growth habitat consisted of decreased GP rates between the Antarctic Peninsula and the South Sandwich Islands at the edge of the optimal thermotolerance range for krill and increased rates in the Bellingshausen Sea, Amundsen Sea and the Ross Sea (**Figure 3c**). The changes in growth habitat area are characterized by a poleward shift of the 5°C and −1°C isotherms (**Figure 3k**), contracting the mean area within the krill growth model's SST range by 12%.

The spatial averages for the anomalies relative to the 1920–1950 period were characterized by an increase in the magnitude of the forced krill GP anomaly to < −0.01 mm day^{-1} by 2100 (**Figure 4a**). Declines in the ensemble mean chlorophyll anomaly accelerated in the mid-century to ∼0.1 mg m^{-3} by 2100 (**Figure 4b**). The forced signal of the SST anomaly showed a continuous trend of rapidly rising temperatures reaching a magnitude of 3°C above the mean by the end of the simulation (**Figure 4c**).

The spatial patterns of natural variability were more pronounced at regional scales (**Figure 3b**) than across the spatial average of the Southern Ocean (**Figure 4a**). The general magnitude of natural variability across the spatial average of the krill GP anomaly was less than 0.005 mm day^{-1}m^{-3} (**Figure 4a**).

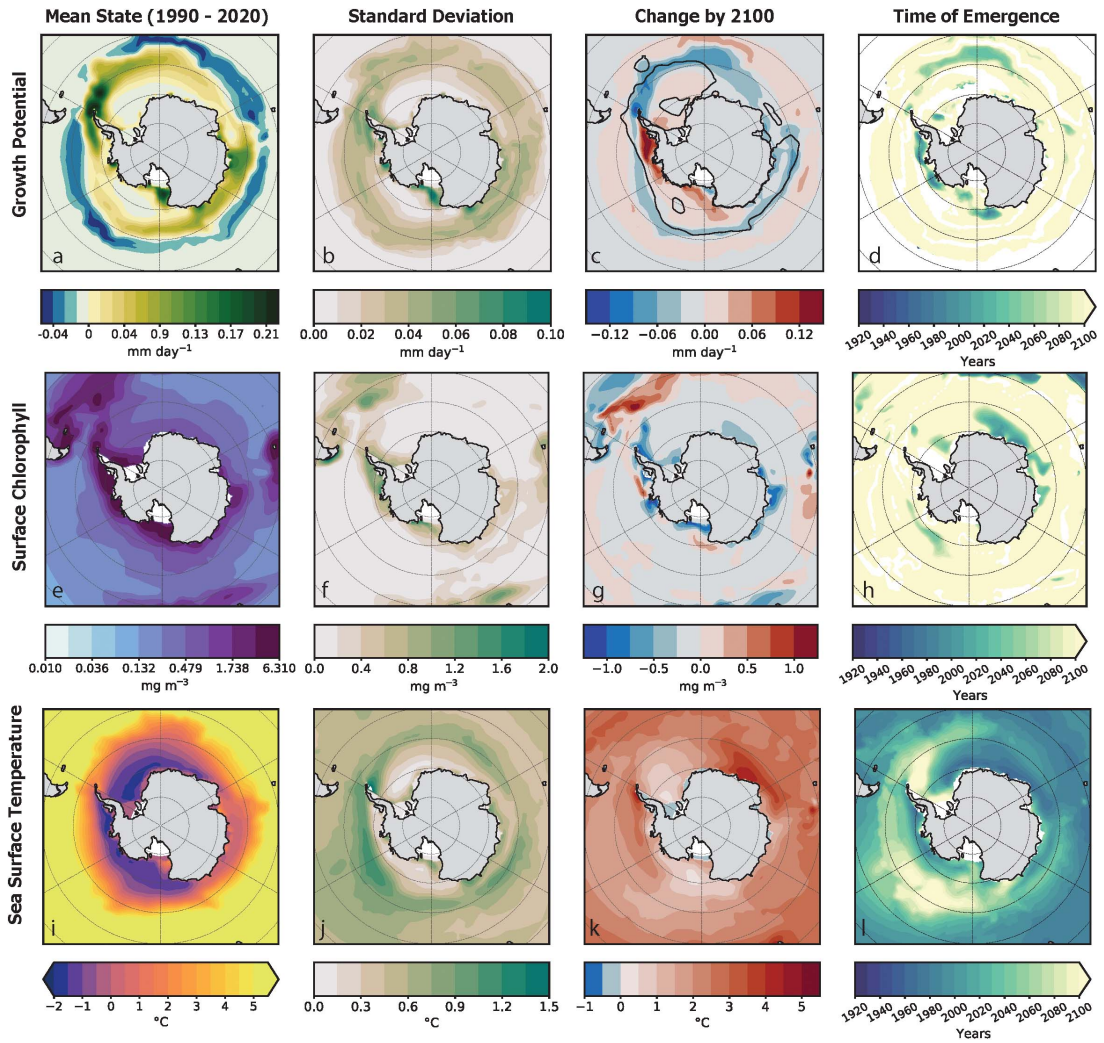

FIGURE 3 | This figure captures the spatial characteristics in the mean state of krill growth potential [top row: **(a–d)**], chlorophyll [middle row: **(e–h)**] and sea surface temperature [bottom row: (i–l)] as simulated by the large ensemble for the austral summer period. The mean state for the current climate (1990–2020) of the is shown for each variable in the leftmost column. Plot **(a)** shows growth potential of krill habitat as the rate growth per day (mm day^{-1}) where habitat that can support krill growth is green and habitat where krill growth is inhibited is blue. The mean state of surface chlorophyll concentration (mg m^{-3}), as shown in plot **(e)**, is plotted on a logarithmic scale. Plot **(i)** illustrates sea surface temperatures (SST) within the optimal temperature range that the empirical growth model was developed (Atkinson et al., 2006). The second column of plots to the left **(b,f,j)** shows the standard deviation of the mean state. The column second to the right **(c,g,k)** is the projected change in the forced signal from the unperturbed climate to the future climate. The difference is shown using a diverging color scale: increasing trends are shown in red and decreasing trends are shown in blue. In plot **(c)**, a black contour line indicates the distribution of habitat with positive krill GP by 2100. The right most column **(d,h,l)** is the year of detection of the "time of emergence" of the forced trend for. Areas in white indicate habitat where a ToE could not be detected. Where the ToE could be detected, the earlier the year of the ToE the darker the color represented on the map.

In contrast, the physical distribution of natural variability in krill GP was characterized by a widespread variability below 0.09 mm day^{-1} with elevated variability along the coastal boundary of growth habitat. The physical distribution of natural variability in krill GP was characterized by areas of increased variability in the frontal zone of the ACC and near the tip of the eastern Antarctic Peninsula (**Figure 3b**). These areas coincided with higher amounts of variability in physical distribution of internal variability in chlorophyll (**Figure 3f**) where the internal variability of chlorophyll ranged up to an order of one higher than the mean state of 0.189 mg m^{-3}. Spatial patterns of variability in SST show higher variability around the boundary of the Polar Front and the eastern tip of Antarctic Peninsula (**Figure 3j**). Across temporal evolution of the spatial average of the anomaly, the magnitude of natural variability was less than 0.5°C (**Figure 4c**).

The trends in krill GP rates illustrate that the forced signal develops increasing dominance (over natural variability) at longer timescales. Spatial estimates of the contribution of natural variability on 20- and 50-year krill GP trends were computed by explicitly separating internal variability from the forced trend (**Figure 5**). Short- and long-term krill GP trends were calculated

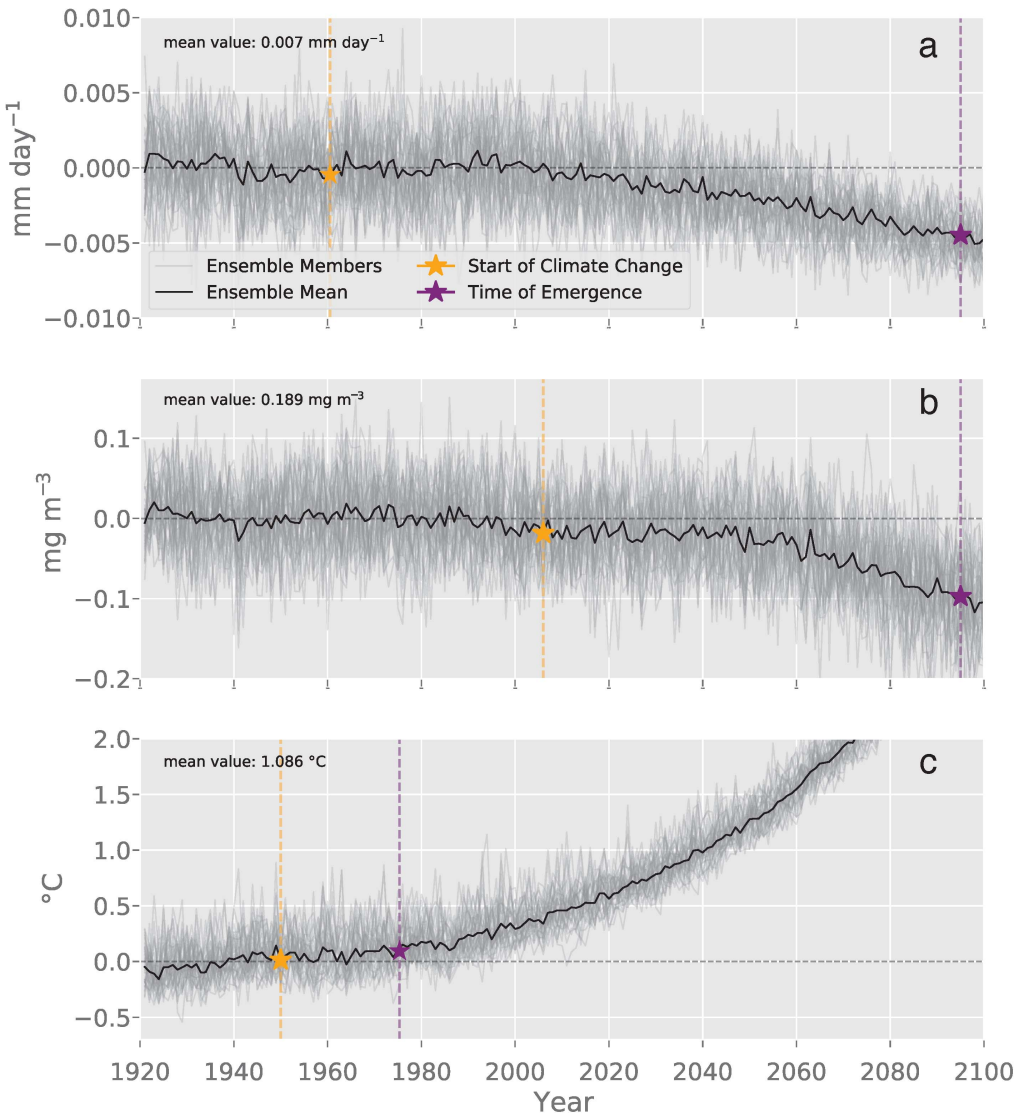

FIGURE 4 | This plot of the spatially averaged modeled DJF fields for the Southern Ocean illustrates the temporal evolution of **(a)** krill growth potential anomaly (mm day^{-1}), **(b)** surface chlorophyll (mg m^3), and **(c)** sea surface temperature (°C). Each ensemble member anomaly is plotted in gray while the black line is the mean ensemble anomaly. The means for each variable are listed in the upper left corner of each plot. The yellow stars indicate the year when the climate change signal was detected (Climate Change Year; GP: 1960, Chl: 2006, SST: 1950). The purple stars indicate the year of detection where trends forced by human-driven climate change can be formally distinguished from natural variability (Year of Detection; GP: 2095, Chl: 2095, SST: 1975) (Eq. 3).

on the spatially resolved model output using a linear least-squares analysis beginning in 2020 and extending to 2040 and 2070, respectively. The forced trends computed over 20 and 50 years are broadly similar in their spatial patterns; the difference is primarily characterized by an intensification of the trend magnitude at the longer timescale and slightly more spatial coherence in the 50-year trend. Decomposing the 20- and 50-year total trends into internal variability and forced signal components illustrated the magnitude of natural variability within the system. Internal variability contributed modestly to 50-year trends but did not display recognizable spatial patterns (**Figures 5g–l**). In some regions, internal variability reinforced the 50-year forced trend, leading to greater rates of change, while in other regions, internal variability worked to oppose the forcing. Overall, 50-year trends in GP were dominated by the forced trend.

The ToE analysis revealed the presence and timing of when the forced signal became distinguishable from internal variability for each variable. The decline in the krill GP trend, due to the forced climate signal, became detectable at 2095 in the Southern Ocean, as did the trend in chlorophyll (**Figures 4a,b**). The earliest detection of the forced signal was observed in the SST anomaly, which became distinguishable from internal variability in 1975 across the Southern Ocean (**Figure 4c**).

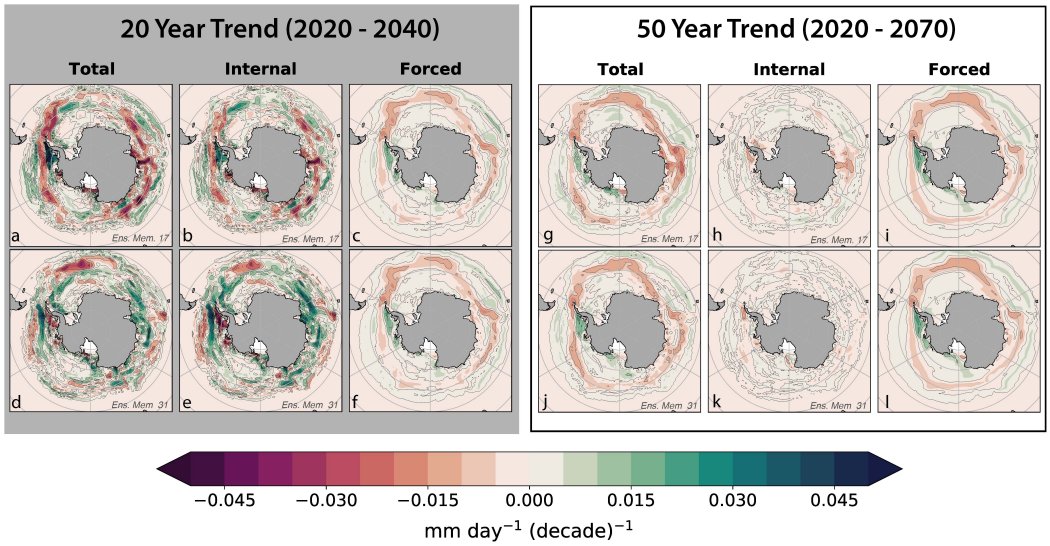

FIGURE 5 | This figure demonstrates the superposition of forced signal and internal variability on the total 20- and 50-year trends of krill GP in austral summer beginning in 2020. Each row is from a separate ensemble member; the top row of plots **(a–c** and **g–i)** are from ensemble member 17 while the bottom row of plots **(d–f** and **j–l)** are from member number 31. These two ensemble members were chosen as exemplary representations from the ensemble. Plot **(a,d)** show the total linear trend in GP for the 20-year while plots **(g,j)** show the 50-year total linear trend. Plots **(b,e)** show the internal variability within the 20-year trend and plots **(h,k)** show the 50-year trend. The forced trend (ensemble mean) of the 20-year trend is shown in plot **(c)** and replicated in **(f)** and the 50-year forced trend is shown in plot **(i)** and replicated in **(l)**. The forced trends are similar between both trend lengths but only drive the spatial coherence in the 50-year total trend, not the 20-year trend.

Spatial distributions of ToE detection indicate that positive and negative regional trends were diagnosed as emergent late in the 21st century for krill GP. The regional forced trend of increased krill GP emerged near the Bellingshausen Sea, Amundsen Sea, and the eastern part of the Ross Sea (**Figure 3e**). Regional declines of the forced trend in krill GP emerged near the WAP and in the mid-Atlantic around the southern boundary of the ACC stretching west to the South Orkney Islands. By late in the 21 century, negative chlorophyll trends were diagnosed as emergent in the eastern Atlantic near the coast (**Figures 3g,h**). The region of emergent negative chlorophyll trends coincided with regions of early emergence of ocean warming trends. In comparison to GP and chlorophyll, the regional trends in SST emerged much earlier in the 21st century. The distribution was characterized by earlier emergence years in the eastern Atlantic and Indian quadrant (0° to 90°E) and coastal zones from the WAP and Bellingshausen Sea and around to the Ross Sea. There was no emergence in SST forced trends by 2100 from the eastern tip of the WAP to the South Sandwich Islands (**Figure 3l**). Areas where trends failed to emerge indicate that the ratio between the forced trend and natural variability was not significant enough to detect separate forced trends.

DISCUSSION

Over the course of the CESM-LE simulation (1920–2100), krill GP rates are projected to decline during the summer season (Dec-Jan), a trend characterized by a poleward contraction of viable habitat (**Figure 3c**). The contraction of growth habitat is most noticeable around krill's current population center from the South Sandwich Islands to the Antarctic Peninsula (Atkinson et al., 2008, 2019). This contraction is a consequence of warming ocean conditions in lower latitudes and the Antarctic Peninsula (**Figure 3i**) and krill's sensitivity to temperature at the upper limits of their thermotolerance (Atkinson et al., 2006; Murphy et al., 2017). In our study, at higher latitudes the increase in forced trend of SST exposed habitat with high chlorophyll concentrations where krill growth had previously been inhibited due to low temperatures ($>-1°C$) (**Figure 3**). As a result, regional growth habitat increased in the Bellingshausen, Amundsen, and Ross Seas. These broad patterns of change in krill growth habitat in our results are reflected in similar studies using ESMs from the CMIP5 project. Within the Atlantic sector, Hill et al. (2013) found that krill growth habitat would be reduced based on ocean warming and reduced chlorophyll. Veytia et al. (2020) found that circumpolar growth habitat was projected to decline in the austral summer over the course of the century and contract toward higher latitudes. Their results, like ours, suggest that projected changes in chlorophyll and SST will reduce krill GP rates in low latitudes but will increase GP rates in higher latitudes.

Natural variability in krill growth habitat is influenced by changes in chlorophyll as well as temperature. Within the Atkinson et al. (2006) growth model, the relationship between growth and chlorophyll is highly nonlinear. Small changes in chlorophyll concentrations have a larger impact on the growth rate than temperatures within the stenothermic range because chlorophyll is the primary driver for krill growth potential and distribution (Ross et al., 2000; Atkinson et al., 2006; Murphy et al., 2017). This is illustrated in the temporal evolution of the

spatial average in krill GP where the fluctuations in the magnitude of internal variability in krill are parallel with chlorophyll until early in the 21st century. Around 2020, the forced trend in krill GP and chlorophyll became more negative until the end of the century (**Figures 4a,b**). While this occurred, the magnitude of variability in krill GP was reduced but magnitude of variability of chlorophyll did not. Decreased variability in krill GP indicates when the forced trend could become dominant over natural variability. We hypothesize that as temperature contracts poleward, fluctuations in the position of the 5°C isotherm led to smaller perturbations in the total area of krill habitat, assuming that circumpolar habitat is well described by a regression with the area encompassed by the isotherm.

Trends associated with the forced signal are unlikely to be reversed on short timescales or can only be reversed through climate intervention strategies. Natural variability, however, implies fluctuations around a nominal mean state. Trends in krill GP are driven by the ratio of the magnitude of natural variability compared to the magnitude of the forced signal. These trends illustrate that the forced signal develops increasing dominance (over natural variability) at longer timescales (**Figure 5**). This is in line with the general understanding that the importance of natural variability is higher at smaller spatial and temporal scales (Hawkins and Sutton, 2012). Additionally, our results are consistent with other studies examining ToE that have found global emergence time scales of 20–30 year for SST and longer scales (50+ years) for surface chlorophyll (Schlunegger et al., 2020). This demonstrates that strong decadal variability is an important feature of the Southern Ocean ecosystem and is likely to dominate the evolution of the system at local to regional scales for the next few decades. From a management perspective, this approach could then be used to inform which climate signal to manage for, on what timescale, and what observational system would be needed to validate the projections.

Our ability to discern the influence of climate change is contingent upon the magnitude of the forced signal in relation to the magnitude of the natural variability. Across the Southern Ocean, the forced trend in krill GP emerges out of the envelope of natural variability late in the 21st century. The spatial patterns of ToE detection highlight the complexities of climate change on krill potential growth habitat: krill GP trends are both increasing and decreasing as a result of human driven climate change. By the mid to late 21st century, an increased krill GP trend emerged in habitat around the Bellingshausen/Amundsen Sea region (**Figure 3**). This result is again similar to projections by the 2016 study that found increased successful spawning habitats for krill in the late 21st century (Piñones and Fedorov, 2016). Currently the Bellingshausen and Amundsen Sea region does not support successful growth or spawning due to insufficient conditions (Piñones and Fedorov, 2016). However, the region has been characterized as habitat for potential future krill recruitment and increased population (Quetin and Ross, 2003) due to increased phytoplankton growth from increased ice-free summer days (Montes-Hugo et al., 2009). Though the GP model used in this study does not account for sea-ice, the spatial trend of increased SST in the Bellingshausen/Amundsen Sea region was diagnosed to emerge in SST by mid to late 21st century.

Declining krill GP rates in the habitat were detected by the late 21st century around the South Sandwich Islands, South Orkney Islands and the tip of the WAP. This region is part of the southwest Atlantic sector (30 to 70°W) of the Atlantic where 70% of the current population of krill is concentrated (Atkinson et al., 2008). Our results suggest that the decline in GP rates could coincide with emergent warming trends along the WAP. A similar projected decline in successful krill spawning habitat was found in the same region by a study using ESMs from the CMIP5 project and an early life cycle krill development model (Piñones and Fedorov, 2016). The 2016 study speculated that this decline was controlled by the significant changes in sea ice advance in the region north of Marguerite Bay (Piñones and Fedorov, 2016). The area around the WAP is considered to be the main seeding region for adult krill in the southwestern Atlantic (Hofmann et al., 1992; Fach et al., 2006; Thorpe et al., 2007, 2019). The significance of declining adult krill growth in the WAP suggests that human driven climate change will result in widespread negative effects on the krill dependent ecosystem. However, the forced changes in krill GP habitat are projected to be largely indistinguishable from natural variability until late the 21st-century.

Limitations

Along with the similarities in the spatial and temporal patterns in krill growth habitat between our results and previous studies using ESMs, there are slight variations in the spatial patterns and krill GP rates in our findings. These differences can be attributed to features of the underlying ESM simulations involved, as well as methodological details associated with the application of the krill model. The krill growth model used in this study was empirically derived using in situ and satellite data for adult krill growth in the summer season and represents a single growth-season. Additionally, the growth model does not properly account for the role of sea ice as it models growth in open ocean when sea ice is absent. Sea ice is thought to play a complex and crucial role in the krill life cycle, recruitment and abundance (Siegel and Loeb, 1995; Atkinson et al., 2004; Nicol, 2006; Thorpe et al., 2007; Piñones and Fedorov, 2016). However, there is minimal quantitative information regarding the relationship between sea ice and summer krill growth.

As an empirical model, the growth potential estimated is primarily descriptive and inherently limited in applicability by the conditions reflected in the dataset used in it's formulation. Additionally, mechanistic knowledge gaps on krill population dynamics in response to environmental drivers currently preclude our ability to develop a model that can simulate the krill life cycle and obtain biomass estimates. Overall, these factors limit our ability to draw conclusions on actual krill biomass and production, but they do not significantly impede our ability to illustrate the projected spatial and temporal trends of climate change and natural variability in krill GP rates.

While our results are broadly consistent with previous studies, ours is the first to consider the effects of natural climate variability explicitly. Multi-model ensembles, like the CMIP5, are composed of multiple models, each with a distinct representation of the mean state and variability. Given the structural differences

between the models, the multi-model ensemble cannot be easily used to explicitly separate natural variability and from forced trends (Solomon et al., 2011). However, the large-ensemble framework used in this study allows for quantification of the uncertainties from internal variability (as found in multi-model ensemble studies), identification of trends climate change and identifying when those trends can be formally distinguished from natural variability.

Because the krill model was applied to the model output offline, the resolution of the model output is limited in its ability to accurately project mean GP values at regional scales. For example, higher regional krill growth rates in some regions like the Bellingshausen Sea region may be partially due to the model's bias for higher chlorophyll concentrations. However, the large ensemble framework assumptions result in a stronger ability to assess the trends and variability. As with any synthetic approach, limitations and caveats exist that stem from coarse model resolution, simplification of a complex system, or inadequate process representation. While these potential caveats are important to consider, they do not undermine our fundamental point regarding the critical role of both natural variability and external forcing in determining the trajectory of the system in coming decades.

Implications

Natural variability is, and will remain, a fundamental reality of the Southern Ocean. It will also remain a challenge for understanding of the ecosystem's response to climate change. Even under perfect observing capabilities, the detection of climate-change signals is limited by the noise of natural variability. Therefore, quantifying the impacts of climate change on a key species like krill requires understanding and separating the influences of the superposition of natural variability and the forced trend. Though our study on krill GP is highly idealized, we found that climate driven trends in krill GP are detectable at basin scales, while strong natural variability challenges detection at local and shorter time scales. These results have several important implications regarding the challenge of detecting and attributing ecological changes to climate change and decision making.

Managing systems characterized by strong natural variability is challenging as the influence of natural variability in climate has the potential to mask or enhance long term trends in climate (Hawkins, 2011) that may be difficult to reverse once they emerge. By providing distinction between influence of natural variability and longer-term climate change trends on the Southern Ocean ecosystem and krill GP, the results and approach presented here can provide insight for informing management as consideration of multi-decadal timescales is imperative for determining if the forced signal is driving change (Hawkins, 2011). We have shown how the influence of natural variability and climate change on circumpolar krill GP depends on time scale. The influence of natural variability dominates the spread of uncertainty in spatial patterns of krill GP. However, longer timescales show that the influence of the forced trend on the contraction of positive krill GP habitat and mean growth potential rates will dominate over the influence of natural variability. This work suggests that in addition to the quantification of climate change impacts, management strategies must explicitly acknowledge that the ecosystem exhibits strong variability. For example, natural variability is likely to primarily impact patterns in krill GP over the next two decades. Natural variability can mask trends in climate that may be difficult to reverse once they emerge. This work suggests that in addition to the quantification of climate change impacts, management strategies must explicitly acknowledge that the Southern Ocean ecosystem exhibits strong variability.

Trends in krill growth potential rates have wide reaching implications for the Antarctic marine ecosystem and it's management. Studies have shown that habitat's ability to support the growth and maintenance of adult krill can be used to identify crucial areas for krill biomass production and high spawning potential (Hill et al., 2013; Murphy et al., 2017). Decreases in summer-time krill GP have negative implications for reproductive performance due to the exponential relationship between adult size and fecundity (Tarling and Johnson, 2006; Siegel and Watkins, 2016). Furthermore, while the poleward shift in growth habitat distribution may not have consequences for growth habitat, it is likely to be inadequate habitat for spawning (Hofmann and Hüsrevoğlu, 2003) or connecting subpopulations (Siegel, 2016). Cascading ecological impacts to the Antarctic marine ecosystem are exasperated by the additional pressure on krill from the fishery (Nicol et al., 2012). Fluctuations in krill productivity pose challenges for current definitions of sustainable catch. For example, seasonal changes in the length of krill are important for interpreting stock structure for fisheries management (Tarling et al., 2016). The changes as a result of climate change and variability in krill productivity and habitat partitioning could cause major consequences for food web linkages, biogeochemical cycling (Cavan et al., 2019), and the krill fishery.

There is wide international recognition of the importance of understanding, and managing for, the impacts of climate variability and climate change on the Antarctic marine ecosystem (Brasier et al., 2019). We believe that the research presented here motivates questions regarding current management priorities. One of the current priorities of the Southern Ocean management body is developing a risk assessment framework to inform the spatial allocation of krill catch (CCAMLR, 2019, para 5.17). The framework development is a part of a long-term ecosystem-based management system for the Antarctic krill fishery. Based on our results, important fluctuations in krill dynamics are likely even in the absence of human-driven warming. If the management strategy envisioned for krill is based on short-term projections, data layers should include the spread of natural variability. When considering long-term projections, the risk assessment could also include one or more layers characterizing long-term outcomes. Consideration of long-term impacts could enhance the management strategy to be more robust or adaptive to the impacts of climate change.

While our approach has oversimplified the complexity involved with sustaining krill populations, the notion of coupling mechanistic ecosystem models to ESMs could provide a more reliable basis for adaptation strategies, risk

analyses, and understanding trade-offs associated with climate change mitigation (Stock et al., 2011; Park et al., 2019). Achieving such an outcome would require coupling the ESM to a krill model that simulates life history dynamics and constraints on growth recruitment and mortality. Nature holds vastly more degrees of freedom than represented in our model and there is significant potential for other mechanisms to arise that fundamentally change the nature of the system's response. A first step in that direction would be to adapt more advanced krill models like Constable and Kawaguchi's model that simulates bioenergetics (Constable and Kawaguchi, 2018). The advancement of this approach will generate new methods for quantifying the impacts of climate change on the Antarctic marine ecosystem. For example, by virtue of the ability to separate the component of change due to natural variability from that associated with the forced trend, the separation enables a theoretical, yet direct, attribution of losses in krill production and yield to climate change (Bonan and Doney, 2018). In turn, these types of attributions could then be used to quantify the cost-benefit of climate mitigation and used to inform long term goals for a flexible management strategy.

Conclusion

The Southern Ocean is a dynamic system and appropriate consideration of the changes projected to accompany climate warming must recognize the important role of natural variability. The research presented here exemplifies a particular application of ESMs, targeted at exploring the specific climate drivers of changes in krill growth potential habitat. Our findings highlight the complexities of the detection and attribution of human-driven climate changes that are superimposed on changes occurring naturally as a result of chaotic dynamics in the climate system. In the context of understanding ecosystem dynamics in the Southern Ocean, the superposition of natural climate variability of force trends is a critical consideration. The basic conclusions of this study are as follows. We have demonstrated how a large ensemble framework can enable explicit assessments of the benefits of climate mitigation to krill habitat and provide perspectives relevant informing for management decisions on timescales ranging from seasons to centuries. We have shown that changes in krill growth potential will be driven by the superposition of natural variability on shorter timescales ($\leq$20 years) but on longer timescales ($\geq$50 years), changes will be driven by the forced trend. Furthermore, we have shown that it will be impossible to distinguish the forced signal from natural variability until deep into the 21st century in krill growth potential. These findings emphasize the need for proactive consideration of natural variability in Southern Ocean management of krill as it can mask trends in climate that may be difficult to reverse once they emerge. Future application of the large ensemble framework can be used to develop projections of krill habitat change inclusive of appropriate uncertainty estimates. In conclusion, both natural variability and externally forced trends will be important determinants of krill habitat over the coming decades. Studies such as this will be relevant and necessary for creating climate-informed management in a marine ecosystem of immense economic and intrinsic value.

DATA AVAILABILITY STATEMENT

The raw data supporting the conclusions of this article will be made available by the authors, without undue reservation.

AUTHOR CONTRIBUTIONS

All authors listed have made a substantial, direct and intellectual contribution to the work, and approved it for publication.

FUNDING

CB and ZS were supported by the Pew Charitable Trusts. ML was supported by NASA grant 19-IDS19-0028.

ACKNOWLEDGMENTS

Supercomputing, analysis, and storage resources were provided by the Computational and Information System Lab at the National Center for Atmospheric Research. We acknowledge high-performance computing support from Yellowstone (ark:/85065/d7wd3xhc) and Cheyenne (doi: 10.5065/D6RX99H) provided by NCAR's Computational and Information Systems Laboratory. The National Center for Atmospheric Research is sponsored by the National Science Foundation. Thanks to Daniel Doak and Nicole Lovenduski for their valuable support and feedback on the manuscript. Thanks also to Anton Van de Putte for providing valuable opportunities to share this work and for his feedback throughout the process. We would also like to thank the reviewers and editor for their time, writing support, and constructive feedback. Lastly, thank you to the CCAMLR Secretariat, Members States and Observers for allowing authors to participate in their meetings. Data from the CESM Large Ensemble publicly available; multiple options for access are described here: https://www.cesm.ucar.edu/projects/community-projects/LENS/data-sets.html.

REFERENCES

Allison, L. C., Johnson, H. L., Marshall, D. P., and Munday, D. R. (2010). Where do winds drive the Antarctic circumpolar current? *Geophys. Res. Lett.* 37:L12605. doi: 10.1029/2010GL043355

Atkinson, A., Hill, S. L., Pakhomov, E. A., Siegel, V., Reiss, C. S., Loeb, V. J., et al. (2019). Krill (*Euphausia superba*) distribution contracts southward during rapid regional warming. *Nat. Clim. Chang.* 9, 142–147. doi: 10.1038/s41558-018-0370-z

Atkinson, A., Shreeve, R. S., Hirst, A. G., Rothery, P., Tarling, G. A., Pond, D. W., et al. (2006). Natural growth rates in Antarctic krill (*Euphausia superba*): II. Predictive models based on food, temperature, body length, sex, and maturity stage. *Limnol. Oceanogr.* 51, 973–987. doi: 10.4319/lo.2006.51.2.0973

Atkinson, A., Siegel, V., Pakhomov, E., and Rothery, P. (2004). Long-term decline in krill stock and increase in salps within the Southern Ocean. *Nature* 432, 100–103. doi: 10.1038/nature02996

Atkinson, A., Siegel, V., Pakhomov, E., Rothery, P., Loeb, V., Ross, R., et al. (2008). Oceanic circumpolar habitats of Antarctic krill. *Mar. Ecol. Prog. Ser.* 362, 1–23. doi: 10.3354/meps07498

Atkinson, A., Siegel, V., Pakhomov, E. A., Jessopp, M. J., and Loeb, V. (2009). A re-appraisal of the total biomass and annual production of Antarctic krill. *Deep Sea Res. 1 Oceanogr. Res. Pap.* 56, 727–740. doi: 10.1016/j.dsr.2008.12.007

Bonan, G. B., and Doney, S. C. (2018). Climate, ecosystems, and planetary futures: the challenge to predict life in Earth system models. *Science* 359:eaam8328. doi: 10.1126/science.aam8328

Bopp, L., Resplandy, L., Orr, J. C., Doney, S. C., Dunne, J. P., Gehlen, M., et al. (2013). Multiple stressors of ocean ecosystems in the 21st century: projections with CMIP5 models. *Biogeosciences* 10, 6225–6245. doi: 10.5194/bg-10-6225-2013

Brady, R. X., Alexander, M. A., Lovenduski, N. S., and Rykaczewski, R. R. (2017). Emergent anthropogenic trends in California current upwelling. *Geophys. Res. Lett.* 44, 5044–5052. doi: 10.1002/2017gl072945

Brasier, M. J., Constable, A., Melbourne-Thomas, J., Trebilco, R., Griffiths, H., Van de Putte, A., et al. (2019). Observations and models to support the first Marine Ecosystem Assessment for the Southern Ocean (MEASO). *J. Mar. Sys.* 197:103182. doi: 10.1016/j.jmarsys.2019.05.008

Cavan, E. L., Belcher, A., Atkinson, A., Hill, S. L., Kawaguchi, S., McCormack, S., et al. (2019). The importance of Antarctic krill in biogeochemical cycles. *Nat. Commun.* 10, 1–13.

CCAMLR (2019). Report of the XXXVIII Meeting of the Commission. Hobart, Tas: Commission for the Conservation of Antarctic Marine Living Resources.

Commission on Geosciences, Environment, and Resources, Climate Research Committee, National Research Council, and Division on Earth and Life Studies (1996). *Natural Climate Variability on Decade-To-Century Time Scales*. Washington, DC: National Academies Press.

Constable, A. (2000). Managing fisheries to conserve the Antarctic marine ecosystem: practical implementation of the Convention on the Conservation of Antarctic Marine Living Resources (CCAMLR). *ICES J. Mar. Sci.* 57, 778–791. doi: 10.1006/jmsc.2000.0725

Constable, A. J., and Kawaguchi, S. (2018). Modelling growth and reproduction of Antarctic krill, *Euphausia superba*, based on temperature, food and resource allocation amongst life history functions. *ICES J. Mar. Sci.* 75, 738–750. doi: 10.1093/icesjms/fsx190

Constable, A. J., Melbourne−Thomas, J., Corney, S. P., Arrigo, K. R., Barbraud, C., Barnes, D. K. A., et al. (2014). Climate change and southern Ocean ecosystems I: how changes in physical habitats directly affect marine biota. *Glob. Chang. Biol.* 20, 3004–3025.

Danabasoglu, G., Bates, S. C., Briegleb, B. P., Jayne, S. R., Jochum, M., Large, W. G., et al. (2012). The CCSM4 ocean component. *J. Clim.* 25, 1361–1389. doi: 10.1175/jcli-d-11-00091.1

Deser, C., Phillips, A., Bourdette, V., and Teng, H. (2012). Uncertainty in climate change projections: the role of internal variability. *Clim. Dyn.* 38, 527–546. doi: 10.1007/s00382-010-0977-x

Doney, S. C., Ruckelshaus, M., Emmett Duffy, J., Barry, J. P., Chan, F., English, C. A., et al. (2012). Climate change impacts on marine ecosystems. *Annu. Rev. Mar. Sci.* 4, 11–37.

Fach, B., Hofmann, E., and Murphy, E. (2002). Modeling studies of Antarctic krill *Euphausia superba* survival during transport across the Scotia Sea. *Mar. Ecol.* 231, 187–203. doi: 10.3354/meps231187

Fach, B. A., Hofmann, E. E., and Murphy, E. J. (2006). Transport of Antarctic krill (*Euphausia superba*) across the Scotia Sea. Part II: krill growth and survival. *Deep Sea Res. 1 Oceanogr. Res. Pap.* 53, 1011–1043. doi: 10.1016/j.dsr.2006.03.007

Feldstein, S. B. (2000). The timescale, power spectra, and climate noise properties of teleconnection patterns. *J. Clim.* 13, 4430–4440. doi: 10.1175/1520-0442(2000)013<4430:ttpsac>2.0.co;2

Flores, H., Atkinson, A., Kawaguchi, S., Krafft, B., Milinevsky, G., Nicol, S., et al. (2012). Impact of climate change on Antarctic krill. *Mar. Ecol. Prog. Ser.* 458, 1–19.

Fogt, R. L., and Marshall, G. J. (2020). The southern annular mode: variability, trends, and climate impacts across the southern hemisphere. *WIREs Clim. Chang.* 11:e652.

Goyal, R., Gupta, A. S., Jucker, M., and England, M. H. (2021). Historical and projected changes in the southern hemisphere surface westerlies. *Geophys. Res. Lett.* 48:e2020GL090849.

Hadley Centre for Climate Prediction and Research (2000). *Hadley Centre Global Sea Ice and Sea Surface Temperature (HadISST)*. doi: 10.5065/XMYE-AN84

Hagen, J. O., Jefferies, R., Marchant, H., Nelson, F., Prowse, T., Vaughan, D. G., et al. (2007). *Polar Regions (Arctic and Antarctic). Cambridge University Press, Contribution of Working Group II: Impacts, Adaptation and Vulnerability Fourth Assessment Report of the Intergovernmental Panel on Climate Change*. Cambridge: Cambridge University Press.

Hasselmann, K. (1976). Stochastic climate models part I. Theory. *Tellus* 28, 473–485. doi: 10.1111/j.2153-3490.1976.tb00696.x

Hasselmann, K. (1993). Optimal fingerprints for the detection of time-dependent climate change. *J. Clim.* 6, 1957–1971. doi: 10.1175/1520-0442(1993)006<1957:offtdo>2.0.co;2

Hawkins, E. (2011). Our evolving climate: communicating the effects of climate variability. *Weather* 66, 175–179. doi: 10.1002/wea.761

Hawkins, E., and Sutton, R. (2009). The potential to narrow uncertainty in regional climate predictions. *Bull. Am. Meteorol. Soc.* 90, 1095–1108. doi: 10.1175/2009bams2607.1

Hawkins, E., and Sutton, R. (2012). Time of emergence of climate signals. *Geophys. Res. Lett.* 39, L01702. doi: 10.1029/2011GL050087

Henley, S. F., Schofield, O. M., Hendry, K. R., Schloss, I. R., Steinberg, D. K., Moffat, C., et al. (2019). Variability and change in the west Antarctic Peninsula marine system: research priorities and opportunities. *Prog. Oceanogr.* 173, 208–237.

Henson, S. A., Beaulieu, C., Ilyina, T., John, J. G., Long, M., Séférian, R., et al. (2017). Rapid emergence of climate change in environmental drivers of marine ecosystems. *Nat. Commun.* 8:14682.

Hill, S. L., Phillips, T., and Atkinson, A. (2013). Potential climate change effects on the habitat of Antarctic krill in the weddell quadrant of the southern ocean. *PLoS One* 8:e72246. doi: 10.1371/journal.pone.0072246

Hobbs, W. R., Massom, R., Stammerjohn, S., Reid, P., Williams, G., and Meier, W. (2016). A review of recent changes in Southern Ocean sea ice, their drivers and forcings. *Glob. Planet. Chang.* 143, 228–250. doi: 10.1016/j.gloplacha.2016.06.008

Hofmann, E., Capella, J. E., Ross, R. M., and Quetin, L. B. (1992). Models of the early life history of *Euphausia superba*—Part I. Time and temperature dependence during the descent-ascent cycle. *Deep Sea Res. A Oceanogr. Res. Pap.* 39, 1177–1200. doi: 10.1016/0198-0149(92)90063-y

Hofmann, E., and Hüsrevoğlu, Y. (2003). A circumpolar modeling study of habitat control of Antarctic krill (*Euphausia superba*) reproductive success. *Deep Sea Res. 2 Top. Stud. Oceanogr.* 50, 3121–3142. doi: 10.1016/j.dsr2.2003.07.012

Hofmann, E., and Lascara, C. (2000). Modeling the growth dynamics of Antarctic krill *Euphausia superba*. *Mar. Ecol. Prog. Ser.* 194, 219–231. doi: 10.3354/meps194219

Holland, M. M., Bailey, D. A., Briegleb, B. P., Light, B., and Hunke, E. (2012). Improved sea ice shortwave radiation physics in CCSM4: the impact of melt ponds and aerosols on arctic sea ice. *J. Clim.* 25, 1413–1430. doi: 10.1175/jcli-d-11-00078.1

Hunke, E. C., and Lipscomb, W. H. (2010). *CICE: The Los Alamos Sea Ice Model Documentation and Software User's Manual Version 4*. Los Alamos, NM: Los Alamos National Lab. (LANL), 76.

Hurrell, J. W., Holland, M. M., Gent, P. R., Ghan, S., Kay, J. E., Kushner, P. J., et al. (2013). The community earth system model: a framework for collaborative research. *Bull. Am. Meteorol. Soc.* 94, 1339–1360.

Kay, J. E., Deser, C., Phillips, A. S., Mai, A., Hannay, C., Strand, G., et al. (2015). The community earth system model (CESM) large ensemble project: a community resource for studying climate change in the presence of internal climate variability. *Bull. Am. Meteorol. Soc.* 96, 1333–1349. doi: 10.1175/bams-d-13-00255.1

Larsen, J. N., Anisimov, O. A., Constable, A., Hollowed, A. B., Maynard, N., Prestrud, P., et al. (2014). *Polar Regions, in: Climate Change 2014–Impacts, Adaptation and Vulnerability: Part B: Regional Aspects: Working Group II*

Contribution to the IPCC Fifth Assessment Report. Cambridge: Cambridge University Press, 1567–1612.

Lawrence, D. M., Oleson, K. W., Flanner, M. G., Fletcher, C. G., Lawrence, P. J., Levis, S., et al. (2012). The CCSM4 land simulation, 1850–2005: assessment of surface climate and new capabilities. *J. Clim.* 25, 2240–2260. doi: 10.1175/jcli-d-11-00103.1

Le Quéré, C., Buitenhuis, E. T., Moriarty, R., Alvain, S., Aumont, O., Bopp, L., et al. (2016). Role of zooplankton dynamics for southern ocean phytoplankton biomass andglobal biogeochemical cycles. *Biogeosciences* 13, 4111–4133. doi: 10.5194/bg-13-4111-2016

Long, M. C., Deutsch, C., and Ito, T. (2016). Finding forced trends in oceanic oxygen. *Glob. Biogeochem. Cycles* 30, 381–397. doi: 10.1002/2015gb005310

Lovenduski, N. S., McKinley, G. A., Fay, A. R., Lindsay, K., and Long, M. C. (2016). Partitioning uncertainty in ocean carbon uptake projections: internal variability, emission scenario, and model structure. *Glob. Biogeochem. Cycles* 30, 1276–1287. doi: 10.1002/2016gb005426

Mayewski, P. A., Meredith, M. P., Summerhayes, C. P., Turner, J., Worby, A., Barrett, P. J., et al. (2009). State of the Antarctic and southern ocean climate system. *Rev. Geophys.* 47:RG1003.

McBride, M. M., Dalpadado, P., Drinkwater, K. F., Godø, O. R., Hobday, A. J., Hollowed, A. B., et al. (2014). Krill, climate, and contrasting future scenarios for Arctic and Antarctic fisheries. *ICES J. Mar. Sci.* 71, 1934–1955. doi: 10.1093/icesjms/fsu002

Meyer, B., Atkinson, A., Bernard, K. S., Brierley, A. S., Driscoll, R., Hill, S. L., et al. (2020). Successful ecosystem-based management of Antarctic krill should address uncertainties in krill recruitment, behaviour and ecological adaptation. *Commun. Earth Environ.* 1, 1–12.

Montes-Hugo, M., Doney, S. C., Ducklow, H. W., Fraser, W., Martinson, D., Stammerjohn, S. E., et al. (2009). Recent changes in phytoplankton communities associated with rapid regional climate change along the western Antarctic Peninsula. *Science* 323, 1470–1473. doi: 10.1126/science.1164533

Murphy, E. J., Cavanagh, R. D., Hofmann, E. E., Hill, S. L., Constable, A. J., Costa, D. P., et al. (2012). Developing integrated models of Southern Ocean food webs: including ecological complexity, accounting for uncertainty and the importance of scale. *Prog. Oceanogr. End End Model. Toward Comp. Anal. Mar. Ecosyst. Org.* 102, 74–92. doi: 10.1016/j.pocean.2012.03.006

Murphy, E. J., Thorpe, S. E., Tarling, G. A., Watkins, J. L., Fielding, S., and Underwood, P. (2017). Restricted regions of enhanced growth of Antarctic krill in the circumpolar Southern Ocean. *Sci. Rep.* 7:6963.

NASA Ocean Biology Processing Group (2018). *SEAWIFS-ORBVIEW-2 Level 3 Binned Chlorophyll Data Version R2018.0*. Greenbelt, MD: NASA Ocean Biology Processing Group, doi: 10.5067/ORBVIEW-2/SEAWIFS/L3B/CHL/2018

Nicol, S. (2006). Krill, currents, and sea ice: *Euphausia superba* and its changing environment. *BioScience* 56, 111–120. doi: 10.1641/0006-3568(2006)056[0111:kcasie]2.0.co;2

Nicol, S., and Foster, J. (2016). "The fishery for antarctic krill: its current status and management regime," in *Biology and Ecology of Antarctic Krill, Advances in Polar Ecology*, ed. V. Siegel (Cham: Springer International Publishing), 387–421.

Nicol, S., Foster, J., and Kawaguchi, S. (2012). The fishery for Antarctic krill–recent developments: krill fishery review. *Fish Fish.* 13, 30–40. doi: 10.1111/j.1467-2979.2011.00406.x

Nicol, S., and Mangel, M. (2018). *The Curious Life of Krill: A Conservation Story from the Bottom of the World*. Washington, DC: Island Press.

Orsi, A. H., Whitworth, T., and Nowlin, W. D. (1995). On the meridional extent and fronts of the Antarctic 802 Circumpolar Current. *Deep Sea Res. Part I: Oceanogr. Res. Pap.* 42, 641–673. doi: 10.1016/0967-0637(95)00021-W

Park, J.-Y., Stock, C. A., Dunne, J. P., Yang, X., and Rosati, A. (2019). Seasonal to multiannual marine ecosystem prediction with a global Earth system model. *Science* 365, 284–288. doi: 10.1126/science.aav6634

Piñones, A., and Fedorov, A. V. (2016). Projected changes of Antarctic krill habitat by the end of the 21st century: changes in Antarctic krill habitat. *Geophys. Res. Lett.* 43, 8580–8589. doi: 10.1002/2016gl069656

Quéré, C. L., Harrison, S. P., Prentice, I. C., Buitenhuis, E. T., Aumont, O., Bopp, L., et al. (2005). Ecosystem dynamics based on plankton functional types for global ocean biogeochemistry models. *Glob. Chang. Biol.* 11, 2016–2040.

Quetin, L., and Ross, R. (2003). Episodic recruitment in Antarctic krill *Euphausia superba* in the Palmer LTER study region. *Mar. Ecol. Prog. Ser.* 259, 185–200. doi: 10.3354/meps259185

Rogers, A. D., Frinault, B. A. V., Barnes, D. K. A., Bindoff, N. L., Downie, R., Ducklow, H. W., et al. (2020). Antarctic futures: an assessment of climate-driven changes in ecosystem structure, function, and service provisioning in the Southern Ocean. *Annu. Rev. Mar. Sci.* 12, 87–120. doi: 10.1146/annurev-marine-010419-011028

Rogers, J. C., and van Loon, H. (1982). Spatial variability of sea level pressure and 500 mb height anomalies over the southern hemisphere. *Mon. Weather Rev.* 110, 1375–1392. doi: 10.1175/1520-0493(1982)110<1375:svoslp>2.0.co;2

Ross, R. M., Quetin, L. B., Baker, K. S., Vernet, M., and Smith, R. C. (2000). Growth limitation in young *Euphausia superba* under field conditions. *Limnol. Oceanogr.* 45, 31–43. doi: 10.4319/lo.2000.45.1.0031

Ryabov, A. B., de Roos, A. M., Meyer, B., Kawaguchi, S., and Blasius, B. (2017). Competition-induced starvation drives large-scale population cycles in Antarctic krill. *Nat. Ecol. Evol.* 1:0177.

Santer, B. D., Mears, C., Doutriaux, C., Caldwell, P., Gleckler, P. J., Wigley, T. M. L., et al. (2011). Separating signal and noise in atmospheric temperature changes: the importance of timescale. *J. Geophys. Res. Atmos.* 116:D22105. doi: 10.1029/2011JD016263

Schlunegger, S., Rodgers, K. B., Sarmiento, J. L., Ilyina, T., Dunne, J. P., Takano, Y., et al. (2020). Time of emergence and large ensemble intercomparison for ocean biogeochemical trends. *Glob. Biogeochem. Cycles* 34:e2019GB006453.

Schmidt, K., Atkinson, A., Steigenberger, S., Fielding, S., Lindsay, M. C. M., Pond, D. W., et al. (2011). Seabed foraging by Antarctic krill: implications for stock assessment, bentho-pelagic coupling, and the vertical transfer of iron. *Limnol. Oceanogr.* 56, 1411–1428. doi: 10.4319/lo.2011.56.4.1411

Siegel, V. (Ed). (2016). *Biology and Ecology of Antarctic krill, Advances in Polar Ecology*. Cham: Springer International Publishing, doi: 10.1007/978-3-319-29279-3

Siegel, V., and Loeb, V. (1995). Recruitment of Antarctic krill *Euphausia superba* and possible causes for its variability. *Mar. Ecol. Prog. Ser.* 123, 45–56. doi: 10.3354/meps123045

Siegel, V., and Watkins, J. L. (2016). "Distribution, Biomass and Demography of Antarctic krill, *Euphausia superba*," in *Biology and Ecology of Antarctic Krill, Advances in Polar Ecology*, ed. V. Siegel (Cham: Springer International Publishing), 21–100. doi: 10.1007/978-3-319-29279-3_2

Solomon, A., Goddard, L., Kumar, A., Carton, J., Deser, C., Fukumori, I., et al. (2011). Distinguishing the roles of natural and anthropogenically forced decadal climate variability: implications for prediction. *Bull. Am. Meteorol. Soc.* 92, 141–156. doi: 10.1175/2010bams2962.1

Stammerjohn, S., Massom, R., Rind, D., and Martinson, D. (2012). Regions of rapid sea ice change: an inter-hemispheric seasonal comparison. *Geophys. Res. Lett.* 39:L06501. doi: 10.1029/2012GL050874

Stammerjohn, S. E., and Maksym, T. (2017). "Gaining (and losing) Antarctic sea ice: variability, trends and mechanisms," in *Sea Ice*, ed. D. N. Thomas (Oxford: Wiley-Blackwell), 261–289. doi: 10.1002/9781118778371.ch10

Stock, C. A., Alexander, M. A., Bond, N. A., Brander, K. M., Cheung, W. W. L., Curchitser, E. N., et al. (2011). On the use of IPCC-class models to assess the impact of climate on living marine resources. *Prog. Oceanogr.* 88, 1–27. doi: 10.1016/j.pocean.2010.09.001

Tarling, G., Hill, S., Peat, H., Fielding, S., Reiss, C., and Atkinson, A. (2016). Growth and shrinkage in Antarctic krill *Euphausia superba* is sex-dependent. *Mar. Ecol. Prog. Ser.* 547, 61–78. doi: 10.3354/meps11634

Tarling, G. A., and Fielding, S. (2016). "Swarming and Behaviour in Antarctic krill," in *Biology and Ecology of Antarctic Krill, Advances in Polar Ecology*, ed. V. Siegel (Cham: Springer International Publishing), 279–319. doi: 10.1007/978-3-319-29279-3_8

Tarling, G. A., and Johnson, M. L. (2006). Satiation gives krill that sinking feeling. *Curr. Biol.* 16, R83–R84.

Thompson, D. W. J., and Wallace, J. M. (2000). Annular modes in the extratropical circulation. Part I: month-to-month variability. *J. Clim.* 13:17.

Thorpe, S., Tarling, G., and Murphy, E. (2019). Circumpolar patterns in Antarctic krill larval recruitment: an environmentally driven model. *Mar. Ecol. Prog. Ser.* 613, 77–96. doi: 10.3354/meps12887

Thorpe, S. E., Murphy, E. J., and Watkins, J. L. (2007). Circumpolar connections between Antarctic krill (*Euphausia superba* Dana) populations: investigating

the roles of ocean and sea ice transport. *Deep Sea Res. 1 Oceanogr. Res. Pap.* 54, 792–810. doi: 10.1016/j.dsr.2007.01.008

Tommasi, D., Stock, C. A., Hobday, A. J., Methot, R., Kaplan, I. C., Eveson, J. P., et al. (2017). Managing living marine resources in a dynamic environment: the role of seasonal to decadal climate forecasts. *Prog. Oceanogr.* 152, 15–49.

Trathan, P. N., and Hill, S. L. (2016). "The Importance of krill Predation in the Southern Ocean," in *Biology and Ecology of Antarctic Krill, Advances in Polar Ecology*, ed. V. Siegel (Cham: Springer International Publishing), 321–350. doi: 10.1007/978-3-319-29279-3_9

Turner, J., Lu, H., White, I., King, J. C., Phillips, T., Hosking, J. S., et al. (2016). Absence of 21st century warming on Antarctic Peninsula consistent with natural variability. *Nature* 535, 411–415. doi: 10.1038/nature18645

Veytia, D., Corney, S., Meiners, K. M., Kawaguchi, S., Murphy, E. J., and Bestley, S. (2020). Circumpolar projections of Antarctic krill growth potential. *Nat. Clim. Chang.* 10, 568–575. doi: 10.1038/s41558-020-0758-4

Watters, G. M., Hinke, J. T., and Reiss, C. S. (2020). Long-term observations from Antarctica demonstrate that mismatched scales of fisheries management and predator-prey interaction lead to erroneous conclusions about precaution. *Sci. Rep.* 10:2314.

Conflict of Interest: The authors declare that the research was conducted in the absence of any commercial or financial relationships that could be construed as a potential conflict of interest.

frontiers in Marine Science

ORIGINAL RESEARCH
published: 02 December 2021
doi: 10.3389/fmars.2021.778121

Environmental Variability and Threshold Model's Predictions for Coral Reefs

Tim Rice McClanahan[1] and Maxwell Kodia Azali[1,2]*

[1] *Wildlife Conservation Society, Global Marine Programs, Bronx, NY, United States,* [2] *Coastal Science and Policy Program, University of California, Santa Cruz, Santa Cruz, CA, United States*

Current models of the future of coral reefs rely on threshold (TM) and multivariate environmental variability models (VM) that vary in how they account for spatial and temporal environmental heterogeneity. Here, a VM based on General Additive Model (GAM) methods evaluated the empirical relationships between coral cover (n = 905 sites pooled to 318 reef cells of the Western and Central Indian Ocean Provinces) and 15 potentially influential variables. Six environmental and one fisheries management variables were selected as significant including SST shape distributions, dissolved oxygen, calcite, and fisheries management. Common predictive variables, including cumulative degree-heating weeks (DHW), pH, maximum light, SST bimodality and rate of rise, and two multivariate metrics were either weak or not significant predictors of coral cover. A spatially-resolved 2020 baseline for future predictions of coral cover within 11,678 reef ~6.25 km^2 cells within 13 ecoregions and 4 fisheries management categories using the 7 top VM variables was established for comparing VM and TM coral cover prediction for the year 2050. We compared the two model's predictions for high and low Relative Concentration Pathway (CMIP5; RCP8.5 and 2.6) scenarios using the four available future-cast SST variables. The excess heat (DHW)-coral mortality relationship of the TM predicted considerably lower coral cover in 2050 than the VM. For example, for the RCP8.5 and RCP2.6 scenarios, the decline in coral for the TM predicted was 81 and 58% compared to a 29 and 20% for the VM among reef cells with >25% coral cover in 2020, if a proposed optimal fisheries management was achieved. Despite differences, coral cover predictions for the VM and TM overlapped in two environmental regions located in the southern equatorial current region of the Indian Ocean. Historical and future patterns of acute and chronic stresses are expected to be more influential than cumulative heat stress in predicting coral cover, which is better accounted for by the VM than the TM.

Keywords: coral reef, climate change, climate model, fisheries, future prediction

Edited by:
Michael Raatz,
Max Planck Institute for Evolutionary Biology, Germany

Reviewed by:
Albert Gabric,
Griffith University, Australia
Keisha D. Bahr,
Texas A&M University Corpus Christi, United States

****Correspondence:***
Tim Rice McClanahan
tmcclanahan@wcs.org

Specialty section:
This article was submitted to Global Change and the Future Ocean, a section of the journal Frontiers in Marine Science

Received: *16 September 2021*
Accepted: *05 November 2021*
Published: *02 December 2021*

Citation:
McClanahan TR and Azali MK (2021) Environmental Variability and Threshold Model's Predictions for Coral Reefs. Front. Mar. Sci. 8:778121. doi: 10.3389/fmars.2021.778121

INTRODUCTION

The ecosystem services provided by coral reefs are under threat from a number of forces of which climate warming, eutrophication, and fishing are among the most wide-spread concerns (Cornwall et al., 2021; Donovan et al., 2021). The two main threatened ecological services are the organic production that produce fisheries and the inorganic production that produces the

calcium carbonate reef framework. Net reef growth is particularly critical for providing shallow-water habitat and shoreline protection, which are threatened by the current rates of sea level rise (Perry et al., 2018). Therefore, the cover of calcifying coral and algal functional groups and the factors that influence them are of concern for societies dependent on the above reef services. This is particularly true in the many tropical regions that are dependent on fisheries and coastal tourism for food and economic security (Spalding et al., 2017; Selig et al., 2019).

Current predictions of generic coral health and cover are based on thermal exposure predictions (van Hooidonk et al., 2020). Predictions are frequently based on climate model's predicted temperature deviations from historical warmest seasonal months from satellite temperature histories and rate of rise in sea-surface temperatures and the production of future "excess heat" (Cornwall et al., 2021). This accumulated excess heat above +1°C of warm-season temperatures is the current threshold model (TM) best-estimate of both the historical and future exposure of corals to thermal stress. This excess-heat model can be modified to include and account for other environmental factors. Common modifications include between-year thermal thresholds, coral acclimation and genetic adaptation rates, light attenuation, and future climate model scenarios (Donner et al., 2005; McManus et al., 2020; Gonzalez-Espinosa and Donner, 2021). Most of this class of models can generally be described as a TM because their core predictions rely on a threshold to provoke the coral stress responses that often but not always coincident with +1°C above summer mean temperatures (Donner, 2011).

Criticisms of threshold models are (1) they poorly account for local variability and environmental contexts (Chollett et al., 2014; McClanahan et al., 2020b), (2) overly reliant in treating exposure as a single latent surface heat stress variable (McClanahan et al., 2019), (3) do not account well for the variable responses in corals to the 1°C hot season threshold or other heat stress metrics (DeCarlo, 2020; McClanahan et al., 2020a), (4) lack the multivariate aspects of stress that include both thermal and non-thermal stress elements (Maina et al., 2011), and 5) rely solely on coral cover responses to heat stress and treat cover as a single pooled entity without taxa-specific niches, life history, or regional characteristics (Cacciapaglia and van Woesik, 2016; Darling et al., 2019; McClanahan et al., 2020a,b). These critiques often arise from models that can generally be described as environmental variability models (VMs).

Defense of the threshold models are that they were created to illuminate the general problem of global climate change on coral reefs and less to make specific local reef-scale predictions. TM should, therefore, help to promote policies and actions to reduce future impacts expected from different human responses and climate scenarios. Yet, modifications of these models are currently being used to identifying climate sanctuaries and prioritize conservation spending (Beyer et al., 2018). There are, however, many cases where these models fail to predict climate-warming disturbances and changes on a large scale, which can undermine the confidence of threshold metrics and usefulness for influencing management policies (McClanahan et al., 2015b; DeCarlo and Harrison, 2019; Kim et al., 2019; Mollica et al., 2019). Moreover, over-reliance on TMs prompts concerns about policy foci, as per the differential efficacy of managing local fisheries, eutrophication, and the global atmospheric commons (Abelson, 2020). If models poorly account for impacts of local human action, the agency for change is centered solely on the global and not local coral reef commons.

Consequently, comparing and considering a new generation of climate change models is needed to address the policy debate and scales of action. Specifically, building and testing models that account for the multivariate nature of chronic and acute stress and coral sensitivity relationships in specific contexts (Mumby et al., 2011). This requires less reliance on core theoretical concepts and greater empiricism in building and testing models that use the power of modern statistical algorithms. A greater diversity of models needs to be created, examined, and competed against each other in terms of their ability to predict local-scale environmental and coral responses. For example, are there missing but potentially important variables that are not being considered by the TMs that might greatly modify the outcomes of climate change? What affects do the five TM simplifications above have on the ability to predict coral cover? In order to begin this process, we explored seldom considered variables that are currently spatially resolved and available to produce a VM option. Our VM examined coral responses in the context of acute and chronic thermal stress and fisheries management in two faunal provinces of the western Indian Ocean (WIO). Thereafter, a common version of the TM that related excess heat and coral mortality was compared with this new VM in terms of their predictions of coral cover in 2050 using Coupled Model Intercomparison Project Phase 5 (CMIP5) global climate model projections.

MATERIALS AND METHODS

This study evaluated the empirical relationships between coral cover and fisheries management and 15 geospatially available and resolved SST and seawater chemistry variables. Model results were then used to predict coral cover within 13 ecoregions of the Western and Central Indian Ocean in 2020 (WIO). The inputs were the significant SST, chemistry variables and fisheries management categories selected by a machine-learning algorithm described below. Thereafter, using the modeled coral cover initial condition in 2020, cover predictions were made for 2050 based on the four future-cast SST variables available for the CMIP5 for low (RCP2.6) and high Relative Concentration Pathway (RCP8.5) scenarios. The two models' predictions in 2050 were then compared to a DHW-coral mortality relationship or threshold model starting with the same 2020 modelled benchmark (Hughes et al., 2018; Cornwall et al., 2021). Finally, we evaluated the potential impacts of a common fisheries sustainability proposals on coral cover by establishing 30% of the cells as fisheries closures and 70% as restricted fishing in each country, which is generally considered a best-practices fisheries policy (O'Leary et al., 2016).

Study Region and Management

The evaluation included the western Indian Ocean coral reefs or western and central Indian Ocean faunal provinces with a

spatial extent of 32°E, 27°S to 73°E −7°N. The United Nations Environmental Program – World Conservation Monitoring Center (UNEP-WCMC) coral reef distribution data were used to create a ∼6.25 km^2 grid of reef cells for the entire region. The map resulted in 11,678 reef cells that were subsequently classified by ecoregion, nation, and the national and local fisheries management status (**Supplementary Table 1**). The cell grid was appropriate for the local nature of reef fishing, management, and encompasses the home range size of most large coral reef fishes and also close to the extent of small-scale fishing movements and gear used in this region (McClanahan and Abunge, 2018). Fishery management classification were either restricted (limited gear often excluding spear guns, explosives, and small-meshed or drag nets) or unrestricted (all gears including spearguns and small-meshed nets used) based on national and local laws but also modified by observations of compliances with restriction (McClanahan et al., 2015a). Legally established closures were classified as low and high compliance based on published literature and personal and stakeholder observations of compliance. The management categories for each cell was based on a combination of legal records and maps, personal observations, and communications with colleagues. The dominant management coverage was recorded in the few locations where the reef area was within more than one management system.

Data Sources

Coral Cover Response Variable

Live coral cover was the biological response used in this model and was retrieved from a large database of coral cover collected in 905 sites from 2005 to 2020 compiled by three experienced observers (T.R. McClanahan, N.A. Muthiga, and N.A.J Graham; **Supplementary Table 2**) and often collected across regional thermal disturbances, such as 2010 and 2016 (McClanahan et al., 2007, 2020a,b). Coral cover data from multiple survey sites within the grid cells were averaged. Where multiple temporal records existed for a site, only the three most recent records were retained, generating a final cell-based pooled dataset of n = 318 per-cell means.

Environmental Variables for Empirical Model

Sea-Surface Temperature Variables

We accessed daily sea-surface temperature (SST) data for the 1985-2020 study period from the U.S. National Oceanic and Atmospheric Administration's Coraltemp v3.1 SST website[1]. These SST data were available at 5-km resolution. From these data, a number of SST metrics were calculated for the period prior to the empirical coral cover sampling and used to develop the empirical coral cover-environmental metrics model. The metrics calculated included the mean, standard deviation, cumulative degree heating weeks (cumDHW), skewness, kurtosis, and a bimodality coefficient found to be strongly related to bleaching (McClanahan et al., 2019).

These variables characterize the temporal structure of temperatures experienced by corals and can act as proxies for either chronic or acute thermal stress. For example, kurtosis is a measure of the thickness of the tails of the SST distribution with negative values indicating increasing thickness. Thus, it represents a measure of the frequency of exposure to SSTs away from the mean and negative values should be associated with some degree of acclimation of corals to unusual temperatures (McClanahan et al., 2020a). Skewness is a measure of the frequency and direction of rare SST events, with high negative and positive values indicating more extreme rare cold and warm SST values. Thus, increased skewness implies more acute stress with more positive values indicating warm and negative values cold extremes. The bimodality coefficient measures the degree of bimodality in SST, and ranges from 0-1, with a value equal to or greater than 0.55 indicating a bimodal or multimodal distribution. Increases in bimodality may represent corals experiencing a stressful 'jump' to extreme temperatures, rather than a more continuous acclimation to thermal variability (McClanahan et al., 2019).

Cumulative Degree Heating Weeks

Degree heating weeks (DHW) were calculated as the sum of positive thermal anomalies (hotspots) greater than 1°C above the historically warmest month (maximum monthly mean) over a 12-week period (Liu et al., 2014) (Equations 1 & 2). Cumulative degree heating weeks were calculated as the sum of the maximum DHW for each year from 1985 – 2020 at a reef location (Equation 3).

$$HS = \begin{cases} SST_{daily} - \text{MMM}, & SST_{daily} > \text{MMM} \\ 0, & SST_{daily} \leq \text{MMM} \end{cases}$$

Equation 1 | Calculation of daily hotspots (HS), which are positive thermal anomalies from observed daily temperatures and the maximum monthly mean climatology (MMM). MMM is the temperature of the historically warmest month.

$$\text{DHW} = \frac{1}{7}\sum_{i=1}^{84}\left(\text{HS}_i, \text{if HS}_i > 1℃\right)$$

Equation 2 | Calculation of Degree Heating Weeks (DHW), which is the accumulation of daily hotspots > 1^0C over a 12-week period.

$$\text{cumDHW} = \sum_{i=1}^{i=35} \text{maximum}\left(\text{DHW}_i\right)$$

Equation 3 | Calculation of cumulative degree heating weeks, which is an aggregated sum of maximum yearly (t) DHW at a reef location from 1985 to 2020.

To understand the geographical variation in the thermal regime across the WIO, we performed a principal components analysis (PCA) and cluster analysis based on thermal stress metrics. We used the 1985-2020 NOAA CRW data to calculate 7 thermal stress metrics for each 6.25 km^2 reef cell, including the mean, standard deviation, cumulative degree heating weeks (cumDHW), skewness, kurtosis, bimodality coefficient, and the SST rate of rise. The SST rate of rise is the linear regression

[1]https://coralreefwatch.noaa.gov/product/5km/index_5km_sst.php

slope of annual mean SST from 1985 – 2020. We conducted a PCA on the 7 thermal stress metrics for 11,678 reef cells using the Factominer package in R (Lê et al., 2008). Subsequently, we conducted a cluster analysis using the clustering large applications algorithm (CLARA) with Euclidean dissimilarities and 50 samples to group coral reef locations based on thermal stress metrics (Kaufman and Rousseeuw, 1990).

Additional Environmental Variables

To broaden the scope of the potential impacts of the environment on coral cover beyond SST, we extracted a number of abiotic variables previously found to influence the distribution and abundance of hard scleractinian corals (Vercammen et al., 2019). Variables extracted from Bio-ORACLE[2] (Tyberghein et al., 2012; Assis et al., 2018) included surface photosynthetically active radiation (PAR), diffuse water-penetration attenuation coefficient at 490nm, calcite concentration, dissolved oxygen, and pH (**Supplementary Table 2**). Bio-ORACLE datasets were obtained from satellite and *in situ* observation collected over various time periods from 1898 to 2009. We extracted values for each cell using the cell's centroid and the data available prior to the field sampling of coral cover. Calcite was estimated from back-scattering light reflectance bands near 443 and 555 nm supported by field measurements and dissolved oxygen from compiled field measurements and interpolation methods.

An additional source of data included values from a multivariate coral climate exposure stress index (Maina et al., 2011). The methods provided both a Climate Stress Model (CSM) including radiation, sediment and also a second option or Global Stress model (GSM) that included reinforcing and reducing variables, such as eutrophication. The CSM and GSM were compared against alternative models that included the above thermal history variables but did not improve the deviance explained and were therefore excluded from the final model.

Variable selection procedures were applied to the above variables that included evaluating the correlations among variables (**Supplementary Figure 1**). Highly correlated variables (Pearson r > 0.70) were extracted for further investigation and excluded from the final model based on previous evaluations of potential causation. For example, the variables of SST-SD, bimodality, and kurtosis were highly correlated and, based on previous variable-selected evaluations and relationships with coral community metrics, kurtosis was selected (Ateweberhan et al., 2018; Zinke et al., 2018; McClanahan et al., 2020a,b). Consequently, we considered fifteen environmental and one fisheries management variable but based on the above selection and preliminary models using AIC criteria, a final model of six environmental and one fisheries management variables is presented.

Modelling Coral Cover Benchmarks

We used a generalized additive model (GAM) as a specific case of a VM, to model the in-situ percent coral cover against the above predictors using a beta distribution and logit link. A beta distribution is appropriate for variables bound between 0-1, thus we divided our percent coral cover by 100 prior to analysis. GAMs are useful for modelling non-linear responses between responses and predictor variables. Therefore, we included smoothing terms to our predictor variables to capture the expected non-linear relationships but limited the knots for the smoothed predictors to five to prevent overfitting. Country was included as a random effect capture to address potential bias in survey effort.

Selection of predictor variables was performed to choose the most parsimonious models using the Akaike Information Criteria (AIC), where models with <2AIC were further compared on basis of the variation explained by the addition of variables. We randomly selected ∼70% of the cell-pooled data (n = 223) to develop the model and reserved the remaining ∼30% (n = 95) to test the accuracy of the model predictions. This procedure was repeated 10 times, where we calculated the average Pearson correlation coefficient, r squared and the mean squared error for all 10 runs (**Supplementary Table 3**). The model was then used to extrapolate hard coral cover predictions in 2020 to the entire planning grid and to 2050 as described below.

Future sea surface temperature data were obtained from the CMIP5 (Taylor et al., 2012) and included simulations of relative concentration pathways (RCP) consistent with the BAU or high (RCP 8.5) and reduced carbon emission (RCP 2.6) scenarios. We extracted daily SST for the 2006 – 2050 period from two global climate models available from NOAA Geophysical Fluid Dynamics Laboratory- CM3 and MIROC5. We averaged the daily SST observations for each cell location from the two CMIP5 models for each RCP scenario to reduce individual model bias. The average daily SST were used to calculate four thermal metrics (mean, skewness, kurtosis, and cumDHW) for the 2020–2050 period for low and high Relative Concentration Pathway (RCP) scenarios. We were unable to forecast the future conditions of dissolved oxygen and calcite because they are not predicted or considered in current RCP scenarios. In present-day models, cumulative DHW was the weakest among the four variables and had a p value of 0.08, or short of formal significance (**Figure 3**). It was, however, retained because it was used in most previous future-cast evaluations, historically found to be statistically significant, and to have similar responses pattern in some other large-sample studies (Darling et al., 2019; McClanahan et al., 2020a). Maps of the distribution of key variables as well as a comparison of the satellite data with selected in situ temperature data are presented (**Supplementary Figures 2**, **3**).

Fisheries Management

The impacts of fisheries management were explored by changing the management systems of each cell and estimating cover values under this new fisheries management in 2050. We chose one common optimal fisheries management system that has been proposed and tested (O'Leary et al., 2016), which is to have 30% of reef area in high compliance closures and 70% having restricted fishing. Thus, we changed the management of the cells in 2050 under both the BAU RCP8.5 and the RCP2.6 carbon emissions reduction scenarios to estimate the coral cover under this optimal fishing scenario. The two scenarios of distributing the 30% reserve and 70% restricted fishing selection at either the regional and national level were explored. The differences were minor and therefore we present the more likely by-country

[2]https://www.bio-oracle.org/

scenario. We present differences in the cumulative frequencies of coral cover for the four scenarios (RCP8.5 and RCP2.6 current management and conservation management) against the 2020 benchmark for each SST cluster.

Predictions and Comparisons of Future Coral Cover Between Models

The predictions and differences in prediction of the GAM's multivariate model and the DHW-mortality model were compared. The DHW-mortality decision is a common decision of TMs used to make future predictions for RCP models (Cornwall et al., 2021). We examined the RCP8.5 and 2.6 DHW prediction for the 2020 to 2050 period to identify the decade that had two or more thermal events greater than 4, 6, 8, and 10 DHW. The coral cover was then reduced using the largest DHW by the proportion established by the empirical DHW-morality relationship reported for the Great Barrier Reef in 2016 (Hughes et al., 2018). Therefore, coral cover was reduced by 39, 60, 67, and 90% for any repeated 4, 6, 8, and 10 DHWs increments. The generality of this response beyond the GBR and over time is unknown but these or similar post-bleaching mortality rates have been used to predict future states of reefs on a large scale (Sheppard, 2003; Cornwall et al., 2021) To simplify the presentation of results, we often compare changes of coral cover above and below 10 and 25% to describe some model outcomes, as the 10% cover has been used as a thresholds for net coral reef growth (Perry et al., 2018) and 25% to achieve maximum fish diversity (Wilson et al., 2009).

RESULTS

Sea-Surface Temperature Distribution Patterns

Sea-surface temperature distribution patterns in the WIO were highly variable, differentiated by most SST metrics, and indicated that sites clustered into six SST groups (**Table 1** and **Figure 1A**). The strongest differentiation (60%) was attributable to the measures of mean, SD, kurtosis, and bimodality that may be considered chronic stress metrics that differ across the cooler and less stable southern to warmer and more stable northern reefs. Cumulative DHW was a weaker differentiating variable and stronger among reef cells with cooler water, high SD, bimodality, and thick-tailed distributions (negative kurtosis) in the central to southern part of this region dominated by the westward-flowing equatorial current (**Figure 1B**). The weaker variation explained by the second axis (19%) was most influenced by SST rate of rise and skewness, or a measure of the frequency of acute stress.

Clusters 1, 2, and 4 located on the left side of the PCA diagram were distinguished by being located in the central to southern WIO and having low water temperatures and high standard deviations, negative kurtosis, and bimodality (**Figure 1**). Cluster 1 was the largest cluster with 4794 reef cells and associated with the dominant northern flow of the Southern Equatorial Current (SEC) system. Cluster 2 was the smallest cluster with 621 cells and associated with southwest Madagascar, which was a location with more stable chronic temperatures but higher right skewness than clusters 1 and 4 cells. Cluster 4 was also a moderately large cluster with 1,463 cells that was broadly distributed from the Mauritius to the African coastline, including the southern Seychelles. This cluster included more reefs on the windward than leeward and southern sides of Madagascar than cluster 1.

Clusters 3, 5, and 6 were located on the right sides of the PCA diagram and distinguished by warm temperature with low metrics of variation or SD, bimodality, DHW and positive kurtosis. Cluster 3 was moderate size cluster with 1,548 cells but largely located along a belt from the Chagos Islands to northern Kenya that included reefs in the northern Seychelles. Cluster 3 was a more moderate set of measurements and a transition between the southern and northern WIO. It was distinguished from other southern WIO reefs by having some negative skewness whereas positive skewness distinguished the northern clusters 5 and 6. Cluster 3 also had high cumDHW similar to clusters 2 and 3. Cluster 5 had a moderate number of 1,004 cells with restricted distributions to the northern Maldives and distinguished by warm water, the strongest right skewness, and low rate of SST rise. Cluster 6 was the second most frequent cluster with 2,248 cells but had restricted distributions to the southern Maldives and fewer cells (70) in the northern Chagos. Clusters 5 and 6 both had warm water and low chronic variation in SST but cluster 5 had a thinner-tailed distribution and more episodic warm water than cluster 6.

Model Results

The variable selection procedure for the VM chose 6 of the 14 environmental variables and fisheries restrictions. Variables not selected included the rate of rise, SD, and bimodality of SST, global and climate stress models, maximum PAR, light attenuation, and pH. The full VM (GAM) with the six selected environmental variables found weak and not statistically significant relationships for CumDHW and country. Therefore, the final predictive model included in order of importance: management, dissolved oxygen, calcite, and mean, skewness, and kurtosis of SST distributions (**Figure 2** and **Supplementary Table 3**). This model explained 40% of the variance, had an adjusted R^2 of 0.35, and was generally supported at this level of prediction by repeated cross validation procedures. All forms of restrictive management had a modest influence of increasing coral cover by 9.3% (SD = 0.6). The observed and predicted patterns were generally consistent across the SST clusters with most of the deviation from expected coral cover among cells occurring at high coral cover levels (i.e., > 60%) among SST clusters 1 and 4 of the southern Indian Ocean (**Supplementary Figure 4**).

Coral cover responses predicted by the VM suggest that cover declined linearly with an increase in SST skewness and kurtosis and also with increasing dissolved oxygen to between 4.4 and 4.6 ml/l, where it becomes less predictive until 4.9 ml/l. The relationship with calcite was hump-shaped with maximum coral coverage at −7 log mol/m^3. The best-fit model for CumDHW and coral cover was also a hump-shaped pattern but with high variance above 30 CumDHW that was likely responsible for the lack of significance and the unpredictable nature of this variable. Mean temperature was also predictive but concave shaped with

TABLE 1 | Summary of the predictions of mean (±SD) coral cover by all reef cells at the (a) ecoregion, (b) nation, (c) fisheries management system, and (d) SST cluster group in 2020 and in 2050 under the RCP2.6 and RCP8.5 scenarios.

Coral cover predictions				**Selected variables**							
(a) Ecoregion	**Coral cover, 2020**	**Coral cover, 2050 (RCP 8.5)**	**Coral cover, 2050 (RCP 2.6)**	**Kurtosis**	**Standard deviation**	**Bimodality coefficient**	**Mean SST**	**Rate of SST rise**	**Skewness**	**Cumulative DHW**	**Frequency of all cells (%)**
Bight of Sofala/Swamp Coast	30.5 (4.83)	18.18 (7.91)	29.77 (9.06)	−1.09 (0.06)	1.55 (0.13)	0.52 (0.02)	26.85 (0.21)	0.015 (0.001)	0.02 (0.02)	50.98 (6.49)	113 (0.97)
Cargados Carajos/Tromelin Island	24.24 (3.45)	30.42 (9.76)	21.35 (2.64)	−1.15 (0.04)	1.68 (0.12)	0.54 (0.01)	26.45 (0.4)	0.025 (0.001)	0.04 (0.04)	81.44 (6.55)	141 (1.21)
Chagos	33.11 (2.36)	4.81 (2.99)	11.05 (5.83)	−0.27 (0.13)	0.9 (0.09)	0.37 (0.02)	28.21 (0.13)	0.022 (0.001)	−0.06 (0.07)	51.39 (5.59)	1457 (12.48)
Delagoa	39.15 (8.43)	7.2 (7.97)	21.53 (10.68)	−1.23 (0.02)	1.85 (0.1)	0.57 (0.01)	25.59 (0.58)	0.01 (0.003)	0.03 (0.04)	25.5 (5.98)	96 (0.82)
East African Coral Coast	35.76 (6.9)	21.89 (5.63)	29.21 (5.59)	−0.98 (0.11)	1.36 (0.06)	0.51 (0.03)	27.28 (0.15)	0.019 (0.003)	−0.13 (0.08)	31.89 (7.62)	2743 (23.49)
Maldives	35.11 (11.08)	27.92 (12.21)	27.01 (13.49)	0.21 (0.15)	0.72 (0.03)	0.35 (0.03)	28.82 (0.1)	0.019 (0.002)	0.3 (0.19)	29.16 (4.2)	3182 (27.25)
Mascarene Islands	38.03 (3.85)	42.41 (5.02)	37.71 (7.34)	−1.26 (0.01)	1.78 (0.01)	0.57 (0.0)	25.72 (0.09)	0.025 (0.001)	0.02 (0.01)	55.36 (10.17)	196 (1.68)
Northern Monsoon Current Coast	14.35 (2.09)	18.57 (1.61)	14.46 (3.35)	−0.58 (0.04)	1.25 (0.02)	0.44 (0.0)	26.94 (0.05)	0.016 (0.005)	0.26 (0.04)	20.16 (4)	130 (1.11)
Seychelles	41.03 (3.87)	13.69 (6.23)	31.73 (10.54)	−0.95 (0.29)	1.52 (0.17)	0.52 (0.06)	27.4 (0.43)	0.018 (0.002)	−0.22 (0.04)	33.63 (9.29)	701 (6.00)
Southeast Madagascar	31.32 (3.55)	19.65 (10.85)	20.82 (8.14)	−1.14 (0.16)	1.65 (0.02)	0.55 (0.03)	25.32 (0.86)	0.014 (0.008)	0.1 (0.11)	42.2 (15.33)	65 (0.56)
Western and Northern Madagascar	35.68 (10.76)	27.18 (10.86)	33.24 (16.77)	−1.17 (0.08)	1.65 (0.25)	0.57 (0.02)	27.1 (0.68)	0.015 (0.007)	−0.11 (0.18)	39.18 (21.95)	2854 (24.44)
(b) Country											
British Indian Ocean Territory	33.11 (2.36)	4.81 (2.99)	11.05 (5.83)	−0.27 (0.13)	0.9 (0.09)	0.37 (0.02)	28.21 (0.13)	0.022 (0.001)	−0.06 (0.07)	51.39 (5.59)	1457 (12.48)
Comoros	31.51 (4.99)	29.54 (5.48)	20.73 (4.55)	−1.16 (0.01)	1.5 (0.01)	0.55 (0.0)	27.55 (0.01)	0.015 (0.001)	−0.12 (0.01)	31.07 (2.05)	238 (2.04)
French Southern Territories	35.87 (6.33)	27.95 (8.99)	32.2 (10.4)	−1.15 (0.02)	1.6 (0.17)	0.54 (0.01)	27.13 (0.51)	0.017 (0.003)	−0.06 (0.07)	50.56 (10.78)	138 (1.18)
Kenya	18.8 (6.53)	17.28 (3.14)	20.01 (5.48)	−0.69 (0.12)	1.25 (0.01)	0.45 (0.01)	26.99 (0.08)	0.017 (0.004)	0.13 (0.13)	21.32 (6.46)	372 (3.19)
Madagascar	34.57 (11.05)	24.59 (9.93)	31.44 (16.01)	−1.18 (0.09)	1.68 (0.27)	0.58 (0.02)	26.94 (0.77)	0.015 (0.008)	−0.1 (0.2)	41.08 (23.93)	2282 (19.54)
Maldives	35.11 (11.08)	27.92 (12.21)	27.01 (13.49)	0.21 (0.15)	0.72 (0.03)	0.35 (0.03)	28.82 (0.1)	0.019 (0.002)	0.3 (0.19)	29.16 (4.2)	3182 (27.25)
Mauritius	32.57 (7.81)	37.22 (9.63)	30.83 (10.04)	−1.21 (0.06)	1.74 (0.1)	0.56 (0.02)	26.03 (0.46)	0.025 (0.001)	0.03 (0.03)	65.19 (15.87)	304 (2.60)
Mayotte	47.11 (3.05)	44.78 (4.19)	56.67 (9.02)	−1.15 (0.01)	1.47 (0.01)	0.55 (0.0)	27.6 (0.03)	0.015 (0.001)	−0.14 (0.01)	26.62 (3.61)	269 (2.30)
Mozambique	37.64 (5.2)	21.47 (7.02)	30.67 (6.35)	−1.07 (0.06)	1.46 (0.13)	0.53 (0.02)	27.09 (0.51)	0.019 (0.004)	−0.1 (0.08)	35.71 (8.38)	1186 (10.16)
Reunion	33.06 (0.99)	43.2 (1.29)	35.7 (5.89)	−1.24 (0.01)	1.78 (0)	0.57 (0.0)	25.79 (0.08)	0.024 (0)	−0.01 (0.01)	71.98 (2.45)	25 (0.21)
Seychelles	41.03 (3.87)	13.69 (6.23)	31.73 (10.54)	−0.95 (0.29)	1.52 (0.17)	0.52 (0.06)	27.4 (0.43)	0.018 (0.002)	−0.22 (0.04)	33.63 (9.29)	701 (6.00)
Tanzania	36.43 (5.4)	21.85 (5.95)	28.62 (5.59)	−0.98 (0.09)	1.35 (0.05)	0.51 (0.02)	27.33 (0.13)	0.018 (0.002)	−0.16 (0.05)	31.52 (7)	1524 (13.05)
(c) Management											
Fished	33.46 (9.03)	22.26 (8)	28.59 (11.54)	−0.58 (0.63)	1.21 (0.42)	0.47 (0.1)	27.77 (0.95)	0.018 (0.005)	0.05 (0.26)	33.73 (14.74)	4903 (41.98)
Restricted	37.26 (10.02)	25.92 (12.9)	29.68 (14.3)	−1.02 (0.28)	1.5 (0.26)	0.53 (0.06)	27.27 (0.66)	0.018 (0.006)	−0.14 (0.11)	37.19 (14.33)	4883 (41.81)
High compliance closures	34.47 (10.37)	27.39 (13.35)	27.13 (12.05)	−1.09 (0.27)	1.65 (0.29)	0.53 (0.06)	26.48 (0.74)	0.021 (0.006)	0 (0.07)	54.38 (25.09)	250 (2.14)
Low compliance closure	34.1 (5.09)	11.9 (14.38)	16.14 (12.8)	−0.29 (0.35)	0.94 (0.24)	0.38 (0.06)	28.16 (0.51)	0.021 (0.003)	−0.01 (0.14)	46.4 (10.78)	1642 (14.06)
(d) SST Clusters											
1	38.14 (7.77)	23.11 (9.07)	31.15 (11.99)	−1.02 (0.14)	1.41 (0.12)	0.53 (0.04)	27.42 (0.26)	0.019 (0.003)	−0.16 (0.1)	31.66 (11.28)	4794 (41.05)
2	22.53 (9.25)	22.22 (13.07)	33.83 (17.79)	−1.13 (0.11)	2 (0.09)	0.56 (0.02)	26.19 (0.74)	0.003 (0.004)	0.18 (0.07)	58.79 (28.97)	621 (5.32)

(Continued)

TABLE 1 | (Continued)

Coral cover predictions				Selected variables							
(a) Ecoregion	Coral cover, 2020	Coral cover, 2050 (RCP 8.5)	Coral cover, 2050 (RCP 2.6)	Kurtosis	Standard deviation	Bimodality coefficient	Mean SST	Rate of SST rise	Skewness	Cumulative DHW	Frequency of all cells (%)
3	32.17 (5.78)	6.17 (4.75)	12.86 (7.93)	−0.31 (0.13)	0.95 (0.13)	0.38 (0.03)	28.11 (0.33)	0.021 (0.003)	−0.05 (0.11)	48.21 (10.84)	1548 (13.26)
4	34.14 (6.08)	26.66 (11.23)	28.59 (10.91)	−1.24 (0.05)	1.72 (0.13)	0.58 (0.02)	26.45 (0.44)	0.019 (0.005)	-0.08 (0.09)	45.86 (17.25)	1463 (12.53)
5	21.35 (4.35)	14.57 (8.39)	10.48 (7.2)	0.41 (0.07)	0.76 (0.02)	0.38 (0.02)	28.73 (0.03)	0.016 (0.001)	0.54 (0.08)	28.95 (2.75)	1004 (8.60)
6	41.18 (6.65)	33.07 (9.74)	33.7 (9.13)	0.11 (0.06)	0.7 (0.02)	0.34 (0.01)	28.86 (0.11)	0.02 (0.002)	0.19 (0.1)	29.97 (6.12)	2248 (19.25)
Total	35.16 (9.24)	22.44 (12.27)	27.26 (13.71)	−0.62 (0.59)	1.23 (0.41)	0.47 (0.1)	27.71 (0.9)	0.018 (0.005)	0.01 (0.24)	36.52 (15.36)	11678 (100.00)

*Results based on the multivariate GAM or environmental variability model (**Figure 2**) and climate variable predictions in 2020 and 2050. Right side of table presents summaries of SST variables mean (±SD) based on satellite data from 1985 to 2018 from NOAA Coraltemp v3.1 SST product. Organized from left to right based on the strength in ordinating the variables among the 6 SST clusters on the first PCA axis.*

the lowest coverage at ∼27°C and increasing at lower and higher temperatures. Fisheries management was a strong effect but this was largely due to increased coral cover with any form of restriction, whether it be restricted gear use or high or low compliance closures.

Future Coral Cover Predictions

The VM was used to predict coral cover in all cells in 2020 and in 2050 for the BAU (RCP8.5), reduced emissions (RCP2.6), and optimal fisheries management scenarios (**Table 1** and **Figures 3**, **4**). Results indicate geographically patchy cover distributions that generally follow the SST cluster groups. In 2020, the predicted mean cover for the whole region was 35.2% (±9.2) in 2020 (**Figure 3A**). The lowest coral cover predictions (<25%) were for northern Kenya and Maldives and south-west Madagascar or more generally in clusters 2 in the south and 5 in the north. The highest cover predictions were for clusters 1 and 6 with intermediate values in clusters 3 and 4 with the exception of most of northern Kenya.

At the regional level in 2050, coral cover by the VM was predicted to decline to 22.4% (±12.3) and become more spatially variable under the BAU scenario (**Figure 3B**). If the low carbon emission plan of RCP2.6 was successfully implemented, an overall higher coral cover values of 27.3% (±13.7) was predicted and some of the high cover reefs were predicted to increase further (**Figures 3C**, **4**). In the BAU scenario, the largest declines by 2050 were predicted for cluster 3 or the Seychelles, Chagos, and northern Kenya but also the northern part of cluster 5 or the Maldives. There was also a high cover loss predicted for most of the southern reefs of the Delagoa and Bight of Sofala/Swamp coast ecoregions of Mozambique from 39.2% (±8.4) to 7.2 (±8.0) and 30.5% (±4.8) to 18.2% (±7.9) cover, respectively. Southeast Madagascar reefs were also predicted to decline considerably to ∼20% for both scenarios. In contrast, the southern region's Mascarene Islands of Mauritius and Reunion, the scenario outcomes were more variable. Reunion Island's coral cover was predicted to increase under both scenarios. Coverage in Mauritius could either decline or increase dependent on the scenario, increasing in the BAU and declining slightly in the reduced carbon emission scenario. Although both climate change scenarios reduced overall coral cover relative to 2020 regional estimates, the reduced emission scenario was predicted to increase coral cover in SST clusters 1, 2, and 3 locations but not in clusters 4, 5, and 6.

Optimal Fisheries Management Scenario

Fishing restrictions consistently increased coral cover predictions relative to the business-as-usual (BAU; RCP8.5) and reduced emissions scenarios (**Figures 3**, **4**). Management induced increases in coral cover were most notable between the 10 and 40% cover predicted in 2020 with maximum increases of around 15% relative to the BAU and 10% by the carbon emissions scenarios. Because of this non-linear initial-condition effect, including fisheries management, had a minor effect on the predicted number of cells having coral cover above 10% relative to the BAU (∼1%) and carbon emission reduction (∼2%) scenarios (**Supplementary Table 4**). The effect was, however, larger for reef

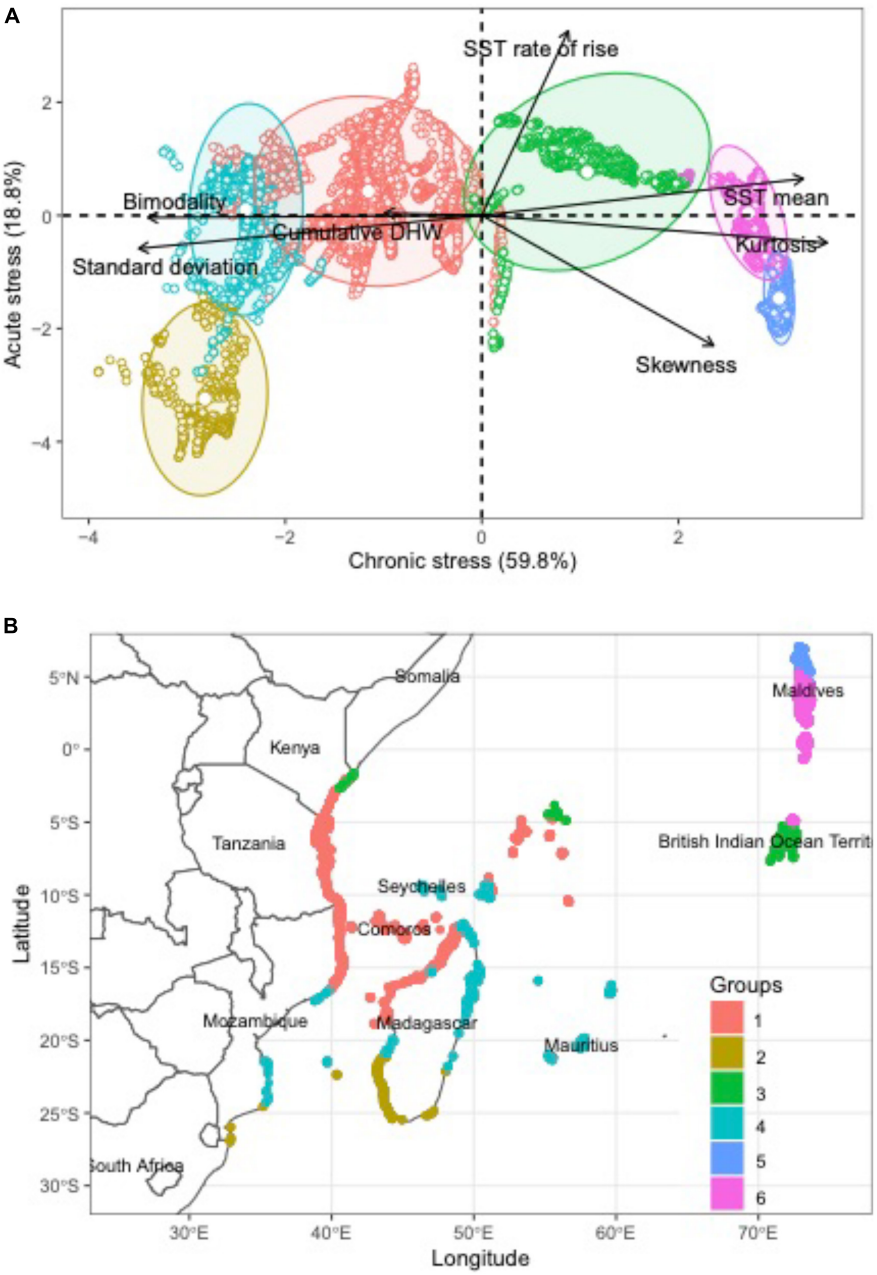

FIGURE 1 | Evaluations of distribution of sea-surface temperatures (SSTs) in the western Indian Ocean. Distribution of sites by **(A)** Principal Component Analysis (PCA) of evaluated SST variables and **(B)** map of the 6 dominant SST clusters distributions.

cells with > 25% cover, increasing by 18% for the BAU and 12% for the reduced emission scenario.

Comparing Models

Comparing the TM with the VM indicates considerable variability in regional-level coral cover predictions (**Table 1** and **Figures 3-5**). Initial coral cover in both models used the same VM-predicted 2020 baseline but cover states in 2050 differed considerably dependent on the two climate change scenarios. Overall, the GAM model predicted higher coral cover in the region by both scenarios. For example, for the RCP8.5 BAU scenarios, the number of cells with coral cover >10% in 2050 was 83% by the GAM and 23% by the DHW-mortality model (**Supplementary Table 4**). Thus, the number of cells with cover <10% increased by 74% for the VM compared to a 14% for the TM.

Reducing carbon emissions in the RCP2.6 scenario increased cover of reefs and cells with >10% cover. The increase was minor (11%) by the TM but more substantial (38.2%) for the VM predictions. If optimal fisheries management were established,

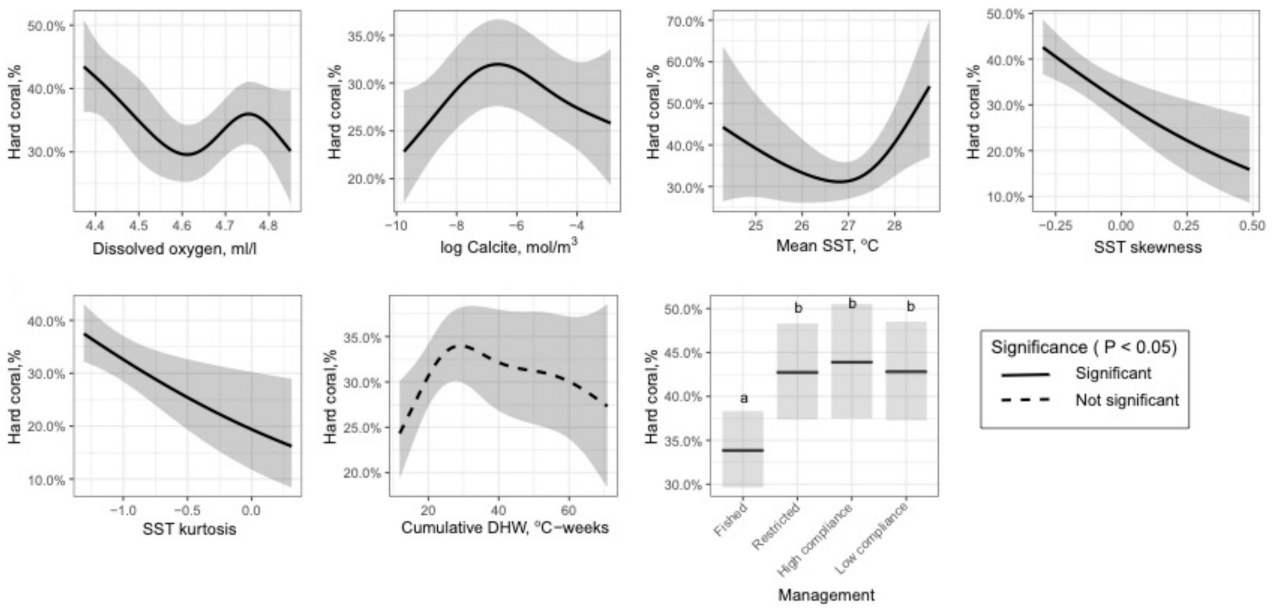

FIGURE 2 | Plots of the best-fit (mean ± 95%) relationships between coral cover and key selected variables identified by the Variability Model (Generalized Additive Model (GAM)).

the increase in number of reefs predicted to have coral cover <10% was reduced to 8.7% of all WIO reefs. Furthermore, the reefs with initial 2020 coral cover >40% were predicted to have more coral cover in 2050 if both restrictive management and emission reductions were implemented.

Prediction were less positive and more divergent between models for corals if the >25% threshold for biodiversity conservation was used. In particular, there was more divergence between scenarios when initial coral cover ranged between 10 and 30%. The 2020 baseline scenario predicted that 87% of reefs had coral cover >25%. The best-cast reduced emissions and increased management of the VM 2050 scenario predicted only 66% and the worst-case TM predicted only 6% of reefs had >25% cover. In a BAU scenario, 60% of the reefs were predicted to fall below 25% or the level where biodiversity was lost. Consequently, while many reefs may maintain net growth if the VM predictions were upheld, there could still be considerable losses in biodiversity without active local and global management. Where there was overlap between the TM and VM model, it was largely in clusters 4 and 5 in the reefs located from northeastern Madagascar to the Tanzanian-Mozambique border region (**Figure 5A**).

The model and 2050 scenario predictions varied considerably within the SST clusters (**Table 1**; **Figure 5** and **Supplementary Table 4**). The TM predictions were that the percentage of reefs with >10% cover was close to zero in clusters 2, 3, and 5 and only clusters 1 and 4 predicted to have ∼42% of the reefs above this net reef growth threshold. Cover was predicted to decline further by the TM when evaluating reefs by the >25% biodiversity threshold with the persistent clusters 1 and 4 having ∼11% of their reefs above 25% and none in all other clusters.

The 2050 predictions for VM RCP8.5 were considerably more optimistic for corals than TM with >85% of the reefs in clusters 1, 2, 4, and 6 having cover >10%. Clusters 3 and 5 were predicted to be the two most affected clusters with only 18 and 65% of reef cells above 10% cover, respectively. The frequency of reefs having coral cover >25% dropped considerably by the VM for this biodiversity threshold. Clusters 1, 2, 4, and 6 were predicted to have between 35 and 79% while predictions for clusters 3 and 5 were 12% and 25% above 25% cover. Fisheries management increased the frequencies above these thresholds, but mostly for the >25% cover threshold. For example, management in the largest clusters 1, 4, and 6 increased the frequency of reefs above this threshold by 25, 22, and 14%, respectively, compared to without management restrictions (**Figure 5A**). Reducing carbon emissions in the RCP2.6 scenario further increased the predicted coral cover, such that only the most disturbed clusters 3 and 5 had significant numbers of reefs with <10% coral cover in 2050.

DISCUSSION

In the WIO region, the empirically-based VM produced a number of outcomes that differed markedly from TM predictions. First, SST heterogeneity in the region was strong and exhibited variable chronic and acute forms of stress that could often be poorly captured solely by a TM mean summer temperature threshold benchmarks. Mean optimal growth and average variances of SSTs, largely the core metrics of the TM, were not significant predictors of coral cover in the WIO, whereas skewness and kurtosis were selected and influential in the final VM. Most of these variables differed among the six large SST clusters dependent on a variety of oceanographic and geographic patterns of current and thermal exposure. Furthermore, there were a number of infrequently considered

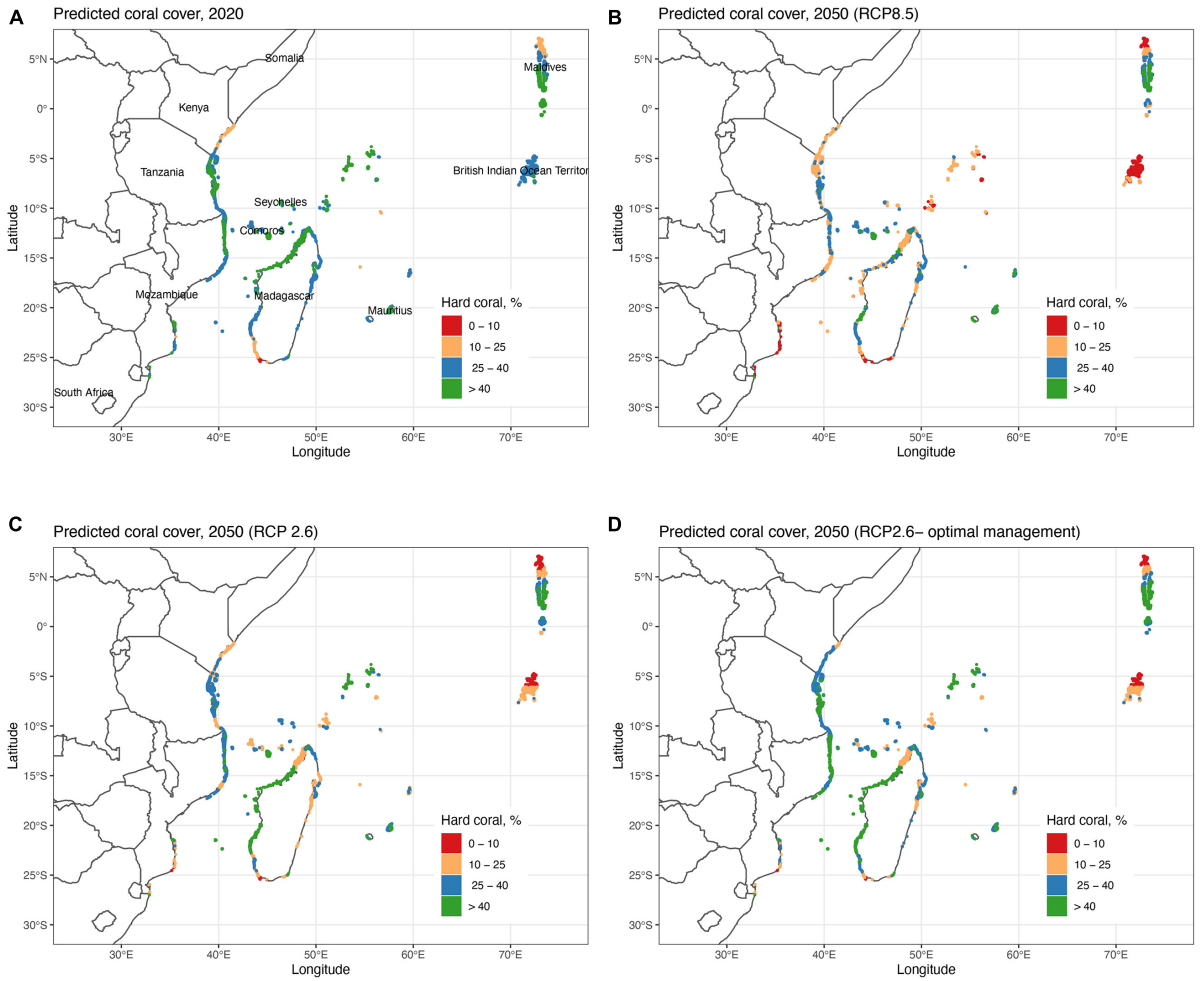

FIGURE 3 | Maps of the predicted coral cover by the Variability Model (VM) **(A)** in 2020 and in 2050 by **(B)** the RCP8.5 model, **(C)** RCP2.6 model, and **(D)** optimal fisheries management (30% closure and 70% restricted fishing) for the RCP2.6 predictions. Cell classifications based on the variables and future predictions of the VM or Generalized Additive Model (GAM) model (**Figure 2**). Note that 2020 predictions are based on 7 and 2050 on 4 variables selected by the GAM model.

variables that were shown to be influential. Most notably, the top variables of dissolved oxygen and calcite concentrations, which should be included in future CMIP evaluates to improve future predictions for coral reefs. The importance of these variables was not peculiar to the WIO. For example, a large modelling study of coral cover in 24 ecoregions of the Coral Triangle found dissolved oxygen to be the single strongest environmental predictor of cover and calcite to be 6^{th} among the 17 variables evaluated (Vercammen et al., 2019). Thus, these variables exhibit similar influences in both regions and are likely to be globally influential rather spatially-restricted drivers of coral cover.

Based on the TM concept and specific application here, coral cover would be expected to decline with cumulative DHW above proposed mortality thresholds. However, large empirical cover compilations have repeatedly found weak, time-since disturbance patterns, or hump-shaped relationships (McClanahan et al., 2015b, 2020a; Darling et al., 2019). The weak hump-shaped relationship found here and in previous studies suggests opposing forces that constrain coral cover within an optimal location, which here and elsewhere was reported at around 30-35 DHW. Consequently, better understanding of thermal stress and its local impacts should illuminate why DHW, as currently used, is infrequently a strong long-term predictor of present and future coral cover (McClanahan et al., 2019, 2020a,b).

The proposed +1°C coral bleaching threshold can appear constant at large scales (Liu et al., 2014). However, this pattern frequently emerges because the +1°C convention was equivalent to 1.73-2.94 SDs for two-thirds of the world's coral reefs (Donner, 2011). Therefore, DHW values are frequently calculated as temperatures ∼ +2SD SST above the mean temperatures. This deviation from the mean should often but not consistently detect bleaching (van Hooidonk and Huber, 2011). However, using DHW stress thresholds in locations outside of where +1°C is approximately equivalent to +2SD-SST results in weaker predictions of bleaching (DeCarlo et al., 2020).

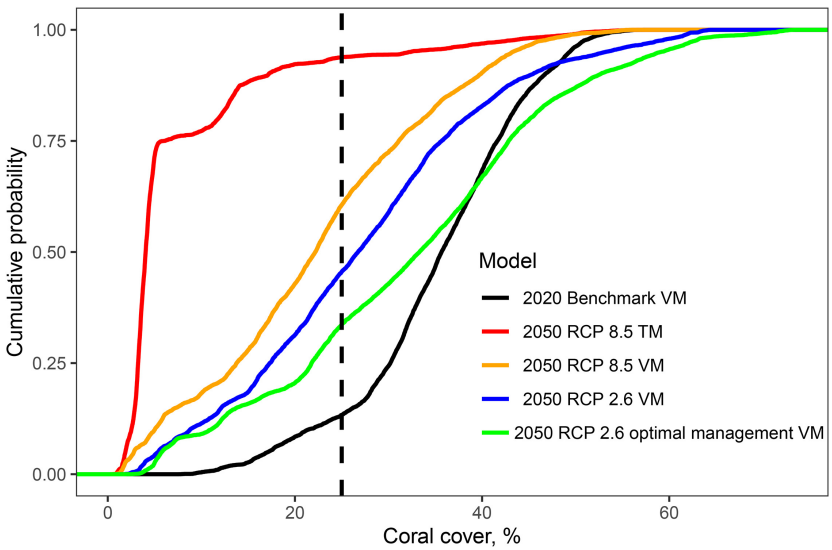

FIGURE 4 | Cumulative frequency distributions showing the cumulative frequencies of coral cover in the 11,678 studied reef cells for the 2020 benchmark prediction of the Variability Model and the four 2050 future scenarios. Scenarios include the Threshold Model (DHW-mortality predictions) for RCP8.5 business-as-usual scenario and the Variability Model for RCP8.5 scenario, RCP2.6 carbon emission reduction scenario, and RCP2.6 with optimal fisheries management system (30 closures and 70% restricted fishing). See **Supplementary Figure 4** for the results presented for each of the 6 SST cluster groups.

More comprehensive evaluations of bleaching have found that removing the +1°C threshold and adding additional variables increased the power to predict bleaching (DeCarlo et al., 2020; Gonzalez-Espinosa and Donner, 2021; Lachs et al., 2021). Moreover, the current DHW metric was expected to become less predictive for bleaching and other coral metrics as corals acclimate, reorganize, and adapt to changing SST conditions (McClanahan, 2017; Hughes et al., 2019). Bleaching represents a stress response to temperatures outside the normal range but is a less accurate measure of mortality (McClanahan, 2004; Welle et al., 2017) - particularly when viewed over time and the subsequent responses in coral mortality and recovery (McClanahan et al., 2015b; Darling et al., 2019). Coral sensitivity to stresses is not constant and appears to be driven by historical differences in SST variability at various temporal scales (Safaie et al., 2018; McClanahan et al., 2020a). Thus, we suggest that the local acute and chronic stress patterns modify the excess thermal stress to produce the hump-shaped DHW-coral cover relationships.

Rare and extreme excess thermal stress, or DHW, will kill corals more than moderate deviations from mean conditions. However, initial warm anomalies will also have a greater impact than subsequent disturbances, as observed in East Africa and the Great Barrier Reef in 2016, 2017, and 2020 (McClanahan, 2017; Hughes et al., 2019). Thus, high coral cover may occur in sites where there is a balance between the forces of acute and chronic stress and acclimation, community change, and genetic adaptation (McClanahan et al., 2020a). The lowest coral cover should occur at the two extremes or outside the optimal location between acute and chronic stress. Therefore, the predicted linear decline in coral cover by the TM was not supported here but rather suggests a weak hump-shaped DHW-coral cover relationship that we believe is more influenced by patterns of chronic and acute stress. The distribution and peak of this hump should vary with historical backgrounds and coral life histories and community structure. The considerable spatial variability in SST cluster or ecoregions suggests that coral responses to climate should be better predicted by empirical models specific to each region. An important caveat is that both models used here did not account for potential future adaptation (acclimation and community and genetic change) or differential recovery rates of corals. As empirical data accumulates specific to each region or SST cluster, the accuracy of predictions should increase beyond those provided by the current larger-scale options. For example, ecoregion has been shown to be strong predictor of coral sensitivity to exposure, even stronger than dissolved oxygen when examined for the Coral Triangle (Vercammen et al., 2019; McClanahan et al., 2020b). Our study was hampered by incomplete and non-random sampling biases at the ecoregion level, which prevented us from using ecoregion as a predictive variable.

Two other key variables of TMs are the mean summer temperature and rate of SST rise, with pH also being a core part of future predictions (Camp et al., 2018). SST rise and pH did not predict the state of coral cover in our empirical study but pH was a significant variable in the Coral Triangle model (Vercammen et al., 2019). Additionally, while mean SST was the 3rd strongest predictor, the relationship found here was u-shaped rather than a decline in cover as mean temperatures increased. That is, the lowest cover was found near moderate tropical SSTs (i.e., 25-27^{o}C) associated with the maximum coral growth (Lough and Cantin, 2014). The implication being that in regions with rapidly changing SST and environmental conditions, locations with optimal mean temperatures failed to maintain coral cover

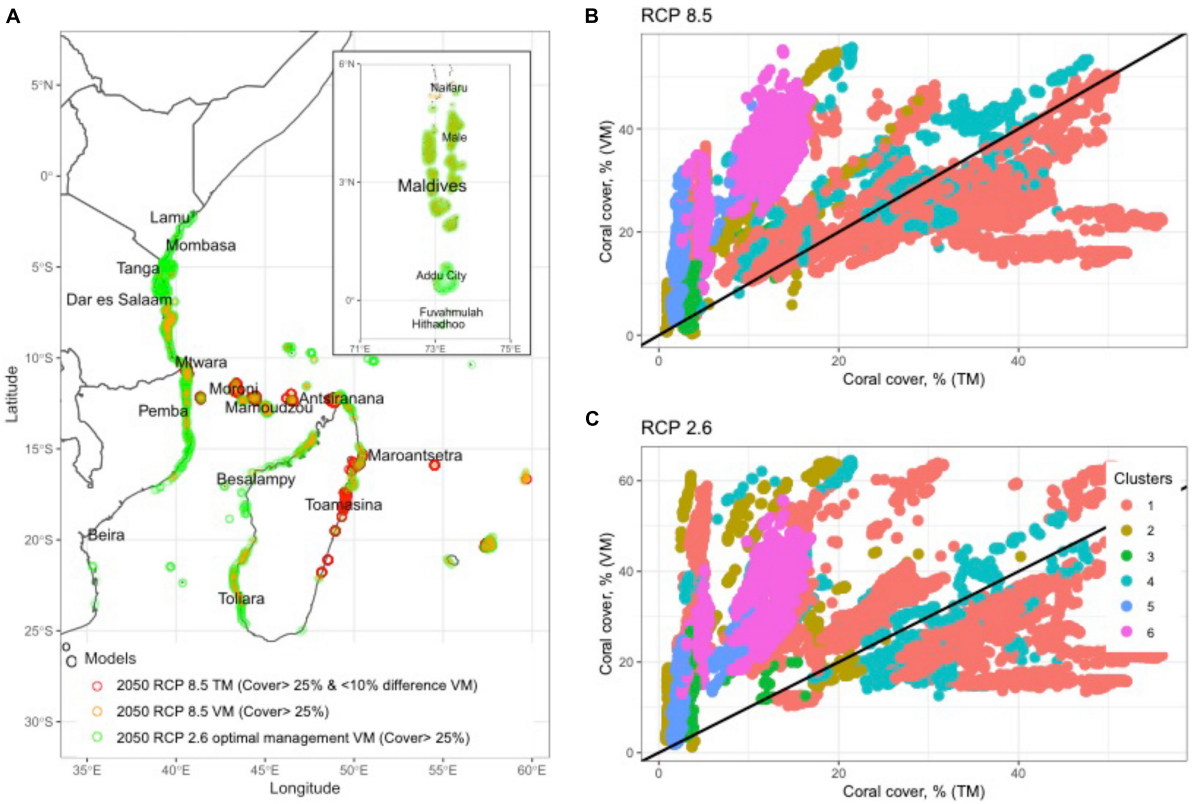

FIGURE 5 | (A) Map plot of three future scenarios and management priority options, which include reef cells selected for (1) coral cover >25% in 2050 for reefs where there is <10% differences between the Threshold (TM) and Variability models (VM), (2) where the business-as-usual (BAU) RCP8.5 predicts >25% coral cover by the VM, and (3) >25% cover with reductions in carbon emissions and optimal fisheries management for the VM. Scatterplot predictions for coral cover comparing the VM and TM predictions in all 11,678 cells in the WIO in 2050 for **(B)** RCP8.5 BAU model in 2050 and **(C)** RCP2.6 carbon reduction scenario. The specific TM presented here is from the DHW-mortality relationships established from observations of DHW and mortality in the GBR during 2016 (Hughes et al., 2018). Cornwall et al. (2021) used this algorithm to estimate coral cover and net reef calcification in 2050 (see methods).

during this period episodic thermal stress These faunal provinces have been undergoing rapid change in recent years, which may be detrimental to corals with narrow optimal growth conditions (McClanahan et al., 2014; Abram et al., 2020).

Less commonly examined metrics not included in TMs were found to be moderate predictors. For example, SST skewness and kurtosis, which were used here as proxies for chronic and acute stress were the 3rd and 4th strongest variables. When evaluated elsewhere, these variables were often among the strongest predictors of a number of coral metrics (Ateweberhan et al., 2018; Zinke et al., 2018; McClanahan et al., 2020a). Cover declined as SST distribution tails became thinner and right skewed, as would be predicted where there is poor acclimation to moderate chronic stress. In some cases, other related proxies, such as daily, seasonal, and annual temperature ranges were good predictors of bleaching and coral cover (Safaie et al., 2018; Vercammen et al., 2019). The maximum and range of SSTs are among the Bio-Oracle SST data options and found to be the 2nd and 3rd strongest environmental variables in predicting coral cover in the Coral Triangle (Vercammen et al., 2019). Consequently, these alternative proxies support the general importance of acute and chronic stress on very broad scales. Including kurtosis and skewness or other appropriate proxies of chronic and acute stress SST metrics, including dissolved oxygen and calcite, should therefore improve predictions

Data distribution variables were shown here to be important but also sensitive to sampling frequency. Therefore, satellite and in situ measurements were likely to differ dependent on the frequency of sampling (McClanahan, 2020; **Supplementary Figure 3**). Less frequently sampled and accurate satellite data may not be able to accurately detect chronic and acute stress (McClanahan and Muthiga, 2021). Satellite data has the distinct advantages of wide coverage and usage for RCP-based predictions, which suggests a need to further consider the satellite proxies that are best at measuring chronic and acute stress. Satellite coverage and CMIP usage allowed us to evaluate a reduced-variable model to make predictions aligned with the metrics currently available. This procedure was useful but less convincing for producing the most accurate predictions expected with the future states of all the variables selected by the GAM. Enough is known about some of these variables that including them in future CMIP models and scenarios is possible and their inclusion should be pursued to improve predictions.

Contextual variables of dissolved oxygen and calcite need to be included in future-cast models to improve predictions. Low dissolved oxygen has been considered a potential stress for corals and other reef invertebrates (Hughes et al., 2020). However, the increasing coral cover with declining or fluctuating oxygen found here suggests a more complicated relationship. The high tolerance to low oxygen among some coral species may explain this pattern. Nevertheless, much remains to be known about how corals respond to the direct and indirect effects of oxygen and how they are associated with other oceanographic and physio-chemical drivers of coral acclimation (Camp et al., 2016). The findings presented here and elsewhere should generate hypotheses for future research (Vercammen et al., 2019). An example of potentially complex relationship is the finding that some coral genes provide co-tolerance to both low oxygen and heat (Alderdice et al., 2021). These investigator's experiments suggested that the upregulation of a hypoxia-inducing factor influenced a coral's tolerance to thermal stress. Clearly, addressing the lack of knowledge, covariance, and the possibility of co-tolerance among stressors should improve understanding and predictions. An unexpected future scenario possibility is that the projected declines in dissolved oxygen with ocean warming could increase tolerance of corals to thermal stress and produce greater resistance than expected to climate change.

The role of fisheries management on coral cover is complex when viewed on a global scale (Graham et al., 2011; Selig et al., 2012; Bates et al., 2019). Nevertheless, previous large compilations of coral cover in the WIO region have shown a weak positive effect of fisheries management on corals but influenced by a number of environmental, ecological, and human use contexts (Ateweberhan et al., 2011; McClanahan et al., 2014; Graham et al., 2020). For example, low compliance reserves and restricted fishing had similar levels of coral cover in the VM. Both fisheries categories have been shown to have similar fish biomass (McClanahan et al., 2015a). Therefore, restrictions on the use of the most destructive gear, such as drag-nets, small-meshed nets, explosives, and spearguns may be important for maintaining coral cover. Cover is likely to be more resistant to modest human fishing disturbances and therefore not requiring the total elimination of local human impacts. If these restriction patterns remain constant or increase further, there could be potential to maintain or increase future coral, particularly in reef already having moderate to high cover.

While our model had modest predictive power, there is still considerable unexplained variation similar to the Coral Triangle model (Vercammen et al., 2019). Unexplained variation based on recent field data is also expected to increase in the future as corals adapt and other unexamined variables influence outcomes of thermal disturbances (McManus et al., 2021). Missing variables is a concern as shown here but also future changes in the disturbances themselves. Changes include a large variety of possible factors that arise for a number of reasons. Not the least is that coral cover is a composite metric that does not include all of the coral organisms and their various life histories, inter-species relationships, and variable responses to stresses (Thompson et al., 2015; Darling et al., 2019; McClanahan et al., 2020a). While cover is the core metric for evaluating reef status, it lacks a considerable amount of life history and stress-response information. Second, is that the grid scale lacks the ability to predict more localized habitat variability. Moreover, the current environmental data are compiled at a coarser scale of ∼9.2-km and therefore limit the potential to evaluate finer-scale resolutions (Assis et al., 2018), Heterogeneity in smaller-scale stress in reef environments, as well as local organismic sensitivity to stress, is evident. Therefore, any gross-scale predictions will fail to capture more resolved variables including habitats, ocean exposure, and depth, among others. Finally, the VM used here reminds us that environmental science can often focus on variables that are assumed to be drivers while failing to examine less considered but potentially important variables. This is evident in the historical focus on water quality parameters that have produced complex, contradictory, and compensatory relationships on coral stress and recovery patterns (MacNeil et al., 2019; Lesser, 2021). Here, eutrophication variables were not examined because they are not widely available on the scale of our study. Nevertheless, future work should consider eutrophication or other proxies to compare their influence relative to calcite and dissolved oxygen. Directed by an incomplete theory, lack of observations, and unobtainable metrics, there is the high possibility for blind spots and unreliable predictions. We see here that the addition of a small number of available variables, such as calcite and dissolved oxygen, had large effects on predictions.

Spatial heterogeneity as uncovered in the SST clustering approach and the consequent future predictions indicate the complexity of potential responses. One notable case of this is the large difference in predictions for clusters 5 and 6 along the Maldives-Chagos islands. Despite their shared oceanic and northern Indian Ocean locations, future predictions were quite sensitive to the patterns of SST skewness along this island chain. Will this observed difference drive changes or will excluded variables of dissolved oxygen, calcite, and others modify outcomes? A large-scale study in 2011 did find lower coral cover in the north compared to the south (Tkachenko, 2015), which is one of the GAM predictions for clusters 5 and 6. These questions are currently unanswerable but could be addressed by further research and monitoring.

This study compared two gross classes of models, the variability and threshold models. It showed how the inclusion of novel environmental variability and empirical relationships can change predictions. The VM predicts less and more spatially variable thermal sensitivity than the TM, which contains fewer influential variables and therefore larger-scale homogeneity in responses to thermal exposure. Predictions overly-reliant on a TM variations and low exposure metrics may have limited spatial applications including identifying the location of sanctuaries. Finding sanctuaries will require expanding and diversifying the suite of ecosystem variables examined for their role in avoidance, resistance, and recovery from climate stresses. The inclusion of five poorly examined variables in the VM produced a more optimistic view of the future than the TM. The heterogeneity of the VM provokes the question of what might be the effect on future predictions for coral reefs by expanding the number

of variables and increasing the spatial resolution of models? Moreover, the efficacy of increasing the quantity, quality, and distribution of field data used to calibrate models. Even large-scale changes, such as global emissions that are expected improve conditions for corals in most regions, were shown to have quite variable consequences for corals among the various SST clusters and management systems. The current failure to understand and evaluate the many sources of variability suggest a need to adopt risk-spreading policies and management decisions.

DATA AVAILABILITY STATEMENT

Environmental data is publicly available and can be found at: https://www.bio.oracle.org/. Coral cover data are available on a formal request to the authors.

AUTHOR CONTRIBUTIONS

TM: conceived the study, collected the field data, supervised the analysis, interpreted the data, and wrote the manuscript. MA: organized the environmental data, undertook the statistical analyses, wrote the methods section, and edited the manuscript. Both authors contributed to the article and approved the submitted version.

FUNDING

TM was supported by the Bloomberg Vibrant Ocean Initiative. MA was supported by the Wildlife Conservation Society's Graduate Scholarship Program through the Beinecke African Conservation Scholarship and the University of California Coastal Science and Policy Program.

ACKNOWLEDGMENTS

The supervision and comments of Mark Carr is greatly appreciated.

SUPPLEMENTARY MATERIAL

The Supplementary Material for this article can be found online at: https://www.frontiersin.org/articles/10.3389/fmars.2021.778121/full#supplementary-material

REFERENCES

Abelson, A. (2020). Are we sacrificing the future of coral reefs on the altar of the "climate change" narrative? *ICES J. Mar. Sci.* 77, 40–45. doi: 10.1093/icesjms/fsz226

Abram, N. J., Wright, N. M., Ellis, B., Dixon, B. C., Wurtzel, J. B., England, M. H., et al. (2020). Coupling of Indo-Pacific climate variability over the last millennium. *Nature* 579, 385–392. doi: 10.1038/s41586-020-2084-4

Alderdice, R., Suggett, D. J., Cárdenas, A., Hughes, D. J., Kühl, M., Pernice, M., et al. (2021). Divergent expression of hypoxia response systems under deoxygenation in reef-forming corals aligns with bleaching susceptibility. *Glob. Change Biol.* 27, 312–326. doi: 10.1111/gcb.15436

Assis, J., Tyberghein, L., Bosch, S., Verbruggen, H., Serrão, E. A., and De Clerck, O. (2018). Bio-ORACLE v2. 0: extending marine data layers for bioclimatic modelling. *Glob. Ecol. Biogeogr.* 27, 277–284. doi: 10.1111/geb.12693

Ateweberhan, M., McClanahan, T. R., Graham, N. A. J., and Sheppard, C. R. C. (2011). Episodic heterogeneous decline and recovery of coral cover in the Indian Ocean. *Coral Reefs* 30, 739–752.

Ateweberhan, M., McClanahan, T. R., Maina, J., and Sheppard, C. (2018). Thermal energy and stress properties as the main drivers of regional distribution of coral species richness in the Indian Ocean. *J. Biogeogr.* 45, 1355–1366.

Bates, A. E., Cooke, R. S. C., Duncan, M. I., Edgar, G. J., Bruno, J. F., Benedetti-Cecchi, L., et al. (2019). Climate resilience in marine protected areas and the 'Protection Paradox'. *Biol. Conserv.* 236, 305–314.

Beyer, H. L., Kennedy, E. V., Beger, M., Chen, C. A., Cinner, J., Darling, E., et al. (2018). Risk-sensitive planning for conserving coral reefs under rapid climate change. *Conserv. Lett.* 11:e12587.

Cacciapaglia, C., and van Woesik, R. (2016). Climate-change refugia: shading reef corals by turbidity. *Glob. Change Biol.* 22, 1145–1154. doi: 10.1111/gcb.13166

Camp, E. F., Schoepf, V., Mumby, P. J., Hardtke, L. A., Rodolfo-Metalpa, R., Smith, D. J., et al. (2018). The future of coral reefs subject to rapid climate change: lessons from natural extreme environments. *Front. Mar. Sci.* 5:4. doi: 10.3389/fmars.2018.00004

Camp, E. F., Suggett, D. J., Gendron, G., Jompa, J., Manfrino, C., and Smith, D. J. (2016). Mangrove and seagrass beds provide different biogeochemical services for corals threatened by climate change. *Front. Mar. Sci.* 3:52. doi: 10.3389/fmars.2016.00052

Chollett, I., Enríquez, S., and Mumby, P. J. (2014). Redefining thermal regimes to design reserves for coral reefs in the face of climate change. *PLoS One* 9:e110634. doi: 10.1371/journal.pone.0110634

Cornwall, C. E., Comeau, S., Kornder, N. A., Perry, C. T., van Hooidonk, R., DeCarlo, T. M., et al. (2021). Global declines in coral reef calcium carbonate production under ocean acidification and warming. *Proc. Natl. Acad. Sci. U.S.A.* 118:e2015265118.

Darling, E. S., McClanahan, T. R., Maina, J., Gurney, G. G., Graham, N. A. J., Januchowski-Hartley, F., et al. (2019). Social–environmental drivers inform strategic management of coral reefs in the Anthropocene. *Nat. Ecol. Evol.* 3, 1341–1350. doi: 10.1038/s41559-019-0953-8

DeCarlo, T. M. (2020). Treating coral bleaching as weather: a framework to validate and optimize prediction skill. *PeerJ* 8:e9449. doi: 10.7717/peerj.9449

DeCarlo, T. M., Carvalho, S., Gajdzik, L., Hardenstine, R. S., Tanabe, L. K., Villalobos, R., et al. (2020). Patterns, drivers, and ecological implications of upwelling in coral reef habitats of the southern Red Sea. *J. Geophys. Res. Oceans* 126:e2020JC016493.

DeCarlo, T. M., and Harrison, H. B. (2019). An enigmatic decoupling between heat stress and coral bleaching on the Great Barrier Reef. *PeerJ* 7:e7473. doi: 10.7717/peerj.7473

Donner, S. D. (2011). An evaluation of the effect of recent temperature variability on the prediction of coral bleaching events. *Ecol. Appl.* 21, 1718–1730. doi: 10.1890/10-0107.1

Donner, S. D., Skirving, W. J., Little, C. M., Oppenheimer, M., and Hoegh-Guldberg, O. (2005). Global assessment of coral bleaching and required rates of adaptation under climate change. *Glob. Change Biol.* 11, 2251–2265.

Donovan, M. K., Burkepile, D. E., Kratochwill, C., Shlesinger, T., Sully, S., Oliver, T. A., et al. (2021). Local conditions magnify coral loss after marine heatwaves. *Science* 372, 977–980. doi: 10.1126/science.abd9464

Gonzalez-Espinosa, P. C., and Donner, S. D. (2021). Cloudiness reduces the bleaching response of coral reefs exposed to heat stress. *Glob. Change Biol.* 27, 3474–3486.

Graham, N. A. J., Nash, K. L., and Kool, J. T. (2011). Coral reef recovery dynamics in a changing world. *Coral Reefs* 30, 283–294. doi: 10.1007/s00338-010-0717-z

Graham, N. A. J., Robinson, J. P. W., Smith, S. E., Govinden, R., Gendron, G., and Wilson, S. K. (2020). Changing role of coral reef marine reserves

in a warming climate. *Nat. Commun.* 11:2000. doi: 10.1038/s41467-020-15863-z

Hughes, D. J., Alderdice, R., Cooney, C., Kühl, M., Pernice, M., Voolstra, C. R., et al. (2020). Coral reef survival under accelerating ocean deoxygenation. *Nat. Clim. Change* 10, 296–307.

Hughes, T. P., Kerry, J. T., Baird, A. H., Connolly, S. R., Dietzel, A., Eakin, C. M., et al. (2018). Global warming transforms coral reef assemblages. *Nature* 556, 492–496. doi: 10.1038/s41586-018-0041-2

Hughes, T. P., Kerry, J. T., Connolly, S. R., Baird, A. H., Eakin, C. M., Heron, S. F., et al. (2019). Ecological memory modifies the cumulative impact of recurrent climate extremes. *Nat. Clim. Change* 9, 40–43. doi: 10.1038/s41558-018-0351-2

Kaufman, L., and Rousseeuw, P. J. (1990). "Clustering large applications (program CLARA)," in *Finding Groups in Data*, (Hoboken, NJ: John Wiley & Sons, Ltd), 126–163. doi: 10.1098/rsta.2019.0394

Kim, S. W., Sampayo, E. M., Sommer, B., Sims, C. A., Gómez-Cabrera, M. D. C., Dalton, S. J., et al. (2019). Refugia under threat: mass bleaching of coral assemblages in high-latitude eastern Australia. *Glob. Change Biol.* 25, 3918–3931. doi: 10.1111/gcb.14772

Lachs, L., Bythell, J. C., East, H. K., Edwards, A. J., Mumby, P. J., Skirving, W. J., et al. (2021). Fine-tuning heat stress algorithms to optimise global predictions of mass coral bleaching. *BioRxiv* [Preprint] doi: 10.1101/2021.1104.1114.439773

Lê, S., Josse, J., and Husson, F. (2008). FactoMineR: an R package for multivariate analysis. *J. Stat. Softw.* 25, 1–18.

Lesser, M. P. (2021). Eutrophication on coral reefs: what is the evidence for phase shifts, nutrient limitation and coral bleaching. *BioScience* biab101. doi: 10.1093/biosci/biab101

Liu, G., Heron, S. F., Eakin, C. M., Muller-Karger, F. E., Vega-Rodríguez, M., Guild, L. S., et al. (2014). Reef-scale thermal stress monitoring of coral ecosystems: new 5-km global products from NOAA coral reef watch. *Remote Sens.* 6, 11579–11606. doi: 10.3390/rs61111579

Lough, J. M., and Cantin, N. E. (2014). Perspectives on massive coral growth rates in a changing ocean. *Biol. Bull.* 226, 187–202. doi: 10.1086/BBLv226n3p187

Maina, J., McClanahan, T. R., Venus, V., Ateweberhan, M., and Madin, J. (2011). Global gradients of coral exposure to environmental stresses and implications for local management. *PLoS One* 6:e23064. doi: 10.1371/journal.pone.0023064

MacNeil, M. A., Mellin, C., Matthews, S., Wolff, N. H., McClanahan, T. R., Devlin, M., et al. (2019). Water quality mediates resilience on the Great Barrier Reef. *Nat. Ecol. Evol.* 3, 620–627.

McClanahan, T. R. (2004). The relationship between bleaching and mortality of common corals. *Mar. Biol.* 144, 1239–1245.

McClanahan, T. R. (2017). Changes in coral sensitivity to thermal anomalies. *Mar. Ecol. Prog. Ser.* 570, 71–85. doi: 10.3354/meps12150

McClanahan, T. R. (2020). "Coral community life histories and population dynamics driven by seascape bathymetry and temperature variability," in *Advances in Marine Biology: Population Dynamics of The Reef Crisis*, eds B. Reigl and P. W. Glynn (London: Academic Press), 291–330. doi: 10.1016/bs.amb.2020.08.003

McClanahan, T. R., and Abunge, C. A. (2018). Demographic variability and scales of agreement and disagreement over resource management restrictions. *Ecol. Soc.* 24:33.

McClanahan, T. R., and Muthiga, N. A. (2021). Oceanic patterns of thermal stress and coral community degradation on the island of Mauritius. *Coral Reefs* 40, 53–74. doi: 10.1007/s00338-020-02015-4

McClanahan, T. R., Ateweberhan, M., Darling, E. S., Graham, N. A. J., and Muthiga, N. A. (2014). Biogeography and change among regional coral communities across the Western Indian Ocean. *PLoS One* 9:e93385. doi: 10.1371/journal.pone.0093385

McClanahan, T. R., Ateweberhan, M., Graham, N. A. J., Wilson, S. K., Sebastián, C. R., Guillaume, M. M., et al. (2007). Western Indian Ocean coral communities: bleaching responses and susceptibility to extinction. *Mar. Ecol. Prog. Ser.* 337, 1–13. doi: 10.3354/meps337001

McClanahan, T. R., Darling, E. S., Maina, J. M., Muthiga, N. A., D 'agata, S., Jupiter, S. D., et al. (2019). Temperature patterns and mechanisms influencing coral bleaching during the 2016 El Niño. *Nat. Clim. Change* 9, 845–851.

McClanahan, T. R., Maina, J., Darling, E. S., Guillaume, M. M. M., Muthiga, N. A., D 'agata, S., et al. (2020b). Large geographic variability in the resistance of corals to thermal stress. *Glob. Ecol. Biogeogr.* 29, 2229–2247. doi: 10.1371/journal.pone.0033353

McClanahan, T. R., Darling, E., Maina, J., Muthiga, N., D 'agata, S., Leblond, J., et al. (2020a). Highly variable taxa-specific coral bleaching responses to thermal stress. *Mar. Ecol. Prog. Ser.* 648, 135–151. doi: 10.3354/meps13402

McClanahan, T. R., Maina, J., and Ateweberhan, M. (2015b). Regional coral responses to climate disturbances and warming is predicted by multivariate stress model and not temperature threshold metrics. *Clim. Change* 131, 607–620. doi: 10.1007/s10584-015-1399-x

McClanahan, T. R., Graham, N. A. J., MacNeil, M. A., and Cinner, J. E. (2015a). Biomass-based targets and the management of multispecies coral reef fisheries. *Conserv. Biol.* 29, 409–417. doi: 10.1111/cobi.12430

McManus, L. C., Forrest, D. L., Tekwa, E. W., Schindler, D. E., Colton, M. A., Webster, M. M., et al. (2021). Evolution and connectivity influence the persistence and recovery of coral reefs under climate change in the Caribbean, Southwest Pacific, and Coral Triangle. *Glob. Change Biol.* 27, 4307–4321. doi: 10.1111/gcb.15725

McManus, L. C., Vasconcelos, V. V., Levin, S. A., Thompson, D. M., Kleypas, J. A., Castruccio, F. S., et al. (2020). Extreme temperature events will drive coral decline in the Coral Triangle. *Glob. Change Biol.* 26, 2120–2133. doi: 10.1111/gcb.14972

Mollica, N. R., Cohen, A. L., Alpert, A. E., Barkley, H. C., Brainard, R. E., Carilli, J. E., et al. (2019). Skeletal records of bleaching reveal different thermal thresholds of Pacific coral reef assemblages. *Coral Reefs* 38, 743–757. doi: 10.1007/s00338-019-01803-x

Mumby, P. J., Elliott, I. A., Eakin, C. M., Skirving, W., Paris, C. B., Edwards, H. J., et al. (2011). Reserve design for uncertain responses of coral reefs to climate change. *Ecol. Lett.* 14, 132–140. doi: 10.1111/j.1461-0248.2010.01562.x

O'Leary, B. C., Winther-Janson, M., Bainbridge, J. M., Aitken, J., Hawkins, J. P., and Roberts, C. M. (2016). Effective coverage targets for ocean protection. *Conserv. Lett.* 9, 398–404. doi: 10.1111/conl.12247

Perry, C. T., Alvarez-Filip, L., Graham, N. A. J., Mumby, P. J., Wilson, S. K., Kench, P. S., et al. (2018). Loss of coral reef growth capacity to track future increases in sea level. *Nature* 558, 396–400. doi: 10.1038/s41586-018-0194-z

Safaie, A., Silbiger, N. J., McClanahan, T. R., Pawlak, G., Barshis, D. J., Hench, J. L., et al. (2018). High frequency temperature variability reduces the risk of coral bleaching. *Nat. Commun.* 9:1671.

Selig, E. R., Casey, K. S., and Bruno, J. F. (2012). Temperature-driven coral decline: the role of marine protected areas. *Glob. Change Biol.* 18, 1561–1570. doi: 10.1111/j.1365-2486.2012.02658.x

Selig, E. R., Hole, D. G., Allison, E. H., Arkema, K. K., McKinnon, M. C., Chu, J., et al. (2019). Mapping global human dependence on marine ecosystems. *Cons. Lett.* 12:e12617. doi: 10.1111/conl.12617

Sheppard, C. R. C. (2003). Predicted recurrences of mass coral mortality in the Indian Ocean. *Nature* 425, 294–297.

Spalding, M., Burke, L., Wood, S. A., Ashpole, J., Hutchison, J., and Zu Ermgassen, P. (2017). Mapping the global value and distribution of coral reef tourism. *Mar. Policy* 82, 104–113.

Taylor, K. E., Stouffer, R. J., and Meehl, G. A. (2012). An overview of CMIP5 and the experiment design. *Bull. Am. Meteorol. Soc.* 93, 485–498. doi: 10.1175/bams-d-11-00094.1

Thompson, J. R., Rivera, H. E., Closek, C. J., and Medina, M. (2015). Microbes in the coral holobiont: partners through evolution, development, and ecological interactions. *Front. Cell. Infect. Microbiol.* 4:176. doi: 10.3389/fcimb.2014.00176

Tkachenko, K. S. (2015). Impact of repetitive thermal anomalies on survival and development of mass reef-building corals in the Maldives. *Mar. Ecol.* 36, 292–304.

Tyberghein, L., Verbruggen, H., Pauly, K., Troupin, C., Mineur, F., and De Clerck, O. (2012). Bio-ORACLE: a global environmental dataset for marine species distribution modelling. *Glob. Ecol. Biogeogr.* 21, 272–281.

van Hooidonk, R., and Huber, M. (2011). Effects of modeled tropical sea surface temperature variability on coral reef bleaching predictions. *Coral Reefs* 31, 121–131. doi: 10.1371/journal.pone.0070400

van Hooidonk, R., Maynard, J., Grimsditch, G., Williams, G., Tamelander, J., Gove, J., et al. (2020). *Projections of Future Coral Bleaching Conditions Using IPCC*

CMIP6 Models: Climate Policy Implications, Management Applications, and Regional Seas Summaries. Nairobi: United Nations Environment Programme.

Vercammen, A., McGowan, J., Knight, A. T., Pardede, S., Muttaqin, E., Harris, J., et al. (2019). Evaluating the impact of accounting for coral cover in large-scale marine conservation prioritizations. *Divers. Distrib.* 25, 1564–1574. doi: 10.1111/ddi.12957

Welle, P. D., Small, M. J., Doney, S. C., and Azevedo, I. L. (2017). Estimating the effect of multiple environmental stressors on coral bleaching and mortality. *PLoS One* 12:e0175018. doi: 10.1371/journal.pone.0175018

Wilson, S. K., Dolman, A. M., Cheal, A. J., Emslie, M. J., Pratchett, M. S., and Sweatman, H. P. A. (2009). Maintenance of fish diversity on disturbed coral reefs. *Coral Reefs* 28, 3–14. doi: 10.1371/journal.pone.0183999

Zinke, J., Gilmour, J. P., Fisher, R., Puotinen, M., Maina, J., Darling, E., et al. (2018). Gradients of disturbance and environmental conditions shape coral community structure for south-eastern Indian Ocean reefs. *Divers. Distrib.* 24, 605–620. doi: 10.1111/ddi.12714

Conflict of Interest: The authors declare that the research was conducted in the absence of any commercial or financial relationships that could be construed as a potential conflict of interest.

frontiers in Marine Science

ORIGINAL RESEARCH
published: 31 January 2022
doi: 10.3389/fmars.2021.812902

Phytoplankton Community Performance Depends on the Frequency of Temperature Fluctuations

Charlotte Kunze[1], Miriam Gerhard[1], Marrit Jacob[2], Niklas Alexander Franke[1], Matthias Schröder[1] and Maren Striebel[1]*

[1] Institute for Chemistry and Biology of Marine Environments (ICBM), Carl-von-Ossietzky University of Oldenburg, Oldenburg, Germany, [2] Faculty of Biology/Chemistry, University of Bremen, Bremen, Germany

With increasing frequency and intensity of climate change events, it is crucial to understand how different components of temperature fluctuations affect the thermal tolerance and performance of marine primary producers. We used a controlled indoor-mesocosm set-up to test the effect of a temperature fluctuation frequency gradient on a natural phytoplankton community. Within a frequency gradient, we allowed the temperature to fluctuate from 18 ± 3°C at different rates (6, 12, 24, 36, and 48 h). The temperature fluctuation frequency gradient was contrasted to a constant temperature treatment with the same mean temperature (18°C). Phytoplankton biomass tended to increase with faster fluctuations but was lowest in the diurnal frequency treatment (24 h). In comparison with constant conditions, diurnal or slower fluctuation frequencies showed lower or comparable performance, whereas faster fluctuations showed higher performance. In addition, minor differences in community structure were observed, but species diversity remained comparable over time. Similarly, resource use efficiency and stoichiometry did not change according to fluctuation frequency treatments. We conclude that the effect of temperature fluctuations on phytoplankton biomass depends on the fluctuation frequency; this suggests that the fluctuation frequency determines how organisms average their environments. However, this trend is not driven by species identity but physiological responses. Our results also indicate that phytoplankton communities may be already well adapted to fluctuating environments and can adjust physiologically to temperature variability.

Keywords: temperature fluctuation, frequency, variability, climate change, phytoplankton, stoichiometry, resource use efficiency, mesocosm experiment

OPEN ACCESS

Edited by:
Christopher Edward Cornwall, Victoria University of Wellington, New Zealand

Reviewed by:
Casey Michael Godwin, University of Michigan, United States
Emily Mae Herstoff, St. Francis College, United States

****Correspondence:***
Charlotte Kunze
Charlotte.kunze@uni-oldenburg.de

Specialty section:
This article was submitted to Global Change and the Future Ocean, a section of the journal Frontiers in Marine Science

Received: *10 November 2021*
Accepted: *30 December 2021*
Published: *31 January 2022*

Citation:
Kunze C, Gerhard M, Jacob M, Franke NA, Schröder M and Striebel M (2022) Phytoplankton Community Performance Depends on the Frequency of Temperature Fluctuations. Front. Mar. Sci. 8:812902. doi: 10.3389/fmars.2021.812902

INTRODUCTION

Across systems and taxa many organisms are exposed to varying temperatures on a regular basis. Temperature variations could include gradual changes in the mean temperature, as well as deterministic or stochastic fluctuations (Moisan et al., 2002; Fujiwara and Takada, 2017). Such fluctuations can trigger functional responses at the organismal level (resource acquisition and allocation) and numerical responses (reproduction) at the level of populations (Chevin et al., 2010; Schaum et al., 2018; Bernhardt et al., 2020; Cabrerizo and Marañón, 2021). Because of the non-linearity of biological responses along the temperature gradient, the consequences of temperature

fluctuations for organisms' performances differ from those observed under constant conditions (i.e., Jensen's inequality) (Jensen, 1906). Additionally, the realized performance of organisms in varying environments depends on their plasticity to respond to such changes (Kremer et al., 2018; Fey et al., 2021).

Acclimation as a specific case of phenotypic plasticity might hereby allow organisms to expand their thermal ranges (Berg and Ellers, 2010; Chevin et al., 2010; Fey et al., 2021) and stabilize population responses in varying environments (Miner et al., 2005; Chevin et al., 2010). Acclimation processes include e.g., altered resource allocation and can be reflected in plankton stoichiometry (Schaum et al., 2018). A divergence in acclimation speed (i.e., gradual plasticity) and phenotypic fitness effects, however, may lead to individual's phenotypes persistently chasing after their environment, severely affecting performance (Kremer et al., 2018; Fey et al., 2021). Thus, the rate of the change and the time of exposure to less optimal temperatures are crucial mediating organisms' performance in changing environments. A growing body of studies have shown that the duration of exposure to above-optimal temperatures can influence organisms' performance and that the thermal range for performance can decrease when exposed to high temperatures for longer time-periods (Rezende et al., 2014; Kingsolver et al., 2015; Kingsolver and Woods, 2016; Kremer et al., 2018). These "time-dependent-effects" can have different impacts on organisms, ranging from positive effects like physiological recovery after a cold period (Colinet et al., 2018), to negative effects reducing survival and growth in ectotherms because of heat stress (Kingsolver and Woods, 2016; Pansch and Hiebenthal, 2019; Wang et al., 2019).

Variability of temperature can be divided into different components, including the magnitude (variance), the frequency, and autocorrelation (predictability of change) (Moisan et al., 2002; Fujiwara and Takada, 2017). Frequency influences not only the time of exposure to different temperatures but also the autocorrelation structure, thus color of noise. Here, autocorrelation structure refers to the relationship between consecutive observations over time and directly influences the predictability of environmental fluctuations across temporal scales, ranging from diurnal to seasonal and annual variation (Halley, 1996; Ripa and Lundberg, 1996; Massie et al., 2015). Indeed, the ability of a population or community to adapt to fluctuating conditions depends on the predictability of change (Ruokolainen et al., 2009; Duncan et al., 2013; Blasius et al., 2020): slower temperature fluctuations are more autocorrelated as a result of a lower rate of change over time and provide more time for acclimation (Koussoroplis et al., 2017; Kremer et al., 2018). Whereas, faster and less autocorrelated (thus less predictable) fluctuations are likely to create mismatches between environmental conditions and acclimation (i.e., gradual plasticity) (Kremer et al., 2018; Fey et al., 2021). Thus, fluctuation frequency is expected to be an important component of variability and, to disentangle its effect from changes in variance, it is essential to test them separately in conceptual experiments, before investigating their combined effect.

While recently the question how fluctuating temperatures influence ectotherm performance in terms of survival, reproduction, and growth has gained increasing attention (e.g., Bernhardt et al., 2018; Schaum et al., 2018; Zhang et al., 2019), only very few studies investigated the effect of fluctuation frequencies (Kremer et al., 2018; Pansch and Hiebenthal, 2019; Wang et al., 2019; Burton et al., 2020), none of them using a gradient design. For example, Kremer et al. (2018) showed that acclimation history as well as fluctuation frequency significantly affected a phytoplankton population and that population densities deviated from the predictions of a rapid acclimation model. Furthermore, both the cold and warm acclimated populations showed the lowest population density in the faster (6 h) fluctuation treatments due to the temporal overlap of plasticity and variability speed. Contrastingly, other studies on ectotherms found a detrimental effect of slower fluctuations with high autocorrelation. In a mytilid study, faster fluctuation frequency (1.5 days) helped to maintain organism's performance whereas slower fluctuation frequency (4.5 days) led to severe reduction in growth rates (Pansch and Hiebenthal, 2019). Similarly, a study on a coccolithophore population found that faster fluctuation frequency (24 h) mitigated the heat stress effects of temperature fluctuations and resulted in lower biomass reduction than slower fluctuation frequency (48 h) (Wang et al., 2019). These contrasting results may be explained by the fact that none of this previous work focused on the frequency of temperature fluctuation as single factor, but instead emphasizes the scale-dependency of temperature fluctuations. Fluctuations can occur over various temporal scales and it is the organism's metabolism (i.e., according to their life span and behavior) which defines how it experiences variability (Jackson et al., 2021). Such perception of changes might influence information transmitted to the next generations; a phenomenon defined as "ecological memory" (Jackson et al., 2021).

Marine phytoplankton have particularly short generation times and thus a short lifespan, which covers a similar timescale as their acclimation rates (Savage et al., 2004; Fey et al., 2021). Delays in plasticity in response to (diurnal) variability might therefore act "*trans*-generational" (Kremer et al., 2018; Rescan et al., 2020). When studying diverse communities, multiple mechanisms take effect, potentially mediating mismatches in realized species performance due to delays in plasticity and community related processes (e.g., complementarity in niche occupancy, competitive exclusion). Phytoplankton shows considerable differences among many traits such as a large range in cell sizes e that directly influences species-specific growth rates (Kerimoglu et al., 2012; Acevedo-Trejos et al., 2013, 2015), a high diversity in morphology (e.g., cell walls, motility), biochemistry (storage products, nutrient uptake mechanisms), and the ability to use the light spectrum differentially (Huisman and Weissing, 1995; Dickman et al., 2006; Kerimoglu et al., 2012). This allows complementary trait distribution and consequently multiple species' co-existence (Hutchinson, 1961; Ebenhöh, 1988). Therefore, diverse communities are expected to buffer the effects of environmental variability on e.g., biomass production (Elmqvist et al., 2003; Bestion et al., 2021). Additionally, environmental variability can affect diversity by promoting species coexistence due to asynchrony in species-specific responses (Yachi and Loreau, 1999; Chesson, 2000;

Loreau and Hector, 2001), or it may lead to species sorting, e.g., the replacement of less tolerant species by smaller, faster-growing taxa with high thermal breadth (Stuart-Smith et al., 2015; Hodapp et al., 2016; Smith et al., 2016; Rasconi et al., 2017; Chen et al., 2019; Bestion et al., 2021).

However, experimental studies investigating the effect of temperature fluctuation on a community level have been limited to single fluctuation scenarios in comparison with a constant regime (Burgmer and Hillebrand, 2011; Rasconi et al., 2017; Gerhard et al., 2019) or different fluctuation magnitudes (Bestion et al., 2021), lacking the consideration of different temperature fluctuation frequencies (over a continuous state-space). While Gerhard et al. (2019) found that reductions in phytoplankton community growth rate were not driven by species identity but a general physiological response to diurnal fluctuations, a few studies reported a change in species dominance as driving mechanism for alterations in phytoplankton community biomass when exposed to fluctuating temperatures in the time period of weeks (Burgmer and Hillebrand, 2011; Rasconi et al., 2017; Cabrerizo et al., 2021).

This raises the question of how phytoplankton communities are affected by alternate temperature fluctuations and whether there is a threshold in fluctuation frequencies after which mismatches in current environmental changes and physiological adjustments due to acclimation occur. Although there are multiple dimensions to temperature variability, this study focuses solely on the effects of different fluctuation frequencies on marine phytoplankton communities. We conducted a controlled indoor mesocosm experiment on a natural plankton community, including phytoplankton and microzooplankton from the North Sea and introduced temperatures that mimic natural conditions during summer (van Aken, 2008; Klein et al., 2019). Temperature treatments were chosen along a frequency gradient, fluctuating every 6, 12, 24, 36 or 48 h with the same amplitude of ±3°C, or remaining constant at 18°C. We chose temperature fluctuation frequencies with ecological relevance, which were faster (6, 12 h), slower (36, 48 h) or matching diurnal fluctuation frequency (24 h). During the experiment, we examined total plankton biomass, phytoplankton biomass and phytoplankton community composition, as well as micro-zooplankton biomass to test the following hypotheses:

H1: Along the fluctuation frequency gradient, phytoplankton performance (estimated as biomass over time) is higher in treatments with slower fluctuation frequency (slower than diurnal) providing more time for phenotypic plasticity (Koussoroplis et al., 2017; Kremer et al., 2018). Thus, a decrease in performance in fast fluctuation frequency treatments (faster than diurnal) is expected because of potential mismatches in variability speed and time required for acclimation (i.e., gradual plasticity) (Kremer et al., 2018; Fey et al., 2021).

H2: A natural and thus highly diverse phytoplankton community might buffer the temperature fluctuation effects on performance through species sorting e.g., toward more tolerant species with wide thermal tolerance (Zhang et al., 2016; Bestion et al., 2021; Cabrerizo et al., 2021). This results in moderate changes in performance among fluctuation frequencies but alterations in the community structure and thus phytoplankton species diversity. Species diversity is expected to decrease with increasing fluctuation frequency resulting in high compositional turnover in faster fluctuation frequency treatments compared to constant conditions (Burgmer and Hillebrand, 2011) and slower fluctuation frequency treatments. These changes in diversity will affect ecosystem functioning and therefore will be reflected in the resource use efficiency of the limiting nutrient, as an index of ecosystem function (Nijs and Impens, 2000; Hodapp et al., 2019).

MATERIALS AND METHODS

Experimental Set-Up

The experiment was conducted in the indoor mesocosm facility of the Institute for Chemistry and Biology of the Marine Environment (ICBM), Wilhelmshaven. The so-called "Planktotrons" are 12 indoor-mesocosms of 600 L each, custom-tailored for plankton studies and made of stainless steel (Gall et al., 2017). To measure plankton community responses to temperature fluctuation frequency over a "continuous state space" (Koussoroplis et al., 2017), we chose an experimental gradient design (**Figure 1**). The fluctuation frequency gradient comprised one constant treatment at 18°C and five fluctuation treatments, which experienced the same mean temperature (of 18°C) as the constant but with 3°C fluctuation every 6, 12, 24, 36, and 48 h (**Figure 1** and see **Supplementary Figure 1** for the complete temperature time series). All treatments were replicated twice. Temperature fluctuated from 15 to 21°C in a sinus curve mimicking the North Sea's natural temperature range during summer but introducing different frequencies (van Aken, 2008; Klein et al., 2019). While many studies used constant conditions as control to compare the experimental treatment to (e.g., Burgmer and Hillebrand, 2011; Zhang et al., 2016; Gerhard et al., 2019), here we included both, a constant treatment as well as a diurnal fluctuation frequency treatment, fluctuating from 15–21°C within 24 h and representing a more realistic control to the experiment (mimicking natural conditions during the experimental season).

The experiment ran for 36 days and started with identical temperature conditions in all Planktotrons (at 18°C) on August 27, 2019. All Planktotrons were inoculated with the same initial plankton community, which was extracted 2 weeks before the experimental start in the German Bight, close to the University of Oldenburg Institute for Chemistry and Biology of the Marine Environment in Wilhelmshaven (53.514031, 8.156335). After extraction, the plankton community was kept in an outdoor basin under natural temperature and light regimes to allow sinking of suspended matter and thus preventing sediment load into the mesocosms. Before filling the mesocosms with 600 liters of the natural plankton community, meso-zooplankton was excluded by filtering through a mesh with 105 μm pore size to minimize grazing pressure on phytoplankton. Zooplankton abundances were counted regularly as a full removal of zooplankton due to its size overlap with larger phytoplankton taxa was not possible.

Light was supplied with an intensity of 119.8–131.3 μmol photons m^{-2} s^{-1} using LEDs with a near-natural light spectrum (IT2040 Evergrow with custom-specific LED composition, see

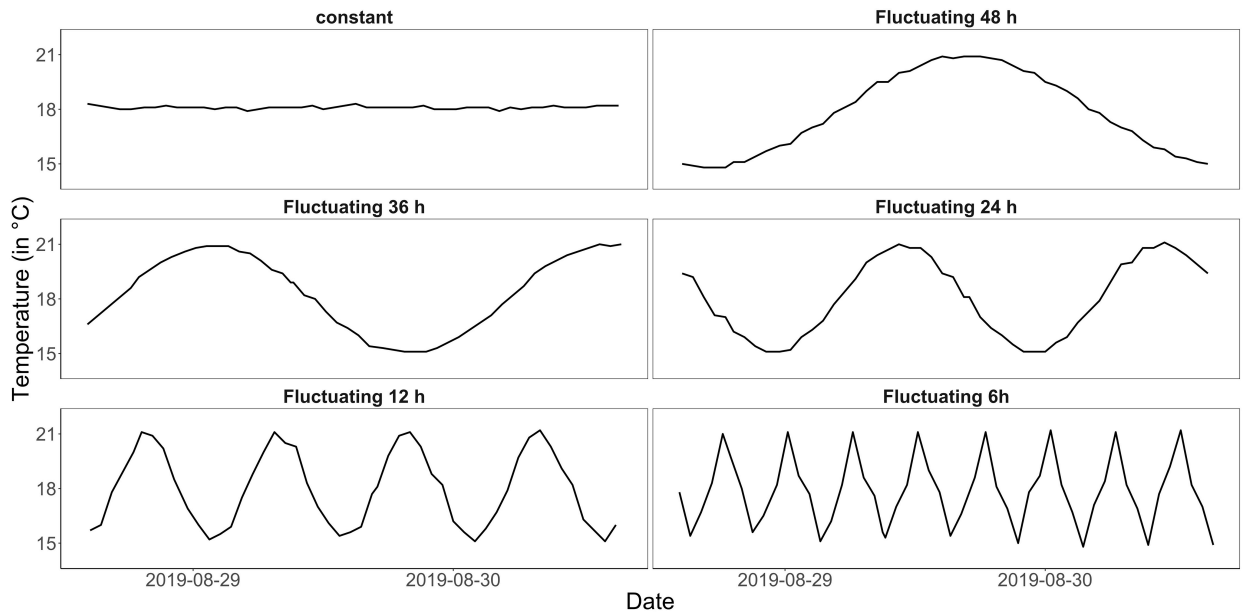

FIGURE 1 | Measured temperature curves for the different treatments (constant control and fluctuation every 6, 12, 24, 36, and 48 h) within 50 h (data shown here for one replicate mesocosm each, from August 28 to August 30; see **Supplementary Figure 1** for a complete temperature time series for each mesocosm). All treatments had the same mean temperature of 18°C and temperature fluctuations had the same amplitude of 3°C, thus were applied over the range of 15–21°C.

Gall et al., 2017) in a 12:12 day:night cycle. Nutrients were supplied continuously to compensate sinking and grazing losses in phytoplankton to maintain constant nutrient availability over the experimental period and, by this reduce potential interactive effects between temperature and nutrients. We added 10% of the start nutrient concentration (NO_3^- 68.6 μg/L, PO_3^- 10.13 μg/L, Si^{2+} 324.25 μg/L measured on August 21, 2019 in the North Sea) daily at every hour using electric "1-channel dosing" pumps (Grotech) and starting at day three after the lag-phase of phytoplankton growth. Stratification of the water column was avoided by increasing the temperature 1–2°C at the bottom of the mesocosms compared to the surface, creating convection in the water column, and keeping homogenous distribution of species and temperature. Additionally, all Planktotrons were mixed using a full electric rotating paddle (Gall et al., 2017) once every hour for 3 min at intermediate intensity (changing the direction of the rotation). Temperature was continuously monitored by PT100 temperature sensors (Gall et al., 2017) in the Planktotrons (**Supplementary Figure 1**).

Sampling and Analysis

Samples to measure phytoplankton and zooplankton biomass and composition as well as dissolved and particulate nutrients were taken every 4th day (starting at day 0 and making a total of 10 samplings). In each sampling, a 6 L integrated water sample across the water column was taken using a tube. Samples were transferred to polyethylene bottles and processed immediately in the laboratory. Phytoplankton and zooplankton samples for microscopic counts were fixed with Lugol's iodine (1% final concentration) and counted using an inverted microscope (Zeiss, Axiovert 10) at 400× magnification (Utermöhl, 1958). Samples for total particulate organic carbon, nitrogen, and phosphorus analysis were filtered onto pre-combusted and acid-washed glass fiber filters (GFC, Whatman) and stored at −80°C in the dark until analysis. Particulate organic phosphorous (POP) was measured using molybdate reaction after sulfuric acid digestion as described in Grasshoff et al. (1999), and particulate organic carbon (POC) and nitrogen (PON) analysis was conducted using a CHN analyzer (Thermo, Flash EA 1112). Particulate silicate (PSi) samples were filtered onto 0.45 μm membrane filters (NC45) and stored in the dark at −80°C before processing samples according to Grasshoff et al. (1999). Dissolved nutrients (PO_4^{3-}, NO_3^-) were determined by a continuous-flow analyzer (Euro EA 3000, HEKAtech GmbH, Wegberg).

Particulate organic carbon measurements were used as an estimation of total plankton biomass (including phytoplankton and zooplankton). For estimating zooplankton and biomass, 6 L water were filtered through a 105 μm mesh and the sample split in equal shares for microscopic abundance determination and CN concentration determination. Phytoplankton biomass was determined by correcting total plankton biomass for zooplankton POC. Molar ratios were calculated using particulate concentrations of C, N, P, and Si. Thus, the stoichiometry of the plankton community was examined using total particulate nutrients, of which zooplankton amounts 6.5% and therefore reflects mainly phytoplankton stoichiometry. To determine if our system was nutrient limited, we calculated the N:P ratio of the dissolved and thus usable fraction of nutrients in the system (**Supplementary Figure 3**). Resource use efficiency (RUE) for the plankton community was calculated as total unit biomass formed (as standing POC) per unit total resource (sum of dissolved and particulate nutrients) for nitrogen and

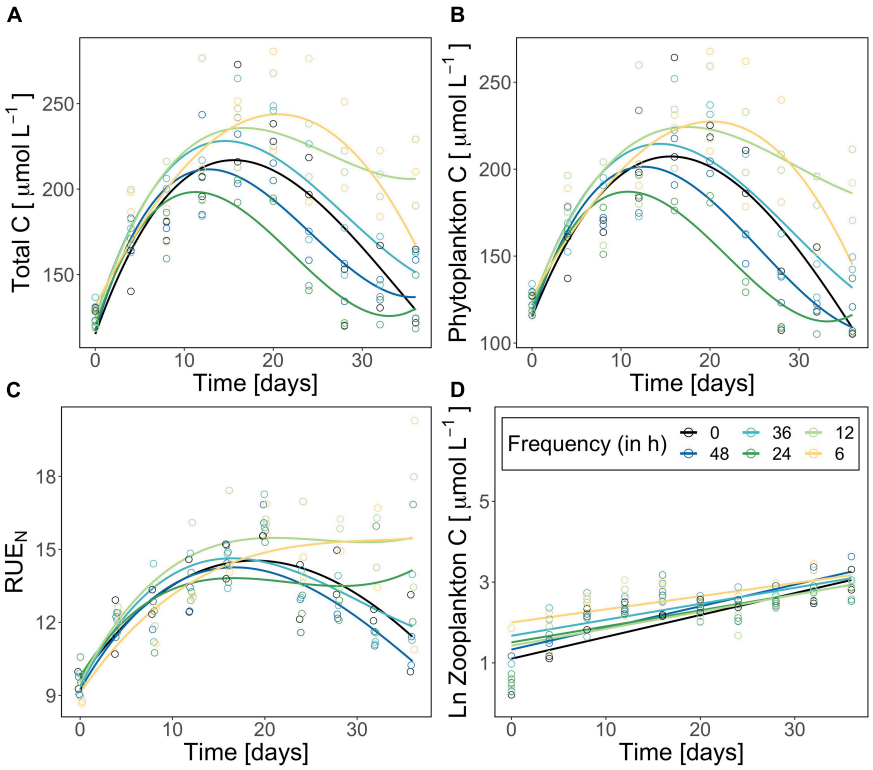

FIGURE 2 | Total plankton biomass (carbon in µmol/L) **(A)**, corrected phytoplankton biomass (carbon in µmol/L) **(B)**, resource use efficiency of nitrogen **(C)**, and ln-transformed zooplankton biomass (carbon in µmol/L) **(D)** during the experiment. The constant treatment is in black, fluctuation treatments are highlighted following a color gradient (dark blue fluctuation every 48 h—yellow fluctuation every 6 h). Each point represents one replicate (n = 2). Please note the different y-scales for panels **(A–C)**. Curves/lines are loess-fits added to visualize the trend over time.

TABLE 1 | Results of the statistical analysis for total Particulate Organic Carbon (POC), phytoplankton POC (total POC corrected for zooplankton carbon as a proxy for phytoplankton biomass), and resource use efficiency of nitrogen (RUE of N) using GAMMs, and zooplankton particulate organic carbon (POC, biomass proxy) using a linear mixed model.

	Total POC		**Phytoplankton (corrected) POC**		**RUE of N**		**Zooplankton POC**	
Transformation		none		none		none		ln
R^2_{adj}		0.60		0.59		0.53		0.42
	Df/edf	***F*(p)**	**Df/edf**	***F*(p)**	**Df/edf**	***F*(p)**	**Df/edf**	***F*(p)**
s(time)	6	38.8 **(< 0.0001)**	1	36.7 **(< 0.0001)**	6	24.8 **(< 0.0001)**	1	38.3 **(< 0.0001)**
Frequency	1 1	5.7 **(0.019)**	6	4.8 **(0.031)**	1	3.7 (0.057)	1	1.6 (0.238)
Time: frequency							1	1.9 (0.168)

Significant effects are indicated in bold.
The R^2 value indicates how much of the observed effects can be explained by the factors.

TABLE 2 | Results of the linear mixed models (LMMs) for phytoplankton compositional structure (species richness, inverse Simpson diversity index, compositional turnover).

	Richness		**Inverse Simpson**		**Compositional turnover**	
Transformation		ln		none		none
R^2_{adj}		0.27		0.07		0.07
	Df/edf	***F*(p)**	**Df/edf**	***F*(p)**	**Df/edf**	***F*(p)**
Time	1	17.8 **(< 0.0001)**	1	0.9 (0.345)	1	0.5 (0.487)
frequency	1	0.7 (0.415)	1	2.2 (0.141)	1	0.05 (0.823)
Time: frequency	1	0.17 (0.686)	1	0.3 (0.560)	1	2.8 (0.096)

Significant effects are indicated in bold.
R^2 value indicates how much of the observed effects can be explained by the factors.

phosphorus (Nijs and Impens, 2000; Ptacnik et al., 2008). RUE of the limiting resource (nitrogen) was used as a proxy for ecosystem functioning (Nijs and Impens, 2000; Hodapp et al., 2019).

Data Analysis

All analyses were performed in R version 4.0.3 (R Core Team, 2020) using the packages *tidyverse* (Wickham et al., 2019), *vegan* (Oksanen et al., 2019), *cowplot* (Wilke, 2019), *mgcv* (Wood, 2011), *lme4* (Bates et al., 2015) and *lubridate* (Grolemund and Wickham, 2011). We analyzed the effect of temperature fluctuation frequency on total plankton, phytoplankton, and zooplankton biomass, as well as phytoplankton diversity, and resource use efficiency of the limiting resource (RUE of nitrogen). To ensure equidistant intervals within the fluctuation frequency gradient, we calculated the fluctuation frequency within 48 h for each treatment. Mixed models were performed including time (experimental day) and fluctuation frequency (within 48 h) as continuous independent variables. The mesocosm ID was introduced as a random component in the models. This allowed us to take the non-independence of the data into account (repeated measures over time) and include potential idiosyncratic effects of experimental units (mesocosms). To account for the non-linear response of phytoplankton biomass, total plankton biomass and RUE of nitrogen over time (**Figure 2**), we used generalized additive mixed models (GAMM) within the *mgcv* package. A thin plate spline smoother (penalized likelihood approach) was included for time and fluctuation frequency was analyzed as linear predictor (n = 120). Only for time a smoother function was included because smoothing the fluctuation frequency resulted in a linear relationship. Introducing only one smoother, we chose a gam model without interaction. Zooplankton biomass did not correlate with phytoplankton biomass (spearman correlation, R = 0.09; p = 0.31; **Supplementary Figure 2**) and was therefore not included as predictor in the phytoplankton model.

To test for fluctuation frequency effects on phytoplankton diversity and zooplankton biomass (as POC), we used linear mixed models (LMMs) within the *lme4* package. Richness, inverse Simpson diversity, and compositional turnover were used as diversity indices for phytoplankton community. Compositional turnover was examined by calculating the Bray-Curtis distance of phytoplankton community composition (vegdist, *vegan* Package) for each treatment over time compared with the starting point. For phytoplankton diversity five samplings were included (n = 60) while for zooplankton biomass data of the 10 samplings were available (n = 120). Species diversity (richness and inverse Simpson) and zooplankton biomass were ln-transformed to get linear relations and meet requirements for LMM analysis (see **Tables 1**, **2**). Differences in community composition (based on species relative abundance) among fluctuation frequency treatments and time were examined by performing an Analysis of Similarity (ANOSIM) using the Bray-Curtis index with 999 permutations. The SIMPER test was used as a *post hoc* test to identify the species explaining differences among treatments.

RESULTS

Temperature Fluctuation Frequency Effects on Plankton Biomass, Stoichiometry and Resource Use Efficiency

Total plankton and phytoplankton biomass significantly changed over time and as an effect of the fluctuation frequency treatment (significant time effect, significant treatment effect; **Table 1**). Total plankton POC (as proxy for plankton biomass) followed a hump-shaped pattern over time, increasing during the first 10–20 days and decreasing afterward. Zooplankton biomass increased significantly over time but did not differ among treatments (**Figure 2**; significant time effect and no effect of frequency, **Table 2**). Phytoplankton biomass followed the same pattern as total plankton biomass since zooplankton represented only 6.5% of total plankton biomass (**Figure 2**), indicating that total plankton reflected the phytoplankton patterns. Fluctuation frequency increased (phyto-)plankton biomass, with faster fluctuations showing the highest concentrations (**Figure 2** and **Table 1**). However, the biomass response was not strictly ordered by the fluctuation frequency and thus, the effect of fluctuation frequency on (phyto-)plankton biomass was only moderate. The fast fluctuation frequency treatments (6, 12 h) resulted in higher biomass than both, the constant treatment and the diurnal fluctuation treatment. In the slow fluctuation frequency treatments (36, 48 h) the biomass was either comparable to the constant treatment or slightly lower. The diurnal fluctuation frequency treatment (24 h) showed the lowest biomass (**Figures 2A,B**).

N:P ratios of dissolved nutrients ranged from 1 to 10 (**Supplementary Figure 3**) indicating that our experimental system was nitrogen limited (Koerselman and Meuleman, 1996). RUE of nitrogen changed significantly over time but did not differ significantly among treatments (significant time effect, **Table 1**). Besides the diurnal fluctuation treatment, RUE of nitrogen (**Figure 2D**) showed similar patterns as the carbon data for total (phyto-)plankton biomass. Molar N:P ratios of particulate nutrients nearly reflected the Redfield ratio (∼16:1) and were comparable in all treatments (**Supplementary Figure 3**). C:Si ratios decreased over time (**Supplementary Figure 4**). Molar C:N ratios followed the same pattern as RUE of nitrogen (**Figure 2D** and **Supplementary Figure 5**), while RUE of phosphorus reflected C:P ratios (**Supplementary Figures 3**, **5**). RUE of nitrogen and C:N ratios in the diurnal fluctuation frequency treatment were higher than or comparable with the slower fluctuation treatments (36h and 48h), and constant conditions over time (**Figure 3** and **Supplementary Figure 5**).

Temperature Fluctuation Frequency Effects on Phytoplankton Community Structure

The phytoplankton community structure was determined as species richness, inverse Simpson index, turnover over time, and species composition. Species richness decreased over time

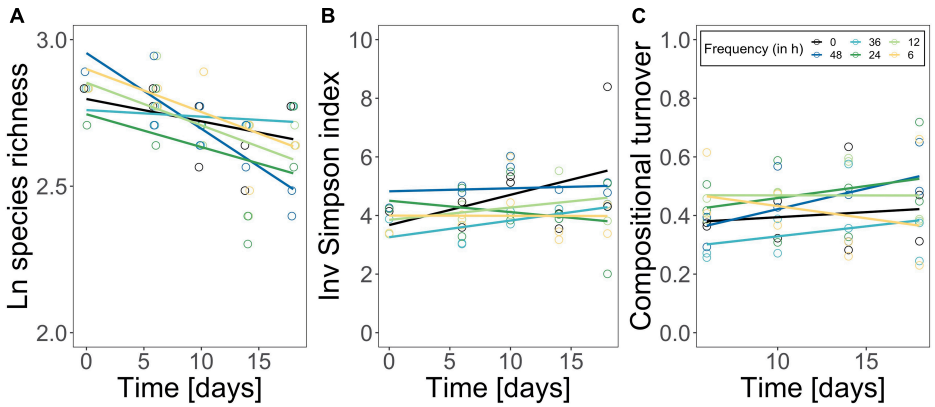

FIGURE 3 | Logarithmized species richness **(A)**, inverse Simpson diversity index **(B)** and compositional turnover (Bray-Curtis distance of phytoplankton community) **(C)** over time. The constant treatment is in black, fluctuation treatments are highlighted following a color gradient (dark blue fluctuation every 48 h—yellow fluctuation every 6 h). Each point represents one replicate (n = 2). Lines represent linear loess-fits added to visualize the trend over time.

from 17 species on average to 13 species on average, but independently of the fluctuation frequency treatments (**Figure 3A**; time effect, **Table 2**). Inverse Simpson index did not change significantly between treatments (**Figure 3B** and **Table 2**) but remained similar over time, suggesting that community evenness was maintained throughout the experiment. Compositional turnover did not change as an effect of treatments or over time (**Figure 3C** and **Table 2**) indicating that there was no change in dominating taxonomic groups due to species sorting. In addition, the performed ANOSIM showed no significant treatment effect, but a significant effect of time (R = 0.35; p = 0.001) on phytoplankton species composition. However, the dissimilarity was low, indicating that the differences over time in relative species abundance were small. Variations in *Cryptomonas* species' abundance explained > 72.6 % of the differences between the initial composition and the end composition in all treatments. Although, *Cryptomonas* species abundance increased in all treatments (**Supplementary Figure 6A**), diatoms were the dominant taxonomic group in the phytoplankton community composition at the beginning and at the end of the experiment in all treatments (**Supplementary Figure 6B**). Most dominant zooplankton groups were calanoid and cyclopoid copepods, and ciliates.

DISCUSSION

To predict how marine phytoplankton communities are affected by variability is one of the major challenges in marine ecology to-date (van de Waal and Litchman, 2020; Cabrerizo and Marañón, 2021). Here, we focused on the single effect of temperature fluctuations on phytoplankton performance and showed that it differed among fluctuation frequencies, even if the amplitude and mean temperature was maintained. Contrary to our expectations in H1 we found that performance increased with increasing fluctuation frequency: fast fluctuations (6, 12 h) showed greater performance, as measured by standing phytoplankton biomass, slow fluctuation frequencies (36, 48 h) had either comparable or slightly lower performance compared to the constant treatment. Whereas the diurnal fluctuation frequency (24 h) had the lowest performance compared to other treatments. Molar N:P ratios as a measure for phytoplankton stoichiometry were comparable in all treatments (rejecting H1). Contrary to our expectations in H2, we found that while species richness changed over time, it did not do so in response to the fluctuation treatments. Simpson diversity index and compositional turnover did not change according to treatments nor over time. Similarity in community structure (diversity and composition) was not supported by similar RUE across experimental treatments. Based on our results, we conclude that changes in standing biomass were driven by physiological responses, not compositional changes in phytoplankton communities.

Exploring H1: Fluctuation Frequency Effects on Phytoplankton Performance (Standing Biomass and Stoichiometry)

The results contradicted our expectations that biomass production is favored by slower temperature fluctuation frequencies and thus the autocorrelation of fluctuations. Instead, standing biomass and resource use efficiency of nitrogen (RUE) (**Figure 2**) was generally higher in faster fluctuation frequency treatments (6, 12 h) and lower in both, diurnal (24 h) and slower (36, 48 h) fluctuation frequency treatments. Our results indicate that effects of temperature fluctuation frequency are dependent on how organisms "average their environments" (Koussoroplis et al., 2017). Encountering suitable temperatures for growth more often might lead to an increase in realized phytoplankton biomass in faster fluctuation frequency treatments (6, 12 h), suggesting that the environment is perceived as if organisms were in more suitable conditions for a longer cumulative period of time (Koussoroplis et al., 2017). Consequently, organisms spend longer consecutive periods of time in less suitable temperatures when experiencing slower fluctuation frequencies (Feder and Hofmann, 1999; Colinet et al., 2018). These time-dependent effects are particularly relevant in studies on ectothermic

populations because the environment has a direct influence on their metabolism (Kingsolver et al., 2015; Colinet et al., 2018; Pansch and Hiebenthal, 2019; Wang et al., 2019). Performance and survival might decrease with increasing duration of exposure to stressful temperatures (Niehaus et al., 2012; Rezende et al., 2014; Kingsolver et al., 2015; Koussoroplis et al., 2017), whereas a brief exposure to suboptimal temperatures may allow for higher subsequent thermal tolerance and survival e.g., due to the expression of heat shock proteins (Feder and Hofmann, 1999; Kingsolver and Woods, 2016). In our experiment, we did not cover stressful temperature ranges but used naturally occurring amplitudes for fluctuation frequency treatments (van Aken, 2008; Klein et al., 2019), suggesting that thermal stress played only a minor role. However, the duration of exposure can influence performance even for temperatures, which are far from extremes (Rezende et al., 2014). We suggest that in our experiment fluctuations with a diurnal frequency or slower (24, 36, 48 h), act to suppress growth due to longer periods in less favorable temperatures compared with faster fluctuation frequencies. Similar to our results, in a mytilid study, organisms could compensate for the exposure to low temperatures if fluctuation frequency was faster, while slower fluctuation frequency led to severe reduction in growth rates (Pansch and Hiebenthal, 2019). In a coccolithophore population slower fluctuation frequencies of 4.5 days significantly reduced performance compared with faster fluctuation frequencies of 1.5 days due to a downregulation of photosynthetic activities during cold phases (Wang et al., 2019).

Reducing the time for plasticity seemed to increase biomass production in our experiment. Plasticity is usually considered to appear during individuals lifespan, thus within one generation (Kremer et al., 2018). Phytoplankton communities, however, cover a large size gradient allowing for differences in growth rates, temperature, and nutrient prevalence (Kerimoglu et al., 2012; Acevedo-Trejos et al., 2013, 2015). One consequence of the broad range of physiological properties is the diversity of responses in physiological adjustments (i.e., phenotypic plasticity). Although we used a diverse natural phytoplankton community with a large size range here, we can assume that phytoplankton generation time is ∼1 day (Savage et al., 2004), meaning that in our experimental setup phytoplankton experienced fluctuations that acted within one generation (6, 12 h fluctuations) as well as across generations (36, 48 h fluctuations). How variability is experienced by the previous and current generation is an important aspect of phenotypic plasticity shaping the interaction between "within- and transgenerational plasticity" (Fox et al., 2019). Temperature fluctuations might therefore mediate ecological memory of phytoplankton communities (Rescan et al., 2020; Jackson et al., 2021). Considering that phytoplankton's lifespan is on a similar timescale as their acclimation rates (Savage et al., 2004; Fey et al., 2021), slower fluctuations may allow for epigenetic plasticity (parental transmission) which affects the performance of the next generation that possess parental environmental information but perform in a novel environment (Guillaume et al., 2016; Kremer et al., 2018; Schaum et al., 2018). This effect may generate a mismatch of acclimated phenotypes and the new current environment, exacerbating the effect of temperature variability (Guillaume et al., 2016) and resulting in lower realized (community) performance (Hanson and Skinner, 2016; Kremer et al., 2018; Fey et al., 2021). Acclimation processes can alter fitness over several generations in the new conditions due to a cost-intensive chase to adjust to the environment suppressing biomass production (Anning et al., 2001; Kremer et al., 2018). For example, Bestion et al. (2021) described substantial effects on phytoplankton performance under large fluctuations when including higher fluctuation amplitudes.

Alterations in (phyto-)plankton community biomass can often be related to changes in resource allocation of the system due to plasticity in responses to changing temperatures (i.e., physiological traits) (Miner et al., 2005; Toseland et al., 2013; De Senerpont Domis et al., 2014). This can be reflected in the community stoichiometry (i.e., molar ratios). Here, N:P ratios nearly reflected the Redfield ratio (∼16) and were comparable among treatments (**Supplementary Figure 5**), suggesting no changes in resource allocation. In addition, carbon:nutrient ratios followed the biomass trends, while dissolved nutrients were low in all treatments (**Supplementary Figure 5**) indicating high nutrient conversion into biomass. We conclude that potential differences in resource allocation were limited due to low nutrient availability (**Supplementary Figure 5**), which reflected natural nutrient concentrations in the North Sea.

Moreover, it is important to note that neither biomass nor resource use efficiency of nitrogen were strictly ordered by the fluctuation frequency gradient. Interestingly, the lowest biomass was detected for the 24 h frequency treatment which correspond to the diurnal fluctuations experienced by the community before the experiment. However, this trend was not reflected in the resource use efficiency of the diurnal fluctuation frequency treatment (**Figure 2**). Our results suggest that there might be other processes involved in how communities adjust to variability in natural systems (i.e., physiological plasticity). When comparing thermal fluctuations with constant conditions in our experiment (**Figure 2**), the differences in biomass support the idea that deviations of expected patterns (i.e., Jensens inequality) (Jensen, 1906) might be detected when considering different frequencies of change (Koussoroplis et al., 2017). Lacking gradient designs and often choosing scenario-based set-ups in ecology, predictions on how scales of environmental change and organisms' generation time may interact are limited. Organisms perceive environmental change at distinct scales according to their generation times, triggering various responses (Jackson et al., 2021). Although we were not able to elaborate on the evolutionary processes in plankton communities here, our results emphasize the importance of testing the different dimensions of variability in single experiments to unravel underlying mechanisms.

Exploring H2: Fluctuation Frequency Effects on Phytoplankton Community Structure and Resource Use Efficiency

Phytoplankton community structure was not significantly affected by temperature fluctuation frequency (**Figure 3**): species richness decreased in all treatments over the experimental period,

likely due to the closed mesocosm set-up preventing species gain by immigration (Hillebrand et al., 2010). Compositional turnover over time was comparable among treatments (**Figure 3**) suggesting no major shifts in phytoplankton community composition driven by the fluctuation frequency gradient (**Supplementary Figure 6**). This was supported by a lack of differences in the species composition among treatments, but diatoms remained the dominant taxonomic group throughout the experiment (**Supplementary Figure 6**). Also, we did not observe a shift in species dominance toward one species with high thermal tolerance, as was reported in other studies (e.g., Zhang et al., 2016; Rasconi et al., 2017; Bestion et al., 2021; Cabrerizo and Marañón, 2021), but diversity (estimated by the inverse Simpson index) was maintained over the experimental period (**Figure 3**). In fact, environmental variability might facilitate species coexistence (Flöder and Sommer, 1999; Loreau and Hector, 2001; Descamps-Julien and Gonzalez, 2005) maintaining high species diversity with the capacity to compensate environmental fluctuations (Elmqvist et al., 2003; Bestion et al., 2021). Additionally, phytoplankton have a large range of complementary traits, therefore species with e.g., a smaller thermal breath are not necessarily outcompeted by their superior competitors if they are able to e.g., use nutrients more efficiently (i.e., niche partitioning) (Hutchinson, 1961; Ebenhöh, 1988). The similarity in community structure (diversity and composition) was also reflected in the resource use efficiency of nitrogen (**Figures 2**, **3**): RUE changed over time but treatment effects were only marginal (**Table 1**). Instead, the resource use efficiency of nitrogen as limiting resource (RUE), a proxy for ecosystem functioning (Nijs and Impens, 2000; Hodapp et al., 2019), was genuinely high (**Figure 2D**). Also, RUE of nitrogen and phosphorus followed the same pattern as molar C:N and C:P ratios (**Figure 2D** and **Supplementary Figures 3**, **5**), respectively, due to a continuous but low nutrient supply in our experiment, which accelerated the incorporation of available nutrients into biomass (**Supplementary Figure 5**). Consequently, effects on compositional structure and general ecosystem functioning were marginal. We conclude that alterations in RUE and differences in standing biomass among the fluctuation frequency treatments did not arise from shifts in compositional structure in our experiment, but that physiological mechanism may have driven the community's responses (Berg and Ellers, 2010; De Senerpont Domis et al., 2014; Gerhard et al., 2019; Barton et al., 2020; Cabrerizo et al., 2021).

In summary, we found differences in biomass along a fluctuation frequency gradient and over time, however, these were not reflected in phytoplankton community structure or resource use efficiency and stoichiometry. Instead, our results suggest that natural marine phytoplankton communities and thus phenotypes of phytoplankton individuals are well adapted to frequencies with naturally relevant amplitudes and might acclimate relatively fast. Trends in biomass might arise from how species average their environment and due to transgenerational effects. However, in our experiment the thermal range of fluctuations might be too small to see substantial effects on performance as were found when including higher fluctuation amplitudes (Kremer et al., 2018; Bestion et al., 2021). In theory, variability effects are expected to be small if species can acclimate fast or fitness benefits of acclimated phenotypes are minor (Fey et al., 2021). However, we did not choose a scenario-based approach for our experiment but aimed to elaborate on the importance of fluctuation frequency impacts. Although, climate change is not expected to alter deterministic variability such as seasonal, diurnal or annual fluctuation, stochastic fluctuations may increase not only in intensity, but also amplitude and frequency, affecting directly the autocorrelation of change and therefore triggering different responses in marine phytoplankton (Ruokolainen et al., 2009; Duncan et al., 2013; Blasius et al., 2020). With proceeding climate change, nutrient limitation will constrain phytoplankton production and ultimately alter the ability to acclimate to variability in phytoplankton (e.g., physiological adjustments due to plasticity) (van de Waal and Litchman, 2020). Also, other abiotic stressors such as pCO_2 and physical processes such as current, mixing and a higher species turnover may amplify the effect of variability.

CONCLUSION

Our study shows that the frequency of temperature fluctuations can significantly alter phytoplankton biomass production. Although, we detected differences in standing biomass among faster fluctuation frequency and slower fluctuation frequency treatments, we did not observe a clear threshold in our frequency gradient after which mismatches in fluctuation frequency and plasticity occur. Furthermore, only minor changes in composition and diversity could be observed, which were reflected in resource use efficiency of nitrogen, indicating that ecosystem functioning could be maintained. We conclude that not compositional shifts, but physiological mechanisms may drive community's responses. Our results suggest that natural marine phytoplankton communities may be more resilient to moderate temperature fluctuations than expected and can quickly adjust to fluctuating environments (Berg and Ellers, 2010; Gerhard et al., 2019). With on-going climate change, however, the unpredictability of temperature change will increase in terms of frequency, intensity, and amplitude, likely constituting a new challenge with the need for high thermal breath and fast plasticity in marine phytoplankton.

DATA AVAILABILITY STATEMENT

The original contributions presented in the study are included in the article/**Supplementary Material**, further inquiries can be directed to the corresponding author/s.

AUTHOR CONTRIBUTIONS

MSc, MSt, and CK designed the experiment. CK, NF, MJ, and MSt conducted the experiments with assistance of MSc. CK and MG conducted the analyses. CK wrote the first draft of

the manuscript with the help of MSt and MG and all authors contributed to revisions.

FUNDING

MSt acknowledges funding by the Deutsche Forschungsgemeinschaft DFG (STR 1383/8-1), MG was supported by the Uruguayan Agency of Investigation and Innovation (ANII: POS_EXT_2015_1_122989), the German Academic Exchange Service (DAAD: 91645020), and H2020 EU-funded project AQUACOSM-Plus (no.: 871081). The establishment of the infrastructure was financed by the Lower Saxony Ministry for Science and Culture (MWK) and the Institute for Chemistry and Biology of the Marine Environment.

ACKNOWLEDGMENTS

We would like to thank Heike Rickels for technical assistance and nutrient measurements, Clara Zeller for help in collecting parts of the data, Dorothee Hodapp for statistical advice and Lutz ter Hell for invaluable technical support. We would also like to thank the Marine Community Ecology class 2019 for support during the experiment and sampling.

SUPPLEMENTARY MATERIAL

The Supplementary Material for this article can be found online at: https://www.frontiersin.org/articles/10.3389/fmars.2021.812902/full#supplementary-material

REFERENCES

Acevedo-Trejos, E., Brandt, G., Bruggeman, J., and Merico, A. (2015). Mechanisms shaping size structure and functional diversity of phytoplankton communities in the ocean. *Sci. Rep.* 5:8918. doi: 10.1038/srep08918

Acevedo-Trejos, E., Brandt, G., Merico, A., and Smith, S. L. (2013). Biogeographical patterns of phytoplankton community size structure in the oceans. *Glob. Ecol. Biogeogr.* 22, 1060–1070. doi: 10.1111/geb.12071

Anning, T., Harris, G., and Geider, R. (2001). Thermal acclimation in the marine diatom chaetoceros calcitrans (Bacillariophyceae). *Eur. J. Phycol.* 36, 233–241. doi: 10.1080/09670260110001735388

Barton, S., Jenkins, J., Buckling, A., Schaum, C. E., Smirnoff, N., Raven, J. A., et al. (2020). Evolutionary temperature compensation of carbon fixation in marine phytoplankton. *Ecol. Lett.* 23, 722–733. doi: 10.1111/ele.13469

Bates, D., Maechler, M., Bolker, B., and Walker, S. (2015). Fitting linear mixed-effects models using lme4. *J. Stat. Softw.* 67, 1–48. doi: 10.18637/jss.v067.i01

Berg, M. P., and Ellers, J. (2010). Trait plasticity in species interactions: a driving force of community dynamics. *Evol. Ecol.* 24, 617–629. doi: 10.1007/s10682-009-9347-8

Bernhardt, J. R., O'Connor, M. I., Sunday, J. M., and Gonzalez, A. (2020). Life in fluctuating environments: adaptation to changing environments. *Philos. Trans. R. Soc. B Biol. Sci.* 375:20190454.

Bernhardt, J. R., Sunday, J. M., Thompson, P. L., Connor, M. I. O., and Bernhardt, J. R. (2018). Nonlinear averaging of thermal experience predicts population growth rates in a thermally variable environment. *Proc. R. Soc. B* 285:20181076. doi: 10.1098/rspb.2018.1076

Bestion, E., Haegeman, B., Alvarez Codesal, S., Garreau, A., Huet, M., Barton, S., et al. (2021). Phytoplankton biodiversity is more important for ecosystem functioning in highly variable thermal environments. *Proc. Natl. Acad. Sci. U.S.A.* 118:e2019591118. doi: 10.1073/pnas.2019591118

Blasius, B., Rudolf, L., Weithoff, G., Gaedke, U., and Fussmann, G. F. (2020). Long-term cyclic persistence in an experimental predator–prey system. *Nature* 577, 226–230. doi: 10.1038/s41586-019-1857-0

Burgmer, T., and Hillebrand, H. (2011). Temperature mean and variance alter phytoplankton biomass and biodiversity in a long-term microcosm experiment. *Oikos* 120, 922–933. doi: 10.1111/j.1600-0706.2010.19301.x

Burton, T., Lakka, H. K., and Einum, S. (2020). Measuring phenotypes in fluctuating environments. *Funct. Ecol.* 34, 606–615. doi: 10.1111/1365-2435.13501

Cabrerizo, M. J., and Marañón, E. (2021). Temperature fluctuations in a warmer environment: impacts on microbial plankton. *Fac. Rev.* 10:9. doi: 10.12703/r/10-9

Cabrerizo, M. J., Marañón, E., Fernández-González, C., Alonso-Núñez, A., Larsson, H., and Aranguren-Gassis, M. (2021). Temperature fluctuation attenuates the effects of warming in estuarine microbial plankton communities. *Front. Mar. Sci.* 8:656282. doi: 10.3389/fmars.2021.656282

Chen, B., Smith, S. L., and Wirtz, K. W. (2019). Effect of phytoplankton size diversity on primary productivity in the North Pacific: trait distributions under environmental variability. *Ecol. Lett.* 22, 56–66. doi: 10.1111/ele.13167

Chesson, P. (2000). Mechanisms of maintenance of species diversity. *Annu. Rev. Ecol. Syst.* 31, 343–366. doi: 10.1146/annurev.ecolsys.31.1.343

Chevin, L. M., Lande, R., and Mace, G. M. (2010). Adaptation, plasticity, and extinction in a changing environment: towards a predictive theory. *PLoS Biol.* 8:e1000357. doi: 10.1371/journal.pbio.1000357

Colinet, H., Rinehart, J. P., Yocum, G. D., and Greenlee, K. J. (2018). Mechanisms underpinning the beneficial effects of fluctuating thermal regimes in insect cold tolerance. *J. Exp. Biol.* 221:jeb164806. doi: 10.1242/jeb.164806

De Senerpont Domis, L. N., Van De Waal, D. B., Helmsing, N. R., Van Donk, E., and Mooij, W. M. (2014). Community stoichiometry in a changing world: combined effects of warming and eutrophication on phytoplankton dynamics. *Ecology* 95, 1485–1495. doi: 10.1890/13-1251.1

Descamps-Julien, B., and Gonzalez, A. (2005). Stable coexistence in a fluctuating environment: an experimental demonstration. *Ecology* 86, 2815–2824.

Dickman, E. M., Vanni, M. J., and Horgan, M. J. (2006). Interactive effects of light and nutrients on phytoplankton stoichiometry. *Oecologia* 149, 676–689. doi: 10.1007/s00442-006-0473-5

Duncan, A. B., Gonzalez, A., and Kaltz, O. (2013). Stochastic environmental fluctuations drive epidemiology in experimental host-parasite metapopulations. *Proc. R. Soc. B Biol. Sci.* 280:20131747. doi: 10.1098/rspb.2013.1747

Ebenhöh, W. (1988). Coexistence of an unlimited number of algal species in a model system. *Theor. Popul. Biol.* 34, 130–144. doi: 10.1016/0040-5809(88)90038-x

Elmqvist, T., Folke, C., Nyström, M., Peterson, G., Bengtsson, J., Walker, B., et al. (2003). Response diversity, ecosystem change, and resilience. *Front. Ecol. Environ.* 1:488–494. doi: 10.1890/1540-9295(2003)001[0488:rdecar]2.0.co;2

Feder, M. E., and Hofmann, G. E. (1999). Heat-shock proteins, molecular chaperones, and the stress response: evolutionary and ecological physiology. *Annu. Rev. Physiol.* 61, 243–282. doi: 10.1146/annurev.physiol.61.1.243

Fey, S. B., Kremer, C. T., Layden, T. J., and Vasseur, D. A. (2021). Resolving the consequences of gradual phenotypic plasticity for populations in variable environments. *Ecol. Monogr.* 91:e01478.

Flöder, S., and Sommer, U. (1999). Diversity in planktonic communities: an experimental test of the intermediate disturbance hypothesis. *Limnol. Oceanogr.* 44, 1114–1119. doi: 10.4319/lo.1999.44.4.1114

Fox, R. J., Donelson, J. M., Schunter, C., Ravasi, T., and Gaitán-Espitia, J. D. (2019). Beyond buying time: the role of plasticity in phenotypic adaptation to rapid environmental change. *Philos. Trans. R. Soc. B: Biol. Sci.* 374.

Fujiwara, M., and Takada, T. (2017). *Environmental Stochasticity. eLS*. Atlanta: American Cancer Society, 1–8.

Gall, A., Uebel, U., Ebensen, U., Hillebrand, H., Meier, S., Singer, G., et al. (2017). Planktotrons: a novel indoor mesocosm facility for aquatic biodiversity and food web research. *Limnol. Oceanogr. Methods* 15, 663–677. doi: 10.1002/lom3.10196

Gerhard, M., Koussoroplis, A. M., Hillebrand, H., and Striebel, M. (2019). Phytoplankton community responses to temperature fluctuations under different nutrient concentrations and stoichiometry. *Ecology* 100:e02834. doi: 10.1002/ecy.2834

Grasshoff, K., Kremling, K., and Ehrhardt, M. (1999). *Methods of Seawater Analysis*, 3rd Edn. Wiley: Hoboken.

Grolemund, G., and Wickham, H. (2011). Dates and times made easy with lubridate. *J. Stat. Softw.* 40, 1–25.

Guillaume, A. S., Monro, K., and Marshall, D. J. (2016). Transgenerational plasticity and environmental stress: do paternal effects act as a conduit or a buffer? *Funct. Ecol.* 30, 1175–1184. doi: 10.1111/1365-2435.12604

Halley, J. M. (1996). Ecology, evolution and 1/f-noise. *Trends Ecol. Evol.* 11, 33–37. doi: 10.1016/0169-5347(96)81067-6

Hanson, M. A., and Skinner, M. K. (2016). Developmental origins of epigenetic transgenerational inheritance. *Environ. Epigenet.* 2, 1–9. doi: 10.1093/eep/dvw002

Hillebrand, H., Soininen, J., and Snoeijs, P. (2010). Warming leads to higher species turnover in a coastal ecosystem. *Glob. Chang. Biol.* 16, 1181–1193. doi: 10.1111/j.1365-2486.2009.02045.x

Hodapp, D., Hillebrand, H., and Striebel, M. (2019). "Unifying" the concept of resource use efficiency in ecology. *Front. Ecol. Evol.* 6, 1–14. doi: 10.3389/fevo.2018.00233

Hodapp, D., Hillebrand, H., Blasius, B., and Ryabov, A. B. (2016). Environmental and trait variability constrain community structure and the biodiversity-productivity relationship. *Ecology* 97, 1463–1474. doi: 10.1890/15-0730.1

Huisman, J., and Weissing, F. J. (1995). Competition for nutrients and light in a mixed water column: a theoretical analysis. *Am. Nat.* 146, 536–564. doi: 10.1086/285814

Hutchinson, G. E. (1961). The paradox of the plankton. *Paradox Plankton* XCV, 51–62. doi: 10.1017/cbo9781139095075.008

Jackson, M. C., Pawar, S., and Woodward, G. (2021). The temporal dynamics of multiple stressor effects: from individuals to ecosystems. *Trends Ecol. Evol.* 36, 402–410. doi: 10.1016/j.tree.2021.01.005

Jensen, J. L. W. V. (1906). Sur les fonctions convexes et les inégalités entre les valeurs moyennes. *Acta Math.* 30, 175–193. doi: 10.1007/bf02418571

Kerimoglu, O., Straile, D., and Peeters, F. (2012). Role of phytoplankton cell size on the competition for nutrients and light in completely mixed systems. *J. Theor. Biol.* 300, 330–343. doi: 10.1016/j.jtbi.2012.01.044

Kingsolver, J. G., Higgins, J. K., and Augustine, K. E. (2015). Fluctuating temperatures and ectotherm growth: distinguishing non-linear and time-dependent effects. *J. Exp. Biol.* 218, 2218–2225. doi: 10.1242/jeb.120733

Kingsolver, J. G., and Woods, H. A. (2016). Beyond thermal performance curves: modeling time-dependent effects of thermal stress on ectotherm growth rates. *Am. Nat.* 187, 283–294. doi: 10.1086/684786

Klein, H., Latarius, K., and Köllner, M. (2019). *3.5.3 Temperaturschichtung und Wärmeinhalt 2018 & 2019. BSH Reports*. Hamburg: Bundesamt für Seeschifffahrt und Hydrographie.

Koerselman, W., and Meuleman, A. F. M. (1996). The vegetation N : P ratio : a new tool to detect the nature of nutrient limitation. *J. Appl. Ecol.* 33, 1441–1450. doi: 10.2307/2404783

Koussoroplis, A. M., Pincebourde, S., and Wacker, A. (2017). Understanding and predicting physiological performance of organisms in fluctuating and multifactorial environments. *Ecol. Monogr.* 87, 178–197.

Kremer, C. T., Fey, S. B., Arellano, A. A., and Vasseur, D. A. (2018). Gradual plasticity alters population dynamics in variable environments: thermal acclimation in the green alga *Chlamydomonas reinhartdii*. *Proc. R. Soc. B Biol. Sci.* 285:20171942. doi: 10.1098/rspb.2017.1942

Loreau, M., and Hector, A. (2001). Partitioning selection and complementarity in biodiversity experiments. *Nature* 412, 72–76. doi: 10.1038/35083573

Massie, T. M., Weithoff, G., Kuckländer, N., Gaedke, U., and Blasius, B. (2015). Enhanced Moran effect by spatial variation in environmental autocorrelation. *Nat. Commun.* 6:5993. doi: 10.1038/ncomms6993

Miner, B. G., Sultan, S. E., Morgan, S. G., Padilla, D. K., and Relyea, R. A. (2005). Ecological consequences of phenotypic plasticity. *Trends Ecol. Evol.* 20, 685–692.

Moisan, J. R., Moisan, T. A., and Abbott, M. R. (2002). Modelling the effect of temperature on the maximum growth rates of phytoplankton populations. *Ecol. Modell.* 153, 197–215. doi: 10.1016/s0304-3800(02)00008-x

Niehaus, A. C., Angilletta, M. J., Sears, M. W., Franklin, C. E., and Wilson, R. S. (2012). Predicting the physiological performance of ectotherms in fluctuating thermal environments. *J. Exp. Biol.* 215, 694–701. doi: 10.1242/jeb.058032

Nijs, I., and Impens, I. (2000). Underlying effects of resource use efficiency in diversity-productivity relationships. *Oikos* 91, 204–208. doi: 10.1034/j.1600-0706.2000.910120.x

Oksanen, J., Blanchet, F. G., Friendly, M., Kindt, R., Legendre, P., McGlinn, D., et al. (2019). *vegan: Community Ecology Package. R package version 2.5-6*. Available online at: https://CRAN.R-project.org/package=vegan.

Pansch, C., and Hiebenthal, C. (2019). A new mesocosm system to study the effects of environmental variability on marine species and communities. *Limnol. Oceanogr. Methods* 17, 145–162. doi: 10.1002/lom3.10306

Ptacnik, R., Solimini, A. G., Andersen, T., Tamminen, T., Brettum, P., Lepistö, L., et al. (2008). Diversity predicts stability and resource use efficiency in natural phytoplankton communities. *Proc. Natl. Acad. Sci. U.S.A.* 105, 5134–5138. doi: 10.1073/pnas.0708328105

Rasconi, S., Winter, K., and Kainz, M. J. (2017). Temperature increase and fluctuation induce phytoplankton biodiversity loss – evidence from a multi-seasonal mesocosm experiment. *Ecol. Evol.* 7, 2936–2946. doi: 10.1002/ece3.2889

R Core Team (2020). *R: A Language and Environment for Statistical Computing*. Vienna: R Foundation for Statistical Computing. Available online at: https://www.R-project.org/

Rescan, M., Grulois, D., Ortega-Aboud, E., and Chevin, L. M. (2020). Phenotypic memory drives population growth and extinction risk in a noisy environment. *Nat. Ecol. Evol.* 4, 193–201. doi: 10.1038/s41559-019-1089-6

Rezende, E. L., Castañeda, L. E., and Santos, M. (2014). Tolerance landscapes in thermal ecology. *Funct. Ecol.* 28, 799–809. doi: 10.1111/1365-2435.12268

Ripa, J., and Lundberg, P. (1996). Noise colour and the risk of population extinctions. *Proc. R. Soc. B Biol. Sci.* 263, 1751–1753. doi: 10.1098/rspb.1996.0256

Ruokolainen, L., Lindén, A., Kaitala, V., and Fowler, M. S. (2009). Ecological and evolutionary dynamics under coloured environmental variation. *Trends Ecol. Evol.* 24, 555–563. doi: 10.1016/j.tree.2009.04.009

Savage, V. M., Gillooly, J. F., Brown, J. H., West, G. B., and Charnov, E. L. (2004). Effects of body size and temperature on population growth. *Am. Nat.* 163, 429–441. doi: 10.1086/381872

Schaum, C. E., Buckling, A., Smirnoff, N., Studholme, D. J., and Yvon-Durocher, G. (2018). Environmental fluctuations accelerate molecular evolution of thermal tolerance in a marine diatom. *Nat. Commun.* 9:1719.

Smith, S. L., Vallina, S. M., and Merico, A. (2016). Phytoplankton size-diversity mediates an emergent trade-off in ecosystem functioning for rare versus frequent disturbances. *Sci. Rep.* 6:34170. doi: 10.1038/srep34170

Stuart-Smith, R. D., Edgar, G. J., Barrett, N. S., Kininmonth, S. J., and Bates, A. E. (2015). Thermal biases and vulnerability to warming in the world's marine fauna. *Nature* 528, 88–92. doi: 10.1038/nature16144

Toseland, A., Daines, S. J., Clark, J. R., Kirkham, A., Strauss, J., Uhlig, C., et al. (2013). The impact of temperature on marine phytoplankton resource allocation and metabolism. *Nat. Clim. Chang.* 3, 979–984. doi: 10.1038/nclimate1989

Utermöhl, H. (1958). Zur vervollkommnung der quantitativen phytoplankton-methodik. *Mitt Int. Ver Limnol.* 9, 1–38. doi: 10.1080/05384680.1958.11904091

van Aken, H. M. (2008). Variability of the water temperature in the western Wadden Sea on tidal to centennial time scales. *J. Sea Res.* 60, 227–234. doi: 10.1016/j.seares.2008.09.001

van de Waal, D. B., and Litchman, E. (2020). Multiple global change stressor effects on phytoplankton nutrient acquisition in a future ocean. *Philos. Trans. R. Soc. B Biol. Sci.* 375, 1–8. doi: 10.1098/rstb.2019.0706

Wang, X., Fu, F., Qu, P., Kling, J. D., Jiang, H., Gao, Y., et al. (2019). How will the key marine calcifier *Emiliania huxleyi* respond to a warmer and more thermally variable ocean? *Biogeosciences* 16, 4393–4409. doi: 10.5194/bg-16-4393-2019

Wickham, H., Averick, M., Bryan, J., Chang, W., McGowan, L., François, R., et al. (2019). Welcome to the tidyverse. *J. Open Source Softw.* 4:1686. doi: 10.21105/joss.01686

Wilke, C. O. (2019). *cowplot: Streamlined Plot Theme and Plot Annotations for 'ggplot2'. R package version 1.0.0*. Available online: https://CRAN.R-project.org/package=cowplot.

Wood, S. N. (2011). Fast stable restricted maximum likelihood and marginal likelihood estimation of semiparametric generalized linear models. *J. R. Stat. Soc. B* 73, 3–36. doi: 10.1111/j.1467-9868.2010.00749.x

Yachi, S., and Loreau, M. (1999). Biodiversity and ecosystem productivity in a fluctuating environment: the insurance hypothesis. *Ecology* 96, 1463–1468. doi: 10.1073/pnas.96.4.1463

Zhang, M., Guan, Y., Qin, B., and Wang, X. (2019). Responses of phytoplankton species to diel temperature fluctuation patterns. *Phycol. Res.* 67, 184–191. doi: 10.1111/pre.12369

Zhang, M., Qin, B., Yu, Y., Yang, Z., Shi, X., and Kong, F. (2016). Effects of temperature fluctuation on the development of cyanobacterial dominance in spring: implication of future climate change. *Hydrobiologia* 763, 135–146. doi: 10.1007/s10750-015-2368-0

Conflict of Interest: The authors declare that the research was conducted in the absence of any commercial or financial relationships that could be construed as a potential conflict of interest.

Publisher's Note: All claims expressed in this article are solely those of the authors and do not necessarily represent those of their affiliated organizations, or those of the publisher, the editors and the reviewers. Any product that may be evaluated in this article, or claim that may be made by its manufacturer, is not guaranteed or endorsed by the publisher.

frontiers in Marine Science

ORIGINAL RESEARCH
published: 24 February 2022
doi: 10.3389/fmars.2021.790241

The Role of Recovery Phases in Mitigating the Negative Impacts of Marine Heatwaves on the Sea Star *Asterias rubens*

Fabian Wolf[1*†], *Katja Seebass*[2†] *and Christian Pansch*[1,3†]

[1] Department of Marine Ecology, GEOMAR Helmholtz Centre for Ocean Research Kiel, Kiel, Germany, [2] Faculty of Mathematics and Natural Sciences, Christian-Albrechts-University Kiel, Kiel, Germany, [3] Department of Environmental and Marine Biology, Åbo Akademi University, Åbo, Finland

OPEN ACCESS

Edited by:
Gretchen E. Hofmann,
University of California,
Santa Barbara, United States

Reviewed by:
Simon Morley,
British Antarctic Survey (BAS),
United Kingdom
Sam Dupont,
University of Gothenburg, Sweden

***Correspondence:**
Fabian Wolf
fabian.wolf.research@gmail.com

†ORCID:
Fabian Wolf
orcid.org/0000-0002-0955-8487
Katja Seebass
orcid.org/0000-0001-6520-7369
Christian Pansch
orcid.org/0000-0001-8442-4502

Specialty section:
This article was submitted to Global Change and the Future Ocean, a section of the journal Frontiers in Marine Science

Received: 06 October 2021
Accepted: 28 December 2021
Published: 24 February 2022

Citation:
Wolf F, Seebass K and Pansch C (2022) The Role of Recovery Phases in Mitigating the Negative Impacts of Marine Heatwaves on the Sea Star Asterias rubens. Front. Mar. Sci. 8:790241. doi: 10.3389/fmars.2021.790241

During recent years, experimental ecology started to focus on regional to local environmental fluctuations in the context of global climate change. Among these, marine heatwaves can pose significant threats to marine organisms. Yet, experimental studies that include fluctuating thermal stress are rare, and if available often fail to base experimental treatments on available long-term environmental data. We evaluated 22-year high-resolution sea surface temperature data on the occurrence of heatwaves and cold-spells in a temperate coastal marine environment. The absence of a general warming trend in the data may in parts be responsible for a lack of changes in heatwave occurrences (frequency) and their traits (intensity, duration, and rate of change) over time. Yet, the retrieved traits for present-day heatwaves ensured most-natural treatment scenarios, enabling an experimental examination of the impacts of marine heatwaves and phases of recovery on an important temperate predator, the common sea star *Asterias rubens*. In a 68-days long experiment, we compared a 37- and a 28-days long heatwave with a treatment that consisted of three consecutive 12-days long heatwaves with 4 days of recovery in between. The heatwaves had an intensity of 4.6°C above climatological records, resulting in a maximum temperature of 23.25°C. We demonstrate that heatwaves decrease feeding and activity of *A. rubens*, with longer heatwaves having a more severe and lasting impact on overall feeding pressure (up to 99.7% decrease in feeding rate) and growth (up to 87% reduction in growth rate). Furthermore, heatwaves of similar overall mean temperature, but interrupted, had a minor impact compared to continuous heatwaves, and the impact diminished with repeated heatwave events. We experimentally demonstrated that mild heatwaves of today's strength decrease the performance of *A. rubens*. However, this echinoderm may use naturally occurring short interruptions of thermal stress as recovery to persist in a changing and variable ocean. Thus, our results emphasize the significance of thermal fluctuations and especially, the succession and timing of heat-stress events.

Keywords: climate change, warming (heating), environmental fluctuation, extreme events, marine heatwaves (MHWs), mitigation, recovery

INTRODUCTION

Anthropogenically induced climate change alters the abiotic conditions for all marine organisms and ecosystems (IPCC, 2021). Thereby, sea surface temperatures (SSTs) are projected to increase by 3°C until the end of this century (IPCC, 2021), which has been shown to negatively impact ecosystems worldwide (Walther et al., 2002; Doney et al., 2012; IPCC, 2021).

Thermal fluctuations are superimposed on this gradual change in temperature, reaching from yearly (seasonal) to daily (day-night) or tidal fluctuations. While colder periods may serve as refuge from heat stress in a fluctuating world, peak temperatures cause high thermal stress temporally (Wahl et al., 2015). Therefore, the examination of natural fluctuations and their extremes is key to understand a system's response to a warming ocean. Among the most important thermal fluctuations, heatwave events are projected to increase in frequency, duration, and intensity worldwide (Oliver et al., 2018), with particular intensification in marginal shallow seas, like the Baltic Sea (Gräwe et al., 2013).

Heatwaves have a high potential of impacting marine ecosystems, by exceeding the thermal limits of species (Oliver et al., 2019; Smale et al., 2019). Much research has been done in tropical systems such as coral reefs, as slight temperature deviations can have massive impacts leading to, e.g., coral bleaching (Le Nohaïc et al., 2017). In coral reef ecosystems, the accumulation of thermal anomalies is used to assess the bleaching potential (degree heating weeks; e.g., Kayanne, 2017). The impact of temperature events on marine ecosystems therefore depends on a heatwave's intensity, but also on traits such as duration (e.g., Oliver et al., 2019) and onset rates (e.g., Genin et al., 2020). Thus, even in temperate regions, with generally higher thermal variability, heatwaves can have strong impacts on marine ecosystems (Pansch et al., 2018; Smale et al., 2019), yet the overall effect strength and direction may strongly depend on the timing of the heatwave event and on the environmental history of the community (Pansch et al., 2018).

Generally, acclimation to environmental change may occur across species, challenging reliable predictions of future ecosystem changes. As shown for multiple simultaneous drivers (Boyd et al., 2018), consecutive stress events (e.g., recurring marine heatwaves) can either have additive, antagonistic or synergistic impacts on species (Gunderson et al., 2016). Antagonistic impacts can mean that a first stressor prepares the organism to respond more adequately when the same stressor recurs, a concept referred to as "stress memory" or "ecological memory" (e.g., Walter et al., 2013; Jackson et al., 2021). At the species level, such processes are triggered by, for example, the expression of heat shock proteins (HSPs, e.g., Todgham et al., 2005; Banti et al., 2008; McBryan et al., 2016), while at the population and the community level, genotype, and species sorting as well as changes in dispersal capacities or species interactions can trigger such "lagged" effects, long after a stress event occurred [as discussed by Jackson et al. (2021)].

Environmental climate change has the potential to drive ecosystem responses if keystone species are impacted (Sanford, 1999). The common sea star (*Asterias rubens*) is such a keystone species in the temperate benthic communities of the Atlantic Ocean, North Sea and Baltic Sea (Vevers, 1949; Budd, 2008). This species is an important part of the ecosystem as it controls the abundance of mussels and thus, the distribution of mussel beds (Gaymer et al., 2001). Mussels, e.g., blue mussels, (*Mytilus* spp.) play an important role as ecosystem engineers by providing habitat for many other species (Norling and Kautsky, 2007; Sadchatheeswaran et al., 2015). Yet, when released from one of their main predators, mussels might outcompete other important structure-forming species like seagrasses and macroalgae by forming large monocultures and thus decreasing overall diversity (Reusch and Chapman, 1997; Dürr and Wahl, 2004).

Even though the importance of environmental variability, including marine heatwaves, is widely acknowledged in the scientific community (Pincebourde et al., 2012; Gunderson et al., 2016; Smale et al., 2019), this aspect is often neglected in experimental ecology. One major problem may be the lack of a universal characterization of variability such as marine heatwave events. In this study, we used a physical (oceanographic) approach suggested by Hobday et al. (2016), which is now widely used in characterizing marine heatwave events globally (Oliver et al., 2019; Smale et al., 2019; Thomsen et al., 2019), thus allowing for a worldwide comparison of events and their impacts. Hobday et al. (2016) defined a heatwave as temperatures that exceed the 90th percentile of a long-term temperature dataset for at least five consecutive days. Our experimental treatments were designed using a 22-years high-resolution (8 mins intervals) SST dataset available for the Kiel Fjord (Wolf et al., 2020). We tested the impact of heatwave events of different duration and frequency on the keystone predator *A. rubens*. We expected a decreased performance of *A. rubens* with increasing duration of the heatwave and a mitigation of heatwave impacts in a scenario that applied successive heatwave events and therefore periods for recovery. In contrast to many existing studies, we measured sea star traits, feeding in particular, at high temporal resolution, allowing for a better approximation of the instant responses of this species to the short-term stress events, explaining long-term consequences.

MATERIALS AND METHODS

The Study System

The Baltic Sea as a semi-enclosed marginal shelf sea, is characterized by its shallow waters with an average depth of 54 m (Leppäranta and Myrberg, 2009). Here, unlike most of the world's oceans, SST is projected to increase by up to 4°C by the end of the century (HELCOM, 2013; 3°C worldwide: IPCC, 2021). Therefore, the Baltic Sea provides an ideal study area as it already shows conditions today that are projected for 2100 in other regions and may thus be considered as "Time Machine" for climate change research (Reusch et al., 2018).

Modeling Heatwave Traits

Extreme event identification and calculation of their traits in different seasons (i.e., frequency, duration, maximum intensity, cumulative intensity, onset rate, and decline rate), was performed

using the "heatwaveR" package (Schlegel and Smit, 2018) in R (R Core Team, 2021), which is based on the heatwave definition by Hobday et al. (2016). The script uses a moving window of 11 days to provide a climatology as well as 90th and 10th percentile thresholds from which heatwave and cold-spell traits are determined, respectively. We used a 22-years high-resolution (8 mins intervals) sea surface (1.8 m depth) temperature dataset from the Kiel Fjord provided by GEOMAR weather station (Wolf et al., 2020). We extracted daily means, which were then implemented into R. The longest period with missing data was between May 25th, 1999 and June 16th, 1999. Therefore, the maximum gap length was set to 23 days into the "heatwaveR" package, in which the temperature was linearly extrapolated.

Using Heatwave Traits for Defining the Experimental Treatments

We applied treatments with summer heatwaves differing in their duration and sequence. The underlying seasonal summer temperature is based on the temperature modeling as described above (i.e., the extracted climatological values) and provided the baseline (*No* heatwave treatment; **Figure 1A**). The *No* heatwave treatment experiences temperatures starting with 16.57°C, maximizing to 18.64°C and ending with 16.69°C. A mean summer heatwave intensity of 4.6°C above seasonality and a maximum onset rate of 0.7°C and decline rate of 1.4°C per day (see bold values in **Supplementary Table 1**) were used as baseline for the applied heatwave treatments. The *Interrupted* heatwave consisted of three single heatwave events of 12 days each above seasonality (**Figure 1B**; 5 or 7 days above the 90th percentile threshold for the first two or the last heatwave, respectively), representing minimum duration as found from the 22-year dataset (see bold values in **Supplementary Table 1**). The heatwaves were separated by four relaxation days in between (**Figure 1B**). Maximum temperatures for each of these three short heatwave events were 22.84, 23.25, and 22.63°C, respectively (**Figure 1B**). To achieve the same overall average temperature of 19.2°C of the *Interrupted* heatwave treatment, the *Present-day* heatwave (**Figure 1C**) had a duration of 28 days above the seasonality (20 days above the 90th percentile threshold) reaching a maximum temperature of 23.25°C. This duration lies within the maximum identified summer heatwave duration of 39 days (**Supplementary Table 1**). The *Extended* heatwave had a duration of 37 days above the seasonality (31 days above the 90th percentile threshold) and is simulating a scenario in which the *Present-day* heatwave is not interrupted by a typical cold-spell (**Figure 1D**). A typical cold-spell in summer has a duration of at least 6 days below the 10th percentile (**Supplementary Table 2**). Such a cold-spell would last for a total of 9 days, when starting and ending at the temperature of the seasonal baseline. This represents the difference in duration between the *Present-day* and *Extended* heatwave treatment, if starting and closing from the seasonal temperature baseline.

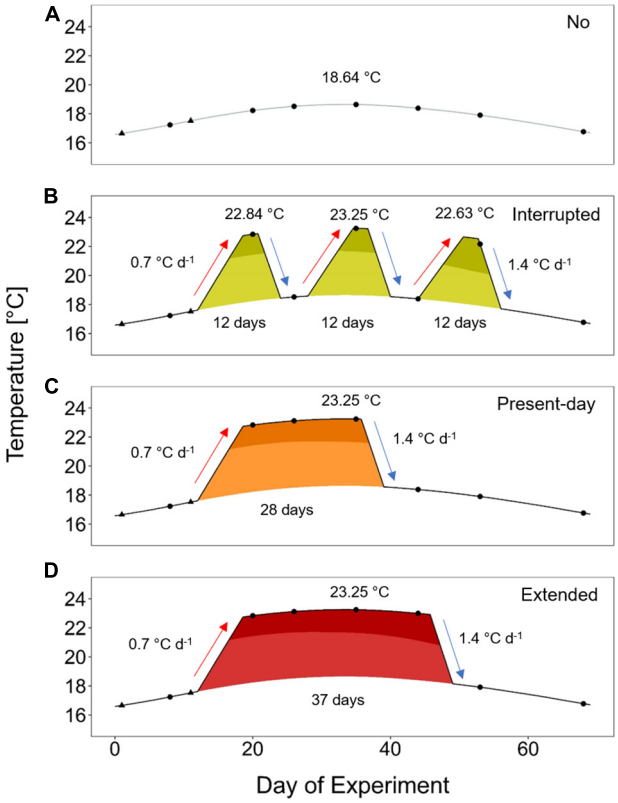

FIGURE 1 | Experimental treatments based on the heatwave definition by Hobday et al. (2016). The treatments followed a smoothed natural summer seasonal temperature profile [*No* heatwave, gray line in panel **(A)**; "climatological values" in Hobday et al. (2016)] or experienced three short heatwaves of 12 days each [*Interrupted*, yellow-green filling in panel **(B)**], a heatwave of 28 days [*Present-day*, orange filling in panel **(C)**] or a heatwave of an extended duration of 37 days [*Extended*, red filling in panel **(D)**]. Durations refer to the period with temperatures above the climatological values. Temperatures above the 90th percentile are shown in a darker shade. All heatwaves had a maximum peak of +4.6°C above the climatological values. Mean temperatures of the *Interrupted* and *Present-day* heatwave treatments were equal. Black triangles represent measuring points for wet weight of *A. rubens*, and black dots indicate additional assessments of righting responses.

Experimental Set-Up

The treatments were applied in the Kiel Indoor Benthocosms (Pansch and Hiebenthal, 2019) from July 5th to September 10th, 2019. The KIBs are a state-of-the-art mesocosm system comprised of twelve 600 L tanks, which served as water baths for each six replicated experimental units (2 L Kautex bottles). Every treatment was applied in two separate and randomly chosen tanks leading to a replication of $n = 12$. Temperature was logged hourly in all ten tanks (EnvLogger, ElectricBlue, Vairão, Portugal; see **Supplementary Figure 1** for attained temperatures). Additionally, temperature was monitored by measuring with a handheld thermometer at least every 3 days (TTX 110 type T, Ebro, Ingolstadt, Germany). Salinity, pH and oxygen concentration were also monitored over the experimental period (Multi 3630 IDS, WTW, Kaiserslautern, Germany; see **Supplementary Figure 2**). Each of the 72 experimental units contained one separate sea star individual. Though six of the experimental units were placed in the same tank, all of

them had a separate water inflow and aeration and were thus considered as independent replicates, yet, potential tank effects were accounted for in the model by including the individual sea star as random factor (see "Data Analysis" below). The temperature in each of the tanks is automatically controlled via chillers and heating elements (Pansch and Hiebenthal, 2019). Due to a short malfunctioning of the system, oxygen levels in the experimental units dropped to circa 2 mg L^{-1} (pH down to 7.1) for one out of 68 days in all treatments (**Supplementary Figure 2**). As this stress was only experienced for a short time, presumably all starfish were impacted equally, and we did not observe any impacts on the sea stars (such short-term hypoxic events are relatively common in the area with 18 days of upwelling favorable winds per summer; Karstensen et al., 2014), we continued with the experiment.

The Study Organism

We collected *A. rubens* individuals in Möltenort, Kiel, Germany (N54°22′57.5″, E010°12′8.8″) on July 1st, 2019. Directly after collection, all sea stars were brought to a climate room and placed inside a 600 L tank with a temperature of 18°C as was measured at the collection site while sampling. The sea stars were fed *ad libitum* with blue mussels. When starting the experiment only sea stars of similar weight (11.3 ± 1.4 g SD) were used.

Response Variables

We measured feeding rate (mg mussel dry weight per day), wet weight change (g) and righting time as a measure for the activity of *A. rubens* (min). For feeding rate, blue mussels (*Mytilus* spp.) between 1.5 and 2 cm shell length were collected the day prior to the feeding at piers next to GEOMAR, Kiel, Germany (N54°19′45.8″, E010°08′56.4″). At each feeding event, mussels inside each experimental unit were replaced with the freshly collected mussels. At the same time, we measured the shell length of consumed mussels (Dial Caliper DialMax Metric, Wiha Division KWB Switzerland). As previously described, the mussel's shell length and tissue dry weight correlate strongly [Supplementary Material in Morón Lugo et al. (2020)]. Therefore, we used this correlation to estimate the dry weight of mussels consumed by the sea stars. Wet weight of the sea stars was measured at the start of the experiment, right before the heatwaves started, before the *Present-day* heatwave started to decline, before the *Extended* heatwave started to decline and at the end of the experiment (**Figure 1**). The righting time was measured by turning the sea star on its aboral side and stopping the time it needed to fully turn back on its oral side (Lawrence and Cowell, 1996). These measurements were taken at the same days as weighing (**Figure 1**) to reduce unnecessary handling stress for the sea stars.

Data Analysis

All data were analyzed using R (R Core Team, 2021).

The trends of extreme event properties were analyzed using Generalized Additive Models (GAMs), applying the function *bam* from the package "mgcv" (Wood, 2017). The models were fitted assuming Gaussian distribution of errors for all parameters, but for frequency of events. As the frequency represents count data, a Poisson distribution of errors was assumed. The smooth terms for all peak dates and months were adjusted using thin plate regression splines, while the smoothing parameters were estimated via Restricted Maximum Likelihood (Wood, 2017). For duration and cumulative intensity an additional autocorrelation factor rho was included in the model.

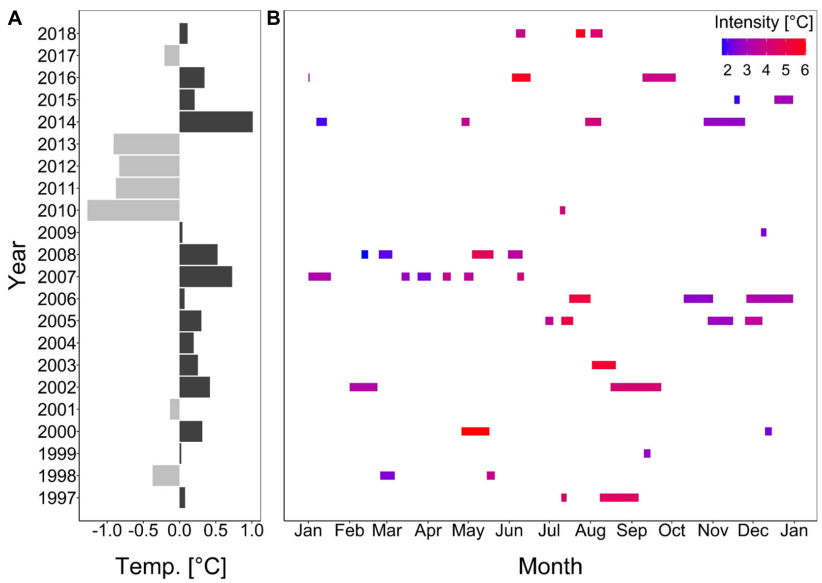

FIGURE 2 | Deviations from annual mean seawater temperature from a 22-year mean (**A**; Wolf et al., 2020) and heatwave durations in different months over the 22-year record **(B)**. Colors in panel **(A)** represent cold (light gray) or warm (dark gray) years, and in panel **(B)** the intensity of the heatwave (i.e., maximum amplitude above the climatological value).

We analyzed the impact of our treatments over time on the performance (feeding rate, wet weight and righting time) of *A. rubens* using sophisticated regression approaches. We used Generalized Additive Mixed-effects Models (GAMMs) for identifying trends in feeding rate and righting time over the course of the experiment. Therefore, the function *bam* from the package "mgcv" (Wood, 2017) was used. We chose GAMMs for feeding rate and righting time as the observed pattern was complex and not linear. The models were fitted assuming Gaussian distribution of errors. The smooth terms for all applied treatments over the experimental period were adjusted using thin plate regression splines, while the smoothing parameters were estimated via REML (Wood, 2017). As all measurements were repeated through time on the same individuals, identity of the respective individual (i.e., replicate) was included as random effect. The temporal trends of the GAMMs in the different treatments were compared using the function *plot_diff* found in the package "itsadug" (van Rij et al., 2020).

TABLE 1 | Generalized Additive Mixed-effect Model (GAMM) and Linear Mixed-effect Model (LMM) results for feeding rate (mg mussel dry weight per day) over 68 days of incubation.

GAMM feeding rate				
Parametric coefficients	***Estimate***	***Std. error***	***t-Value***	***p-Value***
Intercept	55.46	2.36	23.49	**<0.001**
Interrupted	−17.25	2.54	−6.80	**<0.001**
Present-day	−31.33	2.42	−12.93	**<0.001**
Extended	−43.65	2.45	−17.80	**<0.001**
Smooth terms	***Estimated d.f.***	***Reference d.f.***	***F-value***	***p-value***
s (Day of experiment)	1.015	1.028	285.750	**<0.001**
s (Day of experiment): Interrupted	1.952	1.997	15.253	**<0.001**
s (Day of experiment): Present-day	1.990	2.000	54.139	**<0.001**
s (Day of experiment): Extended	1.984	2.000	65.768	**<0.001**
s (Replicate)	0.808	1.000	4.195	**0.023**
LMM feeding rate				
Contrast	***Estimate***	***Std. error***	***d.f.***	***t-Value***	***p-Value***
No:Interrupted	18.700	5.220	42.000	3.585	**0.005**
No:Present-day	30.400	5.110	42.000	5.952	**<0.001**
No:Extended	42.500	5.110	42.000	8.306	**<0.001**
Interrupted:Present-day	11.700	5.110	42.000	2.289	0.117
Interrupted:Extended	23.700	5.110	42.000	4.644	**<0.001**
Present-day:Extended	12.000	5.000	42.000	2.408	0.091

The GAMM for feeding rate had an explained deviance of 54.8%. Significant effects are shown in bold.

In contrast to feeding rate and righting time, the pattern for wet weight was linear, so we applied a Linear Mixed-effect Model (LMM) showing the growth trends over time. Therefore, the function *lmer* from the package "lme4" (Bates et al., 2015) was used, in which the interaction between time and treatment was included, to elucidate the changes over the experimental period subjected to our applied treatments. To account for the repeated measurements of the same individual, we included individual identity as random effect. Identically as for the GAMMs, REML was used to estimate smoothing parameters.

An LMM using REML was applied to identify the impact of the three consecutive heatwaves in the Interrupted heatwave treatment on the average feeding rate during each heatwave event. This was compared to the feeding rate in the No heatwave treatment during the same periods. Therefore, we included the interaction between treatment and the heatwave event as fixed effects, as well as identity of individuals as random effect.

For all response variables an additional LMM was applied using REML to identify the treatment's overall impact at the end of the experiment. In these models, only the treatment as fixed effect and the identity of individuals as random effect were included. The output for all LMMs were generated via the function *emmeans* of the equally named package, in which the contrast analysis is based on a Tukey-test (Lenth, 2020).

The assumptions for all models were thoroughly checked via visual inspection of residual plots.

TABLE 2 | Linear Mixed-effect Model results for the wet weight (g) over 68 days of incubation.

LMM wet weight					
Parametric coefficients	***Estimate***	***Std. Error***	***d.f.***	***t-Value***	***p-Value***
Intercept	10.195	0.899	55.088	11.346	**<0.001**
Interrupted	0.789	1.271	55.088	0.621	0.537
Present-day	0.268	1.245	55.294	0.215	0.830
Extended	2.259	1.245	55.294	1.814	0.075
Day of experiment	0.287	0.011	362.029	26.355	**<0.001**
Interrupted:Day of experiment	−0.111	0.015	362.029	−7.225	**<0.001**
Present-day:Day of experiment	−0.200	0.015	362.061	−13.216	**<0.001**
Extended:Day of experiment	−0.250	0.015	362.061	−16.579	**<0.001**
Contrast	***Estimate***	***Std. error***	***d.f.***	***t-Value***	***p-Value***
No:Interrupted	2.496	1.190	41.900	2.102	0.169
No:Present-day	5.609	1.160	42.000	4.822	**<0.001**
No:Extended	5.134	1.160	42.000	4.413	**<0.001**
Interrupted:Present-day	3.114	1.160	42.000	2.677	**0.050**
Interrupted:Extended	2.638	1.160	42.000	2.268	0.122
Present-day:Extended	−0.476	1.140	42.100	−0.418	0.975

Significant effects are shown in bold.

TABLE 3 | Generalized Additive Mixed-effect Model and LMM results for righting time (min) over 68 days of incubation.

GAMM righting time				
Parametric coefficients	***Estimate***	***Std. error***	***t-Value***	***p-Value***
Intercept	147.577	13.777	10.712	**<0.001**
Present-day	−21.904	19.483	−1.124	0.262
Interrupted	17.506	19.129	0.915	0.361
Extended	83.577	19.129	4.369	**<0.001**
Smooth terms	***Estimated d.f.***	***Reference d.f.***	***F-Value***	***p-Value***
s (Day of experiment)	2.264	2.734	1.487	0.304
s (Day of experiment): Interrupted	1.003	1.006	0.002	0.985
s (Day of experiment): Present-day	3.555	3.864	4.672	**0.004**
s (Day of experiment): Extended	3.776	3.958	9.894	**<0..001**
s (Individual)	0.000	1.000	0.000	0.943
LMM righting time				
Contrast	***Estimate***	***Std. error***	***d.f.***	***t-Value***	***p-Value***
No:Interrupted	0.365	0.473	41.700	0.771	0.867
No:Present-day	−0.283	0.464	42.000	−0.611	0.928
No:Extended	−1.400	0.464	42.000	−3.018	**0.022**
Interrupted:Present-day	−0.648	0.464	42.000	−1.398	0.508
Interrupted:Extended	−1.765	0.464	42.000	−3.805	**0.003**
Present-day:Extended	−1.116	0.454	42.200	−2.457	0.082

The GAMM for feeding rate had an explained deviance of 24.9%. Significant effects are shown in bold.

RESULTS

Heatwave Characteristics and Trends

Between 1997 and 2018, only the onset rate of cold-spells decreased significantly (**Supplementary Figure 3E**). All other parameter of cold-spells as well as heatwaves did not change significantly during this time (**Supplementary Figures 3, 4**). Though, cold-spells tended to increase in duration and cumulative intensity (**Supplementary Figures 3B,D**), while maximum intensity and decline rate tended to decrease (**Supplementary Figures 3C,F**). Cold-spell frequency and all heatwave characteristics on the other hand, did not show any trend (**Supplementary Figures 3A, 4A–F**). Although, date of occurrence of the extreme events did mostly not significantly explain the given trend, the maximum intensity, onset and decline rate for heatwaves as well as cold-spells differed significantly between months (**Supplementary Figures 3C,E,F, 4C,E,F**). Generally, cold years favored cold-spells, whereas warm years favored heatwaves (**Supplementary Figure 5** and **Figure 2**).

Heatwaves usually occur 1.8 times per year with a mean duration of 14.9 days and an intensity of 3.6°C (**Supplementary Table 1**). At the same time, cold-spells occur twice per year on average with a mean duration and intensity of 12.7 days and 3.7°C, respectively (**Supplementary Table 2**). These parameters differ throughout the seasons (**Supplementary Tables 1, 2**).

Feeding Rates Over Time

Sea stars (*A. rubens*) increased their feeding rate over the 68-days experiment but stopped feeding immediately as soon as the heatwave started in both, the *Present-day* and *Extended* heatwave treatments (**Figure 3A**). Yet, sea stars in the *Present-day* heatwave treatment fed on as many mussels as in the *No* heatwave treatment by the end of the experiment (**Figure 3A**). Feeding rates were also reduced in the *Interrupted* heatwave treatment, but less than in the two continuous heatwave treatments (**Figure 3A**). This is also indicated by the non-significant reduction of feeding rates during the first heatwave of the *Interrupted* heatwave treatment (**Figure 4A**). However, the second and third heatwave reduced the feeding rate significantly by 72 and 45%, respectively (**Figures 4B,C**). The reduced performance during heatwaves is further indicated by an overall diminished feeding rate in heatwave treatments, with a more severe impact the longer the event lasted (up to 99.7% decrease in the *Extended* compared to the *No* heatwave treatment; **Figures 3A,B**).

Wet Weights

Growth rates, as indicated by changes in weight, decreased by 39, 70, and 87% in the *Interrupted*, *Present-day* and *Extended* heatwave treatments when compared to the reference treatment (i.e., the *No* heatwave treatment), respectively (slopes of GAMMs in **Figure 3C**). Overall, wet weight only decreased significantly in the *Present-day* and *Extended* heatwave treatments (**Figure 3D**). Similarly to the feeding rates, the effect was more severe in the *Extended* heatwave treatment (**Figures 3C,D**).

Reduced Righting Time During Continuous Heatwaves

Only during the *Present-day* and *Extended* heatwave event the righting time of sea stars (a measure of activity) was significantly increased (i.e., low activity), whereas specimens in the *Interrupted* heatwave treatment did not show a lower activity (**Figure 3E**). Although sea stars were as active after the *Extended* heatwave had ended as before the heatwave had started, there was an overall negative impact of the *Extended* heatwave on the activity of the sea stars (**Figure 3F**).

DISCUSSION

Heatwave Traits and Trends

Marine species are differently impacted by heat stress (e.g., Pansch et al., 2018; Gómez-Gras et al., 2019; Saha et al., 2020; Wahl et al., 2020). Therefore, defining particular temperature thresholds for marine ecosystems at the local scale and globally remains challenging. Corals have been a major research subject for global warming since the 1990s, so that much information is

available to project the impact of heating events on corals (i.e., bleaching) using the concept of degree heating weeks (Liu et al., 2006). However, in order to define species-specific thresholds in diverse communities, one would need thermal performance curves for all species in the system (Schulte et al., 2011). But even if these performance curves were to exist, different traits may have different optima (Wahl et al., 2020). Thus, the whole organism response of the respective species would be a combination from all relevant traits with their potentially different optima resulting in the overall fitness. Therefore, a biology-based methodology for the characterization of heatwaves may not necessarily be the ideal approach. A physical (oceanographic) approach as applied in our study can circumvent the problem by merely focusing on time-series of temperature data and thus, modeling typical vs. extreme conditions in an environment.

Baltic Sea models project an increase in e.g., heatwave duration (Gräwe et al., 2013). Therefore, it is unlikely that the absence of trends in heatwave characteristic in the Kiel Fjord is an actual absence of a trend but rather suggests that our dataset of 22-years may not be sufficient to capture long-term trends in this naturally variable system (Reusch et al., 2018). Fluctuations in the Baltic Sea are not only apparent as extreme events or short-term temperature changes (Pansch and Hiebenthal, 2019), but even as fluctuations on an inter-annual scale as our data highlight. The years 2010–2013 were particularly cold years, which compares well to the extremely low North Atlantic Oscillation index around 2010 (Hurell and National Center for Atmospheric Research Staff, 2020). This anomalous low index (Osborn, 2011) may partly be the reason we did not detect a general warming trend in the time span tested. Yet, warming is the main driver of heatwave trends (Oliver, 2019). Therefore, longer (Hobday et al., 2016) datasets may be required in highly fluctuating systems like the Baltic Sea. This does not only mean that we might have missed existing trends, but also that we may have over- or underestimated some of the heatwave properties. A recent publication by

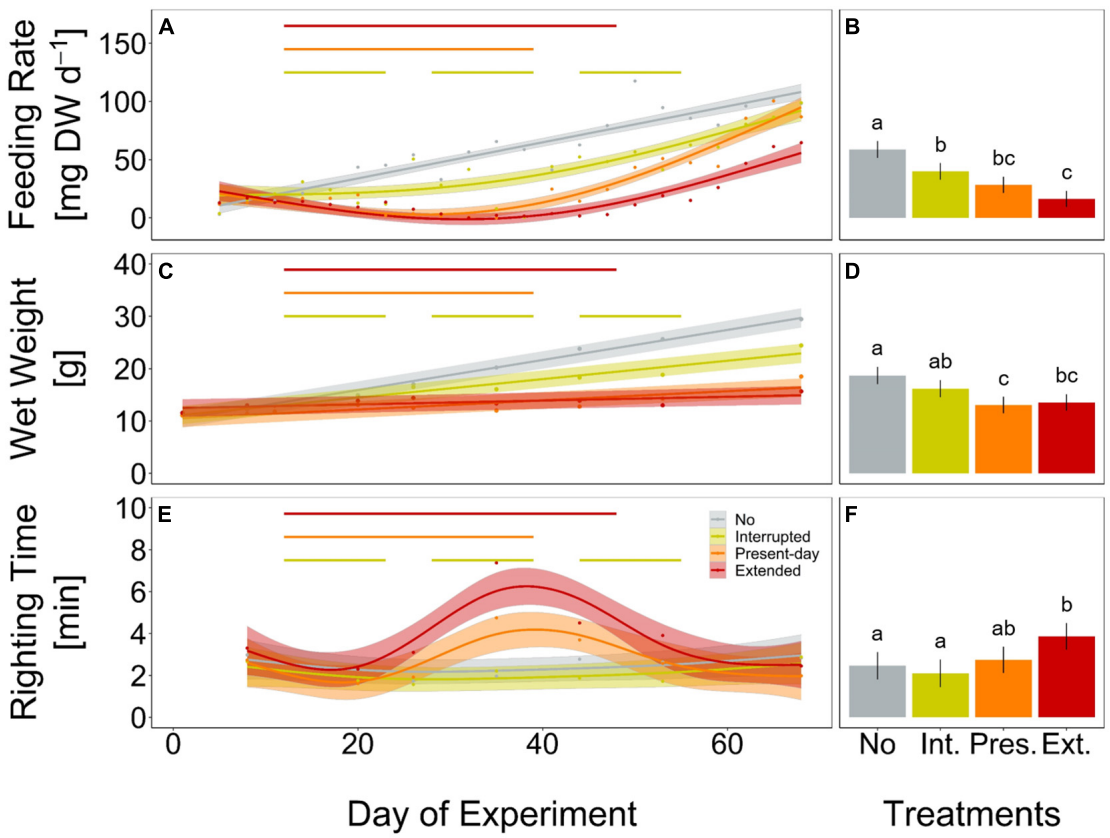

FIGURE 3 | Feeding rate (mg mussel dry weight per day, **A,B**), wet weight (g, **C,D**) and righting time (minutes, **E,F**) of *Asterias rubens* during 68 days of incubation, under No (gray), Interrupted (yellow-green), Present-day (orange), and Extended (red) heatwave treatments (see **Figure 1** for treatment descriptions). Measured data are represented as means for every measurement point [dots in panels **(A,C,E)**] and as overall means with 95% confidence intervals [bars and whiskers in panels **(B,D,F)**]. Temporal trends are modeled using Generalized Additive Mixed-effects Models [GAMM; solid lines in panels **(A,E)**] or Linear Mixed-effects Models [LMM; solid lines in panel **(B)**] and 95% confidence intervals [shaded areas in panels **(A,C,E)**]. The horizontal lines **(A,C,E)** represent the periods of heatwaves (*Interrupted*, *Present-day,* and *Extended*). Significant differences between treatments for feeding rate and righting time **(A,E)** are shown in **Supplementary Figures 6, 7**). Lower case letters in panels **(B,D,F)** represent significant differences between treatments based on Tukey *post hoc* comparisons of LMM. Results shown are based on $n = 12$ (Present-day and Extended) or $n = 11$ (No and Interrupted) replicates. Detailed statistical outcomes are given in **Tables 1**–**3**. See also **Supplementary Figures 8–10** for representation of bar plots and 95% confidence intervals over time.

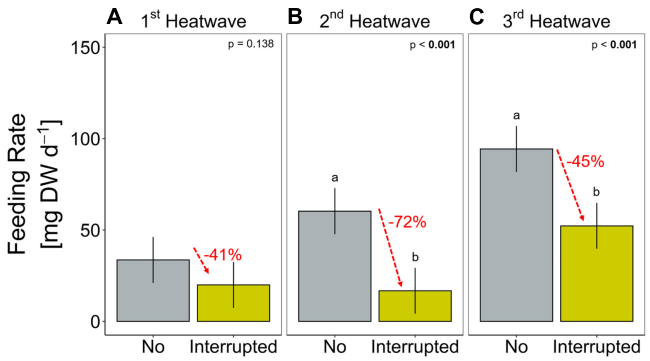

FIGURE 4 | Feeding rate (mg mussel dry weight per day) during each of the three heatwaves of the *Interrupted* heatwave treatment and the respective period in the *No* heatwave treatment (**A**: 1st, **B**: 2nd and **C**: 3rd heatwave period). Data are presented as means (bars) and 95% confidence intervals (whiskers). Lower case letters represent significant differences between treatments based on Tukey *post hoc* comparisons. Percental differences between means are given in red. Detailed statistical outcomes are given in **Table 4**.

Schlegel et al. (2019) investigated how shorter timeseries impact the differently modeled heatwave parameters. Following their findings of the median heatwave properties, our 22-year dataset should likely have 7% more heatwaves, while the duration and maximum intensity should be decreased by 6.4 and 7.3%, respectively. As we chose the heatwave properties for our experiment conservatively, the natural relevance of the study persists, especially as natural heatwaves similar to our *Present-day* and *Extended* heatwave treatment occurred in August 2003 and August 2002, respectively (**Supplementary Figure 11**). Therefore, our experiment provides unique insights into the performance of a keystone predator in times of extreme (and recurring) events.

Heatwaves Reduce the Performance of *Asterias rubens*

Daily temperatures of at least 23.25°C (maximum temperature reached in our experiment) were already measured 89 times in the Kiel Fjord over the past two decades (Wolf et al., 2020). Though not lethal, continuous heatwaves (i.e., *Present-day* and *Extended* heatwave treatments) reduced the performance of the sea star *A. rubens* in feeding, growth, and activity, which confirms previous findings (Rühmkorff et al., unpublished data). Similar impacts and temperature thresholds were also identified for other sea stars (*Pisaster ochraceus*, Pincebourde et al., 2008) and sea urchins (*Heliocidaris erythrogramma*, Minuti et al., 2021). Melzner et al. (personal communication) showed for echinoderms, that thermal stress causes low coelomic oxygen concentrations. Likely, the heatwaves in our experiment led to such a decreased coelomic oxygen concentration in *A. rubens*, so that activity and feeding rate decreased. Consequently, this reduced the growth rate of individuals. Especially, when the heatwaves were extended by 9 days, the impact on sea stars was drastic.

Sea stars in all, but the *Extended* heatwave treatment, fed more at the end compared to the start of the experiment (**Figure 3A**). On the one hand, this indicates the high recovery potential of *A. rubens*, but is likely also driven by the higher energy need of larger sea stars toward the end of the experiment. This elongation is similar to future extrapolation trends of heatwave duration with an increase of 10.3 days by 2100 (Oliver et al., 2018). Pincebourde et al. (2008) likewise demonstrated that longer exposure to heat stress provokes a lasting effect on sea stars. Even when the stress event may be over, echinoderms still suffer from the experienced heat stress by carry over effects (Minuti et al., 2021).

While the more robust prey of sea stars, blue mussels, were shown to survive weeks of exposure to temperatures up to 26°C in the Baltic Sea (Vajedsamiei et al., 2021) or even temperatures up to 41°C for 3 h air exposure in the eastern English Channel (Seuront et al., 2019), temperatures of already 26°C were shown to be 100% lethal for *A. rubens* (Rühmkorff et al., unpublished data). Similarly, Petes et al. (2008) could show that sea stars' mortality is more pronounced in mussel beds that lay closer to the warmer water surface at an intertidal rocky shore, whereas their mussel prey proved to be more resistant to that same heat stress.

Bonaviri et al. (2017) showed that the sea star *Pycnopodia helianthoides* can only control its main prey, the sea urchin *Strongylocentrotus purpuratus*, in a non-warming scenario. Considering the fact that blue mussels are thermally more robust (Vajedsamiei et al., 2021) than sea stars and assuming that sea stars cannot adapt or temporarily migrate to deeper and colder waters, *A. rubens* will hardly be able to control blue mussel abundances (Reusch and Chapman, 1997) in the future Baltic Sea. Thus, a mussel dominated ecosystem might be formed (Reusch and Chapman, 1997), resulting in a restructured benthic community with overall lower diversity. At the same time, we demonstrated that summer heatwaves reduce the weight and thus the size of sea stars. As body size and prey size are strongly correlated in sea stars (Sommer et al., 1999), a heatwave summer would consequently lead to an increased predation on smaller mussels after the heatwaves have ended. This ecosystem-wide impact might be particularly strong for species-poor ecosystems such as the Baltic Sea, unless newcomers add to ecosystem diversity. In this particular case, feeding pressure on similar prey and

TABLE 4 | Linear Mixed-effect Model results for feeding rate (mg mussel dry weight per day) over the three heatwave events in the *Interrupted* heatwave treatment.

LMM feeding rate					
Parametric coefficients	**Estimate**	**Std. error**	***df***	***t*-Value**	***p*-Value**
Intercept	33.609	6.408	55.040	5.245	**<0.001**
Interrupted	−13.655	9.063	55.040	−1.507	0.138
Heatwave No. 2	26.693	8.044	40.000	3.318	**0.002**
Heatwave No. 3	60.729	8.044	40.000	7.550	**<0.001**
Interrupted:Heatwave No. 2	−29.910	11.375	40.000	−2.629	**0.012**
Interrupted:Heatwave No. 3	−28.413	11.375	40.000	−2.498	**0.017**

Significant effects are shown in bold.

prey size, as provoked by the recent invader *Hemigrapsus takanoi* (Nour et al., 2020), may add to ecosystem complexity, with yet unknown consequences. Yet, we conclude that heatwaves affect the keystone predator *A. rubens* with likely ecosystem-wide consequences, especially on the distribution and extent of mussel beds.

Mitigated Impacts by Interrupted Heatwaves

Naturally, an interruption of a heatwave is most likely caused by a cold-spell during an upwelling event at which deeper and colder waters are shoaled to the surface (Lehmann and Myrberg, 2008; Wahl et al., 2021). Though, upwelling events in late summer are often hypoxic (Karstensen et al., 2014) and were shown to negatively impact *A. rubens* (Rühmkorff et al., unpublished data), they can still be beneficial when they interrupt lethal temperature extremes during heatwave events. The importance of cooling events, e.g., large-amplitude internal waves, during heat stress was already demonstrated for tropical systems (Schmidt et al., 2016). In our experiment, sea star individuals subjected to the *Interrupted* heatwaves fed more, were more active, and therefore grew faster than individuals exposed to continuous heatwave treatments. Yet, other fitness consequences such as reproductive success were not measured but could have long-term impacts (Melzner et al., 2020). Overall, this demonstrates that sea stars in temperate regions may quickly recover from thermal stress by using the colder periods in between heatwave events. Or in simpler words, sea stars stop feeding during the heat stress events itself, with a more pronounced impact by longer heatwaves, while resuming to feed normally after the event had ended. In contrast, findings by Morón Lugo et al. (2020), show that repeated short-term excursion into stressful conditions can be detrimental for *A. rubens*. Thus, mean stress levels, but also duration and amplitude of stress events and periods of recovery, will act collectively and determine the overall impact of heat stress in in a future ocean. Additionally, we provide strong evidence that environmental variability such as frequent times of stress recovery may provide a short-term refuge for sea stars from heatwave conditions projected for the future.

We show that the interruption of heatwaves did not only increase the overall performance of the temperate predator *A. rubens* compared to more continuous heat events, but also that the interruption has led to a significantly smaller impact of the third heatwave than the previous event, indicating some potential for acclimation. Other studies already showed that recovery time is very important for a species' and community's stress response (e.g., DeCarlo et al., 2019; Hughes et al., 2019; Nguyen et al., 2020) and this seems to play a crucial role also for the response of *A. rubens* to heatwaves. Our results might thus indicate the potential of *A. rubens* to gain benefits through an ecological stress memory (sensu Jackson et al., 2021). Yet, this needs further investigation, especially on the physiological mechanisms that are involved.

CONCLUSION

An appropriate heatwave characterization can be an extremely important tool for the design of close-to-nature experiments and can therefore help our understanding of the impact of extreme events on single species up to communities and ecosystems. The decreased performance of a temperate keystone predator in response to such simulated heatwaves has likely effects on the whole benthic ecosystem, as their main prey is an ecosystem engineer that may be released from its main predation pressure. At the same time, distinct recovery phases can play an essential role in the heatwave response of the investigated sea star *A. rubens*. The underlying mechanisms that trigger such acclimation and hardening processes still need to be investigated, as well as the question if long-term acclimation to continuous stressors is possible.

DATA AVAILABILITY STATEMENT

All data obtained from the present study are stored at PANGAEA and can be accessed through the following links: https://doi.org/10.1594/PANGAEA.939981 and https://doi.org/10.1594/PANGAEA.939978.

AUTHOR CONTRIBUTIONS

FW and CP initiated and designed the study. FW and KS collected the data. FW analyzed the data and wrote the manuscript. All authors contributed to the article and approved the submitted version.

FUNDING

This study was funded by the Deutsche Forschungs gemeinschaft (DFG; PA2643/2/348431475), through GEOMAR

(Helmholtz-Gemeinschaft) and through Deutsche Bundesstiftung Umwelt (DBU; 20018/553).

ACKNOWLEDGMENTS

We would like to thank Mia Großmann and Sean Kearney for their help during the experiment, including mussel collection, feeding and general maintenance, and Björn Buchholz for help in maintaining the experimental facility.

SUPPLEMENTARY MATERIAL

The Supplementary Material for this article can be found online at: https://www.frontiersin.org/articles/10.3389/fmars.2021.790241/full#supplementary-material

REFERENCES

Banti, V., Loreti, E., Novi, G., Santaniello, A., Alpi, A., and Perata, P. (2008). Heat acclimation and cross-tolerance against anoxia in *Arabidopsis*. *Plant Cell Environ.* 31, 1029–1037. doi: 10.1111/j.1365-3040.2008.01816.x

Bates, D., Mächler, M., Bolker, B., and Walker, S. (2015). Fitting linear mixed-effects models using lme4. *J. Stat. Softw.* 67, 1–48. doi: 10.18637/jss.v067.i01

Bonaviri, C., Graham, M., Gianguzza, P., and Shears, N. T. (2017). Warmer temperatures reduce the influence of an important keystone predator. *J. Anim. Ecol.* 86, 490–500. doi: 10.1111/1365-2656.12634

Boyd, P. W., Collins, S., Dupont, S., Fabricius, K., Gattuso, J.-P., Havenhand, J., et al. (2018). Experimental strategies to assess the biological ramifications of multiple drivers of global ocean change-A review. *Glob. Change Biol.* 24, 2239–2261. doi: 10.1111/gcb.14102

Budd, G. C. (2008). "Asterias rubens Common starfish," in *Marine Life Information Network: Biology and Sensitivity Key Information Reviews*, eds H. Tyler-Walters and K. Hiscock (Plymouth: Marine Biological Association of the United Kingdom).

DeCarlo, T. M., Harrison, H. B., Gajdzik, L., Alaguarda, D., Rodolfo-Metalpa, R., D'Olivo, J., et al. (2019). Acclimatization of massive reef-building corals to consecutive heatwaves. *Proc. Biol. Sci.* 286:20190235. doi: 10.1098/rspb.2019.0235

Doney, S. C., Ruckelshaus, M., Duffy, J. E., Barry, J. P., Chan, F., English, C. A., et al. (2012). Climate change impacts on marine ecosystems. *Annu. Rev. Mar. Sci.* 4, 11–37. doi: 10.1146/annurev-marine-041911-111611

Dürr, S., and Wahl, M. (2004). Isolated and combined impacts of blue mussels (*Mytilus edulis*) and barnacles (*Balanus improvisus*) on structure and diversity of a fouling community. *J. Exp. Mar. Biol. Ecol.* 306, 181–195. doi: 10.1016/j.jembe.2004.01.006

Gaymer, C. F., Himmelman, J. H., and Johnson, L. E. (2001). Distribution and feeding ecology of the seastars *Leptasterias polaris* and *Asterias vulgaris* in the northern Gulf of St Lawrence, Canada. *J. Mar. Biol. Assoc.* 81, 827–843. doi: 10.1017/S0025315401004660

Genin, A., Levy, L., Sharon, G., Raitsos, D. E., and Diamant, A. (2020). Rapid onsets of warming events trigger mass mortality of coral reef fish. *Proc. Natl. Acad. Sci. U.S.A.* 117, 25378–25385. doi: 10.1073/pnas.2009748117

Gómez-Gras, D., Linares, C., de Caralt, S., Cebrian, E., Frleta-Valić, M., Montero-Serra, I., et al. (2019). Response diversity in Mediterranean coralligenous assemblages facing climate change: insights from a multispecific thermotolerance experiment. *Ecol. Evol.* 9, 4168–4180. doi: 10.1002/ece3.5045

Gräwe, U., Friedland, R., and Burchard, H. (2013). The future of the western Baltic Sea: two possible scenarios. *Ocean Dyn.* 63, 901–921. doi: 10.1007/s10236-013-0634-0

Gunderson, A. R., Armstrong, E. J., and Stillman, J. H. (2016). Multiple stressors in a changing world: the need for an improved perspective on physiological responses to the dynamic marine environment. *Annu. Rev. Mar. Sci.* 8, 357–378. doi: 10.1146/annurev-marine-122414-033953

HELCOM (2013). *Climate Change in the Baltic Sea Area: A HELMCOM Thematic Assessment in 2013. Balt. Sea Environ. Proc. 37*. Helsinki: HELCOM.

Hobday, A. J., Alexander, L. V., Perkins, S. E., Smale, D. A., Straub, S. C., Oliver, E. C. J., et al. (2016). A hierarchical approach to defining marine heatwaves. *Prog. Oceanogr.* 141, 227–238. doi: 10.1016/j.pocean.2015.12.014

Hughes, T. P., Kerry, J. T., Connolly, S. R., Baird, A. H., Eakin, C. M., Heron, S. F., et al. (2019). Ecological memory modifies the cumulative impact of recurrent climate extremes. *Nat. Clim. Change* 9, 40–43. doi: 10.1038/s41558-018-0351-2

Hurell, J., and National Center for Atmospheric Research Staff (2020). *The Climate Data Guide: Hurell North Atlantic Oscillation (NAO) Index (Station Based)*. Available online at: https://climatedataguide.ucar.edu/climate-data/hurrell-north-atlantic-oscillation-nao-index-station-based (accessed July 23, 2021).

IPCC (2021). "Climate change 2021: the physical science basis," in *Contribution of Working Group I to the Sixth Assessment Report of the Intergovernmental Panel on Climate Change*, eds V. Masson-Delmotte, P. Zhai, A. Pirani, S. L. Connors, C. Péan, S. Berger, et al. (Geneva: IPCC).

Jackson, M. C., Pawar, S., and Woodward, G. (2021). The temporal dynamics of multiple stressor effects: from individuals to ecosystems. *Trends Ecol. Evol.* 36, 402–410. doi: 10.1016/j.tree.2021.01.005

Karstensen, J., Liblik, T., Fischer, J., Bumke, K., and Krahmann, G. (2014). Summer upwelling at the Boknis Eck time-series station (1982 to 2012) – a combined glider and wind data analysis. *Biogeosciences* 11, 3603–3617. doi: 10.5194/bg-11-3603-2014

Kayanne, H. (2017). Validation of degree heating weeks as a coral bleaching index in the northwestern Pacific. *Coral Reefs* 36, 63–70. doi: 10.1007/s00338-016-1524-y

Lawrence, J. M., and Cowell, B. C. (1996). The righting response as an indication of stress in *Stichaster striatus* (Echinodermata, asteroidea). *Mar. Freshw. Behav. Physiol.* 27, 239–248. doi: 10.1080/10236249609378969

Le Nohaïc, M., Ross, C. L., Cornwall, C. E., Comeau, S., Lowe, R., McCulloch, M. T., et al. (2017). Marine heatwave causes unprecedented regional mass bleaching of thermally resistant corals in northwestern Australia. *Sci. Rep.* 7:14999. doi: 10.1038/s41598-017-14794-y

Lehmann, A., and Myrberg, K. (2008). Upwelling in the Baltic Sea — A review. *J. Mar. Syst.* 74, S3–S12. doi: 10.1016/j.jmarsys.2008.02.010

Lenth, R. V. (2020). *emmeans: Estimated Marginal Means, aka Least Squares means*.

Leppäranta, M., and Myrberg, K. (eds.) (2009). *Physical Oceanography of the Baltic Sea*. Berlin: Springer.

Liu, G., Srong, A. E., Skirving, W. J., and Arzayus, L. F. (2006). "Overview of NOAA coral reef watch program's near-real-time satellite global coral bleaching monitoring activities," in *Proceedings of the 10th International Coral Reef Symposium*, Okinawa, 1783–1793.

McBryan, T. L., Healy, T. M., Haakons, K. L., and Schulte, P. M. (2016). Warm acclimation improves hypoxia tolerance in *Fundulus heteroclitus*. *J. Exp. Biol.* 219, 474–484. doi: 10.1242/jeb.133413

Melzner, F., Buchholz, B., Wolf, F., Panknin, U., and Wall, M. (2020). Ocean winter warming induced starvation of predator and prey. *Proc. Biol. Sci.* 287:20200970. doi: 10.1098/rspb.2020.0970

Minuti, J. J., Byrne, M., Hemraj, D. A., and Russell, B. D. (2021). Capacity of an ecologically key urchin to recover from extreme events: physiological impacts of heatwaves and the road to recovery. *Sci. Total Environ.* 785:147281. doi: 10.1016/j.scitotenv.2021.147281

Morón Lugo, S. C., Baumeister, M., Nour, O. M., Wolf, F., Stumpp, M., and Pansch, C. (2020). Warming and temperature variability determine the performance of two invertebrate predators. *Sci. Rep.* 10:6780. doi: 10.1038/s41598-020-63679-0

Nguyen, H. M., Kim, M., Ralph, P. J., Marín-Guirao, L., Pernice, M., and Procaccini, G. (2020). Stress memory in Seagrasses: first insight into the effects of thermal priming and the role of epigenetic modifications. *Front. Plant Sci.* 11:494. doi: 10.3389/fpls.2020.00494

Norling, P., and Kautsky, N. (2007). Structural and functional effects of *Mytilus edulis* on diversity of associated species and ecosystem functioning. *Mar. Ecol. Prog. Ser.* 351, 163–175. doi: 10.3354/meps07033

Nour, O., Stumpp, M., Morón Lugo, S. C., Barboza, F. R., and Pansch, C. (2020). Population structure of the recent invader *Hemigrapsus takanoi* and prey size selection on Baltic Sea mussels. *Aquat. Invasions* 15, 297–317. doi: 10.3391/ai.2020.15.2.06

Oliver, E. C. J. (2019). Mean warming not variability drives marine heatwave trends. *Clim. Dyn.* 53, 1653–1659. doi: 10.1007/s00382-019-04707-2

Oliver, E. C. J., Burrows, M. T., Donat, M. G., Sen Gupta, A., Alexander, L. V., Perkins-Kirkpatrick, S. E., et al. (2019). Projected marine heatwaves in the 21st century and the potential for ecological impact. *Front. Mar. Sci.* 6:734. doi: 10.3389/fmars.2019.00734

Oliver, E. C. J., Donat, M. G., Burrows, M. T., Moore, P. J., Smale, D. A., Alexander, L. V., et al. (2018). Longer and more frequent marine heatwaves over the past century. *Nat. Commun.* 9:1324. doi: 10.1038/s41467-018-03732-9

Osborn, T. J. (2011). Winter 2009/2010 temperatures and a record-breaking North Atlantic Oscillation index. *Weather* 66, 19–21. doi: 10.1002/wea.660

Pansch, C., and Hiebenthal, C. (2019). A new mesocosm system to study the effects of environmental variability on marine species and communities. *Limnol. Oceanogr. Methods* 28:16. doi: 10.1002/lom3.10306

Pansch, C., Scotti, M., Barboza, F. R., Al-Janabi, B., Brakel, J., Briski, E., et al. (2018). Heat waves and their significance for a temperate benthic community: a near-natural experimental approach. *Glob. Change Biol.* 24, 4357–4367. doi: 10.1111/gcb.14282

Petes, L. E., Mouchka, M. E., Milston-Clements, R. H., Momoda, T. S., and Menge, B. A. (2008). Effects of environmental stress on intertidal mussels and their sea star predators. *Oecologia* 156, 671–680. doi: 10.1007/s00442-008-1018-x

Pincebourde, S., Sanford, E., and Helmuth, B. (2008). Body temperature during low tide alters the feeding performance of a top intertidal predator. *Limnol. Oceanogr.* 53, 1562–1573. doi: 10.4319/lo.2008.53.4.1562

Pincebourde, S., Sanford, E., Casas, J., and Helmuth, B. (2012). Temporal coincidence of environmental stress events modulates predation rates. *Ecol. Lett.* 15, 680–688. doi: 10.1111/j.1461-0248.2012.01785.x

R Core Team (2021). *R: A Language and Environment for Statistical Computing*. Vienna: R Foundation for Statistical Computing.

Reusch, T. B. H., and Chapman, A. R. O. (1997). Persistence and space occupancy by subtidal blue mussel patches. *Ecol. Monogr.* 67:65. doi: 10.2307/2963505

Reusch, T. B. H., Dierking, J., Andersson, H. C., Bonsdorff, E., Carstensen, J., Casini, M., et al. (2018). The Baltic Sea as a time machine for the future coastal ocean. *Sci. Adv.* 4:eaar8195. doi: 10.1126/sciadv.aar8195

Sadchatheeswaran, S., Branch, G. M., and Robinson, T. B. (2015). Changes in habitat complexity resulting from sequential invasions of a rocky shore: implications for community structure. *Biol. Invasions* 17, 1799–1816. doi: 10.1007/s10530-014-0837-4

Saha, M., Barboza, F. R., Somerfield, P. J., Al-Janabi, B., Beck, M., Brakel, J., et al. (2020). Response of foundation macrophytes to near-natural simulated marine heatwaves. *Glob. Change Biol.* 26, 417–430. doi: 10.1111/gcb.14801

Sanford, E. (1999). Regulation of keystone predation by small changes in ocean temperature. *Science (New York N.Y.)* 283, 2095–2097. doi: 10.1126/science.283.5410.2095

Schlegel, R. W., and Smit, A. J. (2018). heatwaveR: a central algorithm for the detection of heatwaves and cold-spells. *J. Open Source Softw.* 3:821. doi: 10.21105/joss.00821

Schlegel, R. W., Oliver, E. C. J., Hobday, A. J., and Smit, A. J. (2019). Detecting marine heatwaves with sub-optimal data. *Front. Mar. Sci.* 6:737. doi: 10.3389/fmars.2019.00737

Schmidt, G. M., Wall, M., Taylor, M., Jantzen, C., and Richter, C. (2016). Large-amplitude internal waves sustain coral health during thermal stress. *Coral Reefs* 35, 869–881. doi: 10.1007/s00338-016-1450-z

Schulte, P. M., Healy, T. M., and Fangue, N. A. (2011). Thermal performance curves, phenotypic plasticity, and the time scales of temperature exposure. *Integr. Comp. Biol.* 51, 691–702. doi: 10.1093/icb/icr097

Seuront, L., Nicastro, K. R., Zardi, G. I., and Goberville, E. (2019). Decreased thermal tolerance under recurrent heat stress conditions explains summer mass mortality of the blue mussel *Mytilus edulis*. *Sci. Rep.* 9:17498. doi: 10.1038/s41598-019-53580-w

Smale, D. A., Wernberg, T., Oliver, E. C. J., Thomsen, M., Harvey, B. P., Straub, S. C., et al. (2019). Marine heatwaves threaten global biodiversity and the provision of ecosystem services. *Nat. Clim. Change* 9:360. doi: 10.1038/s41558-019-0412-1

Sommer, U., Meusel, B., and Stielau, C. (1999). An experimental analysis of the importance of body-size in the seastar-mussel predator-prey relationship. *Acta Oecol.* 20, 81–86. doi: 10.1016/S1146-609X(99)80019-8

Thomsen, M. S., Mondardini, L., Alestra, T., Gerrity, S., Tait, L., South, P. M., et al. (2019). Local extinction of bull kelp (*Durvillaea* spp.) due to a marine heatwave. *Front. Mar. Sci.* 6:84. doi: 10.3389/fmars.2019.00084

Todgham, A. E., Schulte, P. M., and Iwama, G. K. (2005). Cross-tolerance in the tidepool sculpin: the role of heat shock proteins. *Physiol. Biochem. Zool. PBZ* 78, 133–144. doi: 10.1086/425205

Vajedsamiei, J., Wahl, M., Schmidt, A. L., Yazdanpanahan, M., and Pansch, C. (2021). The higher the needs, the lower the tolerance: extreme events may select Ectotherm recruits with lower metabolic demand and heat sensitivity. *Front. Mar. Sci.* 8:660427. doi: 10.3389/fmars.2021.660427

van Rij, J., Wieling, M., Baayen, R. H., and van Rijn, H. (2020). *itsadug: Interpreting Time Series and Autocorrelated Data Using GAMMs*.

Vevers, H. G. (1949). The biology of *Asterias rubens* L: growth and reproduction. *J. Mar. Biol. Assoc.* 28, 165–187. doi: 10.1017/S0025315400055272

Wahl, M., Barboza, F. R., Buchholz, B., Dobretsov, S., Guy-Haim, T., Rilov, G., et al. (2021). Pulsed pressure: fluctuating impacts of multifactorial environmental change on a temperate macroalgal community. *Limnol. Oceanogr.* 33:477. doi: 10.1002/lno.11954

Wahl, M., Buchholz, B., Winde, V., Golomb, D., Guy-Haim, T., Müller, J., et al. (2015). A mesocosm concept for the simulation of near-natural shallow underwater climates: the Kiel Outdoor Benthocosms (KOB). *Limnol. Oceanogr. Methods* 13, 651–663. doi: 10.1002/lom3.10055

Wahl, M., Werner, F. J., Buchholz, B., Raddatz, S., Graiff, A., Matthiessen, B., et al. (2020). Season affects strength and direction of the interactive impacts of ocean warming and biotic stress in a coastal seaweed ecosystem. *Limnol. Oceanogr.* 65, 807–827. doi: 10.1002/lno.11350

Walter, J., Jentsch, A., Beierkuhnlein, C., and Kreyling, J. (2013). Ecological stress memory and cross stress tolerance in plants in the face of climate extremes. *Environ. Exp. Bot.* 94, 3–8. doi: 10.1016/j.envexpbot.2012.02.009

Walther, G.-R., Post, E., Convey, P., Menzel, A., Parmesan, C., Beebee, T. J. C., et al. (2002). Ecological responses to recent climate change. *Nature* 416, 389–395. doi: 10.1038/416389a

Wolf, F., Bumke, K., Wahl, S., Nevoigt, F., Hecht, U., Hiebenthal, C. et al. (2020). High resolution water temperature data between January 1997 and December 2018 at the GEOMAR pier surface. *PANGAEA*. doi: 10.1594/PANGAEA.919186

Wood, S. N. (2017). *Generalized Additive Models*. Boca Raton, FL: CRC Press.

Conflict of Interest: The authors declare that the research was conducted in the absence of any commercial or financial relationships that could be construed as a potential conflict of interest.

Publisher's Note: All claims expressed in this article are solely those of the authors and do not necessarily represent those of their affiliated organizations, or those of the publisher, the editors and the reviewers. Any product that may be evaluated in this article, or claim that may be made by its manufacturer, is not guaranteed or endorsed by the publisher.

frontiers in Marine Science

ORIGINAL RESEARCH
published: 25 March 2022
doi: 10.3389/fmars.2022.858280

Temperature Extremes and Sex-Related Physiology, Not Environmental Variability, Are Key in Explaining Thermal Sensitivity of Bimodal-Breathing Intertidal Crabs

Pedro J. Jimenez[1], *Lyle D. Vorsatz*[1], *Tânia M. Costa*[2] *and Stefano Cannicci*[1,3]*

[1] The Swire Institute of Marine Sciences and Area of Ecology and Biodiversity, School of Biological Sciences, The University of Hong Kong, Hong Kong, Hong Kong SAR, China, [2] Biosciences Institute, São Paulo State University (UNESP), São Vicente, Brazil, [3] Department of Biology, University of Florence, Sesto Fiorentino, Italy

Global temperature increases are predicted to have pronounced negative effects on the metabolic performance of both terrestrial and aquatic organisms. These metabolic effects may be even more pronounced in intertidal organisms that are subject to multiple, abruptly changing abiotic stressors in the land-sea transition zone. Of the available studies targeting the intertidal environment, emphasis has largely been on water-breathing model organisms and this selective focus resulted in limited reliable forecasts on the impact of global warming on primarily air-breathing intertidal species. We investigated the thermal sensitivity of six phylogenetically related fiddler crab species that occupy different microhabitats on intertidal shores from south America and east Asia to test how bimodal-breathing intertidal ectotherms cope with thermal stress. We examined the metabolic physiology and thermal limits of the crabs by measuring their cardiac function and oxygen consumption along a thermal gradient. Their specific thermal microhabitat was also appraised. We found that subtropical fiddler crab species inhabiting vegetated microhabitats have lower upper lethal temperatures and therefore greater thermal sensitivity in comparison to their tropical counterparts. Additionally, females exhibited higher oxygen consumption and lower lethal temperatures in comparison to males. Our results contradict previous predictions that species from higher latitudes that experience greater temperature variability have broader latitudinal distributions, greater phenotypic plasticity and lower thermal sensitivity. Furthermore, the higher thermal sensitivity demonstrated by female fiddler crabs with respect to males strongly suggests a role of both gametogenesis and physiological dimorphism on the thermal performance of tropical and subtropical intertidal organisms. These observations ultimately, advocates for further studies on sex-biased and development-biased thermal sensitivity before drawing any generalizations based on a single sex or life stage.

Keywords: thermal adaptations, fiddler crabs, intertidal organisms, bimodal breathers, thermal physiology, latitudinal gradient, habitat temperature

OPEN ACCESS

Edited by:
Christian Pansch,
Åbo Akademi University, Finland

Reviewed by:
Carolina Madeira,
NOVA University Lisbon, Portugal
Laura Ramajo,
Universidad Católica del Norte, Chile

***Correspondence:**
Stefano Cannicci
cannicci@hku.hk

Specialty section:
This article was submitted to Global Change and the Future Ocean, a section of the journal Frontiers in Marine Science

Received: *19 January 2022*
Accepted: *02 March 2022*
Published: *25 March 2022*

Citation:
Jimenez PJ, Vorsatz LD, Costa TM and Cannicci S (2022) Temperature Extremes and Sex-Related Physiology, Not Environmental Variability, Are Key in Explaining Thermal Sensitivity of Bimodal-Breathing Intertidal Crabs. Front. Mar. Sci. 9:858280. doi: 10.3389/fmars.2022.858280

INTRODUCTION

Intertidal habitats are challenging environments as organisms that colonize them must cope with tidal cycles and high thermal variability (Denny and Paine, 1998; Raffaelli and Hawkins, 1999; Denny et al., 2011). Due to the tides, for instance, organisms occupying the mid-high intertidal zone experience longer periods of emersion and greater thermal fluctuations compared to species present at the low intertidal zone (Williams and Morritt, 1995; Finke et al., 2007). These differences in inundation time often result in spatial patterns of species distribution along a mosaic of specific microhabitats (Peterson, 1991), mainly driven by species-specific thermal tolerances linked to evolutionary plasticity (Stillman and Somero, 1996; Stillman and Somero, 2000; Somero, 2002; Stillman, 2002). In these extremely variable habitats, resident organisms have evolved diverse strategies to mitigate the stress posed by fluctuating environmental conditions over different temporal scales (Viña et al., 2018). These strategies often involve the evolution of plastic morphological (Helmuth et al., 2006b; Harley et al., 2009), physiological (Somero, 2010) and behavioral (Chou et al., 2019) modifications, but local adaptation can play a role in coping with conditions fluctuating at small spatial and temporal scales (Jahnke et al., 2022).

Intertidal shores are also spatially diverse environments that range from bare rock surfaces and mud/sand flats to more structurally complex habitats, such as mangrove forests (Beck, 1998; Vorsatz et al., 2021b). Tidal ranges and local abiotic conditions interact to form complex thermal mosaics across the intertidal zone (Helmuth and Hofmann, 2001; Helmuth, 2002; Helmuth et al., 2006a). Thus, adjacent intertidal microhabitats can have variable microclimates, with areas directly exposed to solar radiation reaching higher temperatures than shaded habitat underneath mangrove trees (Seabra et al., 2011; Chou et al., 2019). This microclimate variability has been shown to influence the thermal tolerance of organisms, with species living in warmer areas showing higher thermal limits but lower physiological plasticity to cope with further warming (Stillman and Somero, 2000).

Temperature is a major factor linked to the life traits and geographic distribution of ectotherms (Roy et al., 1998; Helmuth et al., 2002; Brayard et al., 2005; Somero, 2010). Experienced extreme temperatures, in particular, are regarded as the driving factor that influences their physiological tolerance to heat stress (Pither, 2003; Gaston et al., 2009). Phylogenetic constraints can also drive tolerance traits of species, with phylogenetically related organisms exhibiting similar tolerance to heat stress (Bennett et al., 2021). These phylogenetic signals, also termed niche conservatism (Wiens and Graham, 2005), proved to be particularly important in setting the upper thermal limits of species (Hoffmann et al., 2013), ultimately limiting their phenotypic plasticity and response to climate change (Bennett et al., 2021). Thus, phylogenetic history can play a role in the differential response of intertidal species to fluctuating conditions, but this role was never tested in detail.

Intertidal ectotherms often live close to their thermal limits making these species vulnerable to further temperature increases linked to climate change. Many intertidal crustaceans, mollusks and some fish are bimodal breathers and are able to extract oxygen from both air and water (Mcmahon, 1988; Henry, 1994; Graham, 1997). Due to their thermal physiology and unique respiratory strategies, these organisms are interesting models to investigate the vulnerability of ectotherms to temperature changes. There is, however, a dearth of information on the response of primarily air-breathing intertidal ectotherms to environmental change, with the literature predominantly focused on water-breathing organisms inhabiting rocky shores (e.g. Stillman and Somero, 1996; Stillman and Somero, 2000; Przeslawski et al., 2005; Marshall et al., 2015).

Fiddler crabs (Ocypodidae: Gelasiminae) are represented by an Atlantic-East Pacific (AEP) and an Indo-West Pacific (IWP) clade (Shih et al., 2016a). Crabs from both clades can be found in a wide range of intertidal habitats, such as mud/sand flats and mangrove forests (Crane, 1975), where they experience different thermal environments (Alongi, 1990). Fiddler crabs have functional lungs and are true air breathers (Paoli et al., 2015). They show strong morphological and behavioral differences between sexes. Males have one enlarged cheliped used to court females and fight competitors, which is also useful for thermoregulation (Windsor et al., 2005; Darnell and Munguia, 2011; Darnell et al., 2013). Females have two small chelipeds that they use for feeding (Levinton et al., 1995). This difference in cheliped characteristics cause sex-related constraints on their time-energy budget (Valiela et al., 1974; Darnell et al., 2013), which, ultimately, reflect on the individual thermal physiology (Pörtner, 2012). During the reproductive season female fiddler crabs invest more energy than males to develop their gonads (Yamaguchi, 2003; Hartnoll, 2006; Colpo and López-greco, 2018). The higher energetic investment in reproduction by females is known to constrain their energy budgets, limit growth, increase mortality rates, reduce feeding and hinder other functions (Hartnoll, 2006; Guderley and Pörtner, 2010).

Here, we tested the physiological responses to temperature of six fiddler crab species with tropical and subtropical distributions belonging to two separate phylogenetic clades and from two geographic realms, the IWP and the AEP. We investigated whether fiddler crab species that occupy intertidal habitats with contrasting environmental characteristics could display differences in their thermal limits across sexes. Our hypotheses were: (1) the habitat occupied by ectotherms in physiologically challenging intertidal zones is reflected in their thermal limits, with species living in more thermally stressful environments being better adapted to cope with heat stress; (2) during their extended reproductive season, male and female fiddler crabs have different physiological responses to increasing temperature, with females being more vulnerable due to higher reproductive investment and (3) the phylogenetic distance and evolutionary history of the selected fiddler crabs result in different adaptations in thermal tolerance. Understanding the physiological responses of fiddler crabs to thermal stress can improve our comprehension on the consequences of climate change effects on intertidal

ectotherms. Furthermore, investigating the physiological responses to temperature increase of closely related species from different geographical regions can inform which species are most at risk to climate change.

MATERIALS AND METHODS

Study Areas and Model Species

Two localities, Tung Chung, Hong Kong Special Administrative Region, People's Republic of China and the Itaguaré river mouth, Bertioga, São Paulo State, Brazil, were selected for crab collection. These mangrove areas placed in the IWP and AEP regions, respectively, have very similar thermal and environmental characteristics (**Table S1**).

The Hong Kong fiddler crabs were *Gelasimus borealis*, *Austruca lactea*, and *Paraleptuca splendida*; while the species from Brazil were *Leptuca thayeri*, *L. leptodactyla*, and *L. uruguayensis*. The model species were selected to represent different distributions along a latitudinal and intertidal habitat gradient (**Figure 1**; **Table 1**).

Thirty adult males and 30 females of each species were collected by hand on the mud/sandflats and under the mangrove canopy at both regions. Sampling occurred during the reproductive season, with ovigerous females present in all the sampled fiddler crab populations. Only non-ovigerous females were used in the experiments, because brood care is an energetically costly activity that affects the crabs' physiology (Fernández et al., 2000; Baeza and Fernández, 2002). For each species, the experimental crabs collected belonged to similar size classes, to reduce the variance in size related differences. The carapace width (CW) of the crabs ranged from 17.5 to 23.9 mm in *G. borealis* males and 13.6 to 18.6 mm in females; 15.0 to 18.0 mm in *A. lactea* males and 12.1 to 15.8 mm in females; 14.7 to 19.3 mm in *P. splendida* males and 12.8 to 19.5 in females; 17.7 to 22.6 in *L. thayeri* males and 16.3 to 23.4 in females; 10.6 to 14.4 mm in *L. leptodactyla* males and 8.8 to 11.4 in females; and 8.7 to 11.4 mm in *L. uruguayensis* male and 8.7 to 10.4 mm in females. The collected males had integral chelipeds and collected individuals of both sexes lacked no more than two walking legs, to reduce any effect of crab mutilation on the results. Crabs collected in Hong Kong and Brazil were transported in boxes and buckets with sediment to the facilities of the Swire Institute of Marine Sciences (SWIMS), the University of Hong Kong, and to the Laboratory of Ecology and Animal Behavior (LABECOM), Sao Paulo State University - Coastal Campus,

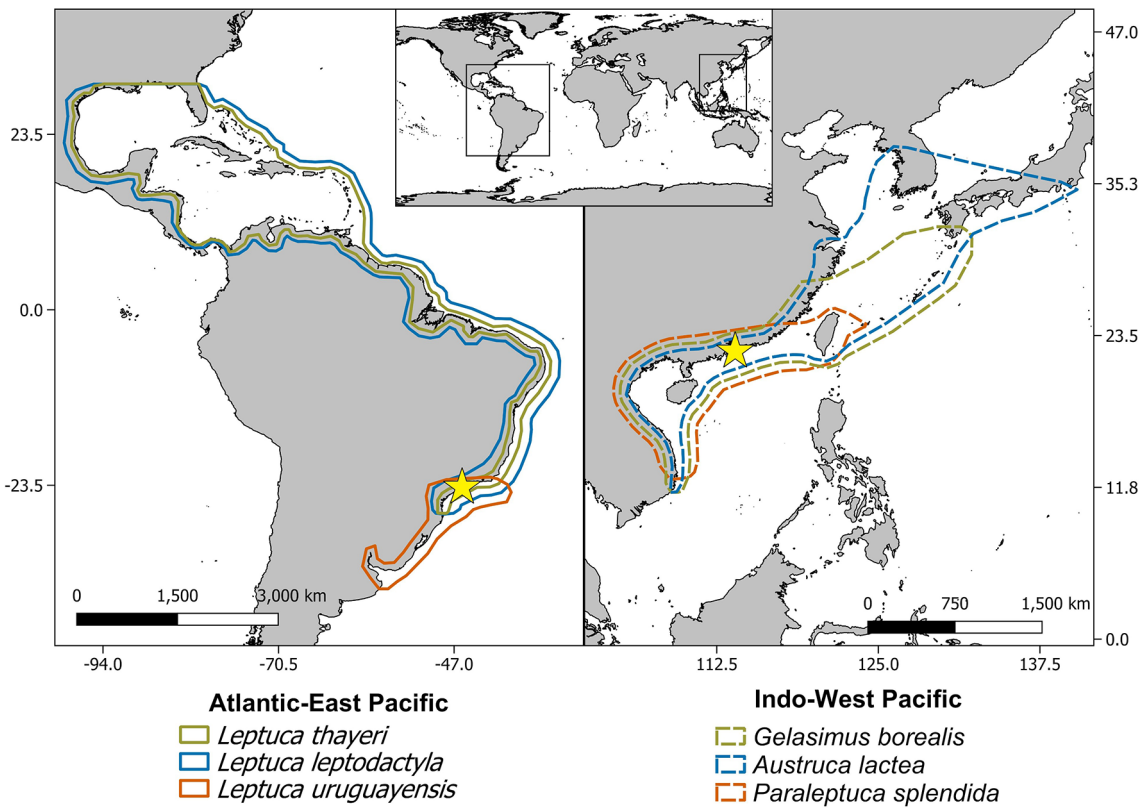

FIGURE 1 | Map showing the latitudinal range of the model species (based on Shih, 2012; Shih et al., 2012; Thurman et al., 2013; Kostina et al., 2016; Shih et al., 2016b; Yuhara et al., 2017). Yellow stars represent the sampling areas: Itaguaré river mouth, Bertioga, São Paulo, Brazil in the Atlantic-East Pacific, and Tung Chung, Hong Kong SAR, PR China in the Indo-West Pacific.

TABLE 1 | Summary of the habitat characteristics where the model species occur.

Region	Species	Habitat
IWP	*Gelasimus borealis*	Exposed sandy to muddy flats at mid-low intertidal levels (Kwok and Tang, 2006)
	Austruca lactea	Exposed open sand flats at high-mid intertidal levels (Kwok and Tang, 2006)
	Paraleptuca splendida	Sandy mudflats, salt marshes and mangroves at mid-high intertidal levels. Also, at landward fringes of sandy beaches (Shih et al., 2012)
AEP	*Leptuca thayeri*	Clay and mud, often associated with vegetation at mid-low intertidal levels (Diele et al., 2010; Thurman et al., 2013)
	Leptuca leptodactyla	Sandy soil, in exposed areas at high-mid intertidal levels (Thurman et al., 2013)
	Leptuca uruguayensis	Firm sandy to silty clay flats at mid-high intertidal levels. Burrows can be exposed but often associated with vegetation (Thurman et al., 2013; Ribeiro et al., 2016)

IWP, Indo-West Pacific; AEP, Atlantic-East Pacific.

respectively. At each institution, crabs were conditioned in three separated outdoor stock tanks, one for each species, measuring 41 × 56 × 78 cm (height × width × length), prepared with a layer of 10 cm of sediment from the sampling sites. In the tanks, water influx was controlled to simulate a semi diurnal tidal regime. Sea water (salinity ~ 34‰) was used for the tide simulation. Fiddler crabs are osmoregulators capable of maintaining their blood osmolarity over a large range of salinities (Lin et al., 2002). These crabs tolerate great variations in salinity across short temporal scales due to the tidal influence, with sea water being well within their tolerance range (Lin et al., 2002; Thurman et al., 2010; Faria et al., 2017). The stock tanks were kept under temperatures similar to the sampling sites, to avoid effects of acclimation in the crabs' physiological responses. No more than 20 crabs were held in each stock tank at once. Since fiddler crabs can have fast acclimation to different thermal conditions (Darnell et al., 2015), experiments were performed within two to 14 days from the sampling date, to avoid effects of long-term captivity on their physiology.

Thermal Characterization of Microhabitats

To measure the soil surface temperature (°C) of the natural environment of the tested species, four iButton® (Maxim Integrated®) thermologgers, waterproofed in silicon glue, were deployed at the two sampling sites, in areas dominated by the different species. In Tung Chung, the thermologgers were deployed during September, at the unshaded intertidal flats, where *G. borealis* and *A. lactea* are found in mixed populations, and at the vegetated area dominated by *P. splendida*. At the Itaguaré river mouth, the thermologgers were deployed in January/February, at the sand flat dominated by *L. leptodactyla*, the vegetated area dominated by *L. uruguayensis*, and at the lower intertidal zone dominated by *L. thayeri*.

Phylogenetic Relationships and Phylogenetic Signal on Thermal Limits

A phylogenetic tree was constructed to investigate phylogenetic relationship between model fiddler crabs. Mitochondrial gene sequences for subunits 16S and 28S ribosomal and cytochrome oxidase subunit I (COI) were obtained from Genbank (Clark et al., 2016) (accession numbers are in **Table S2**) for each of the tested species and for *Ocypode ceratophthalmus*, selected as an outgroup because it belongs to the same family of the fiddler crabs, Ocypodidae, but not to the Gelasiminae subfamily.

Determination of Cardiac Function

Experiments were conducted to determine the heart rate of males and females of the model species in response to temperature (n = 10 for each experimental group, N = 120 specimens). The specimens were placed in 'blacked-out' containers to reduce exposure to visual stimuli. A layer of seawater (salinity 30 ‰) that extended to the height of the crab's ventral surface was added to each holding container to avoid the potential influence of water loss on crab physiology (Burggren et al., 1990; Burggren, 1992). The heart function was measured using a method adapted from Depledge and Andersen (1990). An infrared sensor (Vishay Semiconductors®, CNY70) was attached to each crab's carapace, above the cardiac region, using Blu Tack® adhesive together with cyanoacrylate glue. The sensor was used to record heartbeat signals, which were filtered (Burnett et al., 2013), sent to an oscilloscope (PicoScope® 2204) connected to a computer and recorded with PicoScope 7 software. Individual crabs were placed in individual holding containers positioned in a programmable water bath (Grant® Optima TXF-200 heated circulation bath, Cambridge, UK). The crabs were allowed to recover from handling stress and to acclimate to the initial experimental temperature for 30 min at 25°C. Then, the crabs were exposed to an increasing thermal ramp, starting at 25°C, with a 1°C increase every 20 min until heart function ceased. The initial temperature of 25°C was chosen because it is close to the average minimum air temperature experienced by the crabs at Tung Chung and Itaguaré river mouth during summer The temperature increase was based on the 95th percentile for the temperature variation rate in the vegetated habitats occupied by *L. uruguayensis* and *P. splendida*, 1.2 and 0.8°C each 20 min respectively, thus, mimicking actual conditions and avoiding possible effects of extreme heating rates on the crabs.

Crab body temperatures were corrected in relation to the water bath temperature by employing a method similar to (Levinton et al., 2020). We recorded the body temperature of

crabs subjected to the same temperature-ramp used for the heart rate experiments by means of a temperature probe. For these tests, ten male and female individuals of each model species (N = 120), of comparable size to those in the heart function experiments, were subjected to an identical thermal ramp as previously described. A k-type thermocouple was inserted and fixed in their branchial chambers using Blu Tack® adhesive and cyanoacrylate glue. The thermocouples were connected to a thermometer (Lutron® TM-947SD) that logged the crab body temperature (± 0.1°C) every minute for the duration of the thermal ramp. The temperature inside the water bath was also recorded every minute. Body temperature was then plotted against the water temperature and sex-specific linear regressions were fitted to describe the body/water temperature relationships for each species. The linear regressions were then used to correct body temperature in relation to the temperature within the water bath in the heart function experiment.

Determination of Metabolic Rate

To investigate the basal metabolic rate of the model species in response to increasing temperature, oxygen consumption (MO_2) experiments were conducted on crabs subjected to a thermal ramp. Before the experiments commenced, the carapace and appendages of ten males and females of each of the six species (N = 120) were blotted dry and cleaned with a cotton swab using distilled water and absolute ethanol. The crabs were then allocated to individual ethanol sterilized glass chambers (130 mL), fitted with an oxygen spot sensor (Loligo Systems®, Viborg, Denmark) glued to its inner wall. The respirometry chambers containing the smaller species (*L. leptodactyla* and *L. uruguayensis*) had glass marbles inserted in them, to reduce the volume and ensure an adequate drawdown of oxygen. The total volume of the glass marbles was subsequently subtracted from the chamber volume. All MO_2 measurements were recorded in air, as fiddler crabs are subjected to intense heat stress during their activity periods at low tides (Powers and Cole, 1976; Allen and Levinton, 2014). The chambers were sealed and placed in a water bath (Grant® Optima TXF-200 heated circulation bath). Before the experiment started, the crabs within the chambers were left in the water bath for 30 min at 25°C, to recover from handling stress and acclimate to the initial experimental temperature. Subsequently, the crabs were exposed to a thermal ramp, starting from 25°C up to 50°C, with an increase of 1°C every 20 min. Two oxygen saturation measurements were recorded at each one-minute interval, at every 1°C stepwise increase along the thermal ramp, using a Witrox® oxygen meter (Loligo Systems®), through a fiber optic cable connected to the oxygen spots. The data were then logged on a computer with the Witrox® View software. The MO_2 was then calculated using the difference in oxygen saturation of air between the two points in time. To record the temperature inside the containers, a temperature probe was inserted into an empty and sealed container subjected to the same thermal ramp in parallel with the ones containing the crabs. The recorded temperature was used in the subsequent MO_2 analyses. Chambers without animals (N = 10) were used as blanks, to control for background changes in oxygen saturation in each trial. The absolute values for oxygen saturation changes obtained in the control chambers were then subtracted from the experimental values. Crab volume was also measured using water displacement in graduate cylinders and subtracted from the volume of the chamber upon completion of experiments. Oxygen measurements were taken up to the upper lethal temperatures (LT) obtained for each species from the heart rate experiments. During the experiments, the oxygen saturation inside the chambers never fell below 70%, avoiding hypoxic conditions (Burke, 1979). The crabs used in the experiment were weighted on a precision scale (± 0.001g), and the oxygen consumption was expressed as mg O_2 g^{-1} h^{-1}.

For the cardiac function, body temperature and metabolic rates experiments, crabs were weighed with a precision scale (± 0.001 g) and measured with a dial caliper (CW; ± 0.1 mm). The sizes of the animals used in the experiments are summarized in **Table S3**.

Data Analyses

For the data analyses, the model species were grouped according to their geographic region (factor cluster, IWP and AEP) and the microhabitat they occupy. Thus, *G. borealis* and *L. thayeri* were classified as lower intertidal flat (LI) species, *A. lactea* and *L. leptodactyla* as sand flat (SF) species, and *P. splendida* and *L. uruguayensis* as vegetated area (VG) species. Data analyses were performed in Primer7 and R version 4.0.3 (R core team, 2021).

The temperatures (average, average daily maxima, and minima) were compared among sites (N = 11 days in Hong Kong and N = 14 days in Itaguaré river mouth). To check for differences in temperature, models were constructed with cluster (IWP and AEP) and habitat (unshaded intertidal flat, which comprise lower intertidal and sand flat where *A. lactea* and *G. borealis* coexist, vs vegetated area for Hong Kong, and lower intertidal, sand flat and vegetated area for Brazil) as fixed factors and the temperatures as response variables. The data were not normally distributed (Shapiro-Wilk test, $p < 0.05$) and did not meet the assumptions of homogeneity of variances (Levene test, $p < 0.05$). Euclidean distance matrices were built for each of the response variables. The matrices showed homogeneity of the multivariate dispersion (Betadisper, $p > 0.05$) and were analyzed using a PERMANOVA routine (9999 permutations). When necessary, *post-hoc* pairwise PERMANOVA tests were used to check for differences among experimental groups, with Holm adjusted p values (Holm, 1979). The significance level for all statistical analysis was set as $\alpha = 0.05$.

For the phylogenetic analyses, the mitochondrial gene sequences were aligned with the software mega X (Kumar et al., 2018), using the MUSCLE method (Edgar, 2004). The phylogenetic relationships were estimated using a Bayesian tree. The phylogenetic tree was obtained through conducting a Bayesian Markov Chain Monte Carlo simulation with 100,000,000 generations, sampling parameters every 1000 generations in BEAST v.1.10.4 (Drummond and Rambaut, 2007; Suchard et al., 2018), using a GTR substitution model (Tavaré, 1986), with Γ site heterogeneity model (4 Γ categories) to account for invariable sites (Yang, 1994), using a uncorrelated relaxed clock with log-normal distribution (Drummond et al., 2006) and a tree prior based on Yule Process speciation model (Yule, 1924; Gernhard, 2008). The GTR+I+ Γ model was used because it

leads to accurate phylogenies and ancestral sequences (Abadi et al., 2019). The sampled parameters were examined in Tracer 1.7.1 (Rambaut et al., 2018), where effective sampling size was found to be higher than 1000 for all parameters. The first 10% of the Bayesian analysis were discarded as burn-in trees, and the remaining trees were summarized by Maximum Clade Credibility using the software TreeAnnotator 1.10.4. To account for non-independence of the data that could arise from phylogenetic relationships, a Pagel's λ approach, which assumes a Brownian motion model of trait evolution (Pagel, 1997; Pagel, 1999), was applied to investigate phylogenetic constraints in the recorded physiological traits. Values of Pagel's λ approaching 1 indicate a Brownian model of evolution, where the evolution of a trait is proportional to branch lengths in the phylogenetic tree (Pagel, 1999), while lower values indicate a star phylogeny model of evolution. Pagel's λ was calculated using the package "phytools" (Revell, 2012).

The heart rate (BPM, beats min^{-1}) was determined at one-minute intervals along a thermal ramp and plotted against the temperature. The endpoint of heart function, i.e., when the heart stops beating, was taken as a proxy for LT (Marshall et al., 2010). Then, the LT_{50}, i.e., the median temperature at which 50% of the organisms died was obtained for each species. The Optimum Performance Temperature (OPT), i.e., the temperature where the heart rate is at its maximum, was obtained by applying Lowess smoothers to the heart rate thermal performance curves obtained (smoother span = 0.05, robustifying iterations = 3). The temperature at which the heart rates were at their maximum in the smoothed curve was taken as the OPT. The Arrhenius Breakpoint temperature (ABT), i.e., the temperature at which there is a discontinuity in the slope of the Arrhenius plot and the heart rate rapidly drops (Stillman and Somero, 1996; Marshall et al., 2010; Marshall et al., 2011) was also calculated by plotting the natural log of the heart rates BPM against the inverse Kelvin temperature in Arrhenius form. The ABT was calculated for every individual by piece-wise regression using the package 'segmented' (Muggeo, 2003) on R. As an estimate of vulnerability to climate warming of the studied fiddler crabs, we used the thermal safety margin (TSM) concept (Deutsch et al., 2008). The TSM's of terrestrial and marine ectotherms have been defined and calculated in various ways in the literature and we calculated this margin by subtracting the LT of each species from their maximum experienced habitat temperature, following the definition of Sunday et al. (2014). The data describing OPT, ABT and LT were non-normally distributed (Shapiro-Wilk test, $p < 0.05$). To check for differences in OPT, ABT and LT among experimental groups, Euclidean distance matrices were constructed for each response variable and PERMANOVA (9999 permutations) routines were computed with cluster (IWP and AEP), habitat (LI, SF and VG) and sex (male and female) as fixed factors. The matrices for ABT and LT showed homogeneity of the multivariate dispersion (Betadisper, $p > 0.05$) but not the matrix for OPT (Betadisper, $p < 0.05$). Nonetheless, PERMANOVA was still used, as this routine is robust with non-homogeneous data in balanced designs (Anderson and Walsh, 2013).

Thermal performance curves for MO_2 were fitted for each sex of each species using the R packages 'nls.multstart' (Padfield and Matheson, 2020) and 'rTPC' (Padfield and O'Sullivan, 2020; Padfield et al., 2020). Twenty-one non-linear regression models were constructed to determine the best-fitting TPC for our data (**Table S4**). Using measures of relative fit, Pawar's model for fitting TPC's (Kontopoulos et al., 2018) was selected as the best-fitting model through the Akaike information criterion (AIC) (**Table S4**). For further details about the selected model parameters see Equation S1. Confidence intervals were computed using bootstrapping (case resampling method, 999 iterations). Parameters obtained from the fitted TPC and LT_{50} are shown in **Table S5**.

The MO_2 in response to temperature were compared among model species for each 1°C interval ranging from 26°C until the LT for each species. The differences in MO_2 among species were tested according to four fixed factors: cluster (AEP and IWP), temperature, habitat (LI, SF and VG) and sex (male and female), and individual as a random factor. The data showed a non-normal distribution (Shapiro-Wilk test, $p < 0.05$), therefore a PERMANOVA (9999 permutations) was applied to test the design (Euclidean distances matrix with homogeneity of the multivariate dispersion, Betadisper, $p > 0.05$).

RESULTS

Microhabitats Thermal Characterization

Average daily soil surface temperature variability at the Itaguaré river mouth ranged from 19.6°C to 36.8°C at the *L. thayeri* area, 20.1°C to 45.3°C at the *L. leptodactyla* area, and 20.7°C to 39.7°C at the *L. uruguayensis* area (**Figure 2A**). The temperature at Tung Chung was less variable, ranging from 25.1°C to 37.6°C at the *P. splendida* area and 24.4°C to 44.7°C at the *G. borealis* and *A. lactea* area (**Figure 2B**).

The average soil surface temperature differed between sites and was higher at Tung Chung (PERMANOVA, pseudo-$F_{(1,18795)}$ = 2225.201, $p < 0.005$). Soil surface temperature also differed among habitats (PERMANOVA, pseudo-$F_{(1,18795)}$ = 187.954, $p < 0.005$), with the sand flat experiencing higher temperatures at both sites, followed by the vegetated areas. The lower intertidal shore at Itaguaré river mouth experienced the lowest temperatures among the three habitats ($p < 0.05$, PERMANOVA *post-hoc* test). The average daily soil surface minimum temperature was lower at the Itaguaré river mouth than at Tung Chung (PERMANOVA, pseudo-$F_{(1,59)}$ = 51.398, $p < 0.005$), but was not different among habitats. The average daily maximum soil surface temperature did not differ between the two collection sites (PERMANOVA, pseudo-$F_{(2,59)}$ = 1.350, $p > 0.05$). The maximum temperature however differed among habitats (PERMANOVA, pseudo-$F_{(2,59)}$ = 8.828, $p < 0.005$), with higher temperatures in the sand flats compared to the vegetated areas and lower shores ($p < 0.05$, PERMANOVA *post-hoc* test).

Phylogenetic Relationships and Phylogenetic Signal on Thermal Limits

As expected, the phylogenetic tree constructed to investigate phylogenetic relationship between model fiddler crabs showed that the fiddler crabs from AEP and IWP form two distinct

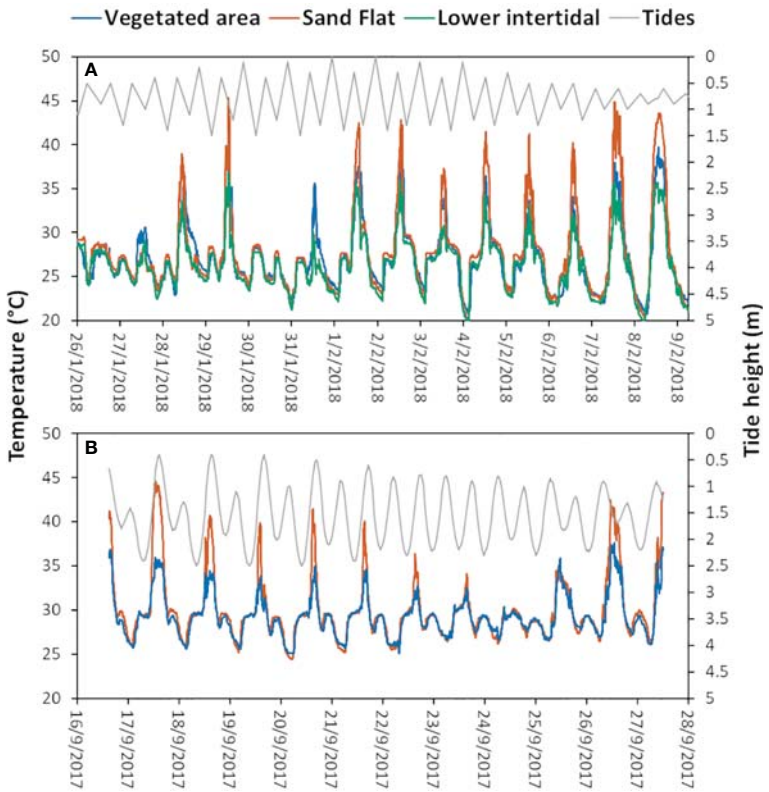

FIGURE 2 | Temperature and tidal regimes recorded at the collection sites during the sampling period. **(A)** Itaguaré river mouth, **(B)** Tung Chung. The orange line in **(B)** represents the mud-sand flat in Tung Chung where both *A. lactea* and *G. borealis* are found in mixed populations.

clades (**Figure 3**). The results related to the possible phylogenetic signal on the physiological traits of the different species are shown in **Table S6**. As there was no significant effect of phylogeny on cardiac function and metabolic rate patterns, the data were treated as independent and phylogeny was not accounted for in further analyses.

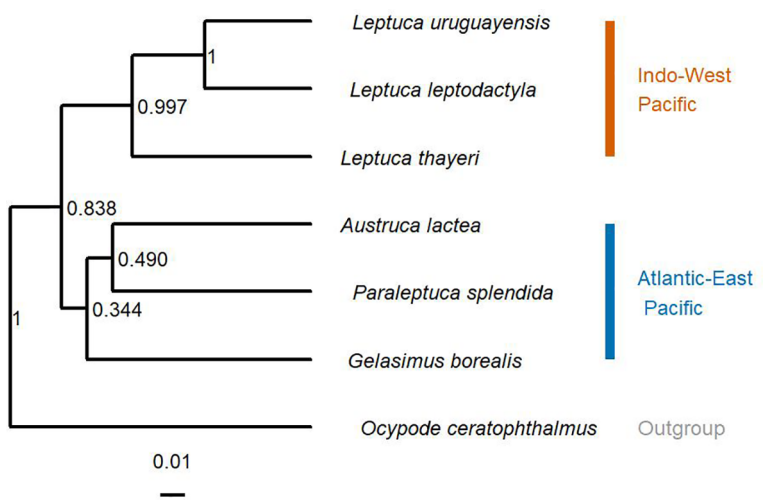

FIGURE 3 | Phylogenetic relationships among species of fiddler crabs from the Atlantic-East Pacific and Indo-West Pacific. *Ocypode ceratophthalmus* is an outgroup. Node numbers are the posterior probability from the Bayesian analysis.

Cardiac Function

There was no significant difference in size when comparing animals of the same sex and species in the heart rate and body temperature experiments (data non-normally distributed, Shapiro-Wilks, $p < 0.05$; and non-homogeneous, Levene Test, $p < 0.05$; Mann-Whitney comparisons, $p > 0.05$).

There was a significant effect of the interaction between the factors cluster and habitat on OPT, ABT and LT among the model species (**Tables S7, S8**). The OPT was similar among the species within clusters and habitat types although *L. uruguayensis* had a lower OPT in comparison to *A. lactea* and *G. borealis* (**Figure 4A**). *Leptuca uruguayensis* had lower ABT and LT compared to the other model species (**Figure 4B**). *Austruca lactea*, had a higher LT compared to *G. borealis*, the lower intertidal species in Hong Kong (**Figure 4C**). Furthermore, there was a significant difference in ABT and LT between sexes (**Table S7**). The model also shows higher LT and ABT in males compared to females (**Figure 5**).

Thermal safety margins were negative for crabs inhabiting exposed areas (**Figure 6**; **Table S8**). *Leptuca leptodactyla*, which inhabits the mid-intertidal zone in the AEP, had the lowest TSM, followed by *G. borealis* and *A. lactea* that occupy the low- and mid-intertidal zone, respectively, in the IWP (**Figure 6**). In the AEP, *L. thayeri*, which occupy the low-intertidal shores, had the highest TSM, followed by *P. splendida* and *L. uruguayensis* that

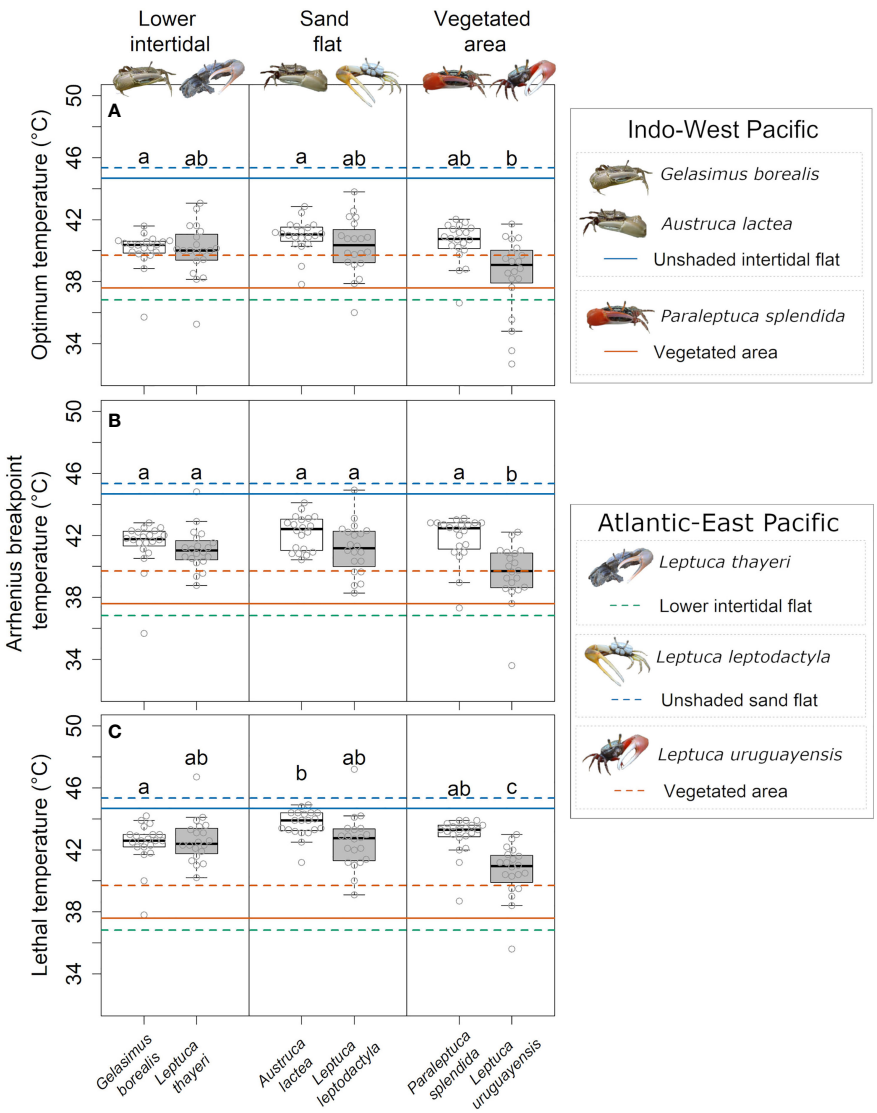

FIGURE 4 | Comparison of: **(A)** Optimum temperature (OPT); **(B)** Arrhenius Breakpoint Temperature (ABT); and **(C)** Lethal temperature (LT) among the model species across habitats. Boxplots show the median, 25th and 75th percentiles, and whiskers are 1.5 times the spread beyond the hinge. White boxes represent Hong Kong species, grey boxes represent Brazilian ones. Circles are the raw data points. Dashed lines and continuous lines represent the maximum temperatures experienced by the model species at the collection sites in Brazil and Hong Kong, respectively. Different letters represent significant differences among species (PERMANOVA pairwise, $p < 0.05$).

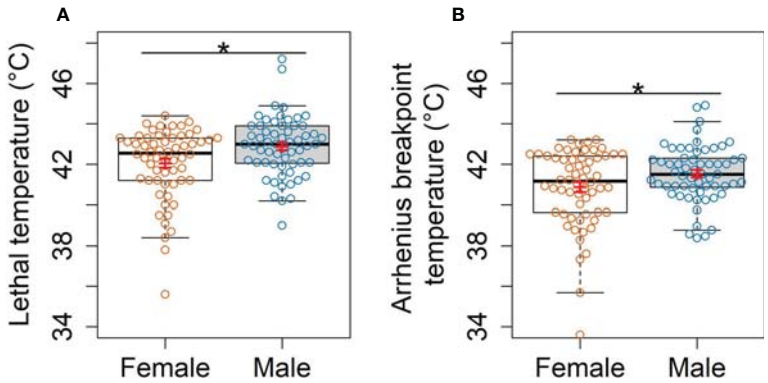

FIGURE 5 | Comparison of: **(A)** Lethal temperature and **(B)** Arrhenius Breakpoint temperature between male and female fiddler crabs. Boxplots show the median, 25th and 75th percentiles, and whiskers are 1.5 times the spread beyond the hinge. White and grey boxes represent females and males, respectively. Orange and blue circles characterize raw data points for females and males, respectively. Red lines show mean and standard errors. Asterisks denote significant differences (PERMANOVA, $p < 0.05$).

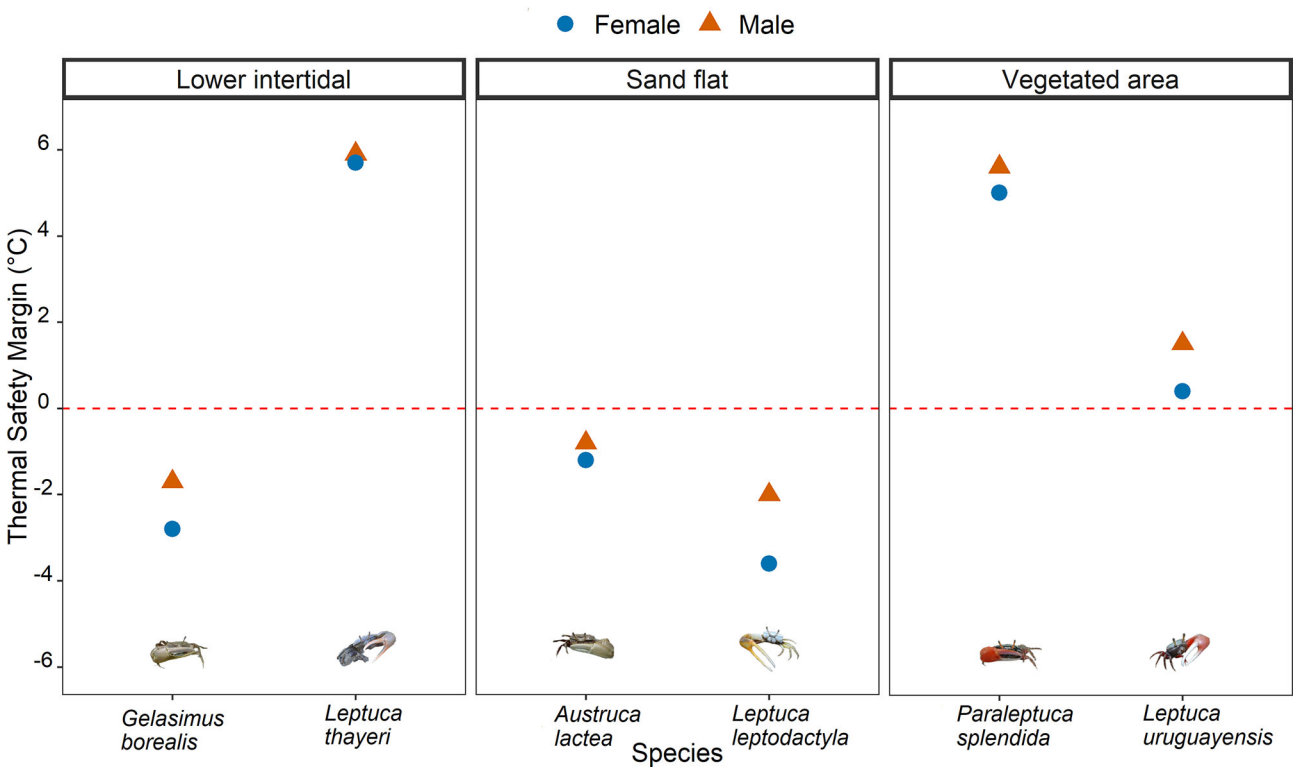

FIGURE 6 | Thermal safety margins of each species across habitats in the present study. Females are represented by blue circles and males are represented by orange triangles. Species on the left of each facet represent the Indo-West Pacific, species on the right of each facet represent the Atlantic East Pacific.

both inhabit vegetated areas at the high-intertidal shore in the IWP and AEP, respectively. Furthermore, females showed consistently lower TSM's for the majority of studied species.

Metabolic Rate

There was a significant effect of the interaction between temperature, cluster, and habitat on MO_2 (**Table S9**). *Leptuca uruguayensis*, showed the highest MO_2, followed by *L. leptodactyla*. These species had higher rates of MO_2 compared to crabs from Hong Kong (**Figure 7**). There was also an effect of the interaction between cluster, habitat, and sex on MO_2 (**Table S9**). The MO_2 differed between males and females in all species (*post-hoc* PERMANOVA, $p < 0.05$). The fitted TPCs for the MO_2 showed lower activation energy in both male and female *L.*

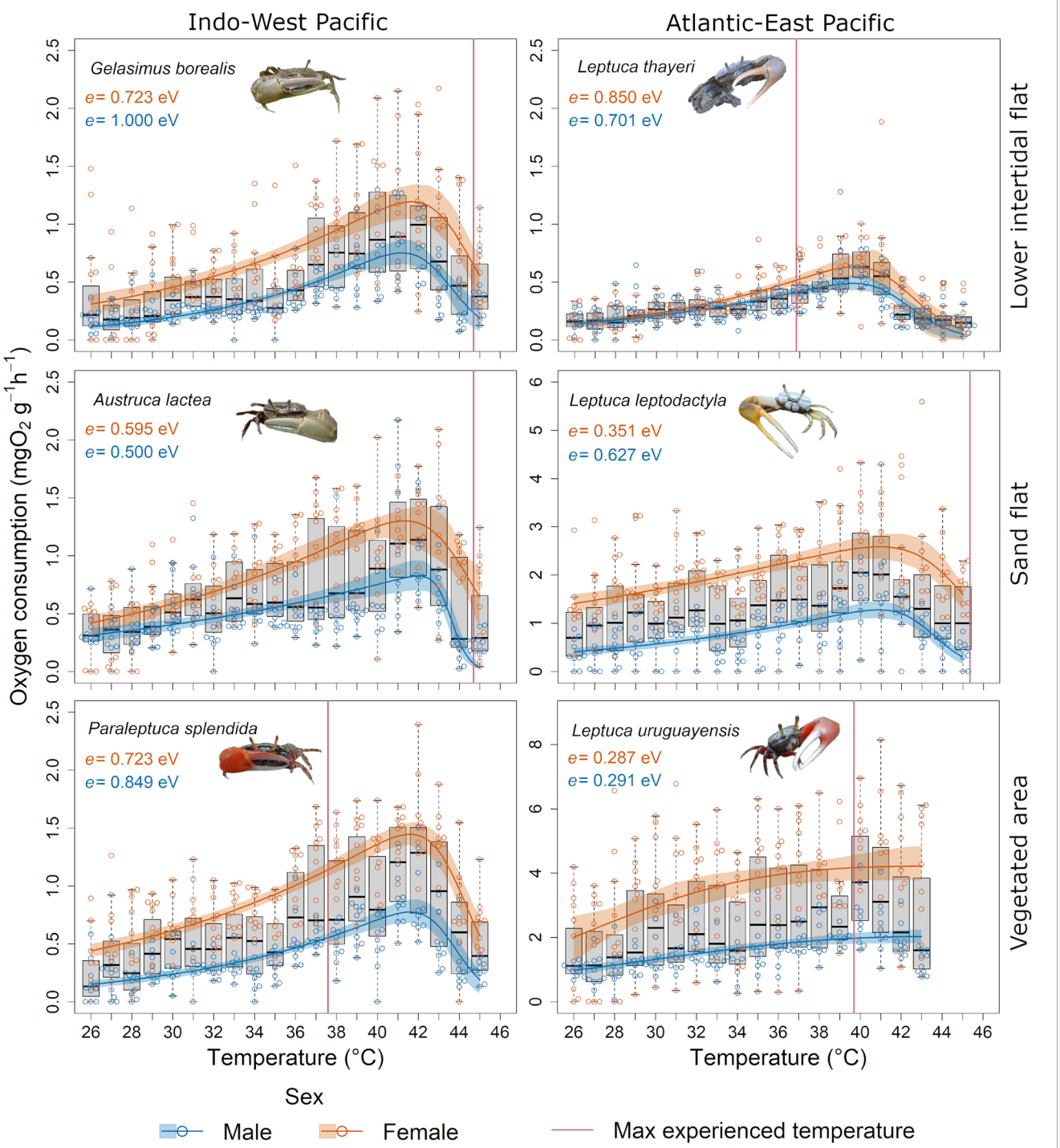

FIGURE 7 | Thermal performance curves and activation energy (e) for the oxygen consumption of the studied fiddler crab species. Boxplots show the median, 25th and 75th percentiles, and whiskers are 1.5 times the spread beyond the hinge of MO_2 for each species. Orange and blue circles characterize raw data points for females and males, respectively. Orange and blue lines characterize raw data points for females and males, respectively. The shading represents the bootstrapped 95% confidence interval around the thermal performance curves.

uruguayensis indicating a higher temperature sensitivity in this species.

DISCUSSION

As a transitional zone between the land and the sea, intertidal habitats are subjected to strong thermal variations and represent a challenging environment that requires adaptations to withstand variable milieus and high thermal stress. Here, using six species of fiddler crabs inhabiting similar thermal habitats along a very wide geographical range, we showed that primarily air-breathing intertidal organisms are indeed adapted to cope with high temperatures. Additionally, we showed that gross latitudinal temperature gradients may in part explain the thermal vulnerability of intertidal species. This macrophysiological conformity is signified by the lower thermal tolerance of species distributed in the subtropics when compared to those in the tropics, even when colonizing similar habitats. More importantly, our data demonstrate that species living in areas where the temperatures exceed their thermal limits are still thriving, casting doubt over the universal use of TSM as predictors for thermal vulnerability in ectotherms, at least for intertidal habitats. We also found differences in thermal sensitivity between sexes of fiddler crabs. This notion strongly suggests refraining from generalizing species-specific patterns of thermal sensitivity based solely on data related to one sex or a single ontogenetic stage.

The physiological performance of ectotherms is governed by temperature dependent processes that either enhance or impair metabolic functions (Brown et al., 2004). Species occupying different habitats in this study had similar thermal limits, indicating that the temperatures experienced by fiddler crabs in their habitats alone do not satisfactorily explain their thermal performance. The high thermal limits of the species inhabiting the exposed area of the shore (such as *A. lactea*, *G. borealis* and *L. leptodactyla*) seem congruent with the Climate Extremes Hypothesis, which postulates that thermal limits are set by the temperature extremes that organisms face in their specific habitats (Pither, 2003; Sunday et al., 2019). The conservation of thermal limits in ectotherm evolutionary history, however, could explain the high thermal tolerance showed by *P. splendida* and *L. thayeri*, despite occupying areas where the upper limit temperatures are lower (Hoffmann et al., 2013; Gutiérrez-Pesquera et al., 2016).

Intertidal crabs derived from marine ancestors maintain functional gills, which enable gaseous exchanges in water (Burggren, 1988). However, fiddler crabs have also evolved an efficient mechanism to breath in air through the development of a functional lung within the gill chambers (Bliss, 1968; Días and Rodríguez, 1977; Farrelly and Greenaway, 1993; Farrelly and Greenaway, 1994; Paoli et al., 2015). Oxygen is less limiting, and gaseous exchange less costly, in air than in water (Giomi et al., 2014), regardless of temperature. Thus, at high temperatures, air-breathing intertidal ectotherms are less constrained by oxygen limitation and show wider thermal tolerances than water breathing ectotherms (Fusi et al., 2016). The broader thermal window allows the maintenance of the animals' aerobic scope at higher temperatures (Fusi et al., 2016) and it is probably a major factor allowing the high thermal tolerance of air-breathing intertidal ectotherms.

The acclimatization of our model crabs to their localized thermal extremes is demonstrated by the variability of their TSM, which was independent of their latitudinal ranges (see, for example, *L. leptodactyla* vs. *L. thayeri* and *A. lactea* vs. *P. splendida*). Even at negative TSM, the Brazilian species with a more tropical latitudinal range colonizing bare intertidal flats actively thrived in thermally stressful conditions, even reproducing during the warmest months of the year (Costa et al., 2006; Bezerra and Matthews-Cascon, 2007; Masunari, 2012). This indicates that TSM; usually calculated by subtracting a proxy for upper thermal limit from a constant metric of experienced temperatures (Sunday et al., 2014; Marshall et al., 2015; Rezende and Bozinovic, 2019; Vinagre et al., 2019; Dahlke et al., 2020), although useful to predict the vulnerability of species to temperature increases, may fail to account for relevant factors involved in thermal tolerance. Moreover, the methods used to estimate TSM are often inconsistent throughout the literature and in many instances ignore local thermal heterogeneity. Additionally, ectotherms often live at supra-lethal temperatures, and behavioral thermoregulation is an essential trait in these animals (Sunday et al., 2014). Fiddler crabs, for example, can thermoregulate by retreating to their burrows (Munguia et al., 2017). Our data confirm that the full understanding of the thermal vulnerability of a particular group of organisms requires a deep knowledge on their behavioral and physiological adaptations, as well as information on possible thermal refugia.

The comparison of species belonging to separate, but closely related, clades revealed similar thermal limits between the two taxa. Our observations do not support the hypothesis that the phylogenetic distance and evolutionary history of fiddler crabs led to different thermal adaptations. Our data, instead, show that the thermal vulnerability of species may not only be related to the experienced temperatures, but also to their latitudinal distribution, since the only truly subtropical species we tested, *L. uruguayensis*, showed significantly lower thermal limits than the other species tested. This indicates that *L. uruguayensis* populations inhabiting the lower latitudinal ranges of its distribution are highly vulnerable to extreme temperature events. Accordingly, this species is more prone to latitudinal shifts or local extinctions at the lower edges of its latitudinal distribution (Thomas, 2010; Hoffmann et al., 2013; Kingsolver et al., 2013). Their populations are also vulnerable to invasions by low latitude species due to temperature increases (Murphy, 2020). Poleward distribution shifts are already occurring in Gelasiminae species (e.g. Perry et al., 2005; Castiglioni et al., 2010; Thurman et al., 2013; Johnson, 2014; Arakaki et al., 2020), and the invasion of low latitude species is projected to affect native populations, due to the very similar ecological characteristics shared by fiddler crab species.

Of course, future latitudinal distribution of these fiddler crabs, and local extinction events of their populations, will not be determined by their thermal vulnerability alone. Being part of the mangrove associated fauna, their vulnerability to the ongoing climatic changes is inherently linked to the resilience of such intertidal forests to global warming and ocean acidification.

Mangrove ecosystems showed to be rather resilient to the ongoing decrease in pH of coastal waters (Alongi, 2008) and their resident fauna proved to be well adapted to the periodic events of hypoxia regularly affecting this habitat, mainly though the evolution of semi-terrestrial adaptations (Fusi et al., 2015; Fusi et al., 2017). At present, the most impacting consequence of climate change for mangrove ecosystems proved to be sea level rise (Gilman et al., 2008; Ellison, 2012), which will also strongly affect the microhabitat of the fiddler crab species we studied. A more holistic approach, taking into account the influence of climate change on their micro-habitat and their food sources is thus necessary to model future distribution of these crabs.

In the present study, sex-specific responses to temperature increases were evident, with females showing greater MO_2 than males. These metabolic differences can be both a consequence of the strong sexual dimorphism of fiddler crabs and of the differential sex-related energy allocation in reproduction common in most animals. During the reproductive season, female fiddler crabs produce large quantities of eggs (Yamaguchi, 2001; Koch et al., 2005; Litulo, 2005; Castiglioni et al., 2007), at energetic costs higher than the ones involved in sperm production (Hartnoll, 2006; Rennie et al., 2008). A large allocation of energy on reproduction reduces the available aerobic scope of organisms (Sokolova, 2013) and it is assumed to reduce their thermal window (Pörtner and Farrell, 2008; Vorsatz et al., 2021a). If female fiddler crabs are more thermally sensitive, they may be the first to succumb to temperature increases, thereby reducing the viability and resilience of populations. Similar results have been observed in spawning fishes (Dahlke et al., 2020) and mangrove crabs (Vorsatz et al., 2021a), suggesting that reproductively active females may constitute an ontogenetic thermal bottleneck in climate change scenarios.

Our data confirmed that bimodal-breathing ectotherms are able to cope with ambient temperatures that regularly reach levels above their thermal limits, showing the efficiency of their thermoregulatory and respiratory mechanisms. These mechanisms allow ectotherms to conform and acclimatize to the conditions they experience, thus supporting the Climate Extremes Hypothesis (Pither, 2003; Bozinovic et al., 2011; Sunday et al., 2019) whereby an ectotherms' thermal tolerance reflects the thermal extremes they face in their habitat along their geographical distribution. Differences in the thermal vulnerability between males and female, however, might also be an important factor in predicting species distributions and the resilience of populations of ectotherms to temperature rises. Indeed, reliable models on the impact of global warming on intertidal species distribution and resilience should include data on both sexes, reproductive biology and different ontogenetic stages, as well as information on local thermal environment. Based on our data, we advocate for the inclusion of physiological traits such as breathing mode and sex-related differences in energy allocation to reproduction in general models aimed to describe and forecast the relationship between thermal sensitivity and the present and future distribution of intertidal species.

DATA AVAILABILITY STATEMENT

All data needed to support the conclusions are present in the article/**Supplementary Material**. Further inquiries can be directed to the corresponding author.

AUTHOR CONTRIBUTIONS

PJ and SC conceived the original idea and designed the methodology. PJ collected the data. PJ and SC analyzed the data. PJ and LV wrote the manuscript. SC and TC revised and edited the manuscript. SC and TC provided funding for the study. All authors contributed critically to the drafts and gave final approval for publication.

FUNDING

This study was funded by the Travel Support for Research Postgraduate Students for International Academic Training/ Research Activities from The University of Hong Kong, by the Faculty of Science Seed fund #104005887.088562.26000.301.01, from the University of Hong Kong, and by the São Paulo Research Foundation (FAPESP) (Costa, TM - #2015/50300-6).

ACKNOWLEDGMENTS

We thank the members of the Integrated Mangrove and Ecology lab of the University of Hong Kong (IMEco Lab) of the Laboratory of Ecology and Animal Behavior of the state University of Sao Paulo (LABECOM) for the field work assistance. We also thank the two reviewers for comments that helped improve the quality of the manuscript.

SUPPLEMENTARY MATERIAL

The Supplementary Material for this article can be found online at: https://www.frontiersin.org/articles/10.3389/fmars.2022.858280/full#supplementary-material

REFERENCES

Abadi, S., Azouri, D., Pupko, T., and Mayrose, I. (2019). Model Selection may Not be a Mandatory Step for Phylogeny Reconstruction. *Nat. Commun.* 10, 934. doi: 10.1038/s41467-019-08822-w

Allen, B. J., and Levinton, J. S. (2014). Sexual Selection and the Physiological Consequences of Habitat Choice by a Fiddler Crab. *Oecologia* 176, 25–34. doi: 10.1007/s00442-014-3002-y

Alongi, D. M. (1990). Community Dynamics of Free-Living Nematodes in Some Tropical Mangrove and Sandflat Habitats. *Bull. Marine Sci.* 46, 358–373.

Alongi, D. M. (2008). Mangrove Forests: Resilience, Protection From Tsunamis, and Responses to Global Climate Change. *Estuarine Coastal Shelf Sci.* 76, 1–13. doi: 10.1016/j.ecss.2007.08.024

Anderson, M. J., and Walsh, D. C. I. (2013). PERMANOVA, ANOSIM, and the Mantel Test in the Face of Heterogeneous Dispersions: What Null Hypothesis Are You Testing? *Ecol. Monogr.* 83, 557–574. doi: 10.1890/12-2010.1

Arakaki, J. Y., Grande, F. R., Arvigo, A. L., Pardo, J. C. F., Fogo, B. R., Sanches, F. H. C., et al. (2020). Battle of the Borders: Is a Range-Extending Fiddler Crab Affecting the Spatial Niche of a Congener Species? *J. Exp. Marine Biol. Ecol.* 532, 151445. doi: 10.1016/j.jembe.2020.151445

Baeza, J. A., and Fernández, M. (2002). Active Brood Care in *Cancer Setosus* (Crustacea: Decapoda): The Relationship Between Female Behaviour, Embryo Oxygen Consumption and the Cost of Brooding. *Funct. Ecol.* 16, 241–251. doi: 10.1046/j.1365-2435.2002.00616.x

Beck, M. W. (1998). Comparison of the Measurement and Effects of Habitat Structure on Gastropods in Rocky Intertidal and Mangrove Habitats. *Marine Ecol. Prog. Ser.* 169, 165–178. doi: 10.3354/meps169165

Bennett, J. M., Sunday, J., Calosi, P., Villalobos, F., Martínez, B., Molina-Venegas, R., et al. (2021). The Evolution of Critical Thermal Limits of Life on Earth. *Nat. Commun.* 12, 1–9. doi: 10.1038/s41467-021-21263-8

Bezerra, L. E. A., and Matthews-Cascon, H. (2007). Population and Reproductive Biology of the Fiddler Crab *Uca Thayeri* Rathbu(Crustacea: Ocypodidae) in a Tropical Mangrove From Northeast Brazil. *Acta Oecologica* 31, 251–258. doi: 10.1016/j.actao.2006.10.003

Bliss, D. E. (1968). Transition From Water to Land in Decapod Crustaceans. *Integr. Comp. Biol.* 8, 355–392. doi: 10.1093/icb/8.3.355

Bozinovic, F., Calosi, P., and Spicer, J. I. (2011). Physiological Correlates of Geographic Range in Animals. *Annu. Rev. Ecol. Evol. Systematics* 42, 155–179. doi: 10.1146/annurev-ecolsys-102710-145055

Brayard, A., Escarguel, G., and Bucher, H. (2005). Latitudinal Gradient of Taxonomic Richness: Combined Outcome of Temperature and Geographic Mid-Domains Effects? *J. Zoological Systematics Evol. Res.* 43, 178–188. doi: 10.1111/j.1439-0469.2005.00311.178

Brown, J. H., Gillooly, J. F., Allen, A. P., Savage, V. M., and West, G. B. (2004). Toward a Metabolic Theory of Ecology. *Ecology* 85, 1771–1789. doi: 10.1890/03-9000

Burggren, W., and Mcmahon, B. R. (1988). *Biology of the Land Crabs* (Cambridge: Cambridge University Press). doi: 10.1017/CBO9780511753428

Burggren, W. W. (1992). Respiration and Circulation in Land Crabs: Novel Variations on the Marine Design. *Am. Zoologist* 32, 417–427. doi: 10.1093/icb/32.3.417

Burggren, W. W., Pinder, A., McMahon, B., Doyle, M., and Wheatly, M. (1990). Heart Rate and Hemolymph Pressure Responses to Hemolymph Volume Changes in the Land Crab *Cardisoma Guanhumi*: Evidence for "Baroreflex" Regulation. *Physiol. Zool.* 63, 167–181. doi: 10.1086/physzool.63.1.30158159

Burke, E. M. (1979). Aerobic and Anaerobic Metabolism During Activity and Hypoxia in Two Species of Intertidal Crabs. *Biol. Bull.* 156, 157–168. doi: 10.2307/1541040

Burnett, N. P., Seabra, R., de Pirro, M., Wethey, D. S., Woodin, S. A., Helmuth, B., et al. (2013). An Improved Noninvasive Method for Measuring Heartbeat of Intertidal Animals. *Limnol. Oceanography: Methods* 11, 91–100. doi: 10.4319/Lom.2013.11.91

Castiglioni, D., da, S., Almeida, A. O., and Bezerra, L. E. A. (2010). More Common Than Reported: Range Extension, Size–Frequency and Sex-Ratio of *Uca* (*Minuca*) *Victoriana* (Crustacea: Ocypodidae) in Tropical Mangroves, Brazil. *Marine Biodiversity Records* 3, 1–7. doi: 10.1017/S1755267210000874

Castiglioni, D., da, S., Negreiros-Fransozo, M. L., and Cardoso, R. C. F. (2007). Breeding Season and Molt Cycle of the Fiddler Crab *Uca Rapax* (Brachyura, Ocypodidae) in a Subtropical Estuary, Brazil, South America. *Gulf Caribbean Res.* 19, 11–20. doi: 10.18785/gcr.1901.02

Chou, C. C., Perez, D. M., Johns, S., Gardner, R., Kerr, K. A., Head, M. L., et al. (2019). Staying Cool: The Importance of Shade Availability for Tropical Ectotherms. *Behav. Ecol. Sociobiol.* 73, 106. doi: 10.1007/s00265-019-2721-9

Clark, K., Karsch-Mizrachi, I., Lipman, D. J., Ostell, J., and Sayers, E. W. (2016). Genbank. *Nucleic Acids Res.* 44, D67–D72. doi: 10.1093/nar/gkv1276

Colpo, K. D., and López-greco, L. S. (2018). Dynamics of Energy Reserves and the Cost of Reproduction in Female and Male Fiddler Crabs. *Zoology* 126, 11–19. doi: 10.1016/j.zool.2018.01.004

Costa, T. M., Silva, S. M. J., and Negreiros-Fransozo, M. L. (2006). Reproductive Pattern Comparison of *Uca Thayeri* Rathbuand U. Uruguayensis Nobil (Crustacea, Decapoda, Ocypodidae). *Braz. Arch. Biol. Technol.* 49, 117–123. doi: 10.1590/S1516-89132006000100014

Crane, J. (1975). *Fiddler Crabs of the World Ocypodidae: Genus* (Uca. Princeton, New Jersey: Princeton University Press). doi: 10.1016/0003-3472(78)90130-6

Dahlke, F. T., Wohlrab, S., Butzin, M., and Pörtner, H.-O. (2020). Thermal Bottlenecks in the Life Cycle Define Climate Vulnerability of Fish. *Science* 369, 65–70. doi: 10.1126/science.aaz3658

Darnell, M. Z., Fowler, K. K., and Munguia, P. (2013). Sex-Specific Thermal Constraints on Fiddler Crab Behavior. *Behav. Ecol.* 24, 997–1003. doi: 10.1093/beheco/art006

Darnell, M. Z., and Munguia, P. (2011). Thermoregulation as an Alternate Function of the Sexually Dimorphic Fiddler Crab Claw. *Am. Nat.* 178, 419–428. doi: 10.1086/661239

Darnell, M. Z., Nicholson, H. S., and Munguia, P. (2015). Thermal Ecology of the Fiddler Crab *Uca Panacea*: Thermal Constraints and Organismal Responses. *J. Thermal Biol.* 52, 157–165. doi: 10.1016/j.jtherbio.2015.06.004

Denny, M. W., Dowd, W. W., Bilir, L., and Mach, K. J. (2011). Spreading the Risk: Small-Scale Body Temperature Variation Among Intertidal Organisms and Its Implications for Species Persistence. *J. Exp. Marine Biol. Ecol.* 400, 175–190. doi: 10.1016/j.jembe.2011.02.006

Denny, M. W., and Paine, R. T. (1998). Celestial Mechanics, Sea-Level Changes, and Intertidal Ecology. *Biol. Bull.* 194, 108–115. doi: 10.2307/1543040

Depledge, M. H., and Andersen, B. B. (1990). A Computer-Aided Physiological Monitoring-System for Continuous, Long-Term Recording of Cardiac Activity in Selected Invertebrates. *Comp. Biochem. Physiol.* 96A, 473–477. doi: 10.1016/0300-9629(90)90664-E

Deutsch, C. A., Tewksbury, J. J., Huey, R. B., Sheldon, K. S., Ghalambor, C. K., Haak, D. C., et al. (2008). Impacts of Climate Warming on Terrestrial Ectotherms Across Latitude. *Proc. Natl. Acad. Sci. U. S. A.* 105, 6668–6672. doi: 10.1073/pnas.0709472105

Días, H., and Rodríguez, G. (1977). The Branchial Chamber in Terrestrial Crabs: A Comparative Study. *Biol. Bull.* 153, 485–504. doi: 10.2307/1540602

Diele, K., Koch, V., Abrunhosa, F. A., de Farias Lima, J., de Jesus de Brito Simith, D., Lima, J. D. F., et al. (2010). "The Brachyuran Crab Community of the Caete Estuary, North Brazil: Species Richness, Zonation and Abundance," in *Mangrove Dynamics and Management in North Brazil*. Eds. U. Saint-Paul and H. Schneider (Berlin: Springer-Verlag Berlin Heidelberg), 251–263. doi: 10.1007/978-3-642-13457-9

Drummond, A. J., Ho, S. Y. W., Phillips, M. J., and Rambaut, A. (2006). Relaxed Phylogenetics and Dating With Confidence. *PloS Biol.* 4, 699–710. doi: 10.1371/journal.pbio.0040088

Drummond, A. J., and Rambaut, A. (2007). BEAST: Bayesian Evolutionary Analysis by Sampling Trees. *BMC Evol. Biol.* 7, 1–8. doi: 10.1186/1471-2148-7-214

Edgar, R. C. (2004). MUSCLE: Multiple Sequence Alignment With High Accuracy and High Throughput. *Nucleic Acids Res.* 32, 1792–1797. doi: 10.1093/nar/gkh340

Ellison, J. C. (2012). "Mangrove Swamps: Causes of Decline and Mortality," in *Forest Decline: Causes and Impacts*. Ed. J. A. Jenkins (New York: Nova Science Publishers), 39–68.

Faria, S. C., Provete, D. B., Thurman, C. L., and Mcnamara, J. C. (2017). Phylogenetic Patterns and the Adaptive Evolution of Osmoregulation in Fiddler Crabs (Brachyura, *Uca*). *PloS One* 2, 1–19. doi: 10.1371/journal.pone.0171870

Farrelly, C. A., and Greenaway, P. (1993). Land Crabs With Smooth Lungs: Grapsidae, Gecarcinidae, and Sundathelphusidae Ultrastructure and Vasculature. *J. Morphol.* 215, 245–260. doi: 10.1002/jmor.1052150306

Farrelly, C. A., and Greenaway, P. (1994). Gas Exchange Through the Lungs and Gills in Air-Breathing Crabs. *J. Exp. Biol.* 187, 113–130. doi: 10.1242/jeb.187.1.113

Fernández, M., Bock, C., and Pörtner, H.-O. (2000). The Cost of Being a Caring Mother: The Ignored Factor in the Reproduction of Marine Invertebrates. *Ecol. Lett.* 3, 487–494. doi: 10.1046/j.1461-0248.2000.00172.x

Finke, G. R., Navarrete, S. A., and Bozinovic, F. (2007). Tidal Regimes of Temperate Coasts and Their Influences on Aerial Exposure for Intertidal Organisms. *Marine Ecol. Prog. Ser.* 343, 57–62. doi: 10.3354/meps06918

Fusi, M., Babbini, S., Giomi, F., Fratini, S., Daniele, F. D., Christopher, D., et al. (2017). Thermal Sensitivity of the Crab *Neosarmatium Africanum* in Tropical and Temperate Mangroves on the East Coast of Africa. *Hydrobiologia* 803, 251–263. doi: 10.1007/s10750-017-3151-1

Fusi, M., Cannicci, S., Daffonchio, D., Mostert, B., Pörtner, H.-O., and Giomi, F. (2016). The Trade-Off Between Heat Tolerance and Metabolic Cost Drives the Bimodal Life Strategy at the Air-Water Interface. *Sci. Rep.* 6, 19158. doi: 10.1038/srep19158

Fusi, M., Giomi, F., Babbini, S., Daffonchio, D., Mcquaid, C. D., Porri, F., et al. (2015). Thermal Specialization Across Large Geographical Scales Predicts the Resilience of Mangrove Crab Populations to Global Warming. *Oikos* 124, 784–795. doi: 10.1111/oik.01757

Gaston, K. J., Chown, S. L., Calosi, P., Bernardo, J., Bilton, D. T., Clarke, A., et al. (2009). Macrophysiology: A Conceptual Reunification. *Am. Nat.* 174, 595–612. doi: 10.1086/605982

Gernhard, T. (2008). The Conditioned Reconstructed Process. *J. Theor. Biol.* 253, 769–778. doi: 10.1016/j.jtbi.2008.04.005

Gilman, E. L., Ellison, J., Duke, N. C., and Field, C. (2008). Threats to Mangroves From Climate Change and Adaptation Options: A Review. *Aquat. Bot.* 89, 237–250. doi: 10.1016/j.aquabot.2007.12.009

Giomi, F., Fusi, M., Barausse, A., Mostert, B., Pörtner, H.-O., and Cannicci, S. (2014). Improved Heat Tolerance in Air Drives the Recurrent Evolution of Air-Breathing. *Proc. R. Soc. B* 281, 20132927. doi: 10.1098/rspb.2013.2927

Graham, J. B. (1997). *Air-Breathing Fishes. 1st Ed* (London: Academic Press). doi: 10.1016/B978-0-12-294860-2.X5000-4

Guderley, H., and Pörtner, H. O. (2010). Metabolic Power Budgeting and Adaptive Strategies in Zoology: Examples From Scallops and Fish. *Can. J. Zool.* 88, 753–763. doi: 10.1139/Z10-039

Gutiérrez-Pesquera, L. M., Tejedo, M., Olalla-Tárraga, M. A., Duarte, H., Nicieza, A., and Solé, M. (2016). Testing the Climate Variability Hypothesis in Thermal Tolerance Limits of Tropical and Temperate Tadpoles. *J. Biogeography* 43, 1166–1178. doi: 10.1111/jbi.12700

Harley, C. D. G., Denny, M. W., MacH, K. J., and Miller, L. P. (2009). Thermal Stress and Morphological Adaptations in Limpets. *Funct. Ecol.* 23, 292–301. doi: 10.1111/j.1365-2435.2008.01496.x

Hartnoll, R. G. (2006). Reproductive Investment in Brachyura. *Hydrobiologia* 557, 31–40. doi: 10.1007/s10750-005-9305-6

Helmuth, B. (2002). How do We Measure the Environment? Linking Intertidal Thermal Physiology and Ecology Through Biophysics. *Integr. Comp. Biol.* 42, 837–845. doi: 10.1093/icb/42.4.837

Helmuth, B., Broitman, B. R., Blanchette, C., Gilman, S., Halpin, P., Harley, C. D., et al. (2006a). Mosaic Patterns of Thermal Stress in the Rocky Intertidal Zone: Implications for Climate Change. *Ecol. Monogr.* 76, 461–479. doi: 10.1890/0012-9615(2006)076[0461:MPOTSI]2.0.CO;2

Helmuth, B., Harley, C. D. G., Halpin, P. M., O'Donnell, M., Hofmann, G. E., and Blanchette, C. a (2002). Climate Change and Latitudinal Patterns of Intertidal Thermal Stress. *Science* 298, 1015–1017. doi: 10.1126/science.1076814

Helmuth, B. S. T. T., and Hofmann, G. E. (2001). Microhabitats, Thermal Heterogeneity, and Patterns of Physiological Stress in the Rocky Intertidal Zone. *Biol. Bull.* 201, 374–384. doi: 10.2307/1543615

Helmuth, B., Mieszkowska, N., Moore, P., and Hawkins, S. J. (2006b). Living on the Edge of Two Worlds: Forecasting the Responses of Rocky Intertidal Ecosystems to Climate Change. *Annu. Rev. Ecol. Systematics* 37, 373–404. doi: 10.2307/annurev.ecolsys.37.091305.30000015

Henry, R. P. (1994). Morphological, Behavioral, and Physiological Characterization of Bimodal Breathing Crustaceans. *Integr. Comp. Biol.* 34, 205–215. doi: 10.1093/icb/34.2.205

Hoffmann, A. A., Chown, S. L., and Clusella-Trullas, S. (2013). Upper Thermal Limits in Terrestrial Ectotherms: How Constrained Are They? *Funct. Ecol.* 27, 934–949. doi: 10.1111/j.1365-2435.2012.02036.x

Holm, S. (1979). A Simple Sequentially Rejective Multiple Test Procedure. *Scandinavian J. Stat* 6, 65–70.

Jahnke, M., Moknes, P., le Moan, A., Martens, G. A., and Jonsson, P. R. (2022). Seascape Genomics Identify Adaptive Barriers Correlated to Tidal Amplitude in the Shore Crab *Carcinus Maenas*. *Mol. Ecol.* 1–15. doi: 10.1111/mec.16371

Johnson, D. S. (2014). Fiddler on the Roof: A Northern Range Extension for the Marsh Fiddler Crab *Uca Pugnax*. *J. Crustacean Biol.* 34, 671–673. doi: 10.1163/1937240X-00002268

Kingsolver, J. G., Diamond, S. E., and Buckley, L. B. (2013). Heat Stress and the Fitness Consequences of Climate Change for Terrestrial Ectotherms. *Funct. Ecol.* 27, 1415–1423. doi: 10.1111/1365-2435.12145

Koch, V., Wolff, M., and Diele, K. (2005). Comparative Population Dynamics of Four Fiddler Crabs (Ocypodidae, Genus *Uca*) From a North Brazilian Mangrove Ecosystem. *Marine Ecol. Prog. Ser.* 291, 177–188. doi: 10.3354/meps291177

Kontopoulos, D. G., García-Carreras, B., Sal, S., Smith, T. P., and Pawar, S. (2018). Use and Misuse of Temperature Normalisation in Meta-Analyses of Thermal Responses of Biological Traits. *PeerJ* 2018, 1–18. doi: 10.7717/peerj.4363

Kostina, E. E., Tsurpalo, A. P., and Gulbin, V. v. (2016). "The Species Composition and Distribution of Macrobenthic Communities in the Intertidal Zone of Vietnam," in *Biodiversity of the Western Part of the South China Sea*, vol. 502. Eds. A. v Adrianov and K. A. Lutaenko (Vladivostok: Dalnauka).

Kumar, S., Stecher, G., Li, M., Knyaz, C., and Tamura, K. (2018). Mega X: Molecular Evolutionary Genetics Analysis Across Computing Platforms. *Mol. Biol. Evol.* 35, 1547–1549. doi: 10.1093/molbev/msy096

Kwok, W. P. W., and Tang, W. (2006). Fiddler Crabs in Hong Kong – An Overview. *Hong Kong Biodiversity* 12, 1–7.

Levinton, J. S., Judge, M. L., and Kurdziel, J. P. (1995). Functional Differences Between the Major and Minor Claws of Fiddler Crabs (*Uca*, Family Ocypodidae, Order Decapoda, Subphylum Crustacea): A Result of Selection or Developmental Constraint? *J. Exp. Marine Biol. Ecol.* 193, 147–160. doi: 10.1016/0022-0981(95)00115-8

Levinton, J. S., Volkenborn, N., Gurr, S., Correal, K., Villacres, S., Seabra, R., et al. (2020). Temperature-Related Heart Rate in Water and Air and a Comparison to Other Temperature-Related Measures of Performance in the Fiddler Crab *Leptuca Pugilator* (Bosc 1802). *J. Thermal Biol.* 88, 102502. doi: 10.1016/j.jtherbio.2019.102502

Lin, H.-C., Su, Y., and Su, S.-H. (2002). A Comparative Study of Osmoregulation in Four Fiddler Crabs (Ocypodidae: *Uca*). *Zoological Sci.* 19, 643–650. doi: 10.2108/zsj.19.643

Litulo, C. (2005). Population Structure and Reproductive Biology of the Fiddler Crab *Uca Urvillei* (Brachyura: Ocypodidae) in Maputo Bay (South Mozambique). *J. Natural History* 39, 2307–2318. doi: 10.1080/00222930502005688

Marshall, D. J., Dong, Y., Mcquaid, C. D., and Williams, G. A. (2011). Thermal Adaptation in the Intertidal Snail *Echinolittorina Malaccana* Contradicts Current Theory by Revealing the Crucial Roles of Resting Metabolism. *J. Exp.* 214, 3649–3657. doi: 10.1242/jeb.059899

Marshall, D. J., McQuaid, C. D., and Williams, G. A. (2010). Non-Climatic Thermal Adaptation: Implications for Species' Responses to Climate Warming. *Biol. Lett.* 6, 669–673. doi: 10.1098/rsbl.2010.0233

Marshall, D. J., Rezende, E. L., Baharuddin, N., Choi, F., and Helmuth, B. (2015). Thermal Tolerance and Climate Warming Sensitivity in Tropical Snails. *Ecol. Evol.* 5, 5905–5919. doi: 10.1002/ece3.1785

Masunari, S. (2012). Hood Construction as an Indication of the Breeding Period of the Fiddler Crab *Uca* (*Leptuca*) *Leptodactyla* Rathbu(Decapoda, Ocypodidae) From Guaratuba Bay, Southern Brazil. *Crustaceana* 85, 1153–1169. doi: 10.1163/156854012X651277

Mcmahon, R. F. (1988). Respiratory Response to Periodic Emergence in Intertidal Molluscs. *Integr. Comp. Biol.* 28, 97–114. doi: 10.1093/icb/28.1.97

Muggeo, V. M. R. (2003). Estimating Regression Models With Unknown Break-Points. *Statist. Med.* 22, 3055–3071. doi: 10.1002/sim.1545

Munguia, P., Backwell, P. R. Y., and Darnell, M. Z. (2017). Thermal Constraints on Microhabitat Selection and Mating Opportunities. *Anim. Behav.* 123, 259–265. doi: 10.1016/j.anbehav.2016.11.004

Murphy, J. T. (2020). Climate Change, Interspecific Competition, and Poleward vs. Depth Distribution Shifts: Spatial Analyses of the Eastern Bering Sea Snow and Tanner Crab (*Chionoecetes Opilio* and *C. Bairdi*). *Fisheries Res.* 223, 105417. doi: 10.1016/j.fishres.2019.105417

Padfield, D., and Matheson, G. (2020) *Nls.Multstart: Robust Non-Linear Regression Using AIC Scores*. Available at: https://cran.r-project.org/package=nls.multstart.

Padfield, D., and O'Sullivan, H. (2020) *Rtpc: Functions for Fitting Thermal Performance Curves*. Available at: http://github.com/padpadpadpad/rTPC.

Padfield, D., O'Sullivan, H., and Pawar, S. (2020). Rtpc and Nls.Multstart: A New Pipeline to Fit Thermal Performance Curves in R. *bioRxiv* 12, 16. doi: 10.1101/2020.12.16.423089

Pagel, M. (1997). Inferring Evolutionary Processes From Phylogenies. *Zool. Scripta* 26, 331–348. doi: 10.1111/j.1463-6409.1997.tb00423.x

Pagel, M. (1999). Inferring the Historical Patterns of Biological Evolution. *Nature* 401, 877–884. doi: 10.1038/44766

Paoli, F., Wirkner, C. S., and Cannicci, S. (2015). The Branchiostegal Lung of *Uca Vocans* (Decapoda: Ocypodidae): Unreported Complexity Revealed by Corrosion Casting and Microct Techniques. *Arthropod Structure Dev.* 44, 622–629. doi: 10.1016/j.asd.2015.09.006

Perry, A. L., Low, P. J., Ellis, J. R., and Reynolds, J. D. (2005). Climate Change and Distribution Shifts in Marine Fishes. *Science* 308, 1912–1915. doi: 10.1126/science.1111322

Peterson, C. H. (1991). Intertidal Invertebrates Zonation in Sand and Mud. *Am. Scientist* 79, 236–249.

Pither, J. (2003). Climate Tolerance and Interspecific Variation in Geographic Range Size. *Proc. R. Soc. B: Biol. Sci.* 270, 475–481. doi: 10.1098/rspb.2002.2275

Pörtner, H.-O. (2012). Integrating Climate-Related Stressor Effects on Marine Organisms: Unifying Principles Linking Molecule to Ecosystem-Level Changes. *Marine Ecol. Prog. Ser.* 470, 273–290. doi: 10.3354/meps10123

Pörtner, H.-O., and Farrell, A. P. (2008). Physiology and Climate Change. *Science* 322, 690–692. doi: 10.1126/science.1163156

Powers, L. W., and Cole, J. F. (1976). Temperature Variation in Fiddler Crab Microhabitats. *J. Exp. Marine Biol. Ecol.* 21, 141–157. doi: 10.1016/0022-0981(76)90035-6

Przeslawski, R., Davis, A. R., and Benkendorff, K. (2005). Synergistic Effects Associated With Climate Change and the Development of Rocky Shore Molluscs. *Global Change Biol.* 11, 515–522. doi: 10.1111/j.1365-2486.2005.00918.x

Raffaelli, D., and Hawkins, S. (1999). doi: 10.2307/1352485

Rambaut, A., Drummond, A. J., Xie, D., Baele, G., and Suchard, M. A. (2018). Posterior Summarization in Bayesian Phylogenetics Using Tracer 1.7. *Systematic Biol.* 67, 901–904. doi: 10.1093/sysbio/syy032

R core team. (2021). *R: A Language and Environment for Statistical Computing*. Available at: https://www.r-project.org/.

Rennie, M. D., Purchase, C. F., Lester, N., Collins, N. C., Shuter, B. J., and Abrams, P. A. (2008). Lazy Males? Bioenergetic Differences in Energy Acquisition and Metabolism Help to Explain Sexual Size Dimorphism in Percids. *J. Anim. Ecol.* 77, 916–926. doi: 10.1111/j.1365-2656.2008.01412.x

Revell, L. J. (2012). Phytools: An R Package for Phylogenetic Comparative Biology (and Other Things). *Methods Ecol. Evol.* 3, 217–223. doi: 10.1111/j.2041-210X.2011.00169.x

Rezende, E. L., and Bozinovic, F. (2019). Thermal Performance Across Levels of Biological Organization. *Philos. Trans. R. Soc. B: Biol. Sci.* 374, 20180549. doi: 10.1098/rstb.2018.0549

Ribeiro, P. D., Christy, J. H., Nuñez, J. D., and Iribarne, O. O. (2016). Hood Building Dynamics and Mating Mode in the Temperate Fiddler Crab *Uca Uruguayensis* Nobil. *J. Crustacean Biol.* 36, 507–514. doi: 10.1163/1937240X-00002440

Roy, K., Jablonski, D., Valentine, J. W., and Rosenberg, G. (1998). Marine Latitudinal Diversity Gradients: Tests of Causal Hypotheses. *Proc. Natl. Acad. Sci. U. S. A.* 95, 3699–3702. doi: 10.1073/pnas.95.7.3699

Seabra, R., Wethey, D. S., Santos, A. M., and Lima, F. P. (2011). Side Matters: Microhabitat Influence on Intertidal Heat Stress Over a Large Geographical Scale. *J. Exp. Marine Biol. Ecol.* 400, 200–208. doi: 10.1016/j.jembe.2011.02.010

Shih, H.-T. (2012). Distribution of Fiddler Crabs in East Asia, With a Note on the Effect of the Kuroshio Current. *Kuroshio Sci.* 6, 83–89.

Shih, H.-T., Lee, J. H., Ho, P. H., Liu, H. C., Wang, C. H., Suzuki, H., et al. (2016b). Species Diversity of Fiddler Crabs, Genus *Uca Leach* 1814 (Crustacea: Ocypodidae), From Taiwan and Adjacent Islands, With Notes on the Japanese Species. *Zootaxa* 4083, 57–82. doi: 10.11646/zootaxa.4083.1.3

Shih, H.-T., Ng, P. K. L., Davie, P. J. F., Schubart, C. D., Türkay, M., Naderloo, R., et al. (2016a). Systematics of the Family Ocypodidae Rafinesqu(Crustacea: Brachyura), Based on Phylogenetic Relationships, With a Reorganization of Subfamily Rankings and a Review of the Taxonomic Status of Uca Leach 1814, *Sensu Lato* and Its Subgenera. *Raffles Bull. Zool.* 64, 139–175.

Shih, H.-T., Ng, P. K. L., Wong, K. J. H., and Chan, B. K. K. (2012). Gelasimus Splendidus Stimpson, 1858 (Crustacea: Brachyura: Ocypodidae), a Valid Species of Fiddler Crab From the Northern South China Sea and Taiwan Strait. *Zootaxa* 3490, 30–37. doi: 10.11646/zootaxa.3490.1.2

Sokolova, I. M. (2013). Energy-Limited Tolerance to Stress as a Conceptual Framework to Integrate the Effects of Multiple Stressors. *Integr. Comp. Biol.* 53, 597–608. doi: 10.1093/icb/ict028

Somero, G. N. (2002). Thermal Physiology and Vertical Zonation of Intertidal Animals: Optima, Limits, and Costs of Living. *Integr. Comp. Biol.* 42, 780–789. doi: 10.1093/Icb/42.4.780

Somero, G. N. (2010). The Physiology of Climate Change: How Potentials for Acclimatization and Genetic Adaptation Will Determine "Winners" and "Losers." *J. Exp. Biol.* 213, 912–920. doi: 10.1242/jeb.037473

Stillman, J. H. (2002). Causes and Consequences of Thermal Tolerance Limits in Rocky Intertidal Porcelain Crabs, Genus *Petrolisthes*. *Integr. Comp. Biol.* 42, 790–796. doi: 10.1093/icb/42.4.790

Stillman, J. H., and Somero, G. N. (1996). Adaptation to Temperature Stress and Aerial Exposure in Congeneric Species of Intertidal Porcelain Crabs (Genus *Petrolisthes*): Correlation of Physiology, Biochemistry and Morphology With Vertical Distribution. *J. Exp. Biol.* 1855, 1845–1855. doi: 10.1073/pnas.93.20.10855

Stillman, J. H., and Somero, G. N. (2000). A Comparative Analysis of the Upper Thermal Tolerance Limits of Eastern Pacific Porcelain Crabs, Genus *Petrolisthes*: Influences of Latitude, Vertical Zonation, Acclimation, and Phylogeny. *Physiol. Biochem. Zool.* 73, 200–208. doi: 10.1086/316738

Suchard, M. A., Lemey, P., Baele, G., Ayres, D. L., Drummond, A. J., and Rambaut, A. (2018). Bayesian Phylogenetic and Phylodynamic Data Integration Using BEAST 1.10. *Virus Evol.* 4, vey016. doi: 10.1093/ve/vey016

Sunday, J. M., Bates, A. E., Kearney, M. R., Colwell, R. K., Dulvy, N. K., Longino, J. T., et al. (2014). Thermal-Safety Margins and the Necessity of Thermoregulatory Behavior Across Latitude and Elevation. *Proc. Natl. Acad. Sci. U. S. A.* 111, 5610–5615. doi: 10.1073/pnas.1316145111

Sunday, J. M., Bennett, J. M., Calosi, P., Clusella-Trullas, S., Gravel, S., Hargreaves, A. L., et al. (2019). Thermal Tolerance Patterns Across Latitude and Elevation. *Philos. Trans. R. Soc. B: Biol. Sci.* 374, 20190036. doi: 10.1098/rstb.2019.0036

Tavaré, S. (1986). Some Probabilistic and Statistical Problems in the Analysis of DNA Sequences. *Am. Math. Society: Lectures Mathematics Life Sci.* 17, 57–86.

Thomas, C. D. (2010). Climate, Climate Change and Range Boundaries. *Diversity Distributions* 16, 488–495. doi: 10.1111/j.1472-4642.2010.00642.x

Thurman, C. L., Faria, S. C., and McNamara, J. C. (2013). The Distribution of Fiddler Crabs (*Uca*) Along the Coast of Brazil: Implications for Biogeography of the Western Atlantic Ocean. *Marine Biodiversity Records* 6, e1. doi: 10.1017/S1755267212000942

Thurman, C. L., Hanna, J., and Bennett, C. (2010). Ecophenotypic Physiology: Osmoregulation by Fiddler Crabs (*Uca* Spp.) From the Northern Caribbean in Relation to Ecological Distribution. *Marine Freshwater Behav. Physiol.* 43, 339–356. doi: 10.1080/10236244.2010.526407

Valiela, I., Babiec, D. F., Atherton, W., Seitzinger, S., and Krebs, C. (1974). Some Consequences of Sexual Dimorphism: Feeding in Male and Female Fiddler Crabs, *Uca Pugnax* (Smith). *Biol. Bull.* 147, 652–660. doi: 10.2307/1540748

Viña, N., Bascur, M., Guzmán, F., Riera, R., Paschke, K., and Urzúa, Á. (2018). Interspecific Variation in the Physiological and Reproductive Parameters of Porcelain Crabs From the Southeastern Pacific Coast: Potential Adaptation in Contrasting Marine Environments. *Comp. Biochem. Physiol. Part A: Mol. Integr. Physiol.* 226, 22–31. doi: 10.1016/j.cbpa.2018.07.006

Vinagre, C., Dias, M., Cereja, R., Abreu-Afonso, F., Flores, A. A. V., and Mendonça, V. (2019). Upper Thermal Limits and Warming Safety Margins of Coastal Marine Species – Indicator Baseline for Future Reference. *Ecol. Indic.* 102, 644–649. doi: 10.1016/j.ecolind.2019.03.030

Vorsatz, L. D., Mostert, B. P., McQuaid, C. D., Cannicci, S., and Porri, F. (2021a). Thermal Sensitivity in Dual-Breathing Ectotherms: Embryos and Mothers Determine Species' Vulnerability to Climate Change. *Limnol. Oceanography Lett.* doi: 10.1002/lol2.10225

Vorsatz, L. D., Pattrick, P., and Porri, F. (2021b). Quantifying the *in Situ* 3-Dimensional Structural Complexity of Mangrove Tree Root Systems: Biotic and Abiotic Implications at the Microhabitat Scale. *Ecol. Indic.* 121, 107154. doi: 10.1016/j.ecolind.2020.107154

Wiens, J. J., and Graham, C. H. (2005). Niche Conservatism: Integrating Evolution, Ecology, and Conservation Biology. *Annu. Rev. Ecol. Evol. Systematics* 36, 519–539. doi: 10.1146/annurev.ecolsys.36.102803.095431

Williams, G. A., and Morritt, D. (1995). Habitat Partitioning and Thermal Tolerance in a Tropical Limpet, Cellana Grata. *Marine Ecol. Prog. Ser.* 124, 89–103. doi: 10.3354/meps124089

Windsor, A., Crowe, M., and Bishop, J. (2005). Determination of Temperature Preference and the Role of the Enlarged Cheliped in Thermoregulation in Male Sand Fiddler Crabs, *Uca Pugilator*. *J. Thermal Biol.* 30, 37–41. doi: 10.1016/j.jtherbio.2004.06.006

Yamaguchi, T. (2001). The Breeding Period of the Fiddler Crab, *Uca Lactea* (Decapoda, Brachyura, Ocypodidae) in Japan. *Crustaceana* 74, 285–293. doi: 10.1163/156854001505523

Yamaguchi, T. (2003). Seasonal Changes in the Energy Content of Females of the Fiddler Crab, *Uca Lactea*, Especially During the Reproductive Period. *Crustaceana* 76, 1371–1397. doi: 10.1163/156854003323009867

Yang, Z. (1994). Maximum Likelihood Phylogenetic Estimation From Dna Sequences With Variable Rates Over Sites: Approximate Methods. *J. Mol. Evol.* 39, 306–314. doi: 10.1007/BF00160154

Yuhara, T., Yokooka, H., and Taru, M. (2017). Range Extension of the Sesarmid Crab *Clistocoeloma Villosum* Along the Eastern Pacific Coast of the Izu Peninsula, Japan. *Marine Biodiversity Records* 10, 1–5. doi: 10.1186/s41200-017-0122-1

Yule, G. U. (1924). A Mathematical Theory of Evolution, Based on the Conclusions of Dr. J. C. Willis, F.R.s. *Philos. Trans. R. Soc. B* 213, 21–87. doi: 10.1098/rstb.1925.0002

Conflict of Interest: The authors declare that the research was conducted in the absence of any commercial or financial relationships that could be construed as a potential conflict of interest.

Publisher's Note: All claims expressed in this article are solely those of the authors and do not necessarily represent those of their affiliated organizations, or those of the publisher, the editors and the reviewers. Any product that may be evaluated in this article, or claim that may be made by its manufacturer, is not guaranteed or endorsed by the publisher.

frontiers in Marine Science

ORIGINAL RESEARCH
published: 25 March 2022
doi: 10.3389/fmars.2022.824624

Phytoplankton Response to Different Light Colors and Fluctuation Frequencies

Sebastian Neun[1†], Nils Hendrik Hintz[1†], Matthias Schröder[2] and Maren Striebel[1]*

[1] Institute for Chemistry and Biology of the Marine Environment (ICBM), Carl von Ossietzky University of Oldenburg, Wilhelmshaven, Germany, [2] Institute for Chemistry and Biology of the Marine Environment (ICBM), Carl von Ossietzky University of Oldenburg, Oldenburg, Germany

OPEN ACCESS

Edited by:
Christopher Edward Cornwall, Victoria University of Wellington, New Zealand

Reviewed by:
Douglas Andrew Campbell, Mount Allison University, Canada
C.-Elisa Schaum, University of Hamburg, Germany
Martina Andrea Doblin, University of Technology Sydney, Australia

***Correspondence:**
Nils Hendrik Hintz
nils.hendrik.hintz@uol.de

[†] These authors have contributed equally to this work and share first authorship

Specialty section:
This article was submitted to Global Change and the Future Ocean, a section of the journal Frontiers in Marine Science

Received: 29 November 2021
Accepted: 09 February 2022
Published: 25 March 2022

Citation:
Neun S, Hintz NH, Schröder M and Striebel M (2022) Phytoplankton Response to Different Light Colors and Fluctuation Frequencies. Front. Mar. Sci. 9:824624. doi: 10.3389/fmars.2022.824624

The natural environment of phytoplankton is variable in manifold ways. Light, as essential resource for photosynthetic phytoplankton, fluctuates in its intensity (quantity) as well as spectrum (quality) over great temporal scales in aquatic ecosystems. To elucidate the significance of temporal heterogeneity in available light spectrum for phytoplankton, we analyzed the growth of four marine North Sea species (chlorophyte *Tetraselmis* sp., cryptophyte *Rhodomonas salina*, cyanobacteria *Pseudanabaena* sp., raphidophyte *Fibrocapsa japonica*), in monoculture as well as the dynamics of these species in pairwise competition experiments under blue and green light. These species were chosen as they differ in their absorption of light, the colors were chosen to contrast the absorption by chlorophylls (blue), carotenoids (partially green) and phycobiliproteins (green). Light colors were either supplied constantly or along a gradient of fluctuation frequencies (hourly to weekly alternation) between blue and green but always with the same photon flux density. When constantly supplied (no change in color), the color of light led to significant differences in growth rates and carrying capacities of the species, with *Pseudanabaena* sp. being the only one profiting from green light. Under alternating light color, the maximum growth rate of *R. salina* was higher with faster light color fluctuations, but lower for *Pseudanabaena* sp. and did not show significant trends for *F. japonica* and *Tetraselmis* sp. Accordingly, competition was significantly affected by the light color treatments, under constant as well as fluctuating supply conditions. However, we did not detect considerable changes in competitive outcomes between fluctuating light colors vs. constant light color supply. As the underwater light in natural ecosystems is rather variable than constant, our results of fluctuations within the light spectrum highlight their frequency-dependent effects on growth and competition. While fluctuating light colors affect the growth and capacity of species, our tested fluctuations did not have major effects on species competition.

Keywords: phytoplankton, light spectrum, fluctuations, frequency, PAR, growth rate, carrying capacity, competition

INTRODUCTION

As primary producers, phytoplankton considerably affect processes like the cycling of elements (Falkowski et al., 1998) and control the food webs by limiting the growth of nearly all higher trophic levels (e.g., Falkowski, 2012). Aquatic primary production strongly depends on the availability of light and nutrients (Falkowski, 1994; Field et al., 1998; Elser et al., 2007). In water, light intensity is attenuated exponentially with depth due to absorption and scattering processes by water molecules, particulate and dissolved organic matter (Stomp et al., 2007a; Kirk, 2011). Moreover, the attenuation of light is wavelength-dependent, based on the optical properties of water and creates a vertical gradient in underwater light colors. Thus, in clear water bodies like the open oceans, the light absorption by water molecules themselves shift the watercolor bluish (Stomp et al., 2007a; Kirk, 2011). Thereupon, in coastal seas and lakes high loads of organic matter can lead to a dominance of brownish wavelengths and the light absorption by phytoplankton can color the water more greenish (Morel, 1980; Stomp et al., 2007a; Kirk, 2011). Characterized by its intensity, i.e., quantity, and wavelengths, i.e., light quality, the variability in light influences not only the productivity but also the distribution (horizontally as well as vertically) and diversity of phytoplankton (Wall and Briand, 1979; Falkowski, 1994; Holtrop et al., 2021).

Furthermore, natural environments are fluctuating at multiple scales and affect the living organisms in manifold ways (Bernhardt et al., 2020), with particularly high fluctuations in light. The fastest light fluctuations underwater are those induced by surface ripples as they briefly focus and diffuse the incident light, similar to a lens, within seconds (Dera and Gordon, 1968; Walsh and Legendre, 1983; Falkowski, 1984). Slower causes of light fluctuations are a changing cloud cover in the range of minutes and diurnal changes (Walsh and Legendre, 1983; Ferris and Christian, 1991). Aquatic organisms further encounter light intensity fluctuations induced by semi-diurnal tidal changes and phytoplankton species are subjected to light variations, both quantitatively and qualitatively, due to vertical mixing in the timespan of minutes to hours (Denman and Gargett, 1983; Walsh and Legendre, 1983; Falkowski, 1984). Moreover, with future predictions of altered water temperatures, wind conditions and precipitation pattern the light availability and light fluctuation for phytoplankton is expected to change as well due to climate change (Saros et al., 2012; Sydeman et al., 2014; Somavilla et al., 2017; Dutkiewicz et al., 2019).

With having pigments of different properties and quantity, phytoplankton possess structures to absorb the prevailing light as efficiently as possible, even under sub-optimal conditions. These pigments harvest the light photons of the photosynthetic active radiation (PAR) according to their absorption characteristics and transfer their energy to the light reaction of photosynthesis (Falkowski and Raven, 2007; Roy et al., 2011).

The chlorophylls have two absorption peaks, one in the blue of 400–500 nm and one in the red of 600–700 nm of the light spectrum, but almost no absorption of green light between 500 and 600 nm (Kirk, 2011; Croce and van Amerongen, 2014). Carotenoids, however, absorb in the short-wavelength region between 300 and 500 nm and thus, contrary to the chlorophylls, to a small extent in the green part (Kirk, 2011). Phycobiliproteins occur in Rhodophyta, Cryptophyta, and Cyanophyta and are, except a few carotenoids, the only pigments absorbing the PAR in the "green gap" at 500–600 nm (Croce and van Amerongen, 2014).

Because of their different light absorption characteristics, species-specific pigment compositions and thus light-harvesting strategies may allow the coexistence of phytoplankton species along the vertical light gradient (Wall and Briand, 1979; Stomp et al., 2007b; Holtrop et al., 2021). Indeed, several studies showed that for calm conditions the vertical distribution of phytoplankton species within the water column can be linked to the available light quality (Bidigare et al., 1990; Stomp et al., 2007b; Hickman et al., 2009), indicating that the outcome of phytoplankton competition for light is not determined solely by the given light intensity but also by the availability of different wavelengths.

This adds a complete additional dimension to the high diversity in morphology such as size or motility and biochemistry such as storage products or nutrient uptake mechanisms of phytoplankton as a potential explanation of Hutchinson's "paradox of the plankton" (Hutchinson, 1961). An underexplored mechanism for the high diversity in phytoplankton might be this twofold multi-dimensionality, both of the variable supply by light fluctuations and the use, i.e., light acquisition traits. Hutchinson supposed that in nature the assumed steady-state never occurs as environmental changes are faster than the process of competitive exclusion (Hutchinson, 1961). Thus, temporal variability in an environment may be an important aspect preventing competitive exclusion (Richerson et al., 1970; Tilman et al., 1982). Although there is great evidence that varying light conditions do support the biodiversity of phytoplankton (Litchman, 1998, 2003; Flöder et al., 2002; Flöder and Burns, 2005), evidence for a linkage between fluctuating light spectrum and phytoplankton competition is rare. Stomp et al. (2008) showed that light color fluctuations are an important factor for the coexistence of phytoplankton species, especially those with periods that are comparable with weather-induced light fluctuations. For fluctuations in light color, no coexistence was observed but species with a flexible phenotype had a clear advantage under fluctuating light colors. However, competition of phytoplankton, especially eukaryotic species, under fluctuating light color is still barely examined.

Luimstra et al. (2020) showed that the photosynthetic efficiency is also a function of light color. They studied competition between a green alga and a cyanobacterium, both harvesting different ranges of the light's spectrum, under mixtures of blue and red light. As long as blue light was available, the green alga competitively excluded the cyanobacterium and the cyanobacterium won competition only under 100% red light so that coexistence was never observed, but the color of light determined the competition outcome. Thus, coexistence under white light cannot be expected in general although two species absorb in two different regions of the light spectrum (Luimstra et al., 2020; Tan et al., 2020).

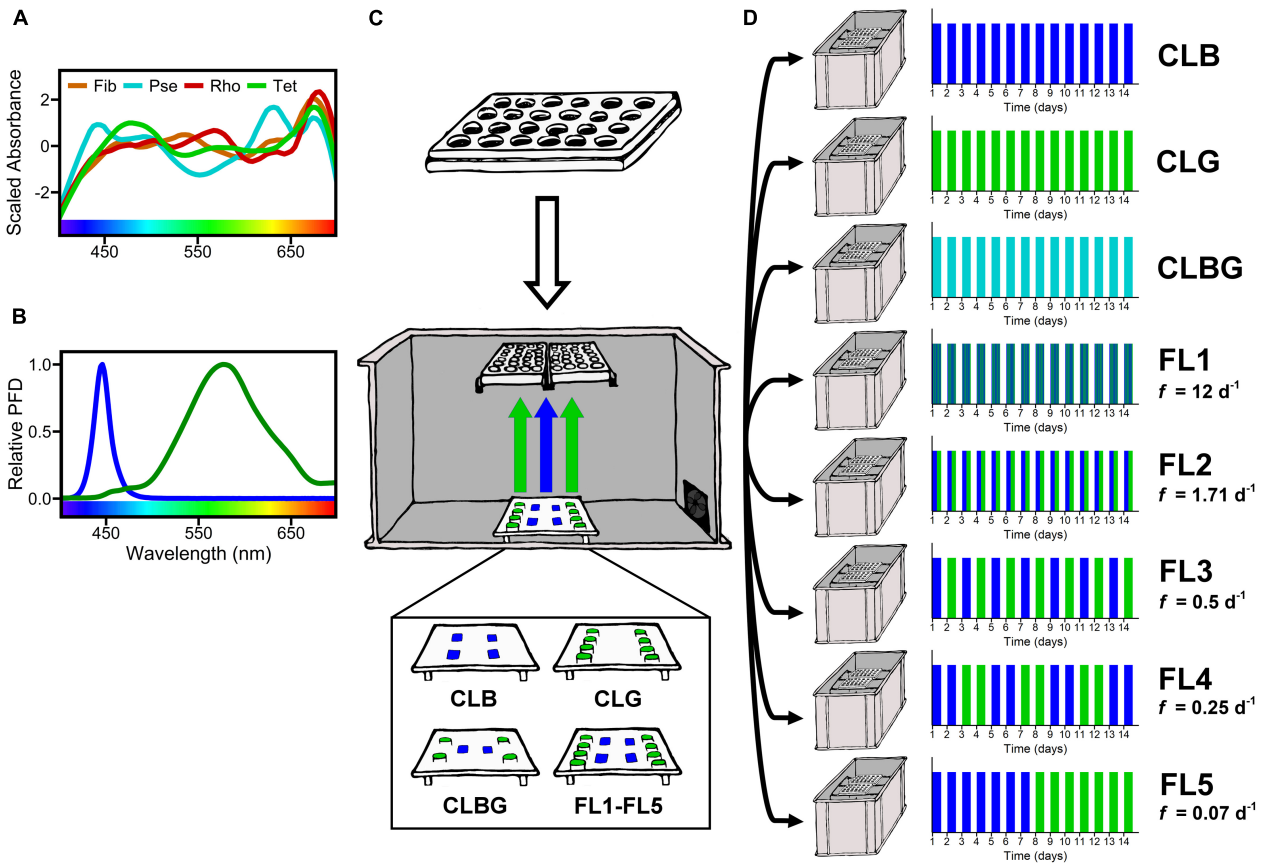

FIGURE 1 | Scheme of experimental setup. **(A)** Species absorption spectra scaled by z-transformation and **(B)** the supplied light spectra in relative photon flux density (PFD). The supplied light was adjusted to 50 μmol photons m^{-2} s^{-1} integrated over the PAR range for each treatment. **(C)** Experimental setup by placing two culture microwell plates above the LED array in combinations according to the treatments. Uniformly distribution of LEDs, sufficient distance and a reflective coating of the boxes' walls and lid ensured a homogenous light distribution for all positions. Temperature control was implied by the opening at the right side of the opaque box. **(D)** Treatments time schedule stating the fluctuation frequency (f) for an example duration of 14 days. Treatments were considered as "constant" (CLB, CLG, CLBG) if the applied spectrum did not alternate and "fluctuating" if the spectrum alternated (between blue and green) throughout the experiment. They were conducted in replicates of 6 for monocultures and 4 for pairwise species mixtures for each treatment and box, respectively.

The impact of temporal variations in light quality is a remaining question but may be an important contribution explaining the coexistence of phytoplankton species. In aquatic environments with intense vertical mixing, calm conditions are the exception rather than the rule. Therefore, we conducted a laboratory experiment with four marine phytoplankton species, showing different light-absorption and investigated their growth under two different light colors, blue and green in monoculture as well as in two-species mixtures. Light was supplied constantly as well as fluctuating with different frequencies to test the effect of fluctuating light color on growth and competition of the species. We tested the following hypotheses:

H1: The performance of phytoplankton species depends on species-specific light-harvesting strategies under blue and green light conditions. That is, a higher performance is expected for species possessing a complementary pigment composition and thus can use the light spectrum provided more efficiently as compared to other species.

H2: Species showing differences in the performance under blue and green light will be negatively affected by light fluctuations, both in monoculture and mixed culture, as the usable light is reduced on average over time. However, outcomes will depend on the frequency of light fluctuations. The negative effect should disappear for high frequencies as short periods of unsuitable light can be outlasted.

H3: In general, if two species compete for the same light spectrum, the species with the higher growth rate will dominate. If two species use blue and green light differently, resulting in dissimilar performances, they can coexist under blue-green light.

MATERIALS AND METHODS

Phytoplankton

Species were selected according to their light-harvesting properties by means of light absorption. The chlorophyte

Tetraselmis sp. (in following abbreviated as *Tet*) and the raphidophyte *Fibrocapsa japonica* (*Fib*) were chosen and suggested as species, potentially favoring blue light. As potentially green-light using species, the cryptophyte *Rhodomonas salina* (*Rho*) and the cyanobacterium *Pseudanabaena* sp. (*Pse*) were selected, both known to contain phycoerythrin. Strains of the latter species are further known for being able to adjust their cellular pigment ratio of phycoerythrin:phycocyanin with light quality (Tandeau de Marsac, 1977; Bryant and Cohenbazire, 1981; Stomp et al., 2008). All phytoplankton species were originally isolated from the German bight in the North Sea. They were pre-cultivated in f/2 medium according to Guillard and Ryther (1962) and Guillard (1975) at 18°C and under the same white light with an intensity of about 30 µmol photons m^{-2} s^{-1} and a day:night cycle of 12:12 h.

Experimental Setup

For the experiment, cultures were grown in f/2 medium (Guillard and Ryther, 1962; Guillard, 1975) using transparent 24-well cell culture plates (Greiner Bio-One) in opaque boxes (**Figure 1**). The temperature was kept constant at 20°C. We applied constant light treatments with blue (CLB), green (CLG) and blue-green (CLBG) light, as well as five fluctuating light treatments (FL) with light fluctuating between blue and green light with the following frequencies (**Figure 1**): 1 h blue/1 h green: frequency = 12 day^{-1}, 7 h blue/7 h green: frequency = 1.71 day^{-1}, 1 d blue/1 d green: frequency = 0.5 day^{-1}, 2 d blue/2 d green: frequency = 0.25 day^{-1}, 7 d blue/7 d green: frequency = 0.07 day^{-1}. All light treatments experienced a day:night cycle of 14:10 h that refers to light intensity. Day:night cycle of light intensity (14:10 h) and temperatures were monitored with temperature/light data loggers (HOBO Pendant MX2202, Onset). As it was not possible to randomize the plates' wells within the setup, we used a maximal number of replicates (6 for each monoculture and 4 for each mixture, per box and respective treatment) which were placed across two well plates per box. Within the boxes, well plates were illuminated from below with small high-power light-emitting diodes (LEDs). Blue light was obtained from single-colored blue LEDs with a peak emission at 445 nm (Csspm1.14, OSRAM), overlapping greatly with the regarding chlorophyll peak. For green light, white LEDs (Highpower 1W 3,000–4,000°K, World Trading Net GmbH & Co. KG) were covered with a green light transmission foil (LEE Filter 088, LEE Filters Worldwide), resulting in a peak emission at approximately 575 nm. This matches with reported absorption values of phycoerythrin in *Rho* (545–565 nm, e.g., da Silva et al., 2009; Heidenreich and Richardson, 2020) and *Pse* (560–570 nm, e.g., Stomp et al., 2008; Acinas et al., 2009). Due to differences in total light output between the blue LEDs and the white LEDs with the light filter, the number of LEDs per box were adapted. By the uniformly distribution of LEDs, a sufficient distance to the well plates as well as reflective coating of the boxes' walls and lids a homogeneous light distribution was ensured for all positions. The light output was measured as photon flux density (µmol photons m^{-2} s^{-1}) with a spherical PAR-sensor (US-SQS/L Submersible Spherical Micro Quantum Sensor, Walz, with LI-250A, LI-COR), integrating the irradiance over the PAR range (400-700 nm). Photon flux density was set to 50 µmol photons m^{-2} s^{-1} in total for each light treatment, by adjusting the LEDs via constant current reduction (KSQ1000 V2.0, KT-Elektronik GmbH). This has the advantage of stepless adjusting without inducing high-frequent fluctuations (Schulze et al., 2017). The light fluctuations as well as the day:night cycle were programmed with a microcontroller (Arduino Nano, Arduino AG). Accurate timing was specified with a connected real-time clock (DS1307, LC Technology).

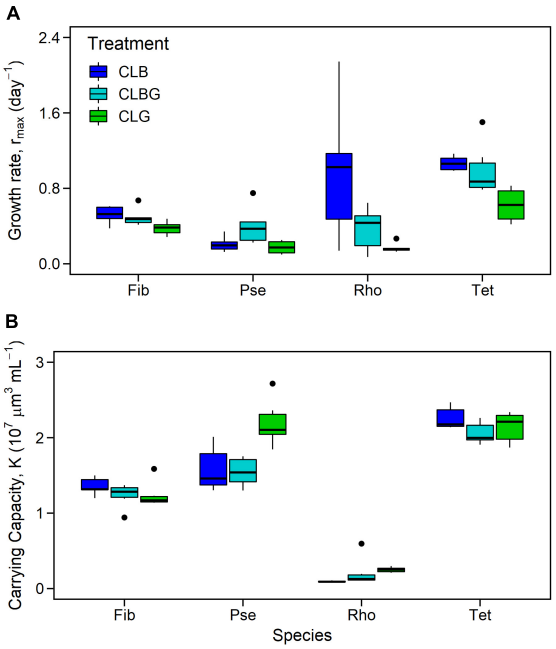

FIGURE 2 | Maximum growth rate **(A)** and carrying capacity **(B)** for monocultures [*Fibrocapsa japonica* (Fib), *Pseudanabaena* sp. (Pse), *Rhodomonas salina* (Rho), and *Tetraselmis* sp. (Tet)] under constant light. Colors indicate constant light treatment (CLB, constant blue light; CLBG, constant blue-green light; CLG, constant green light).

Sampling and Measurements

The experiment lasted 16 days. Each well in the culture plates was filled with a total volume of 2 mL and all monocultures as well as mixed cultures were inoculated with the same biovolume concentration of $1.2*10^6$ μm^3 mL^{-1}. Consequently, biovolume concentrations of the respective species in mixed culture were half of that in monoculture. Species-specific biovolume was estimated based on geometric shapes by measuring the size parameter of at least 20 randomly chosen cells according to Hillebrand et al. (1999) and Olenina et al. (2006).

Daily measurements included blank-subtracted optical density (OD_{450nm}) (**Supplementary Figure 1**) as well as *in vivo* absorption spectra (300–805 nm, in steps of 1 nm, as absorbance per wavelength, see **Supplementary Figure 3**) using a microplate reader (Synergy H1, BioTek). Before measurements, culture plates were shaken gently to homogenize the cultures. Every 4 days 10% of the cultures were sampled and exchanged with

TABLE 1 | Monocultures under constant light.

ANOVA	Log(r_{max})		Log(K)	
Effect	***F***	***p***	***F***	***p***
Species	25.6	**<0.001**	537.9	**<0.001**
Treatment	12.3	**<0.001**	11.1	**<0.001**
Species * Treatment	3.4	**<0.01**	8.3	**<0.001**
***Post-hoc* test**				
Species comparison	**diff**	***p* adj**	**diff**	***p* adj**
Pse-Fib	–0.692	**<0.001**	0.312	**<0.001**
Rho-Fib	–0.351	0.128	–2.088	**<0.001**
Tet-Fib	0.631	**<0.001**	0.525	**<0.001**
Rho-Pse	0.341	0.147	–2.401	**<0.001**
Tet-Pse	1.323	**<0.001**	0.213	**<0.05**
Tet-Rho	0.983	**<0.001**	2.614	**<0.001**
Treatment comparison				
CLBG-CLB	–0.108	0.709	0.100	0.268
CLG-CLB	–0.633	**<0.001**	0.294	**<0.001**
CLG-CLBG	–0.524	**<0.001**	0.194	**<0.01**

*Two-factorial ANOVA of log-transformed maximum growth rates (r_{max}) and carrying capacity (K) with F and p-values (species df = 3, treatment df = 2, species*treatment df = 6, residuals df = 60) and summary of post-hoc tests (Tukey HSD) for differences between phytoplankton species and light treatments. Both growth parameters were obtained by logistic growth curve fits. For each comparison, differences in mean (diff) and adjusted p-values (p adj) are shown. Significant effects ($p < 0.05$) are highlighted in bold. Species were abbreviated as Fib, Fibrocapsa japonica; Rho, Rhodomonas salina; Pse, Pseudanabaena sp.; and Tet, Tetraselmis sp. Treatment abbreviations indicate constant CLB, blue light; CLG, constant green light and CLBG, constant blue-green light in simultaneous supply.*

fresh, sterile medium to compensate culture volume loss and avoid nutrient limitation. Samples were fixed with Lugol's iodine solution and microscopically counted (DM IL inverted microscope, Leica) to monitor population dynamics and respective proportions in mixtures. Monocultures were not counted but checked for contaminations by other species.

Statistical Analysis

Based on daily OD_{450nm} measurements, logistic growth curves were fitted per experimental unit to predict the parameters of maximum growth rate (r_{max}) and carrying capacity (K) (Eq. 1) of monocultures and mixed cultures with N_0 as the OD_{450nm} at the beginning and t the day of the experiment (**Supplementary Figure 2**).

$$OD_{450nm} = \frac{K \times N_0}{\left(N_0 + (K - N_0) \times e^{-r_{\max} \times t}\right)} \quad (1)$$

Carrying capacities were converted from OD measurements into biovolume concentration ($mm^3\ mL^{-1}$) based on dilution series and microscopic determinations to clarify differences between species. Linear regression models were fitted to test for a linear relationship for these calibrations for each monoculture. For two-species mixtures, linear relationships between the experimentally measured optical density values and counted cell concentrations were calculated. Analysis of variances (ANOVA) were conducted to test for significant treatment effects on r_{max} and K, including treatment and species as independent variables. Significant differences among treatments and species under constant light were tested using *post-hoc* tests (Tukey HSD test). For fluctuations (as frequency day^{-1}) we estimated linear relationships between fluctuation frequency and r_{max} or K, respectively. A significant fit of the linear regression slope indicated whether the r_{max} or K were positively or negatively correlated to fluctuation frequency. A positive correlation indicated a higher r_{max} or K, respectively, with higher fluctuation frequency, i.e., the faster the light color fluctuated. ANOVA assumptions of normality and homoscedasticity were checked by Shapiro-Wilk-Test and Levene's test, respectively. If necessary, log transformation was applied to fit the assumptions.

All statistical results were interpreted as significant for a significance level of $\alpha = 0.05$ and all statistical analysis were performed with R version 4.0.2 (R Project for Statistical Computing, RRID:SCR_001905, R Core Team, 2020). Fitting of logistic growth curves and ANOVA was performed with the "stats" package (R Core Team, 2020). Levene's test for homoscedasticity was performed with the "car" package (Fox and Sanford, 2019). All plots were done with the "ggplot2" package (Wickham, 2016).

RESULTS

Monoculture Performance Under Constant Light—Growth and Carrying Capacity

Maximum growth rates (r_{max}) and carrying capacities (K) were significantly affected by the light treatments (**Figure 2**, significant treatment effect, **Table 1**) and showed species-specific responses (**Figure 2**, species and species * treatment effect, **Table 1**). In general, highest r_{max} were observed under blue light whereas green light resulted in species' lowest r_{max} (**Figure 2**). *Post-hoc* tests revealed that phytoplankton r_{max} did not differ significantly between the blue and blue-green light treatments (**Figure 2A** and **Table 1**), however, r_{max} under green vs. blue light as well as r_{max} under green vs. blue-green were significantly different (**Figure 2A** and **Table 1**). K was overall highest affected by green light (**Figure 2B**, significant treatment effects and treatment comparison, **Table 1**) but did not differ between blue and blue-green light.

Species comparison showed that *Tetraselmis* sp. (*Tet*) had significantly higher r_{max} than all other species and *Fibrocapsa japonica* (*Fib*) significantly higher r_{max} than *Pseudanabaena* sp. (*Pse*), while the r_{max} did not significantly differ between the other species comparisons. In contrast, species K were overall species-specific, meaning significant differences for all species comparison were obtained (**Table 1**), with the highest K for *Tet*.

Monoculture Performance Under Fluctuating Light—Growth and Carrying Capacity

Frequency effects of light color fluctuation on r_{max} and K of phytoplankton monocultures depended on the species identity

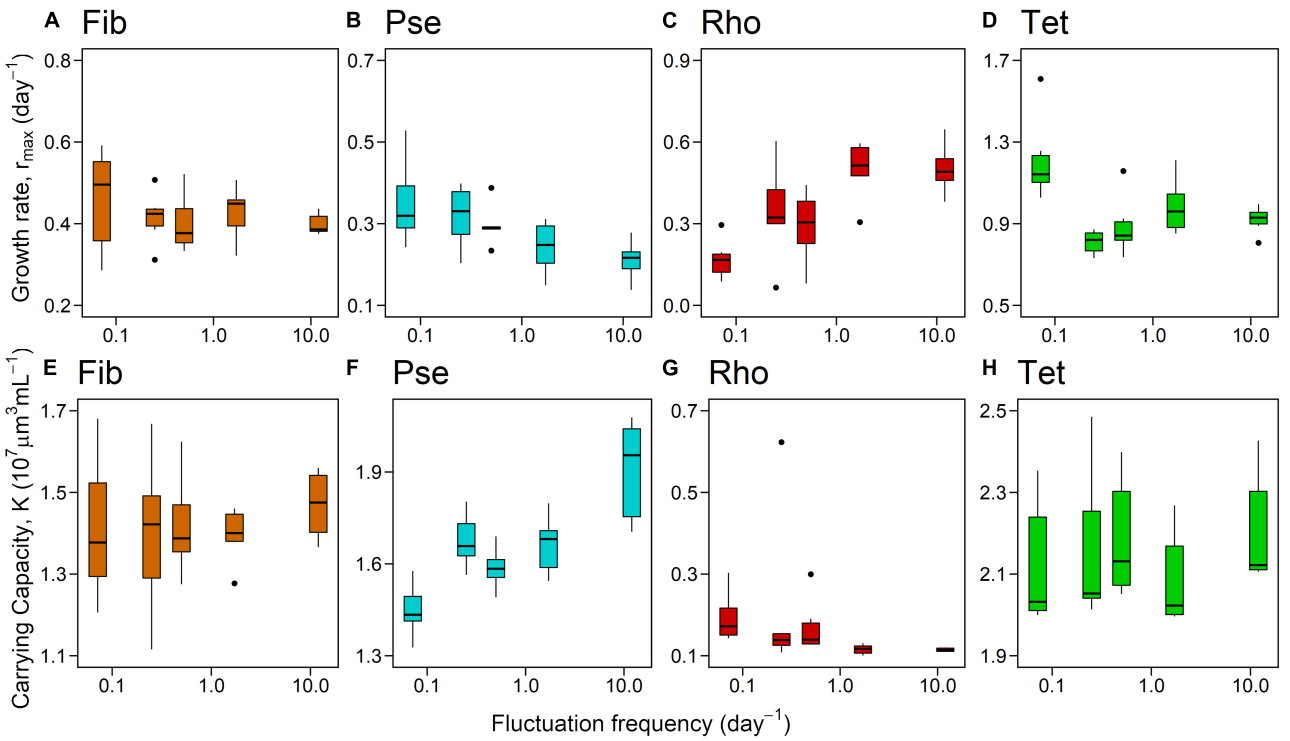

FIGURE 3 | Maximum growth rate **(A–D)** and carrying capacity **(E–H)** for monocultures related to fluctuation frequency (displayed as fluctuation frequency per day on log-scale). **(A)**: *Fibrocapsa japonica* (Fib), **(B)**: *Pseudanabaena* sp. (Pse), **(C)**: *Rhodomonas salina* (Rho), and **(D)**: *Tetraselmis* sp. (Tet).

(**Figures 3**, **4** and **Table 2**, significant interactive effect of species * frequency). While r_{max} of *Fib* was not affected by light fluctuations and K only marginally positive affected (**Figures 3A,E** and **Table 2**) growth rates of *Pse* decreased with increasing fluctuation frequency whereas carrying capacity increased with fluctuation frequency (**Figures 3B,F** and **Table 2**). Maximum growth rates of *Rhodomonas salina* (*Rho*) increased with faster frequency of light fluctuation (**Figure 3C** and **Table 2**) while no significant effect of fluctuation frequency on K (although a decreasing trend) was observed (**Figure 3G** and **Table 2**). Maximum growth rates and K of *Tet* tended to increase with faster frequency of light fluctuation (**Figures 3D,H** and **Table 2**), however, as the lowest fluctuation frequency resulted in highest growth rate (first week of experiment exposed to blue light before switched to green) this trend was not significant (**Figures 3D**, **4A** and **Table 2**).

Mixed Culture Performance Under Constant Light—Growth, Capacity and Species Proportion

Maximum growth rates as well as K of the two-species mixtures, as total response of both species together (*Fib*+*Tet*, *Pse*+*Rho*, *Pse*+*Tet*, and *Rho*+*Tet*), were significantly affected by light treatment and species mixture (**Table 2**), with highest r_{max} under blue light and lowest r_{max} under the green light treatment while K was significantly higher under green light compared to blue light (**Figure 5**, significant treatment effects and treatment comparison, **Table 3**).

The two-species mixtures reflect the performance of the included species, mixtures containing *Tet* generally performed better than others while mixtures containing *Rho* showed lower performance than other mixtures (**Figure 5**, species mixture comparison, **Table 3**).

Furthermore, the light treatment effects (light color) also depended on the containing species, thus mixed cultures including *Tet* had overall higher r_{max} under blue light than under blue-green and lowest under green light while such light effects on r_{max} were not observed in other mixtures.

The two-species mixtures' K was mainly species-specific, thus mixtures including *Tet* had highest K while mixtures containing *Rho* had lowest K compared to other mixtures (**Figure 5**, species mixture comparison, **Table 3**). The light treatment effects, in terms of light color, of the two-species mixtures' K only existed between blue and green light treatments (**Figure 5** and **Table 3**).

Mixed Culture Performance Under Fluctuating Light—Growth, Capacity, and Species Proportion

Frequency of blue-green light fluctuations significantly affected r_{max} and K of species mixtures (**Figure 6** and **Table 4**). While the overall growth rates of mixtures decreased with increasing frequency (**Figure 6** and **Table 4**), the slopes of fitted linear relationships between growth rates and frequency of individual

mixtures were not significant except for *Pse+Tet* (**Figure 7A** and **Table 4**). K was significantly affected by frequency and species mixture, here K increased significantly with increasing fluctuation frequency for *Pse+Rho*, *Pse+Tet*, and *Rho+Tet* (**Figure 7B** and **Table 4**).

Composition of Mixed Cultures—Relative Biovolume Under Constant and Fluctuating Light Colors

In mixture under constant light conditions, almost all combinations showed significant effects of the supplied light (except *Fib+Rho*, **Figure 8** and **Table 5**). While *Pse* showed significantly lower relative biovolume under blue light compared to blue-green and highest relative biovolume under green light in mixture (**Figure 8** and **Table 5**), the respective other species contained in the two-species mixture showed the opposed effect. The light treatment dependent relative biovolume of the other species generally reflected the preferences observed in monoculture, however, it depended also on the combination of species. *Rho* showed higher relative biovolume under blue light when combined with *Pse* while *Rho* showed higher relative biovolume under green light when combined with *Tet* (**Figure 8**). Similar to the observations under constant light, *Tet* was the dominating species in mixed cultures under fluctuating light conditions.

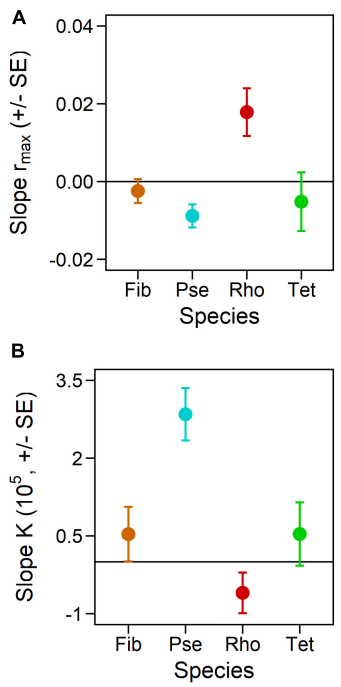

FIGURE 4 | Slopes from the relations between fluctuation frequency and responses in maximum growth rates **(A)** and carrying capacities **(B)** of the monocultures, calculated based on linear regressions. A positive correlation indicates a higher r_{max} or K, respectively, with higher fluctuation frequency, i.e., the faster the light color fluctuated. Error bars represent standard error of calculated regression slopes.

DISCUSSION

Species Performance Under Constant Light

Our results show that performance of phytoplankton species clearly depends on the wavelength of the supplied light, which is in great overlap with previous studies (Luimstra et al., 2018; Heidenreich and Richardson, 2020; Tan et al., 2020). For all phytoplankton species, except for the cyanobacterium *Pseudanabaena* sp. (*Pse*), highest growth rates were observed under blue compared to green light supply. We considered *Tetraselmis* sp. (*Tet*) and *Fibrocapsa japonica* (*Fib*) as blue-light using species, both having higher absorption and higher maximum growth rates under blue light than under green light. *Pse* and *Rhodomonas salina* (*Rho*) were considered as species using blue as well as green light due to the pigment phycoerythrin. However, these species did not show higher growth under green light than *Tet* and *Fib,* whereas the capacity within these species was highest under green light. That is, species performances depended on their light-harvesting strategies, but we did not observe that species with green-light absorbing pigments have consequently higher growth under green light than species without such pigments, which conflicts with our first hypothesis (H1). Thus, species-specific performance was most relevant before treatment specific effects came into play, treatment effects, however, reflected the light absorption traits.

TABLE 2 | Monocultures under fluctuating light.

ANOVA	r_{max}		K	
Effect	***F***	***p***	***F***	***p***
Frequency	0.017	0.895	10.411	**<0.01**
Species	161.106	**<0.001**	1,293.198	**<0.001**
Species * Frequency	5.077	**<0.01**	7.915	**<0.001**
Species (*df*)	**Slope (± se)**	***p***	**Slope (± se)**	***p***
Fib (28)	–0.0024 (0.0031)	0.434	$0.0053*10^7$ ($0.0053*10^7$)	0.318
Pse (28)	–0.0088 (0.0030)	**<0.01**	$0.0285*10^7$ ($0.0050*10^7$)	**<0.001**
Rho (28)	0.0179 (0.0061)	**<0.01**	$-0.0060*10^7$ ($0.0039*10^7$)	0.138
Tet (28)	–0.0052 (0.0075)	0.498	$0.0054*10^7$ ($0.0061*10^7$)	0.387
Tet without lowest frequency (22)	0.0036 (0.0051)	0.490	$0.0048*10^7$ ($0.0064*10^7$)	0.468

*Two-factorial ANOVA of log-transformed maximum growth rates (r_{max}) and carrying capacity (K) with F and p-values (species df = 3, treatment df = 1, species*treatment df = 3, residuals df = 112 per species). Both growth parameters were obtained by logistic growth curve fits. The lower part of the table gives slopes of single linear regression estimating the relationship between fluctuation frequency and r_{max} or K, respectively. p adj. value indicates fit. Slope calculation for Tet was performed twice, excluding its slowest fluctuation frequency (0.071 day^{-1}) as its exponential growth phase was before the first change of light color in the second approach for comparison. Significant effects ($p < 0.05$) are highlighted in bold. Species were abbreviated as Fib, Fibrocapsa japonica; Rho, Rhodomonas salina; Pse, Pseudanabaena sp.; and Tet, Tetraselmis sp.*

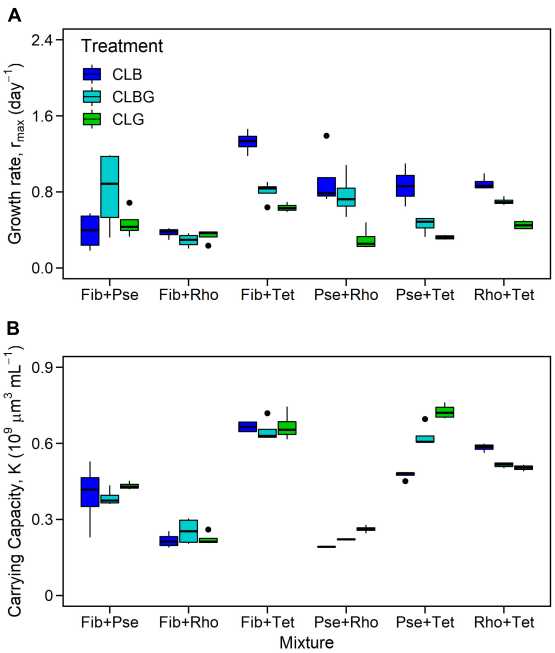

FIGURE 5 | Maximum growth rate **(A)** and carrying capacity **(B)** for two-species mixtures. Colors indicate constant light treatments (CLB, constant blue light; CLBG, constant blue-green light; CLG, constant green light).

In our experiment, the chlorophyte *Tet* was observed as fast-growing species, showing the overall highest maximum growth rates, irrespective of the light treatments. This corresponds to the meta-analysis of Schwaderer et al. (2011) who examined that (freshwater) chlorophytes are generally characterized by high growth rates. We found that light color affected the maximum growth rates of *Tet* but not the carrying capacity. *Tet* is not known to possess pigments absorbing the green light efficiently which affected the r_{max}. Here, small emission of orange-red light at 600–650 nm, although the treatment was peaking in green, probably overlapped with the second absorption peak of chlorophyll and thus sufficed growth of *Tet* which later reached a similar K than under blue light. Nevertheless, Abiusi et al. (2014) also reported growth of a *Tetraselmis* species (*T. suecica*) under blue and green light, similar to our results.

Maximum growth rates of the raphidophyte *Fib* were significantly lower under green light than under blue light but carrying capacities did not differ between the treatments. Besides chlorophyll *a* and *c*, *Fib* is known to possess several carotenoids as accessory light-harvesting pigments, i.a. fucoxanthin (Guidi-Rontani et al., 2010), which in part absorbs green light as well (e.g., Dubinsky and Stambler, 2009). With that, *Fib* could have used the green light in our treatments, leading to the similar carrying capacities under the blue and green light.

The cryptophyte species *Rho* showed large differences in maximum growth rates, with higher growth under blue light than under green light. These results are consistent with other studies on the genus of *Rhodomonas* (Heidenreich and Richardson, 2020; Latsos et al., 2021). Absorption spectra (**Supplementary Figure 3**) showed that *Rho* absorbs blue and red light, likely due to the chlorophylls *a* and *c* as well as green light by phycoerythrin (Lawrenz and Richardson, 2017; Heidenreich and Richardson, 2020). The performance of *Pse* was clearly different from the other species, as its growth rates were highest under constant blue-green light. Furthermore, maximum growth rates did not significantly differ between blue and green light. Carrying capacities, however, were significantly higher under green light than under the other constant light treatments. Lower growth of cyanobacteria under blue light compared to green or red light was also reported in other studies(e.g., Bland and Angenent, 2016; Luimstra et al., 2018; Tan et al., 2020). Based on our measured absorption spectra characteristics (**Supplementary Figure 3**) this can be related to the diverse set of pigments common in *Pse*, namely chlorophyll

TABLE 3 | Two-species mixtures under constant light.

ANOVA	**Log(r_{max})**		**K**	
Effect	**F**	***p***	**F**	***p***
Species mixture	16.8	**<0.001**	247.2	**<0.001**
Treatment	24.9	**<0.001**	7.7	**<0.01**
Species * Treatment	5.5	**<0.001**	7.8	**<0.001**
***Post-hoc* test**				
Species comparison	**diff**	***p* adj**	**diff (× 10^9)**	***p* adj**
Fib+Rho—Fib+Pse	–0.397	**<0.05**	–0.174	**<0.001**
Fib+Tet—Fib+Pse	0.592	**<0.001**	0.255	**<0.001**
Pse+Rho—Fib+Pse	0.171	0.669	–0.180	**<0.001**
Pse+Tet—Fib+Pse	0.027	0.999	0.204	**<0.001**
Rho+Tet—Fib+Pse	0.302	0.104	0.128	**<0.001**
Fib+Tet—Fib+Rho	0.989	**<0.001**	0.430	**<0.001**
Pse+Rho—Fib+Rho	0.567	**<0.001**	–0.006	0.999
Pse+Tet—Fib+Rho	0.424	**<0.01**	0.378	**<0.001**
Rho+Tet—Fib+Rho	0.699	**<0.001**	0.303	**<0.001**
Pse+Rho—Fib+Tet	–0.421	**<0.01**	–0.435	**<0.001**
Pse+Tet—Fib+Tet	–0.565	**<0.001**	–0.051	**<0.05**
Rho+Tet—Fib+Tet	–0.290	0.131	–0.127	**<0.001**
Pse+Tet—Pse+Rho	–0.144	0.805	0.384	**<0.001**
Rho+Tet—Pse+Rho	0.131	0.858	0.309	**<0.001**
Rho+Tet—Pse+Tet	0.275	0.171	–0.076	**<0.001**
Treatment comparison				
CLBG-CLB	–0.183	0.070	0.020	0.214
CLG-CLB	–0.558	**<0.001**	0.047	**<0.001**
CLG-CLBG	–0.376	**<0.001**	0.026	0.078

*Two-factorial ANOVA of log-transformed maximum growth rates (r_{max}) and carrying capacity (K) with F and p-values (species mixture df = 5, treatment df = 2, species*treatment df = 10, residuals df = 54) and summary of post-hoc tests (Tukey HSD) for differences between two-species-mixes and light treatments. Both growth parameters were obtained by logistic growth curve fits. For each comparison, differences in mean (diff) and adjusted p-values (p adj) are shown. Significant effects ($p < 0.05$) are highlighted in bold. Species are abbreviated as Fib (Fibrocapsa japonica), Rho (Rhodomonas salina), Pse (Pseudanabaena sp.), and Tet (Tetraselmis sp.). Treatment abbreviations indicate constant CLB, blue light; CLG, constant green light; and CLBG, constant blue-green light in simultaneous supply.*

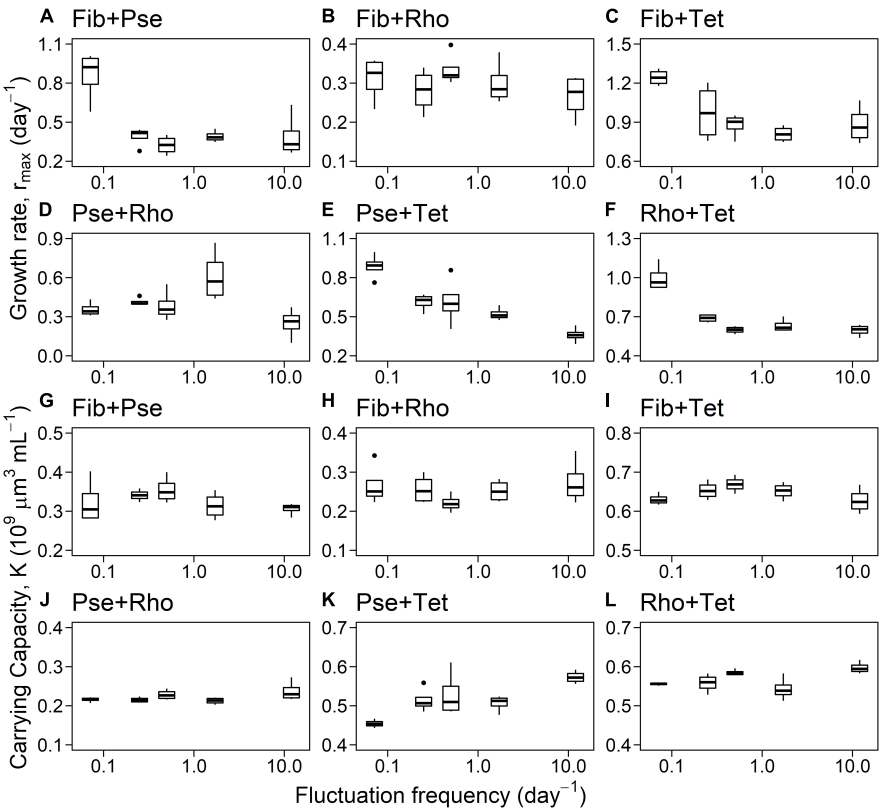

FIGURE 6 | Maximum growth rates **(A–F)** and carrying capacity **(G–L)** for two-species mixtures related to fluctuation frequency (log-scale).

a absorbing blue and red light, phycoerythrin absorbing green light, and phycocyanin absorbing orange-red light (Stomp et al., 2008; Acinas et al., 2009), suggesting that the cyanobacterium is a good competitor under different light colors. However, Luimstra et al. (2018) elucidated that, in contrast to species with chlorophyll-based pigment complexes like chlorophytes, cyanobacteria with their phycobiliproteins have a lower light-harvesting efficiency for blue light due to an imbalance in the photosystems. Thus, corresponding with Heidenreich and Richardson (2020) it seems likely that phycobiliproteins are not very effective in light-harvesting but allow the species to widen the window of absorbable wavelengths. This might explain why we did not detect higher growth responses of phycoerythrin-containing species under green light compared to species without such pigments (rejecting H1).

Species Performance Under Fluctuating Light

Monoculture experiments under constant light showed that blue and green light resulted in significant differences in the growth responses of *Fib*, *Rho*, and *Tet*, respectively. Thus, the assumption was that fluctuations between blue and green light would, depending on the frequency, also affect species performance. Our experiment revealed that fluctuations in the available light spectrum do not necessarily affect phytoplankton growth in monocultures but there are species able to tolerate these fluctuations. Generally, species maximum growth rates depended more on fluctuation frequency than species carrying capacities did. As for *Fib*, neither maximum growth rates nor carrying capacities were affected by fluctuation frequency, this supports the previous implication that the effects of the light colors on growth of *Fib* were not strong. Maximum growth rates of the other species were all significantly affected by the fluctuation frequency but not always in the same direction. While growth rates of *Tet* and *Rho* were higher with faster fluctuations, those of *Pse* decreased with increasing fluctuation frequency. Carrying capacities showed the opposite picture with those of *Rho* decreasing while the others were either increasing or not affected by fluctuation frequency. For *Pseudanabaena* sp., having the capability of complementary chromatic adaptation, Stomp et al. (2008) suggested that there might be a threshold for light color fluctuations above which it could benefit from this phenotypic plasticity. Thus, for their used strain of *Pseudanabaena* sp., fluctuations between green and red light in the order of hours were too fast for the species to acclimate. The used fluctuation frequencies in our experiment might also have been too fast for such a chromatic adaptation and in addition, the blue light color treatment we used (alteration between green and blue) did not match the phycobilin's absorption range (compared to red as in Stomp et al., 2008).

Our experiment showed that growth and capacity of phytoplankton species can be affected by the frequency of

TABLE 4 | Two-species mixtures under fluctuating light.

ANOVA	r_{max}		K	
Effect	**F**	***p***	**F**	***p***
Frequency	17.5	**<0.001**	5.5	**<0.05**
Species	41.5	**<0.001**	654.2	**<0.001**
Species * Frequency	1.0	0.411	4.9	**<0.001**
Species (*df*)	**Slope (± se)**	***p***	**Slope (± se)**	***p***
Fib+Pse	–0.0111 (0.0112)	0.337	$-2.574*10^6$ ($1.694*10^6$)	0.1461
Fib+Rho	–0.0036 (0.0026)	0.178	$2.167*10^6$ ($2.024*10^6$)	0.2984
Fib+Tet	–0.0112 (0.0094)	0.248	$-1.986*10^6$ ($1.218*10^6$)	0.1203
Pse+Rho	–0.0142 (0.0073)	0.068	$1.630*10^6$ ($0.687*10^6$)	**<0.05**
Pse+Tet	–0.0283 (0.0074)	**<0.01**	$6.464*10^6$ ($1.895*10^6$)	**<0.01**
Rho+Tet	–0.0137 (0.0075)	0.086	$3.032*10^6$ ($1.112*10^6$)	**<0.05**

*Two-factorial ANOVA of log-transformed maximum growth rates (r_{max}) and carrying capacity (K) with F and p-values (species df = 5, treatment df = 1, species*treatment df = 5, residuals df = 108). The lower part of the table gives slopes of linear regression estimating the relationship between fluctuation frequency and r_{max} or K, respectively. p adj. value indicates fit. Significant effects ($p < 0.05$) are highlighted in bold. Species were abbreviated as Fib, Fibrocapsa japonica; Rho, Rhodomonas salina; Pse, Pseudanabaena sp.; and Tet, Tetraselmis sp.*

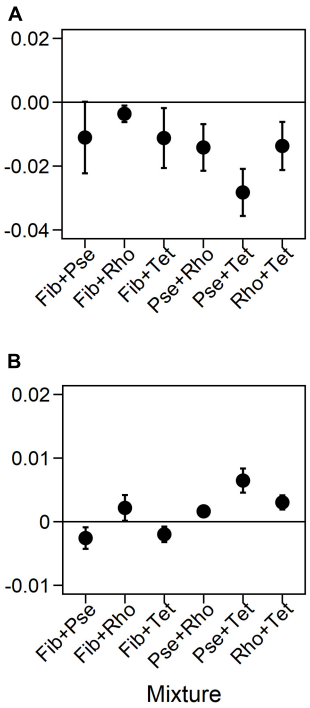

FIGURE 7 | Slopes from the relations between fluctuation frequency and responses in maximum growth rates **(A)** and carrying capacities **(B)** of the two-species mixtures. Error bars represent standard error.

fluctuating light colors but there are also species being unaffected (here *Fib* and *Tet*) which confirms partially hypothesis H2. Species showed positive and negative responses in performances to fluctuation frequency.

Competition Outcomes

According to the first part of hypothesis H3, we expected that a species with a higher growth rate for a certain light color would dominate in competition with a species, having a lower growth rate. However, the results of our experiment showed that species-specific growth rates measured in monocultures—at certain light color conditions—could not be used directly to predict the competition outcome for all mixtures. While *Tet* was observed as fast-growing species, showing overall highest maximum growth rates and carrying capacities under constant light treatment, this was reflected in the competitive outcomes in mixed cultures. On the other hand, *Rho* became a dominant species when it was mixed with *Fib* under all constant light treatments contrariwise to the observed growth traits of the species in monoculture. Thus, our results of the mixed cultures with *Fib* and *Rho* as well as the *Fib* and *Pse* mixture results conflict with hypothesis H3, as growth in mixture could not be predicted by the performance at different light colors in monocultures. It emphasizes that further factors affecting competition, such as the light characteristics and species light-use efficiencies (cf. Huisman and Weissing, 1994; Stomp et al., 2004; Luimstra et al., 2020) needs to be included.

Our hypothesis that species using blue and green light differently would be able to coexist when both light colors are supplied simultaneously was thus not supported by our results but may be explained by species light-use efficiencies (rejecting H3). Under blue-green and green light, *Pse* competitively excluded *Fib*, despite the higher maximum growth rates and carrying capacities of *Fib* in monoculture compared to those of *Pse*. This coincides again with the results of Luimstra et al. (2018) that cyanobacteria have a lower light use efficiency for blue light.

Fluctuation frequency significantly affected the population dynamics in almost all two-species mixtures, however, effects of species-specific competition were more pronounced than the effects of fluctuation frequency. According to hypothesis H2, we expected that maximum growth rates and carrying capacities in species mixtures depended on fluctuation frequency if at least one species showed differences in growth under blue and green light in monoculture, respectively. This was confirmed by all mixtures, except that of *Fib* and *Rho* showing no effect of fluctuation frequency on maximum growth rate.

Implications of Light Color Fluctuations on the Performance of Different Species

The phytoplankton species analyzed here were originally isolated from the North Sea, a habitat which has encountered severe changes in temperature (Belkin, 2009), nutrient concentrations (Radach et al., 1990; Philippart et al., 2000) and loads of organic matter (Evans et al., 2005; Dupont and Aksnes, 2013; Binding et al., 2015; Capuzzo et al., 2015; Leech et al., 2018). The phytoplankton light absorption in the North Sea is characterized by large peaks in the blue and red wavebands

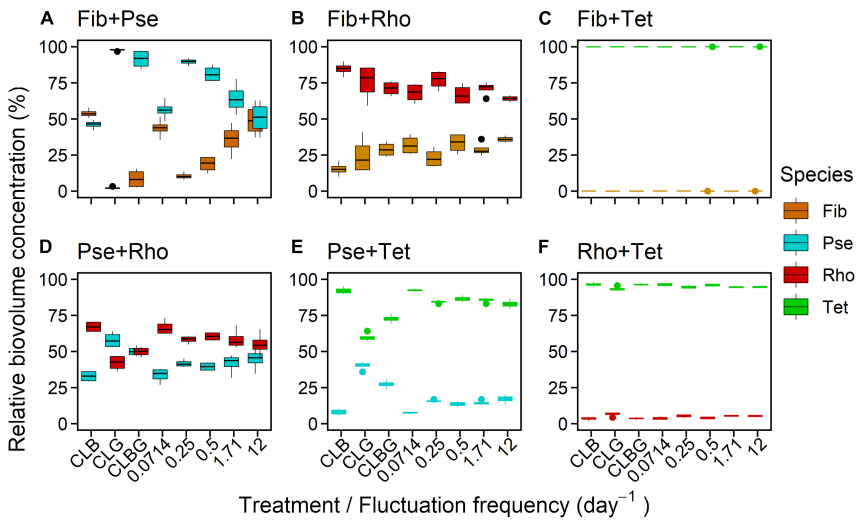

FIGURE 8 | Species-specific contribution to total biovolume (%) under constant and fluctuating conditions for two-species mixtures **(A–F)** after the experiment (16 days). Colors indicate the species in combination. The distance of both species' biovolumes indicates the extent of domination. Values of 100 and 0%, respectively, indicate exclusion. Positions on the *x*-axis were slightly shifted for better visibility.

TABLE 5 | ANOVA outcomes (*F* and *p*-values given) testing for effects of constant and fluctuating light on the relative proportion of species in the two-species mixtures.

Mixture	Constant treatments		Fluctuating treatments	
	$F_{(2,\ 9)}$	*p*	$F_{(1,\ 18)}$	*p*
Pse-Fib	185.92	**<0.001**	8.20	**<0.05**
Fib-Rho	2.83	0.111	3.36	0.083
Fib-Tet	4.57	**<0.05**	0.12	0.735
Pse-Rho	36.26	**<0.001**	3.72	0.0695
Pse-Tet	140.31	**<0.001**	6.19	**<0.05**
Rho-Tet	8.02	**<0.05**	1.61	0.220

Species were abbreviated as Fib, Fibrocapsa japonica; Rho, Rhodomonas salina; Pse, Pseudanabaena sp.; and Tet, Tetraselmis sp. Significant effects ($p < 0.05$) are highlighted in bold.

whereas green light is less absorbed (Babin et al., 2003). Green light, however, is expected to provide a significant niche for growth of small cyanobacteria due to their well-suited set of phycobiliproteins (e.g., Stomp et al., 2007b; Holtrop et al., 2021). In our study, we observed that blue and green light lead to significant differences in growth of our phytoplankton species, belonging to three different phytoplankton phyla. Whereas all eukaryotic species had lower growth rates under green light than under blue light, only the cyanobacterium (*Pse*) grew similarly well under both light colors. These species-specific results indicate that shifts in watercolor will likely affect phytoplankton growth, depending on species light-harvesting strategies (Luimstra et al., 2018; Tan et al., 2020). As the estimated effects in monocultures did not necessarily predict competition outcomes, yet provide insight on potential changes in community compositions, experiments using mixtures and thus including species competition are essential. *Pse* was the only species in our experiment which benefited from the provided green light in competition with other species, highlighting the nature of cyanobacteria to be competitively advanced in aquatic ecosystems with altered light spectra (Scheffer et al., 1997; Lebret et al., 2018; Luimstra et al., 2020). However, the species chosen for this experiment might not be representative for certain phytoplankton groups and light absorption is expected to differ in general between species. Nevertheless, in water bodies with a less pronounced turbidity but strong vertical mixing processes, phytoplankton will encounter not only a shift but a high temporal variability in light conditions, both quantitatively and qualitatively. These mixing processes occur within the order of hours to days (e.g., Denman and Gargett, 1983) and thus greatly overlap with the tested light fluctuations here. Together with the large number of studies, demonstrating that growth of phytoplankton species is strongly affected by light intensity fluctuations, depending on species-specific traits (Nicklisch, 1998; Litchman, 2000; Guislain et al., 2019) we can contribute with this first attempt, that growth of phytoplankton species is also affected by fluctuations in light color although responses seem to be species-specific. The importance of light quality for natural phytoplankton populations is of increasing concern as several studies are reporting decreasing water clarity and shifts in underwater light spectra of coastal seas and lakes (Evans et al., 2005; Dupont and Aksnes, 2013; Binding et al., 2015; Capuzzo et al., 2015; Leech et al., 2018). Moreover, in future scenarios the patterns and frequencies of mixing processes are expected to change and affect phytoplankton (Saros et al., 2012; Sydeman et al., 2014; Somavilla et al., 2017). First studies show that such spectral shifts and altered light availability will likely affect phytoplankton growth and community structure (e.g., Thrane et al., 2014; Lebret et al., 2018; Mustaffa et al., 2020), emphasizing the importance of light as a dynamic environmental factor for the phytoplankton in aquatic ecosystems.

CONCLUSION

Our experimental outcomes demonstrate that shifts in watercolor within natural systems will likely affect phytoplankton growth, depending on species light-harvesting strategies. *Pseudanabaena* sp. benefited from the provided green light in competition with other species, highlighting the nature of cyanobacteria to be competitively advanced in aquatic ecosystems with such light spectra. Despite the frequency of fluctuation resulting in significant effects, the competition outcome under fluctuating light was outweighed by the combination of competitors, hence outcomes being species-specific. Nevertheless, the fluctuation in light color significantly influenced the species dynamics in mixed cultures and the light color use efficiency thus should be considered as important species-specific trait among others (as e.g., light-absorption properties, maximum growth rates, carrying capacities) to influence the outcomes of phytoplankton competition for light. The reported results here may be the first step to improve knowledge about the significance of fluctuating light conditions for phytoplankton growth and competition, not only in intensity but also in the quality of light.

DATA AVAILABILITY STATEMENT

The raw data supporting the conclusions of this article will be made available by the authors, without undue reservation.

AUTHOR CONTRIBUTIONS

NH and MSt designed the experiment. SN, NH, and MSc constructed the experimental setup. SN, MSt, and NH conducted the experiment. SN and MSt analyzed the data and drafted the manuscript, with input from all co-authors. All authors contributed to the article and approved the submitted version.

FUNDING

The project was funded by the German Research Foundation (DFG: STR 1383/5-1 and WA 2445/13-1).

ACKNOWLEDGMENTS

We thank Julian Zeller for supporting sampling and analysis. We also thank the editor and reviewers for their constructive comments on the manuscript.

SUPPLEMENTARY MATERIAL

The Supplementary Material for this article can be found online at: https://www.frontiersin.org/articles/10.3389/fmars.2022.824624/full#supplementary-material

REFERENCES

Abiusi, F., Sampietro, G., Marturano, G., Biondi, N., Rodolfi, L., D'Ottavio, M., et al. (2014). Growth, photosynthetic efficiency, and biochemical composition of *Tetraselmis suecica* F&M-M33 grown with LEDs of different colors. *Biotechnol. Bioeng.* 111, 956–964. doi: 10.1002/bit.25014

Acinas, S. G., Haverkamp, T. H. A., Huisman, J., and Stal, L. J. (2009). Phenotypic and genetic diversification of *Pseudanabaena* spp. (cyanobacteria). *ISME J.* 3, 31–46. doi: 10.1038/ismej.2008.78

Babin, M., Stramski, D., Ferrari, G. M., Claustre, H., Bricaud, A., Obolensky, G., et al. (2003). Variations in the light absorption coefficients of phytoplankton, nonalgal particles, and dissolved organic matter in coastal waters around Europe. *J. Geophys. Res. Oceans* 108:3211. doi: 10.1029/2001jc000882

Belkin, I. M. (2009). Rapid warming of large marine ecosystems. *Prog. Oceanogr.* 81, 207–213. doi: 10.1016/j.pocean.2009.04.011

Bernhardt, J. R., O'Connor, M. I., Sunday, J. M., and Gonzalez, A. (2020). Life in fluctuating environments. *Philos. Trans. R. Soc. B Biol. Sci.* 375:20190454. doi: 10.1098/rstb.2019.0454

Bidigare, R. R., Marra, J., Dickey, T. D., Iturriaga, R., Baker, K. S., Smith, R. C., et al. (1990). Evidence for phytoplankton succession and chromatic adaptation in the Sargasso Sea during spring 1985. *Mar. Ecol. Prog. Ser.* 60, 113–122. doi: 10.3354/meps060113

Binding, C. E., Greenberg, T. A., Watson, S. B., Rastin, S., and Gould, J. (2015). Long term water clarity changes in North America's Great Lakes from multi-sensor satellite observations. *Limnol. Oceanogr.* 60, 1976–1995. doi: 10.1002/lno.10146

Bland, E., and Angenent, L. T. (2016). Pigment-targeted light wavelength and intensity promotes efficient photoautotrophic growth of Cyanobacteria. *Bioresour. Technol.* 216, 579–586. doi: 10.1016/j.biortech.2016.05.116

Bryant, D. A., and Cohenbazire, G. (1981). Effects of chromatic illumination on Cyanobacterial Phycobilisomes evidence for the specific induction of a second pair of Phycocyanin subunits in *Pseudanabaena* 7409 grown in red light. *Eur. J. Biochem.* 119, 415–424. doi: 10.1111/j.1432-1033.1981.tb05624.x

Capuzzo, E., Stephens, D., Silva, T., Barry, J., and Forster, R. M. (2015). Decrease in water clarity of the southern and central North Sea during the 20th century. *Glob. Chang. Biol.* 21, 2206–2214. doi: 10.1111/gcb.12854

Croce, R., and van Amerongen, H. (2014). Natural strategies for photosynthetic light harvesting. *Nat. Chem. Biol.* 10, 492–501. doi: 10.1038/nchembio.1555

da Silva, A. F., Lourenco, S. O., and Chaloub, R. M. (2009). Effects of nitrogen starvation on the photosynthetic physiology of a tropical marine microalga *Rhodomonas* sp (Cryptophyceae). *Aquat. Bot.* 91, 291–297. doi: 10.1016/j.aquabot.2009.08.001

Denman, K. L., and Gargett, A. E. (1983). Time and space scales of vertical mixing and advection of phytoplankton in the upper ocean. *Limnol. Oceanogr.* 28, 801–815. doi: 10.4319/lo.1983.28.5.0801

Dera, J., and Gordon, H. R. (1968). Light field fluctuations in the photic zone. *Limnol. Oceanogr.* 13, 697–699. doi: 10.4319/lo.1968.13.4.0697

Dubinsky, Z., and Stambler, N. (2009). Photoacclimation processes in phytoplankton: mechanisms, consequences, and applications. *Aquat. Microb. Ecol.* 56, 163–176. doi: 10.3354/ame01345

Dupont, N., and Aksnes, D. L. (2013). Centennial changes in water clarity of the Baltic Sea and the North Sea. *Estuar. Coast. Shelf Sci.* 131, 282–289. doi: 10.1016/j.ecss.2013.08.010

Dutkiewicz, S., Hickman, A. E., Jahn, O., Henson, S., Beaulieu, C., and Monier, E. (2019). Ocean colour signature of climate change. *Nat. Commun.* 10:578. doi: 10.1038/s41467-019-08457-x

Elser, J. J., Bracken, M. E. S., Cleland, E. E., Gruner, D. S., Harpole, W. S., Hillebrand, H., et al. (2007). Global analysis of nitrogen and phosphorus limitation of primary producers in freshwater, marine and terrestrial ecosystems. *Ecol. Lett.* 10, 1135–1142. doi: 10.1111/j.1461-0248.2007.01113.x

Evans, C. D., Monteith, D. T., and Cooper, D. M. (2005). Long-term increases in surface water dissolved organic carbon: observations, possible causes and environmental impacts. *Environ. Pollut.* 137, 55–71. doi: 10.1016/j.envpol.2004.12.031

Falkowski, P. G. (1984). Physiological responses of phytoplankton to natural light regimes. *J. Plankton Res.* 6, 295–307. doi: 10.1093/plankt/6.2.295

Falkowski, P. G. (1994). The role of phytoplankton photosynthesis in global biogeochemical cycles. *Photosynth. Res.* 39, 235–258. doi: 10.1007/BF00014586

Falkowski, P. G. (2012). The power of plankton. *Nature* 483, S17–S20. doi: 10.1038/483S17a

Falkowski, P. G., and Raven, J. A. (2007). *Aquatic Photosynthesis*. Princeton, NJ: Princeton University Press.

Falkowski, P. G., Barber, R. T., and Smetacek, V. (1998). Biogeochemical controls and feedbacks on ocean primary production. *Science* 281, 200–206. doi: 10.1126/science.281.5374.200

Ferris, J. M., and Christian, R. (1991). Aquatic primary production in relation to microalgal responses to changing light: a review. *Aquat. Sci.* 53, 187–217. doi: 10.1007/bf00877059

Field, C. B., Behrenfeld, M. J., Randerson, J. T., and Falkowski, P. (1998). Primary production of the biosphere: integrating terrestrial and oceanic components. *Science* 281, 237–240. doi: 10.1126/science.281.5374.237

Flöder, S., and Burns, C. W. (2005). The influence of fluctuating light on diversity and species number of nutrient-limited phytoplankton. *J. Phycol.* 41, 950–956. doi: 10.1111/j.1529-8817.2005.00124.x

Flöder, S., Urabe, J., and Kawabata, Z. (2002). The influence of fluctuating light intensities on species composition and diversity of natural phytoplankton communities. *Oecologia* 133, 395–401. doi: 10.1007/s00442-002-1048-8

Fox, J. W., and Sanford, W. (2019). *An R Companion to Applied Regression*. Thousand Oaks, CA: Sage.

Guidi-Rontani, C., Maheswari, U., Jabbari, K., and Bowler, C. (2010). Comparative ecophysiology and genomics of the toxic unicellular alga *Fibrocapsa japonica*. *New Phytol.* 185, 446–458. doi: 10.1111/j.1469-8137.2009.03074.x

Guillard, R. R. L. (1975). "Culture of phytoplankton for feeding marine invertebrates," in *Culture of Marine Invertebrate Animals*, eds W. L. Smith and M. H. Chanley (New York, NY: Plenum Publishing), 29–60.

Guillard, R. R. L., and Ryther, J. H. (1962). Studies of marine planktonic diatoms. I. *Cyclotella nana* Hustedt, and *Detonula confervacea* (Cleve) Gran. *Can. J. Microbiol.* 8, 229–239. doi: 10.1139/m62-029

Guislain, A., Beisner, B. E., and Kohler, J. (2019). Variation in species light acquisition traits under fluctuating light regimes: implications for non-equilibrium coexistence. *OIKOS* 128, 716–728. doi: 10.1111/oik.05297

Heidenreich, K. M., and Richardson, T. L. (2020). Photopigment, absorption, and growth responses of marine cryptophytes to varying spectral irradiance. *J. Phycol.* 56, 507–520. doi: 10.1111/jpy.12962

Hickman, A. E., Holligan, P. M., Moore, C. M., Sharples, J., Krivtsov, V., and Palmer, M. R. (2009). Distribution and chromatic adaptation of phytoplankton within a shelf sea thermocline. *Limnol. Oceanogr.* 54, 525–536. doi: 10.4319/lo.2009.54.2.0525

Hillebrand, H., Dürselen, C. D., Kirschtel, D., Pollingher, U., and Zohary, T. (1999). Biovolume calculation for pelagic and benthic microalgae. *J. Phycol.* 35, 403–424. doi: 10.1046/j.1529-8817.1999.3520403.x

Holtrop, T., Huisman, J., Stomp, M., Biersteker, L., Aerts, J., Grébert, T., et al. (2021). Vibrational modes of water predict spectral niches for photosynthesis in lakes and oceans. *Nat. Ecol. Evol.* 5, 55–66. doi: 10.1038/s41559-020-01330-x

Huisman, J., and Weissing, F. J. (1994). LIGHT-LIMITED GROWTH AND COMPETITION FOR LIGHT IN WELL-MIXED AQUATIC ENVIRONMENTS – AN ELEMENTARY MODEL. *Ecology* 75, 507–520. doi: 10.2307/1939554

Hutchinson, G. E. (1961). The paradox of the plankton. *Am. Nat.* 95, 137–145. doi: 10.1086/282171

Kirk, J. T. O. (2011). *Light and Photosynthesis in Aquatic Ecosystems*. Cambridge: Cambridge University Press.

Latsos, C., van Houcke, J., Blommaert, L., Verbeeke, G. P., Kromkamp, J., and Timmermans, K. R. (2021). Effect of light quality and quantity on productivity and phycoerythrin concentration in the cryptophyte *Rhodomonas* sp. *J. Appl. Phycol.* 33, 729–741. doi: 10.1007/s10811-020-02338-3

Lawrenz, E., and Richardson, T. L. (2017). Differential effects of changes in spectral irradiance on photoacclimation, primary productivity and growth in *Rhodomonas salina* (Cryptophyceae) and *Skeletonema costatum* (Bacillariophyceae) in simulated blackwater environments. *J. Phycol.* 53, 1241–1254. doi: 10.1111/jpy.12578

Lebret, K., Langenheder, S., Colinas, N., Ostman, O., and Lindstrom, E. S. (2018). Increased water colour affects freshwater plankton communities in a mesocosm study. *Aquat. Microb. Ecol.* 81, 1–17. doi: 10.3354/ame01858

Leech, D. M., Pollard, A. I., Labou, S. G., and Hampton, S. E. (2018). Fewer blue lakes and more murky lakes across the continental US: implications for planktonic food webs. *Limnol. Oceanogr.* 63, 2661–2680. doi: 10.1002/lno.10967

Litchman, E. (1998). Population and community responses of phytoplankton to fluctuating light. *Oecologia* 117, 247–257. doi: 10.1007/s004420050655

Litchman, E. (2000). Growth rates of phytoplankton under fluctuating light. *Freshw. Biol.* 44, 223–235. doi: 10.1046/j.1365-2427.2000.00559.x

Litchman, E. (2003). Competition and coexistence of phytoplankton under fluctuating light: experiments with two cyanobacteria. *Aquat. Microb. Ecol.* 31, 241–248. doi: 10.3354/ame031241

Luimstra, V. M., Schuurmans, J. M., Verschoor, A. M., Hellingwerf, K. J., Huisman, J., and Matthijs, H. C. P. (2018). Blue light reduces photosynthetic efficiency of cyanobacteria through an imbalance between photosystems I and II. *Photosynth. Res.* 138, 177–189. doi: 10.1007/s11120-018-0561-5

Luimstra, V. M., Verspagen, J. M. H., Xu, T., Schuurmans, J. M., and Huisman, J. (2020). Changes in water color shift competition between phytoplankton species with contrasting light-harvesting strategies. *Ecology* 101:e02951. doi: 10.1002/ecy.2951

Morel, A. (1980). In-water and remote measurements of ocean color. *Boundary Layer Meteorol.* 18, 177–201. doi: 10.1007/bf00121323

Mustaffa, N. I. H., Kallajoki, L., Biederbick, J., Binder, F. I., Schlenker, A., and Striebel, M. (2020). Coastal ocean darkening effects via Terrigenous DOM addition on plankton: an indoor mesocosm experiment. *Front. Mar. Sci.* 7:547829. doi: 10.3389/fmars.2020.547829

Nicklisch, A. (1998). Growth and light absorption of some planktonic cyanobacteria, diatoms and Chlorophyceae under simulated natural light fluctuations. *J. Plankton Res.* 20, 105–119. doi: 10.1093/plankt/20.1.105

Olenina, I., Hajdu, S., Edler, L., Andersson, A., Wasmund, N., Busch, S., et al. (2006). Biovolumes and size-classes of phytoplankton in the Baltic Sea. *HELCOM Baltic Sea Environ. Proc.* 106, 1–144.

Philippart, C. J. M., Cadée, G. C., van Raaphorst, W., and Riegman, R. (2000). Long-term phytoplankton-nutrient interactions in a shallow coastal sea: algal community structure, nutrient budgets, and denitrification potential. *Limnol. Oceanogr.* 45, 131–144. doi: 10.4319/lo.2000.45.1.0131

R Core Team (2020). *R: A Language and Environment for Statistical Computing*. Vienna: R Foundation for Statistical Computing.

Radach, G., Berg, J., and Hagmeier, E. (1990). Long-term changes of the annual cycles of meteorological, hydrographic, nutrient and phytoplankton time series at Helgoland and at LV ELBE 1 in the German Bight. *Cont. Shelf Res.* 10, 305–328. doi: 10.1016/0278-4343(90)90054-P

Richerson, P., Armstrong, R., and Goldman, C. R. (1970). Contemporaneous disequilibrium, a new hypothesis to explain the "Paradox of the Plankton". *Proc. Natl. Acad. Sci. U.S.A.* 67, 1710–1714. doi: 10.1073/pnas.67.4.1710

Roy, S., Llewellyn, C. A., Egeland, E. S., and Johnsen, G. (2011). *Phytoplankton Pigments: Characterization, Chemotaxonomy, and Applications in Oceanography*. Cambridge: Cambridge University Press.

Saros, J. E., Stone, J. R., Pederson, G. T., Slemmons, K. E., Spanbauer, T., Schliep, A., et al. (2012). Climate-induced changes in lake ecosystem structure inferred from coupled neo- and paleoecological approaches. *Ecology* 93, 2155–2164. doi: 10.1890/11-2218.1

Scheffer, M., Rinaldi, S., Gragnani, A., Mur, L. R., and van Nes, E. H. (1997). On the dominance of filamentous cyanobacteria in shallow, Turbid Lakes. *Ecology* 78, 272–282.

Schulze, P. S. C., Guerra, R., Pereira, H., Schuler, L. M., and Varela, J. C. S. (2017). Flashing LEDs for microalgal production. *Trends Biotechnol.* 35, 1088–1101. doi: 10.1016/j.tibtech.2017.07.011

Schwaderer, A. S., Yoshiyama, K., de Tezanos Pinto, P., Swenson, N. G., Klausmeier, C. A., and Litchman, E. (2011). Eco-evolutionary differences in light utilization traits and distributions of freshwater phytoplankton. *Limnol. Oceanogr.* 56, 589–598. doi: 10.4319/lo.2011.56.2.0589

Somavilla, R., Gonzalez-Pola, C., and Fernandez-Diaz, J. (2017). The warmer the ocean surface, the shallower the mixed layer. How much of this is true? *J. Geophys. Res. Oceans* 122, 7698–7716. doi: 10.1002/2017JC013125

Stomp, M., Huisman, J., de Jongh, F., Veraart, A. J., Gerla, D., Rijkeboer, M., et al. (2004). Adaptive divergence in pigment composition promotes phytoplankton biodiversity. *Nature* 432, 104–107. doi: 10.1038/nature03044

Stomp, M., Huisman, J., Stal, L. J., and Matthijs, H. C. P. (2007a). Colorful niches of phototrophic microorganisms shaped by vibrations of the water molecule. *ISME J.* 1, 271–282. doi: 10.1038/ismej.2007.59

Stomp, M., Huisman, J., Voros, L., Pick, F. R., Laamanen, M., Haverkamp, T., et al. (2007b). Colourful coexistence of red and green picocyanobacteria in lakes and seas. *Ecol. Lett.* 10, 290–298. doi: 10.1111/j.1461-0248.2007.01026.x

Stomp, M., van Dijk, M. A., van Overzee, H. M. J., Wortel, M. T., Sigon, C. A. M., Egas, M., et al. (2008). The timescale of phenotypic plasticity and its impact on competition in fluctuating environments. *Am. Nat.* 172, E169–E185. doi: 10.1086/591680

Sydeman, W. J., Garcia-Reyes, M., Schoeman, D. S., Rykaczewski, R. R., Thompson, S. A., Black, B. A., et al. (2014). Climate change. Climate change and wind intensification in coastal upwelling ecosystems. *Science* 345, 77–80. doi: 10.1126/science.1251635

Tan, X., Zhang, D. F., Duan, Z. P., Parajuli, K., and Hu, J. Y. (2020). Effects of light color on interspecific competition between *Microcystis aeruginosa* and *Chlorella pyrenoidosa* in batch experiment. *Environ. Sci. Pollut. Res.* 27, 344–352. doi: 10.1007/s11356-019-06650-5

Tandeau de Marsac, N. (1977). Occurrence and nature of chromatic adaptation in cyanobacteria. *J. Bacteriol.* 130, 82–91. doi: 10.1128/jb.130.1.82-91.1977

Thrane, J. E., Hessen, D. O., and Andersen, T. (2014). The absorption of light in lakes: negative impact of dissolved organic carbon on primary productivity. *Ecosystems* 17, 1040–1052. doi: 10.1007/s10021-014-9776-2

Tilman, D., Kilham, S. S., and Kilham, P. (1982). Phytoplankton community ecology – The role of limiting nutrients. *Annu. Rev. Ecol. Syst.* 13, 349–372. doi: 10.1146/annurev.es.13.110182.002025

Wall, D., and Briand, F. (1979). Response of lake phytoplankton communities to in situ manipulations of light intensity and colour. *J. Plankton Res.* 1, 103–112. doi: 10.1093/plankt/1.1.103

Walsh, P., and Legendre, L. (1983). Photosynthesis of natural phytoplankton under high frequency light fluctuations simulating those induced by sea surface waves. *Limnol. Oceanogr.* 28, 688–697. doi: 10.4319/lo.1983.28.4.0688

Wickham, H. (2016). *ggplot2: Elegant Graphics for Data Analysis*. New York, NY: Springer-Verlag.

Conflict of Interest: The authors declare that the research was conducted in the absence of any commercial or financial relationships that could be construed as a potential conflict of interest.

Publisher's Note: All claims expressed in this article are solely those of the authors and do not necessarily represent those of their affiliated organizations, or those of the publisher, the editors and the reviewers. Any product that may be evaluated in this article, or claim that may be made by its manufacturer, is not guaranteed or endorsed by the publisher.

frontiers | Frontiers in Marine Science

MINI REVIEW
published: 16 June 2022
doi: 10.3389/fmars.2022.864797

Adaptive Strategies and Evolutionary Responses of Microbial Organisms to Changing Oceans

Bovern Suchart Arromrak, Zhenzhen Li and Juan Diego Gaitán-Espitia *

School of Biological Sciences and The Swire Institute of Marine Sciences, The University of Hong Kong, Hong Kong, Hong Kong SAR, China

Environmental variability is an intrinsic characteristic of nature. Variability in factors such as temperature, UV, salinity, and nutrient availability can influence structural and functional properties of marine microbial organisms. This influence has profound implications for biochemical cycles and the ecosystem services provided by the oceans. In this review we discuss some of the most relevant mechanisms underpinning adaptive strategies of microbial organisms in variable and dynamic oceans. We assess the extent to which the magnitude and rate of environmental change influence plastic phenotypic adjustments and evolutionary trajectories of microbial populations. This understanding is fundamental for developing better predictions regarding microbial dynamics at ecological and evolutionary time-scales and in response to climate change.

Keywords: phenotypic plasticity, adaptive evolution, phytoplankton, bacteria, climate change, environmental change

OPEN ACCESS

Edited by:
Michael Raatz,
Max Planck Institute for Evolutionary Biology, Germany

Reviewed by:
Francisca C. García,
King Abdullah University of Science and Technology, Saudi Arabia
Giannina Hattich,
Åbo Akademi University, Finland

***Correspondence:**
Juan Diego Gaitán-Espitia
juadiegaitan@gmail.com

Specialty section:
This article was submitted to Global Change and the Future Ocean, a section of the journal Frontiers in Marine Science

Received: *28 January 2022*
Accepted: *23 May 2022*
Published: *16 June 2022*

Citation:
Arromrak BS, Li Z and Gaitán-Espitia JD (2022) Adaptive Strategies and Evolutionary Responses of Microbial Organisms to Changing Oceans. Front. Mar. Sci. 9:864797. doi: 10.3389/fmars.2022.864797

INTRODUCTION

Oceans are highly variable environments. These systems are characterized by marked fluctuations in environmental conditions (e.g., salinity, pH, temperature, nutrients, irradiance), that operate at different temporal (second to decades) and spatial scales (millimeters to kilometers), creating heterogenous seascapes (Boyd et al., 2016a; Rodríguez-Romero et al., 2022). Such fluctuations modulate the environmental envelope (i.e., a set of environmental variables and conditions that favours species occurrence; **Figures 1A, B**) of marine microbial communities (Boyd et al., 2010), their distribution and ecological dynamics (Brun et al., 2015), as well as their structure and function across time and space (Tinta et al., 2015; Hutchins and Fu, 2017; Di Pane et al., 2022). However, marine microbes are not static units as they can display a range of biological strategies to short-term changes in environmental conditions such as those occurring at time-scales approximating microbial division times (i.e., within generations; **Figure 1C**) (Litaker et al., 1993). These strategies mainly involve non-genetic phenotypic adjustments (i.e., phenotypic plasticity) that allow microbes to actively respond to the physiological challenges imposed by environmental fluctuations at such time-scales (Chevin et al., 2013; Schaum et al., 2013; Boyd et al., 2016a; Collins et al., 2020). For instance, short-term fluctuations (e.g., diurnal cycles) in drivers such as underwater irradiance (light intensity/quality), temperature and/or nutrient availability can potentially induce stressful conditions to marine microorganisms, triggering compensatory behavioral (e.g., vertical migration; Aumack et al., 2014) and metabolic (e.g., photosynthetic activity; Gaidarenko et al., 2019) adjustments. The outcome of these phenotypic responses can be adaptive, neutral or maladaptive

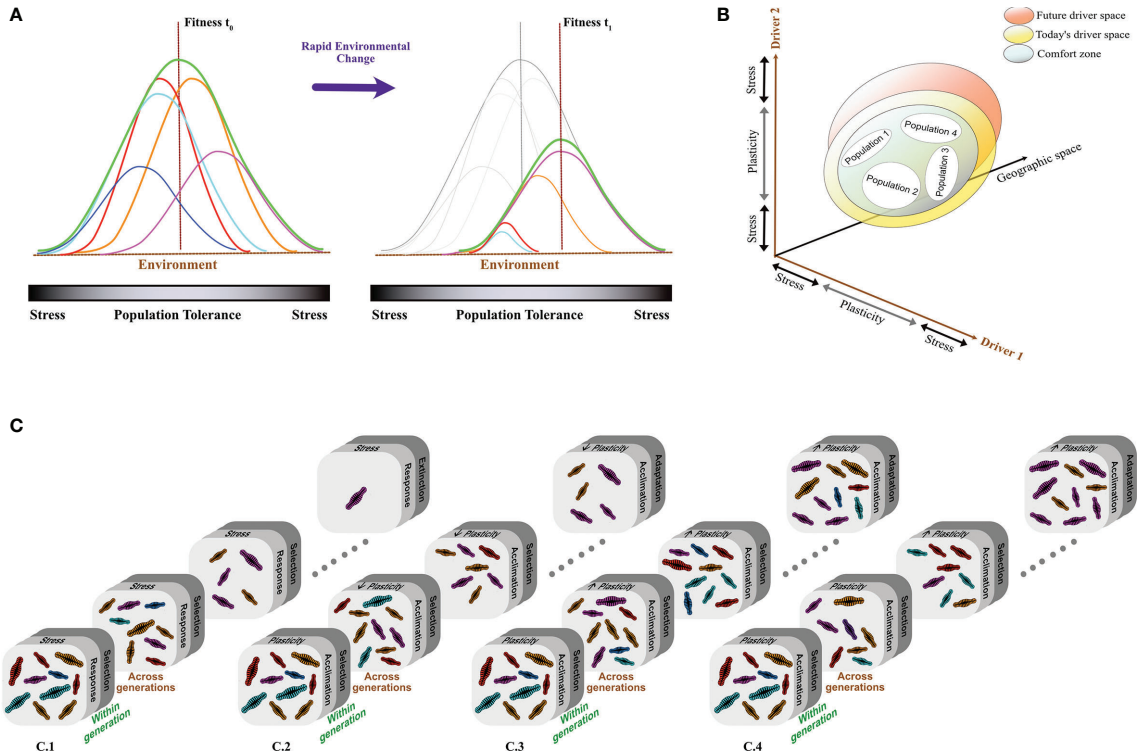

FIGURE 1 | Ecological and evolutionary dynamics of marine microbial organisms in variable and dynamic oceans. **(A)** The overall fitness of a population (green curve) is a function of the tolerances and capacity for plastic adjustments of individual genotypes/strains (colour curves). This function determines the adaptive capacity of a population to persist after rapid environmental changes. **(B)** These changes involve more than one driver at the time. In a population, the balance between tolerances, plasticity and stress for each driver determines its ecological niche and helps to predict the capacity to respond to future environmental changes. Different populations can be locally adapted as result of differences in the environmental conditions and the variability they experience. This can explain the geographic differences in the capacity for phenotypic plasticity and adaptive potential (e.g., narrower or closer to their tolerance limits). **(C)** Populations with contrasting differences in the capacity for plastic adjustments, tolerances and potential for adaptive evolution in response to environmental changes show divergent ecological and evolutionary dynamics (within and across generations). Rapid reduction of genetic diversity and high extinction risk is expected for populations with limited phenotypic plasticity inhabiting stable environments where only one driver changes (C.1). If plasticity is present, it can buffer the influence of selection mitigating population decline and extinction (C.2). Fluctuating environments are hypothesised to facilitate plasticity promoting the maintenance of phenotypic/genetic diversity as a consequence of reduced strength of directional selection (C.3). However, if multiple drivers are interacting and changing in these environments, selection is going to be stronger accelerating the fixation of "optimal" phenotypes (more tolerant to directional changes in dominant drivers; C.4).

(i.e., not adjusting adequately to the new environment) depending on the interaction with other environmental drivers (e.g., light x salinity; Sauer et al., 2002) and the overall effect on organismal fitness (Chevin et al., 2013). Although plasticity provides a mechanism for adaptation to changing environments (e.g., Schaum et al., 2013; Kremer et al., 2018), there are limits for plastic responses (DeWitt et al., 1998; Fox et al., 2019; Gill et al., 2022), beyond which genetic adjustments are required to persist (Fox et al., 2019; Gaitán-Espitia and Hobday, 2021). These responses (i.e., adaptive evolution) are particularly relevant if unfavorable environmental changes are difficult to track (unpredictable or occur too rapidly) and persist beyond few generations (Chevin et al., 2013; Bernhardt et al., 2020; Collins et al., 2020). Nevertheless, the ability to undergo these adjustments varies within and across populations (**Figures 1B, C**) depending on the presence of genetic variation for ecologically important traits (Chevin et al., 2013; Godhe and Rynearson, 2017), and on the strength (e.g., the intensity of selection increases with the number of drivers) and form/direction of natural selection (e.g., directional selection under ocean warming; **Figure 1C**) (Brennan et al., 2017; Collins et al., 2020; Walworth et al., 2020). These components of selection are ultimately determined by the magnitude and rate of environmental change (Gaitán-Espitia et al., 2017a; Collins et al., 2020). Consequently, inadequate responses (e.g., neutral or maladaptive) to unfavorable conditions (i.e., where selection is strong and induce significant loss of fitness) can drive population declines and local extinctions (**Figure 1C**). Contrarily, adaptive responses to stress due to environmental change may lead to phenotypic and genetic changes associated to the evolution of tolerance to novel conditions *via* increased physiological resistance levels, behavioral (e.g., vertical migration) and life-history (e.g., dormancy) avoidance of the stressful conditions. These adaptive evolutionary responses can allow the maintenance of biodiversity and the persistence of populations despite the negative effects on fitness initially induced by

environmental change (**Figure 1C**) (Boyd et al., 2016a; Schaum et al., 2016; Schluter et al., 2016; Fox et al., 2019; Collins et al., 2020; Walworth et al., 2020). In this review, we discuss some of the most relevant mechanisms underpinning the adaptive strategies of microbial organisms and their evolutionary responses and outcomes in variable and dynamic oceans.

SHORT-TERM RESPONSES: ADAPTIVE STRATEGIES TO ENVIRONMENTAL VARIABILITY

Phenotypic plasticity offers a fundamental mechanism for marine microbes to cope with short-time environmental fluctuations, allowing them to track environmental changes and escape local extinction (**Figure 1C**) (Chevin et al., 2013). This capacity for rapid phenotypic adjustments is considered to be shaped by the level of environmental variability experienced by populations (e.g., higher plasticity in organisms from more heterogeneous environments; Boyd et al., 2016a), and the predictability of environmental change (e.g., lower plasticity in less predictable environments; Schaum and Collins, 2014; Bernhardt et al., 2020; Leung et al., 2020; Gill et al., 2022) (**Figure 2**). Here, we described three common short-term adaptive plastic responses of microbial organisms (i.e. direct environmental sensing-response, anticipatory-memory response, and diversified bet-hedging strategy) to environmental fluctuation (**Figure 2**). While the mechanisms are described individually in the next section, they are not mutually exclusive, as microbes may combine two or three strategies depending on the magnitude and rate of environmental variability (i.e., the strength and direction of selection).

Adaptive Plasticity *via* Sense-Response Regulatory Mechanisms

The most common mechanism employed by marine microbes to cope with environmental changes is modulated at the transcriptional level where a specific environmental stimuli/condition triggers the expression of a specific phenotype (sensing-regulatory response) (**Figure 2E**; Forsman, 2015; Bonamour et al., 2019). For prokaryotes, plasticity in their responses to environmental stimuli is primarily mediated by the two-component signal transduction systems (TCS) (Capra and Laub, 2012; Held et al., 2019). While there are variants to the prokaryotic TCS, the canonical systems are structured by two conserved components called the histidine protein kinases (HPK) and response regulator (RR) (Zschiedrich et al., 2016; Busby, 2019). Although TCS are prevalent in prokaryotes, these signaling elements have also been co-opted to meet the needs of signal transduction in microbial eukaryotes (Schaller et al., 2011). For these organisms, the gene expression/repression activity often involves more complex regulatory networks than those seen in the prokaryotic TCS (Madhani, 2013; Cruz de Carvalho et al., 2016). Nevertheless, in both domains, organisms share some similarity in their plastic responses to environmental stimuli evidenced by the initiation of transcription *via* RNA polymerase (Andrews, 2017).

A classic system for the study of sensing-regulatory response as an adaptive strategy to short-term scale environmental change comes from the nutrient limitation research. Nutrient limitation or exhaustion is a prevailing environmental challenge often experienced by microbes, rendering them constantly changing between feast and famine states (Suzuki et al., 2004; Rozen and Belkin, 2005; Cruz de Carvalho et al., 2016; Andrews, 2017). One of the solutions "wield" by microbes to cope with fluctuations in nutrients is through transcriptional reprogramming (Brown et al., 2014). For example, upon sensing limitation in the nitrogen (N) supply in surrounding environment, prokaryotic microbes can display a global alteration in gene expression, shifting from growth-associated transcriptomes to growth-arrested stationary-phase transcriptomes (Brown et al., 2014; Switzer et al., 2018). This is an important mechanism for conservation and allocation of resources mainly for cellular maintenance and repairing activities under unfavorable conditions. In photosynthetic microbes, similar adaptive regulatory mechanisms to cope with short-term fluctuations in nutrient availability have been documented (Suzuki et al., 2004; Bender et al., 2014; Cruz de Carvalho et al., 2016; Matthijs et al., 2017). Under these conditions (i.e., fluctuations in phosphate or nitrogen), photosynthetic microbes such as cyanobacteria and diatoms can activate sensory stress response and signaling systems that combine "bacterial CTS" (Suzuki et al., 2004; Cruz de Carvalho et al., 2016) with more complex pathways (e.g., nutrient recycling, carbohydrate and fatty acid metabolism; Bender et al., 2014), and non-coding regulatory systems (e.g., long intergenic nonprotein coding RNAs; Cruz de Carvalho et al., 2016). Comparable signaling-regulatory responses have been documented in marine diatoms exposed to fluctuations in salinity (Krell et al., 2008) and irradiance (Depauw et al., 2012), in which complex signal transduction cascades and regulatory processes, including transcriptional and post-transcriptional networks, second messengers, and chromatin remodeling are activated as part of the adaptive response (Krell et al., 2008; Depauw et al., 2012).

Adaptive Plasticity *via* Anticipatory and Memory Mechanisms

Some microbes have evolved the ability to anticipate future conditions as a result of evolving in highly predictable environments (**Figure 2D**; Johnson et al., 2008; Tagkopoulos et al., 2008; Gill et al., 2022). For example, several species of marine diatoms can cope with highly variable light conditions, as they possess suitable molecular systems that allow them to perceive, respond to, and anticipate light variations (Sauer et al., 2002; Depauw et al., 2012; Aumack et al., 2014; Serôdio, 2021). The capacity to anticipate daily changes in illumination was explained by the endogenous circadian clock in marine diatoms, a biological system that could be linked to light-driven gene expression regulatory mechanisms (Depauw et al., 2012). The anticipatory mechanism explains behavioural plastic responses of marine microbes to changes in environmental conditions. For instance, photosynthetic microbes in marine sediments exhibit vertical migrations characterized by rhythmic and synchronized movement of cells upward towards the surface of the sediment at the beginning of daytime periods of

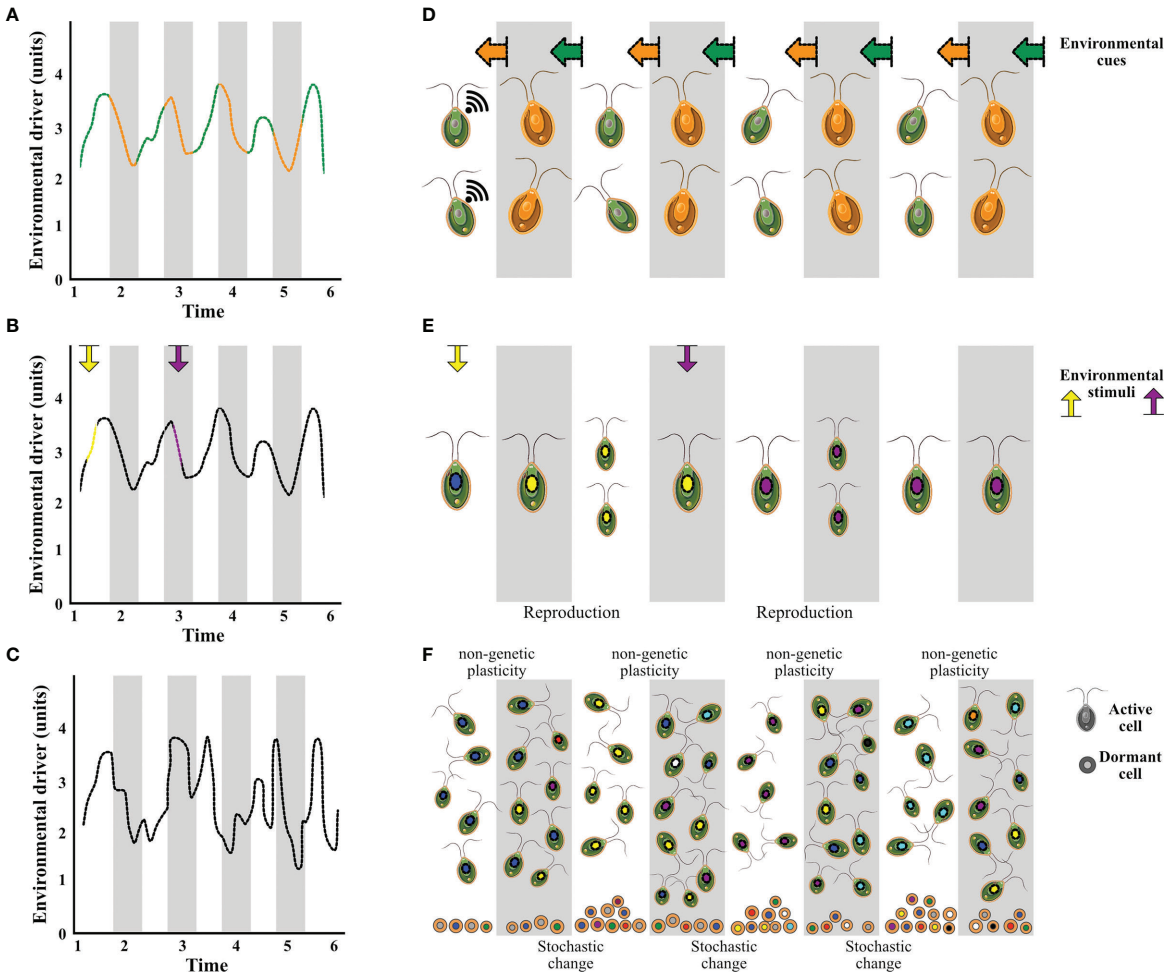

FIGURE 2 | Adaptive strategies of marine microbes to cope with short-term environmental variability are influenced by the level of predictability (High: **A, B**; Low: **C**) of environmental change. Anticipatory and memory mechanisms **(D)** in which microbes can sense environmental cues (arrows in orange and green linked to predictable environmental changes, **(A)** that allow them to adjust phenotypically in an anticipatory manner. Direct environmental sensing-respond mechanisms **(E)** in which microbes exhibit phenotypic responses that correspond to their environmental condition/stimulus (yellow and purple, **B**). **(F)** Seed banks representing the diversified bet-hedging (a.k.a. stochastic phenotypic switching) strategy, in which microbes produce long-term resting stages that act as a genetic and phenotypic reservoir that protect populations against unpredictable future conditions **(C)**.

low tide, followed by the downward migration in anticipation of tidal flood or night (Serôdio, 2021). It has been documented that the disruption of the anticipatory ability can negatively impact the capacity of microbes for physiological adjustments with consequences on ecological dynamics and the fitness of microbial populations (Woelfle et al., 2004).

Another example of anticipatory response of microbes to environmental fluctuations is represented by the capacity of storing "memories" or "past historical experiences" and impart this "knowledge" to the next generation (Casadesús and D'Ari, 2002; Zacharioudakis et al., 2007; Dragosits et al., 2013; Norman et al., 2013; Shimizu, 2013). For example, prokaryotes have shown the existence of a memory-driven anticipatory mechanism that helps microbes to cope with fluctuating carbon sources (e.g. glucose and fructose) (Lambert and Kussel, 2014). When the preferred carbon source (glucose) is exhausted, prokaryotic microbes activate the lac operon (i.e. a set of multiple genes that are responsible for the production of lac protein), in order to use lactose (Östling et al., 1991). However, in normal circumstances, there is a lag phase before these microbes are able to utilize lactose, which can be at an unintended fitness disadvantage in a competitive environment. To overcome this drawback, the bacteria can adopt a phenotypic memory-like mechanism, where the stable intracellular lac protein present in parental cells can be transmitted across dividing daughter cells (Lambert and Kussel, 2014). When prokaryotic cells are adapted to fluctuating carbon sources microbes can continuously express genes required for lactose metabolism (i.e. even after the lac operon inducer is removed), removing the need for regulatory responses (i.e. signal transduction and gene activation/repression) (Lambert and Kussel, 2014). Consequently, this adaptive strategy reduces the metabolic transition in lag phase, thereby increasing microbial fitness in this environment, simply with quicker response

for lactose metabolism. Ecological memory is also hypothesized to be important for the tolerance and fitness of photosynthetic microbes to changing oceans, particularly when the environmental signal is cyclic and reliable. In symbiotic dinoflagellates, for example, thermal priming (e.g., past exposure to increased temperatures and heat stress) enhance heat tolerance and photosynthetic performance during heatwaves (Middlebrook et al., 2012). It has been suggested that this type of acquired tolerance through stress memory is modulated by epigenetic modifications that alter gene expression (e.g., DNA methylation, histone modifications and non-coding micro RNAs), and that these can be transmitted across generations (Bossdorf et al., 2008; Walworth et al., 2021a). However, thermal priming does not always enhance performance and fitness for eukaryotic microbes. For instance, in a Southern Ocean diatom, heat-primed populations exhibited higher levels of mortality during heatwaves than populations without pre-exposure to sub-lethal temperatures (Samuels et al., 2021). These findings suggest the existence of more complex mechanisms regulating the ecological memory of past stress in eukaryotic microbes.

Adaptive Plasticity *via* Bet-Hedging Mechanism

Phenotypic plasticity may not always be an effective strategy to cope with environmental change, particularly when fluctuations in environmental conditions are unpredictable (Veening et al., 2008; Grimbergen et al., 2015; Leung et al., 2020; Gill et al., 2022). Under these conditions, natural selection may favour a strategy where a single genotype produces a range of phenotypes each generation but without responding in a specific way to the prevailing conditions but ensuring the survival of sub-populations that will be adaptive to a future condition (**Figure 2F**; Ackermann, 2015). This mechanism is known as diversified bet-hedging strategy or stochastic phenotypic switching (Veening et al., 2008; Grimbergen et al., 2015; Ellegaard and Ribeiro, 2018). In marine microbes, the maintenance of a seed bank is often hypothesized to constitute a bet-hedging strategy in which long-term resting stages (or propagules) are an insurance against an unpredictable future (Ellegaard and Ribeiro, 2018). For example, some species of diatoms and dinoflagellates are able to survive environmental fluctuations that exceed the tolerance range for vegetative cells through the formation of resting cells (spores/cysts), resuming vegetative growth under favourable conditions (Godhe and Rynearson, 2017; Ellegaard and Ribeiro, 2018). In dinoflagellates, these resting stages are mainly produced as part of their sexual reproduction, which appears to be another form of stress avoidance as it is initiated by unfavourable conditions (e.g., nutrient limitation x suboptimal temperature; Tang and Gobler, 2015; Borowitzka, 2018; Ellegaard and Ribeiro, 2018). Resting cysts of dinoflagellates also contribute to population dynamics influencing rapid shifts in genetic diversity (through genetic recombination) and geographic expansion (Tang and Gobler, 2015). In diatoms, resting cells are not initiated by sexual reproduction but by physiological stress (Borowitzka, 2018; Ellegaard and Ribeiro, 2018). In this case, the formation of resting cells is activated by the upregulation of ferritin (an iron binding protein), a process that triggers the morphological transformation from fusiform to ovoid cells, the decrease in growth rates, the excretion of exopolymeric substances, the upregulation of stress resistance proteins and the increase of nitrate reserves (Liu et al., 2022). Although this adaptive strategy represents a loss of genetic material for marine microbes in the short term (i.e., many of the resting stages never germinate), sacrificing mean fitness for reduced variability in fitness over time, it is described as an effective strategy for risk-spreading, for persistence through longer periods of adverse conditions, and for preparing for an unpredictable future (Ellegaard and Ribeiro, 2018). Despite the important ecological role of the bet-hedging strategy for marine microbes (i.e., influencing population persistence), there is no clear consensus about its role in evolutionary dynamics (Rengefors et al., 2017). Generally, resting stages are considered to weaken the effect of selection and slow down adaptive evolution (Hairston and De Stasio, 1988) by lengthening the generation time of microorganisms, potentially delaying the manifestation of novel mutations (Lennon and Jones, 2011). Contrarily, dormant cells can act as genetic reservoirs that speed up adaptive evolution by increasing phenotypic and genetic variation, which in turn influence the adaptive potential and the response to selection (Kremp et al., 2016; Rengefors et al., 2017).

LONG TERM RESPONSES: ADAPTIVE EVOLUTION IN FLUCTUATING ENVIRONMENTS

Predictable fluctuating marine environments are expected to promote adaptive phenotypic plasticity (**Figure 2**) (Schaum and Collins, 2014; Leung et al., 2020; Gill et al., 2022) at the cost of delaying genetic adaptation (Walworth et al., 2020). However, in environments where changes are less predictable and occur extremely rapidly for organisms to track and adjust phenotypically, plasticity is not promoted (Leung et al., 2020). Under these conditions, genetic adaptation may be the only mechanism that allows species and populations to persist locally (Gaitán-Espitia and Hobday, 2021). Although the link between environmental variability and marine microbial evolution is still poorly understood, in this section we aim to provide glimpses of factors and mechanisms modulating adaptive evolutionary dynamics of microbes in dynamic oceans.

Empirical evidences based on experimental evolution have shown that microbial populations can rapidly adapt to environmental changes (single- and multi-driver environments), throughout, for instance, intraspecific strain sorting and genetic changes (Lohbeck et al., 2012; Hoppe et al., 2018; Wolf et al., 2019). Notwithstanding, the evolutionary responses of microbes to environmental fluctuations are conditioned by the number and identity of the interacting drivers involved (Brennan et al., 2017). Faster rates of adaptation have been documented with increased number of drivers as a result of the increase in the strength of selection (Brennan et al., 2017). However, the effect of drivers on selection is not additive as only few (e.g., temperature, nutrients) explain most of the phenotypic and evolutionary changes observed (Brennan and Collins, 2015; Boyd et al., 2016a; Brennan et al., 2017; Feng et al., 2020). Particularly, temperature has been identified as

one of the most dominant drivers modulating phenotypic and genetic responses in marine microorganisms comprising broad evolutionary backgrounds (Boyd et al., 2016b; Brennan et al., 2017; Barton et al., 2020; Cabrerizo et al., 2022). This important and dominant influence across microbial life forms is perhaps explained by the existence of "universal" thermodynamic constraints that limit the pace of life and the thermal window for biochemical performance (Angilletta et al., 2010). Fluctuations in dominant drivers such as temperature can also modulate the rate of adaptation and the evolutionary trajectories of marine microbes. For example, a study by Schaum et al. (2018) showed that marine diatoms can exhibit rapid evolutionary divergence and adaptation to high temperatures when populations have evolved under fluctuating environments. Here, the temporary restoration of benign heat level conditions increased population size and therefore the probability of fixing beneficial mutations required for adaptation (Schaum et al., 2018). These characteristics and their influence on adaptive evolution to changes in temperature have been linked to the "complexity" of microbial organisms in which species with small genomes (e.g., prokaryotes) have higher rates of adaptation (e.g., compensatory evolutionary shifts on metabolic traits) to warming compared to "more complex" microbes with larger genomes (Barton et al., 2020).

The rate of adaptation to changing marine environments is also regulated by evolutionary trade-offs (Gaitán-Espitia J. et al., 2017). These trade-offs reflect the costs and constraints for evolutionary change (O'Donnell et al., 2018; Aranguren-Gassis et al., 2019; Lindberg and Collins, 2020; Walworth et al., 2020), and can alter the trajectories of populations across fitness landscapes, delaying or blocking them to reach a global fitness optimum (Gaitán-Espitia J. et al., 2017; Gaitán-Espitia and Hobday, 2021). Because evolutionary trade-offs are difficult to demonstrate in nature, some proxies are used to asses them. These include selection experiments (e.g., Jin et al., 2022), and the analysis of functional/phenotypic and genetic correlations (e.g., Argyle et al., 2021; Walworth et al., 2021b). In the marine diatom *Chaetoceros simplex*, a trade-off from a functional correlation between high-temperature tolerance and increased nitrogen requirements is suggested to underlie the inhibited thermal adaptation under nitrogen limitation conditions (Aranguren-Gassis et al., 2019). Similarly, in the marine diatom *Phaeodactylum tricornutum*, adaptation to high CO_2 was mediated by a functional trade-off in which populations decreased metabolic rates while maintaining the carbon allocation and growth (i.e., fitness; Jin et al., 2022). In marine bacteria, evolutionary trade-offs have been documented when comparing strains growing in natural constant and fluctuating environments. In coastal systems, bacteria carry significantly more environmental stimuli sensing genes than strains in oligotrophic systems (e.g., open ocean; Held et al., 2019). This represents a functional trade-off due to the elevated cost of maintenance of signal transduction systems (TCS) for strains in coastal areas (i.e. dynamic and fluctuating) compared to strains in oceanic (i.e. relatively constant) environment (Mackey et al., 2015). Other evolutionary trade-offs are mostly documented as a result of challenging conditions, these trade-offs can also exist under ameliorated conditions, as evidenced in the study by Lindberg and Collins (2020). In this work, populations of *Chlamydomonas reinhardtii* evolved to allocate a smaller proportion of carbon to growth while increasing their ability to tolerate and metabolise reactive oxygen species (ROS; Lindberg and Collins, 2020).

CONCLUSION

Understanding how microbes cope with and adapt to variability in their environments is fundamental for understanding their ecological resilience and adaptive potential in the face of anthropogenic climate change. Unfortunately, most of the mechanistic understanding regarding the environmental-molecular-evolutionary link underpinning the short- and long-term adaptive responses discussed here, have been based on changes in one or two environmental drivers. However, environmental variation and climate change involve multivariate changes (Boyd et al., 2015) that can alter the ecological and evolutionary significance of genetic and non-genetic responses in marine microbes. From the phenotypic plasticity perspective, it is unclear to what extent the number of changing drivers and the type of interactions (i.e., additive, antagonistic or synergetic) can alter the capacity of natural populations to employ plastic strategies such as direct sense-response, anticipatory/memory and bet-hedging. Moreover, we do not know if these responses are differentially modulated across time and space, depending on the level of environmental variation (e.g., higher production of resting cells in more variable environments; lower ecological memory in less variable environments), the existence of physiological constraints (e.g., capacity and costs for activation and maintenance of sensing-regulatory mechanisms), and the signal/duration of the molecular mechanisms underpinning such responses (e.g., different epigenetic factors have different lasting effects). From an evolutionary perspective, we know that fluctuating environments are likely to generate more dynamic adaptive fitness landscapes compared to constant environments. However, in most of the experimental evolution studies, the dynamics have been assessed in stable conditions of one or two drivers, which are characterised by a static local fitness optimum (Steinberg and Ostermeier, 2016). This limits our capacity to understand and predict the tempo and mode of evolution of microbes in fluctuating, multi-driver environments.

AUTHOR CONTRIBUTIONS

JDGE and BA conceived the idea and designed the work. BA led the manuscript writing with feedback and input from ZL and JDGE. All authors contributed to the article and approved the submitted version.

FUNDING

JDGE was supported by the Research Grants Council (ECS 27124318) of Hong Kong.

REFERENCES

Ackermann, M. (2015). A Functional Perspective on Phenotypic Heterogeneity in Microorganisms. *Nat. Rev. Microbiol.* 13, 497–508. doi: 10.1038/nrmicro3491

Andrews, J. H. (2017). Comparative Ecology of Microorganisms and Macroorganisms. *2nd Edn.* New York: Springer Science+Business Media LLC.

Angilletta, M. J.Jr, Huey, R. B., and Frazier, M. R. (2010). Thermodynamic Effects on Organismal Performance: Is Hotter Better? *Physiol. Biochem. Zool.* 83 (2), 197–206. doi: 10.1086/648567

Aranguren-Gassis, M., Kremer, C. T., Klausmeier, C. A., and Litchman, E. (2019). Nitrogen Limitation Inhibits Marine Diatom Adaptation to High Temperatures. *Ecol. Lett.* 22, 1860–1869. doi: 10.1111/ele.13378

Argyle, P. A., Walworth, N. G., Hinners, J., Collins, S., Levine, N. M., and Doblin, M. A. (2021). Multivariate Trait Analysis Reveals Diatom Plasticity Constrained to a Reduced Set of Biological Axes. *ISME Commun.* 1 (1), 1–11. doi: 10.1038/s43705-021-00062-8

Aumack, C. F., Juhl, A. R., and Krembs, C. (2014). Diatom Vertical Migration Within Land-Fast Arctic Sea Ice. *J. Mar. Syst.* 139, 496–504. doi: 10.1016/j.jmarsys.2014.08.013

Barton, S., Jenkins, J., Buckling, A., Schaum, C. E., Smirnoff, N., Raven, J. A., et al. (2020). Evolutionary Temperature Compensation of Carbon Fixation in Marine Phytoplankton. *Ecol. Lett.* 23 (4), 722–733. doi: 10.1111/ele.13469

Bender, S. J., Durkin, C. A., Berthiaume, C. T., Morales, R. L., and Armbrust, E. V. (2014). Transcriptional Responses of Three Model Diatoms to Nitrate Limitation of Growth. *Front. Mar. Sci.* 1, 1–15. doi: 10.3389/fmars.2014.00003

Bernhardt, J. R., O'Connor, M. I., Sunday, J. M., and Gonzalez, A. (2020). Life in Fluctuating Environments. *Philos. Trans. R. Soc. B* 375 (1814), 20190454. doi: 10.1098/rstb.2019.0454

Bonamour, S., Chevin, L.-M., Charmantier, A., and Teplitsky, C. (2019). Phenotypic Plasticity in Response to Climate Change: The Importance of Cue Variation. *Philos. Trans. R. Soc B Biol. Sci.* 374, 1–12. doi: 10.1098/rstb.2018.0178

Borowitzka, M. A. (2018). The 'Stress' Concept in Microalgal Biology—Homeostasis, Acclimation and Adaptation. *J. Appl. Phycol.* 30 (5), 2815–2825. doi: 10.1007/s10811-018-1399-0

Bossdorf, O., Richards, C. L., and Pigliucci, M. (2008). Epigenetics for Ecologists. *Ecol. Lett.* 11, 106–115. doi: 10.1111j.1461-0248.2007.01130.x

Boyd, P., Cornwall, C. E., Davison, A., Doney, S. C., Fourquez, M., Hurd, C. L., et al. (2016a). Biological Responses to Environmental Heterogeneity Under Future Ocean Conditions. *Glob. Change Biol.* 22 (8), 2633–2650. doi: 10.1111/gcb.13287

Boyd, P. W., Dillingham, P. W., McGraw, C. M., Armstrong, E. A., Cornwall, C. E., Feng, Y. Y., et al. (2016b). Physiological Responses of a Southern Ocean Diatom to Complex Future Ocean Conditions. *Nat. Climate Change* 6 (2), 207–213. doi: 10.1038/nclimate2811

Boyd, P. W., Lennartz, S. T., Glover, D. M., and Doney, S. C. (2015). Biological Ramifications of Climate-Change-Mediated Oceanic Multi-Stressors. *Nat. Climate Change* 5 (1), 71–79. doi: 10.1038/nclimate2441

Boyd, P. W., Strzepek, R., Fu, F., and Hutchins, D. A. (2010). Environmental Control of Open-Ocean Phytoplankton Groups: Now and in the Future. *Limnol. Oceanogr.* 55 (3), 1353–1376. doi: 10.4319/lo.2010.55.3.1353

Brennan, G., Colegrave, N., and Collins, S. (2017). Evolutionary Consequences of Multidriver Environmental Change in an Aquatic Primary Producer. *Proc. Natl. Acad. Sci. U. S. A.* 114, 9930–9935. doi: 10.1073/pnas.1703375114

Brennan, G., and Collins, S. (2015). Growth Responses of a Green Alga to Multiple Environmental Drivers. *Nat. Clim. Change.* 5 (9), 892–897. doi: 10.1038/nclimate2682

Brown, D. R., Barton, G., Pan, Z., Buck, M., and Wigneshweraraj, S. (2014). Nitrogen Stress Response and Stringent Response are Coupled in Escherichia Coli. *Nat. Commun.* 5, 1–8. doi: 10.1038/ncomms5115

Brun, P., Vogt, M., Payne, M. R., Gruber, N., O'brien, C. J., Buitenhuis, E. T., et al. (2015). Ecological Niches of Open Ocean Phytoplankton Taxa. *Limnol. Oceanogr.* 60 (3), 1020–1038. doi: 10.1002/lno.10074

Busby, S. J. W. (2019). Transcription Activation in Bacteria: Ancient and Modern. *Microbiol. (United Kingdom)* 165, 386–395. doi: 10.1099/mic.0.000783

Cabrerizo, M., Medina-Sánchez, J., González-Olalla, J., Sánchez-Gómez, D., and Carrillo, P. (2022). Microbial Plankton Responses to Multiple Environmental Drivers in Marine Ecosystems With Different Phosphorus Limitation Degrees. *Sci. Total Environ.* 816, 151491. doi: 10.1016/j.scitotenv.2021.151491

Capra, E. J., and Laub, M. T. (2012). Evolution of Two-Component Signal Transduction Systems. *Annu. Rev. Microbiol.* 66, 325–347. doi: 10.1146/annurev-micro-092611-150039

Casadesús, J., and D'Ari, R. (2002). Memory in Bacteria and Phage. *BioEssays* 24, 512–518. doi: 10.1002/bies.10102

Chevin, L. M., Collins, S., and Lefèvre, F. (2013). Phenotypic Plasticity and Evolutionary Demographic Responses to Climate Change: Taking Theory Out to the Field. *Funct. Ecol.* 27 (4), 967–979. doi: 10.1111/j.1365-2435.2012.02043.x

Collins, S., Boyd, P. W., and Doblin, M. A. (2020). Evolution, Microbes, and Changing Ocean Conditions. *Ann. Rev. Mar. Sci.* 12, 181–208. doi: 10.1146/annurev-marine-010318-095311

Cruz de Carvalho, M. H., Sun, H. X., Bowler, C., and Chua, N. H. (2016). Noncoding and Coding Transcriptome Responses of a Marine Diatom to Phosphate Fluctuations. *New Phytol.* 210 (2), 497–510. doi: 10.1111/nph.13787

Depauw, F. A., Rogato, A., D'Alcalá, M. R., and Falciatore, A. (2012). Exploring the Molecular Basis of Responses to Light in Marine Diatoms. *J. Exp. Bot.* 63, 1575–1591. doi: 10.1093/jxb/ers005

DeWitt, T. J., Sih, A., and Wilson, D. S. (1998). Costs and Limits of Phenotypic Plasticity. *Trends Ecol. Evol.* 13 (2), 77–81. doi: 10.1016/S0169-5347(97)01274-3

Di Pane, J., Wiltshire, K. H., McLean, M., Boersma, M., and Meunier, C. L. (2022). Environmentally Induced Functional Shifts in Phytoplankton and Their Potential Consequences for Ecosystem Functioning. *Global Change Biol.* 28 (8), 2804–2819. doi: 10.1111/gcb.16098

Dragosits, M., Mozhayskiy, V., Quinones-Soto, S., Park, J., and Tagkopoulos, I. (2013). Evolutionary Potential, Cross-Stress Behavior and the Genetic Basis of Acquired Stress Resistance in Escherichia Coli. *Mol. Syst. Biol.* 9, 1–13. doi: 10.1038/msb.2012.76

Ellegaard, M., and Ribeiro, S. (2018). The Long-Term Persistence of Phytoplankton Resting Stages in Aquatic 'Seed Banks.'. *Biol. Rev.* 93, 166–183. doi: 10.1111/brv.12338

Feng, Y., Roleda, M. Y., Armstrong, E., Summerfield, T. C., Law, C. S., Hurd, C. L., et al. (2020). Effects of Multiple Drivers of Ocean Global Change on the Physiology and Functional Gene Expression of the Coccolithophore Emiliania Huxleyi. *Global Change Biol.* 26 (10), 5630–5645. doi: 10.1111/gcb.15259

Forsman, A. (2015). Rethinking Phenotypic Plasticity and its Consequences for Individuals, Populations and Species. *Heredity (Edinb).* 115, 276–284. doi: 10.1038/hdy.2014.92

Fox, R. J., Donelson, J. M., Schunter, C., Ravasi, T., Gaita, J. D., and Fox, R. J. (2019). Beyond Buying Time: The Role of Plasticity in Phenotypic Adaptation to Rapid Environmental Change. *Proc. R. Soc B Biol. Sci.* 374 (1768), 20180174. doi: 10.1098/rstb.2018.0174

Gaidarenko, O., Sathoff, C., Staub, K., Huesemann, M. H., Vernet, M., and Hildebrand, M. (2019). Timing Is Everything: Diel Metabolic and Physiological Changes in the Diatom Cyclotella Cryptica Grown in Simulated Outdoor Conditions. *Algal Res.* 42, 101598. doi: 10.1016/j.algal.2019.101598

Gaitán-Espitia, J. D., and Hobday, A. J. (2021). Evolutionary Principles and Genetic Considerations for Guiding Conservation Interventions Under Climate Change. *Glob. Change Biol.* 27, 475–488. doi: 10.1111/gcb.15359

Gaitán-Espitia, J. D., Marshall, D. J., Dupont, S., Bacigalupe, L. D., Bodrossy, L., and Hobday, A. J. (2017a). Geographical Gradients in Selection can Reveal Genetic Constraints for Evolutionary Responses to Ocean Acidification. *Biol. Lett.* 13, 20160784. doi: 10.1098/rsbl.2016.0784

Gaitán-Espitia, J. D., Villanueva, P. A., Lopez, J., Torres, R., Navarro, J. M., and Bacigalupe, L. D. (2017b). Spatio-Temporal Environmental Variation Mediates Geographical Differences in Phenotypic Responses to Ocean Acidification. *Biol. Lett.* 13 (2), 20160865. doi: 10.1098/rsbl.2016.0865

Gill, R. L., Collins, S., Argyle, P. A., Larsson, M. E., Fleck, R., and Doblin, M. A. (2022). Predictability of Thermal Fluctuations Influences Functional Traits of a Cosmopolitan Marine Diatom. *Proc. R. Soc. B Biol. Sci.* 289 (1973), 20212581. doi: 10.1098/rspb.2021.2581

Godhe, A., and Rynearson, T. (2017). The Role of Intraspecific Variation in the Ecological and Evolutionary Success of Diatoms in Changing Environments. *Philos. Trans. R. Soc. B: Biol. Sci.* 372 (1728), 20160399. doi: 10.1098/rstb.2016.0399

Grimbergen, A. J., Siebring, J., Solopova, A., and Kuipers, O. P. (2015). Microbial Bet-Hedging: The Power of Being Different. *Curr. Opin. Microbiol.* 25, 67–72. doi: 10.1016/j.mib.2015.04.008

Hairston, N. G. Jr, and De Stasio, B. T.Jr. (1988). Rate of Evolution Slowed by a Dormant Propagule Pool. *Nature* 336 (6196), 239–242. doi: 10.1038/336239a0

Held, N. A., Mcilvin, M. R., Moran, D. M., Laub, M. T., and Saito, A. (2019). Unique Patterns and Biogeochemical Relevance of Two- Component Sensing in Marine Bacteria. *mSystems* 4, 1–16. doi: 10.1128/mSystems.00317-18

Hoppe, C. J. M., Wolf, K. K. E., Schuback, N., Tortell, P. D., and Rost, B. (2018). Compensation of Ocean Acidification Effects in Arctic Phytoplankton Assemblages. *Nat. Clim. Change* 8, 529–533. doi: 10.1038/s41558-018-0142-9

Hutchins, D. A., and Fu, F. (2017). Microorganisms and Ocean Global Change. *Nat. Microbiol.* 2, 17058. doi: 10.1038/nmicrobiol.2017.58

Jin, P., Ji, Y., Huang, Q., Li, P., Pan, J., Lu, H., et al. (2022). A Reduction in Metabolism Explains the Trade-Offs Associated With the Long-Term Adaptation of Phytoplankton to High CO2 Concentrations. *New Phytol.* 233 (5), 2155–2167. doi: 10.1111/nph.17917

Johnson, C. H., Mori, T., and Xu, Y. (2008). A Cyanobacterial Circadian Clockwork. *Curr. Biol.* 18, 816–825. doi: 10.1016/j.cub.2008.07.012

Krell, A., Beszteri, B., Dieckmann, G., Glöckner, G., Valentin, K., and Mock, T. (2008). A New Class of Ice-Binding Proteins Discovered in a Salt-Stress-Induced cDNA Library of the Psychrophilic Diatom Fragilariopsis Cylindrus (Bacillariophyceae). *Eur. J. Phycol.* 43 (4), 423–433. doi: 10.1080/09670260802348615

Kremer, C. T., Fey, S. B., Arellano, A. A., and Vasseur, D. A. (2018). Gradual Plasticity Alters Population Dynamics in Variable Environments: Thermal Acclimation in the Green Alga Chlamydomonas Reinhartdii. *Proc. R. Soc. B: Biol. Sci.* 285 (1870), 20171942. doi: 10.1098/rspb.2017.1942

Kremp, A., Oja, J., LeTortorec, A. H., Hakanen, P., Tahvanainen, P., Tuimala, J., et al. (2016). Diverse Seed Banks Favour Adaptation of Microalgal Populations to Future Climate Conditions. *Environ. Microbiol.* 18 (2), 679–691. doi: 10.1111/1462-2920.13070

Lambert, G., and Kussel, E. (2014). Memory and Fitness Optimization of Bacteria Under Fluctuating Environments. *PloS Genet.* 10, e1004556. doi: 10.1371/journal.pgen.1004556

Lennon, J. T., and Jones, S. E. (2011). Microbial Seed Banks: The Ecological and Evolutionary Implications of Dormancy. *Nat. Rev. Microbiol.* 9 (2), 119–130. doi: 10.1038/nrmicro2504

Leung, C., Rescan, M., Grulois, D., and Chevin, L. M. (2020). Reduced Phenotypic Plasticity Evolves in Less Predictable Environments. *Ecol. Lett.* 23 (11), 1664–1672. doi: 10.1111/ele.13598

Lindberg, R. T., and Collins, S. (2020). Quality–quantity Trade-Offs Drive Functional Trait Evolution in a Model Microalgal 'Climate Change Winner.' *Ecol. Lett.* 23, 780–790. doi: 10.1111/ele.13478

Litaker, W., Duke, C. S., Kenney, B. E., and Ramus, J. (1993). Short-Term Environmental Variability and Phytoplankton Abundance in a Shallow Tidal Estuary. II. Spring and Fall. *Mar. Ecol. Prog. Ser.* 94, 141–154. doi: 10.3354/meps094141

Liu, X., Wang, L., Wu, S., Zhou, L., Gao, S., Xie, X., et al. (2022). Formation of Resting Cells is Accompanied With Enrichment of Ferritin in Marine Diatom Phaeodactylum Tricornutum. *Algal Res.* 61, 102567. doi: 10.1016/j.algal.2021.102567

Lohbeck, K. T., Riebesell, U., and Reusch, T. B. (2012). Adaptive Evolution of a Key Phytoplankton Species to Ocean Acidification. *Nat. Geosci.* 5 (5), 346–351. doi: 10.1038/ngeo1441

Mackey, K. R. M., Post, A. F., McIlvin, M. R., Cutter, G. A., John, S. G., Saito, M. A., et al. (2015). Divergent Responses of Atlantic Coastal and Oceanic Synechococcus to Iron Limitation. *Proc. Natl. Acad. Sci. U. S. A.* 112, 9944–9949. doi: 10.1073/pnas.1509448112

Madhani, H. D. (2013). The Frustrated Gene: Origins of Eukaryotic Gene Expression. *Cell* 155, 744. doi: 10.1016/j.cell.2013.10.003

Matthijs, M., Fabris, M., Obata, T., Foubert, I., Franco-Zorrilla, J. M., Solano, R., et al. (2017). The Transcription Factor Bzip14 Regulates the TCA Cycle in the Diatom Phaeodactylum Tricornutum. *EMBO J.* 36, 1559–1576. doi: 10.15252/embj.201696392

Middlebrook, R., Anthony, K. R., Hoegh-Guldberg, O., and Dove, S. (2012). Thermal Priming Affects Symbiont Photosynthesis But Does Not Alter Bleaching Susceptibility in Acropora Millepora. *J. Exp. Mar. Biol. Ecol.* 432, 64–72. doi: 10.1016/j.jembe.2012.07.005

Norman, T. M., Lord, N. D., Paulsson, J., and Losick, R. (2013). Memory and Modularity in Cell-Fate Decision Making. *Nature* 503, 481–486. doi: 10.1038/nature12804

O'Donnell, D. R., Hamman, C. R., Johnson, E. C., Kremer, C. T., Klausmeier, C. A., and Litchman, E. (2018). Rapid Thermal Adaptation in a Marine Diatom Reveals Constraints and Trade-Offs. *Global Change Biol.* 24 (10), 4554–4565. doi: 10.1111/gcb.14360

Östling, J., Goodman, A., and Kjelleberg, S. (1991). Behaviour of IncP-1 Plasmids and a miniMu Transposon in a Marine Vibrio Sp.: Isolation of Starvation Inducible Lac Operon Fusions. *FEMS Microbiol. Lett.* 86 (1), 83–93. doi: 10.1111/j.1574-6968.1991.tb04797.x

Rengefors, K., Kremp, A., Reusch, T. B., and Wood, A. M. (2017). Genetic Diversity and Evolution in Eukaryotic Phytoplankton: Revelations From Population Genetic Studies. *J. Plankton Res.* 39 (2), 165–179. doi: 10.1093/plankt/fbw098

Rodríguez-Romero, A., Gaitán-Espitia, J. D., Opitz, T., and Lardies, M. A. (2022). Heterogeneous Environmental Seascape Across a Biogeographic Break Influences the Thermal Physiology and Tolerances to Ocean Acidification in an Ecosystem Engineer. *Biodiversity Distributions*, 1–12. doi: 10.1111/ddi.13478

Rozen, Y., and Belkin, S. (2005). Survival of Enteric Bacteria in Seawater. *Ocean. Heal. Pathog. Mar. Environ.* 25, 93–107. doi: 10.1007/0-387-23709-7_4

Samuels, T., Rynearson, T. A., and Collins, S. (2021). Surviving Heatwaves: Thermal Experience Predicts Life and Death in a Southern Ocean Diatom. *Front. Mar. Sci.* 9. doi: 10.3389/fmars.2021.600343

Sauer, J., Wenderoth, K., Maier, U. G., and Rhiel, E. (2002). Effects of Salinity, Light and Time on the Vertical Migration of Diatom Assemblages. *Diatom. Res.* 17 (1), 189–203. doi: 10.1080/0269249X.2002.9705538

Schaller, G. E., Shiu, S. H., and Armitage, J. P. (2011). Two-Component Systems and Their Co-Option for Eukaryotic Signal Transduction. *Curr. Biol.* 21, R320–R330. doi: 10.1016/j.cub.2011.02.045

Schaum, C. E., Buckling, A., Smirnoff, N., Studholme, D. J., and Yvon-Durocher, G. (2018). Environmental Fluctuations Accelerate Molecular Evolution of Thermal Tolerance in a Marine Diatom. *Nature Communications* 9 (1), 1–14. doi: 10.1038/s41467-018-03906-5

Schaum, C. E., Buckling, A., Smirnoff, N., Studholme, D. J., and Yvon-Durocher, G. (2018a). Environmental fluctuations accelerate molecular evolution of thermal tolerance in a marine diatom. *Nature Communications* 9 (1), 1–14.

Schaum, C. E., Rost, B., and Collins, S. (2016). Environmental Stability Affects Phenotypic Evolution in a Globally Distributed Marine Picoplankton. *ISME J.* 10, 75–84. doi: 10.1038/ismej.2015.102

Schaum, E., Rost, B., Millar, A. J., and Collins, S. (2013). Variation in Plastic Responses of a Globally Distributed Picoplankton Species to Ocean Acidification. *Nat. Climate Change* 3 (3), 298–302. doi: 10.1038/nclimate1774

Schluter, L., Lohbeck, K. T., Gro ger, J. P., Riebesell, U., and Reusch, T. B. H. (2016). Long-Term Dynamics of Adaptive Evolution in a Globally Important Phytoplankton Species to Ocean Acidification. *Sci. Adv.* 2, e1501660–e1501660. doi: 10.1126/sciadv.1501660

Serôdio, J. (2021). Diatom Motility: Mechanisms, Control and Adaptive Value. *Diatom. Glid. Motil.*, 159–183. doi: 10.1002/9781119526483.ch7

Shimizu, K. (2013). Regulation Systems of Bacteria Such as Escherichia Coli in Response to Nutrient Limitation and Environmental Stresses. *Metabolites* 4, 1–35. doi: 10.3390/metabo4010001

Steinberg, B., and Ostermeier, M. (2016). Environmental Changes Bridge Evolutionary Valleys. *Sci. Adv.* 2 (1), e1500921. doi: 10.1126/sciadv.1500921

Suzuki, S., Ferjani, A., Suzuki, I., and Murata, N. (2004). The SphS-SphR Two Component System is the Exclusive Sensor for the Induction of Gene Expression in Response to Phosphate Limitation in Synechocystis. *J. Biol. Chem.* 279 (13), 13234–13240. doi: 10.1074/jbc.M313358200

Switzer, A., Evangelopoulos, D., Figueira, R., de Carvalho, L. P. S., Brown, D. R., and Wigneshweraraj, S. (2018). A Novel Regulatory Factor Affecting the Transcription of Methionine Biosynthesis Genes in Escherichia Coli Experiencing Sustained Nitrogen Starvation. *Microbiol. (United Kingdom)* 164, 1457–1470. doi: 10.1099/mic.0.000683

Tagkopoulos, I., Liu, Y.-C., and Tavazoie, S. (2008). Predictive Behavior Within Microbial Genetic Networks. *Science* 320, 1313–1317. doi: 10.1126/science.1154456

Tang, Y. Z., and Gobler, C. J. (2015). Sexual Resting Cyst Production by the Dinoflagellate Akashiwo Sanguinea: A Potential Mechanism Contributing to the Ubiquitous Distribution of a Harmful Alga. *J. Phycol.* 51 (2), 298–309. doi: 10.1111/jpy.12274

Tinta, T., Vojvoda, J., Mozetič, P., Talaber, I., Vodopivec, M., Malfatti, F., et al. (2015). Bacterial Community Shift is Induced by Dynamic Environmental Parameters in a Changing Coastal Ecosystem (Northern Adriatic, Northeastern Mediterranean Sea)–A 2-Year Time-Series Study. *Environ. Microbiol.* 17 (10), 3581–3596. doi: 10.1111/1462-2920.12519

Veening, J. W., Smits, W. K., and Kuipers, O. P. (2008). Bistability, Epigenetics, and Bet-Hedging in Bacteria. *Annu. Rev. Microbiol.* 62, 193–210. doi: 10.1146/annurev.micro.62.081307.163002

Walworth, N. G., Hinners, J., Argyle, P. A., Leles, S. G., Doblin, M. A., Collins, S., et al. (2021b). The Evolution of Trait Correlations Constrains Phenotypic Adaptation to High CO2 in a Eukaryotic Alga. *Proc. R. Soc. B* 288 (1953), 20210940. doi: 10.1098/rspb.2021.0940

Walworth, N. G., Lee, M. D., Dolzhenko, E., Fu, F. X., Smith, A. D., Webb, E. A., et al. (2021a). Long-Term M5c Methylome Dynamics Parallel Phenotypic Adaptation in the Cyanobacterium Trichodesmium. *Mol. Biol. Evol.* 38 (3), 927–939. doi: 10.1093/molbev/msaa256

Walworth, N. G., Zakem, E. J., Dunne, J. P., Collins, S., and Levine, N. M. (2020). Microbial Evolutionary Strategies in a Dynamic Ocean. *Proc. Natl. Acad. Sci. U. S. A.* 117, 5943–5948. doi: 10.1073/pnas.1919332117

Woelfle, M. A., Ouyang, Y., Phanvijhitsiri, K., and Johnson, C. H. (2004). The Adaptive Value of Circadian Clocks: An Experimental Assessment in Cyanobacteria. *Curr. Biol.* 14, 1481–1486. doi: 10.1016/j.cub.2004.08.023

Wolf, K. K. E., Romanelli, E., Rost, B., John, U., Collins, S., Weigand, H., et al. (2019). Company Matters: The Presence of Other Genotypes Alters Traits and Intraspecific Selection in an Arctic Diatom Under Climate Change. *Glob. Change Biol.* 25, 2869–2884. doi: 10.1111/gcb.14675

Zacharioudakis, I., Gligoris, T., and Tzamarias, D. (2007). A Yeast Catabolic Enzyme Controls Transcriptional Memory. *Curr. Biol.* 17, 2041–2046. doi: 10.1016/j.cub.2007.10.044

Zschiedrich, C. P., Keidel, V., and Szurmant, H. (2016). Molecular Mechanisms of Two-Component Signal Transduction. *J. Mol. Biol.* 428, 3752–3775. doi: 10.1016/j.jmb.2016.08.003

Conflict of Interest: The authors declare that the research was conducted in the absence of any commercial or financial relationships that could be construed as a potential conflict of interest.

Publisher's Note: All claims expressed in this article are solely those of the authors and do not necessarily represent those of their affiliated organizations, or those of the publisher, the editors and the reviewers. Any product that may be evaluated in this article, or claim that may be made by its manufacturer, is not guaranteed or endorsed by the publisher.

frontiers | Frontiers in Marine Science

BRIEF RESEARCH REPORT
published: 21 June 2022
doi: 10.3389/fmars.2022.883265

Thermal Fluctuations Yield Sex-Specific Differences of Ingestion Rates of the Littoral Mysid *Neomysis integer*

Laura M. Hennigs[*†], *Konstanze Bergunder*[*†], *Erik Sperfeld* and *Alexander Wacker*

Animal Ecology, Zoological Institute and Museum, University of Greifswald, Greifswald, Germany

Shallow aquatic environments are characterized by strong environmental variability. For ectotherms, temperature is the main driver of metabolic activity, thus also shaping performance. Ingestion rates in mysids are fast responses, influenced by metabolic and behavioral activity. We examined ingestion rates of the mysid *Neomysis integer*, collected in the Baltic Sea, after one-week exposure to different constant and fluctuating temperature regimes (5, 10, 15, 20°C and 9 ± 5, 14 ± 5°C, respectively). To investigate possible differences between sexes, thermal performance curves (TPCs) were established for female and male mysids based on ingestion rates measured at constant temperatures. TPCs of ingestion rates at constant temperatures differed between sexes, with female mysids showing a higher total ingestion rate as well as a higher thermal optimum compared to male mysids. Females showed reduced ingestion rates when exposed to fluctuating temperatures around their thermal optimum, whereas ingestion of male mysids was not reduced when exposed to fluctuating temperatures. The observed sex-specific differences might be related to potentially higher lipid and energy demands of the females. We suggest future studies should investigate males and females to improve our understanding about impacts of environmental variability on natural populations.

Keywords: nonlinear averaging, fluctuations, variable environments, thermal performance curves, sex-specific effects, time-dependent effects, brackish Mysida

OPEN ACCESS

Edited by:
Christopher Edward Cornwall, Victoria University of Wellington, New Zealand

Reviewed by:
Jonathan Y.S. Leung, University of Adelaide, Australia
Kaitlyn Lowder, The Ocean Foundation, United States

****Correspondence:***
Laura M. Hennigs
laura.hennigs@uni-greifswald.de
Konstanze Bergunder
konstanze.bergunder@uni-greifswald.de

[†]These authors have contributed equally to this work and share first authorship

Specialty section:
This article was submitted to Global Change and the Future Ocean, a section of the journal Frontiers in Marine Science

Received: *24 February 2022*
Accepted: *28 April 2022*
Published: *21 June 2022*

Citation:
Hennigs LM, Bergunder K, Sperfeld E and Wacker A (2022) Thermal Fluctuations Yield Sex-Specific Differences of Ingestion Rates of the Littoral Mysid Neomysis integer. Front. Mar. Sci. 9:883265. doi: 10.3389/fmars.2022.883265

INTRODUCTION

Natural environments are characterized by variability at various temporal and spatial scales. Variability of abiotic factors in shallow brackish habitats can occur as fluctuations in temperature, salinity, nutrients, light availability, oxygen, and pH (Boyd & Hutchins, 2012; Franz et al., 2019). Variability is induced by various processes, such as seasons, day-night cycles, radiation, tides, currents, wind, and up- and downwelling, or even by the biological activity of organisms (Feely et al., 2008; Hurd et al., 2011; Cornwall et al., 2013; Saderne et al., 2013). The temporal scales at which variability affects environmental conditions range from seconds/minutes over days up to months (e.g. Gunderson et al., 2016), and are especially important in relation to the timescale organisms experience them (Jackson et al., 2021).

Temperature is the primary driver of metabolic rates in ectotherms, thus affecting both physiological and fitness traits of marine ectotherms. An increase in temperature accelerates most physiological processes within tolerance limits (Newell and Branch, 1980). Traditionally, the performance of ectotherms at different temperatures is determined by exposing organisms to constant temperature treatments along a thermal gradient (Huey and Stevenson, 1979; Schulte et al., 2011). From this, thermal performance curves (TPCs) can be deduced that may vary in shape depending on the measured trait, but performance usually peaks around a thermal optimum, followed by a rapid decline (Dowd et al., 2015). Different nonlinear mathematical models have been used to fit the thermal performance data, ranging from negative quadratic to more complex functions (Angilletta, 2006). Such TPCs and the mathematical principle of nonlinear averaging, often also known as Jensen's Inequality (**Supplementary Box 1**; Jensen, 1906; Ruel and Ayres, 1999), can be used to predict performance in variable environments if time-dependent effects do not play a large role. For instance, population growth rates of a green alga under fluctuating temperatures could be sufficiently predicted by non-linear averaging using a TPC measured at constant temperatures (Bernhardt et al., 2018). Another study on the bivalve *Mytilus*, combining two experiments at different time scales, could predict long-term performance at fluctuating temperatures on the basis of short-term functioning (feeding) measured at constant temperatures using nonlinear averaging (Vajedsamiei et al., 2021). These studies also confirm the theory based on Jensen's Inequality that performance is smaller in fluctuating compared to constant temperatures (of the same mean) when fluctuations range in the concave part of the generally non-linear, unimodal TPC (**Supplementary Box 1**; Jensen, 1906).

Despite these examples of successfully using Jensen's Inequality to predict performance in fluctuating environments, limitations of this method have been described. Koussoroplis et al. (2019) showed that non-linear averaging is suitable only at particular fluctuation frequencies to predict effects of resource variability. Additionally, duration and order of exposure to temperature events can affect ectotherm performance (Kingsolver et al., 2015), as well as other time-dependent effects, such as stress, acclimation, compensation, use of reserves, or the interplay among several (co-)varying factors (Koussoroplis et al., 2017). Stress responses can be beneficial short-term but may reduce organism performance at longer time scales, whilst acclimation may amplify or buffer fluctuation effects, depending on the frequency of change in relation to acclimation speed of the organism (Kingsolver et al., 2015; Koussoroplis et al., 2017). Predicting the direction of time-dependent effects and differentiating between time-dependent effects and Jensen's Inequality is still a challenge (Kingsolver et al., 2015).

For the next decades, extreme events like storms, heavy precipitation or marine heatwaves are predicted to occur with increasing magnitude and frequency (IPCC, 2021). This will change established variability patterns of temperature, but the effects on organisms are largely unexplored. Therefore, there is a need to incorporate effects of fluctuations when studying species' functioning and performance in a changing world with variability (Vasseur et al., 2014). Fluctuating temperature showed substantial effects on the performance of marine organisms (Bernhardt et al., 2018; Vajedsamiei et al., 2021), which can differ between species depending on the shape of the TPC and whether the thermal mean is on the convex, concave or linear part of the TPC. For instance, Morón Lugo et al. (2020) observed decreased feeding of the sea star *Asterias rubens* under warming and an additional increased stress response under thermal fluctuation. In contrast, feeding of the crab *Hemigrapsus takanoi* was unaffected by thermal fluctuations. This suggests that thermal fluctuations have been situated in the linear part of *H. taganoi*'s TPC, leading to no effect, whereas they have been situated in the concave part of *A. rubens*'. Whether responses to fluctuating temperatures also differ within aquatic species, e.g. amongst sexes, genotypes or ontogenetic stages, remains to be explored. In particular, we are not aware of any study investigating sex-specific differences in fluctuation effects on performance of marine invertebrates so far. However, if sex-specific differences in response to changing temperature regimes exist, changes in the sex ratio and thus to consequences for population dynamics and ultimately food web functioning are expected. To fill this knowledge gap, we investigate the effect of thermal fluctuations on the performance of male and female *Neomysis integer* as important littoral mysid species of Baltic Sea food webs.

We collected male and female mysids from a brackish estuary of the Baltic Sea and measured their ingestion rates after exposing them to different constant and fluctuating temperatures in the laboratory. Here, ingestion rate serves as an estimate of the organism's performance, combining short-term responses of its metabolic capacity and behavior that ultimately affect longer-term responses such as growth and reproduction. Based on the mysids' responses measured at constant temperatures, a TPC was established ($TPC_{Constant}$) and used to calculate a TPC that predicts performance under fluctuating temperature conditions ($TPC_{Fluctuation}$) using non-linear averaging. We also measured ingestion rates of mysids that experienced daily temperature fluctuations and compared these responses to the two different TPC types. We hypothesize that ingestion rates show a unimodal response across the temperature gradient as typically observed for many other performance traits. We further hypothesize that ingestion rates of mature females should be higher than those of males as mature females require more energy for egg production. Since metabolic rates, and thus the energy demand of *N. integer*, are higher in warmer temperatures (Weisse and Rudstam 1989, Fockedey et al., 2006), we expect more pronounced differences in females' and males' energy demands, and consequently ingestion rates, at warmer temperatures. We hypothesize lower ingestion rates of mysids that experienced temperature fluctuations compared to constant temperatures based on Jensen's Inequality principle, which predicts lower mean performance in fluctuating environments within the concave range of the TPC. Any deviation from the prediction based on Jensen's Inequality (i.e., our $TPC_{Fluctuation}$), whether positive or negative, will point to effects of biological processes, such as stress responses or short-term acclimation.

METHODS

The Mysid *Neomysis integer*

Mysids are an important component in the food web of coastal zones, linking benthic and pelagic systems by nutrient exchange and biomass transfer (Roast et al., 1998). They can switch between two feeding modes (suspension and raptorial feeding), allowing them to feed on detritus and phytoplankton, but also to actively select zooplankton (Viitasalo and Rautio, 1998). In turn, they serve as a protein-rich (>70% of dry weight, Raymont et al., 1968) food source for higher trophic levels. We used *Neomysis integer* Leach, 1814 (Mysidacea: mysidae) in our experiments. *N. integer* occurs in the hyperbenthic zones of estuaries and is also abundant in shallow coastal waters of the Baltic Sea (Margoński and Maciejewska, 1999). In estuaries and brackish water systems, such as the Greifswalder Bodden, thermal variability occurs on both daily and seasonal scales (Seifert, 1938; Schiewer, 2008).

Collection and Laboratory Conditions

N. integer were collected at water depths <0.5 m in a shallow bay (coordinates: 54.097495, 13.455123) of the Greifswalder Bodden, in the southwest of the Baltic Sea on 04th May 2021. At collection, the water temperature was 11.3°C and the salinity was 7.5 psu. The bay is very shallow (<5 m), making it likely that mysids can experience strong thermal variability at short time scales. To avoid acute stress responses, especially in the warmer temperature treatments of the experiment, 150 mysids were kept in a climate chamber at constant 15°C for the next 16 days. Mysids stayed in aerated 40 L-aquaria and were fed ad libitum with freshly-hatched *Artemia salina* nauplii and fish pellets (MultiFit). The culture medium consisted of a 50:50% mixture of artificial seawater (Tropic Marin Pro-Reef Salt) and filtered (0.2 µm) water from the sample site. The salinity was set to 10 psu, somewhat higher than the ambient value, to establish a reference for future experiments and for comparative purposes with other experimental studies (e.g. Roast et al., 1999; Roast et al., 2000). At least 50% of this culture medium was exchanged every 3-4 days. The light regime in the climate chamber and during experiments was set to a 12:12 h dark: light photoperiod.

Temperature Treatments

Before the ingestion measurements, mysids were exposed simultaneously for 7 days to 4 constant temperature treatments and to 2 fluctuating temperature treatments (**Figure 1**). They were kept in 6 L-aquaria placed in different climate cabinets under the respective treatment temperature (1 climate cabinet per treatment) and fed ad libitum with freshly-hatched *A. salina* nauplii. Mysids in constant treatments were kept on 5 (♂ n = 13; ♀ n = 4), 10 (♂ n = 15; ♀ n = 2), 15 (♂ n = 5; ♀ n = 1), or 20°C (♂ n = 3; ♀ n = 10), whereas mysids in the two fluctuating treatments experienced 9 ± 5°C (♂ n = 12; ♀ n = 5) and 14 ± 5°C (♂ n = 11; ♀ n = 6) with a frequency of once per day (see **Figure 2** for shape of the temperature fluctuation profile). The amplitude of ± 5°C was chosen to elicit a response and is likely larger than what the animals would experience on a diurnal basis in the environment. Highly controllable and precise climate cabinets were used (± 0.5 Kelvin) to avoid potential differences caused by cabinet identity.

Ingestion Rate Measurements

Vivid *N. integer* were starved for one day prior to the measurements of ingestion rates (Lindén and Kuosa, 2004). Ingestion rates of *N. integer* individuals from both the constant and fluctuating treatments were measured in the respective constant mean temperatures of 5, 10, 15, and 20°C, and in case of the fluctuating treatments when temperature was close to the respective mean value. One climate cabinet was used for each constant mean temperature. Ingestion rates of mysids from the fluctuating treatments were measured in the same climate cabinets as ingestion rates of mysids from the respective constant temperature treatment to ensure comparability. For the measurements, *N. integer* were placed individually in small beakers containing 50 ml of the culture medium described above at an initial food density of 30 A. *salina* nauplii. After 1.5 h, *N. integer* individuals were removed and stored in ethanol for later sex and length determination. The remaining *A. salina* nauplii were counted, and ingestion rates per mysid per hour were calculated (**Figure 1**). The sex of the mysids was identified based on sexual characteristics using a stereo-microscope. All females had a developed marsupium. Body length (from the base of eyestalks to the end of the last abdominal segment, excluding uropods and telson; Fockedey et al., 2005) was determined from photographs using the software ImageJ (mean body length ± SD, females: 11.11 ± 1.65 mm, males: 9.46 ± 0.87 mm). Since all mysids used in the experiment were adults and were sampled in May, i.e. at the beginning of the growing season providing ample of food, we expected all individuals being in a reproductive state.

Data Analyses

Data analyses were performed in R version 4.0.2 (R Core Team, 2020). Individual ingestion rates at constant temperatures were analyzed using Analysis of Covariance (ANCOVA) with a negative quadratic function of temperature as continuous independent variable and sex of animals as factor. Preliminary inspection of the data revealed that our data were distributed rather in the upper part of the TPC above a potential inflection point where the second derivative of the TPC is always negative, i.e. the concave downward part of the TPC. For this region, a negative quadratic function is a reasonable simplification and fits the typical unimodal responses in ectotherm TPCs (Angilletta, 2006). The full model was simplified based on AIC using the R function *step()*. A potential decrease of the ingestion rates measured under fluctuating temperatures was tested against the performance prediction of the ANCOVA for the respective constant temperature with a one-sided, one sample t-test. We also tested for any deviation from the performance predicted under fluctuating temperature by performing a two-sided, one sample t-test.

To calculate ingestion rates predicted at fluctuating temperature regimes, we used the deviations of the actually realized temperatures (measured in the climate cabinet) from the mean temperature of the 9 ± 5°C fluctuation treatment. This treatment was chosen exemplary since the realized temperature deviations from the mean in the 14 ± 5°C treatment were very similar and resulted in similar calculated ingestion rates at the end. In detail, we conducted the following steps (**Figure 2**):

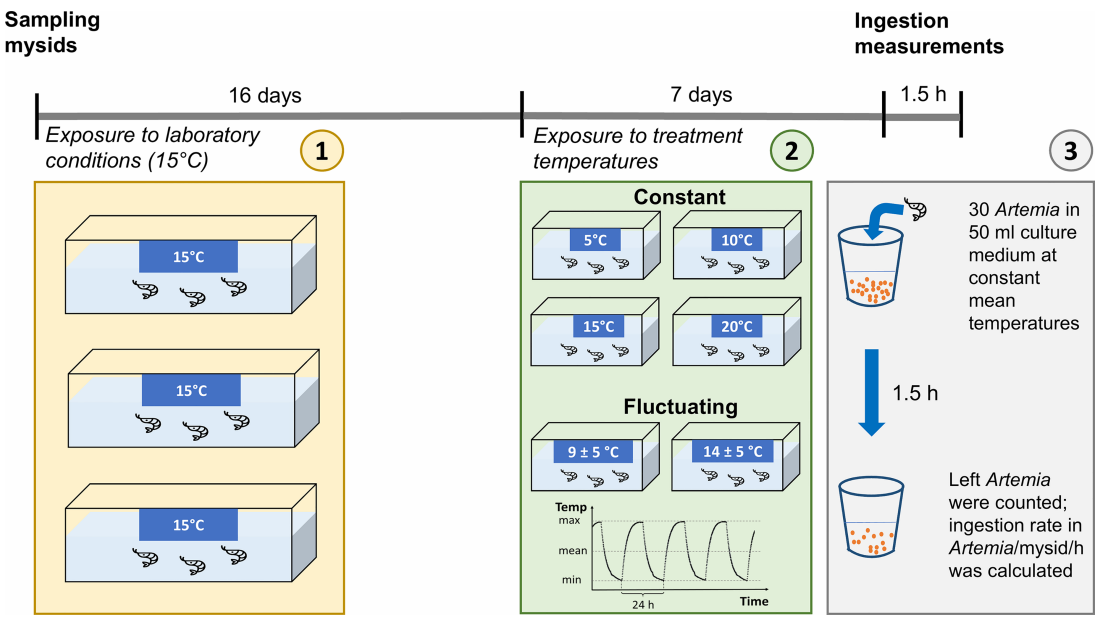

FIGURE 1 | Scheme of the experimental set-up and time schedule. Mysids were exposed to laboratory conditions for 16 days at constant 15°C before they were randomly distributed and exposed to the treatment temperature regimes. For the ingestion experiment, mysids were placed individually in beakers containing 30 *Artemia* nauplii. After 1.5 h, mysids were removed and remaining *Artemia* were counted for the calculation of the ingestion rates (*Artemia*/mysid/hour).

Preparation of Simulated Temperature Data

1.) The temperature fluctuation regime realized in the 9 ± 5°C treatment was logged every 5 min during the experiment (Onset, HOBO Pendant logger). From this temperature profile, the realized mean temperature ($\bar{T}$) was calculated. $\bar{T}$ was subtracted from every single value of the realized temperature profile to obtain deviations from the mean temperature across time in the fluctuation regime.

2.) A thermal gradient ranging from 0 to 25°C in increments of 0.1° C steps was simulated. The single values of this gradient were used as simulated mean temperatures ($\overline{T_n}$) for the predictions of ingestions rates under fluctuating temperature (**Figure 2F**).

3.) To each of these $\overline{T_n}$, we added the deviations across time which were calculated in step 1. This procedure provided simulated fluctuating temperature profiles with the same deviations from the mean temperature as in our experimental treatments, but for all $\overline{T_n}$ along the simulated thermal gradient (0 to 25°C).

Calculation of Ingestion Rates Predicted at Fluctuating Temperature

4.) For every temperature of each of these temperature fluctuation profiles (cf. **Figure 2B**), we calculated the predicted instantaneous performance $g(T)$ (**Figure 2C**, lower plot), based on the $TPC_{Constant}$, over time in steps of every 5 mins, $g(t)$ (**Figure 2D**).

5.) From these predicted values across the temperature fluctuation regime, we calculated the mean ingestion rate over time ($\overline{g(t)}$, **Figure 2E**). The $\overline{g(t)}$, was calculated for each $\overline{T_n}$ along the simulated thermal gradient described in step 2 (**Figure 2F**). The resulting mean ingestion rates under fluctuating temperature ($\overline{g(T_n)}$), were added as $TPC_{Fluctuation}$ to the figure showing also the $TPC_{Constant}$.

RESULTS

Sex-Specific Ingestion Rates at Constant Temperatures

Under constant temperature conditions, ingestion rates of *N. integer* showed a unimodal relationship to temperature for both sexes (**Figure 3A**), characterizing a $TPC_{Constant}$ that can be well described by a negative quadratic function (ANCOVA; $F_{1,48}$ = 5.02, p = 0.030). The female $TPC_{Constant}$ reached a higher maximum than the male $TPC_{Constant}$ (**Figure 3A**, sex: $F_{1,48}$ = 5.44, p = 0.024), and the thermal optimum (14.1°C and 10.7°C for females and males, respectively) was shifted towards higher temperatures (interaction Temp × Sex, $F_{1,48}$ = 9.03, p = 0.004).

Thermal Fluctuation Effect on Sex-Specific Ingestion Rates

The measured ingestion rates of female mysids exposed to the 14 ± 5°C regime (**Figure 3B**, open symbol), close to their thermal optimum, were lower than the ingestion value predicted by the $TPC_{Constant}$ (one-sided t-test, p = 0.018), but did not deviate positively or negatively from the value of the $TPC_{Fluctuation}$ (two-sided t-test, p = 0.11). For female mysids exposed to the 9 ± 5°C

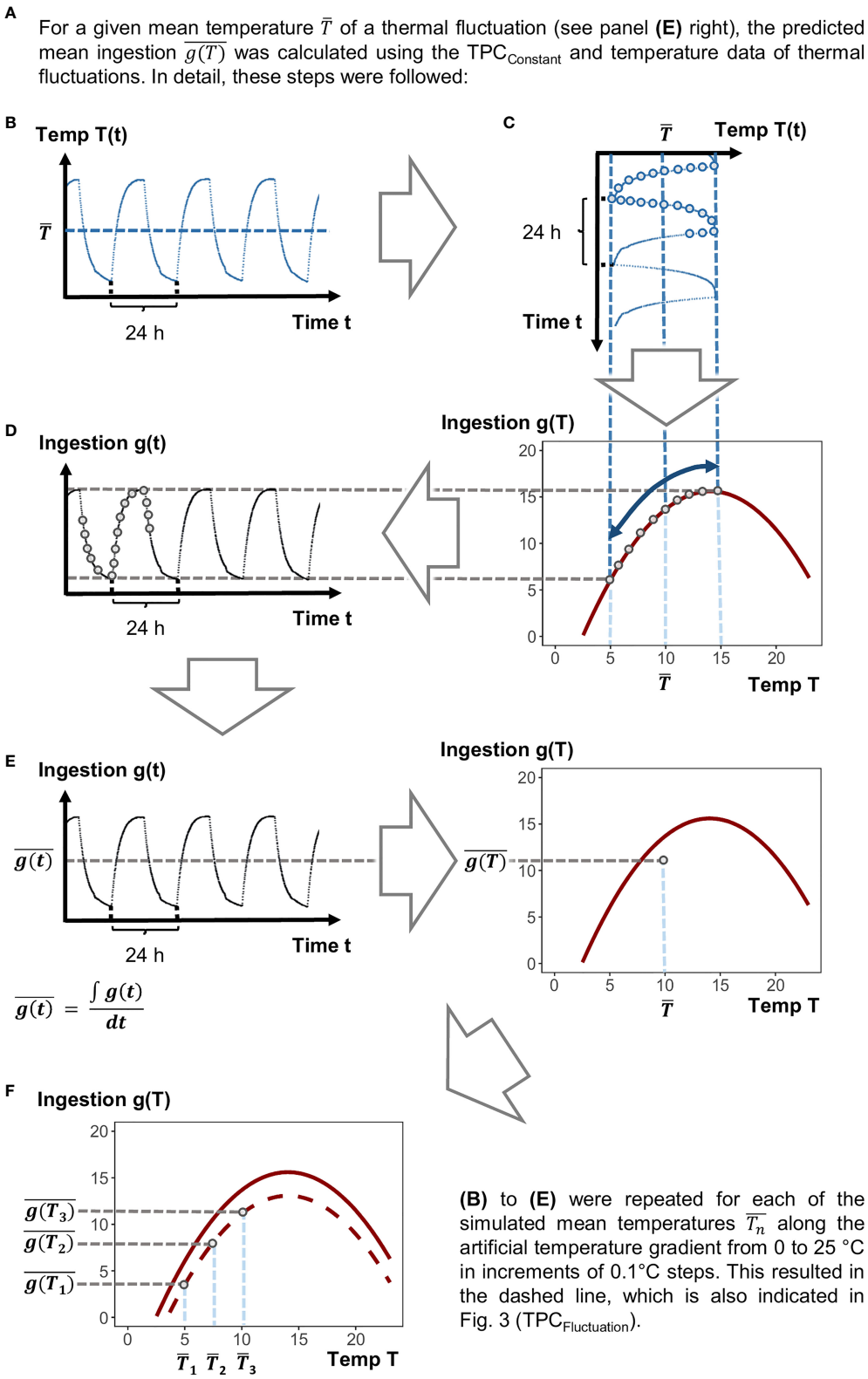

FIGURE 2 | Schematic figure showing how to predict ingestion rates at fluctuating conditions on the basis of ingestion rates measured at constant temperatures. References to and explanations for labels **(A–F)** are given in the main text.

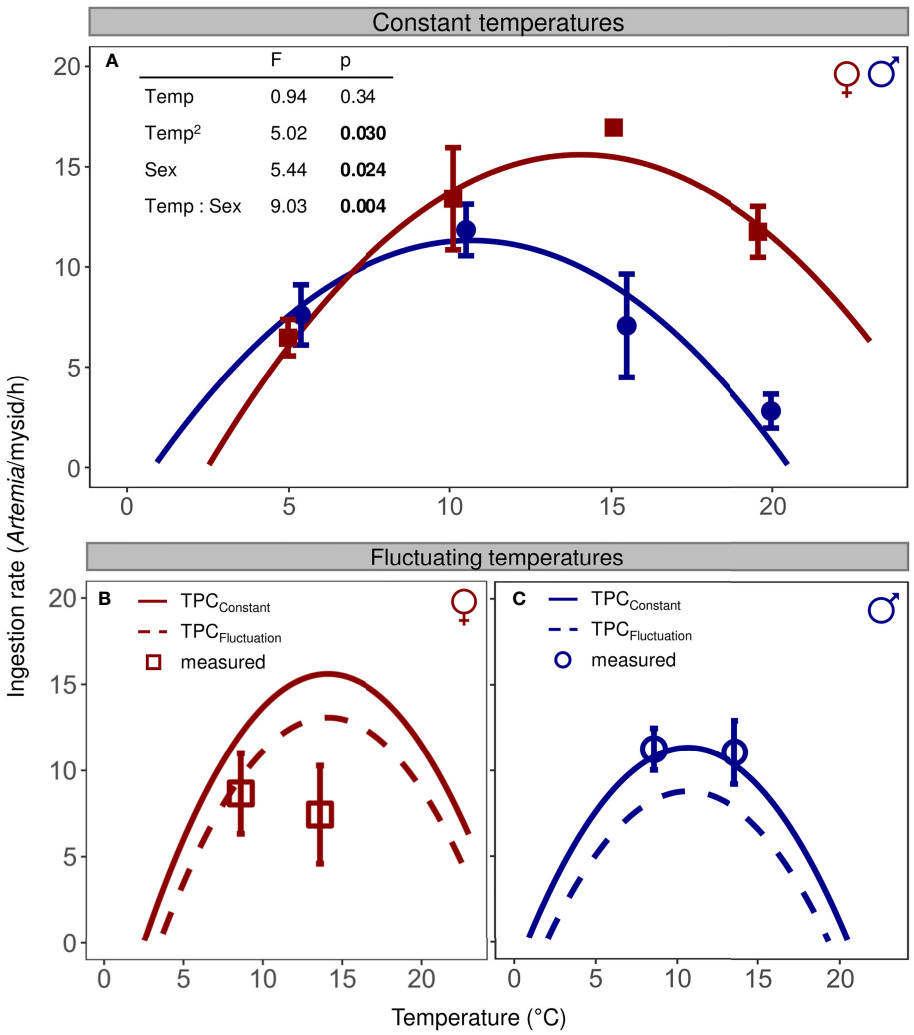

FIGURE 3 | Sex-specific ingestion rates of *N. integer* exposed to **(A)** constant temperatures (filled symbols, mean ± SE) and **(B, C)** fluctuating temperature conditions (open symbols). **(A)** $TPC_{Constant}$ for females (red squares) and males (blue circles) were calculated based on estimates of an ANCOVA model with a negative quadratic function (see table inlet) fitted through ingestion rates measured at constant temperature. **(B, C)** Ingestion rates predicted for fluctuating temperature conditions ($TPC_{Fluctuation}$) were calculated using non-linear averaging based on the $TPCs_{Constant}$.

regime, ingestion rates neither decreased compared to the value of the $TPC_{Constant}$ (one-sided t-test, $p = 0.11$) nor did they deviate from the corresponding $TPC_{Fluctuation}$ value (two-sided t-test, $p = 0.72$). In contrast to females, the ingestion rates of male mysids exposed to fluctuating temperatures (**Figure 3C**) were very similar to the values predicted by the $TPC_{Constant}$ for both corresponding temperatures (9 and 14°C, one-sided t-tests, $p > 0.63$) and did also not deviate from the two values of the $TPC_{Fluctuation}$ (two-sided t-tests, $p > 0.10$).

DISCUSSION

Summary of Results

Our study showed first results that temperature fluctuations can affect ingestion rates, a process influenced by metabolism and behavior of marine crustaceans, and that differences in responses even occur between females and males of the same population. In our case, we found evidence for differences in sex-specific ingestion rates of *N. integer*. At constant temperatures, the thermal optimum of ingestion rates based on fitted TPCs was higher for females than for males, and at warmer temperatures, females showed higher ingestion rates than males. Temperature fluctuations of ± 5°C around the observed thermal optimum led to reduced ingestion rates for females, but not for males, when compared to ingestion rates observed at constant temperature.

Sex-Specific Ingestion Rates Under Constant Temperatures

In our study, ingestion rates of female and male mysids show a unimodal pattern across the tested temperature range, reflecting

the expected non-linear nature of TPCs (e.g. Angilletta, 2006; Dowd et al., 2015). Whilst the $TPC_{Constant}$ for females and males showed similar responses to lower temperatures, sex-specific differences were apparent at higher temperatures (**Figure 3A**). Female mysids showed both a higher thermal optimum and higher total ingestion at the optimum temperature compared to males. Simmons & Knight (1975) described sex-specific differences in performance for the mysid *Neomysis intermedia* under various temperature and salinity that were weight-dependent. The respiratory response of *N. intermedia* was also dependent on the status of gravidity (Simmons and Knight, 1975). Similarly, Simmons and Knight (1975) indicated linkages between the respiration of mysids and the level of reproduction. The higher ingestion rates of females observed at higher temperatures in our study could be therefore related to the reproductive status of the used individuals. For females, such a relation between a higher ingestion and a higher energy demand for reproduction, in form of glycogen, has also been discussed for other marine invertebrates, such as the oyster *Pinctada* (Chávez-Villalba et al., 2013). Further, Winkler and Greve (2002) found that mysids' reproduction rates and growth factors for smaller females seem to be higher at 15°C than at 10°C, resulting in shorter intermoult periods, which could lead to higher energy demands and thus to higher ingestion rates at 15°C compared to 10°C, as observed in our study. In the context of reproduction, a higher lipid demand, necessary for gamete production, may have led to the observed higher thermal optimum of females and their higher total ingestion of *Artemia*. Support for this assumption arises from a previous study showing that ovigerous females of *N. integer* contained almost double the amount of lipids compared to males due to the lipid-rich eggs (Linford, 1965). The lipid content and the energy budget were dependent on the season and therefore also influenced by variations in prey and temperature (Linford, 1965; Verslycke and Janssen, 2002). The lipid amount also correlates with the wet weight of an animal, with sex-specific relative lipid concentrations (Linford, 1965). This may also have led to the observed higher ingestion rates of females compared to males in our study, as female *N. integer* were slightly larger than males. However, the relationship between ingestion rates and length in the different temperature treatments was neither significant for females nor for males ($p > 0.4$). Alternatively, differences in ingestion rates between males and females may be influenced by differences in thermal tolerance. For instance, lower thermal tolerance in males compared to females may explain lower ingestion rates of males at higher temperatures. So far, however, nothing is known about sex-specific differences in thermal tolerance of mysids based on fitness-related traits such as growth rate or survival, making it difficult to draw conclusions about this option.

Similar to our observed ingestion rates for females, Roast et al. (2000) observed a significant increase of egestion rates for *N. integer* with increasing temperature up to 15°C. In another study, Roast et al. (1999) found an interactive effect of temperature and sex on respiration, with males showing a higher oxygen consumption than females. Even though we also found a significant interaction between temperature and sex, our results showed the opposite pattern, with higher ingestion rates of females observed at higher temperature. However, Roast et al. (1999) did not measure feeding in their study, and therefore the direct link between respiration and feeding rates in *N. integer* remains unclear. In studies using the blue mussel *Mytilus*, it was shown that respiration and feeding are two different functional traits, which at times are decoupled from each other, suggesting that they should be compared with caution (Vajedsamiei et al., 2021).

Females Are Negatively Affected by Thermal Fluctuations Around Their Optimum, Whilst Males Are Not

Ingestion rates of female *N. integer* exposed to temperature fluctuations around their optimum were lower than ingestion rates at constant temperature, but not lower than ingestion rates predicted under thermal fluctuations, suggesting females behaved as predicted by Jensen's Inequality. In contrast, ingestion rates of male mysids exposed to fluctuating temperatures were similar to the values of the $TPC_{Constant}$ (**Figure 3C**). This suggests that males are not affected by time-dependent effects of thermal fluctuations, whilst females were affected by such effects at their thermal optimum. Based on our current knowledge, we can only speculate that males instantaneously respond to the changing conditions and therefore show a $TPC_{constant}$-predicted ingestion rate, while females deviate as they either are capable of cognitively integrating their feeding behavior across the temperature fluctuations or suffer from some time-dependent effect, such as a stress-related response.

The longer-term thermal histories of females and males used in our study should be similar as *N. integer* lives in swarms (Lindén, 2007), and our animals were collected from the same swarm. Swarms might experience similar temperatures in the field, but could also show sex-dependent habitat preferences (Vesakoski et al., 2008). The extent of thermal variability the mysids actually experience in the study region, in particular in high spatial and temporal resolution, is a matter of further investigations.

Perspectives and Conclusions

There are many different types of thermal variability in natural environments. Thermal fluctuations are not as regular or periodic as in laboratory studies, but rather stochastic (e.g. Pansch et al., 2018) and vertical or horizontal movements of mobile ectotherms can change the amplitudes and frequencies of fluctuations they experience (Koussoroplis et al., 2019). Further complexity is also added by the interplay of temperature with other factors, such as acidification, hypoxia, food availability, that may all vary in time and space (Cornwall et al., 2013; Comeau et al., 2014; Koussoroplis and Wacker, 2016). Thus, there is a lot to learn about predicting ectotherm performance in naturally fluctuating multifactorial systems, especially in the context of changing variability patterns and frequencies of extreme events due to climate change. To our knowledge, this study is the first investigating a TPC for mysids' ingestion rates under constant temperatures, and combining it with ingestion

rates under fluctuating conditions. We observed differences in ingestion rates between females and males in warmer temperatures at constant conditions and that females responded to temperature fluctuations whilst males did not. Investigations on the underlying mechanisms, that may be related to the reproductive status or other physiological differences in females and males, are of considerable interest for future research. We further advise caution when using TPCs based on measurements in constant conditions to predict performance in fluctuating environments, since time-dependent effects such as stress-induced damage or compensation can influence the ectotherms' responses at variable conditions. Since we observed differences in sex-specific ingestion rates within one species, we propose that future studies should put more emphasis on studying potential differences between female and male individuals of studied populations. This would allow a better understanding of variation observed in thermal performance curves and possible effects of fluctuating conditions, and is crucial for improved predictions of species' performance under climate change.

DATA AVAILABILITY STATEMENT

The original contributions presented in the study are included in the article/**Supplementary Material**. Further inquiries can be directed to the corresponding authors.

AUTHOR CONTRIBUTIONS

All authors contributed to conception and design of the study. LMH and KB acquired the data. All authors performed the statistical analysis. LMH and KB wrote the first draft of the manuscript. All authors contributed to manuscript revision, read, and approved the submitted version.

ACKNOWLEDGMENTS

We thank Hamam Aflok for help in the laboratory and Christin Park who ensured that all laboratory work could be conducted in time and as planned. KB and LMH are associated with the DFG graduate college and Research Training Group (RTG 2010) 'Biological RESPONSEs to Novel and Changing Environments'. We acknowledge support for the Article Processing Charge by the German Research Foundation and the Open Access Publication Fund of the University of Greifswald. We are grateful to the reviewers for their constructive comments which improved previous versions of the manuscript.

SUPPLEMENTARY MATERIAL

The Supplementary Material for this article can be found online at: https://www.frontiersin.org/articles/10.3389/fmars.2022.883265/full#supplementary-material

REFERENCES

Angilletta, M. J. (2006). Estimating and Comparing Thermal Performance Curves. *J. Therm. Biol.* 31, 541–545. doi: 10.1016/j.jtherbio.2006.06.002

Bernhardt, J. R., Sunday, J. M., Thompson, P. L., and O'Connor, M. I. (2018). Nonlinear Averaging of Thermal Experience Predicts Population Growth Rates in a Thermally Variable Environment. *Proc. R. Soc. B.: Biol. Sci.* 285, 20181076. doi: 10.1098/rspb.2018.1076

Boyd, P. W., and Hutchins, D. A. (2012). Understanding the Responses of Ocean Biota to a Complex Matrix of Cumulative Anthropogenic Change. *Mar. Ecol. Prog. Ser.* 470, 125–135. doi: 10.3354/meps10121

Chávez-Villalba, J., Soyez, C., Aurentz, H., and Le Moullac, G. (2013). Physiological Responses of Female and Male Black-Lip Pearl Oysters *(Pinctada Margaritifera)* to Different Temperatures and Concentrations of Food. *Aquat. Liv. Resour.* 26, 263–271. doi: 10.1051/alr/2013059

Comeau, S., Edmunds, P. J., Spindel, N. B., and Carpenter, R. C. (2014). Diel Pco_2 Oscillations Modulate the Response of the Coral *Acropora Hyacinthus* to Ocean Acidification. *Mar. Ecol. Prog. Ser.* 501, 99–111. doi: 10.3354/meps10690

Cornwall, C. E., Hepburn, C. D., McGraw, C. M., Currie, K. I., Pilditch, C. A., Hunter, K. A., et al. (2013). Diurnal Fluctuations in Seawater pH Influence the Response of a Calcifying Macroalga to Ocean Acidification. *Proc. R. Soc. B.: Biol. Sci.* 280, 20132201. doi: 10.1098/rspb.2013.2201

Dowd, W. W., King, F. A., and Denny, M. W. (2015). Thermal Variation, Thermal Extremes and the Physiological Performance of Individuals. *J. Exp. Biol.* 218, 1956–1967. doi: 10.1242/jeb.114926

Feely, R. A., Sabine, C. L., Hernandez-Ayon, J. M., Ianson, D., and Hales, B. (2008). Evidence for Upwelling of Corrosive "Acidified" Water Onto the Continental Shelf. *Science* 320, 1490–1492. doi: 10.1126/science.1155676

Fockedey, N., Ghekiere, A., Bruwiere, S., Janssen, C., and Vincx, M. (2006). Effect of Salinity and Temperature on the Intra-Marsupial Development of the Brackish Water Mysid *Neomysis integer* (Crustacea: Mysidacea). *Mar. Biol.* 148, 1339–1356. doi: 10.1007/s00227-005-0160-9

Fockedey, N., Mees, J., Vangheluwe, M., Verslycke, T., Janssen, C. R., and Vincx, M. (2005). Temperature and Salinity Effects on Post-Marsupial Growth of Neomysis Integer (Crustacea: Mysidacea). *J. Exp. Mar. Biol. Ecol.* 326, 27–47. doi: 10.1016/j.jembe.2005.05.005

Franz, M., Lieberum, C., Bock, G., and Karez, R. (2019). Environmental Parameters of Shallow Water Habitats in the SW Baltic Sea. *Earth Syst. Sci. Data* 11, 947–957. doi: 10.5194/essd-11-947-2019

Gunderson, A. R., Armstrong, E. J., and Stillman, J. H. (2016). Multiple Stressors in a Changing World: The Need for an Improved Perspective on Physiological Responses to the Dynamic Marine Environment. *Ann. Rev. Mar. Sci.* 8, 357–378. doi: 10.1146/annurev-marine-122414-033953

Huey, R. B., and Stevenson, R. D. (1979). Integrating Thermal Physiology and Ecology of Ectotherms: A Discussion of Approaches. *Am. Zool.* 19, 357–366. doi: 10.1093/icb/19.1.357

Hurd, C. L., Cornwall, C. E., Currie, K., Hepburn, C. D., McGraw, C. M., Hunter, K. A., et al. (2011). Metabolically Induced pH Fluctuations by Some Coastal Calcifiers Exceed Projected 22nd Century Ocean Acidification: A Mechanism for Differential Susceptibility? *Global Change Biol.* 17, 3254–3262. doi: 10.1111/j.1365-2486.2011.02473.x

IPCC (2021). "Summary for Policymakers", in *Climate Change 2021: The Physical Science Basis. Contribution of Working Group I to the Sixth Assessment Report of the Intergovernmental Panel on Climate Change*. Eds. V. Masson-Delmotte, P. Zhai, A. Pirani, S. L. Connors, C. Péan, S. Berger, N. Caud, Y. Chen, L. Goldfarb, M. I. Gomis, M. Huang, K. Leitzell, E. Lonnoy, J. B. R. Matthews, T. K. Maycock, T. Waterfield, O. Yelekçi, R. Yu and B. Zhou (Cambridge, United Kingdom and New York, NY, USA: Cambridge University Press) pp. 3–32. doi: 10.1017/9781009157896.001

Jackson, M. C., Pawar, S., and Woodward, G. (2021). The Temporal Dynamics of Multiple Stressor Effects: From Individuals to Ecosystems. *Trends Ecol. Evol.* 36, 402–410. doi: 10.1016/j.tree.2021.01.005

Jensen, J. L. W. V. (1906). Sur Les Fonctions Convexes Et Les Inégalités Entre Les Valeurs Moyennes. *Acta Math.* 30, 175–193. doi: 10.1007/BF02418571

Kingsolver, J. G., Higgins, J. K., and Augustine, K. E. (2015). Fluctuating Temperatures and Ectotherm Growth: Distinguishing Non-Linear and Time-Dependent Effects. *J. Exp. Biol.* 218, 2218–2225. doi: 10.1242/jeb.120733

Koussoroplis, A.-M., Pincebourde, S., and Wacker, A. (2017). Understanding and Predicting Physiological Performance of Organisms in Fluctuating and

Multifactorial Environments. *Ecol. Monogr.* 87, 178–197. doi: 10.1002/ecm.1247

Koussoroplis, A.-M., Schälicke, S., Raatz, M., Bach, M., and Wacker, A. (2019). Feeding in the Frequency Domain: Coarser-Grained Environments Increase Consumer Sensitivity to Resource Variability, Covariance and Phase. *Ecol. Lett.* 22, 1104–1114. doi: 10.1111/ele.13267

Koussoroplis, A.-M., and Wacker, A. (2016). Covariance Modulates the Effect of Joint Temperature and Food Variance on Ectotherm Life-History Traits. *Ecol. Lett.* 19, 143–152. doi: 10.1111/ele.12546

Lindén, E. (2007). The More the Merrier: Swarming as an Antipredator Strategy in the Mysid *Neomysis Integer*. *Aquat. Ecol.* 41, 299–307. doi: 10.1007/s10452-006-9055-1

Lindén, E., and Kuosa, H. (2004). Effects of Grazing and Excretion by Pelagic Mysids (*Mysis* Spp.) on the Size Structure and Biomass of the Phytoplankton Community. *Hydrobiologia* 514, 73–78. doi: 10.1023/B:hydr.0000018207.42449.fb

Linford, E. (1965). Biochemical Studies on Marine Zooplankton: II. Variations in the Lipid Content of Some Mysidacea. *ICES J. Mar. Sci.* 30, 16–27. doi: 10.1093/icesjms/30.1.16

Margoński, P., and Maciejewska, K. (1999). The Distribution, Abundance and Biomass of *Mysis Mixta* and *Neomysis Integer* (Crustacea: Mysidacea) in the Open Waters of the Southern Baltic Sea. *Bull. Sea. Fish. Inst. Gdynia.* 147, 23–35.

Morón Lugo, S. C., Baumeister, M., Nour, O. M., Wolf, F., Stumpp, M., and Pansch, C. (2020). Warming and Temperature Variability Determine the Performance of Two Invertebrate Predators. *Sci. Rep.* 10, 6780. doi: 10.1038/s41598-020-63679-0

Newell, R. C., and Branch, G. (1980). The Influence of Temperature on the Maintenance of Metabolic Energy Balance in Marine Invertebrates. *Adv. Mar. Biol.* 17, 329–396. doi: 10.1016/S0065-2881(08)60304-1

Pansch, C., Scotti, M., Barboza, F. R., Al-Janabi, B., Brakel, J., Briski, E., et al. (2018). Heat Waves and Their Significance for a Temperate Benthic Community: A Near-Natural Experimental Approach. *Global Change Biol.* 24, 4357–4367. doi: 10.1111/gcb.14282

Raymont, J. E. G., Austin, J., and Linford, E. (1968). Biochemical Studies on Marine Zooplankton V. The Composition of the Major Biochemical Fractions in *Neomysis Integer*. *J. Mar. Biol. Assoc. Unit. Kingd.* 48, 735–760. doi: 10.1017/S002531540001924X

R Core Team (2020). "R: A language and environment for statistical computing, *R Foundation for Statistical Computing*. (Vienna, Austria). Available at: https://www.R-project.org/.

Roast, S. D., Widdows, J., and Jones, M. B. (1998). The Position Maintenance Behaviour of *Neomysis Integer* (Peracarida: Mysidacea) in Response to Current Velocity, Substratum and Salinity. *J. Exp. Mar. Biol. Ecol.* 220, 25–45. doi: 10.1016/S0022-0981(97)00082-8

Roast, S. D., Widdows, J., and Jones, M. B. (1999). Respiratory Responses of the Estuarine Mysid *Neomysis Integer* (Peracarida: Mysidacea) in Relation to a Variable Environment. *Mar. Biol.* 133, 643–649. doi: 10.1007/s002270050504

Roast, S. D., Widdows, J., and Jones, M. B. (2000). Egestion Rates of the Estuarine Mysid *Neomysis Integer* (Peracarida: Mysidacea) in Relation to a Variable Environment. *J. Exp. Mar. Biol. Ecol.* 245, 69–81. doi: 10.1016/S0022-0981(99)00152-5

Ruel, J. J., and Ayres, M. P. (1999). Jensen's Inequality Predicts Effects of Environmental Variation. *Trends Ecol. Evol.* 14, 361–366. doi: 10.1016/S0169-5347(99)01664-X

Saderne, V., Fietzek, P., and Herman, P. M. J. (2013). Extreme Variations of Pco2 and pH in a Macrophyte Meadow of the Baltic Sea in Summer: Evidence of the Effect of Photosynthesis and Local Upwelling. *PloS One* 8, e62689. doi: 10.1371/journal.pone.0062689

U. Schiewer (Ed.) (2008). *Ecology of Baltic Coastal Waters* (Berlin: Springer), 428p.

Schulte, P. M., Healy, T. M., and Fangue, N. A. (2011). Thermal Performance Curves, Phenotypic Plasticity, and the Time Scales of Temperature Exposure. *Integr. Comp. Biol.* 51, 691–702. doi: 10.1093/icb/icr097

Seifert, R. (1938). Die Bodenfauna Des Greifswalder Boddens. Ein Beitrag Zur Ökologie Der Brackwasserfauna. *Z. Für. Morpholog. Und. Ökolog. Der. Tiere.* 34, 221–271. doi: 10.1007/BF00408759

Simmons, M. A., and Knight, A. W. (1975). Respiratory Response of *Neomysis Intermedia* (Crustacea: Mysidacea) to Changes in Salinity, Temperature and Season. *Comp. Biochem. Physiol. – Part A.: Physiol.* 50, 181–193. doi: 10.1016/S0010-406X(75)80223-4

Vajedsamiei, J., Melzner, F., Raatz, M., Morón, S., and Pansch, C. (2021). Cyclic Thermal Fluctuations can be Burden or Relief for an Ectotherm Depending on Fluctuations' Average and Amplitude. *Funct. Ecol.* 35, 2483– 2496. doi: 10.1111/1365-2435.13889

Vasseur, D. A., DeLong, J. P., Gilbert, B., Greig, H. S., Harley, C. D. G., McCann, K. S., et al. (2014). Increased Temperature Variation Poses a Greater Risk to Species Than Climate Warming. *Proc. R. Soc. B.: Biol. Sci.* 281, 20132612. doi: 10.1098/rspb.2013.2612

Verslycke, T., and Janssen, C. R. (2002). Effects of a Changing Abiotic Environment on the Energy Metabolism in the Estuarine Mysid Shrimp *Neomysis Integer* (Crustacea: Mysidacea). *J. Exp. Mar. Biol. Ecol.* 279, 61–72. doi: 10.1016/S0022-0981(02)00339-8

Vesakoski, O., Boström, C., Ramsay, T., and Jormalainen, V. (2008). Sexual and Local Divergence in Host Exploitation in the Marine Herbivore *Idotea Baltica* (Isopoda). *J. Exp. Mar. Biol. Ecol.* 367, 118–126. doi: 10.1016/j.jembe.2008.09.006

Viitasalo, M., and Rautio, M. (1998). Zooplanktivory by *Praunus Flexuosus* (Crustacea: Mysidacea): Functional Responses and Prey Selection in Relation to Prey Escape Responses. *Mar. Ecol. Prog. Ser.* 174, 77–87. doi: 10.3354/meps174077

Weisse, T., and Rudstam, L. G. (1989). Excretion and Respiration Rates of *Neomysis integer* (Mysidaceae): Effects of Temperature, Sex and Starvation. *Hydrobiologia* 178, 253–258. doi: 10.1007/BF00006032

Winkler, G., and Greve, W. (2002). Laboratory Studies of the Effect of Temperature on Growth, Moulting and Reproduction in the Co-Occurring Mysids *Neomysis integer* and *Praunus flexuosus*. *Mar. Ecol. Prog. Ser.* 235, 177–188. doi: 10.3354/meps235177

Conflict of Interest: The authors declare that the research was conducted in the absence of any commercial or financial relationships that could be construed as a potential conflict of interest.

Publisher's Note: All claims expressed in this article are solely those of the authors and do not necessarily represent those of their affiliated organizations, or those of the publisher, the editors and the reviewers. Any product that may be evaluated in this article, or claim that may be made by its manufacturer, is not guaranteed or endorsed by the publisher.

Advantages of publishing in Frontiers

OPEN ACCESS
Articles are free to read for greatest visibility and readership

FAST PUBLICATION
Around 90 days from submission to decision

HIGH QUALITY PEER-REVIEW
Rigorous, collaborative, and constructive peer-review

TRANSPARENT PEER-REVIEW
Editors and reviewers acknowledged by name on published articles

Frontiers
Avenue du Tribunal-Fédéral 34
1005 Lausanne | Switzerland

Visit us: www.frontiersin.org
Contact us: frontiersin.org/about/contact

REPRODUCIBILITY OF RESEARCH
Support open data and methods to enhance research reproducibility

DIGITAL PUBLISHING
Articles designed for optimal readership across devices

FOLLOW US
@frontiersin

IMPACT METRICS
Advanced article metrics track visibility across digital media

EXTENSIVE PROMOTION
Marketing and promotion of impactful research

LOOP RESEARCH NETWORK
Our network increases your article's readership